

DEGRADATION OF DIETHANOLAMINE SOLUTIONS BY CARBONYL SULPHIDE AND CARBON
DISULPHIDE

by

OLUKAYODE FATAI DAWODU

B.Sc. (CHEM. ENG.), UNIVERSITY OF IFE, NIGERIA, 1982

M.Sc. (CHEM. ENG.), UNIVERSITY OF IFE, NIGERIA, 1985

A THESIS SUBMITTED IN PARTIAL FULFILMENT OF

THE REQUIREMENTS FOR THE DEGREE OF

DOCTOR OF PHILOSOPHY

in

THE FACULTY OF GRADUATE STUDIES

DEPARTMENT OF CHEMICAL ENGINEERING

We accept this thesis as conforming

to the required standard

THE UNIVERSITY OF BRITISH COLUMBIA

SEPTEMBER 1991

© OLUKAYODE F. DAWODU, 1991

In presenting this thesis in partial fulfilment of the requirements for an advanced degree at the University of British Columbia, I agree that the Library shall make it freely available for reference and study. I further agree that permission for extensive copying of this thesis for scholarly purposes may be granted by the head of my department or by his or her representatives. It is understood that copying or publication of this thesis for financial gain shall not be allowed without my written permission.

Department of CHEMICAL ENGINEERING

The University of British Columbia
Vancouver, Canada

Date OCTOBER 3, 1991

ABSTRACT

The common industrial practice of using aqueous solutions of diethanolamine (DEA) for the removal of impurities such as carbon dioxide (CO_2), hydrogen sulphide (H_2S), carbonyl sulphide (COS) and carbon disulphide (CS_2) from natural, refinery and manufactured gases often entails irreversible reactions between the solvent and the impurities. This phenomenon is referred to as amine degradation and it not only constitutes a loss of the amine but may contribute to operational problems such as foaming, corrosion and fouling.

Degradation of DEA by COS and CS_2 was studied by using a 600 mL stainless steel reactor under the following conditions: DEA concentration 10 - 40 wt%; temperature 120 - 195 $^{\circ}\text{C}$; COS partial pressure 345 - 1172 kPa; CS_2 volume 2.5 - 10.5 mL (CS_2 /DEA mole ratio of 0.055 - 0.233). An analytical procedure consisting of gas chromatography (GC) and gas chromatography/mass spectroscopy (GC/MS) was used to identify over 20 compounds in the partially degraded DEA solutions. The major degradation products are monoethanolamine (MEA), bis hydroxyethyl ethylenediamine (BHEED), bis hydroxyethyl piperazine (BHEP), hydroxyethyl oxazolidone (HEOD), hydroxyethyl imidazolidone (HEI), tris hydroxyethyl ethylenediamine (THEED) and bis hydroxyethyl imidazolidone (BHEI); as well as a dithiocarbamate salt (in the case of the CS_2 -DEA systems). In addition, both COS and CS_2 induced degradation formed solid products which were characterized on the basis of solubility, melting point, elemental composition, solid probe GC/MS and infrared analysis. The number of degradation compounds in the COS -DEA

and CS₂-DEA systems is large when compared with the three major degradation compounds found in CO₂-DEA systems; this demonstrates that the former systems are distinct and more complicated than the latter system.

When COS or CS₂ was contacted with aqueous DEA solution, hydrolysis occurred and H₂S, CO₂, COS and, possibly, CS₂ together with their related ionic species were present in the system. Solubility and hydrolysis experiments were therefore conducted to establish the equilibrium composition of the COS-DEA system prior to the commencement of degradation. A modified Kent-Eisenberg (K/E) model which was developed to correlate the experimental data, showed good agreement between the experimental results and model predictions. Since the K/E and previous models were limited to amine-CO₂ and/or H₂S systems, the present modified K/E model which incorporates COS, is a significant improvement.

The rate of degradation of DEA was found to increase with temperature, DEA concentration, COS partial pressure and CS₂ volume. On the basis of the experiments conducted to evaluate the contributions of the various compounds in the partially degraded solutions, reaction schemes were developed for the formation of 18 degradation compounds in the COS-DEA and CS₂-DEA systems. Despite the complexity of the reactions, the overall degradation of DEA was well represented by a first order reaction for the present experimental conditions. A mathematical model based on the major reaction schemes was developed to estimate the concentrations of DEA and the major degradation compounds in the COS-DEA system.

Contrary to literature information, experiments conducted with gas mixtures of CO_2 and H_2S showed that H_2S enhanced the rate of DEA degradation. A direct result of the combined effects of H_2S and CO_2 on alkanolamines was the production of the corresponding lower order alkanolamines from higher order ones. The resulting mixed amine solution increases the routes for degradation compared to single amine solutions. The study therefore provides an indication of what to expect in terms of degradation when mixtures of alkanolamines are used for gas sweetening.

TABLE OF CONTENTS

ABSTRACT	ii
LIST OF TABLES	xi
LIST OF FIGURES	xiii
ACKNOWLEDGEMENTS	xxii
CHAPTER	
1 INTRODUCTION	1
1.1 OBJECTIVES OF THE PRESENT STUDY	6
2 LITERATURE REVIEW	7
2.1 PROPERTIES OF CARBONYL SULPHIDE AND CARBON DISULPHIDE	7
2.2 ABSORPTION OF ACIDIC GASES IN AQUEOUS ALKANOLAMINE SOLUTIONS	8
2.2.1 CARBON DIOXIDE AND HYDROGEN SULPHIDE	8
2.2.2 CARBONYL SULPHIDE	9
2.2.3 CARBON DISULPHIDE	15
2.3 EQUILIBRIUM REACTIONS OF ACID GASES IN AMINE SOLUTIONS	15
2.3.1 REACTIONS OF HYDROGEN SULPHIDE	15
2.3.2 REACTIONS OF CARBON DIOXIDE	16
2.3.3 REACTIONS OF CARBONYL SULPHIDE	18
2.3.4 REACTIONS OF CARBON DISULPHIDE	20
2.4 DEGRADATION OF DIETHANOLAMINE SOLUTIONS	22
2.4.1 DEGRADATION OF DIETHANOLAMINE BY CARBON DIOXIDE	22

2.4.2	DEGRADATION OF DIETHANOLAMINE BY CARBONYL SULPHIDE	28
2.4.3	DEGRADATION OF DIETHANOLAMINE BY CARBON DISULPHIDE	29
2.5	LIMITATIONS OF THE PREVIOUS COS-DEA AND CS ₂ -DEA DEGRADATION STUDIES	30
2.6	ANALYSIS OF DEGRADED ALKANOLAMINE SOLUTIONS	32
3	EXPERIMENTAL APPARATUS AND PROCEDURE	34
3.1	REACTOR	34
3.2	MATERIALS	35
3.3	EXPERIMENTAL PROCEDURE	37
3.4	SAMPLING	39
3.5	OPERATING CONDITIONS	40
3.6	ANALYTICAL PROCEDURE	41
3.7	TECHNIQUES USED TO IDENTIFY THE DEGRADATION PRODUCTS	42
3.7.1	GAS CHROMATOGRAPHIC (GC) ANALYSIS	43
3.7.2	GAS CHROMATOGRAPHIC/MASS SPECTROMETRIC (GC/MS) ANALYSIS	43
3.7.3	GC/MS ANALYSIS OF SILYLATED DERIVATIVES	45
3.7.4	GC ANALYSIS OF DEGRADED MIXTURE SPIKED WITH SUSPECTED COMPOUNDS	46
3.8	EXPERIMENTAL DESIGN	47
4	IDENTIFICATION OF DEGRADATION PRODUCTS	50
4.1	PRELIMINARY EXPERIMENTS	50
4.1.1	EFFECTS OF ELEVATED TEMPERATURES	50

4.1.2	SURFACE EFFECTS	51
4.1.3	EFFECTS OF STIRRER SPEED	53
4.1.4	REPRODUCIBILITY	53
4.2	DEGRADATION PRODUCTS RESULTING FROM	
	COS-DEA INTERACTIONS	54
4.3	DEGRADATION PRODUCTS RESULTING FROM	
	CS ₂ -DEA INTERACTIONS	76
4.4	CHARACTERIZATION OF THE SOLID PRODUCTS	78
4.4.1	SOLUBILITY	79
4.4.2	MELTING POINT	79
4.4.3	ELEMENTAL ANALYSIS	80
4.4.4	MASS SPECTRAL ANALYSIS	82
4.4.5	INFRA-RED ANALYSIS	86
5	EFFECTS OF OPERATING VARIABLES	90
5.1	COS-DEA SYSTEM	90
5.1.1	EFFECTS OF INITIAL DEA CONCENTRATION	90
5.1.2	EFFECTS OF TEMPERATURE	109
5.1.3	EFFECTS OF INITIAL COS PARTIAL PRESSURE	124
5.2	CS ₂ -DEA SYSTEM	135
5.2.1	EFFECTS OF INITIAL DEA CONCENTRATION	135
5.2.2	EFFECTS OF TEMPERATURE	149
5.2.3	EFFECTS OF INITIAL VOLUME OF CS ₂	161
6	EXPERIMENTS DESIGNED TO ELUCIDATE REACTION MECHANISMS	172
6.1	EFFECTS OF MIXED GASES	172
6.2	EFFECTS OF OXYGEN	183
6.3	EFFECTS OF DEGRADATION COMPOUNDS	185

6.3.1	EFFECT OF ETHANOL	185
6.3.2	EFFECT OF ACETALDEHYDE	186
6.3.3	EFFECT OF ACETIC ACID	189
6.3.4	EFFECT OF ACETONE	191
6.3.5	EFFECT OF BUTANONE	191
6.3.6	EFFECT OF ETHYLENE GLYCOL	192
6.3.7	EFFECTS OF THE ALKYL ALKANOLAMINES	192
6.3.8	EFFECT OF WATER	200
6.3.9	EFFECT OF MONOETHANOLAMINE	202
6.3.10	EFFECT OF BHEED	204
7	SOLUBILITY AND HYDROLYSIS OF CARBONYL SULPHIDE	205
7.1	THEORY	206
7.2	EXPERIMENTAL EQUIPMENT AND PROCEDURE	212
7.2.1	PROCEDURE	212
7.2.2	ACID GAS LOADINGS	214
7.2.3	GAS ANALYSIS	215
7.2.3	SOLUBILITY DETERMINATION AT LOW TEMPERATURES	217
7.2.5	HYDROLYSIS AT ELEVATED TEMPERATURES	219
7.3	RESULTS AND DISCUSSION OF SOLUBILITY AND HYDROLYSIS RUNS	220
7.3.1	SOLUBILITY OF COS IN DEA SOLUTIONS AT LOW TEMPERATURES	221
7.3.2	HYDROLYSIS OF COS IN DEA SOLUTIONS AT ELEVATED TEMPERATURES	226
7.3.3	MODEL PREDICTIONS	235

	7.3.4	REPRODUCIBILITY238
	7.3.5	COS BALANCE238
8		REACTION MECHANISMS240
	8.1	COS-DEA DEGRADATION240
	8.1.1	FORMATION OF MONOETHANOLAMINE (MEA)240
	8.1.2	FORMATION OF ACETALDEHYDE AND KETONES243
	8.1.3	FORMATION OF ACETIC ACID244
	8.1.4	FORMATION OF ETHYL AMINOETHANOL (EAE)246
	8.1.5	FORMATION OF DIETHYL DISULPHIDE246
	8.1.6	FORMATION OF SUBSTITUTED PYRIDINES247
	8.1.7	FORMATION OF ETHYLDIETHANOLAMINE (EDEA)248
	8.1.8	FORMATION OF N,N,N'-TRIS HYDROXYETHYL ETHYLENEDIAMINE (THEED)249
	8.1.9	FORMATION OF BIS HYDROXYETHYL ETHYLENEDIAMINE (BHEED)250
	8.1.10	FORMATION OF N,N'-BIS HYDROXYETHYL PIPERAZINE (BHEP) AND N-HYDROXYETHYL PIPERAZINE (HEP)251
	8.1.11	FORMATION OF N-HYDROXYETHYL OXAZOLIDONE (HEOD)	251
	8.1.12	FORMATION OF N,N'-BIS HYDROXYETHYL IMIDAZOLIDONE (BHEI)252
	8.1.13	FORMATION OF N-HYDROXYETHYL IMIDAZOLIDONE (HEI)	253
	8.1.14	FORMATION OF N-HYDROXYETHYL ACETAMIDE (HEA)	...254
	8.1.15	FORMATION OF ETHANETHIOIC ACID-(S- (HYDROXYETHYL) AMINO) METHYL ESTER (ETAHEAME)254
	8.2	CS ₂ -DEA DEGRADATION255
	8.3	FORMATION OF THE SOLID PRODUCT257

9	KINETIC MODEL FOR DEA DEGRADATION	258
9.1	COS INDUCED DEGRADATION OF DEA	258
9.2	CS ₂ INDUCED DEGRADATION OF DEA	267
10	CONCLUSIONS AND RECOMMENDATIONS	270
10.1	CONCLUSIONS	270
10.1.1	COS INDUCED DEGRADATION	270
10.1.2	CS ₂ INDUCED DEGRADATION	273
10.2	RECOMMENDATIONS	274
	NOMENCLATURE	277
	REFERENCES	280
	APPENDICES	287
A.1	ALKANOLAMINES COMMONLY USED INDUSTRIALLY	287
A.2	SYNTHESIS OF SELECT DEGRADATION COMPOUNDS	289
B.1	CALIBRATION OF THE GAS CHROMATOGRAPH	293
B.2	MASS SPECTRA OF MINOR DEGRADATION COMPOUNDS	308
C	EXPERIMENTAL CONCENTRATIONS	317
D	COMPARISON BETWEEN EXPERIMENTAL AND PREDICTED CONCENTRATIONS	338
E	ERROR AND SENSITIVITY ANALYSIS	358
F	PROGRAM LISTINGS	365

LIST OF TABLES

TABLE

2.1	SELECTED PHYSICAL PROPERTIES OF COS AND CS ₂	8
4.1	REPRODUCIBILITY AND EFFECT OF STIRRER SPEED IN COS-DEA SYSTEMS	54
4.2	DEGRADATION COMPOUNDS DETECTED IN COS-DEA SYSTEMS AND THEIR RETENTION TIMES IN THE GC	59
4.3	ELEMENTAL COMPOSITIONS OF THE SOLIDS FORMED IN THE COS-DEA SYSTEMS	81
4.4	ELEMENTAL COMPOSITIONS OF THE SOLIDS FORMED IN THE CS ₂ -DEA SYSTEMS	81
4.5	FUNCTIONAL GROUPS ASSIGNMENTS IN THE SOLIDS FORMED IN THE COS-DEA AND CS ₂ -DEA SYSTEMS	89
6.1	CONTRIBUTIONS OF OXYGEN TO DEGRADATION IN THE COS-DEA SYSTEM	184
6.2	CONCENTRATIONS OF DEA AND THE LOW BOILING DEGRADATION COMPOUNDS IN THE REGULAR AND EDEA-SPIKED RUNS	196
6.3	CONCENTRATIONS OF DEA AND THE LOW BOILING DEGRADATION COMPOUNDS IN THE REGULAR AND EAE-SPIKED RUNS	197
7.1	FITTING CONSTANTS IN THE HENRY'S LAW EXPRESSION FOR THE COS-DEA SYSTEM (T = 20 - 50 °C)	223
7.2	HENRY'S CONSTANTS FOR THE SOLUBILITY OF COS IN WATER	223
7.3	EQUILIBRIUM DATA FOR THE HYDROLYSIS OF COS IN AQUEOUS DEA SOLUTIONS (COMPOSITIONS ARE EXPRESSED IN MILLIMOLES)	224

7.4	EQUILIBRIUM DATA FOR THE HYDROLYSIS OF COS IN AQUEOUS DEA SOLUTIONS (LIQUID PHASE CONCENTRATIONS ARE EXPRESSED IN MOLE/MOLE DEA)	225
7.5	PREDICTED AND EXPERIMENTAL ACID GAS LOADINGS	239
C.1 - C.20	CONCENTRATIONS OF COMPOUNDS IN THE COS-DEA SYSTEMS	317
C.21 - C.36	CONCENTRATIONS OF COMPOUNDS IN THE CS ₂ -DEA SYSTEMS	327
C.37 - C.43	CONCENTRATIONS OF COMPOUNDS IN OTHER SYSTEMS	335
D.1 - D.18	COMPARISON BETWEEN EXPERIMENTAL AND PREDICTED CONCENTRATIONS	338
D.19 - D.20	RATE CONSTANTS OBTAINED FROM THE OPTIMIZATION ROUTINE	356
E.1	NITROGEN BALANCE FOR THE DEGRADATION RUNS	359
E.2	MAXIMUM DEVIATIONS IN THE DEA CONCENTRATIONS REPORTED FOR THE DEGRADATION RUNS	361
E.3	DEVIATIONS BETWEEN THE EXPERIMENTAL AND FITTED VALUES OF THE PROTONATION, CARBAMATE AND THIOCARBAMATE EQUILIBRIUM CONSTANTS	362
E.4	COMPARISON OF PROTONATION (K_1) AND CARBAMATE (K_2) CONSTANTS FROM THE KENT-EISENBERG AND MODIFIED KENT-EISENBERG MODELS	362
E.5	SENSITIVITY OF THE OBJECTIVE FUNCTION TO CHANGES IN THE RATE CONSTANTS FOR THE COS-DEA SYSTEMS (% CHANGE IN k_i = + 20%)	363
E.6	SENSITIVITY OF THE OBJECTIVE FUNCTION TO CHANGES IN THE RATE CONSTANTS FOR THE COS-DEA SYSTEMS (% CHANGE IN k_i = - 20%)	364

LIST OF FIGURES

Figure

1.1	Typical alkanolamine sweetening unit	4
3.1	Sketch of the reactor	36
3.2	Set-up for the CS ₂ -DEA degradation experiments	38
4.1	Chromatograms of partially degraded DEA solutions of 4M initial concentration (a: 180 °C, 0.34 MPa COS; b: 150 °C, 0.34 MPa COS; c: 120 °C, 0.68 MPa COS)	52
4.2	Chromatograms showing gradual formation of degradation products in a COS-DEA system (4M DEA, 180 °C, 0.34 MPa COS)	55
4.3	Mass spectra of peak 1 identified as Acetone (a: EI spectrum; b: EI reference spectrum; c: CI spectrum)	60
4.4	Mass spectra of peak 2 identified as Butanone (a: EI spectrum; b: EI reference spectrum; c: CI spectrum)	61
4.5	Mass spectra of peak 3 identified as MEA (a: EI spectrum; b: EI reference spectrum; c: CI spectrum; d: CI spectrum of the silyl derivative)	62
4.6	Mass spectra of peak 4 identified as EAE (a: EI spectrum; b: EI reference spectrum; c: CI spectrum)	63
4.7	Mass spectra of peak 5 identified as DEA (a: EI spectrum; b: EI reference spectrum; c: CI spectrum; d: CI spectrum of the silyl derivative)	64
4.8	Mass spectra of peak 6 identified as EDEA (a: EI spectrum; b: EI reference spectrum; c: CI spectrum; d: CI spectrum of the silyl derivative)	65
4.9	Mass spectra of peak 7 identified as HEA (a: EI spectrum; b: EI reference spectrum; c: CI spectrum; d: CI spectrum of the silyl derivative)	66
4.10	Mass spectra of peak 8 identified as HEP (a: EI spectrum; b: EI reference spectrum; c: CI spectrum; d: CI spectrum of the silyl derivative)	67
4.11	Mass spectra of peak 9 identified as ETHEAME (a: EI spectrum; b: CI spectrum; c: CI spectrum of silyl derivative)	68

4.12	Mass spectra of peak 10 identified as BHEED (a: EI spectrum; b: EI reference spectrum; c: CI spectrum; d: CI spectrum of the silyl derivative).	69
4.13	Mass spectra of peak 11 identified as BHEP (a: EI spectrum; b: EI reference spectrum; c: CI spectrum; d: CI spectrum of the silyl derivative)	70
4.14	Mass spectra of peak 12 identified as HEOD (a: EI spectrum; b: EI reference spectrum; c: CI spectrum; d: CI spectrum of the silyl derivative)	71
4.15	Mass spectra of peak 13 identified as HEI (a: EI spectrum; b: EI reference spectrum; c: CI spectrum; d: CI spectrum of the silyl derivative)	72
4.16	Mass spectra of peak 14 identified as THEED (a: EI spectrum; b: EI reference spectrum; c: CI spectrum; d: CI spectrum of the silyl derivative)	73
4.17	Mass spectra of peak 15 identified as BHEI (a: EI spectrum; b: EI reference spectrum; c: CI spectrum; d: CI spectrum of the silyl derivative)	74
4.18	Chromatograms of partially degraded DEA solutions of 3M initial concentration degraded with 10 mL of CS ₂ for 48 hours (a: 180 °C; b: 165 °C; c: 150 °C)	77
4.19	EI and CI mass spectra of the solid formed in the COS-DEA system	84
4.20	EI and CI mass spectra of the solid formed in the CS ₂ -DEA system	85
4.21	Infra-red trace of the solid formed in the COS-DEA system	87
4.22	Infra-red trace of the solid formed in the CS ₂ -DEA system	88
5.1	DEA concentration as a function of initial DEA concentration and time (P _{COS} = 0.34 MPa, T = 120 °C)	92
5.2	DEA concentration as a function of initial DEA concentration and time (P _{COS} = 0.34 MPa, T = 150 °C)	93
5.3	DEA concentration as a function of initial DEA concentration and time (P _{COS} = 0.34 MPa, T = 165 °C)	94
5.4	Overall degradation rate constant as a function of initial DEA concentration and temperature (P _{COS} = 0.34 MPa)	95

5.5	Initial degradation rate as a function of initial DEA concentration and temperature ($P_{\text{COS}} = 0.34 \text{ MPa}$)97
5.6	Acetone concentration as a function of initial DEA concentration and time ($P_{\text{COS}} = 0.34 \text{ MPa}$, $T = 165 \text{ }^{\circ}\text{C}$)98
5.7	Butanone concentration as a function of initial DEA concentration and time ($P_{\text{COS}} = 0.34 \text{ MPa}$, $T = 165 \text{ }^{\circ}\text{C}$)99
5.8	MEA concentration as a function of initial DEA concentration and time ($P_{\text{COS}} = 0.34 \text{ MPa}$, $T = 165 \text{ }^{\circ}\text{C}$)100
5.9	BHEED concentration as a function of initial DEA concentration and time ($P_{\text{COS}} = 0.34 \text{ MPa}$, $T = 165 \text{ }^{\circ}\text{C}$)102
5.10	BHEP concentration as a function of initial DEA concentration and time ($P_{\text{COS}} = 0.34 \text{ MPa}$, $T = 165 \text{ }^{\circ}\text{C}$)103
5.11	HEOD concentration as a function of initial DEA concentration and time ($P_{\text{COS}} = 0.34 \text{ MPa}$, $T = 165 \text{ }^{\circ}\text{C}$)104
5.12	HEI concentration as a function of initial DEA concentration and time ($P_{\text{COS}} = 0.34 \text{ MPa}$, $T = 165 \text{ }^{\circ}\text{C}$)105
5.13	THEED concentration as a function of initial DEA concentration and time ($P_{\text{COS}} = 0.34 \text{ MPa}$, $T = 165 \text{ }^{\circ}\text{C}$)106
5.14	BHEI concentration as a function of initial DEA concentration and time ($P_{\text{COS}} = 0.34 \text{ MPa}$, $T = 165 \text{ }^{\circ}\text{C}$)107
5.15	DEA concentration as a function temperature and time ($P_{\text{COS}} = 0.34 \text{ MPa}$, $\text{DEA}_0 = 4\text{M}$)110
5.16	DEA concentration as a function temperature and time ($P_{\text{COS}} = 0.34 \text{ MPa}$, $\text{DEA}_0 = 3\text{M}$)111
5.17	DEA concentration as a function temperature and time ($P_{\text{COS}} = 0.34 \text{ MPa}$, $\text{DEA}_0 = 2\text{M}$)112
5.18	Arrhenius plots of the overall degradation rate constant ($P_{\text{COS}} = 0.34 \text{ MPa}$)113
5.19	Butanone concentration as a function of temperature and time ($P_{\text{COS}} = 0.34 \text{ MPa}$, $\text{DEA}_0 = 3\text{M}$)114
5.20	Acetone concentration as a function of temperature and time ($P_{\text{COS}} = 0.34 \text{ MPa}$, $\text{DEA}_0 = 3\text{M}$)115
5.21	MEA concentration as a function of temperature and time ($P_{\text{COS}} = 0.34 \text{ MPa}$, $\text{DEA}_0 = 3\text{M}$)116

5.22	BHEED concentration as a function of temperature and time ($P_{\text{COS}} = 0.34 \text{ MPa}$, $\text{DEA}_0 = 3\text{M}$)	117
5.23	BHEP concentration as a function of temperature and time ($P_{\text{COS}} = 0.34 \text{ MPa}$, $\text{DEA}_0 = 3\text{M}$)	118
5.24	HEOD concentration as a function of temperature and time ($P_{\text{COS}} = 0.34 \text{ MPa}$, $\text{DEA}_0 = 3\text{M}$)	119
5.25	HEI concentration as a function of temperature and time ($P_{\text{COS}} = 0.34 \text{ MPa}$, $\text{DEA}_0 = 3\text{M}$)	120
5.26	THEED concentration as a function of temperature and time ($P_{\text{COS}} = 0.34 \text{ MPa}$, $\text{DEA}_0 = 3\text{M}$)	121
5.27	BHEI concentration as a function of temperature and time ($P_{\text{COS}} = 0.34 \text{ MPa}$, $\text{DEA}_0 = 3\text{M}$)	122
5.28	DEA concentration as a function of initial COS partial pressure and time ($\text{DEA}_0 = 3\text{M}$, $T = 150 \text{ }^\circ\text{C}$)	125
5.29	Acetone concentration as a function of initial COS partial pressure and time ($\text{DEA}_0 = 3\text{M}$, $T = 150 \text{ }^\circ\text{C}$)	126
5.30	Butanone concentration as a function of initial COS partial pressure and time ($\text{DEA}_0 = 3\text{M}$, $T = 150 \text{ }^\circ\text{C}$)	127
5.31	MEA concentration as a function of initial COS partial pressure and time ($\text{DEA}_0 = 3\text{M}$, $T = 150 \text{ }^\circ\text{C}$)	128
5.32	BHEED concentration as a function of initial COS partial pressure and time ($\text{DEA}_0 = 3\text{M}$, $T = 150 \text{ }^\circ\text{C}$)	129
5.33	BHEP concentration as a function of initial COS partial pressure and time ($\text{DEA}_0 = 3\text{M}$, $T = 150 \text{ }^\circ\text{C}$)	130
5.34	HEOD concentration as a function of initial COS partial pressure and time ($\text{DEA}_0 = 3\text{M}$, $T = 150 \text{ }^\circ\text{C}$)	131
5.35	HEI concentration as a function of initial COS partial pressure and time ($\text{DEA}_0 = 3\text{M}$, $T = 150 \text{ }^\circ\text{C}$)	132
5.36	THEED concentration as a function of initial COS partial pressure and time ($\text{DEA}_0 = 3\text{M}$, $T = 150 \text{ }^\circ\text{C}$)	133
5.37	BHEI concentration as a function of initial COS partial pressure and time ($\text{DEA}_0 = 3\text{M}$, $T = 150 \text{ }^\circ\text{C}$)	134
5.38	DEA concentration as a function of initial DEA concentration and time (CS_2 volume = 6 mL, $T = 120 \text{ }^\circ\text{C}$, CS_2/DEA mole ratios = 0.10 - 0.20)	136

5.39	DEA concentration as a function of initial DEA concentration and time (CS_2 volume = 6 mL, $T = 150^\circ\text{C}$, CS_2/DEA mole ratios = 0.10 - 0.20)	137
5.40	DEA concentration as a function of initial DEA concentration and time (CS_2 volume = 6 mL, $T = 165^\circ\text{C}$, CS_2/DEA mole ratios = 0.10 - 0.20)	138
5.41	Overall degradation rate constant for CS_2 -DEA systems as a function of initial DEA concentration and temperature (CS_2 volume = 6mL, CS_2/DEA mole ratios = 0.10 - 0.20)	139
5.42	Initial degradation rate as a function of initial DEA concentration and temperature (CS_2 volume = 6mL, CS_2/DEA mole ratios = 0.10 - 0.20)	140
5.43	MEA concentration as a function of initial DEA concentration and time (CS_2 volume = 6 mL, $T = 165^\circ\text{C}$, CS_2/DEA mole ratios = 0.10 - 0.20)	142
5.44	BHEED concentration as a function of initial DEA concentration and time (CS_2 volume = 6 mL, $T = 165^\circ\text{C}$, CS_2/DEA mole ratios = 0.10 - 0.20)	143
5.45	BHEP concentration as a function of initial DEA concentration and time (CS_2 volume = 6 mL, $T = 165^\circ\text{C}$, CS_2/DEA mole ratios = 0.10 - 0.20)	144
5.46	HEOD concentration as a function of initial DEA concentration and time (CS_2 volume = 6 mL, $T = 165^\circ\text{C}$, CS_2/DEA mole ratios = 0.10 - 0.20)	145
5.47	HEI concentration as a function of initial DEA concentration and time (CS_2 volume = 6 mL, $T = 165^\circ\text{C}$, CS_2/DEA mole ratios = 0.10 - 0.20)	146
5.48	THEED concentration as a function of initial DEA concentration and time (CS_2 volume = 6 mL, $T = 165^\circ\text{C}$, CS_2/DEA mole ratios = 0.10 - 0.20)	147
5.49	BHEI concentration as a function of initial DEA concentration and time (CS_2 volume = 6 mL, $T = 165^\circ\text{C}$, CS_2/DEA mole ratios = 0.10 - 0.20)	148
5.50	DEA concentration as a function of temperature and time ($\text{DEA}_0 = 4\text{M}$, CS_2 volume = 6 mL, CS_2/DEA mole ratio = 0.10)	150
5.51	DEA concentration as a function of temperature and time ($\text{DEA}_0 = 3\text{M}$, CS_2 volume = 6 mL, CS_2/DEA mole ratio = 0.13)	151

5.52	DEA concentration as a function of temperature and time (DEA ₀ = 2M, CS ₂ volume = 6 mL, CS ₂ /DEA mole ratio = 0.20)	152
5.53	Arrhenius plots for the overall degradation rate constant as a function of initial CS ₂ volume	153
5.54	MEA concentration as a function of temperature and time (DEA ₀ = 3M, CS ₂ volume = 6 mL, CS ₂ /DEA mole ratio = 0.13)	154
5.55	BHEED concentration as a function of temperature and time (DEA ₀ = 3M, CS ₂ volume = 6 mL, CS ₂ /DEA mole ratio = 0.13)	155
5.56	BHEP concentration as a function of temperature and time (DEA ₀ = 3M, CS ₂ volume = 6 mL, CS ₂ /DEA mole ratio = 0.13)	156
5.57	HEI concentration as a function of temperature and time (DEA ₀ = 3M, CS ₂ volume = 6 mL, CS ₂ /DEA mole ratio = 0.13)	157
5.58	HEOD concentration as a function of temperature and time (DEA ₀ = 3M, CS ₂ volume = 6 mL, CS ₂ /DEA mole ratio = 0.13)	158
5.59	BHEI concentration as a function of temperature and time (DEA ₀ = 3M, CS ₂ volume = 6 mL, CS ₂ /DEA mole ratio = 0.13)	159
5.60	THEED concentration as a function of temperature and time (DEA ₀ = 3M, CS ₂ volume = 6 mL, CS ₂ /DEA mole ratio = 0.13)	160
5.61	DEA concentration as a function of initial CS ₂ volume and time (DEA ₀ = 3M, T = 165 °C)	163
5.62	MEA concentration as a function of initial CS ₂ volume and time (DEA ₀ = 3M, T = 165 °C)	164
5.63	BHEED concentration as a function of initial CS ₂ volume and time (DEA ₀ = 3M, T = 165 °C)	165
5.64	BHEP concentration as a function of initial CS ₂ volume and time (DEA ₀ = 3M, T = 165 °C)	166
5.65	HEOD concentration as a function of initial CS ₂ volume and time (DEA ₀ = 3M, T = 165 °C)	167
5.66	HEI concentration as a function of initial CS ₂ volume and time (DEA ₀ = 3M, T = 165 °C)	168
5.67	BHEI concentration as a function of initial CS ₂ volume and time (DEA ₀ = 3M, T = 165 °C)	169
5.68	THEED concentration as a function of initial CS ₂ volume and time (DEA ₀ = 3M, T = 165 °C)	170

6.1	DEA concentrations as a function of time and gas composition (DEA ₀ = 3M, T = 165 °C)	175
6.2	BHEP concentrations as a function of time and gas composition (DEA ₀ = 3M, T = 165 °C)	176
6.3	HEOD concentrations as a function of time and gas composition (DEA ₀ = 3M, T = 165 °C)	177
6.4	THEED concentrations as a function of time and gas composition (DEA ₀ = 3M, T = 165 °C)	178
6.5	MEA concentrations as a function of time and gas composition (DEA ₀ = 3M, T = 165 °C)	179
6.6	BHEED concentrations as a function of time and gas composition (DEA ₀ = 3M, T = 165 °C)	180
6.7	HEI concentrations as a function of time and gas composition (DEA ₀ = 3M, T = 165 °C)	181
6.8	BHEI concentrations as a function of time and gas composition (DEA ₀ = 3M, T = 165 °C)	182
6.9	Chromatograms of partially degraded DEA solutions of 3M initial concentrations degraded with 10.5 mL of CS ₂ at 180 °C (a: regular run; b: ethanol-spiked run)	187
6.10	Chromatograms of partially degraded DEA solutions of 3M initial concentrations degraded with 10.5 mL of CS ₂ at 180 °C (a: regular run; b: acetaldehyde-spiked run)	188
6.11	Chromatograms of partially degraded DEA solutions of 3M initial concentration degraded with 10.5 mL of CS ₂ at 180 °C (a: regular run; b: acetic acid-spiked run)	190
6.12	Chromatogram of partially degraded EAE solution of 1M initial concentration degraded with 10.5 mL of CS ₂ at 180 °C	193
6.13	Chromatogram of partially degraded EDEA solution of 1M initial concentration degraded with 10.5 mL of CS ₂ at 180 °C	194
6.14	EI mass spectrum of the compound identified as Ethyl amine in the partially degraded EAE solution	198
6.15	EI mass spectrum of the compound identified as Ethyl acetamide in the partially degraded EAE solution	198

6.16	EI mass spectrum of the compound identified as Ethyl thiazolidone in the partially degraded EAE solution	199
6.17	EI mass spectrum of the compound identified as Ethyl thiazolidone-2-thione in the partially degraded EAE solution	199
6.18	Concentrations of DEA as a function of time in aqueous and non-aqueous sytems in contact with 345 kPa of COS at 150 °C	201
7.1	Gas trapping set-up	216
7.2	Chromatogram showing a typical separation by the Chromosil 310 teflon packed column	218
7.3	Henry's constant as a function of temperature for COS in aqueous DEA solutions	222
7.4	H ₂ S liquid loading as a function of initial COS partial pressure and DEA concentration at 120 °C	227
7.5	CO ₂ liquid loading as a function of initial COS partial pressure and DEA concentration at 120 °C	228
7.6	Selectivity as a function of temperature and DEA concentration	229
7.7	Partial pressure of H ₂ S as a function of liquid loading and temperature for a 30 wt% DEA solution	231
7.8	Partial pressure of CO ₂ as a function of liquid loading and temperature for a 30 wt% DEA solution	232
7.9	Henry's constant for H ₂ S in aqueous DEA solutions containing also CO ₂ and COS	233
7.10	Henry's constant for CO ₂ in aqueous DEA solutions containing also H ₂ S and COS	234
A.1	Structure of amines	288
B.1	Calibration curve for acetone	295
B.2	Calibration curve for butanone	296
B.3	Calibration curve for MEA	297
B.4	Calibration curve for DEA	298
B.5	Calibration curve for BHEED	299

B.6	Calibration curve for BHEP300
B.7	Calibration curve for HEOD301
B.8	Calibration curve for HEI302
B.9	Calibration curve for THEED303
B.10	Calibration curve for BHEI304
B.11	Calibration curve for CO ₂305
B.12	Calibration curve for COS306
B.13	Calibration curve for H ₂ S307
B.14	Sample and library EI spectra of methanol308
B.15	Sample and library EI spectra of ethanol309
B.16	Sample and library EI spectra of acetaldehyde310
B.17	Sample and library EI spectra of acetic acid311
B.18	Sample and library EI spectra of methyl pyridine312
B.19	Sample and library EI spectra of diethyl disulphide313
B.20	Sample and library EI spectra of 1,2 dithiane314
B.21	Sample and library EI spectra of ethyl methyl pyridine315
B.22	Mass spectra of EHEP (a: EI; b: CI)316

ACKNOWLEDGEMENTS

I wish to express my gratitude to the following for their various contributions towards the completion of my doctoral program:

- Professor Axel Meisen for his supervision, guidance and encouragements, particularly during the difficult moments of this work;
- Professor Larry Weiler for his help with the reaction mechanisms and other chemistry-related aspects of this work;
- My wife, Adeyinka, and my sons, Ayoyinka and Olaniyi, for their love, understanding and sacrifice;
- My parents, brothers and sisters for their love and moral support. In particular, I gratefully acknowledge the efforts of my mother and mother-in-law in taking care of our sons while my wife and I pursued our academic goals;
- The Canadian Commonwealth Scholarship and Fellowship Plan for the scholarship to pursue my doctorate program, as well as the Natural Sciences and Engineering Research Council of Canada for the grant(s) to purchase equipments and supplies;

Finally, I thank God for giving me the health and stamina to complete the program.

CHAPTER 1

INTRODUCTION

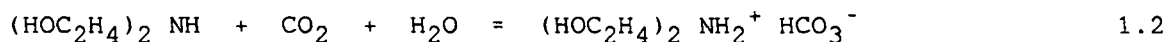
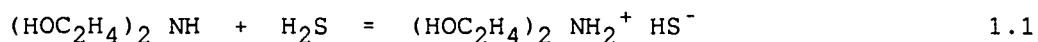
Natural gas consists essentially of methane, with other hydrocarbons such as ethane and propane being present in considerably lower amounts. In addition to these hydrocarbons, the other constituents are commonly referred to as contaminants and they include carbon dioxide, hydrogen sulphide and water. In natural gas reservoirs containing large amounts of carbon dioxide and hydrogen sulphide, it is also usual to find other impurities such as carbonyl sulphide and carbon disulphide albeit at quite low concentrations. Carbonyl sulphide and carbon disulphide also occur as impurities in refinery and synthesis gases, particularly those derived from coal conversion and catalytic and thermal cracking processes. Their concentrations in these gas streams vary from a few parts per million (ppm) to about 1% (1).

The removal of impurities is necessary for reasons of toxicity, corrosivity and environmental regulations. The extent of removal depends on the end use of the clean gas, but typical environmental requirements for hydrogen sulphide is $0.00557\text{g H}_2\text{S/m}^3$ of natural gas, while the total sulphur content could be as high as 0.2228g /m^3 of natural gas (1).

A variety of purification or sweetening processes are being used for the removal of acidic contaminants. These include dry bed, direct conversion, physical, chemical and speciality solvent processes. By far the most widely used purification processes are the chemical solvent processes utilizing alkanolamines as the solvent. Alkanolamines are

amino derivatives of alcohols or alcohol derivatives of ammonia, and thus possess dual functionality. The hydroxyl group increases the molecular weight of the amine, resulting in a reduced vapour pressure and increased water solubility, while the needed alkalinity in aqueous solutions to cause the absorption of acidic gases is provided by the amino group. The amines commonly used in industry are monoethanolamine (MEA) and diethanolamine (DEA). Other less common ones are diglycolamine (DGA), diisopropanolamine (DIPA), methyldiethanolamine (MDEA), triethanolamine (TEA) and sterically hindered amines such as 2-amino-methyl propanol (AMP). The structural formulae of these amines are given in Appendix A1. The popularity of alkanolamines in gas treating is a result of their ability to reduce the concentrations of the contaminants to levels lower than those economically achievable with other methods. There are currently over 1400 alkanolamine plants in use world wide (2).

The absorption of the acidic impurities is enhanced by reversible chemical reactions with the amine. Such reactions are summarized for DEA as follows:



The reversibility of these reactions form the basis of the sweetening operation and affords continuous use of the amine solution over long periods of time.

The use of alkanolamines for gas sweetening dates back to 1930 when Bottoms (3) was granted a patent covering triethanolamine. A

typical alkanolamine sweetening unit is shown in Figure 1.1. Feed gas enters the absorber from the bottom and contacts a downward stream of an aqueous solution of an alkanolamine at low temperature and elevated pressure. The solvent absorbs the impurities in the gas, leaving a cleaner (sweeter) gas exiting the absorber at the top. Usually, a scrubber is installed before the absorber to remove particulate matter and entrained liquids from the feed gas. Another scrubber after the absorber removes amine droplets entrained in the sweet gas. The "rich" amine solution leaving the bottom of the absorber is flashed to remove dissolved hydrocarbons and passed through a heat exchanger before entering the stripper at elevated temperature. A counter current flow of steam strips off the absorbed gases leaving a "lean" amine solution to exit the stripper. The lean amine solution is passed through a series of heat exchangers to reduce its temperature before returning to the absorber for another cycle. Activated carbon columns are usually installed upstream of the absorber to remove impurities and foam-inducing surface active materials from a slip stream of the lean amine solution. The overhead products of the stripping column are passed through a condenser to remove water which is returned as reflux to the stripper. The effluent gases, depending on their composition, may undergo further treatment such as sulphur recovery in a Claus unit. The treated gas leaving the top of the absorber is usually passed through a glycol dehydration unit to remove water and entrained alkanolamine. In some plants, a mixture of alkanolamine and glycol is used in the absorber, to simultaneously remove impurities and water from the feed gas.

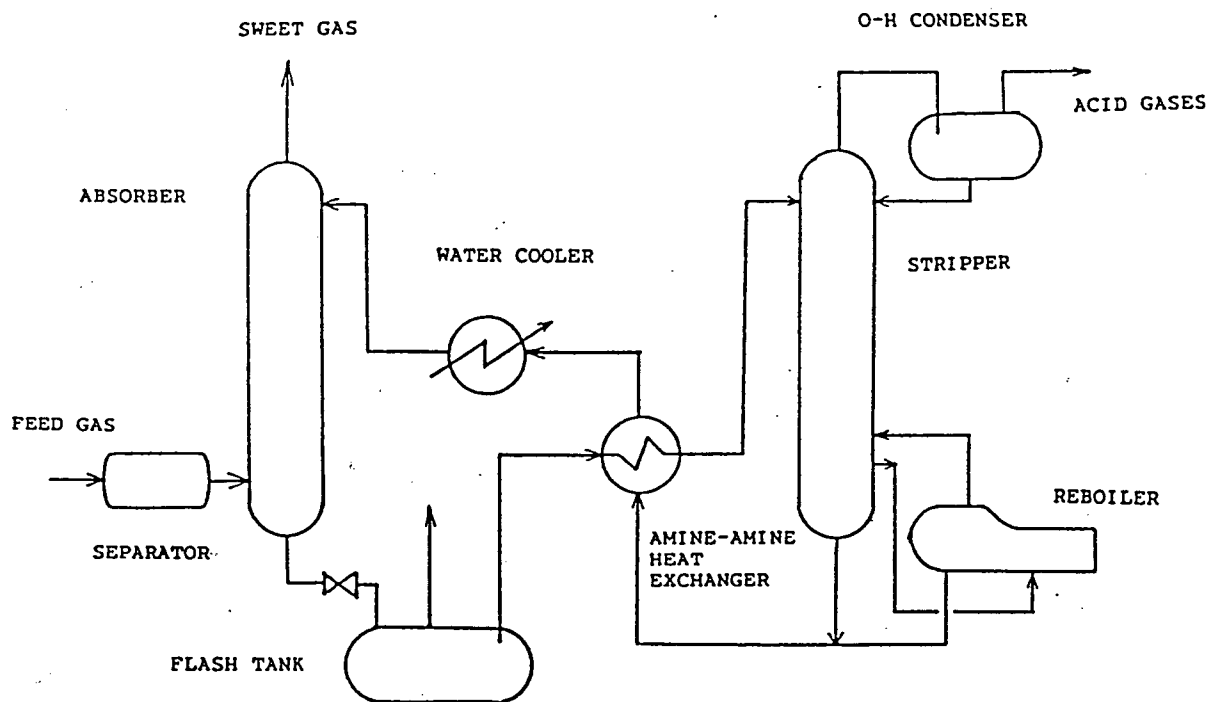


Figure 1.1: Typical alkanolamine sweetening unit.

In spite of their resistance to chemical breakdown, plant and laboratory reports indicate that, on prolonged use, alkanolamines are transformed into undesirable products from which the amine is not easily recovered. This phenomenon, commonly referred to as "amine degradation", not only leads to amine losses, but may also contribute to operational problems such as foaming (4,5,17), corrosion (6-8) and fouling (9).

The degradation of DEA by CO_2 has been studied quite extensively (9-18) and there is evidence that the degradation proceeds primarily via amine carbamate (e.g. $(\text{HOC}_2\text{H}_4)_2\text{NCOO}^-\text{H}^+$) which may be formed by the direct reaction of carbon dioxide with amines. Since hydrogen sulphide is incapable of forming carbamate-type compounds, it is generally agreed that hydrogen sulphide does not cause amine degradation. The results reported by Choy (12) and Kim and Sartori (13) suggest that hydrogen sulphide in the presence of carbon dioxide actually hinders amine degradation. By contrast, relatively little is known about the degradation of DEA by carbonyl sulphide and carbon disulphide. Orbach and Selleck (19) and Pearce et. al. (20) were unable to detect appreciable amounts of degradation compounds in COS-DEA systems and they concluded that unlike MEA, DEA is not degraded by COS. It has been estimated that 10 - 20% of the COS-MEA reaction leads to non-regenable products (20). DEA is therefore the preferred choice for treating gas streams containing COS. Osenton and Knight (21) reported that CS_2 reacted with DEA to form primarily a dithiocarbamate salt from which the amine could not be easily recovered.

These conclusions notwithstanding, there are three reasons (expatiated in Chapter 2) to believe that COS and CS_2 are capable of

degrading DEA. First, COS and CS₂ may be hydrolysed to H₂S and CO₂ with the latter causing the well known CO₂-induced degradation. Second, previously used reaction times were too short. Third, the analytical techniques used in the past were inadequate.

As the supply of sweet gas and light crude oil declines, more sour deposits containing appreciable amounts of COS and CS₂ are being processed. The present study was therefore conducted to provide qualitative and quantitative information on the interactions of COS and CS₂ with DEA, particularly in regard to the degradation of the amine.

1.1 OBJECTIVES OF THE PRESENT STUDY

The principal objectives of the present study may be stated as follows:

1. To identify the reaction products and to propose reaction mechanisms when COS and CS₂ are separately contacted with aqueous solutions of diethanolamine.
2. To determine the effects of temperature, pressure and solution concentration on the reactions.
3. To identify the reaction products and to propose reaction mechanisms when mixtures of COS, CO₂ and H₂S are contacted with aqueous DEA solutions.
4. To develop predictive kinetic models for amine degradation resulting from COS and CS₂ exposure.

CHAPTER 2

LITERATURE REVIEW

This review emphasises studies concerning the COS-DEA and CS₂-DEA systems. The interactions of the other impurities such as CO₂ and H₂S with DEA and other amines are also included because, as will be shown in later chapters, the partially degraded DEA solutions contain mixtures of amines and acid gases.

2.1 PROPERTIES OF CARBONYL SULPHIDE AND CARBON DISULPHIDE

Carbonyl sulphide and carbon disulphide are colourless compounds which exist as a gas and liquid respectively, at standard temperature and pressure. Some selected physical properties are shown in Table 2.1. A review paper by Ferm (22) and The Encyclopedia of Chemical Technology (23) provide more extensive coverage of the properties and chemistry of COS. Other properties of CS₂ as well as its reactions are also listed in The Encyclopedia of Chemical Technology (24).

Carbon dioxide and hydrogen sulphide are more common than COS. Their properties are not discussed here, but may be found in most chemistry texts and encyclopediae (25,26).

Table 2.1: Selected physical properties of COS and CS₂.

Properties	COS	CS ₂
Molecular Weight	60.0	76.0
Specific Gravity*	2.485	1.263
Boiling Point (°C)	- 50.2	46.2
Melting Point (°C)	-138.2	-111.53
Critical Temperature (°C)	105.0	273.0
Critical Pressure (MPa)	6.129	7.699

*COS and CS₂ values refer to air and water, respectively.

2.2 ABSORPTION OF ACIDIC GASES IN AQUEOUS ALKANOLAMINE SOLUTIONS

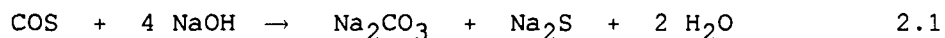
2.2.1 CARBON DIOXIDE AND HYDROGEN SULPHIDE

Several studies have been conducted on the absorption or solubility of CO₂ and H₂S in alkanolamine solutions. Some of those on DEA solutions are listed in references (27-35). The studies cover a wide range of operating conditions and provide equilibrium data essential for the modelling and simulation of acid gas plants. These data, together with the reactions between the acid gases and the alkanolamine solutions, have been used to develop thermodynamic models to predict the equilibrium compositions in acid gas-alkanolamine-water systems (36-41).

Since the focus of the present study is on the degradation of DEA, the equilibrium models are not reviewed. Detailed critiques of the earlier models have been presented by Austgen et al. (41). However, a shortcoming of all the models is that they are limited to CO_2 and/or H_2S - amine systems. Consequently, there is a need for models which accomodate other impurities such as COS and/or CS_2 . Such a model, based on the Kent and Eisenberg (39) approach, is presented in Chapter 7.

2.2.2 CARBONYL SULPHIDE

Early attempts at removing COS from gas streams were generally based on its hydrolysis in aqueous sodium hydroxide (NaOH) according to the overall equation:



One such method was described by Schultze et al. (42) but the hydrolysis was slow and required long contact times to go to completion. Johnson et al. (43) found that the hydrolysis could be accelerated by using aqueous mixtures of MEA and NaOH. The MEA acts as a catalyst; it forms a thiocarbamate with the COS, which is then hydrolysed by NaOH thereby regenerating the MEA. These methods consumed NaOH due to the difficulty in regenerating it from sodium sulphide (Na_2S) and sodium carbonate (Na_2CO_3).

The use of alkanolamines was regarded as a better alternative since they are effective in absorbing CO_2 and H_2S and the amine is easily regenerated. Schultze and Short (44) described a method utilizing MEA impregnated on a bed of alumina for the absorption of COS from liquid propane and butane. It was reported that the system removed COS from a stream originally containing 0.002 wt% COS, but the COS was irreversibly bound to the MEA. Kearns and Beamer (45) also used aqueous solutions containing 10 - 60 wt% MEA to absorb COS from a gas stream and found that the MEA was irreversibly transformed to diethanolurea. As a result of the substantial amine losses that occur from the irreversible reactions of MEA with COS, DEA is generally a preferred choice for treating gases containing COS. Nevertheless, the choice of DEA for processing COS bearing streams has been controversial in the past. Kerns and Beamer (45) and Reed (46) claimed that DEA is inert to COS and cannot effectively remove COS from gas streams even though they did not provide details of their experimental conditions. On the other hand, Easthagen et al. (47) reported that 99% of carbonyl sulphide in gaseous hydrocarbons can be removed by treatment with aqueous DEA and that the spent solution is easily regenerated by steam stripping. Other studies have also shown that DEA absorbs COS from gas streams (19,20). Pearce et al. (20) passed COS into aqueous DEA solutions and analyzed them by gas chromatography. Carbonyl sulphide was detected in the solution and this was taken as an indication that DEA absorbs COS directly and not its hydrolysis products. Orbach and Selleck (19) contacted a gas stream containing 1 mole% COS in N_2 alternately with aqueous solutions containing 20% MEA and 35 wt% DEA at room temperature. The gas and

solvents flowed countercurrently in a 25 mm I.D. glass column packed to a height of 40 cm with 6 mm O.D. glass Raschig rings. The gas leaving the column was analysed with an infra-red spectrophotometer set to a wavelength of 4.87 microns where the absorption coefficient of COS is $9.18 \times 10^{-3} \text{ mm Hg}^{-1} \text{ cm}^{-1}$. It was found that both MEA and DEA solutions absorbed COS from the gas stream but more COS was absorbed by the DEA solution.

The absorption of COS in amine and alkali solutions was reported by Sharma and Danckwerts (48). The experimental data obtained from various contacting devices such as a wetted wall column, stirred cell and jet apparatus showed that most of the amines absorbed COS. At 25 °C, the second order reaction rate constants for the amine-COS reaction ($k_{\text{AM-COS}}$) was approximately 1% of the rate constant for the corresponding amine-CO₂ reactions. The ratio was only 0.25% in the case of MEA. Less common amines such as methyl aminoethanol (MAE) and ethyl aminoethanol (EAE) gave better results than either MEA or DEA in the absorption of COS. The rate constants obtained for these amines were 250 and 220 L/(mole s) respectively, as opposed to 16 and 11 L/(mole s) for MEA and DEA, respectively.

Rahman (49) has studied the absorption of acid gases in anhydrous alkanolamines. CO₂, H₂S, COS and mercaptans were contacted with MEA, DEA, DGA, DIPA and MDEA in a Claisen distillation flask at initial pressures up to 20 psig. The temperature in the flask was not controlled, but depended on the heats of reactions. Temperature and pressure variations were recorded during the experiments which lasted 1 hour. All alkanolamines were found to absorb COS as indicated by the

drop in the total pressure within the reaction vessel. Analysis of samples of the amine-COS systems by ^{13}C NMR spectroscopy revealed the presence of the respective thiocarbamates. Although the study was able to establish the species in the amine solutions, the data pertained only to anhydrous systems and are therefore of little industrial relevance.

The physical solubility of a gas in a solvent with which it reacts cannot be determined directly. Al-Ghawas et al (50) therefore used the N_2O analogy originally proposed by Clarke (51) to determine the physical solubility of COS in 0 - 30 wt% aqueous MDEA solutions at 20 to 40 °C and 1 atm pressure. The ratio of the Henry's constants for the solubility of COS and N_2O ($H^\circ_{\text{COS}}/H^\circ_{\text{N}_2\text{O}}$) in water and 15.5 wt% ethylene glycol solutions were first determined at 25°C. The difference in the ratios for both systems was found to be only 0.26%. It was then assumed that this ratio was the same for all temperatures and amine solutions. The Henry's constants for the solubility of COS in aqueous MDEA solutions were then determined from the expression:

$$H_{\text{COS}} = H^\circ_{\text{COS}}/H^\circ_{\text{N}_2\text{O}} \times H_{\text{N}_2\text{O}}$$

where H°_i and H_i refer to the Henry's constant for the solubility of gas i in water and aqueous MDEA solutions, respectively.

The Henry's constants were found to range from 3.941 kPa m^3/mol for water at 20 °C to 7.554 kPa m^3/mol for 30.21 wt% MDEA solution at 40 °C. The temperature variation of the Henry's constant was well correlated by the Arrhenius expression. Since the focus of the study was the kinetics of the COS-MDEA reaction, only physical solubility and

diffusivity data were reported. No information was provided on the total solubility of COS in MDEA solutions.

It was recently reported (52) that the absorption of COS into alkaline solutions could be enhanced by using a second emulsified liquid phase. A theoretical enhancement factor was defined as the ratio of the specific rate of absorption in the base, with and without the second emulsified liquid phase. Enhancement factors of 2.5 and 4.0 respectively were achieved using toluene (20% v/v) and 2-propanol (50% v/v) as the second emulsified liquid phases in sodium hydroxide solution at 30 °C. There was no indication whether such enhancements could be achieved in alkanolamine systems. The operational difficulties which may accompany the use of emulsions, were not discussed either.

Reilly et al. (89) have also reported that the rate of absorption of COS in MDEA solutions was enhanced by heterocyclic amine additives. Enhancements factors up to 8 fold were obtained for the range of additives concentrations investigated. The additives produced little or no enhancements in the corresponding CO₂ systems.

Other alkanolamines such as DIPA (53) and DGA (54) are used for absorbing COS without incurring appreciable amine loss but their industrial acceptance is still quite limited. Singh and Bullin (55) studied the kinetics of the reaction between COS and aqueous DGA over a temperature range of 307 - 322 K and pressure range of 345 - 414 kPa. They used a perfectly mixed flow reactor operated with continuous gas and liquid feeds. The composition of the amine solution leaving the absorber was determined by gas chromatography. Although the hydrolysis of COS produces equimolar amounts of CO₂ and H₂S, the GC analysis

recorded insignificant levels of CO_2 . The latter may be due to its consumption in the degradation of DGA. The rates of reaction were calculated by dividing the sum of the molar flow rates of COS (and the H_2S from the hydrolysis reaction) by the volume of the reactor; they were found to be much higher than those for the $\text{COS-H}_2\text{O}$ reaction (56). This led to the conclusion that DGA was catalysing the hydrolysis of COS. A similar effect has also been reported for other amines (57). The COS-DGA reaction was second order; it was first order with respect to the amine and COS concentrations. The second order reaction rate constants obeyed the Arrhenius expression. At 27°C , the value was $0.0023 \text{ m}^3/(\text{mol s})$ compared to $0.166 \text{ m}^3/(\text{mol s})$ (49) and at most $0.016 \text{ m}^3/(\text{mol s})$ (48,57). The latter was inferred from the rate constant reported at 25°C for the reaction of COS with MEA, a primary amine that reacts faster than DGA. The reported values differ significantly but it is difficult to make a direct comparison of the rate constants for acid gas-amine reactions in aqueous and non-aqueous amine systems because of the differences in diffusivity, ionic strength, nature of gas-liquid interface and physical solubility. The combined effects of these factors may explain the higher values found by Rahman.

It is clear from the foregoing that COS is absorbed directly into amine solutions and not its hydrolysis products. However, compared to CO_2 and H_2S , very little work has been reported on the total solubility of COS in amine solutions. The few studies on COS-amine systems cover narrow temperature ranges below 50°C . It is not surprising therefore that Vapour-Liquid-Equilibrium (VLE) models to date, are limited to aqueous amine- CO_2 - H_2S systems.

2.2.3 CARBON DISULPHIDE

Osenton and Knight (21) contacted CS_2 vapour with aqueous alkanolamine solutions and used changes in system pressure to establish the rates of absorption of CS_2 into alkanolamine solutions. The rates of absorption followed the order Sulfinol > 25% DEA > 20% MEA. Sulfinol is a mixture of DIPA and a physical solvent. As in the case of COS, equilibrium data for the solubility of CS_2 in amine solutions are lacking.

2.3 EQUILIBRIUM REACTIONS OF ACID GASES IN AMINE SOLUTIONS

When acid gases are absorbed into alkanolamine solutions, ionic species are generated and various equilibria, which are discussed in the following sections, are established.

2.3.1 REACTIONS OF HYDROGEN SULFIDE

Hydrogen sulphide in aqueous amine solutions dissociates into H^+ and HS^- :



The proton is transferred to the amine virtually instantaneously (2,58):



where R' and R'' represent H and / or -C₂H₄OH, depending on the class of amine, while R represents -C₂H₄OH.

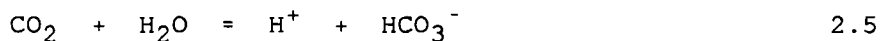
The bisulphide ion can dissociate further:



However, this reaction occurs only in highly basic solutions (pH > 12) and can usually be disregarded for alkanolamine solutions contacting acid gases (2,58).

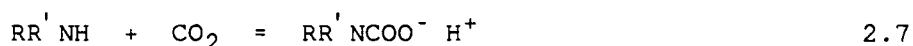
2.3.2 REACTIONS OF CARBON DIOXIDE

The equilibria in CO₂-amine systems can be represented by the following series of equations:

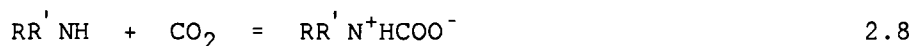


Reaction 2.5 has been shown to be catalysed by bases (37,58,59). The protons (or hydrogen ions) react with the amines to form protonated amines according to equation 2.3.

In addition, a direct reaction occurs between CO₂ and primary and secondary amines to form carbamates:



It has been postulated that this equation may involve two steps; a zwitterion intermediate is first formed which by virtue of its instability, is easily deprotonated in the presence of a base (B) to form the carbamate (60):

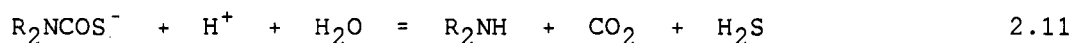
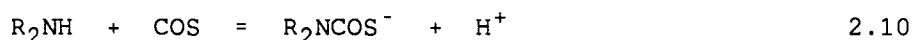


Equation 2.8 is the rate determining step since the deprotonation of the zwitterion (Eq. 2.9) is instantaneous (59,60). Reaction 2.7 is much faster than the hydration of CO_2 (eq. 2.5) and represents the major mode of interaction between CO_2 and primary or secondary amines.

Tertiary amines have no labile hydrogen atoms and are therefore unable to form carbamates. Absorption of CO_2 in such amines proceeds via Eqs. 2.5 and 2.6. They are able to absorb H_2S at a faster rate and are thus used for the selective absorption of hydrogen sulphide. Methyldiethanolamine (MDEA) is widely used for this purpose (61-63).

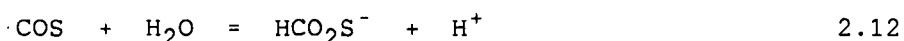
2.3.3 REACTIONS OF CARBONYL SULPHIDE

Sharma (57) postulated that, because of the structural similarities of CO_2 and COS, their reactions with amines are similar. The relevant equations for the COS-DEA system would therefore be:



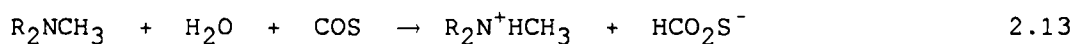
Equation 2.10 represents the thiocarbamate formation. Primary and secondary amines undergo this reaction. In the case of MEA, the thiocarbamate may be further transformed into degradation products from which the amine is not easily recovered (19,20,64). It has been estimated that 10 to 20% of the MEA reacting with COS is lost in such irreversible reactions (20). Equation 2.11 is the COS hydrolysis reaction. It has been represented in this form since most of the COS in solution was absorbed as thiocarbamate and also to indicate that the hydrolysis of COS is catalyzed by the DEA. Rahman (49) and Rahman et al. (65) confirmed through NMR spectroscopy, the presence of the respective carbamates, thiocarbamates and protons in anhydrous alkanolamine-acid gas systems. The H_2S and CO_2 produced via Eq. 2.11 then initiate the reactions shown in Eqs. 2.2 - 2.4 and 2.5 - 2.7, respectively.

Al-Ghawas et al. (50) have suggested that COS may be hydrated like CO_2 by forming a thio-bicarbonate ion:



The existence of HCO_2S^- in solution was not proven directly but was inferred from spectroscopic observations. A mixture of CO_2 and H_2S was bubbled through an aqueous solution of MDEA and COS was bubbled through another aqueous MDEA solution. Both solutions, when inspected spectrophotometrically, were found to absorb at different wavelengths; the solution exposed to COS absorbed at 518 nm, whereas the other solution absorbed at 503 nm. It is known that CO_2 and H_2S in solution give rise to HCO_3^- and HS^- , respectively. If hydrolysis of COS is the

predominant reaction in the COS-MDEA solution, the solution should absorb at the same wavelength as the MDEA solution exposed to CO_2 and H_2S . The observed differences in absorption wavelengths were attributed to the existence of another species, i.e. HCO_2S^- . The overall reaction for the COS-MDEA system was postulated as:



The second order rate constant k_2 , was given by the expression:

$$k_2 = 4198.74 \exp (-4575.80/T).$$

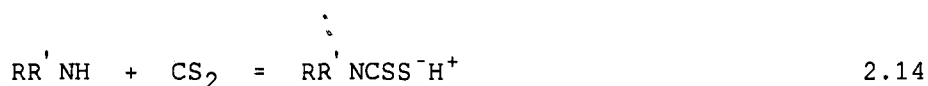
The units of k_2 and T are $\text{m}^3/\text{mol s}$ and Kelvin (K) respectively.

It is therefore clear that an aqueous COS-amine system at equilibrium, consists of the amine, CO_2 , H_2S , unhydrolysed COS and their derived species such as protonated amine, carbamates, thiocarbamates, hydrogen ions and bicarbonate ions. The selectivity of the amine for these gases will establish the equilibrium composition of the system.

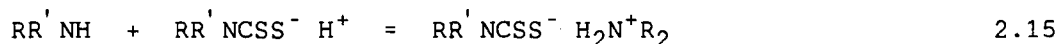
2.3.4 REACTIONS OF CARBON DISULPHIDE

Osenton and Knight (21) used thin layer chromatography to confirm that CS_2 reacts with aqueous alkanolamine solutions. In their work, 7 mL of CS_2 were added to 40 mL of aqueous amine solutions and the resulting mixture was stirred for a short time. Samples of the aqueous layer of

the mixture were then spotted on a silica gel TLC plate and developed in methanol. Subsequent inspection of the plate in iodine or U.V. light showed, in all cases, the presence of a new compound in addition to the starting materials. This compound was reported as amine dithiocarbamate, the product of the CS₂-amine reaction:



The amine dithiocarbamate reacts further in the presence of excess amine to give the dithiocarbamate salt of the amine:



Kothari and Sharma (66) have determined the kinetic parameters of the reaction of CS₂ with aqueous amine solutions using stirred cells. The amine solutions were contacted with CS₂ in the vapour and liquid states at temperatures between 5 and 30 °C. The kinetic parameters were estimated by applying the penetration theory equation to the experimental data, and were found to be independent of the state of the CS₂ and speed of agitation above 25 r.p.m. The rate constants obtained for the amine-CS₂ reactions obeyed the Arrhenius expression. Diethanolamine was the only alkanolamine investigated and a rate constant of 0.10 L/g-mole-s was reported for the CS₂-DEA reaction at 30 °C. By comparing the second order rate constants ($k_{\text{AM-CS}_2}$) with published rate constants for the corresponding CO₂-amine it was found that:

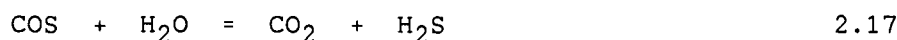
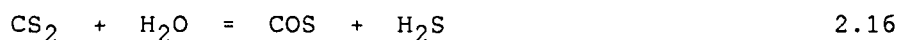
$$k_{\text{AM-CO}_2} / k_{\text{AM-CS}_2} = 2 \times 10^4.$$

Since $k_{\text{AM-CO}_2} / k_{\text{AM-COS}} = 1 \times 10^2$ (57), it follows that

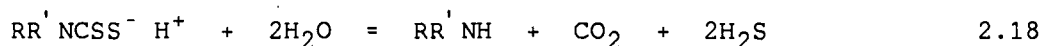
$$k_{\text{AM-COS}} / k_{\text{AM-CS}_2} = 2 \times 10^2.$$

The ratios of the reaction rate constants indicate that the rates of reaction follow the order: $k_{\text{AM-CO}_2} > k_{\text{AM-COS}} > k_{\text{AM-CS}_2}$.

Carbon disulphide also undergoes hydrolysis in aqueous solutions producing COS, CO₂ and H₂S (24). The overall reactions are:



CS₂ hydrolysis may also occur via the amine dithiocarbamate:

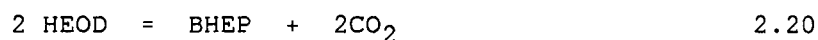


The CO₂/H₂S ratio is therefore 1/2 compared with 1/1 for COS hydrolysis.

2.4 DEGRADATION OF DIETHANOLAMINE SOLUTIONS

2.4.1 DEGRADATION OF DIETHANOLAMINE BY CARBON DIOXIDE

The degradation of DEA by carbon dioxide was first reported by Polderman and Steele (10). Two compounds, bis hydroxyethyl piperazine (BHEP) and hydroxyethyl oxazolidone (HEOD) were detected in the degraded solution. It was suggested that these compounds were formed as follows:



Later, Hakka et al. (11) identified another compound, tris hydroxyethyl ethylene diamine (THEED) in a degraded DEA solution, but offered no mechanism for its formation. Other more detailed studies have since been published (9, 12-18).

Choy (12) conducted degradation experiments using a stainless steel reactor at temperatures between 165 and 180 °C and CO₂ pressures of up to 4238 kPa. Analysis of the solutions by gas chromatography indicated a number of products, but only BHEP was conclusively identified. It was reported that the initial overall DEA degradation could be represented by first order kinetics even though the rate constant was a function of the initial DEA concentration.

Kennard (16) as well as Kennard and Meisen (14) reported results of degradation experiments conducted in a 600 mL stainless steel reactor. Aqueous solutions containing 5 - 100 wt% of DEA were subjected to CO₂ pressures up to 4.1 MPa at temperatures ranging from 90 - 205°C. A total of 12 products were identified in the degraded solutions, the major ones being BHEP, HEOD and THEED. The following simplified mechanism, supported by experimental observations, was suggested for the formation of the major degradation products:



The initial rate of DEA degradation was found to increase with DEA concentration, temperature and CO₂ partial pressure; these observations

agreed with those of Choy (12). A pseudo first order kinetic model was developed to predict the rate of degradation and the formation of the major degradation compounds. The HEOD formation (Eq. 2.21) was assumed to be irreversible and the influence of CO_2 partial pressure on the kinetics was eliminated by establishing the pressure beyond which CO_2 loading was constant. Thus the kinetic model was restricted to the ranges: DEA concentration of 0 - 100 wt%; temperatures of 90 - 175 °C; CO_2 loadings > 0.2g / g DEA. CO_2 was neither consumed nor formed in the degradation process and was therefore suggested as catalysing the process.

Kim and Sartori (13) conducted degradation experiments at 100 and 120°C using 3.2M aqueous DEA solutions containing various amounts of CO_2 and/or H_2S . The solutions were put in sealed stainless steel ampoules which were then immersed in a temperature controlled bath. The rate of degradation increased with increasing CO_2 loadings, producing BHEP, HEOD and THEED as the major degradation compounds. A scheme suggesting successive reactions was put forth to account for the formation of the degradation compounds:



Rate constants for the reaction steps were determined at 100 and 120°C. Again, the catalytic role of CO_2 was noted while H_2S exerted essentially no effect. It should be noted that the ratio of CO_2 to H_2S solution

loading in the only mixed gas run reported was 36.7. The extremely low H_2S loading might explain the similar initial rate of degradation obtained in the corresponding run conducted with CO_2 alone.

Chakma (18) and Chakma and Meisen (9) have reported degradation of DEA by CO_2 in a heat transfer loop. The rate of degradation increased with temperature, DEA concentration and CO_2 partial pressure, but decreased with solution flow rate. The mechanism suggested by Kennard and Meisen (14) was used to develop a mathematical model for the degradation. However, unlike in the previous case (14), CO_2 was explicitly included in the rate expressions so that the model could cover a wider range of operating conditions. In essence, the formation of HEOD and THEED was governed by second order kinetics while BHEP formation was first order as shown below:



The rate constants were reported as functions of temperature.

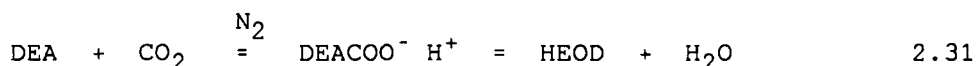
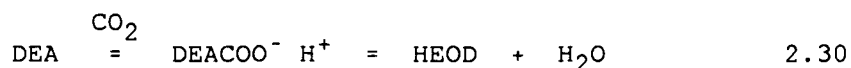
Hsu and Kim (15) used a gas chromatograph coupled to a mass spectrometer (GC/MS) to identify higher molecular weight triamino degradation compounds in aqueous DEA solutions degraded by CO_2 . The mixture was first derivatized to make the compounds more volatile and thus amenable to GC/MS analysis. The procedure for the derivatization

consisted of saturating the partially degraded solution with potassium carbonate to remove water, followed by extraction with isopropyl alcohol. The alcohol was then evaporated to obtain a dehydrated oily material. 1 mL of anhydrous pyridine, 0.2 mL of hexamethyl disilazane and 0.1 mL of trimethylchlorosilane were added to the oil and the resulting mixture was vigorously shaken for 30 s and kept at room temperature for over 5 min until derivatization was complete. In addition to DEA, HEOD, BHEP and THEED three other compounds, 3-(-(bis(2-hydroxyethyl)-amino)ethyl)-2-oxazolidone (HAO), N-(2-(N,N-bis(2-hydroxyethyl)amino)ethyl)-N'-(2-hydroxyethyl)piperazine (HAP) and N,N,N',N''-tetrakis(2-hydroxyethyl)diethylenetriamine (THEDT) were identified and reaction mechanisms were proposed for their formation.

Chakma (18) reported that the above procedure was not always selective, sometimes resulting in the derivatisation of both the alcohol and amino groups in alkanolamines. Instead of a mixture of chemicals, Chakma used trimethyl silyl imidazole (TSIM) to derivatize partially degraded MDEA solutions. Only the hydroxyl groups were derivatized and derivatization was complete within 30 minutes. The selective derivatization made it possible to infer the number of hydroxyl groups in the underivatized compounds.

Smith and Younger (17), in a more practical approach, offered some helpful hints on the design and operation of gas plants to avoid or minimise problems such as foaming, corrosion and degradation. They reported that 10 of 19 plants investigated experienced some degradation, the products being BHEP, residual salts, thiosulphates and probably TEA.

These studies have provided appreciable insight into alkanolamine degradation due to carbon dioxide. The degradation is believed to occur primarily via amine carbamates which may be formed by the direct reaction of CO_2 with amines. Since H_2S is incapable of forming carbamate-type compounds, it is generally agreed that H_2S does not cause amine degradation. Choy (12) and Kim and Sartori (13) have reported findings which suggest that H_2S in the presence of CO_2 actually hinders amine degradation. The difference in the mechanisms suggested by Kim and Sartori (13) and Kennard and Meisen (14) is in the formation of THEED. In order to determine which of the mechanisms better represents THEED formation, the equilibrium between HEOD and DEA under CO_2 -rich and CO_2 -limiting conditions as represented below, is re-examined:



In the CO_2 -rich system (Eq. 2.30), the equilibrium will always favour HEOD production and can be maintained by the transformation of excess DEA carbamate (DEACOO^-) or HEOD to other products such as THEED. However, the high CO_2 loading reduces the basicity of the solution and the transformation of HEOD to THEED, a reaction which involves ring breakage, may be slightly hindered. On the other hand, the reaction of DEA with DEACOO^- to form THEED as proposed by Kennard and Meisen will proceed well. In support of this assertion is the finding of Kennard and Meisen that the HEOD concentration increased only slightly in an aqueous

solution of DEA and HEOD that was saturated with CO_2 and maintained at 175°C for 8 hr.

In the nitrogen or CO_2 -limiting case (Eq. 2.31), the equilibrium lies to the left in favour of DEA and DEACOO^- formation. The equilibrium is maintained by the reaction of excess DEACOO^- with DEA to form THEED. Data reported by Kim and Sartori showed that in an aqueous solution containing HEOD and DEA at 120°C , the HEOD concentration decreased by 0.4 M while the DEA and THEED concentrations increased by 0.03 M and 0.20 M, respectively. If the mechanism of Kennard and Meisen is correct the 0.2 M THEED could be produced from 0.2 moles/L each of DEA and DEACOO^- , both of which account for the 0.4 M drop in HEOD concentration. Using the mechanism by Kim and Sartori, the concentration data implies that the 0.2M THEED was produced from 0.2 moles of HEOD and DEA. The remaining 0.2 M drop in HEOD is that lost in the reversal to carbamate. The latter keeps the DEA concentration approximately constant since GC analysis does not distinguish between free amine and amine carbamate. Thus HEOD reversal to DEACOO^- and its reaction with DEA to form THEED would proceed at the same rates, a situation that would disrupt the equilibrium in Eq. 2.31. The mechanism of Kennard and Meisen therefore appears to be the more applicable one to the CO_2 limiting case.

In summary, the mechanism postulated by Kennard and Meisen appears to represent both the CO_2 limiting and non-limiting systems whereas the mechanism by Kim and Sartori is partially applicable to the latter but not the former case. Since amine degradation in sweetening units occurs mostly at high temperatures, a condition that limits CO_2 loadings, the

Kennard and Meisen mechanism is therefore more appropriate for industrial situations.

2.4.2 DEGRADATION OF DIETHANOLAMINE BY CARBONYL SULPHIDE

Compared with CO₂-induced degradation, little work has been reported on the COS-alkanolamine degradation reactions (19,20). Orbach and Selleck (19) contacted pure COS with 20 wt% MEA and 35 wt% DEA solutions in a bench-scale pilot plant simulating a typical, continuous absorption-regeneration process. The absorber and regenerator were operated at 40 °C and 104 °C, respectively. Periodic analysis of the amine solutions using Kjeldahl analysis and acid titration revealed that, while MEA was substantially degraded, no loss of alkalinity occurred in the DEA solution over 8 hours. Although the authors reported the formation of some extraneous products, they were "too small for isolation and characterization". Believing that these products could be formed from small quantities of MEA in the initial DEA solution, they concluded that COS does not degrade DEA.

Pearce et al. (20) contacted, in a batch-mode, pure COS with 20 wt% DEA solutions at temperatures ranging from 40 to 120 °C. The solutions were subsequently analyzed by infrared and mass spectroscopy. Minor quantities of ethanol and oxazolidone were detected. However, these quantities were insignificant compared with those formed when MEA was subjected to COS under similar operating conditions. Pearce et al. (20) also contacted COS with DEA continuously using an approach analogous to that of Orbach and Selleck (19). The concentrations of the

DEA solutions at the start and end of the experiments were determined by wet chemical analysis and found to be essentially the same. This again led to the conclusion that COS does not degrade DEA. A further conclusion was that COS underwent significant hydrolysis as revealed by the presence of CO_2 and H_2S in the regenerator off gas and the DEA solution leaving the absorber.

2.4.3 DEGRADATION OF DIETHANOLAMINE BY CARBON DISULPHIDE

The only substantive study on alkanolamine degradation by CS_2 was conducted by Osenton and Knight (21). They contacted 40 mL of a 25 wt% aqueous DEA solution with 7 mL of CS_2 for 3 hours in a stirred vessel at 25 °C. Titration of the solution for free amine and dithiocarbamate contents revealed the complete conversion of amine to the amine salt of dithiocarbamic acid (see eq. 2.14). When the reaction mixture was boiled for 1 hour and analyzed in the same manner, only 20% of the DEA was recovered from the dithiocarbamate salt. Using MEA instead of DEA, Osenton and Knight found that about 40% of the initial MEA was recovered upon boiling. They also detected oxazolidone-2-thione amongst the reaction products, contrary to the findings of Pearce et al. (20) who did not detect any degradation compounds in MEA/ CS_2 systems. It should be noted that while Osenton and Knight contacted CS_2 directly with MEA, Pearce et al. based their conclusions on a field test of an MEA plant which processed gas containing COS and CS_2 . The assumption was made that the plant's MEA loss was due to the MEA-COS reaction only. Since COS and CS_2 exist in p.p.m concentrations in sour industrial gases, it is

possible that, in the field test, the CS_2 -MEA reactions resulted in degradation product concentration too low to be detected by the mass spectroscopic analysis. This may be the reason for the contradictory findings.

2.5 LIMITATIONS OF THE PREVIOUS COS-DEA AND CS_2 -DEA DEGRADATION STUDIES

Conclusions of some earlier studies notwithstanding, there are three basic reasons to believe that degradation may occur in COS-DEA and CS_2 -DEA systems.

First, recent studies on the CO_2 -MDEA system have shown that degradation is possible via amine protonation as well as carbamate formation (18). Since COS and CS_2 hydrolyze in aqueous systems to give H_2S and CO_2 , significant concentrations of H^+ and CO_2 may result to induce the degradation of DEA via protonated DEA and DEA carbamate.

Second, it has been reported that the COS-DEA and CS_2 -DEA reactions forming thiocarbamate and dithiocarbamate respectively, are two and five orders of magnitude slower than the CO_2 -DEA reaction yielding DEA carbamate (57,66). Since CO_2 -induced degradation of DEA occurs primarily via DEA carbamate, it is likely that the COS and CS_2 induced degradation of DEA via the thiocarbamates and dithiocarbamates respectively, are correspondingly slower. For instance, it was found that at 120°C , a CO_2 partial pressure of 4.1 MPa and an initial DEA concentration of 30 wt%, it took almost 20 hours to obtain a 5% reduction in the amine concentration and only one degradation compound was formed in appreciable quantities (16). When the degradation

experiments were conducted for extended periods of up to 30 days at low temperatures (11,13,14,16) or for eight hours at elevated temperatures (14,16), significant decreases in amine concentrations were recorded and more degradation compounds were formed. Since Orbach and Selleck (19) and Osenton and Knight (21) conducted their DEA degradation experiments over just 8 and 4 hours, respectively, it is not surprising that significant amounts of degradation compounds could not be detected. (The durations of the experimental runs performed by Pearce et al. (20) were not clearly indicated.)

Third, the analytical techniques used previously may not have been sufficiently sensitive to detect the compounds arising from the degradation reactions. The difference between Kjeldahl total nitrogen and free amine determinations were often used to establish the extent of amine inactivation. Polderman et al. (4) have noted some inconsistencies in this approach. Values obtained for total nitrogen includes nitrogen from the amine as well as its nitrogenous degradation compounds. Acid titrations to determine free amine concentration provide erroneous results since the degradation compounds are basic and some of them are titrated as well. Therefore, it may be concluded that values obtained from the difference of the two analyses may not be reliable estimates of the degree of amine inactivation.

2.6 ANALYSIS OF DEGRADED ALKANOLAMINE SOLUTIONS

Earlier attempts to analyze degraded amine solutions used methods such as potentiometric titration (67), acid titration and Kjeldahl total nitrogen determination (4,68), fractional distillation and crystallization (10). These methods were generally unsuccessful for reasons such as lack of reproducibility, inability to separate degradation compounds, decomposition of amines and degradation compounds at elevated temperatures. Derivatization prior to gas chromatographic analysis has also been tried (69,70,71). Although fairly successful, gas chromatographic analysis of derivatized degraded amine solutions suffers some drawbacks. These were outlined by Saha et al. (72) and include: time consuming procedures of preparing derivatives, incomplete derivatisation, instability of derivatives over long periods and in the presence of water, and long period of analysis. As a result, they developed a direct gas chromatographic technique using a column packed with Tenax GC, a porous polymer based on 2,6-diphenyl paraphenylene oxide (73). This column successfully separated a mixture of MEA, DEA and TEA in about 8 minutes. The use of the Tenax GC column was extended to the analysis of degraded DEA solutions (13,74) and Kennard and Meisen (74) have reported the detailed analytical conditions for the analysis. However, while Kennard and Meisen (74) reported good resolution of peaks, Kim and Sartori (13) were unable to separate some degradation compounds with the Tenax GC column alone. To overcome this problem, each analysis was repeated with a 5% SE 30/Chrom-GHP column. The lack of separation could have been due to the shorter column length (2 ft) used

in the study, as opposed to the 6 ft column used by Kennard and Meisen (74).

A gas chromatographic method involving a combination of columns has also been reported by Robbins and Bullin (75). Tenax GC and Porapak Q columns were connected in series for the analysis of amine solutions containing acid gases, hydrocarbons and water. The Tenax column separated the amine from the other components which were further separated by the Porapak Q column and detected by a thermal conductivity detector (TCD). A switching valve in the set up was used to bypass the Porapak column once the lighter components had eluted. This was done to protect the Porapak column from irreversible adsorption or deactivation by the amine. Good resolution was obtained for CO_2 , H_2S , H_2O and MDEA within 10 minutes. The concentrations of the acid gases obtained from the GC analysis were in good agreement with the values obtained from wet chemical methods. This method is able to simultaneously determine the concentrations of acid gases as well as the amine and its degradation products. However, care should be taken in the handling of samples from degradation runs conducted at high temperatures and pressure, to prevent flashing of the acid gases and hence erroneous acid gas loadings.

Chakma (18) as well as Chakma and Meisen (76) have also used Tenax GC columns for the analysis of degraded DEA and MDEA solutions.

CHAPTER 3

EXPERIMENTAL APPARATUS AND PROCEDURE

3.1 REACTOR

The degradation experiments were carried out using a 600 mL stainless steel reactor (model 4560, Parr Instrument Co. Ill., U.S.A.), shown in Figure 3.1. Its main features and accessories are described below:

1. A pressure gauge for monitoring the pressure within the reactor.
2. A J-type thermocouple in a 316 stainless steel well, to monitor the temperature within the reactor.
3. A close fitting, quartz fabric heating mantle in an insulated aluminium housing, attached to a stand to enable movement up or down as desired.
4. An automatic heater/temperature controller (model 4813EB, Parr Instrument Co., Ill., U.S.A.). The controller maintains the system temperature within $\pm 0.5^{\circ}\text{C}$ of the set point by regulating the power supply to the mantle. An indicator within the controller assembly displays the system temperature in terms of the magnitude of the deviation from the set point. The temperature limits of the reactor are room temperature and 400°C .
5. A stainless steel stirrer, driven by a variable speed motor at speeds up to 600 r.p.m.

6. Liquid sampling, gas inlet and gas outlet valves. A 1/8" sample tube connected to the gas inlet/liquid sampling port enables the supply of gas to and the withdrawal of liquid from the reactor.
7. A rupture disc which breaks when the pressure within the reactor exceeds the rating of the disc. The rating of the disc on the reactor is 13.78 MPa (2000 psi) at 400 °C.
8. A stainless steel cooling coil for rapid cooling of the reactor when necessary.
9. A pyrex liner to reduce contact between the reactants and the inner walls of the reactor.

3.2 MATERIALS

DEA (>99% purity) was purchased from Aldrich Chemical Co., Inc. (Milwaukee, WI). CS₂ (>99% purity) was purchased from BDH Chemicals Inc. (Vancouver, BC). COS was supplied by Matheson Inc (Edmonton, AB) with the following purity expressed in mole percent: COS - 97.7%, CO₂ - 1.4%, CS₂ - 0.19%, H₂S - 0.01%, O₂ - 0.1%, CO &/or N₂ - 0.6%. Nitrogen (>99% purity) was purchased from Medigas Ltd. (Vancouver, BC). The compounds used for the calibration of the gas chromatograph were purchased from Aldrich Chemical Co., Inc. (Milwaukee, WI) with the exception of HEOD, THEED and BHEI which were unavailable and had to be synthesized in the laboratory. Procedures for their synthesis are described in Appendix A2.

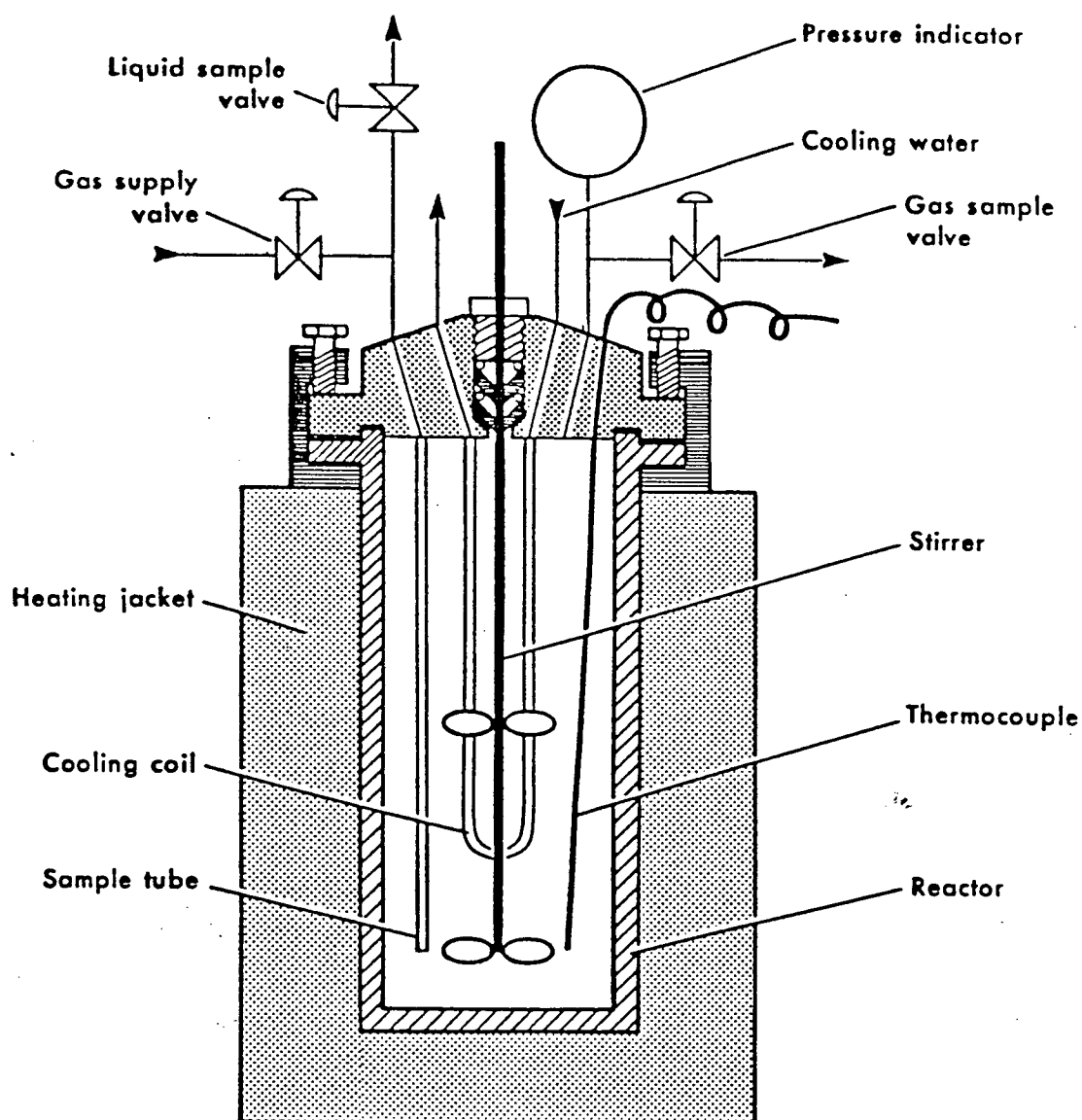


Figure 3.1: Sketch of the reactor.

3.3 EXPERIMENTAL PROCEDURE

Typically, 250 mL of an aqueous DEA solution with the desired concentration was placed in the reactor before sealing it. The stirrer was turned on at a speed of 120 r.p.m and air was purged from the reactor by passing nitrogen through it for about 15 min. The gas inlet and outlet valves were closed and the heater was turned on to bring the reactor to the desired operating temperature. Once steady state had been achieved, the pressure within the reactor was recorded as the initial pressure. This pressure is the sum of the vapour pressure of the amine solution and the pressure due to the residual nitrogen in the reactor. COS was then introduced through a stainless steel pressure hose connected to the pressurized COS cylinder. It was necessary to warm the COS cylinder to about 45 °C to increase the pressure within the cylinder beyond the normal value of 1.1 MPa (160 psi) at room temperature. The regulator on the COS cylinder was set so that the difference between the final and initial pressures in the reactor corresponded to the desired partial pressure of COS for the run. The COS line was left open and connected throughout the experiments to ensure a continuous supply of COS to the reactor. A check valve on the COS line prevented backflow even when the pressure in the reactor rose beyond the delivery pressure set with the regulator.

In the case of CS₂ runs, a known volume of CS₂ was placed in a 40 mL stainless steel cylinder which was connected to the reactor, and

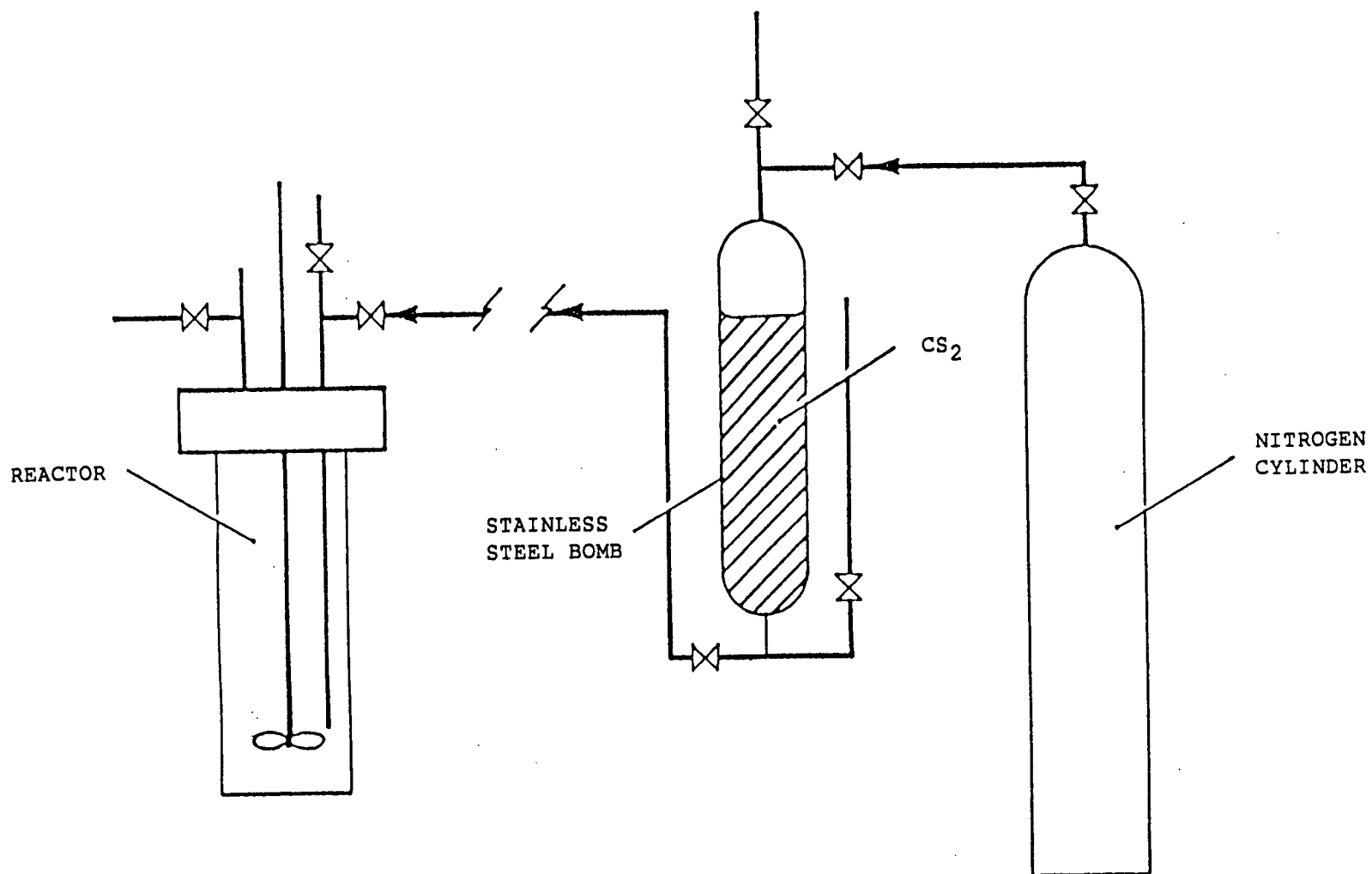


Figure 3.2: Set-up for the CS₂-DEA degradation experiments.

forced into the reactor with nitrogen. The delivery pressure of the nitrogen cylinder was regulated to achieve a constant total pressure in all the runs. The experimental set-up is shown in Figure 3.2.

3.4 SAMPLING

The gas sampling line was a 1/8" stainless steel tube fitted with inlet and outlet valves. Gas from the reactor was first trapped between the inlet valve of the sampling line and the gas outlet valve on the reactor. With the outlet valve of the sampling line closed, the inlet valve was opened to transfer the gas sample to the line. The sample was subsequently withdrawn with a 10 mL "pressure-lok" syringe by inserting the syringe through a septum in the "swagelok" fitting connected to the outlet valve of the sampling line. This arrangement was sufficient to reduce the pressure of the sample and make it possible to collect the sample without difficulties. Expansion of the sample in the syringe during sampling, further reduced the pressure. Prior to sampling, the sampling line was purged with the sample gas.

Liquid samples were collected with a 2 mL stainless steel coil fitted with inlet and outlet valves. The pressure in the reactor was sufficient to force liquid samples into the sampling coil once the sampling valve on the reactor and the inlet valve of the sampling coil were opened, while the outlet valve of the coil was closed. About 3 mL of solution were purged to ensure that the sample is representative of the reactor solution. With all valves closed, the sampling coil was disconnected and rapidly cooled to room temperature by immersing it in

ice-cold water. The sample was then transferred into a covered glass vial ready for analysis. The sampling coil was then flushed with water and air dried. It was then ready for subsequent use.

3.5 OPERATING CONDITIONS

The degradation experiments were conducted under the following operating conditions:

1. DEA concentration 10 - 40 wt% (appr. 1 - 4 M)

This range was chosen to cover the 10 - 35 wt% range commonly used industrially. A few runs were done at initial DEA concentration of 60 wt% to explore the effect of high amine concentrations on the rate of degradation.

2. Temperature 120 - 195 °C

Industrial DEA plants operate at regeneration temperatures of about 120 °C. Part of the amine solution is exposed to temperatures as high as 140 °C, especially at the reboiler surfaces. Temperatures as high as 195 °C have been used in this study merely to increase the rate of the reactions. In addition, since the reaction mechanism may change with operating temperature, a sufficiently wide range of temperature needs to be covered.

3. COS partial pressure 0.3 - 1.17 MPa
CS₂ volume 2.5 - 10.5 mL
(0.055 - 0.233 mole CS₂/mole DEA)

It is recognised that these ranges are much higher than those normally encountered industrially. They have been chosen to obtain measurable quantities of degradation compounds within a reasonable time. It should be noted that the CS₂/DEA mole ratios are much lower than 1.195 which was used by Osenton and Knight (21). They therefore represent plant conditions more closely.

4. Volume of DEA solution 250 mL

This volume was considered sufficient so that sample withdrawals (10 x 5 mL) will have no significant effect on the volume of the liquid reactant. In addition, enough space is left in the reactor for the gas. Chakma (18) reported similar MDEA concentrations in two runs conducted with initial solution volumes of 100 and 250 mL.

3.6 ANALYTICAL PROCEDURE

A Hewlett-Packard Gas Chromatograph (Model 5830A) equipped with an integrator terminal, was used to separate the various constituents of the reactor samples. The concentrations of the constituent compounds were determined from previously prepared calibration curves (see

Appendix B). The principal operating conditions used in the present study were:

Column	Tenax (GC and TA)., 60/80 mesh packed in a 9' x 1/8" stainless steel column (supplied by SUPELCO Inc., Oakville, Ont.)
Detector	H ₂ flame ionization (FID)
Detector Temperature	300 °C
Temperature Program	Isothermal at 150 °C for 0.5 minutes, then raising it to 300 °C at the rate of 8 °C/min
Carrier gas	N ₂ at 23 mL/min
Injection Temperature	300 °C
Sample volume	0.001 mL

These conditions are similar to those used by Kennard and Meisen (74) and Chakma and Meisen (76).

The identity of the degradation compounds cannot not be confirmed by the GC analysis alone. A combination of the techniques described below was employed. Other analytical techniques were used in order to identify the solid reaction products.

3.7 TECHNIQUES USED TO IDENTIFY THE DEGRADATION PRODUCTS

In order to identify the products of the degradation reactions, four successive methods were used:

3.7.1 GAS CHROMATOGRAPHIC (GC) ANALYSIS

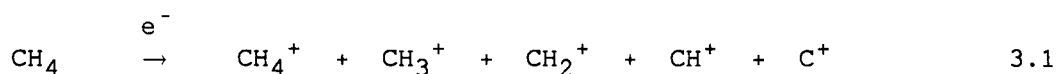
This analysis provides the concentrations and the retention times of the compounds. The latter should remain approximately constant under the same analytical conditions, assuming little or no column deterioration.

3.7.2 GAS CHROMATOGRAPHIC/MASS SPECTROMETRIC (GC/MS) ANALYSIS

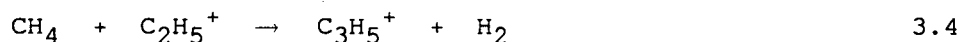
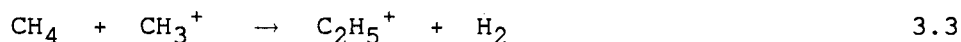
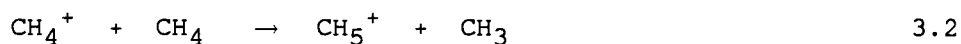
The GC/MS system consists of a gas chromatograph coupled to a mass spectrometer. The unit used in this study was a Hewlett-Packard, Model 5985B. In the analysis of a mixture of compounds, the gas chromatograph vaporises and fractionates an injected sample of the mixture. The vapour fractions eluting from the GC column flow into the ion source of the mass spectrometer. The ion source, maintained at high temperature and vacuum pressure, produces electrons from a hot tungsten filament which bombards the incoming vapour fractions, thereby causing ionisation and fragmentation of the molecules. The resulting mixture of ions is accelerated through an electric field into the ion collector system where they are separated according to their mass to charge (m/e) ratio. The charge carried by each ion produces an electric current that is detected by an electrometer and then amplified and recorded. This record of the numbers of different kinds of ions is called the mass spectrum. The uniqueness of the molecular fragmentation assists with the identification of compounds because no two compounds ionise and fragment

in exactly the same manner. The mass spectrum is therefore, a "finger print" of each compound.

The mass spectrometer can be operated in the Electron Impact (EI) or Chemical Ionisation (CI) modes. In the EI mode, the ion source voltage is about 70 eV and the system pressure is between 10^{-5} and 10^{-7} mm Hg. Each molecule flowing across the ion source is fragmented by direct bombardment with electrons. This bombardment generates numerous ions as the voltage applied is sufficient to rupture many bonds in the molecules. In the CI mode, the molecules to be fragmented are diluted with excess reagent gas, usually methane. At the normal system pressure, methane is bombarded with a stream of electrons which results in ionisation and fragmentation (77):

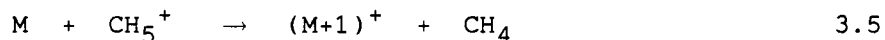


By maintaining the ion source at a higher pressure (usually 0.5 - 1 mm Hg) than the rest of the system, ion-molecule reactions occur by collision:



CH_5^+ is usually the most abundant of these ions. These positive ions are then used to ionize the molecules of a sample. Due to the high methane

to sample ratio (typically 10^3), ionization of the molecule occurs via ion - molecule collisions:



Other reactions causing proton abstraction $(M-1)^+$ and loss of water $(M+1-18)^+$ may also occur. Since these collisions occur at lower energies than direct electron bombardment, less fragmentation of the molecules occurs. Thus the CI spectrum displays a prominent (usually the most abundant) protonated molecular ion $(M+1)^+$, from which the molecular weight of the compound may be inferred.

3.7.3 GC/MS ANALYSIS OF SILYLATED DERIVATIVES

To gain insight into the structure of the degradation products, the mass spectra of the compounds in a silylated sample of the degraded solution were also obtained. Silylation is a form of derivatization whereby silyl groups are introduced into molecules to replace active hydrogen atoms. The silyl groups can also replace metals in salts (78).

The silylation was performed with trimethyl silyl imidazole (TSIM) following Chakma's procedure (18). 5 mL of a degraded solution were placed in a glass vial and saturated with potassium carbonate to dehydrate the sample. Isopropyl alcohol was then added to extract the degradation compounds from the mixture. The extract was transferred to another vial where the alcohol was removed by evaporation, leaving a

viscous oil. An excess of TSIM was added to the oil, the mixture was thoroughly shaken and left for at least 1 hour at room temperature to ensure complete derivatization. The derivatized sample was then analysed by GC/MS. A fused silica megabore column (50% phenyl methyl silicone, 0.53 mm ID x 10 m) was used to separate the mixture because Tenax G.C. proved to be unsuitable. Since TSIM attacks primarily hydroxyl groups, the CI spectra could be used to determine the molecular masses of the silylated compounds and hence the number of hydroxyl groups per molecule. The silylating trimethyl silicon ion (TMS) has a molecular mass of 73 and replaces the hydrogen in -OH groups. Thus silylation of a compound increases its molecular mass by $72n$, where n is the number of hydroxyl groups in the compound.

3.7.4 GC ANALYSIS OF DEGRADED MIXTURES SPIKED WITH SUSPECTED COMPOUNDS

GC/MS analysis provided information on the possible identities of the unknown compounds in degraded solutions. Pure forms of the suspected compounds were purchased or synthesized and then used to spike the sample. The spiked sample of the degraded solution was then analysed by gas chromatography. An increase in the peak area of the corresponding peak provided strong proof that the peak represents the unknown compound.

In summary, the steps followed to identify the degradation compounds were:

1. Determination of the retention times under standard GC operating conditions.
2. Obtaining the EI and CI mass spectra from the GC/MS analysis. The CI spectra provided the molecular weights of the unknowns, while the EI spectra were compared with literature spectra (15,16,18,79,80).
3. Determination of the number of hydroxyl groups in the unknown compounds by comparing the CI spectra of the silylated derivatives and unsilylated compounds.
4. Comparing the retention times of the suspected and the unknown compounds under the same GC operating conditions.

3.8 EXPERIMENTAL DESIGN

Experiments were designed in stages that reflect the stated objectives of the study:

1. Identification of reaction products

Two runs each were conducted for the COS-DEA and CS₂-DEA systems at the boundary temperatures indicated in section 3.5, to ascertain that the reaction products at the high temperature are similar to those produced at the low temperature. The runs will also serve to verify the fact that the high temperature merely increases the rates of the reactions. However, differences observed in the product spectra for the low and

high temperature runs for the CS₂-DEA system necessitated another run at 165 °C.

2. Effects of operating conditions

Runs were conducted as shown below, to determine the effects of temperature, solution concentration, initial COS partial pressure and initial CS₂ volume on the degradation reactions:

DEA CONC.	TEMPERATURE (°C)											
(wt%)	195	190	180	175	170	165	160	150	135	130	127	120
40			*, +			*, +	*	*, +	*		*	+
30		*	*, +	+	*	*, +	*	*, +	*	*, +	*	+
20	*		*			*, +		*, +		*, +	*	
10			*			*						

where * and + denote COS-DEA and CS₂-DEA runs, respectively.

The runs were conducted with an initial COS partial pressure of 345 kPa or an initial CS₂ volume of 6 or 10.5 mL. It should be noted that some of the runs were conducted with a glass lined reactor and are only suitable for qualitative explanations.

The above runs were only able to show the effects of temperature and DEA concentration. A separate set of runs was conducted to determine the effects of COS partial pressure and CS₂ volume on the reactions. The conditions used for these runs are:

DEA concentration	30 wt%
COS partial pressure	345, 759, 1172 kPa
CS ₂ volume	2.5, 6.0, 10.5 mL
Temperature	150 °C for the COS runs 165 °C for the CS ₂ runs

3. Effects of mixed gas phase

The original intention was to conduct runs using a mixture of CO₂, COS and CS₂ in the gas phase. While it was possible to obtain a gas mixture of COS and CO₂, there was no way to include CS₂ in the mixture and maintain its concentration throughout the runs. Since COS and CS₂ are eventually hydrolysed to CO₂ and H₂S, a better choice was to use a mixture consisting of the two latter gases. The results from the use of a CO₂/H₂S gas mixture also augment the scanty data reported in the literature on the degradation effects of such mixtures. The operating conditions and compositions of the gas mixtures used for these runs are discussed in Chapter 6.

4. Additional and special runs

Some duplicate runs were conducted to ascertain reproducibility. It was also found necessary to conduct more runs to elucidate the reaction mechanisms and determine the equilibrium distribution of the acid gases in the reactor. These runs are discussed in detail in Chapters 6 and 7, respectively.

CHAPTER 4

IDENTIFICATION OF DEGRADATION PRODUCTS

4.1 PRELIMINARY EXPERIMENTS

Before proceeding with the main experimental programme, it was necessary to conduct preliminary experiments aimed at evaluating the effects of certain operating variables on the degradation reactions.

4.1.1 EFFECTS OF ELEVATED TEMPERATURES

Elevated temperatures were used in this study to speed up the degradation reactions. The results obtained under such conditions will only have industrial relevance if the alkanolamines are not thermally degraded and the reaction products are similar to those obtained at the lower temperatures commonly used in industry. Thermal degradation experiments, conducted by heating aqueous solutions of DEA under a blanket of nitrogen, revealed the following: at 150 °C no change in solution composition was observed over a period of 220 hours; at 165 °C no change occurred over 60 hours; at 180 °C thermal degradation was negligible up to 80 hours. Since most of the high temperature degradation runs were conducted over 48 hour periods, the influence of thermal degradation on the results can be disregarded. Kennard (16) also found thermal degradation to be negligible when aqueous DEA

solutions were maintained at 205 °C for 8 hours under a blanket of nitrogen.

Typical chromatograms of aqueous DEA solutions degraded in the presence of COS are shown in Figs. 4.1a to 4.1c. The qualitative similarity of the figures is obvious. This suggests that the basic reaction mechanism is not affected by temperature. Since industrial DEA regenerators operate at reboiler temperatures of up to 140 °C, the products obtained in this study should also be formed under industrial conditions.

4.1.2 SURFACE EFFECTS

Two runs were performed with and without the pyrex liner in the reactor. The results indicated very similar products, suggesting that the liner did not affect the reaction mechanism. Since the solution was in contact with the stainless steel stirrer in both cases, it is also clear that the reactions were not influenced by the difference in the solid surface areas.

However, the liner caused a temperature gradient within the reactor. The result of this was the transfer of water from the amine solution into the annulus, thereby increasing the concentration of the amine. The use of the liner was therefore discontinued and a new set of runs (C.1 - C.43 in appendix C) was conducted.

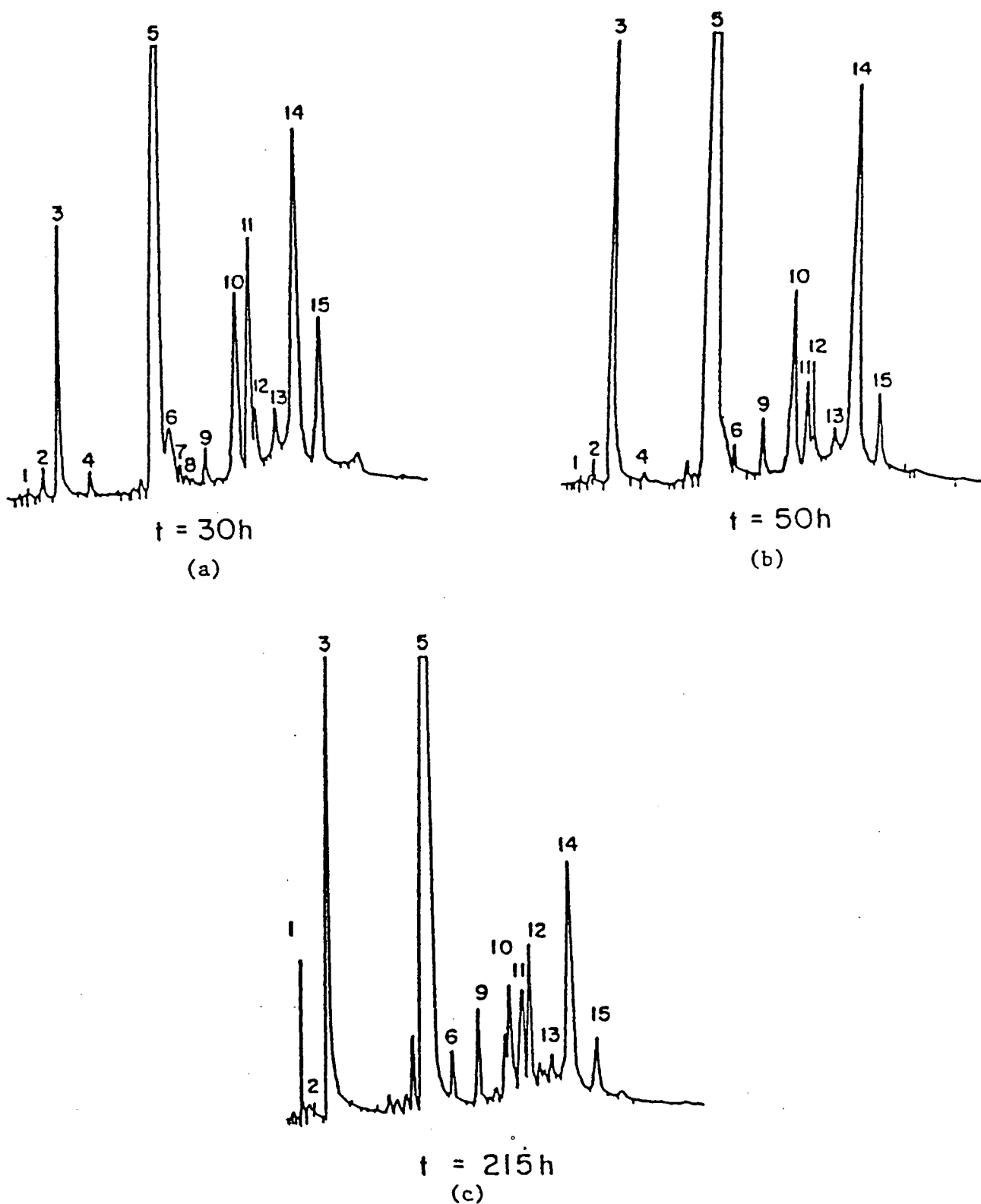


Figure 4.1: Chromatograms of partially degraded DEA solutions of 4M initial concentration (a: $180\text{ }^{\circ}\text{C}$, 0.34 MPa COS ; b: $150\text{ }^{\circ}\text{C}$, 0.34 MPa COS ; c: $120\text{ }^{\circ}\text{C}$, 0.68 MPa COS).

4.1.3 EFFECTS OF STIRRER SPEED

Stirring speed influences the rate of mass transfer between the gas and liquid phases. It was reported previously (16,18) that the rate of degradation is slow and that changes in stirrer speed do not affect degradation rates in CO_2 -amine systems. Since the present study involves COS and CS_2 which hydrolyse to produce H_2S and CO_2 , it was decided to re-examine the effect of stirrer speed and hence the rates of mass transfer on degradation. The DEA concentrations in two runs performed at stirrer speeds of 120 and 180 r.p.m. are shown in columns 2 and 3 of Table 4.1. The deviations in the concentrations are generally less than $\pm 4\%$. This confirms that the change in stirrer speed did not affect the rate of degradation. The run at 180 r.p.m was terminated after 30 hours because of a leakage from the reactor.

4.1.4 REPRODUCIBILITY

Columns 2 and 4 of Table 4.1 also show DEA concentrations for two runs performed two weeks apart but under the same operating conditions. The deviations between concentrations are generally less than 2% and therefore lend confidence to the reproducibility of the experimental and analytical procedures.

Table 4.1: Reproducibility and effect of stirrer speed in COS-DEA degradation ($\text{DEA}_0 = 3 \text{ M}$, $T = 150^\circ\text{C}$, $P_{\text{COS}} = 345 \text{ kPa}$).

Time (h)	DEA CONCENTRATION AT DIFFERENT STIRRER SPEEDS (moles/L)		
	120 rpm	180 rpm	120 rpm
0	3.01	2.98	3.00
2	3.06	2.96	2.98
4	2.91	2.91	2.86
8	2.83	2.84	2.77
12	2.76	2.78	2.69
24	2.47	2.53	2.45
30	2.31	2.31	2.30
36	2.18		2.17
48	1.93		1.91

4.2 DEGRADATION PRODUCTS RESULTING FROM COS-DEA INTERACTIONS

Figure 4.2 contains chromatograms showing the gradual formation of reaction products in a typical run conducted with a 40 wt% DEA solution, at a COS partial pressure of 0.34 MPa and a temperature of 180°C in the glass lined reactor. The gradual formation of reaction products is obvious. In addition, it was noted that the samples became more pungent and viscous as the degradation progressed. Some particulate matter was also found in the samples.

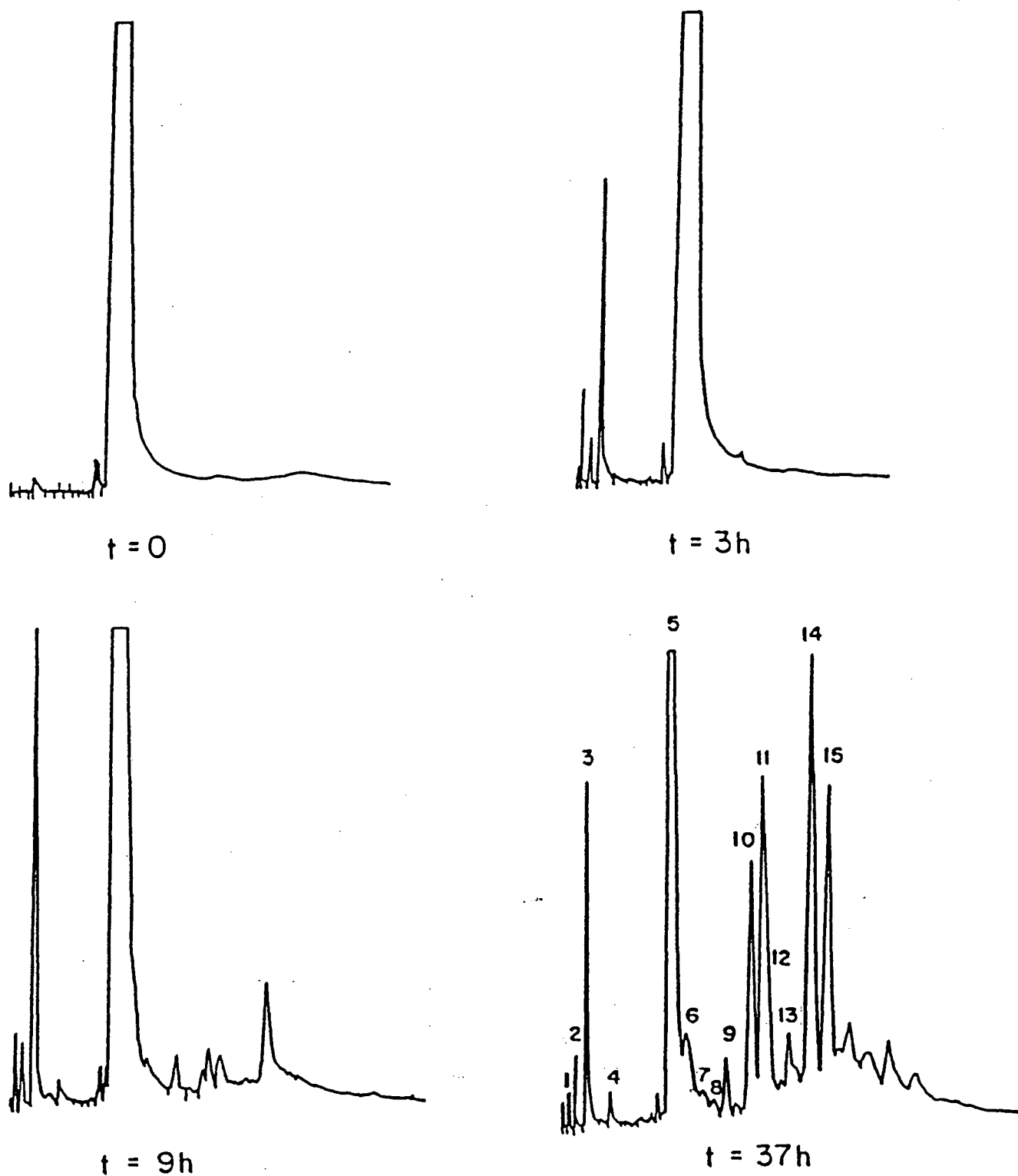


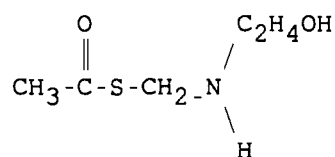
Figure 4.2: Chromatograms showing gradual formation of degradation products in a COS-DEA system (4M DEA, 180 °C, 0.34 MPa COS).

By following the techniques described in section 3.7, the compounds responsible for the peaks labelled in Fig. 4.1 were identified and are listed in Table 4.2. The symbols M^* and $n\text{ OH}$ in Table 4.2 refer to the molecular weight of the derivatized compound and the number of hydroxyl groups in the compound. It should be noted that the retention times depend, to some extent, on the concentrations of the compounds and the age of the column. The corresponding mass spectra are shown in Figures 4.3 to 4.17. For compounds whose mass spectra were not in the computer's data base, the library EI spectra refer to the spectra of the pure compounds purchased or synthesized in the laboratory, depending on their commercial availability.

A consistent pattern in the fragmentation of these hydroxyl-amino compounds is the loss of hydroxymethyl radicals (m/e 31) from the parent compounds to produce, in general, the most abundant ions. Ions of mass 30 for MEA, 58 for EAE, 74 for DEA, 72 for HEA, 102 for EDEA, 143 for BHEP and BHEI, 100 for HEOD, 99 for HEI and HEP were generated in this manner. In the case of BHEED and THEED, hydroxymethyl radicals were also lost, but the principal fragmentation resulted from the cleavage of the C-C bond between two nitrogen atoms giving the most abundant ions with mass 74 for BHEED (N,N' isomer) and 118 for THEED. Water molecules were also lost in the fragmentation. For example, ions of mass 74 lost water to give ions with mass 56 in the case of DEA. The molecular ion peaks are not prominent in most of the EI spectra because of the ease with which the hydroxymethyl groups break from the molecules. The characteristic peaks in the CI spectra of the hydroxyl amino compounds are produced by the $[M+H]^+$, $[M+C_2H_5]^+$ and $[M+H-H_2O]^+$ ions. For the silyl

derivatives, the CI spectra show prominent $[M+H]^+$, $[M+C_2H_5]^+$ and $[M-CH_3]^+$ ions. The $[M-CH_3]^+$ ion is characteristic of the silylating agent (TSIM).

The previous, tentative identification (100) of peak 9 as bis-hydroxyethyl amino ethanol (BHEAE) now appears to be invalid. The compound has a molecular mass of 149 as indicated by its CI spectrum (Figure 4.11). Its silyl derivative has a molecular mass of 221 which suggests that it contains one hydroxyl group. The EI spectrum shows the ion with mass 74 as the most abundant. Loss of the characteristic hydroxymethyl radical does not produce a prominent peak even though the compound appears to have an hydroxyethyl attachment (deduced from ion 74). This, in addition to the prominent ion of mass 89 in the CI spectrum, suggests that the compound is not very stable and fragments on electron bombardment to give ions with mass 89 or, more likely, 74. Based on the presently available information, the most likely structure for this compound is:



The name of the compound is ethanethioic acid S - [(2-hydroxyethyl) amino] methyl ester. Its abbreviation is ETAHEAME. This compound is not available commercially and it was therefore not possible to compare its retention time under the present GC conditions with that of peak 9. Time and resources did not permit its synthesis during the present study.

It also appears that triethanolamine (TEA) was formed as a degradation compound but could not be clearly separated from BHEED under the analytical conditions used. This supposition arises from the fact that the GC analysis of the silyl derivatives showed a peak before BHEED, having a molecular weight of 365. This would suggest an underivatized hydroxyl amino compound with a molecular weight of 149 and three hydroxyl groups. Triethanolamine fits this structure.

Table 4.2: Degradation compounds detected in the COS-DEA system.

Peak	Retention Time (min)	Characteristic EI ions	Molecular Weight M	M*	n OH (M*-M)/72	Identity
1	1.4 - 1.5	43, 58	58			ACETONE
2	2.2 - 2.3	29, 43, 57, 72	72			BUTANONE
3	3.1 - 3.3	30, 42, 61	61	133	1	MEA
4	5.2 - 5.3	30, 56, 74 42, 58, 89	89	161	1	EAE
5	9.2 - 10.0	45, 56, 74	105	249	2	DEA
6	10.9 - 11.1	30, 56, 74, 102 45, 58, 88, 133	133	277	2	EDEA
7	11.5 - 11.6	30, 60, 73 43, 72, 85	103	175	1	HEA
8	12.0 - 12.1	42, 70, 112 56, 88, 130	130	202	1	HEP
9	13.4 - 13.5	56, 74, 118 61, 89, 149	149	221	1	ETAHEAME
10	15.2 - 15.5	44, 74, 100, 56, 88, 118, 127	148	292	2	BHEED
11	16.2 - 16.6	42, 70, 100, 125 56, 88, 113, 143 156, 174	174	318	2	BHEP
12	16.7 - 16.9	42, 74, 100 56, 88, 131	131	203	1	HEOD
13	18.2 - 18.4	42, 70, 99 56, 85, 130	130	202	1	HEI
14	19.7 - 19.8	42, 70, 100, 130 56, 88, 118, 143 174	192	408	3	THEED
15	21.0 - 21.3	42, 70, 114, 143 56, 99, 130, 174	174	318	2	BHEI

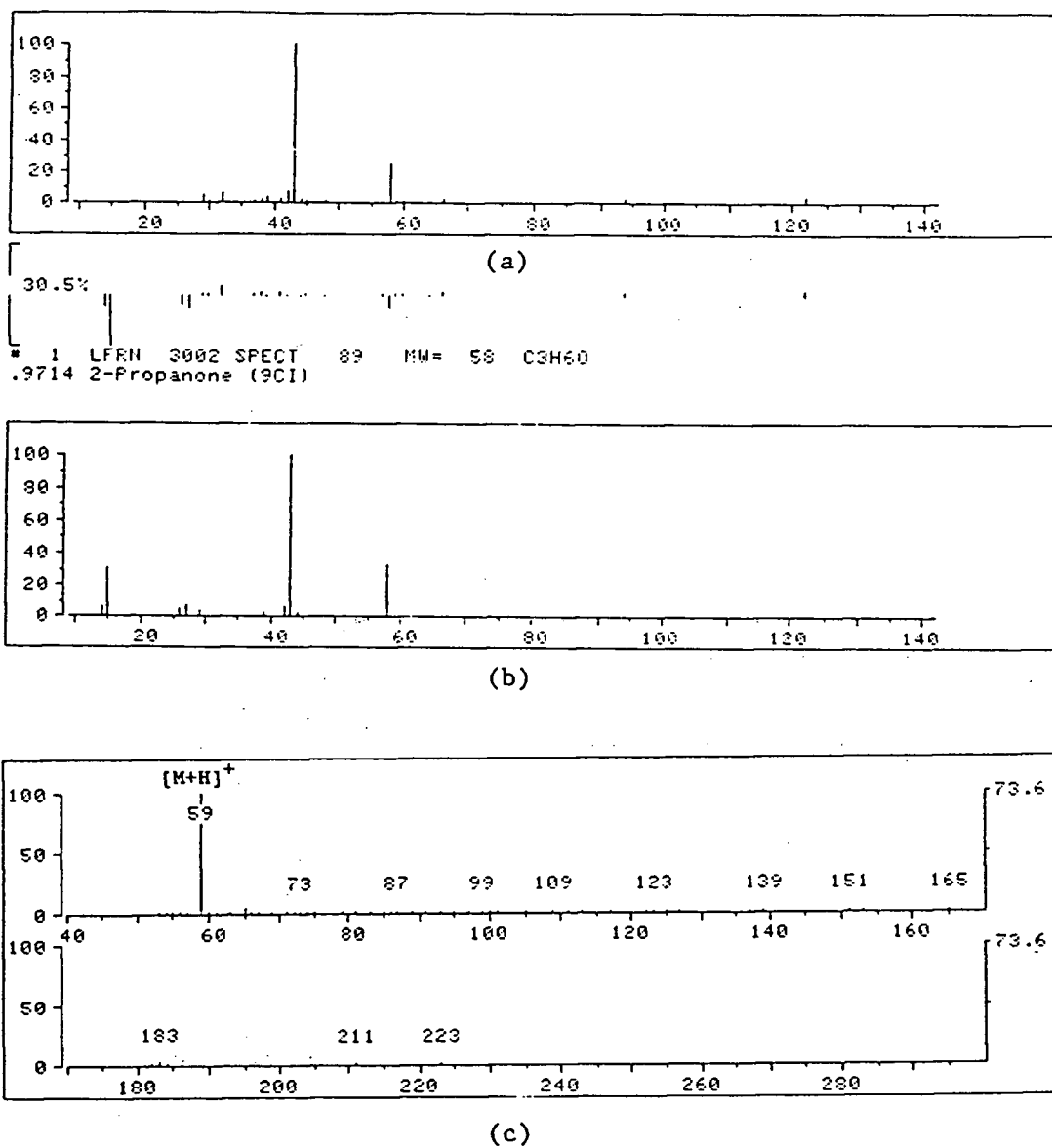


Figure 4.3: Mass spectra of peak 1 identified as Acetone
(a: EI spectrum; b: EI reference spectrum;
c: CI spectrum).

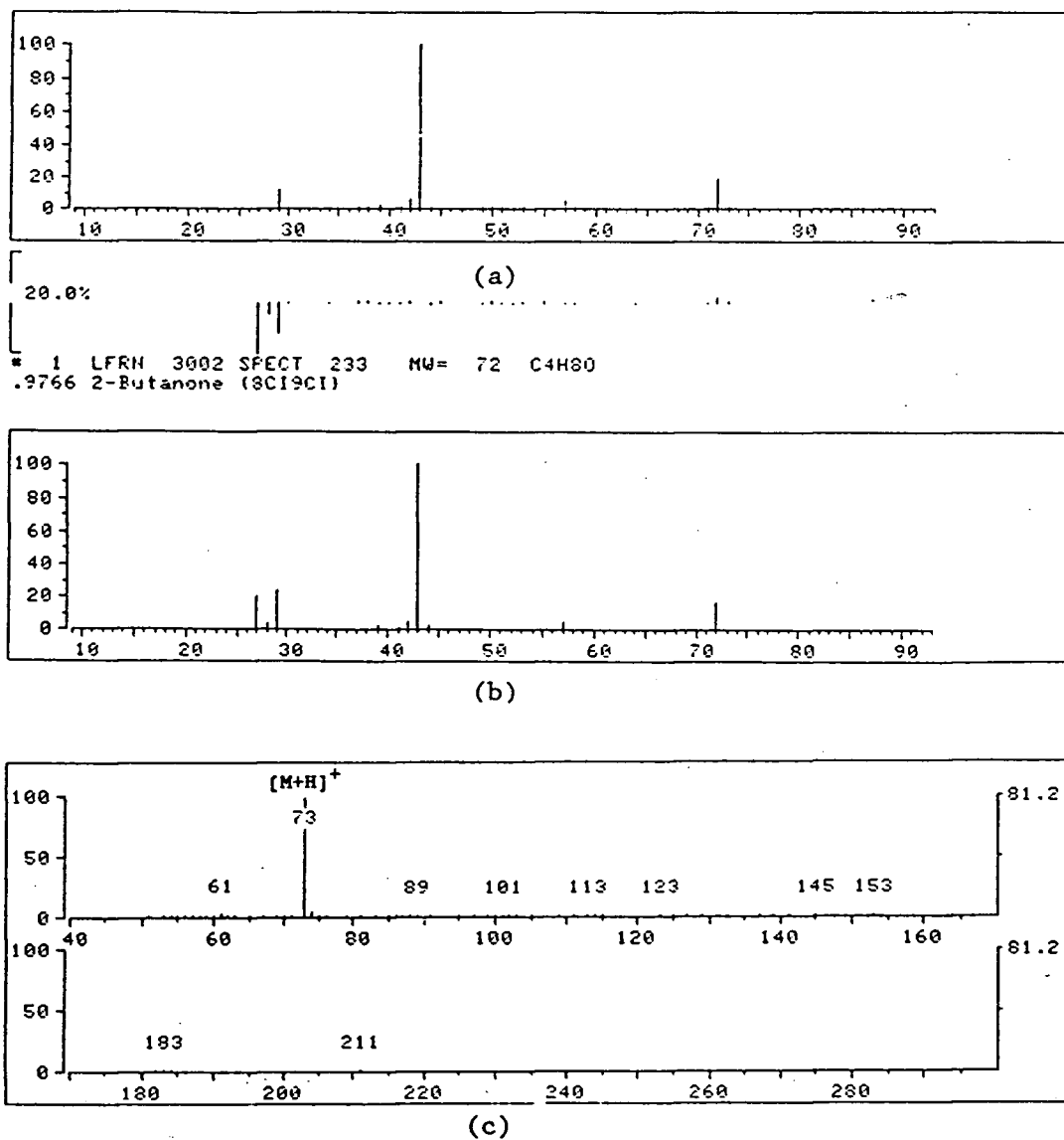
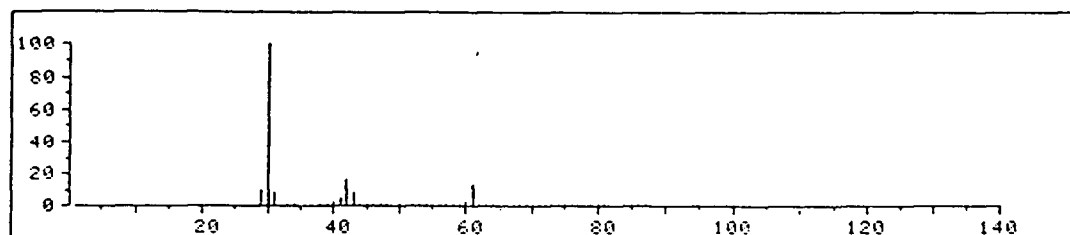
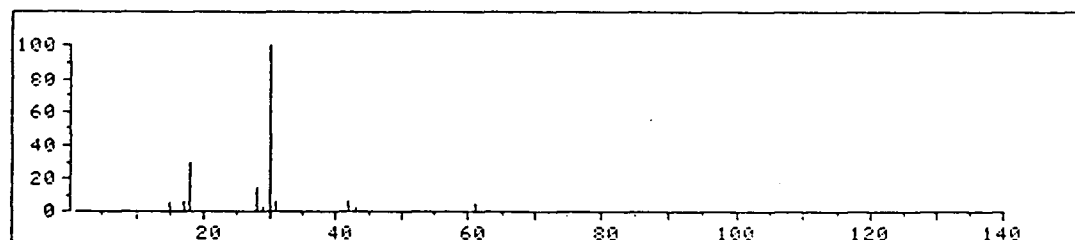


Figure 4.4: Mass spectra of peak 2 identified as Butanone
(a: EI spectrum; b: EI reference spectrum;
c: CI spectrum).

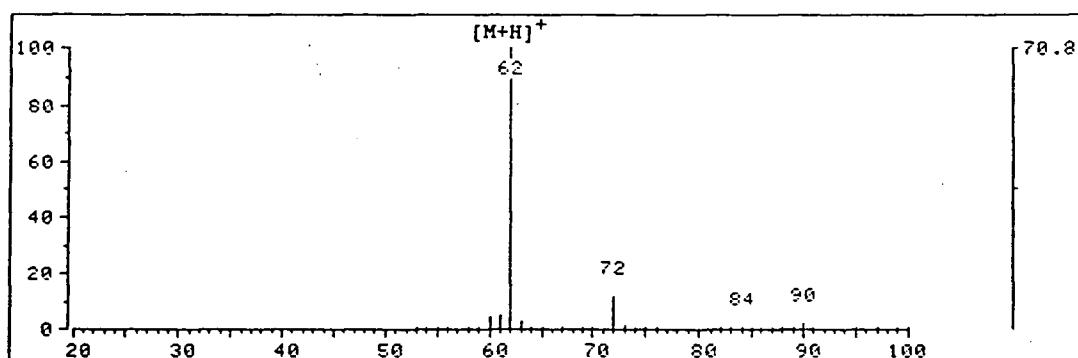


(a)

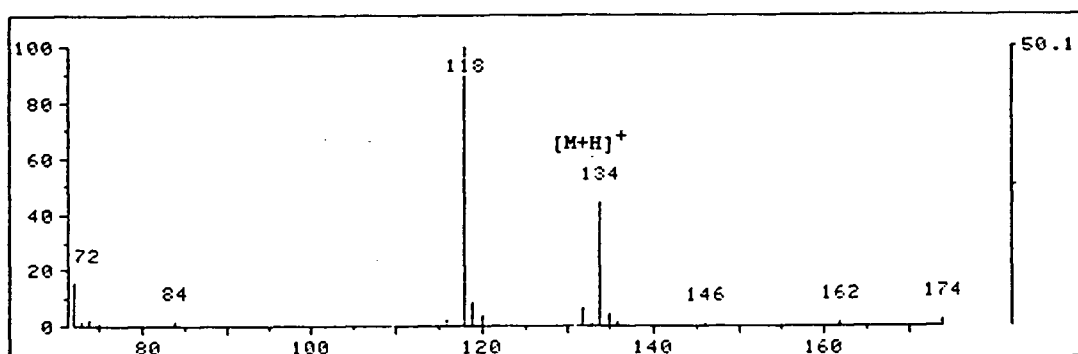
29.9%
 2 LFRH 3002 SPECT 125 MW= 61 C2H7NO
 .8100 Ethanol, 2-amino- (8CI9CI)



(b)

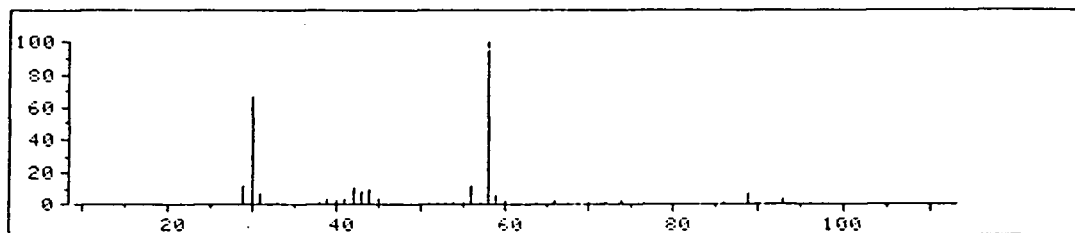


(c)

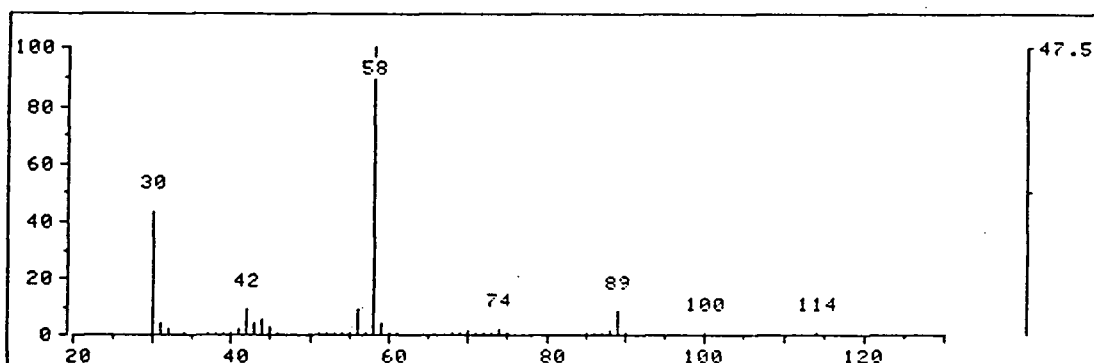


(d)

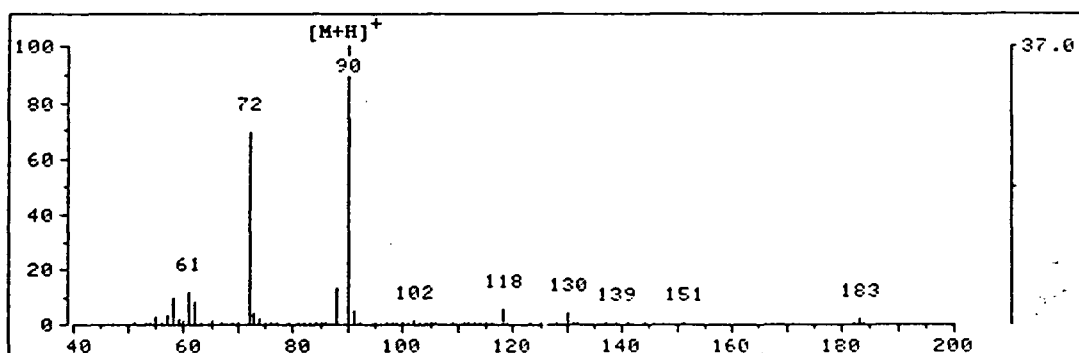
Figure 4.5: Mass spectra of peak 3 identified as MEA (a: EI spectrum; b: EI reference spectrum; c: CI spectrum; d: CI spectrum of the silyl derivative).



(a)

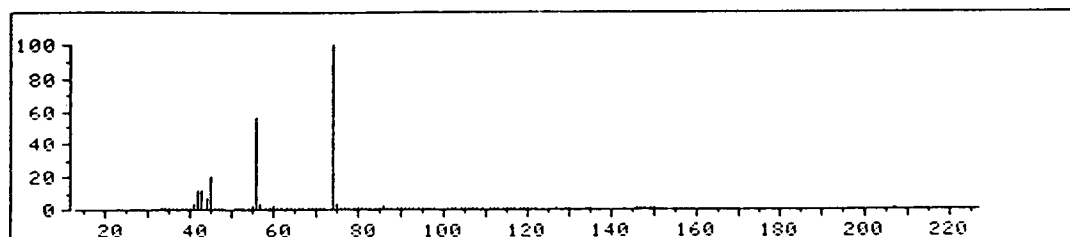


(b)



(c)

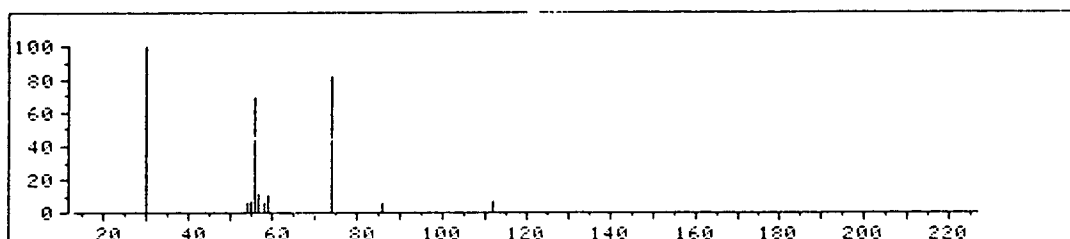
Figure 4.6: Mass spectra of peak 4 identified as EAE (a: EI spectrum; b: EI reference spectrum; c: CI spectrum).



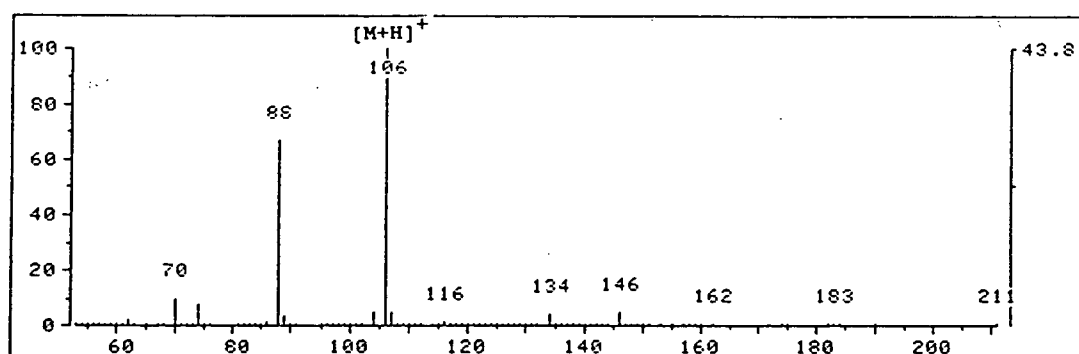
(a)

100.0%

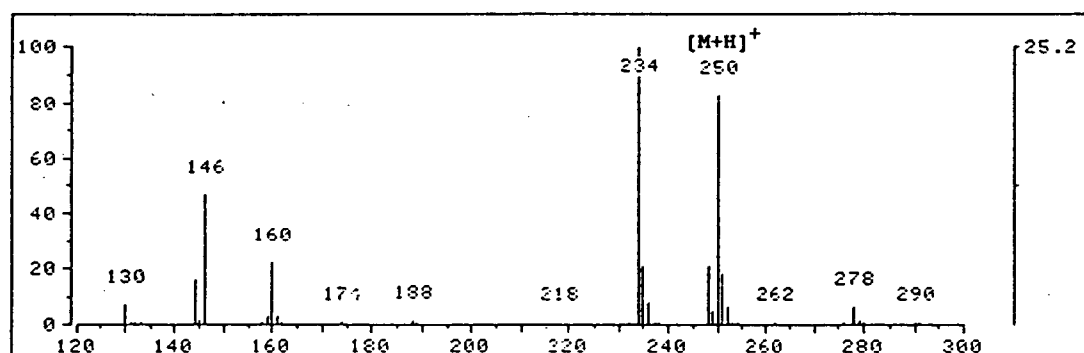
1 LFRN 3002 SPECT 1457 MW= 105 C4H11NO2
 .9754 Ethanol, 2,2'-iminobis- (9CI)



(b)

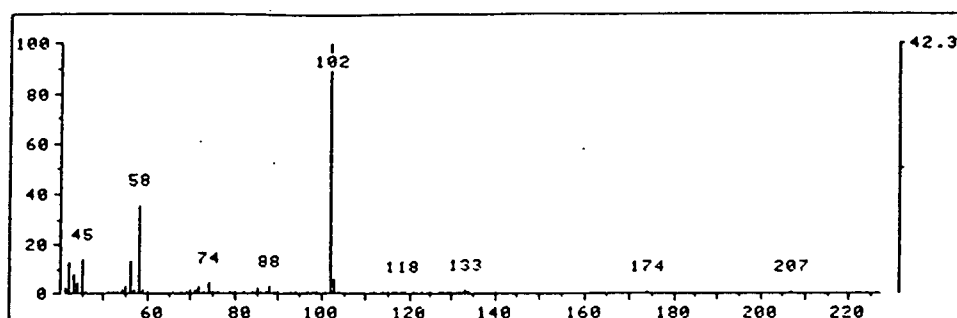


(c)

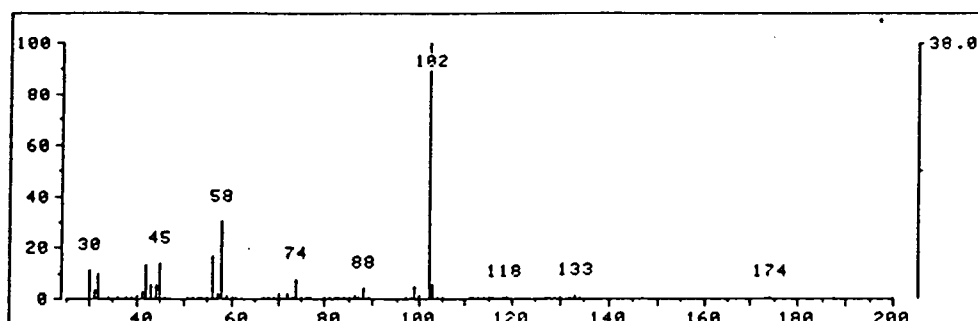


(d)

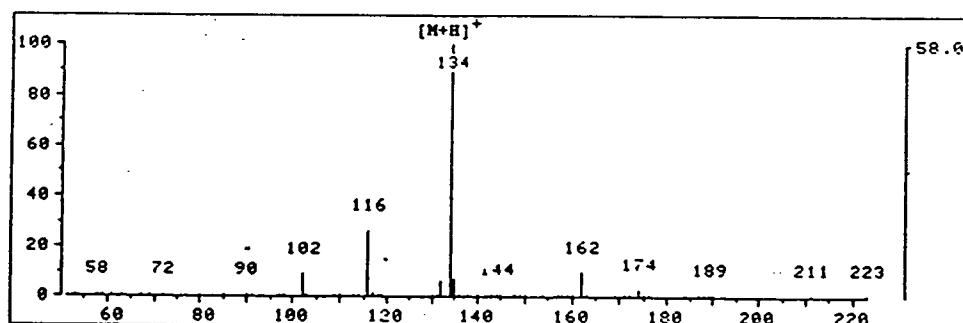
Figure 4.7: Mass spectra of peak 5 identified as DEA (a: EI spectrum; b: EI reference spectrum; c: CI spectrum; d: CI spectrum of the silyl derivative).



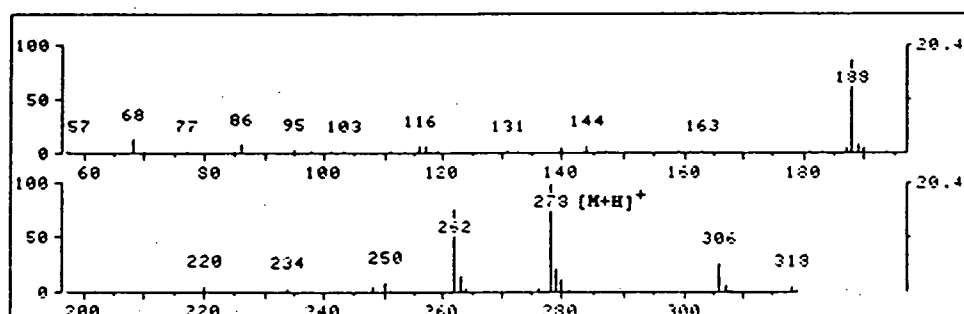
(a)



(b)

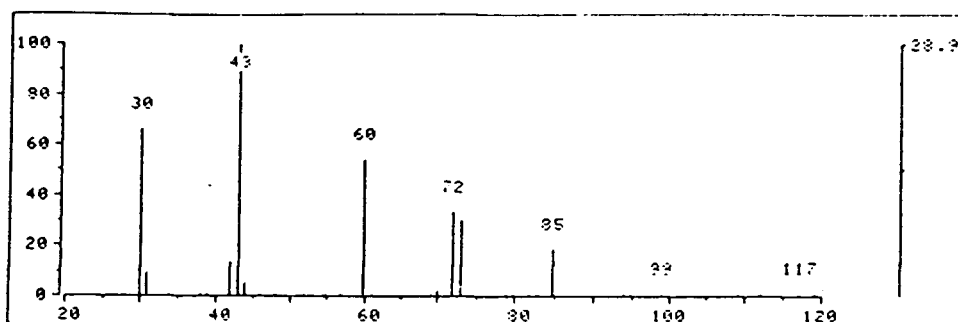


(c)

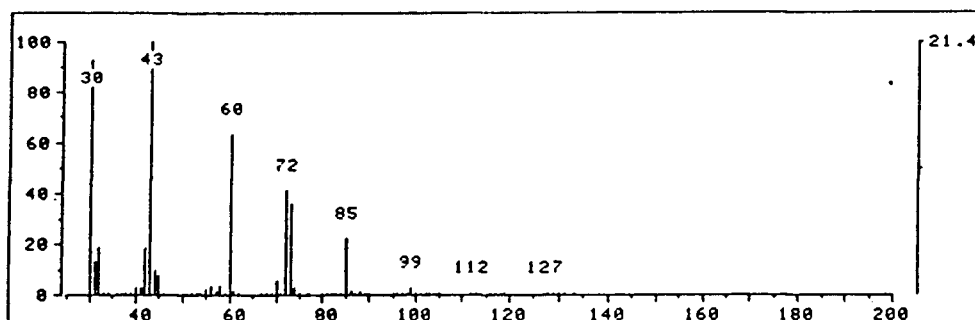


(d)

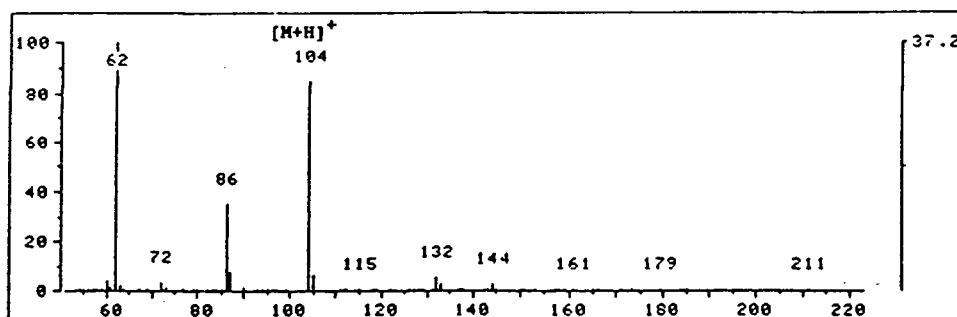
Figure 4.8: Mass spectra of peak 6 identified as EDEA (a: EI spectrum; b: EI reference spectrum; c: CI spectrum; d: CI spectrum of the silyl derivative).



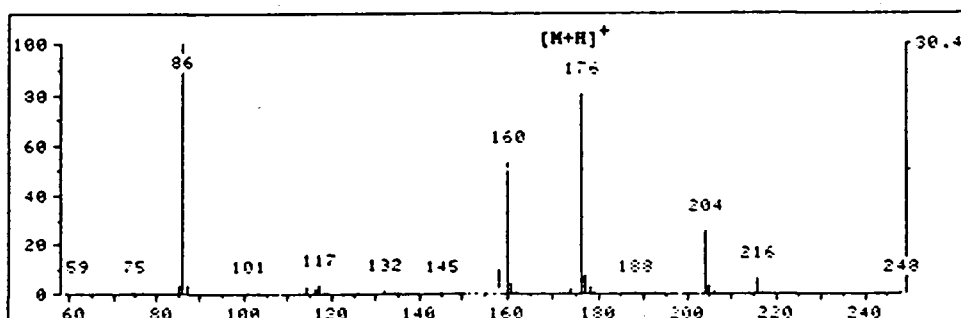
(a)



(b)

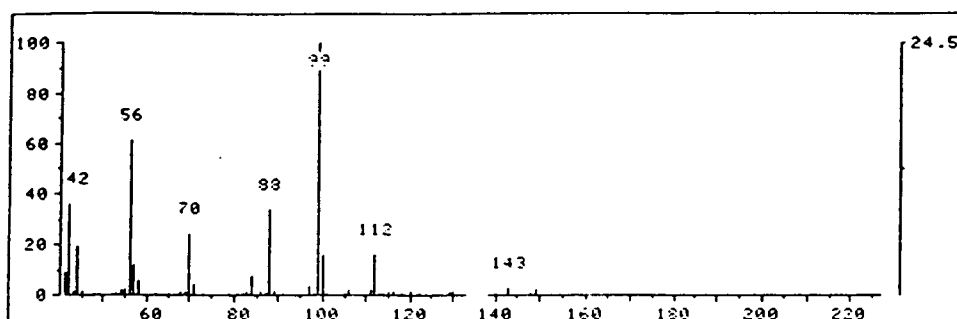


(c)

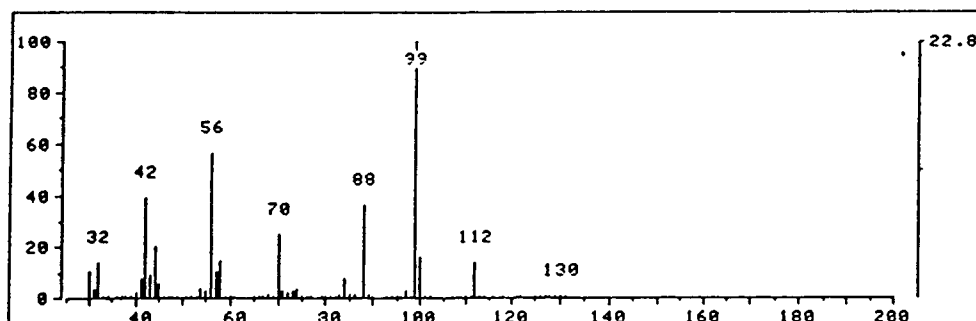


(d)

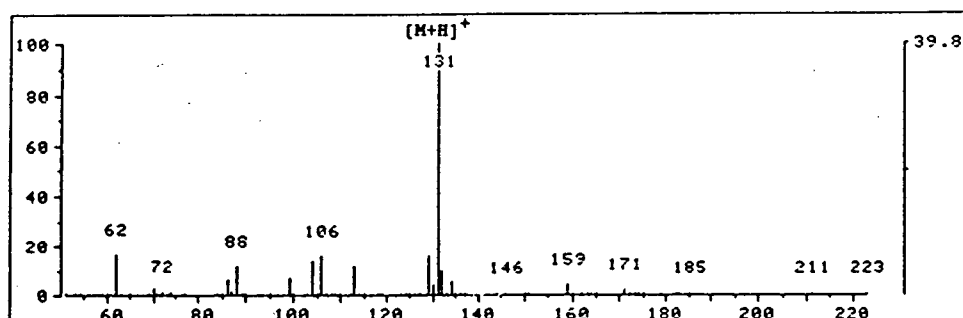
Figure 4.9: Mass spectra of peak 7 identified as HEA (a: EI spectrum; b: EI reference spectrum; c: CI spectrum; d: CI spectrum of the silyl derivative).



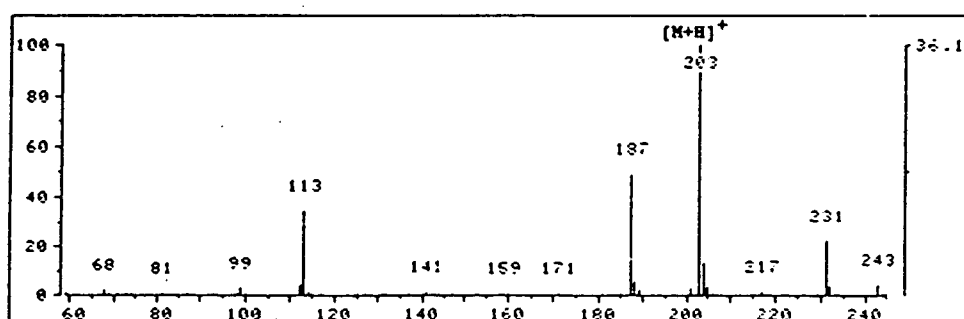
(a)



(b)

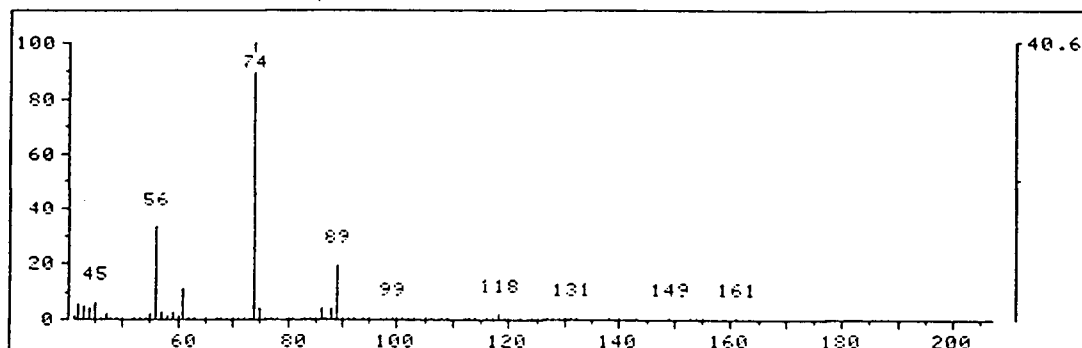


(c)

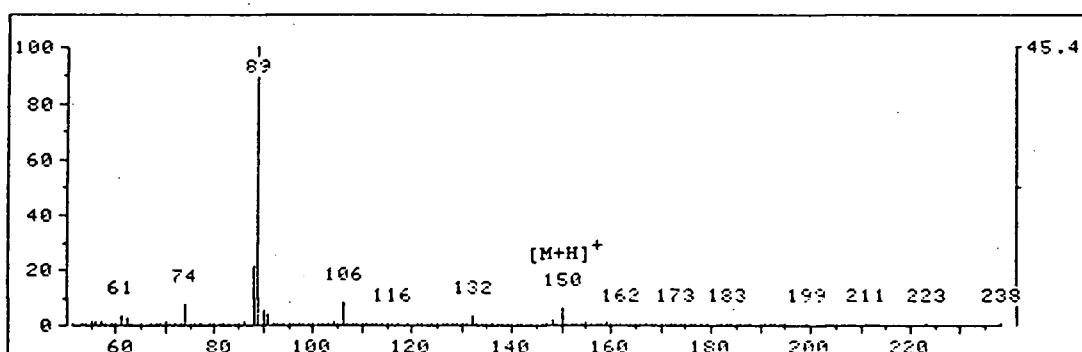


(d)

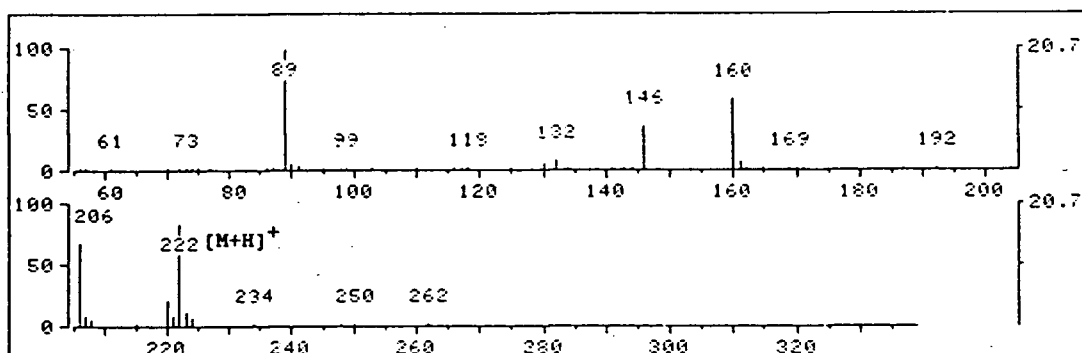
Figure 4.10: Mass spectra of peak 8 identified as HEP (a: EI spectrum; b: EI reference spectrum; c: CI spectrum; d: CI spectrum of the silyl derivative).



(a)

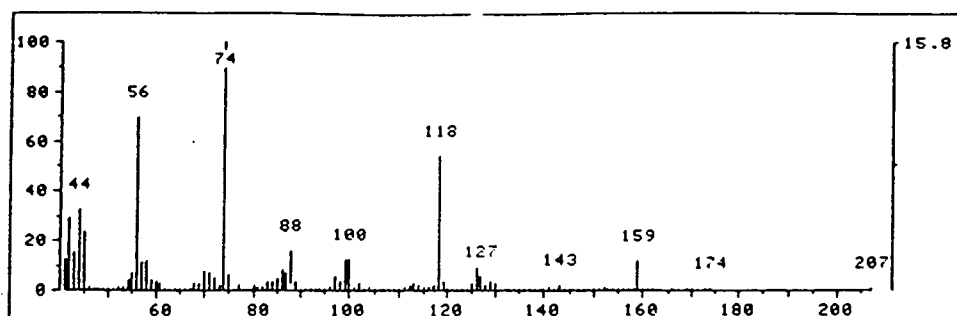


(b)

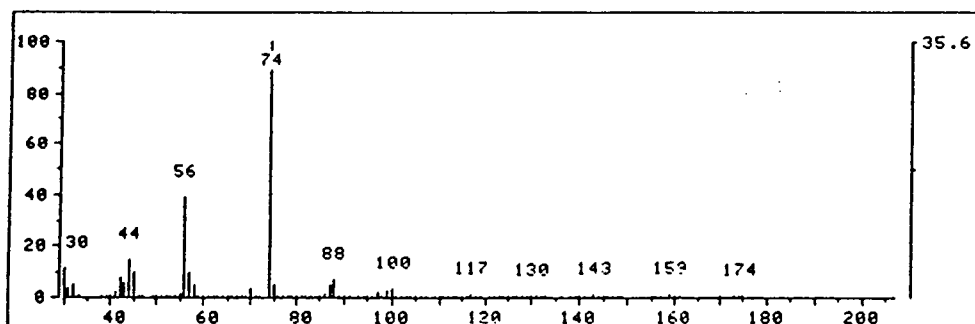


(c)

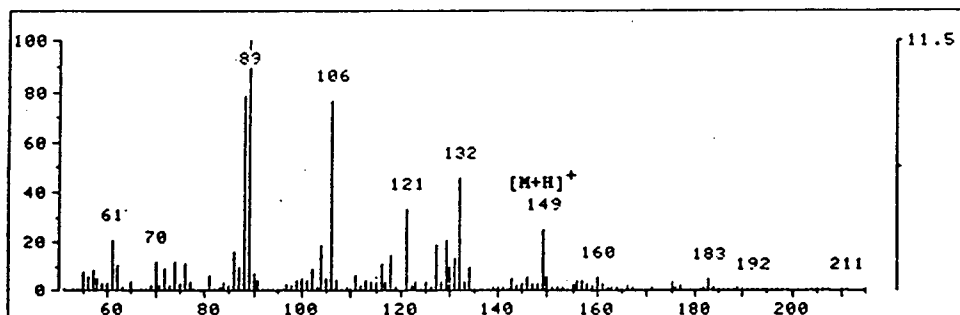
Figure 4.11: Mass spectra of peak 9 identified as ETAHEAME
 (a: EI spectrum; b: CI spectrum; c: CI spectrum of silyl derivative).



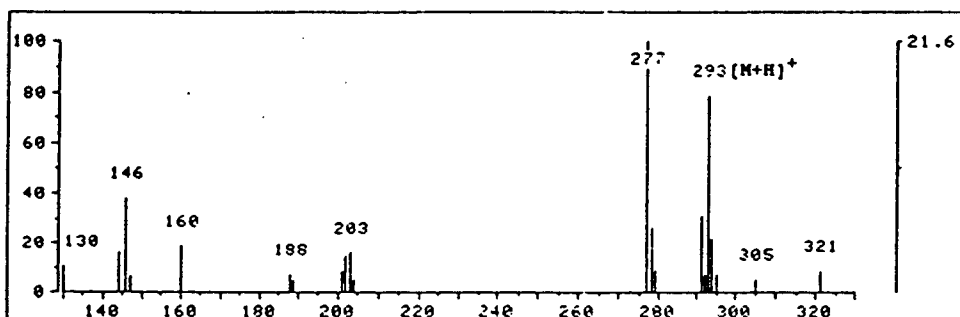
(a)



(b)

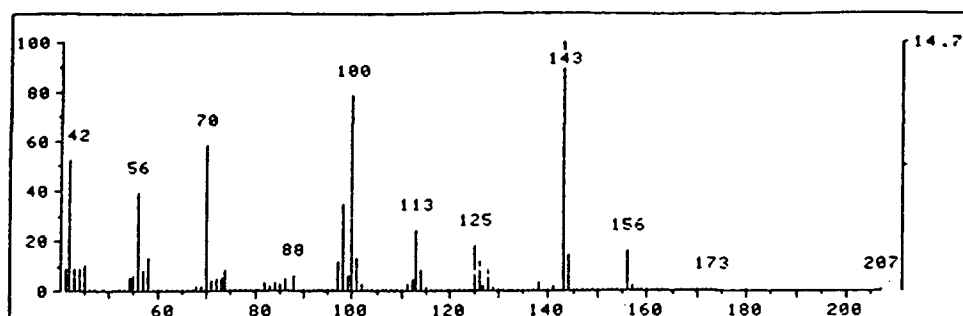


(c)

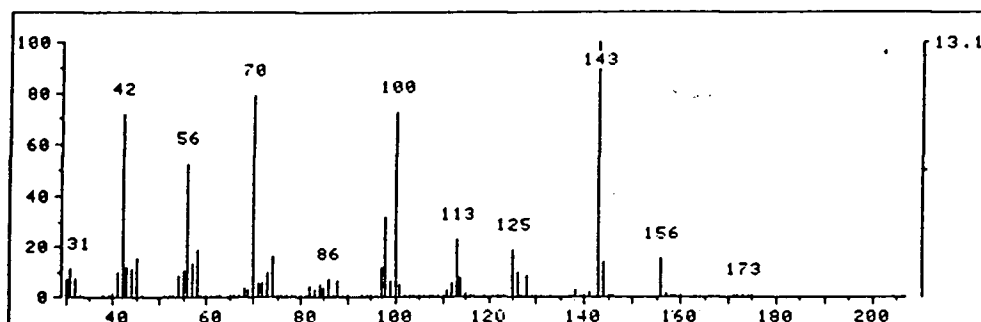


(d)

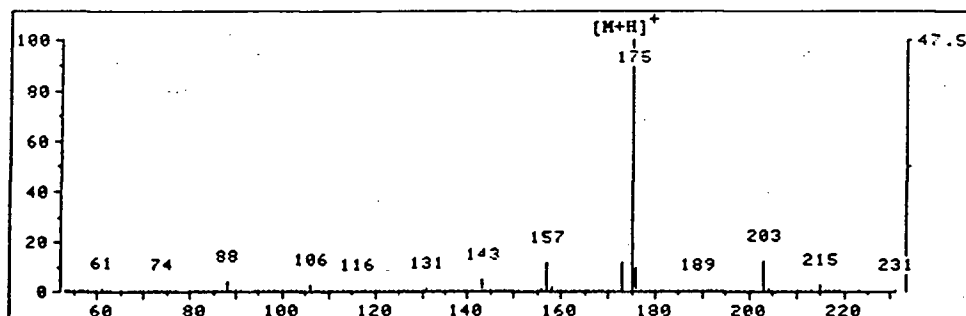
Figure 4.12: Mass spectra of peak 10 identified as BHEED
 (a: EI spectrum; b: EI reference spectrum;
 c: CI spectrum; d: CI spectrum of the silyl derivative).



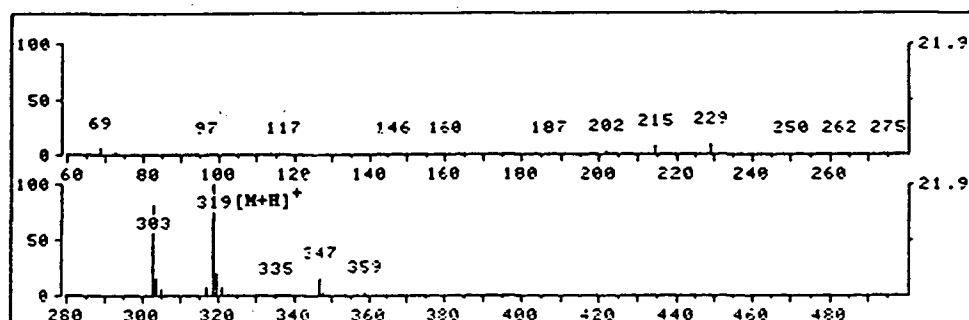
(a)



(b)

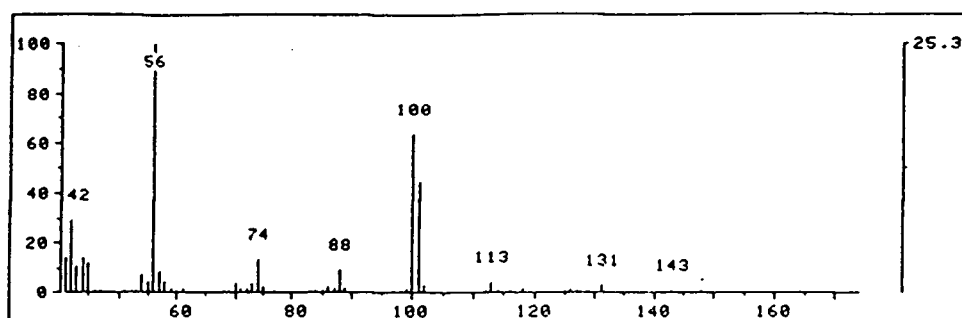


(c)

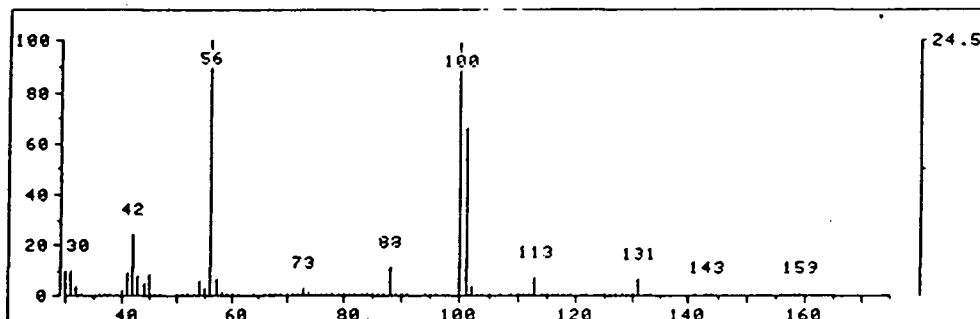


(d)

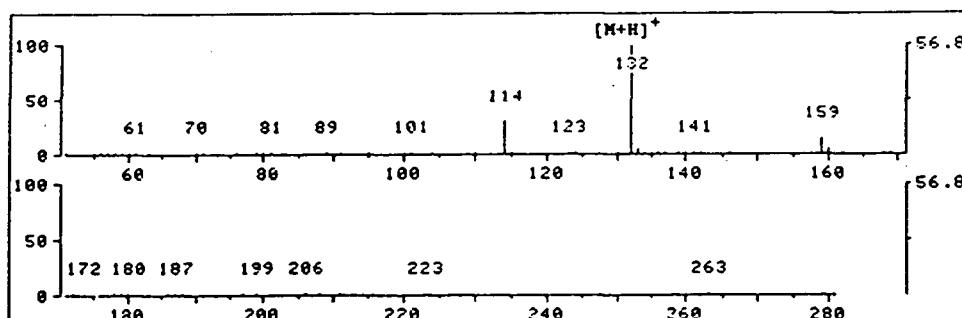
Figure 4.13: Mass spectra of peak 11 identified as BHEP (a: EI spectrum; b: EI reference spectrum; c: CI spectrum; d: CI spectrum of the silyl derivative).



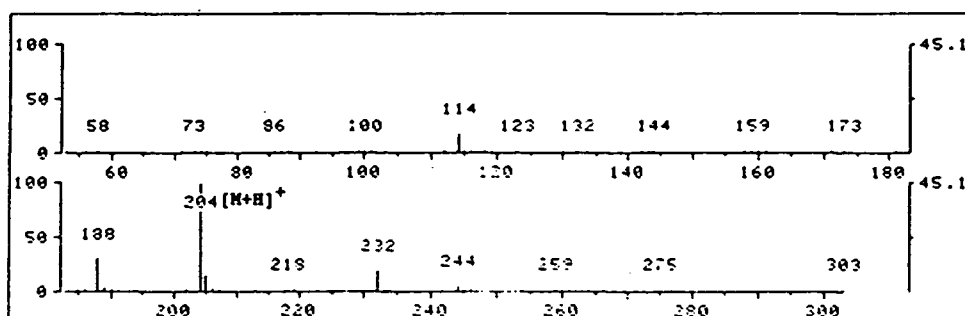
(a)



(b)

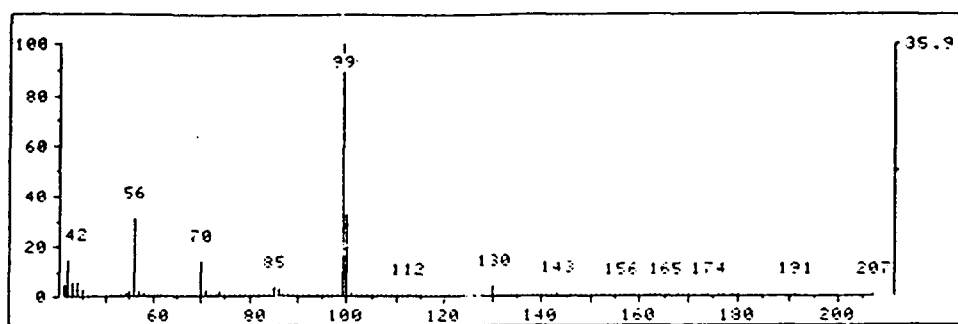


(c)

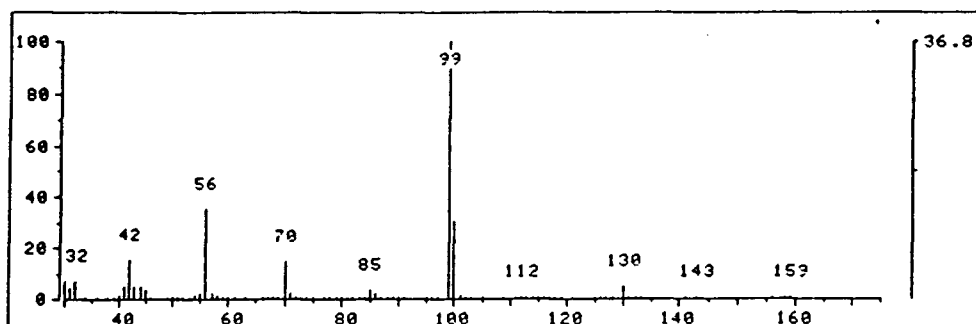


(d)

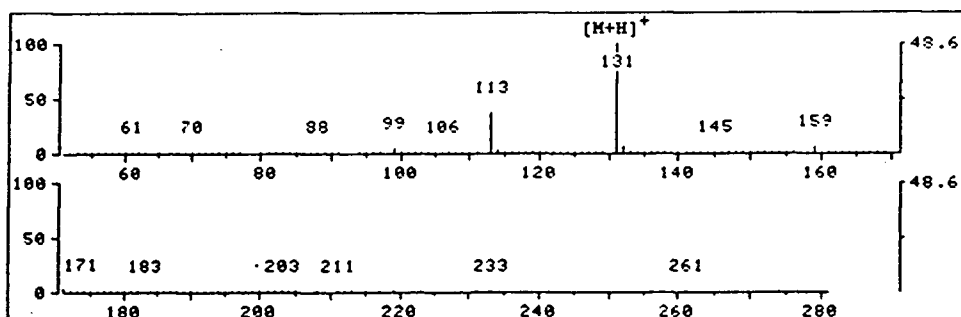
Figure 4.14: Mass spectra of peak 12 identified as HEOD (a: EI spectrum; b: EI reference spectrum; c: CI spectrum; d: CI spectrum of the silyl derivative).



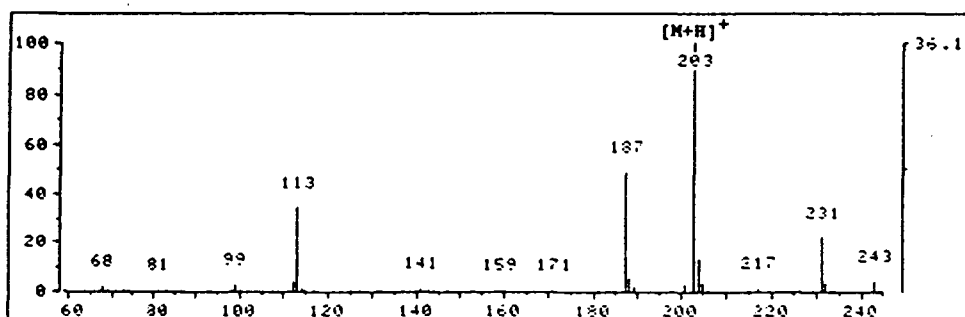
(a)



(b)

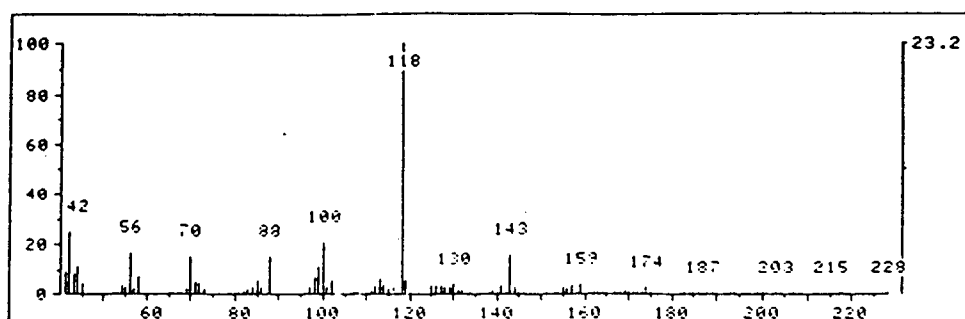


(c)

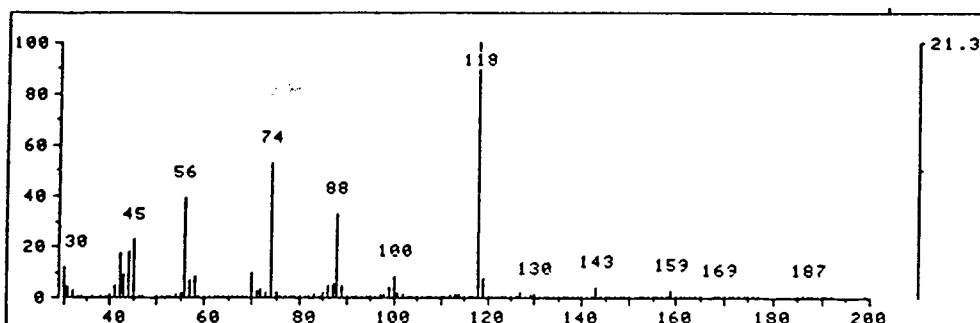


(d)

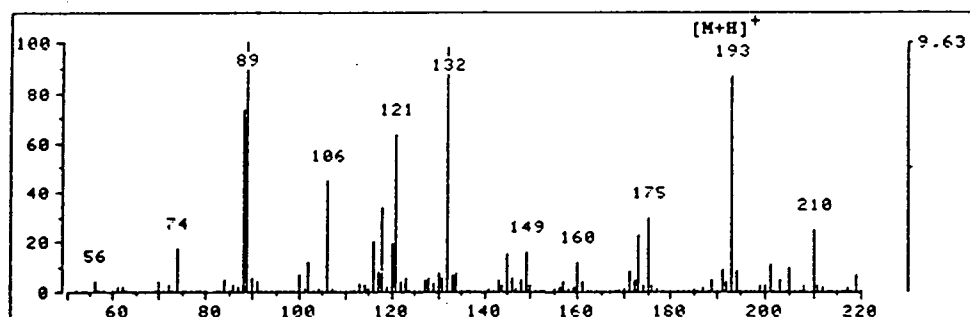
Figure 4.15: Mass spectra of peak 13 identified as HEI (a: EI spectrum; b: EI reference spectrum; c: CI spectrum; d: CI spectrum of the silyl derivative).



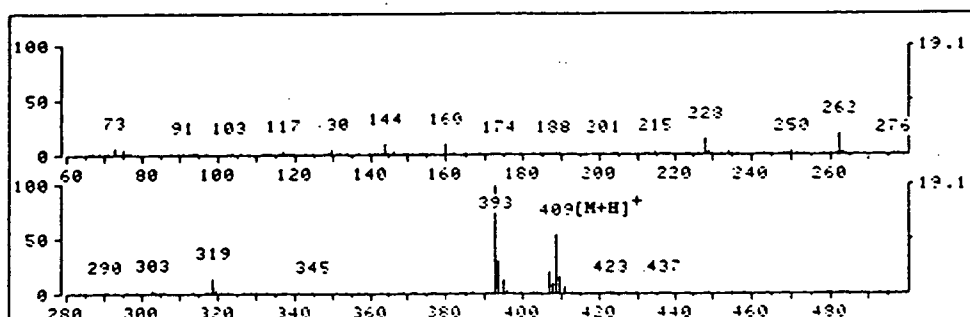
(a)



(b)

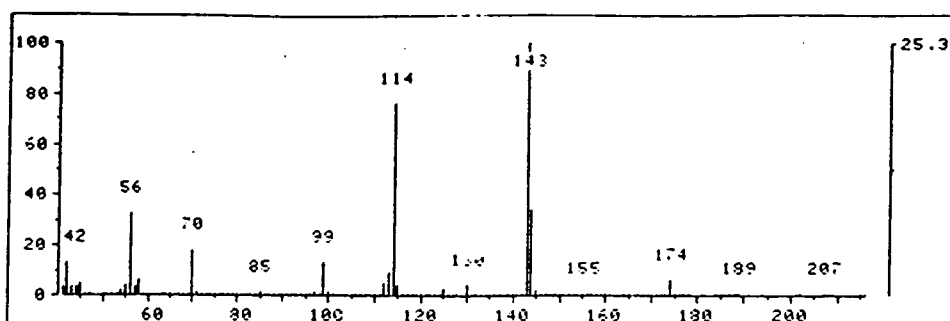


(c)

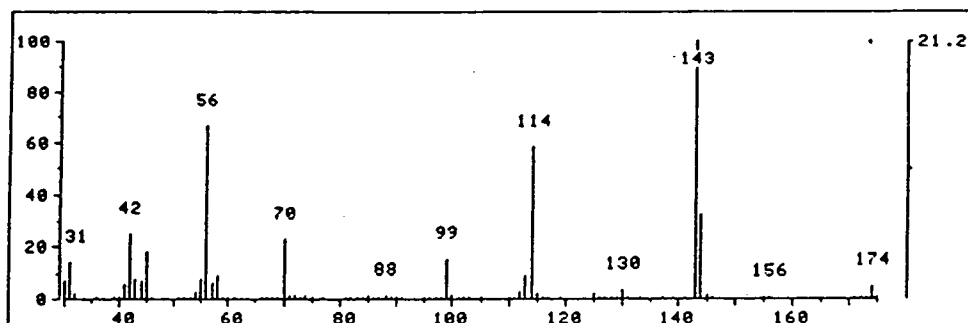


(d)

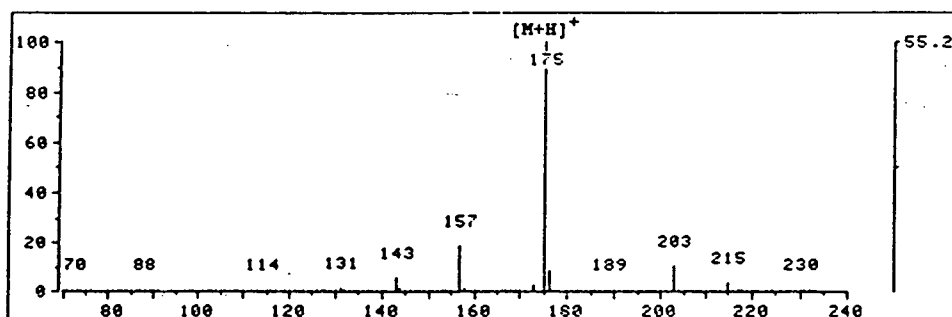
Figure 4.16: Mass spectra of peak 14 identified as THEED
 (a: EI spectrum; b: EI reference spectrum;
 c: CI spectrum; d: CI spectrum of the silyl derivative).



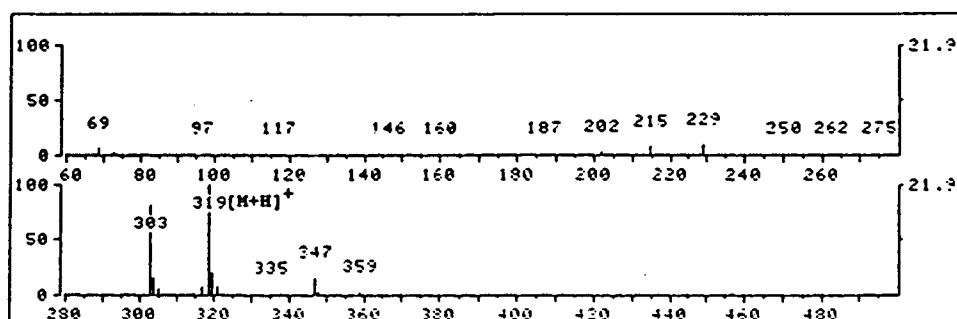
(a)



(b)



(c)



(d)

Figure 4.17: Mass spectra of peak 15 identified as BHEI (a: EI spectrum; b: EI reference spectrum; c: CI spectrum; d: CI spectrum of the silyl derivative).

The degradation compounds may be conveniently grouped into two categories: low-boiling degradation compounds which elute before DEA and high-boiling degradation compounds which elute after DEA. Other low-boiling degradation compounds include methanol, ethanol, acetaldehyde and/or ethylene oxide, acetic acid, methyl pyridine, diethyl disulphide, ethyl methyl pyridine and 1,2 dithiane. These compounds are not included in Table 4.2, but their EI spectra are shown in Appendix B2. Methanol, ethanol, acetaldehyde being very volatile, were not properly separated during the GC analyses and they were barely visible in the chromatograms. Their presence in the degraded solutions was deduced from the GC/MS analysis. Acetic acid eluted from the Tenax GC column just before butanone. In most of the analyses, it was embedded in the butanone peak. Methyl pyridine, ethyl methyl pyridine, diethyl disulphide and 1,2 dithiane peaks were visible and well separated but were formed in very low concentrations.

Qualitative analysis of the gas phase showed ethanol, acetone, butanone, pentanone, hexanone and some of the low boiling degradation compounds found in the liquid phase.

In addition to the water soluble degradation compounds, an insoluble, light brown solid product was also formed. Tests conducted to identify the solid are discussed below.

The present results are at variance with some previous findings (19,20). However, it is important to note that the degradation reactions proceed slowly. Even under the most severe conditions used in this study (40% DEA, 190 °C), only the low boiling degradation compounds were formed in appreciable quantities within the first 6 hours. At 120 °C,

only the low boiling degradation compounds were detected within the first 24 hours. As pointed out earlier, perhaps the inability of the previous investigators to detect degradation compounds in COS/DEA systems was due to the short experimental durations and their analytical techniques.

4.3 DEGRADATION PRODUCTS RESULTING FROM CS₂-DEA INTERACTIONS

Figures 4.18a-c show chromatograms of runs conducted with 10.5 mL CS₂ and 250 mL of 3M aqueous DEA solutions at 180, 165 and 150 °C, respectively. Runs conducted at temperatures between 165 and 120 °C (e.g. Figs. 4.18b and 4.18c) gave similar products and samples of the solutions had a lighter colour, less pungent odour and greater solids content due to the formation of the dithiocarbamate salt, than the corresponding COS-DEA samples. It was necessary to centrifuge the samples from the CS₂-DEA runs before injecting them into the gas chromatograph. At 180 °C, the reaction mechanism appears to be more complex because more products were formed in significant quantities. Furthermore, the samples were deep brown and possessed a very pungent odour. The pressure in the reactor was also found to increase by about 0.45 to 0.55 MPa (70 to 80 psi) within 3 hours, compared with approximately 0.07 to 0.15 MPa for the corresponding COS-DEA runs.

These results indicate that, unlike the COS-DEA system, some reaction steps in the CS₂-induced degradation of DEA are affected by temperature. The resemblance between Figs. 4.18a and 4.1a-c suggests

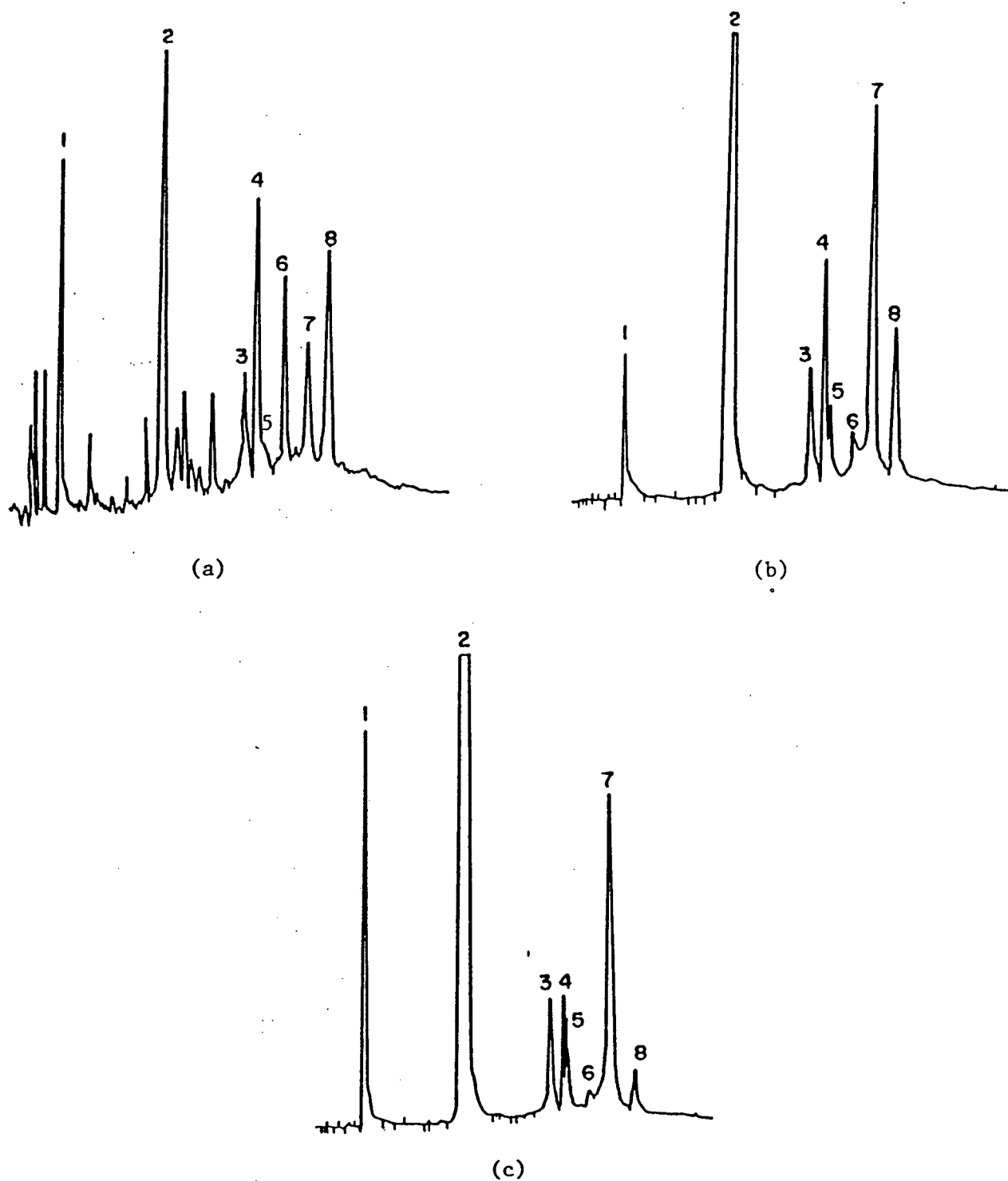


Figure 4.18: Chromatograms of partially degraded DEA solutions of 3M initial concentration degraded with 10 mL of CS₂ for 48 hours (a: 180 °C; b: 165 °C; c: 150 °C).

that degradation in the CS₂-DEA system at 180 °C is preceded by hydrolysis of CS₂ to COS with the latter causing COS-induced degradation.

Following the analytical procedure described earlier, the peaks labelled 1 to 8 in Fig. 4.18 were identified as MEA, DEA, BHEED, BHEP, HEOD, HEI, THEED and BHEI, respectively. MEA was the only low boiling compound of significance detected in CS₂-DEA systems at temperatures below 165°C.

A solid material was also produced by the CS₂-DEA systems. Solids produced in runs conducted at temperatures of 165 °C and below, had a beige colour whereas the solids recovered from runs conducted at 180 °C were yellowish brown and similar to those of the COS runs.

4.4 CHARACTERIZATION OF THE SOLID PRODUCTS

The solids recovered from all the COS runs and the CS₂ runs conducted at 180 °C were yellowish brown in colour. Liquid samples withdrawn from both sets of runs also had the same yellowish brown appearance. GC/MS analysis of the centrifuged liquid samples revealed that they contain the same compounds. In view of these similarities, both systems are believed to be undergoing similar reactions. As for the CS₂ runs conducted at temperatures of 165 °C and below, the recovered solid had a beige colour while the liquid samples were colourless and did not contain any ketones. The solid formed fine powders on grinding, unlike the solids generated from the COS runs and CS₂ runs at 180 °C

which were sticky. In order to characterize the solid materials from the CS₂-DEA and COS-DEA systems, the following tests were conducted.

4.4.1 SOLUBILITY

The solubility of the solids in a variety of solvents such as water, ethanol, methanol, toluene, diethyl ether, acetone and carbon disulphide was examined. Both the COS and CS₂ generated solids were found to be insoluble in these solvents even when the solvents were heated to boiling. However, dimethyl formamide at boiling temperature (153 °C) was able to dissolve the solids but precipitation occurred as soon as the solutions were cooled. The insoluble nature of the solid suggests that it is a polymeric material.

4.4.2 MELTING POINT

The melting points of the solids were determined with a Kofler Hot Stage Microscope. The set up consisted of the Kofler hot bench mounted on a Wild Heitz microscope, a thermometer to monitor the temperature of the hot bench and a regulating transformer which controlled the rate of heating. Controlled illumination of the microscope was achieved with an on-line voltage regulator.

A tiny chip of solid to be analysed was placed on a slide which was then centred on the hot bench. The heating rate and hence temperature of the hot bench was controlled by a series resistance connecting the hot bench to the main power supply. The resistance was

set in such a manner that the temperature of the hot bench rose by 4 °C/min. While the bench was heated, the state of the solid was monitored by viewing the sample at a magnification of 100. At the outset, the sample appeared as a black dot in the field of the microscope. At the melting temperature, the sample became fluid and the field became illuminated. The temperature indicated on the thermometer was recorded as the melting point of the sample. Four determinations were made for each sample and the average temperatures were recorded. The COS generated solid melted in the range 124 °C to 138 °C with most of it melting above 135 °C. The CS₂ solid generated at temperatures below 165 °C had a narrower melting range of 138 °C and 144 °C. The size of the melting ranges suggest that the CS₂ generated solid is less contaminated than the COS generated solid. Since the boiling temperature of dimethyl formamide exceeds the melting points of the solids, their apparent dissolution in the boiling solvent was due to melting. Therefore the solids can be considered insoluble in dimethyl formamide.

4.4.3 ELEMENTAL ANALYSIS

The elemental composition of the solids was determined by the Canadian Microanalytical Laboratory, New Westminster, BC, and the results are shown in Tables 4.3 and 4.4.

The compositions of the solids seem to depend on the conditions used for the degradation runs. The percentage of sulphur decreased with increasing temperature while the reverse was the case for the other

Table 4.3: Elemental compositions of solids formed in the COS-DEA systems

ELEMENT	COMPOSITIONS (wt%)			
	150 °C		180 °C	
	wt%	mole%	wt%	mole%
C	41.95	28.31	44.11	29.07
H	7.08	57.34	7.26	57.41
N	1.76	1.02	2.94	1.66
O	2.87	1.45	3.94	1.95
S	46.92	11.88	40.14	9.92
TOTAL	100.58	100.00	98.39	100.00

Table 4.4: Elemental compositions of solids formed in the CS₂-DEA systems.

ELEMENT	COMPOSITIONS (wt%)			
	150 °C		180 °C	
	wt%	mole%	wt%	mole%
C	38.97	26.88	48.00	29.32
H	6.95	57.53	7.89	57.84
N	3.09	1.83	4.44	2.32
O	4.92	2.55	6.19	2.84
S	43.35	11.21	33.49	7.67
TOTAL	97.28	100.00	100.01	100.00

elements. The changes were generally more pronounced for the solids generated in the CS₂ runs. This trend could be due to the fact that, except for sulphur, all other elements are contained in the amine whose initial concentration increases with operating temperature (due to increased evaporation of water). In the same vein, increasing temperature limits the solubility of COS and CS₂ and consequently the amount of sulphur available for reactions in the liquid phase. The ratios of the elements could be calculated from the elemental analysis shown in Tables 4.3 and 4.4. For example, in the solid generated in the COS runs at 180 °C, the C/S, C/H, C/N, S/O, N/O, C/O, H/N and H/O ratios are 2.93, 0.50, 17.50, 5.09, 0.85, 14.93, 34.57 and 29.48, respectively. These ratios transform approximately to an empirical formula of C₁₅H₃₀NOS₅ (E.W 400). Using the same calculations, the formula C₁₄H₃₀NOS₆ (E.W 420) can be derived for the solids recovered from the CS₂ system at 150 °C. The higher molecular weight of the CS₂ solid would imply a higher melting point as confirmed by the melting point determinations.

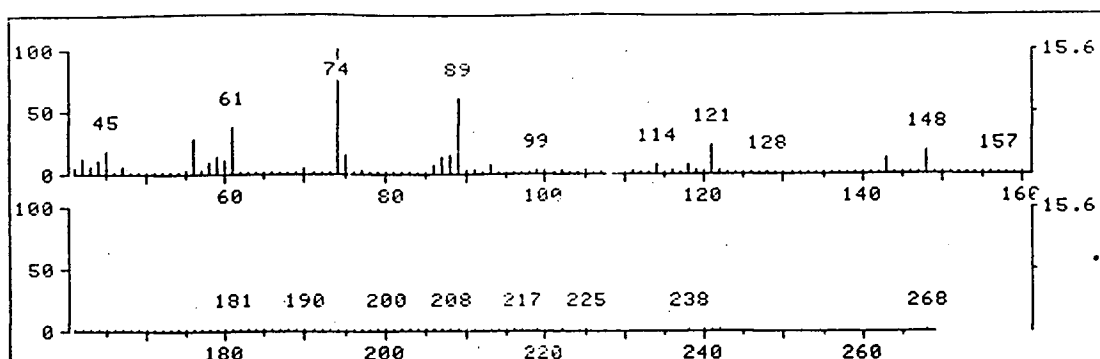
4.4.4 MASS SPECTRAL ANALYSIS

Solid probe EI and CI mass spectral analyses were performed on the solid products to determine their fragmentation patterns as well as their molecular weights. Both solids produced similar traces as shown in Figures 4.19 and 4.20. The CS₂ solid trace is for the solid generated in the CS₂ run at 150 °C. Although the EI spectra resemble the library spectrum of acetic acid - mercapto - 1,2 ethanediyl ester (C₆H₁₀O₄S₂)

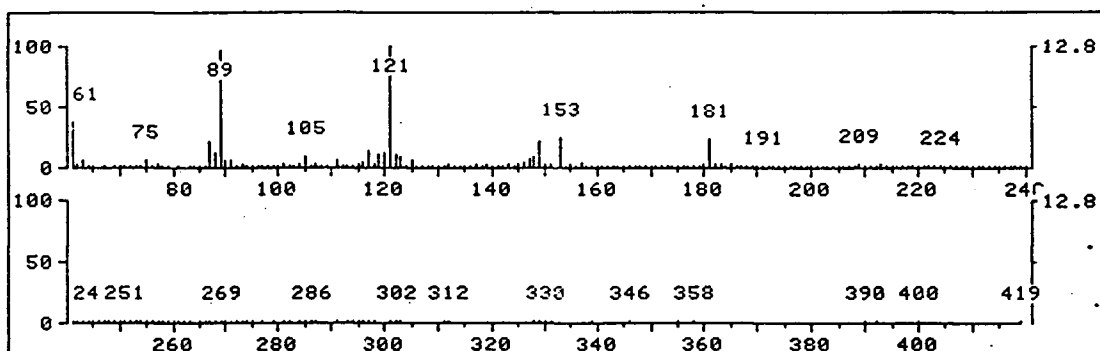
with a molecular weight of 210, the elemental composition of this compound is at variance with the results of the elemental analysis. Hence the identity of the solids is different from that suggested by the library of mass spectra.

The fragmentation pattern in the CI spectra show successive losses of ions of masses 28 and 32. Since the solids are rich in sulphur, the ion of mass 32 is most likely due to elemental sulphur. The ion of mass 28 could either be a carbonyl group ($C=O$) or an ethenyl (C_2H_4) group. However, the very low oxygen to sulphur ratio in the solids, the almost equal number of losses of masses 28 and 32 and the high carbon content of the solids, point to an ethenyl group as the fragmenting group with mass 28. It is difficult to identify a molecular ion peak from the CI traces because of the low abundances of the high molecular weight ions. The most abundant peak has a mass of 121, suggesting a molecular weight of 120. The high melting point of the solids is inconsistent with this molecular weight. Furthermore, the absence of ions of mass 149 ($M+29$) makes a molecular mass of 120 very unlikely.

The pattern of successive losses of masses 28 and 32 in the CI spectra suggests a fragile linear structure containing several covalent bonds with sulphur interspersed between the ethenyl groups. The ease of bond breakage is, perhaps, the reason for not having a prominent molecular ion peak. The similarities in the mass spectrum of the solids is another indication that the solids have similar structures.

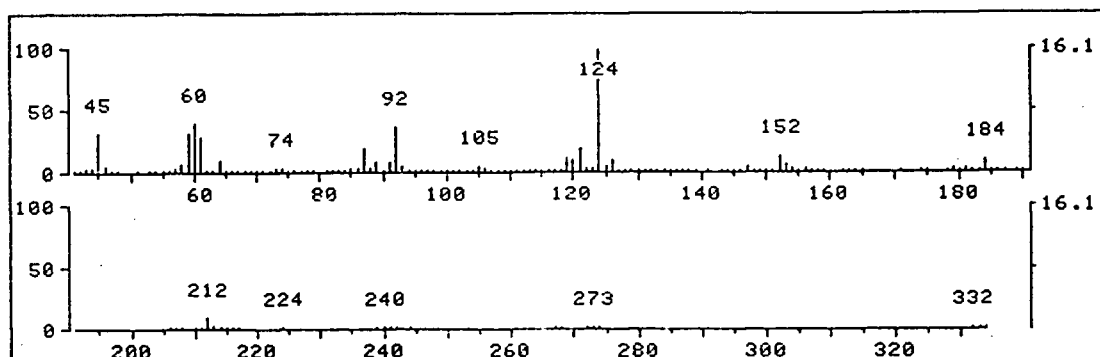


(a)

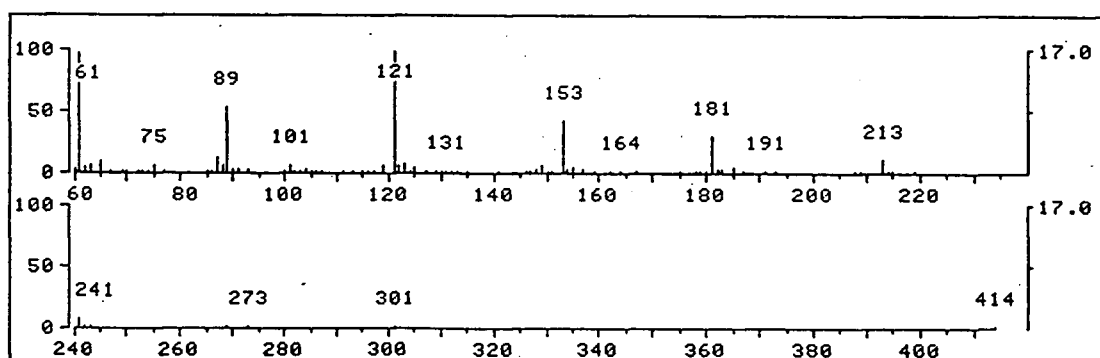


(b)

Figure 4.19: Mass spectra of the solid formed in the COS-DEA system
(a: EI spectrum; b: CI spectrum).



(a)



(b)

Figure 4.20: Mass spectra of the solid formed in the CS₂-DEA system (a: EI spectrum; b: CI spectrum).

4.4.5 INFRA-RED ANALYSIS

To gain insight into the functional groups of the solid compounds, infra red (IR) absorption traces were obtained using KBr pellets in a Bomem - Michelson 100 spectrophotometer. The resulting traces are shown in Figures 4.21 and 4.22. Again there are obvious similarities in the absorption wavelenghts of both solids. It should be noted that the absorbances in the traces are of weak to medium intensities since the transmittance scale is from 78.7% to 102.75%, a range of only 24%. Table 4.5 shows a possible assignment of functional groups to the absorption bands in the IR traces.

The dependency of the composition of the solid on the operating temperature suggests that the solids are probably not pure compounds but a mixture. If this is the case, then it is more appropriate to consider the solids as chemically derived organic fouling deposits. It could also be that, in spite of the similarities in the results from the other analyses, the solids are different compounds belonging to the same homologous series.

The analyses conducted have enabled the identification of the fragments or functional groups that occur in the solid products. The insoluble nature of the solids as well as their level of purity, posed problems that prevented further analysis and conclusive identification.

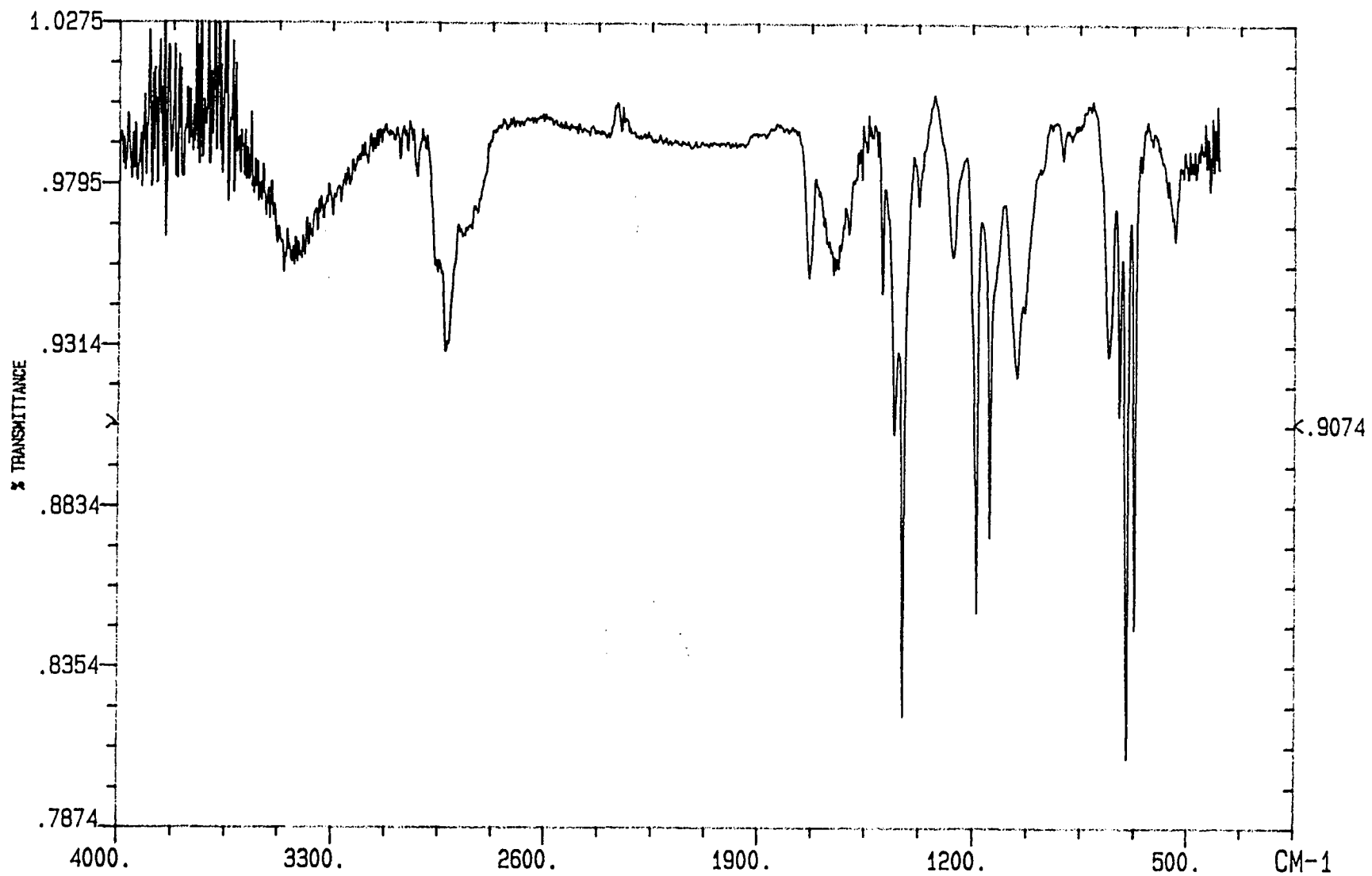


Figure 4.21: Infra-red trace of the solid formed in the COS-DEA system.

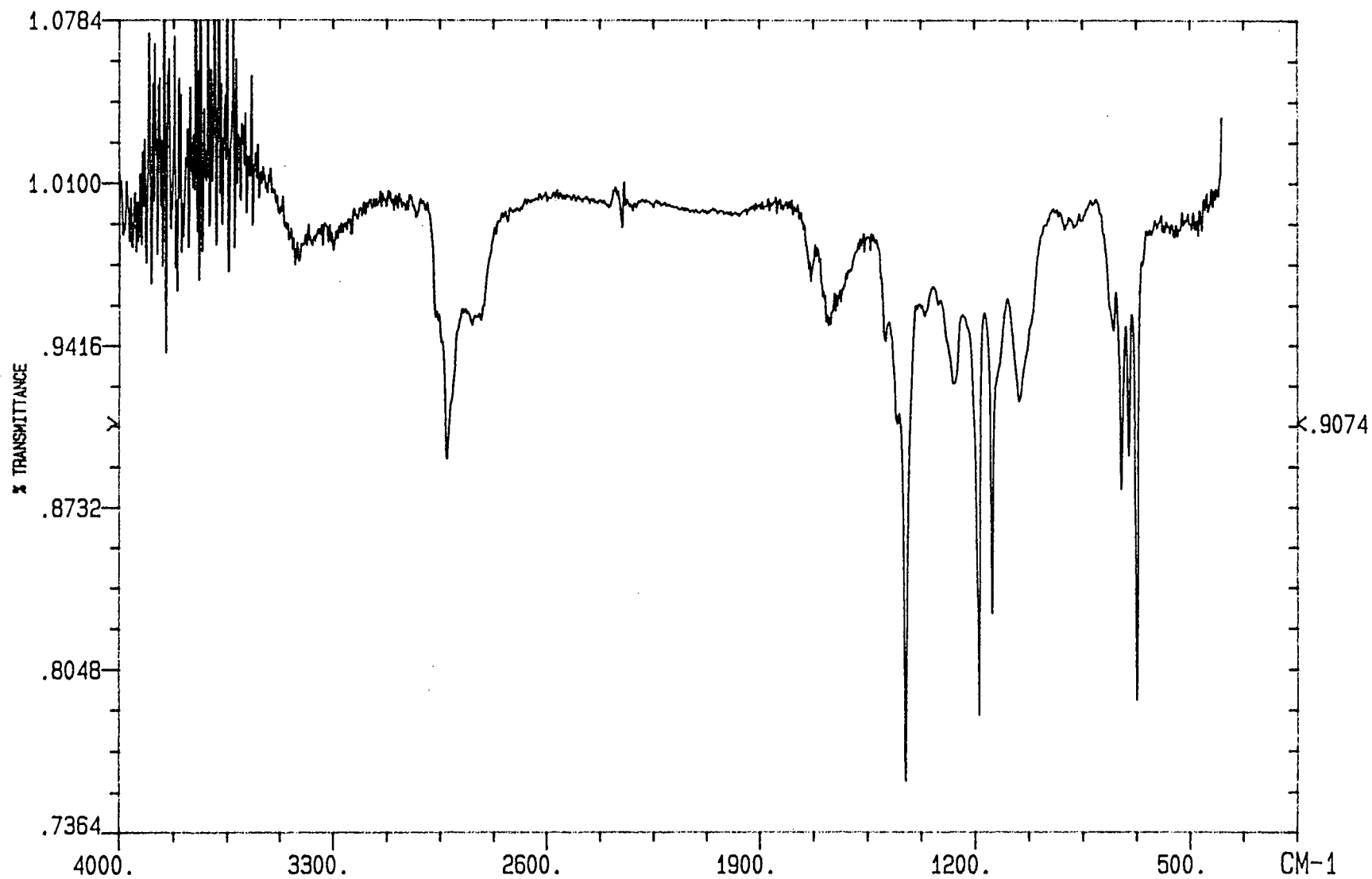


Figure 4.22: Infra-red trace of the solid formed in the CS_2 -DEA system.

Table 4.5: Functional group assignments for the solids formed in the COS-DEA and CS₂-DEA systems.

LITERATURE IR (81,82)		SAMPLE IR	
GROUP	BAND (cm ⁻¹)	BAND (cm ⁻¹)	ASSIGNMENT
CH ₂ -S-CH ₂	670 - 760 (m)	672, 698 (m)	CH ₂ -S-CH ₂
-SH	815 - 930 (w)	910 (w)	-SH
	2420 - 2600 (w)	2500 (w)	-SH
CH ₂ -NH-CH ₂	3100 - 3500 (m)	3422 (w-m)	CH ₂ -NH-CH ₂
	1480 - 1580 (w)	1492 (w)	
	1100 - 1200 (m)	1187 (m)	
	1080 - 1150 (m)	1143 (m)	
-(CH ₂) ₁	770 - 785 (w-m)		
-(CH ₂) ₂	735 - 745 (w-m)	755 (w)	-(CH ₂) _n
-(CH ₂) ₃	725 - 735 (w-m)	721 (w-m)	2 ≤ n ≤ 4
-(CH ₂) ₄	720 - 725 (w-m)	721 (w-m)	
-CH ₂ OH	1400 - 1460 (w)	1424 (m)	-CH ₂ OH
	1260 - 1350 (w)	1264 (w)	
	1010 - 1090 (s)	1053 (w)	
	3100 - 3500 (s)	3422 (w-m)	

The letters m, s, w in parenthesis, refer to absorbances of moderate, strong and weak strengths, respectively.

CHAPTER 5

EFFECTS OF OPERATING VARIABLES ON DEA DEGRADATION

The effects of initial DEA concentration, temperature, COS partial pressure and CS₂ volume on the degradation reactions are discussed with particular reference to DEA and the major degradation products. The observed trends are interpreted not only to highlight the effects that changes in the operating conditions have on the rates of degradation of DEA and the formation of degradation products, but also an attempt is made to distinguish terminal reaction products from reaction intermediates. Such distinction will eventually simplify the development of reaction mechanisms.

5.1 COS-DEA SYSTEM

5.1.1 EFFECTS OF INITIAL DEA CONCENTRATION

The overall degradation of DEA may be represented by:



The rate of degradation may be written as:

$$d[\text{DEA}]/dt = -k_{\text{DEA}} [\text{DEA}]^n \quad 5.2$$

where n is the order of reaction and k_{DEA} is the overall degradation rate constant.

For first order reactions, Eq. 5.2 reduces to:

$$\ln [\text{DEA}]_t = \ln [\text{DEA}]_0 - k_{\text{DEA}} t \quad 5.3$$

Eq. 5.2 may also be written in the form:

$$\log\{-d[\text{DEA}]/dt\} = \log k_{\text{DEA}} + n \log [\text{DEA}] \quad 5.4$$

According to Eq. 5.3, a semilogarithmic plot of DEA versus time should be linear with a slope corresponding to the degradation rate constant.

Figures 5.1 to 5.3 show the effect of initial DEA concentration on the degradation of the amine at 127, 150 and 165 °C, respectively. The plots are linear and thus confirm that the overall degradation of DEA follows first order kinetics at those temperatures.

The rate of degradation increases with amine concentration up to 4M. Between 4 and 6M initial concentrations, the rate of degradation decreases (see Fig. 5.4). At an initial concentration of 6M, the amine is in excess of water. Under such conditions, the reactions that generate the ions which induce degradation are hindered and consequently the rate of degradation falls. Kennard (16) and Chakma (18) observed similar effects in CO₂-DEA and CO₂-MDEA systems, respectively.

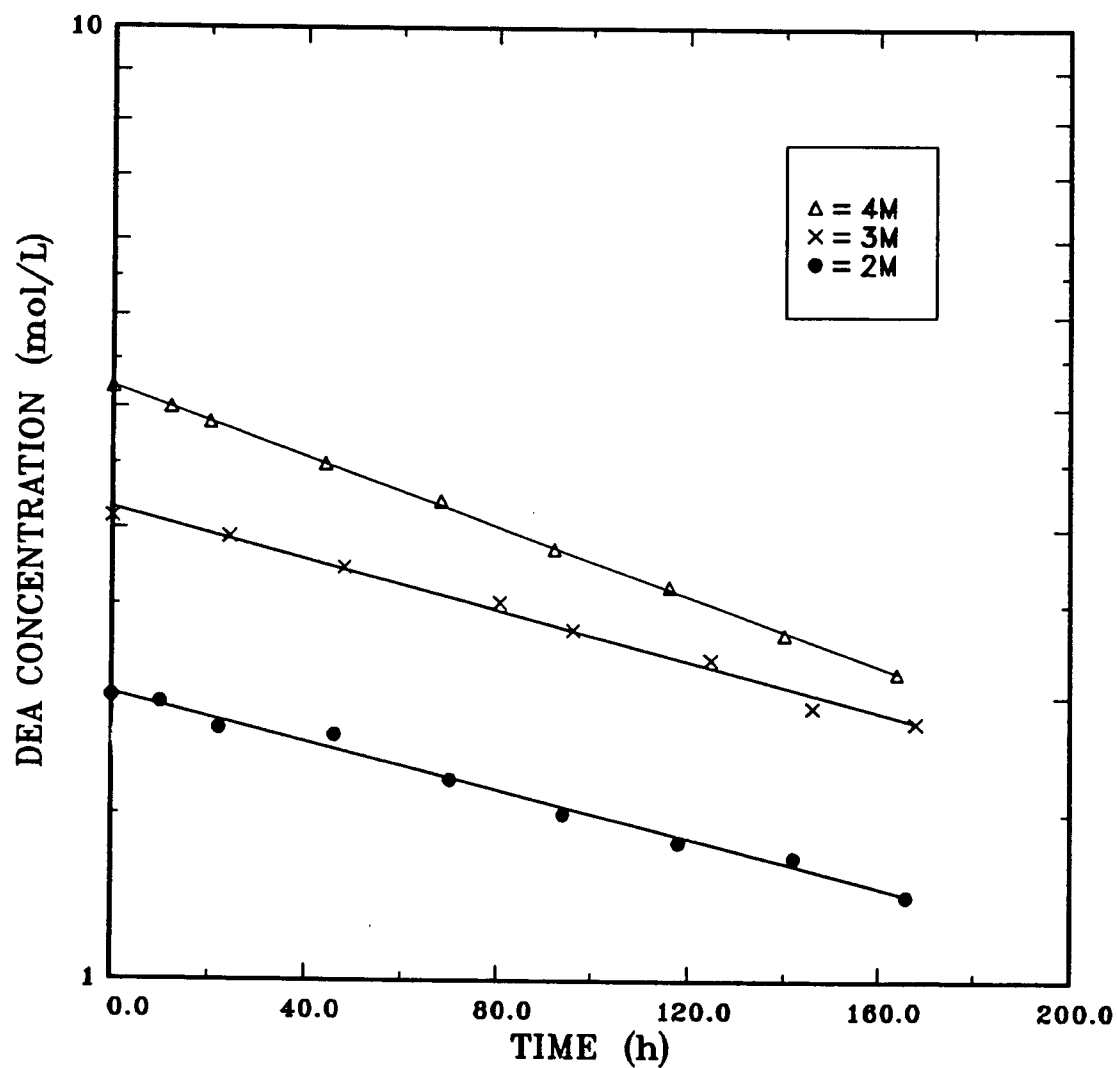


Figure 5.1: DEA concentration as a function of initial DEA concentration and time ($P_{COS} = 0.34$ MPa, $T = 127$ °C).

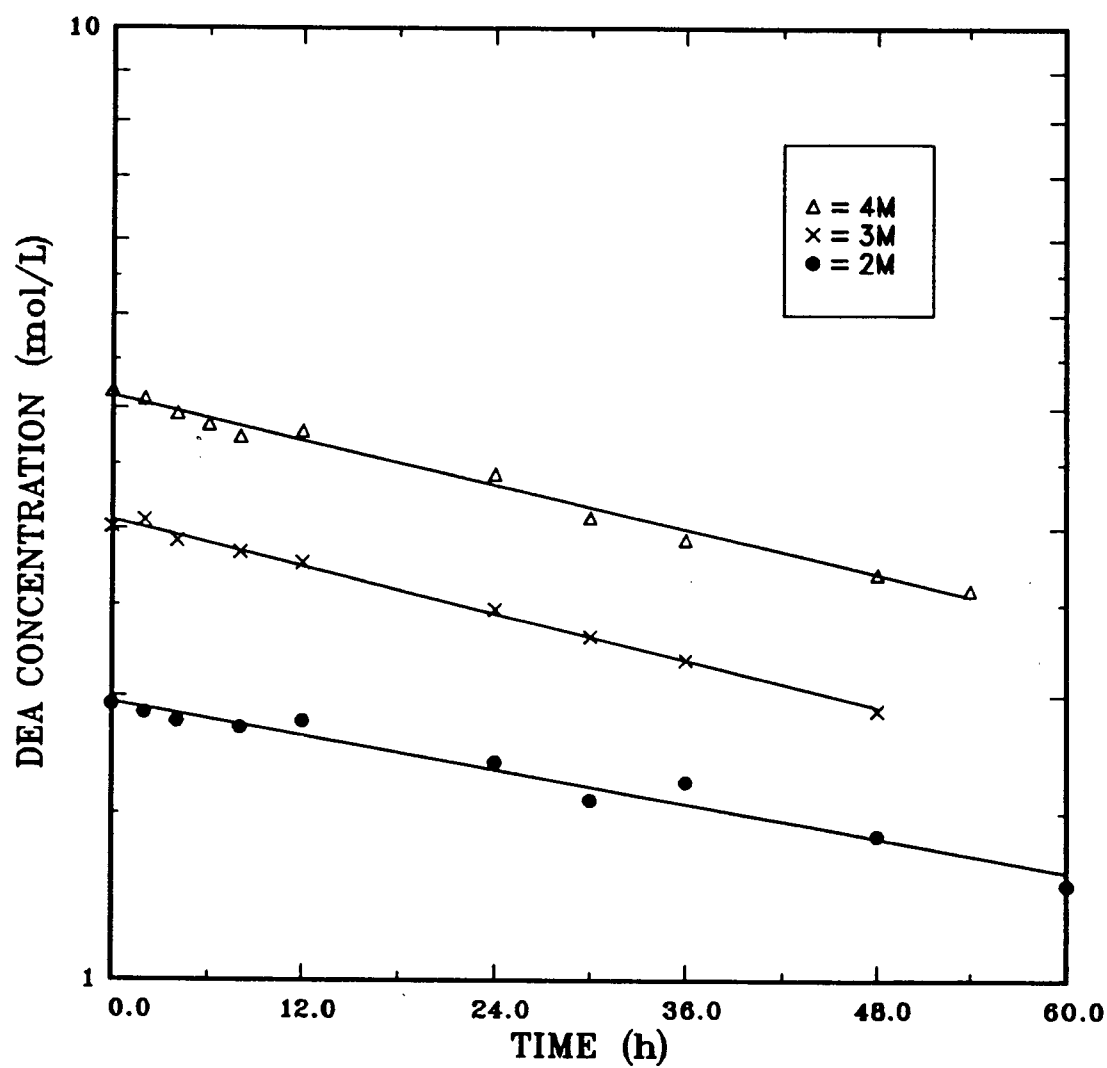


Figure 5.2: DEA concentration as a function of initial DEA concentration and time ($P_{\text{COS}} = 0.34$ MPa, $T = 150$ °C).

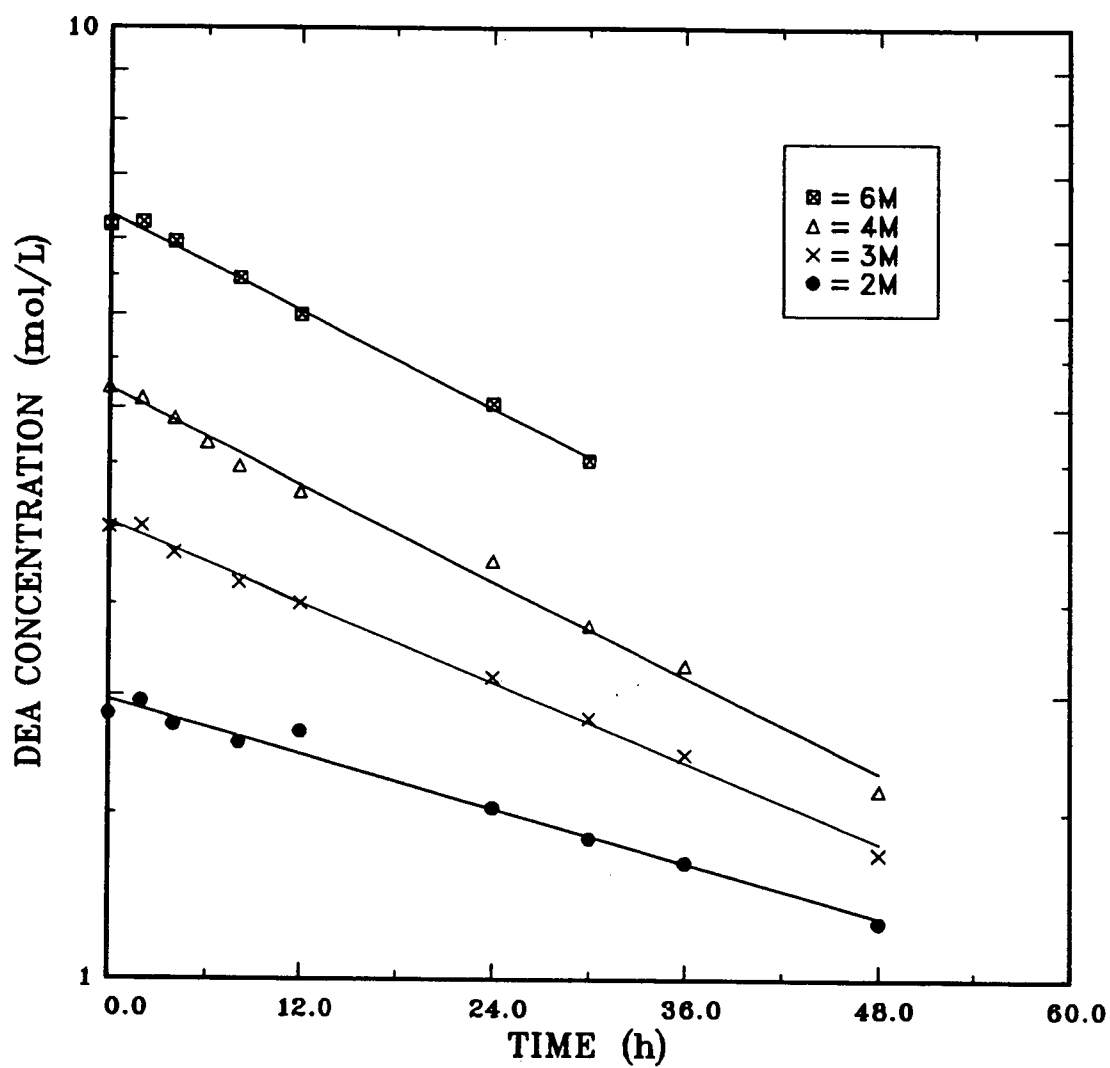


Figure 5.3: DEA concentration as a function of initial DEA concentration and time ($P_{\text{COS}} = 0.34 \text{ MPa}$, $T = 165 \text{ }^{\circ}\text{C}$).

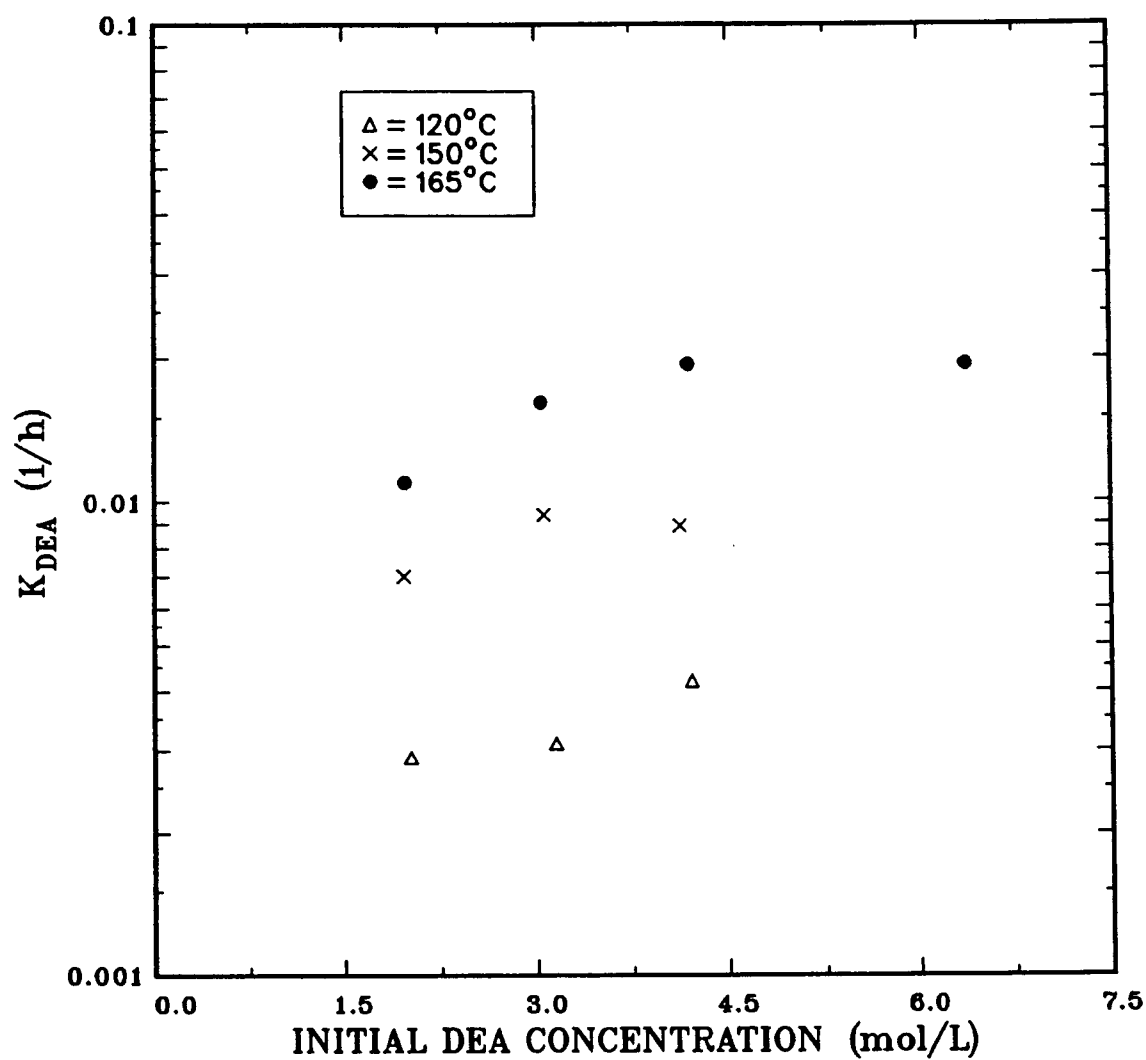


Figure 5.4: Overall degradation rate constant as a function of initial DEA concentration and temperature ($P_{\text{COS}} = 0.34 \text{ MPa}$).

The role of water on amine degradation is further addressed in chapter 6.

The initial rate of degradation ($-d[\text{DEA}]/dt$) may be plotted against the initial DEA concentration on a log-log scale. In accordance with Eq. 5.4, the slopes of such plots correspond to the order of reaction. A least squares fit of the plots in Fig. 5.5 produced slopes of approximately 1.4. This further confirms that the rate of degradation may be represented, in an appropriate manner, by a first order expression. The first order representation is only apparent since the rate constant is dependent on the initial DEA concentration.

Figure 5.6 shows that the rate of formation of acetone increases with initial DEA concentration. At each DEA concentration and within the durations of the experiments, the acetone concentration attains a maxima followed by a decline to an equilibrium value which appears to be independent of the initial DEA concentration. The presence of maxima suggests that acetone is an intermediate and undergoes further reaction.

The butanone concentration increases with initial DEA concentration and time (see Fig. 5.7). For DEA concentrations between 3 and 6M, the maximum or final butanone concentration is independent of the initial DEA concentration. At an initial concentration of 2M, butanone concentration is still on the rise throughout the duration of the experiment.

It should be noted that the reported acetone and butanone concentrations correspond to the liquid phase. Analysis of some gas samples indicated the presence of these compounds in significant

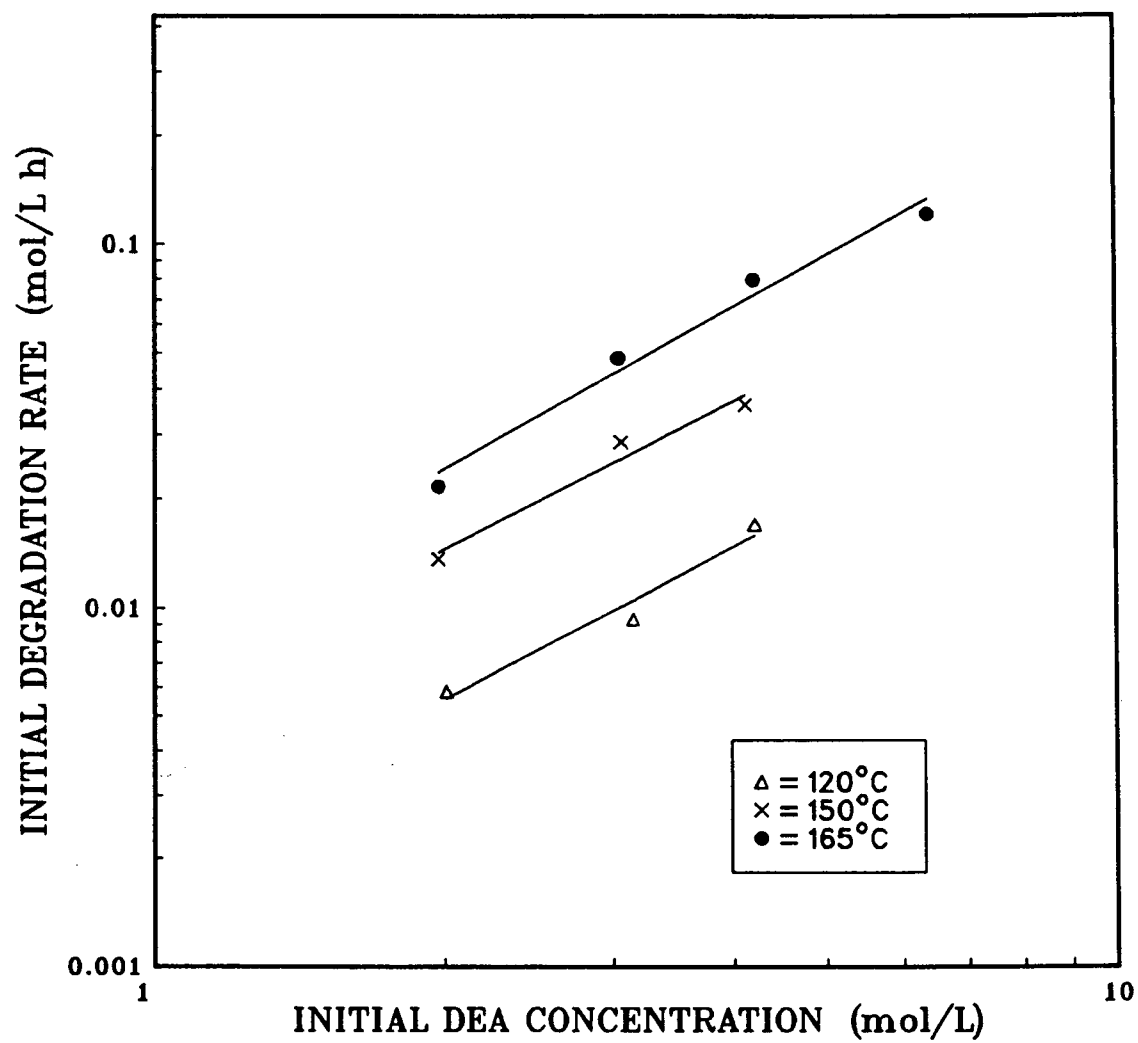


Figure 5.5: Initial degradation rate as a function of initial DEA concentration and temperature ($P_{\text{COS}} = 0.34$ MPa).

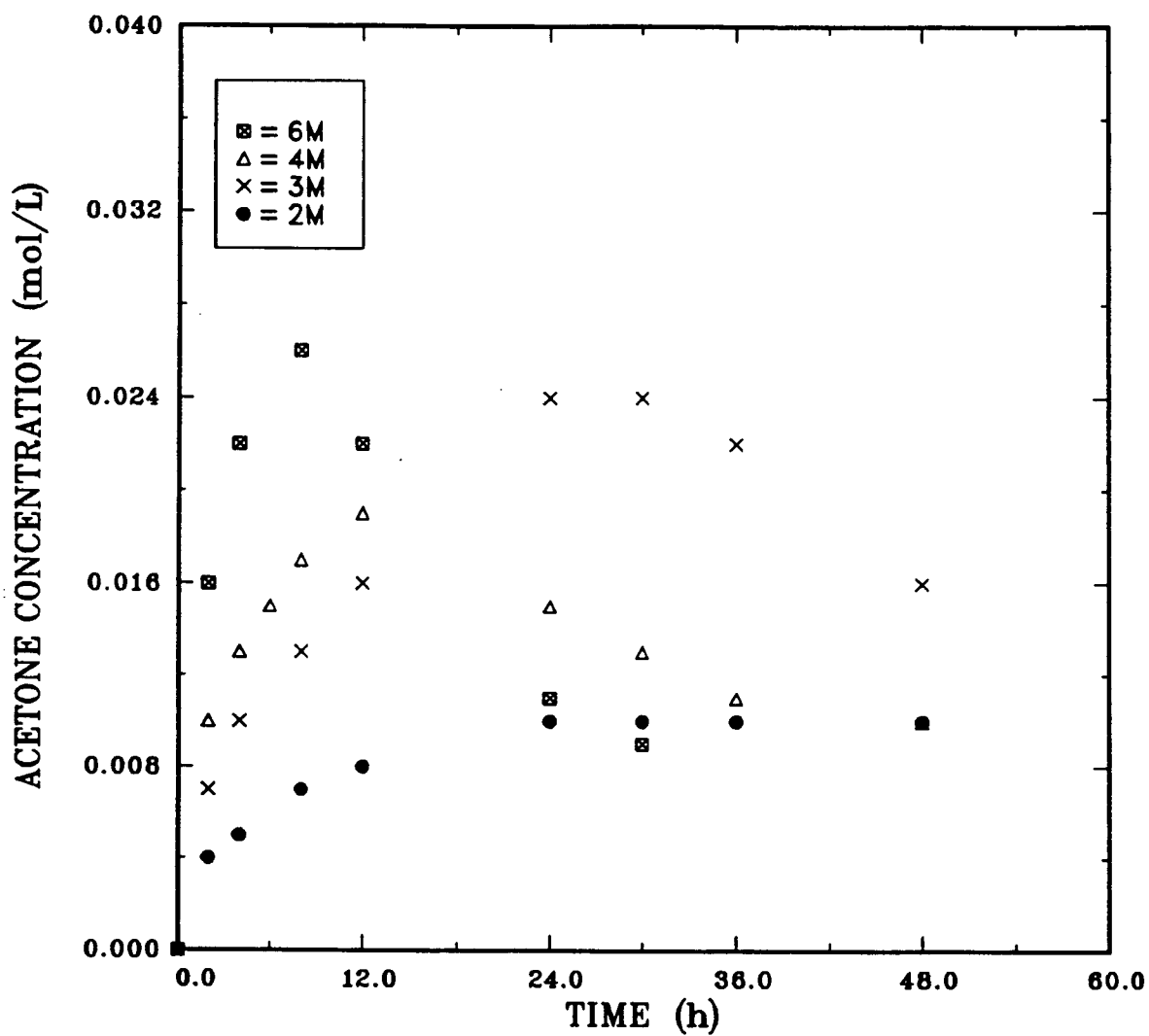


Figure 5.6: Acetone concentration as a function of initial DEA concentration and time ($P_{\text{COS}} = 0.34 \text{ MPa}$, $T = 165 \text{ }^{\circ}\text{C}$).

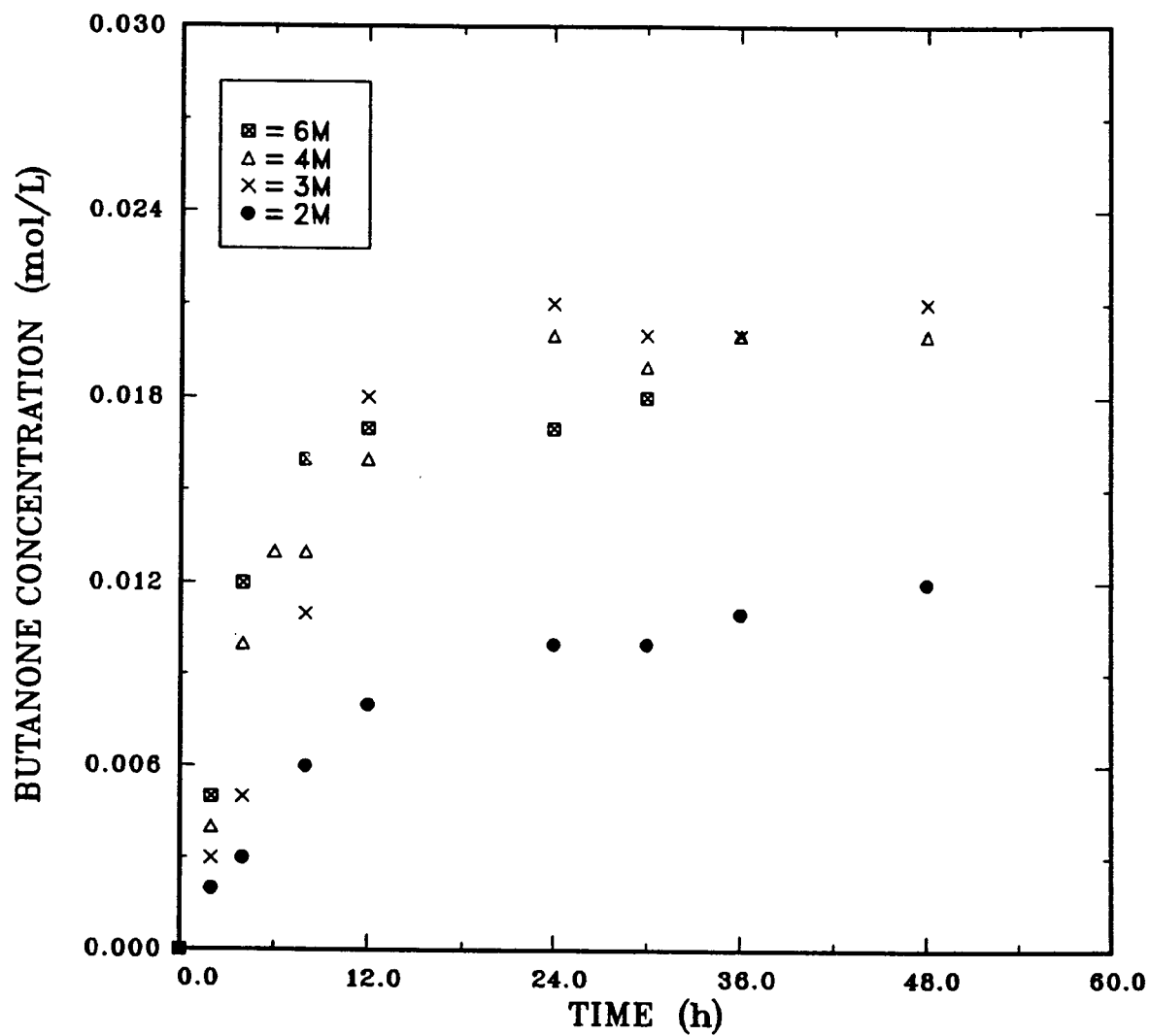


Figure 5.7: Butanone concentration as a function of initial DEA concentration and time ($P_{\text{COS}} = 0.34$ MPa, $T = 165$ °C).

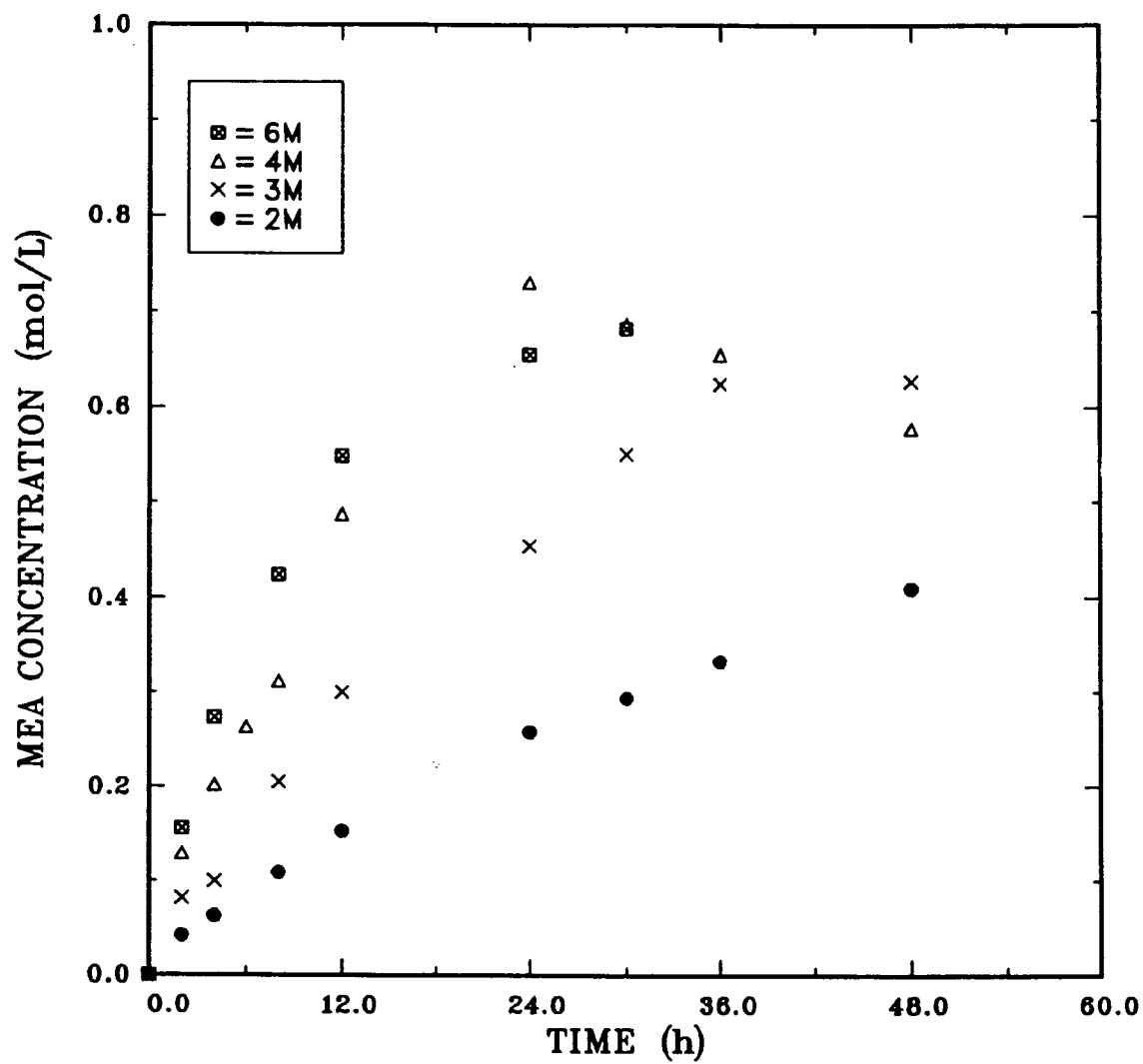


Figure 5.8: MEA concentration as a function of initial DEA concentration and time ($P_{\text{COS}} = 0.34$ MPa, $T = 165$ °C).

quantities in the gas-phase as well. However, it was not possible to determine their concentrations due to analytical difficulties arising from condensation within the gas sampling line and in the syringe during and after sample withdrawals, respectively. Hence, the total amounts of acetone and butanone produced are greater than the plots show.

As shown by Fig. 5.8, the initial rate of MEA production and maximum MEA concentration increase with initial DEA concentration. At later stages, the trend is reversed suggesting that the depletion of MEA is enhanced by increased DEA concentration. This may be due to the fact that the equilibrium solubility of the acid gases that induce degradation increase with DEA concentration. The presence of the maxima also implies that MEA is not a terminal product, but undergoes further reactions.

The concentration-time plots for high boiling compounds (BHEED, BHEP, HEOD, HEI, THEED, BHEI) are shown in Figs. 5.9 to 5.14, respectively. The concentrations of these compounds were found to increase with initial DEA concentration. It has been reported (16) that HEOD is formed from DEA carbamate (DEACOO^-), the concentration of the latter being largely dictated by the equilibrium solubility of CO_2 . Therefore, the HEOD concentration should increase with DEA concentration as shown in Fig. 5.11, since the equilibrium solubility of CO_2 increases with DEA concentration. The presence of HEOD in the degraded solution is an indication of COS hydrolysis. The fact that HEOD concentration increased throughout the duration of the runs suggests that the equilibrium between $\text{DEACOO}^- \text{H}^+$ and HEOD takes longer to be established in the COS-DEA system than in the CO_2 -DEA system. This may be due to

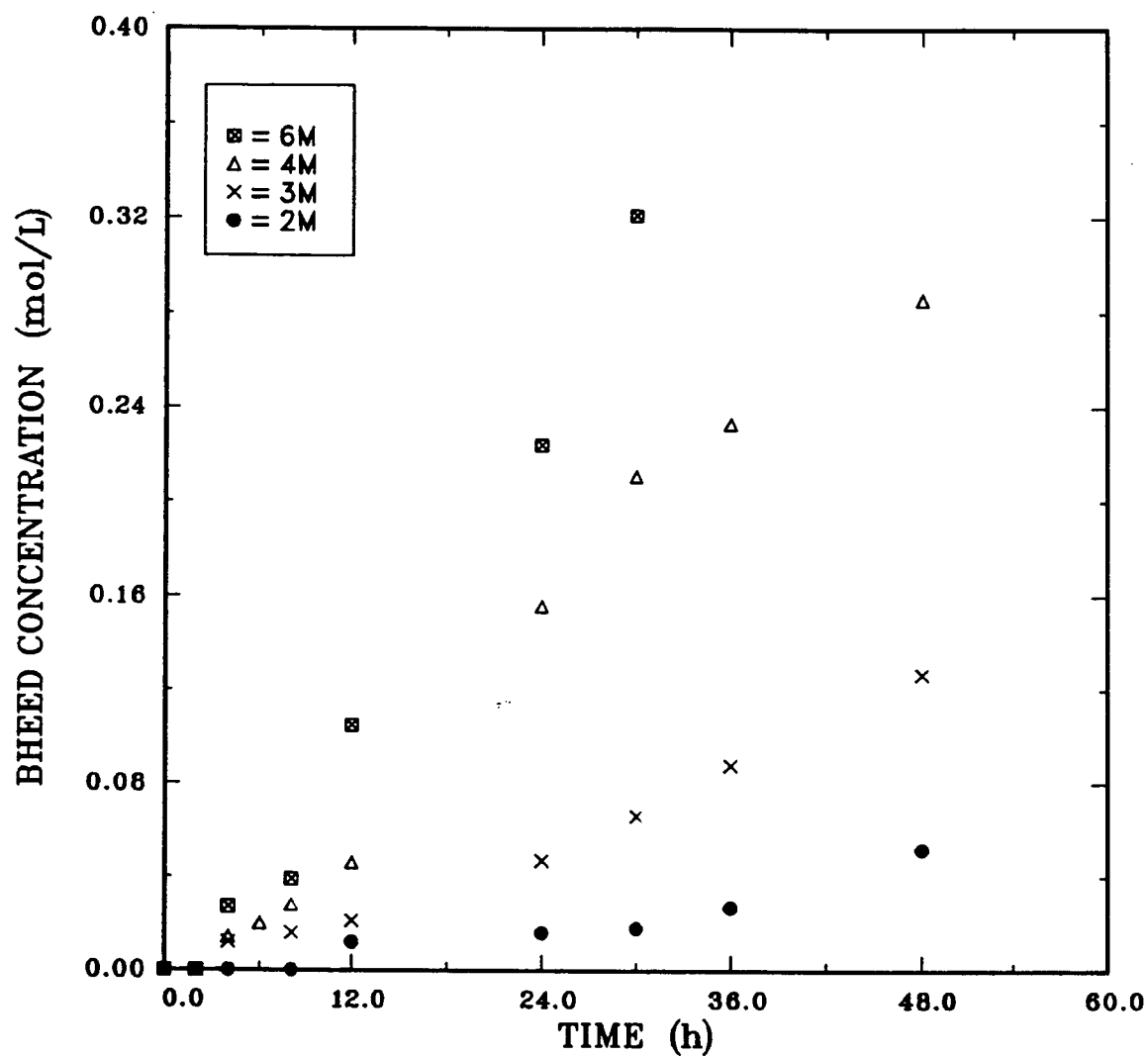


Figure 5.9: BHEED concentration as a function of initial DEA concentration and time ($P_{\text{COS}} = 0.34$ MPa, $T = 165$ °C).

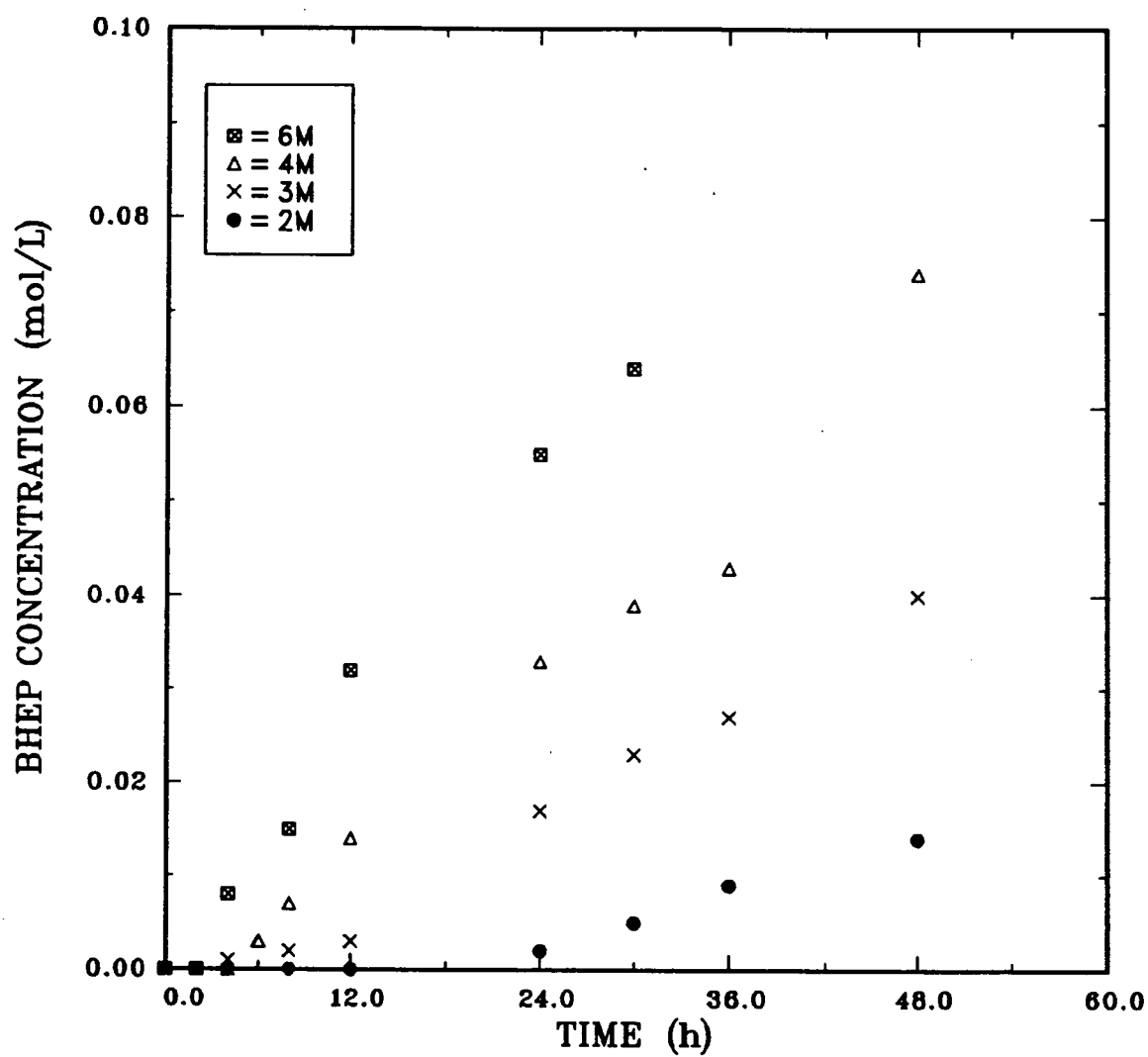


Figure 5.10: BHEP concentration as a function of initial DEA concentration and time ($P_{\text{COS}} = 0.34 \text{ MPa}$, $T = 165 \text{ }^{\circ}\text{C}$).

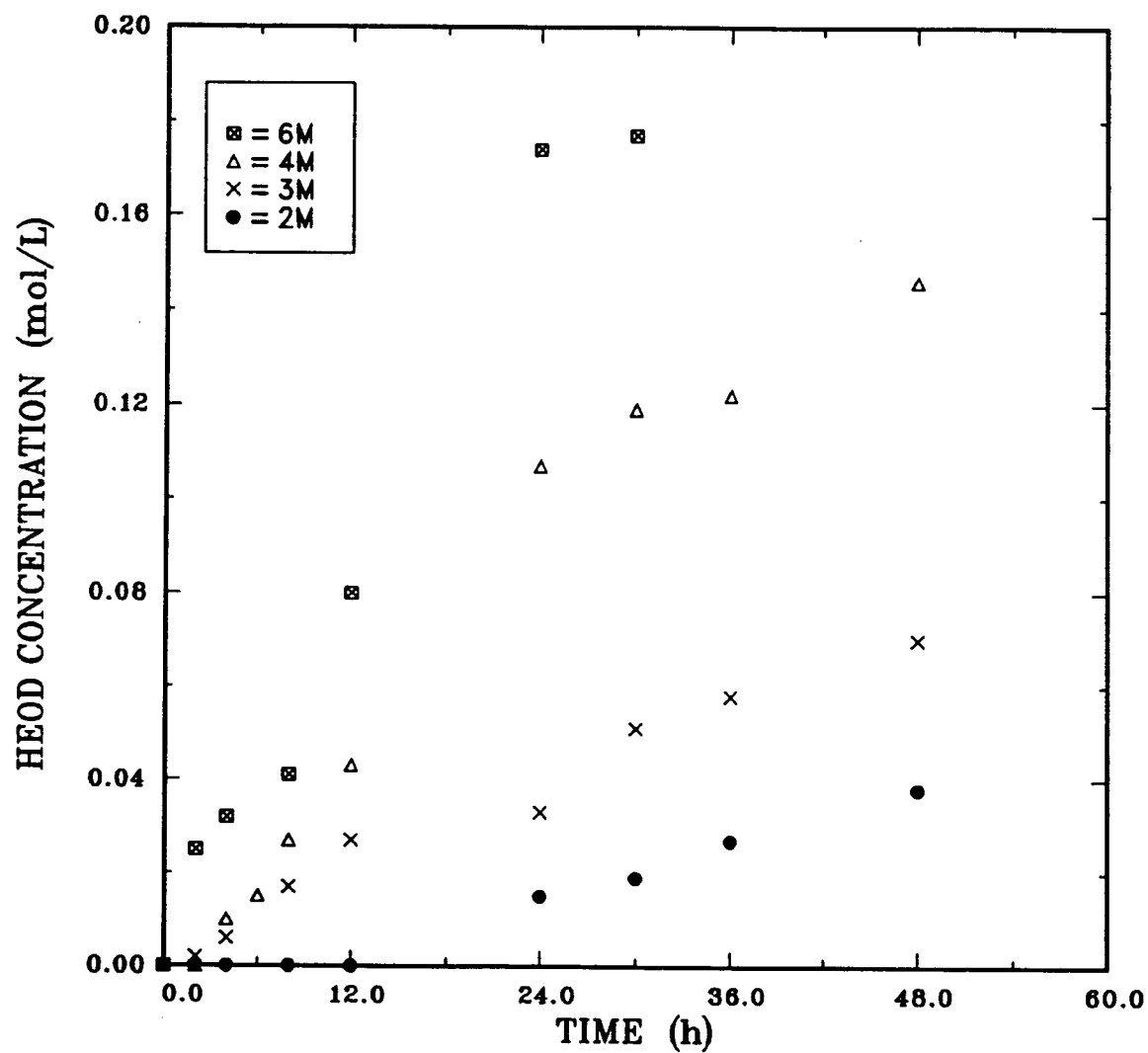


Figure 5.11: HEOD concentration as a function of initial DEA concentration and time ($P_{\text{COS}} = 0.34 \text{ MPa}$, $T = 165 \text{ }^{\circ}\text{C}$).

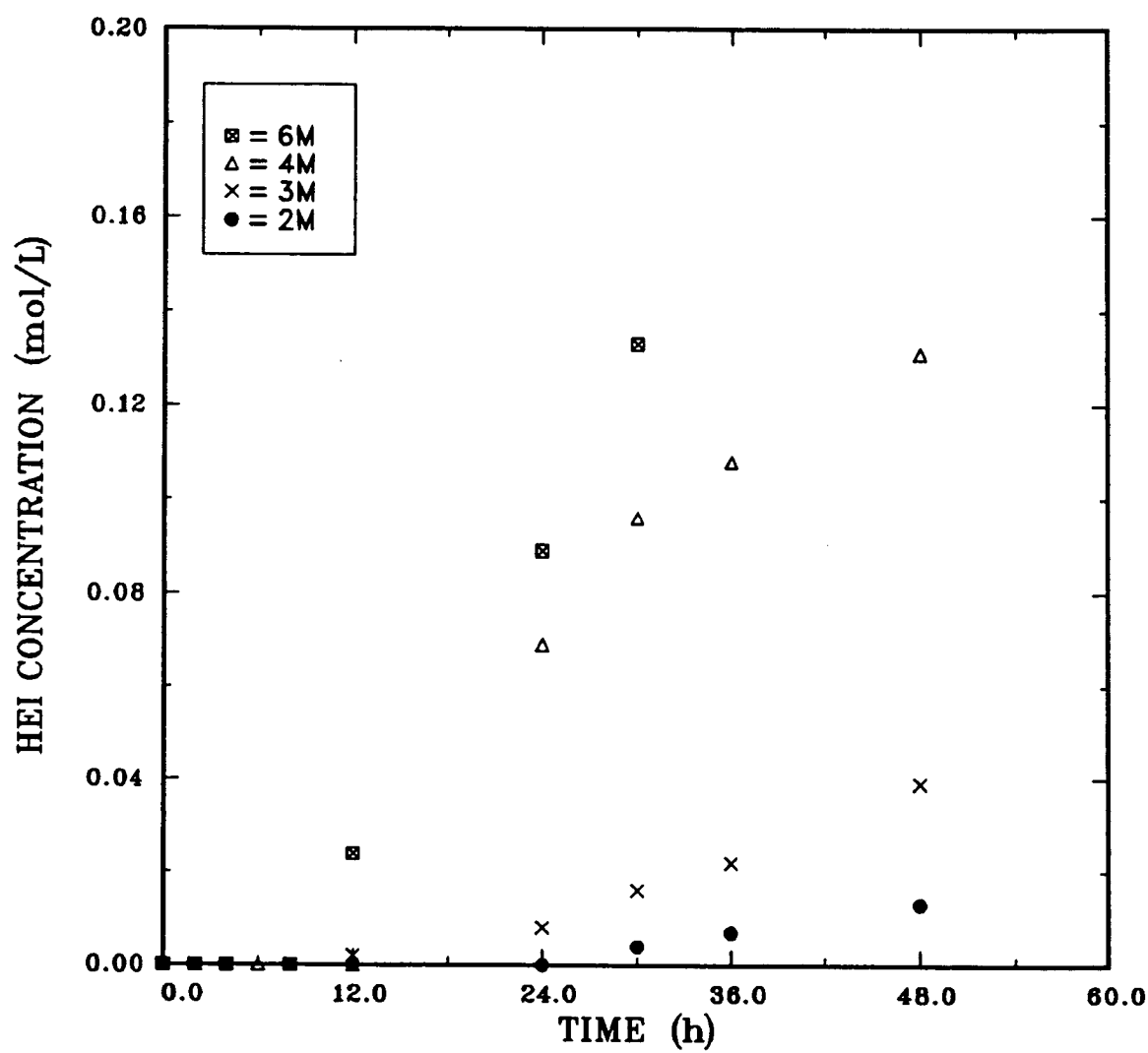


Figure 5.12: HEI concentration as a function of initial DEA concentration and time ($P_{\text{COS}} = 0.34 \text{ MPa}$, $T = 165 \text{ }^{\circ}\text{C}$).

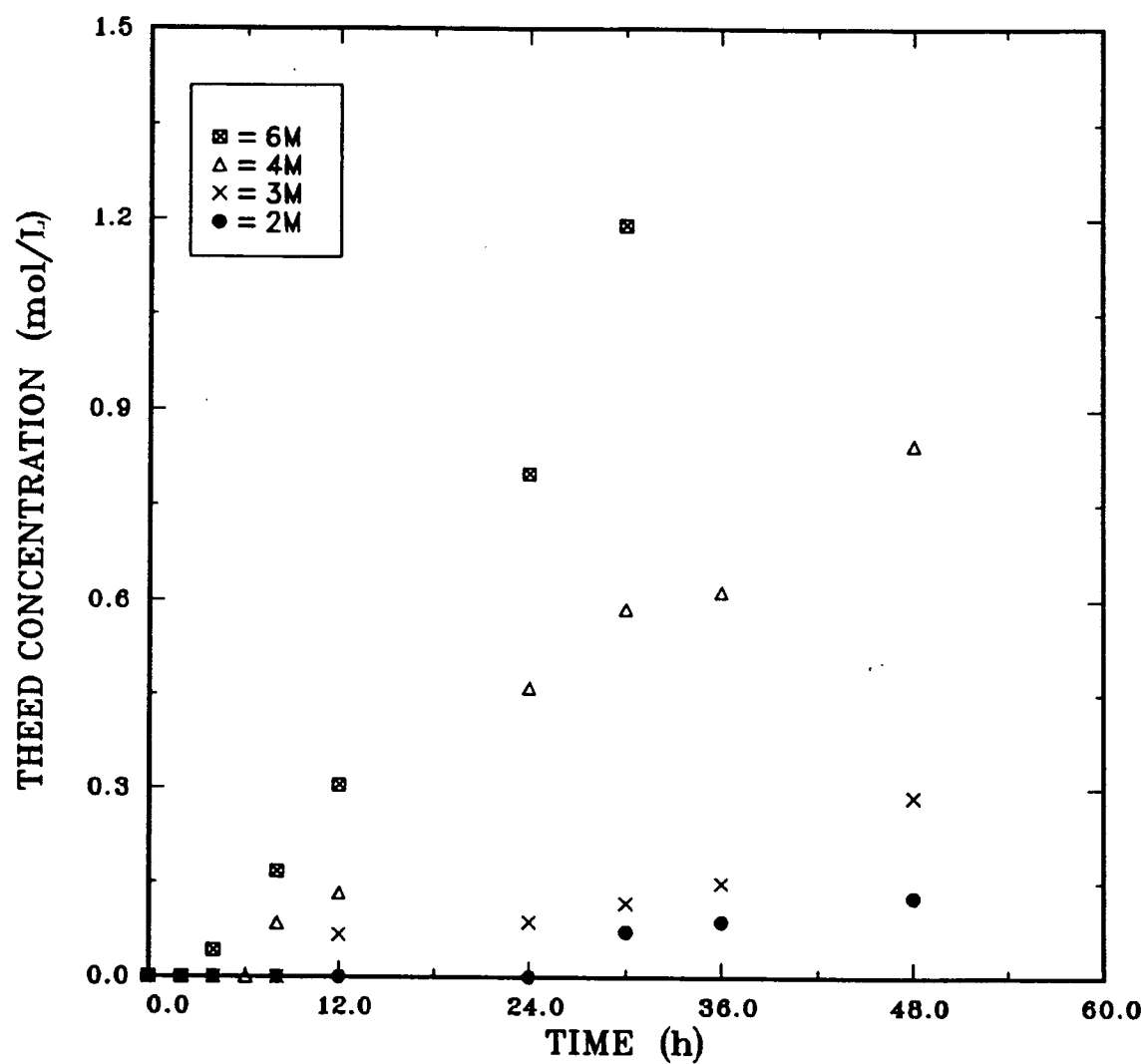


Figure 5.13: THEED concentration as a function of initial DEA concentration and time ($P_{\text{COS}} = 0.34 \text{ MPa}$, $T = 165 \text{ }^{\circ}\text{C}$).

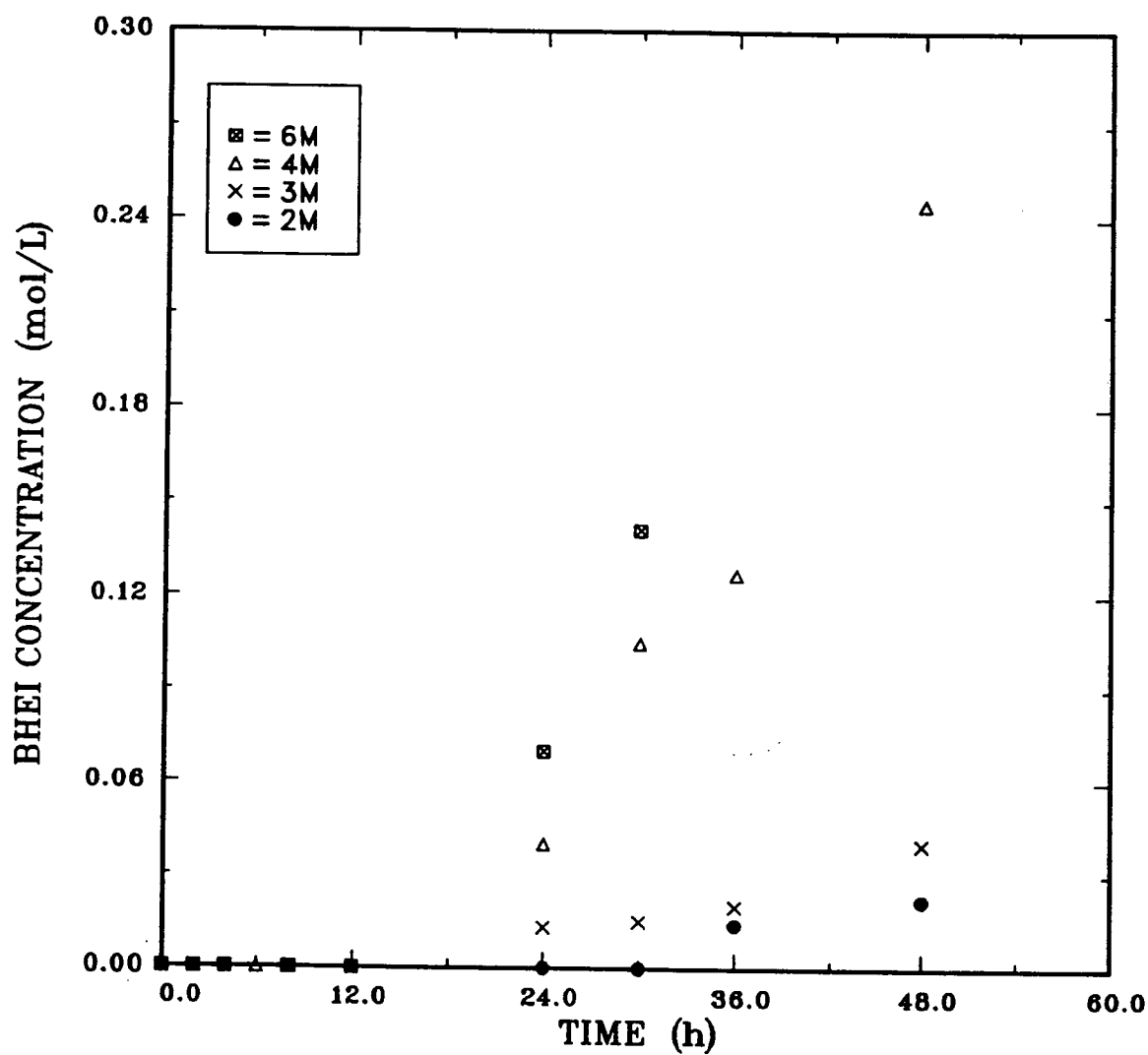


Figure 5.14: BHEI concentration as a function of initial DEA concentration and time ($P_{\text{COS}} = 0.34$ MPa, $T = 165$ °C).

the differences in the rate of degradation in both systems or due to the lower partial pressures of COS which were typically 10% of the partial pressures of CO_2 used in the CO_2 -DEA systems (14). The lack of maxima in the HEOD concentration profile also supports the conclusion by Kennard and Meisen (14) that HEOD is a final product and not an intermediate as suggested by Kim and Sartori (13).

It is pertinent to point out that for true first order reactions, the rate constant is independent of the initial concentration of reactants. The dependency of k_{DEA} on the initial DEA concentration observed in the present study can be explained in terms of the analytical procedure employed as well as solution composition. At constant COS partial pressure and temperature, the equilibrium solubility of COS and the ratio of free amine to ionised amine are functions of the initial amine concentration. For different initial DEA concentrations, this ratio is not necessarily the same as the ratio of the initial DEA concentrations. At the high temperatures used, the free amine concentration exceeds the concentration of the amine in the protonated carbamate or thiocarbamate forms. Since degradation is induced by ionic species, especially the carbamates, the DEA concentration in Eqs. 5.1 - 5.3 should be the ionic concentration. However, the GC analysis provides only the total DEA concentration as it cannot distinguish between the various forms of DEA in solution. Thus, when the equations are written in terms of total DEA concentration, the dependency of k_{DEA} on the initial DEA concentration is inevitable.

5.1.2 EFFECTS OF TEMPERATURE

Figures 5.15 to 5.17 show the DEA concentrations as a function of time for various temperatures and initial DEA concentrations of 40 wt%, 30 wt% and 20 wt% (approx. 4, 3 and 2M), respectively. The rates of degradation increase with temperature. As shown by Fig. 5.18, the degradation rate constants, k_{DEA} obey the Arrhenius expression and thus confirm the notion of first order reaction kinetics.

The rate of production and final concentration of butanone increase with temperature (Fig. 5.19). The levelling off observed in butanone concentrations suggest that the compound may be a terminal product or the reaction by which it is produced, attains equilibrium.

As shown by Fig. 5.20 and 5.21 respectively, the rates of production and depletion of acetone and MEA increase with temperature. Hence their final concentrations are inversely related to temperature. At 150 °C, the plots do not show maxima because the rates of depletion are much lower than the rates of production.

The rate of production of BHEED increases with temperature and the high temperature plots in Fig. 5.22 show maxima. BHEED may therefore be regarded as an intermediate product, reacting further to form other compounds. The rates of such reactions appear to be very low at temperatures below 165 °C. This explains the absence of maxima at such temperatures for the durations of the experiments.

Rates of production and final concentrations of BHEP increase with temperature as shown by Fig. 5.23. BHEP thus behaves as a terminal product as previously reported (13,14).

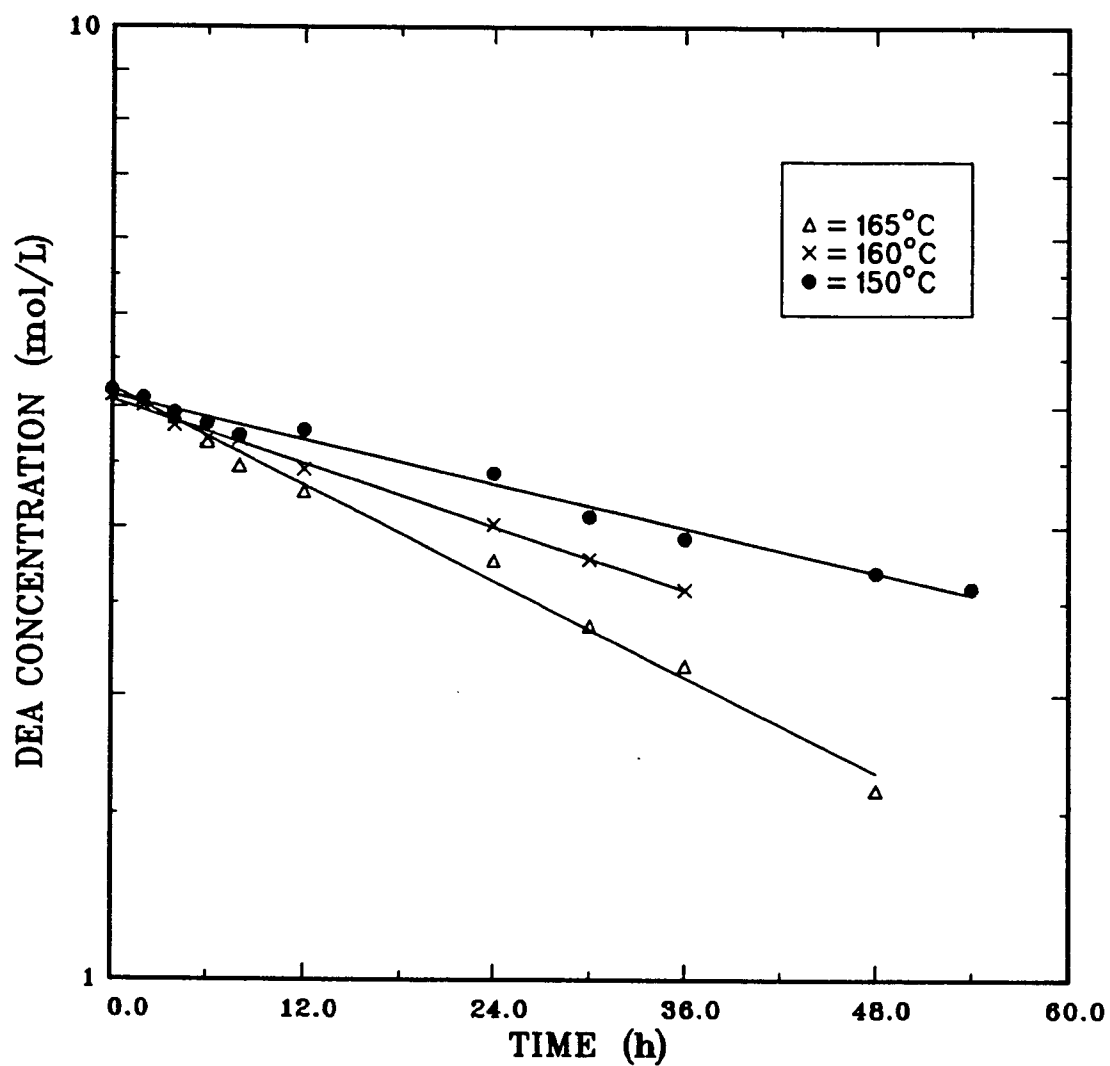


Figure 5.15: DEA concentration as a function temperature and time
($P_{\text{COS}} = 0.34 \text{ MPa}$, $\text{DEA}_0 = 4\text{M}$).

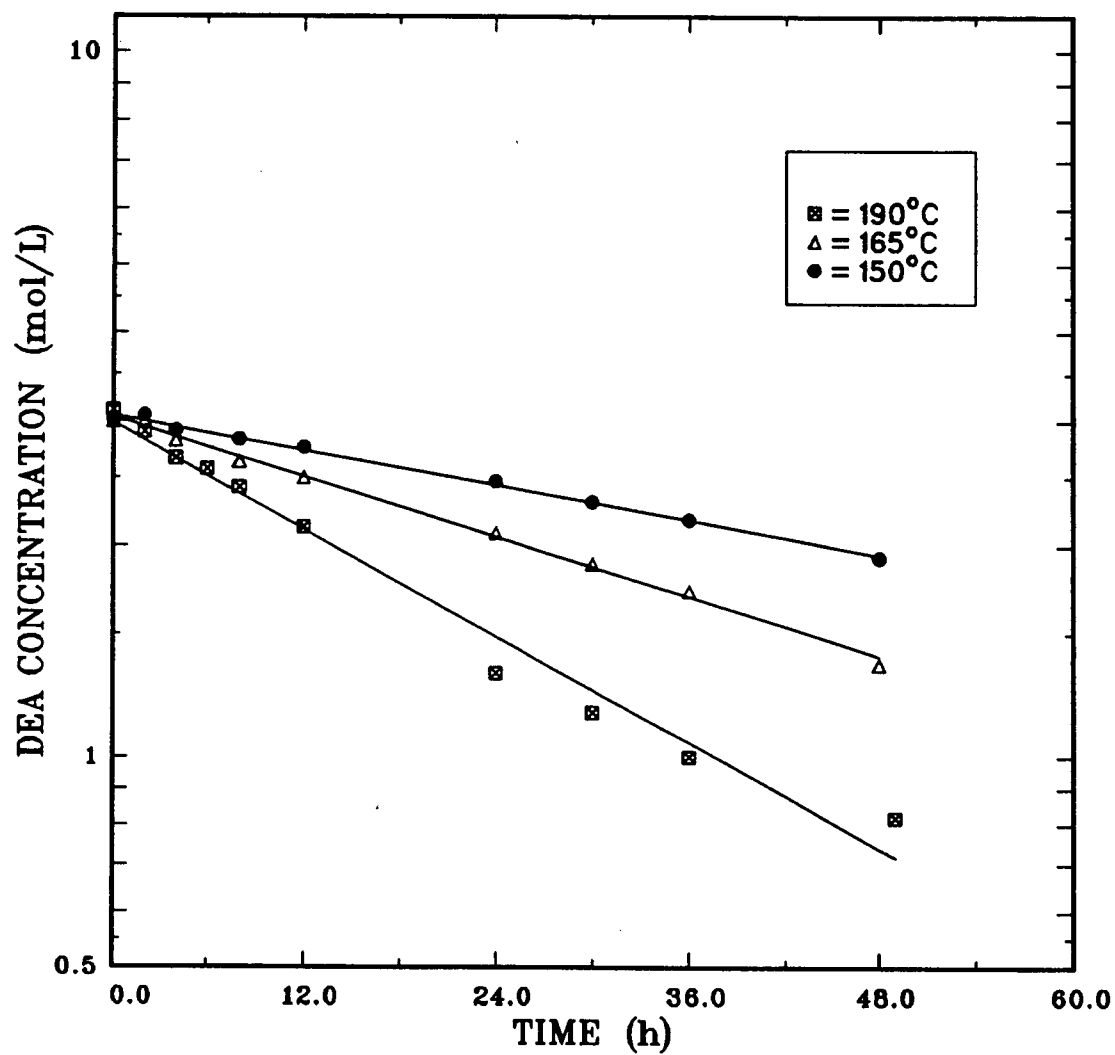


Figure 5.16: DEA concentration as a function temperature and time
($P_{\text{COS}} = 0.34 \text{ MPa}$, $\text{DEA}_0 = 3\text{M}$).

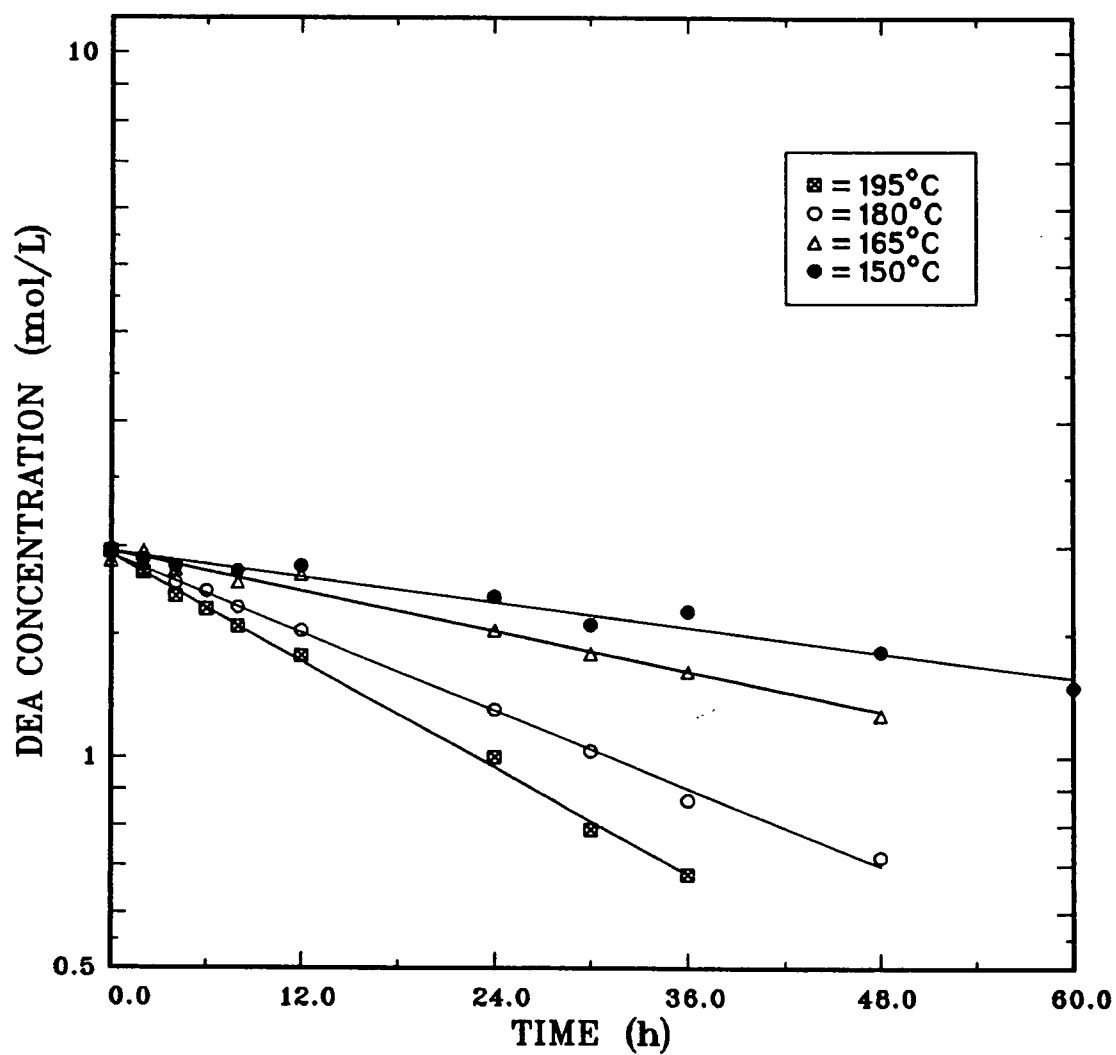


Figure 5.17: DEA concentration as a function temperature and time
 ($P_{\text{COS}} = 0.34 \text{ MPa}$, $\text{DEA}_0 = 2\text{M}$).

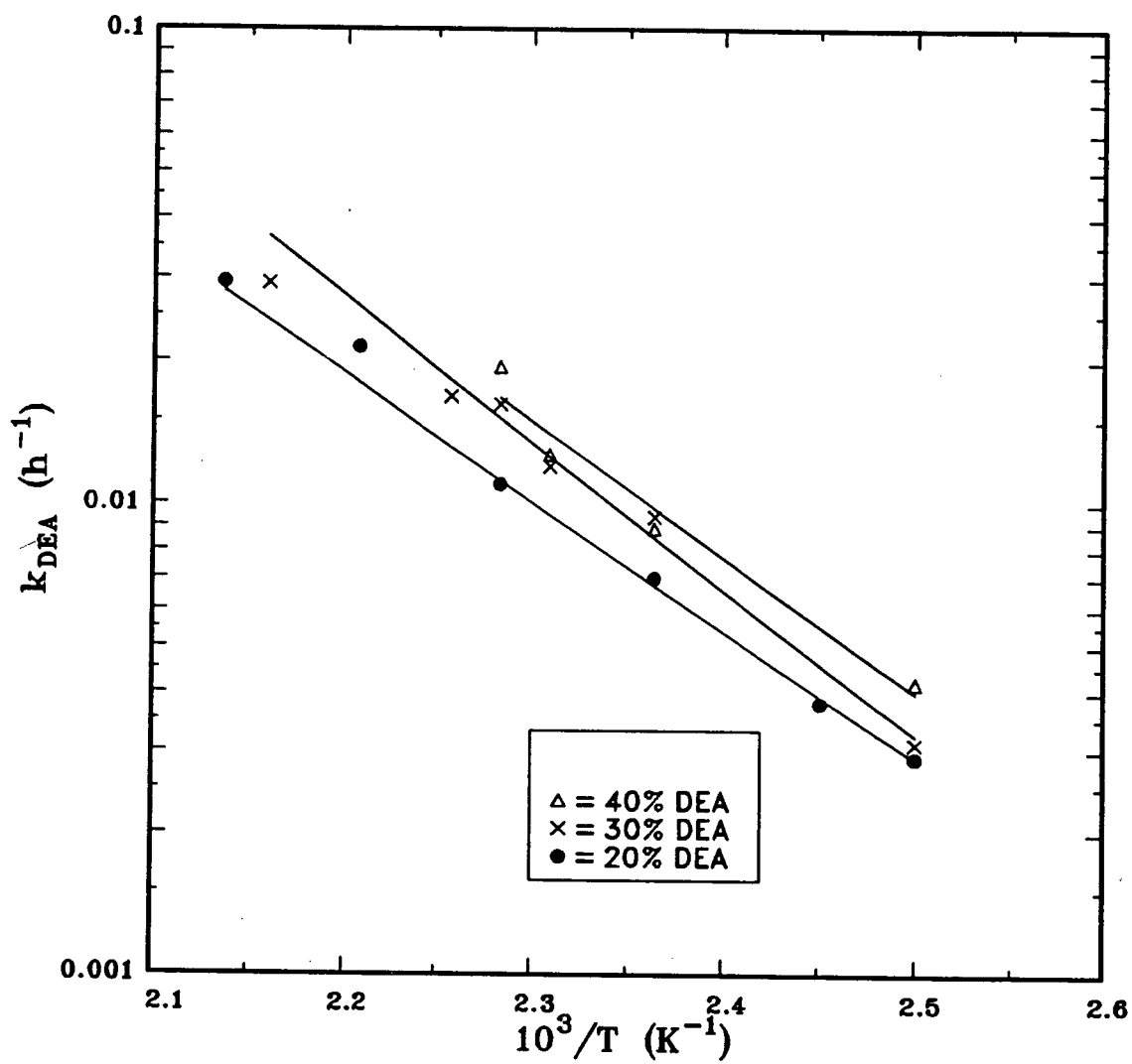


Figure 5.18: Arrhenius plots of the overall degradation rate constant ($P_{\text{COS}} = 0.34$ MPa).

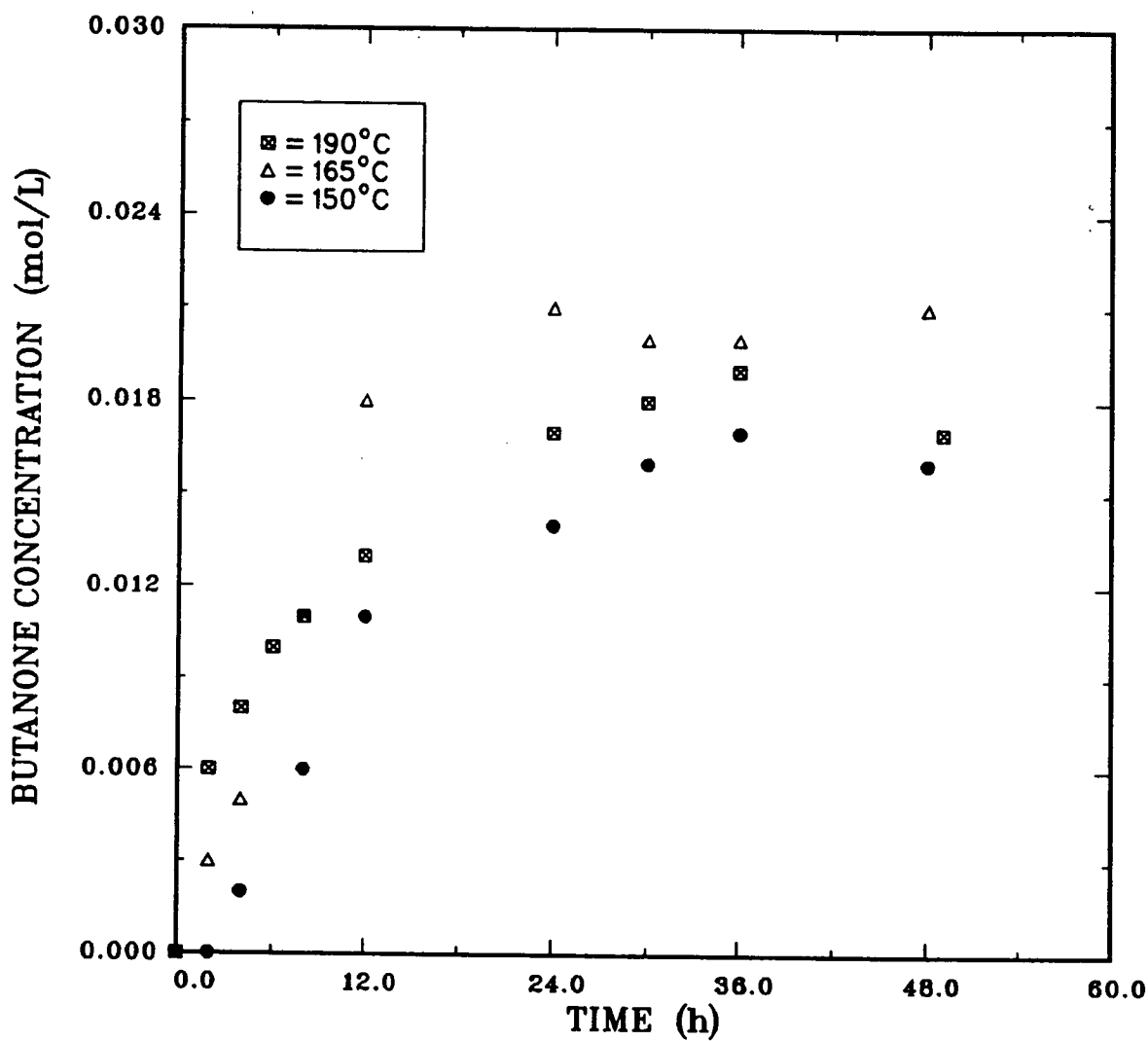


Figure 5.19: Butanone concentration as a function temperature and time ($P_{\text{COS}} = 0.34 \text{ MPa}$, $\text{DEA}_0 = 3\text{M}$).

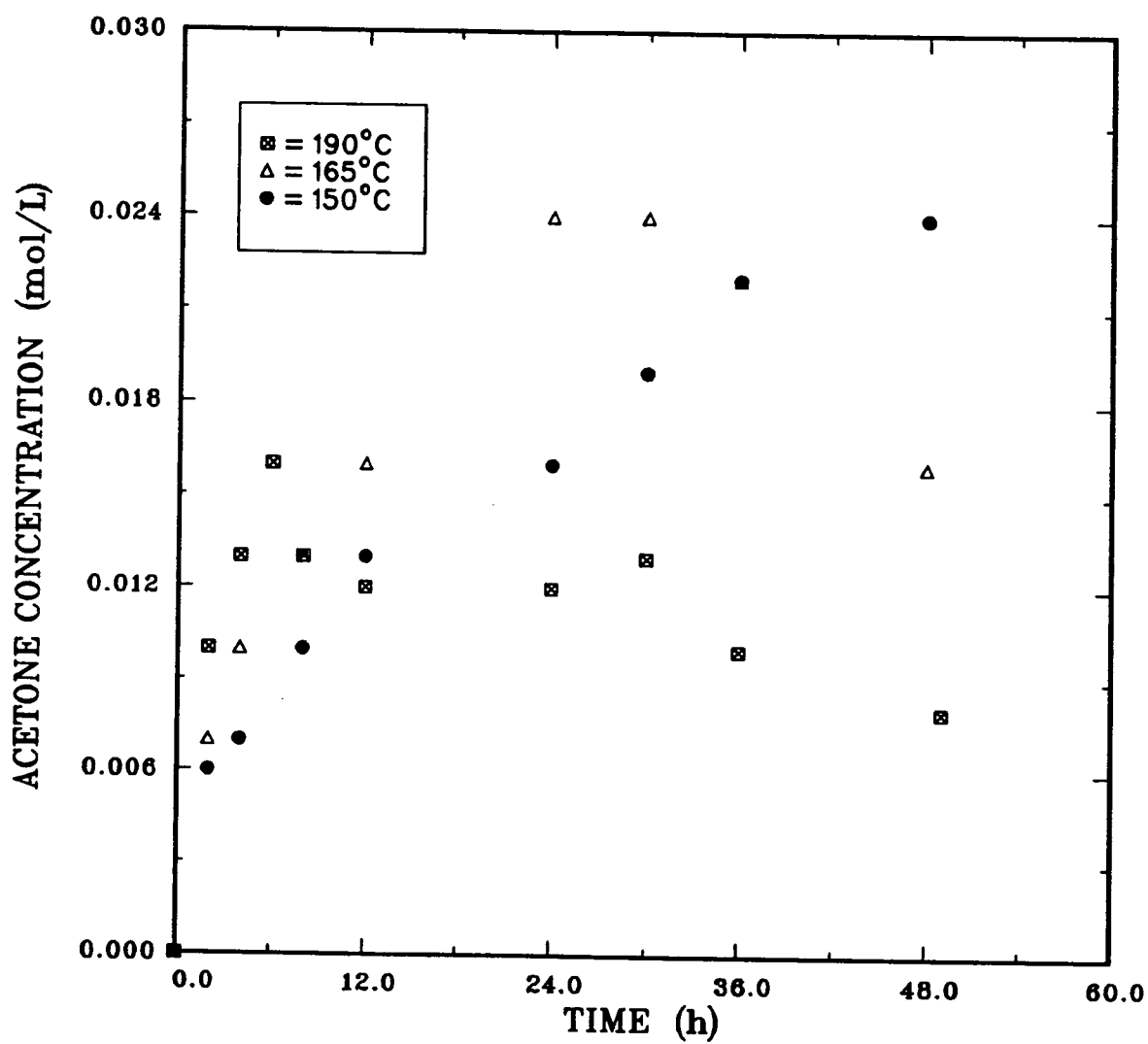


Figure 5.20: Acetone concentration as a function temperature and time ($P_{\text{COS}} = 0.34$ MPa, $\text{DEA}_0 = 3\text{M}$).

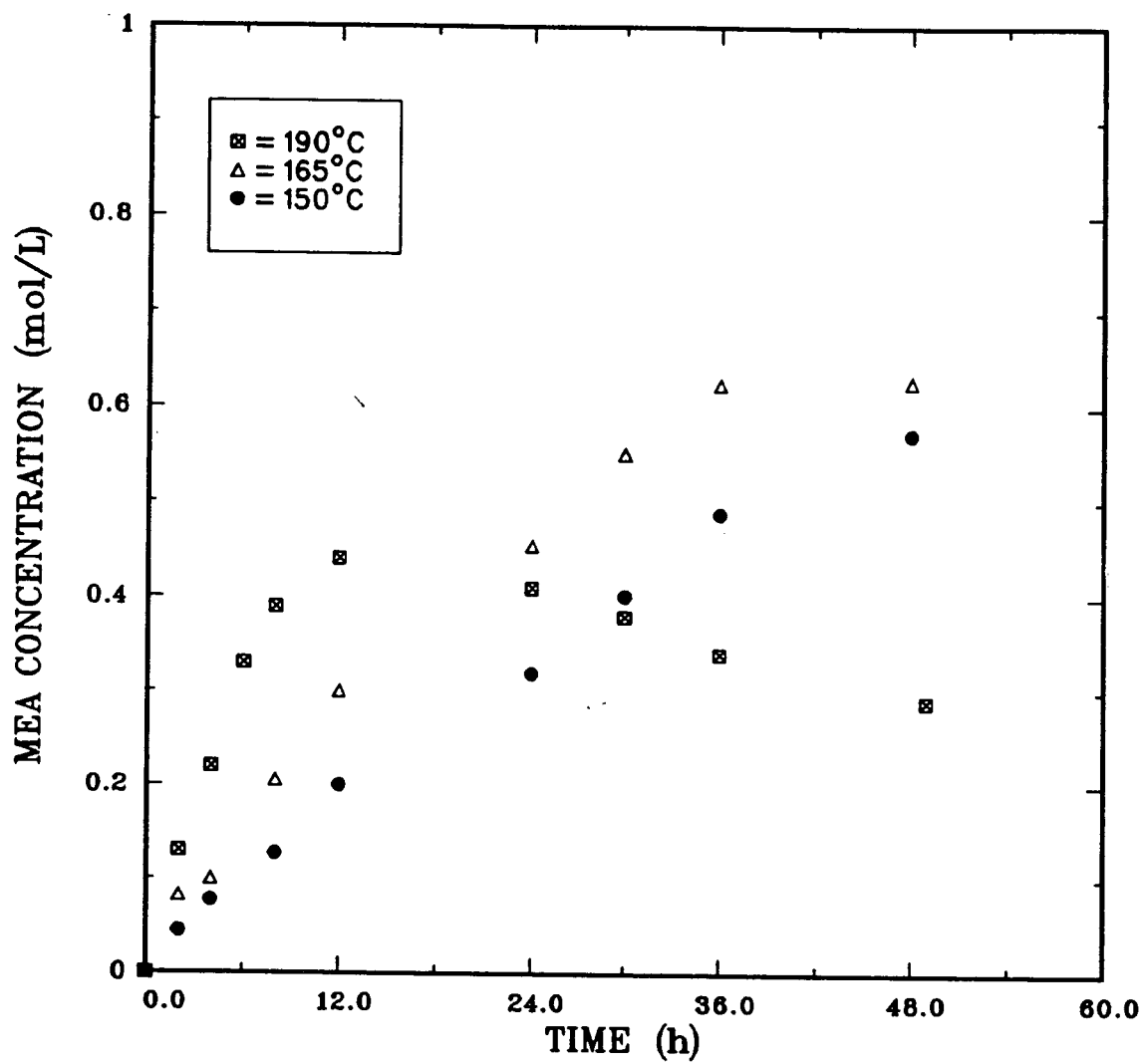


Figure 5.21: MEA concentration as a function temperature and time
($P_{\text{COS}} = 0.34$ MPa, $\text{DEA}_0 = 3\text{M}$).

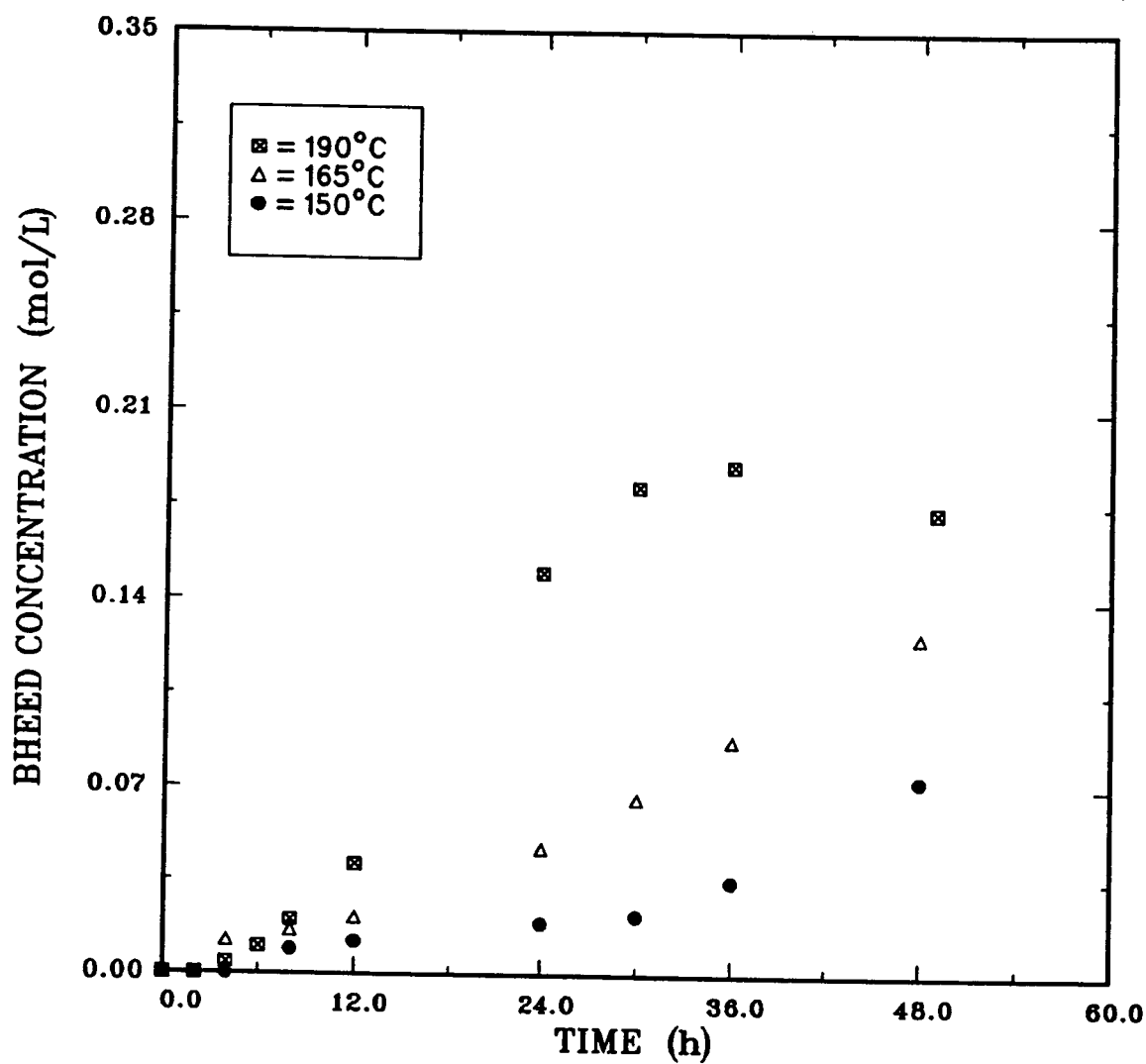


Figure 5.22: BHEED concentration as a function temperature and time ($P_{\text{COS}} = 0.34 \text{ MPa}$, $\text{DEA}_0 = 3\text{M}$).

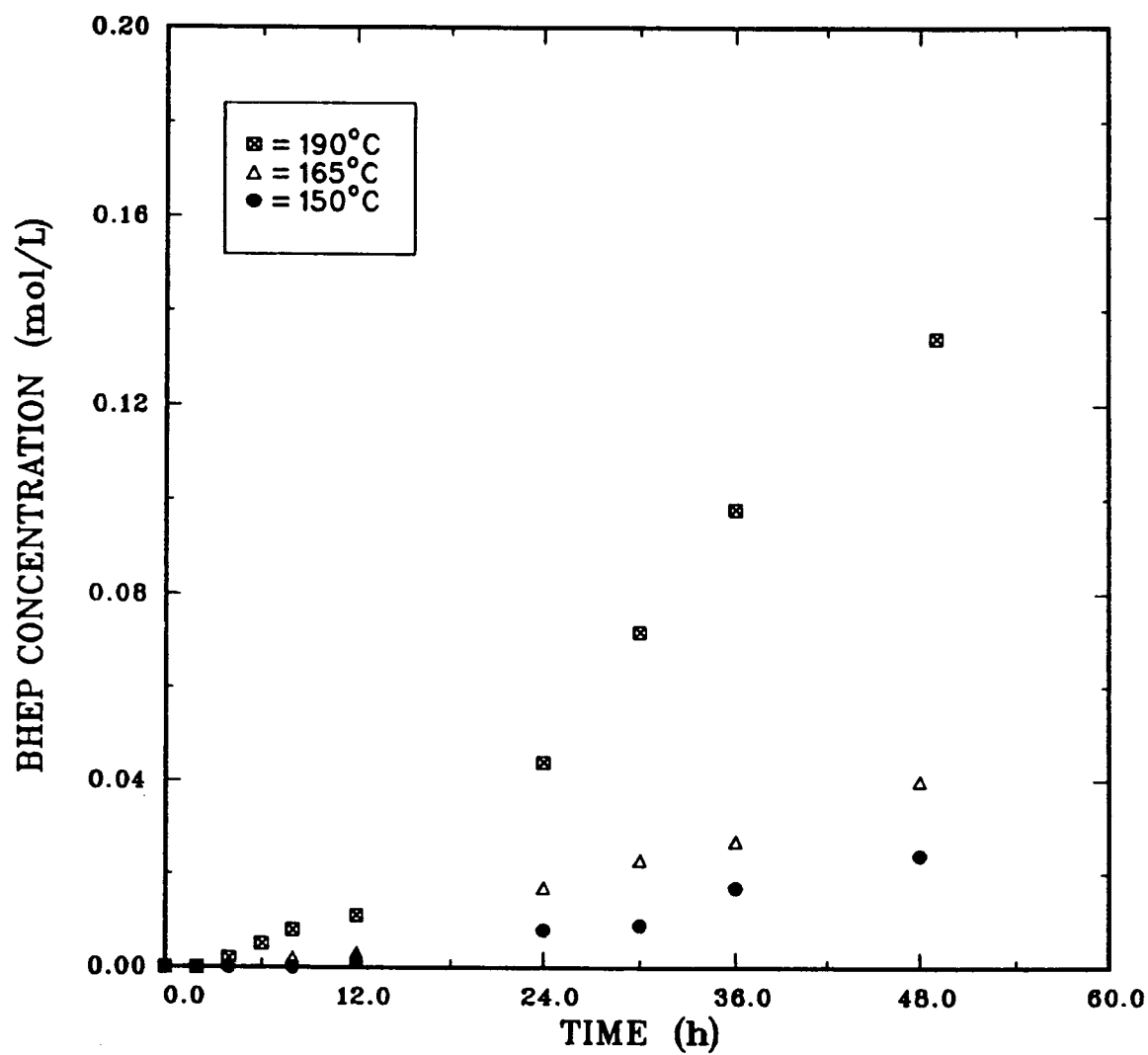


Figure 5.23: BHEP concentration as a function temperature and time
($P_{\text{COS}} = 0.34 \text{ MPa}$, $\text{DEA}_0 = 3\text{M}$).

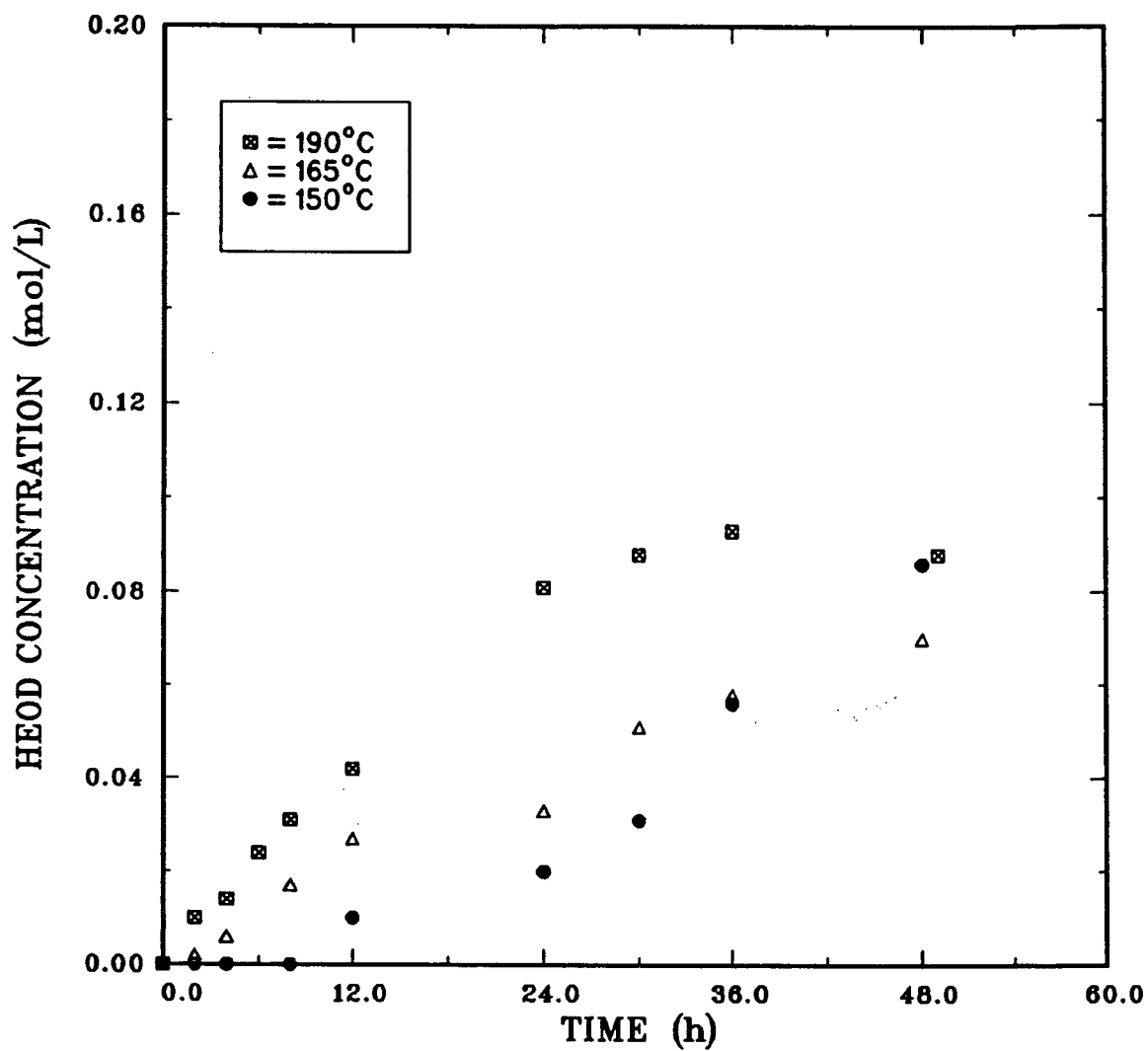


Figure 5.24: HEOD concentration as a function temperature and time
($P_{\text{COS}} = 0.34 \text{ MPa}$, $\text{DEA}_0 = 3\text{M}$).

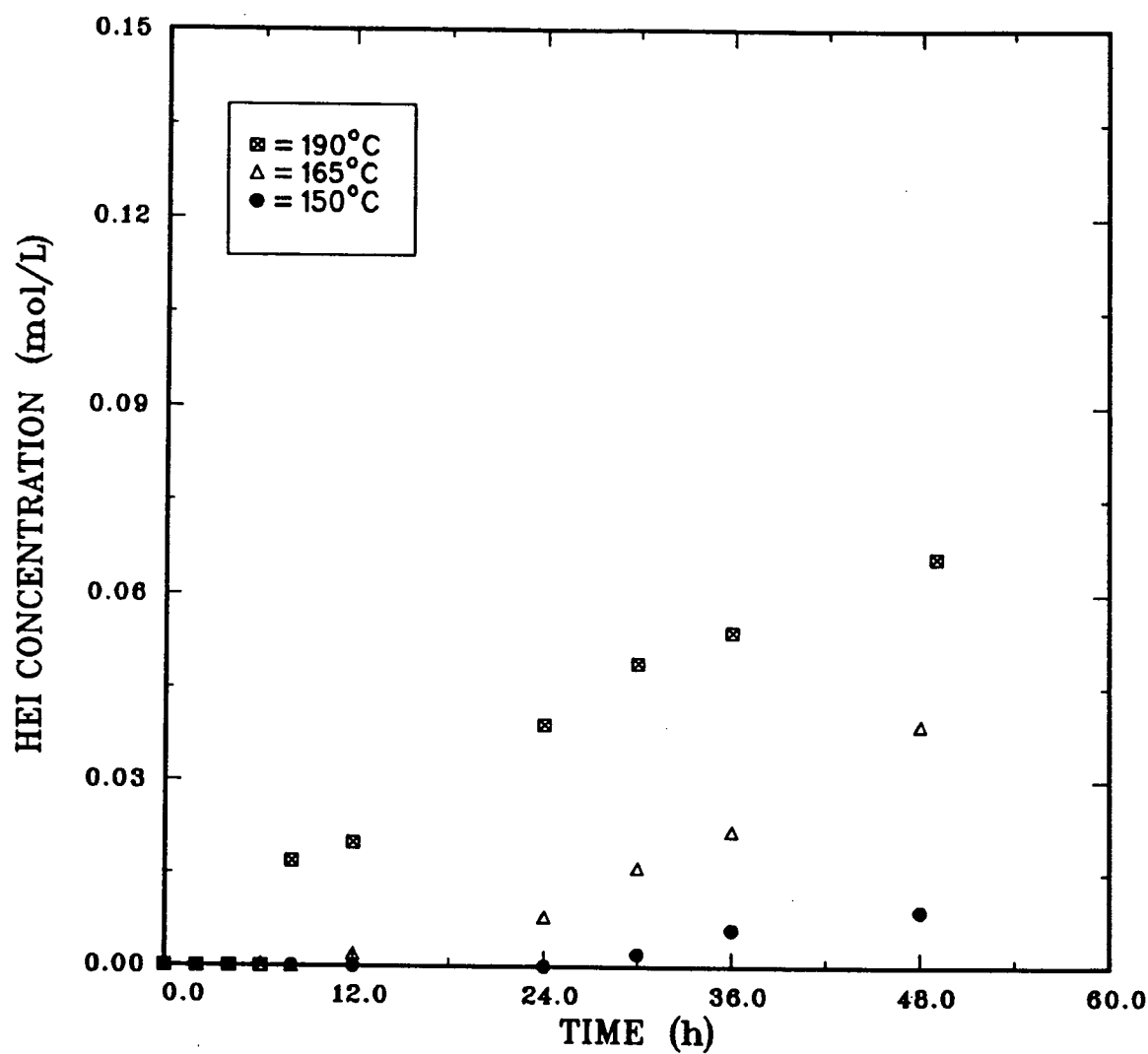


Figure 5.25: HEI concentration as a function temperature and time
($P_{\text{COS}} = 0.34 \text{ MPa}$, $\text{DEA}_0 = 3\text{M}$).

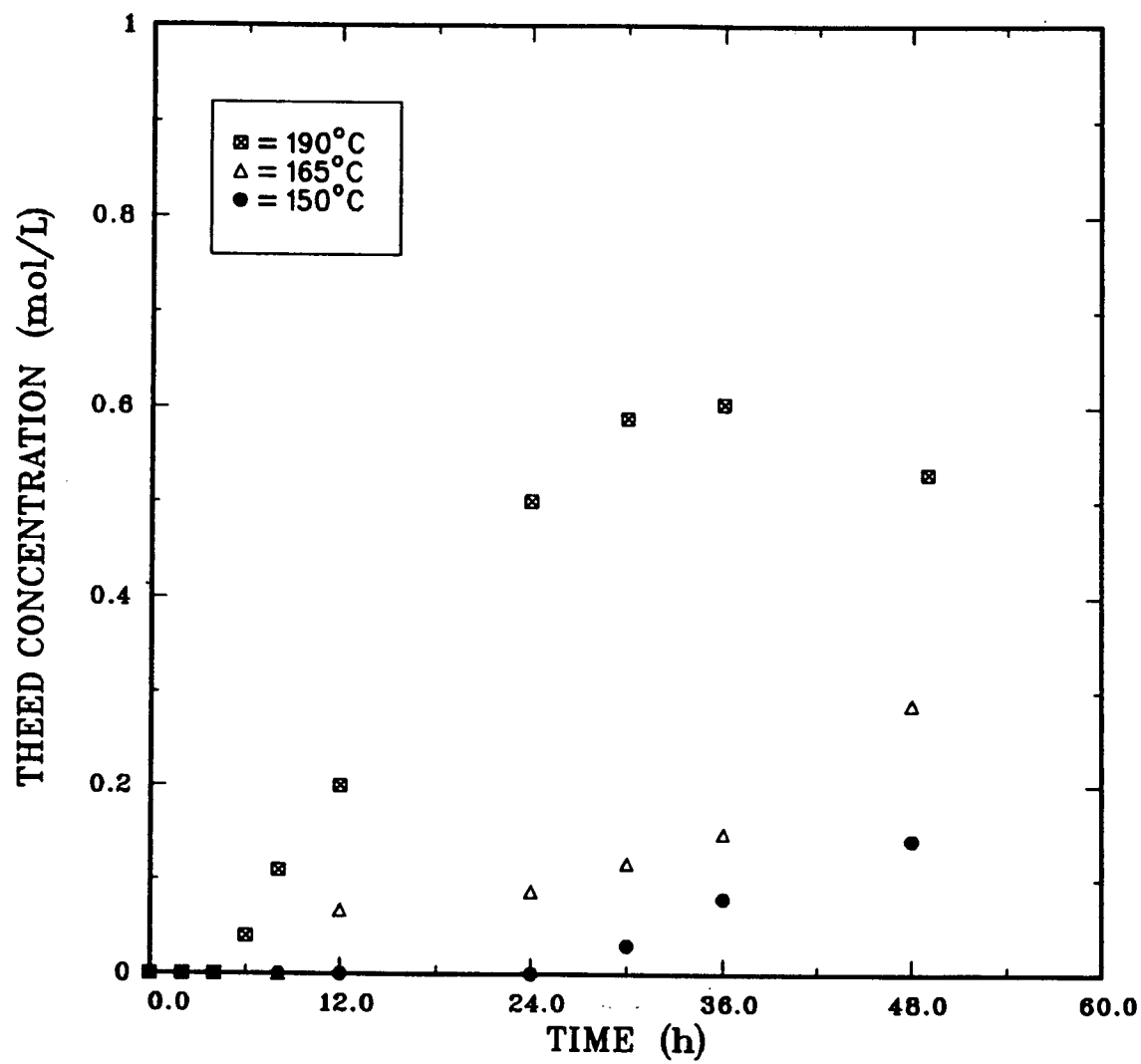


Figure 5.26: THEED concentration as a function temperature and time
($P_{\text{COS}} = 0.34 \text{ MPa}$, $\text{DEA}_0 = 3\text{M}$).

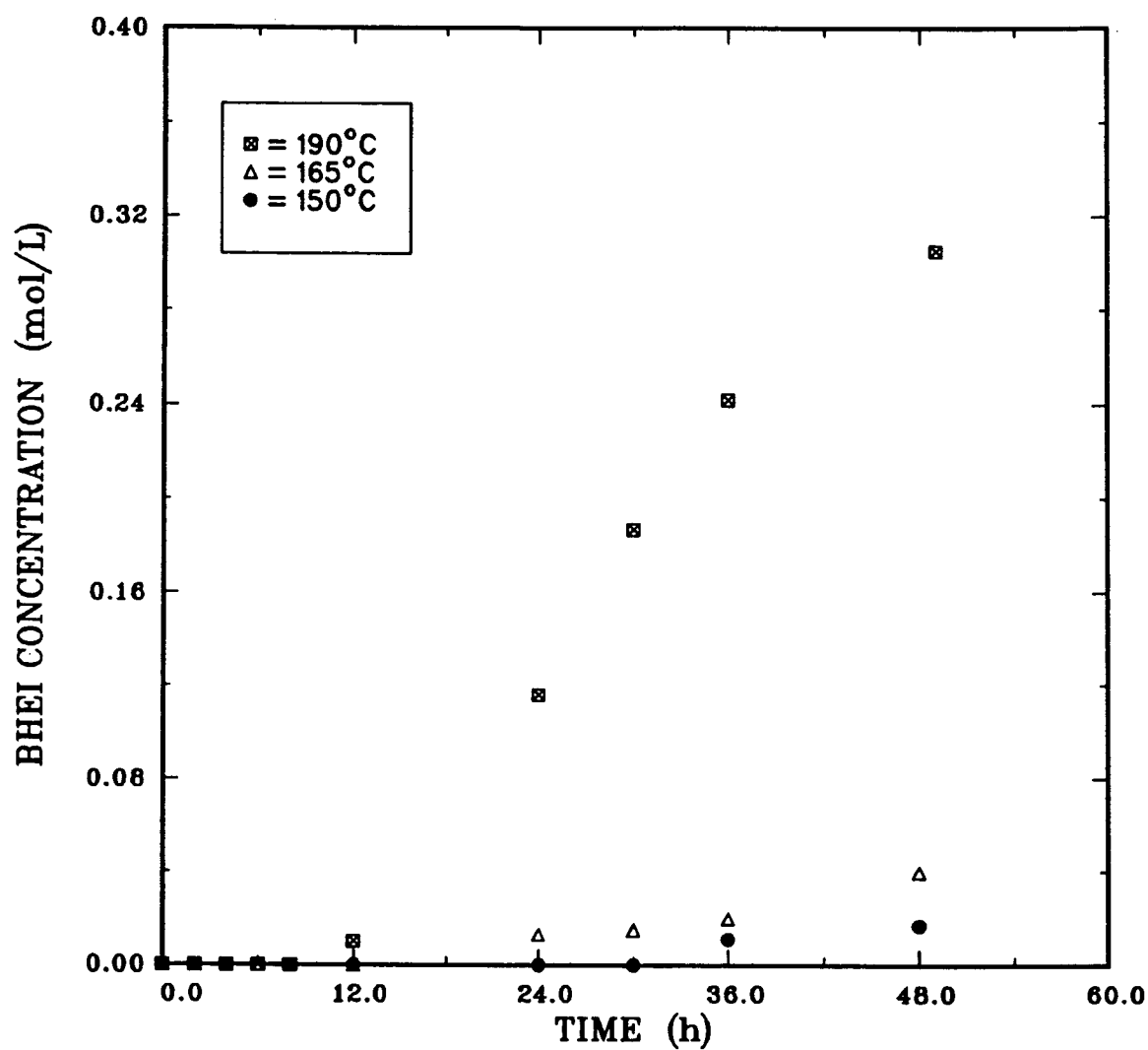


Figure 5.27: BHEI concentration as a function temperature and time
($P_{\text{COS}} = 0.34$ MPa, $\text{DEA}_0 = 3\text{M}$).

For the CO_2 -DEA system, Kennard (16) found that the HEOD production attained equilibrium and that the final concentrations decrease with increasing temperature. Figure 5.24 shows that equilibrium was not attained at $T \leq 165^\circ\text{C}$. However, at 165°C , the HEOD production appears to level off to a final concentration lower than that obtained at 150°C . Such approach to equilibrium was also observed in the runs conducted with an initial DEA concentration of 20 wt% and at low temperatures (see Tables C.14 and C.15). The initial rate of HEOD production, on the other hand, increased with temperature. This trend is consistent with the mechanism that HEOD is produced from DEA carbamate (DEACOO^-) which, in turn, is a function of the equilibrium CO_2 solubility. Although the rate of transformation of DEA carbamate to HEOD increases with temperature (see initial rates of HEOD production), the final concentration is dependent on the equilibrium CO_2 solubility which is inversely related to temperature. Hence, the equilibrium HEOD concentration should decrease as temperature increases.

The HEI production and final concentration increase with temperature as shown in Fig. 5.25.

Figure 5.26 shows that the rate of production and depletion of THEED increase with temperature. Hence at high temperatures, maxima result. It has been reported that THEED dehydrates to BHEP (13,14). The data shown by Fig. 5.26 are consistent with the conclusion that THEED is an intermediate product.

The rate of production and final concentration of BHEI increase with temperature. No maxima are indicated by Fig. 5.27. Therefore, BHEI may be considered a terminal product. At temperatures above 165°C , the

BHEI concentration increases significantly. The rate of decline of the compound producing BHEI should be correspondingly high at such temperatures. The depletion of BHEED exhibits this trait. BHEED may therefore be the intermediate product from which BHEI is formed.

5.1.3 EFFECTS OF INITIAL COS PARTIAL PRESSURE

It is shown in chapter 7 that the equilibrium solubility of COS and the concentrations of the ionic species that induce degradation increase with initial COS partial pressure. Consequently, the rate of depletion of DEA increases with initial COS partial pressure as shown by Fig. 5.28.

The effects of initial COS pressure on the production of acetone and butanone are shown by Figs. 5.29 and 5.30, respectively. The rates of production of both compounds increase with the initial COS partial pressure. The final concentration of acetone also increases with the initial COS partial pressure, but a drop in final concentration was observed for butanone as the pressure rose to 1171 kPa. Butanone may be depleted via some reactions, the rates of which increase with COS partial pressure.

The rate of production of MEA and its final concentration increase with initial COS partial pressure. The increase is less pronounced for pressure increase from 759 to 1171 kPa, probably because MEA is an intermediate product and its rate of depletion increases with COS partial pressure (see Fig. 5.31).

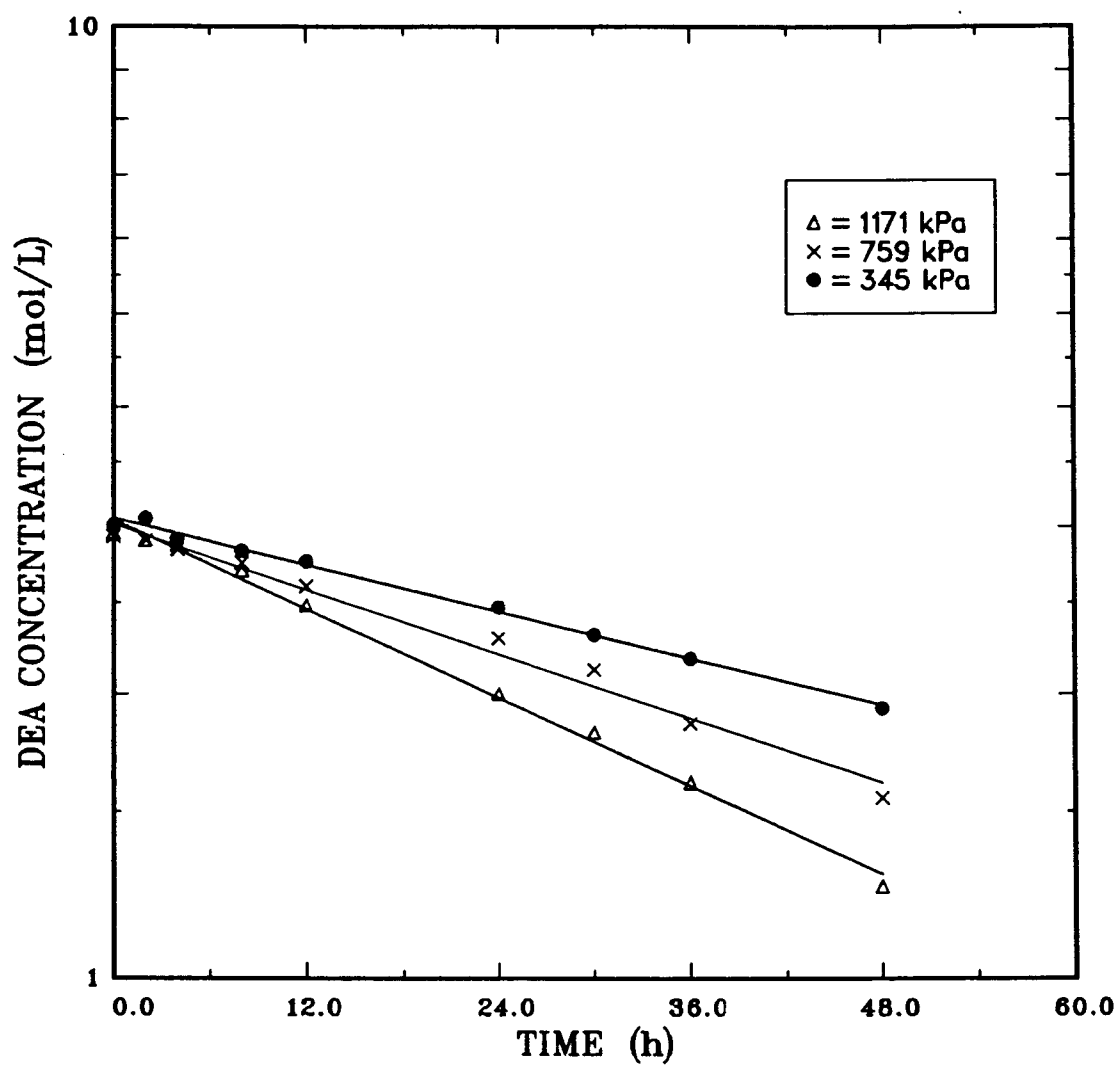


Figure 5.28: DEA concentration as a function of initial COS partial pressure and time ($\text{DEA}_0 = 3\text{M}$, $T = 150^\circ\text{C}$).

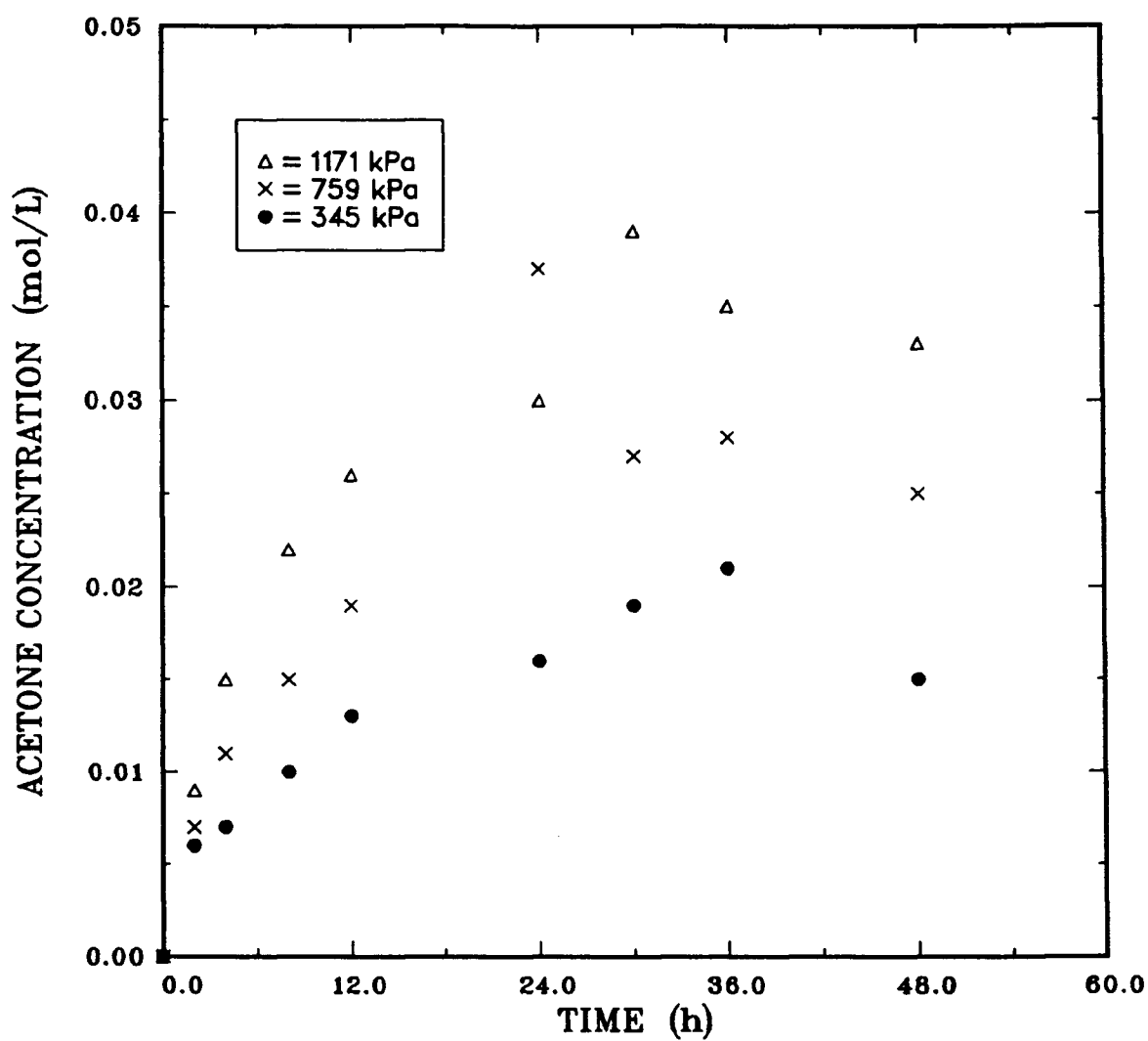


Figure 5.29: Acetone concentration as a function of initial COS partial pressure and time ($\text{DEA}_0 = 3\text{M}$, $T = 150^\circ\text{C}$).

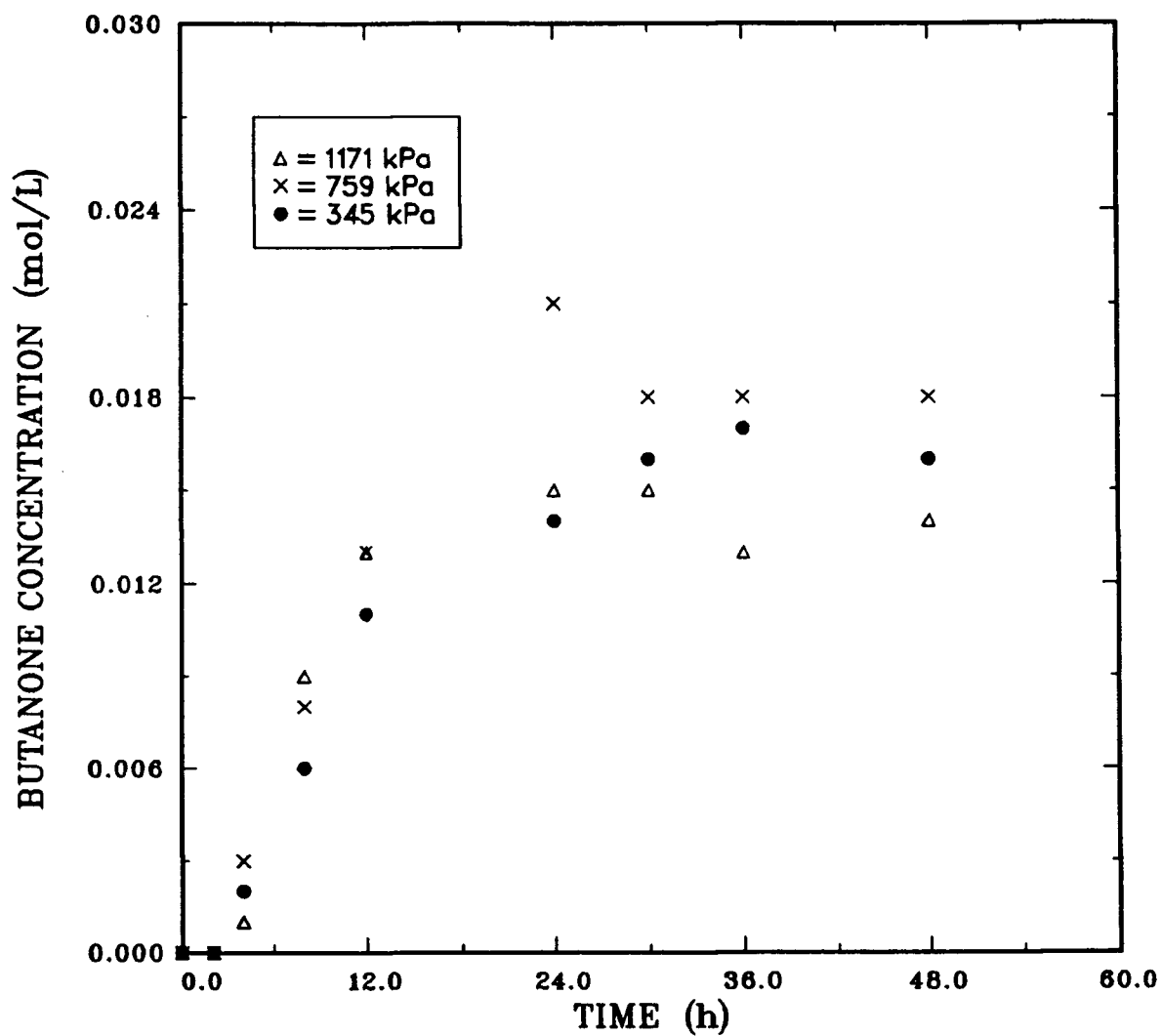


Figure 5.30: Butanone concentration as a function of initial COS partial pressure and time ($\text{DEA}_0 = 3\text{M}$, $T = 150^\circ\text{C}$).

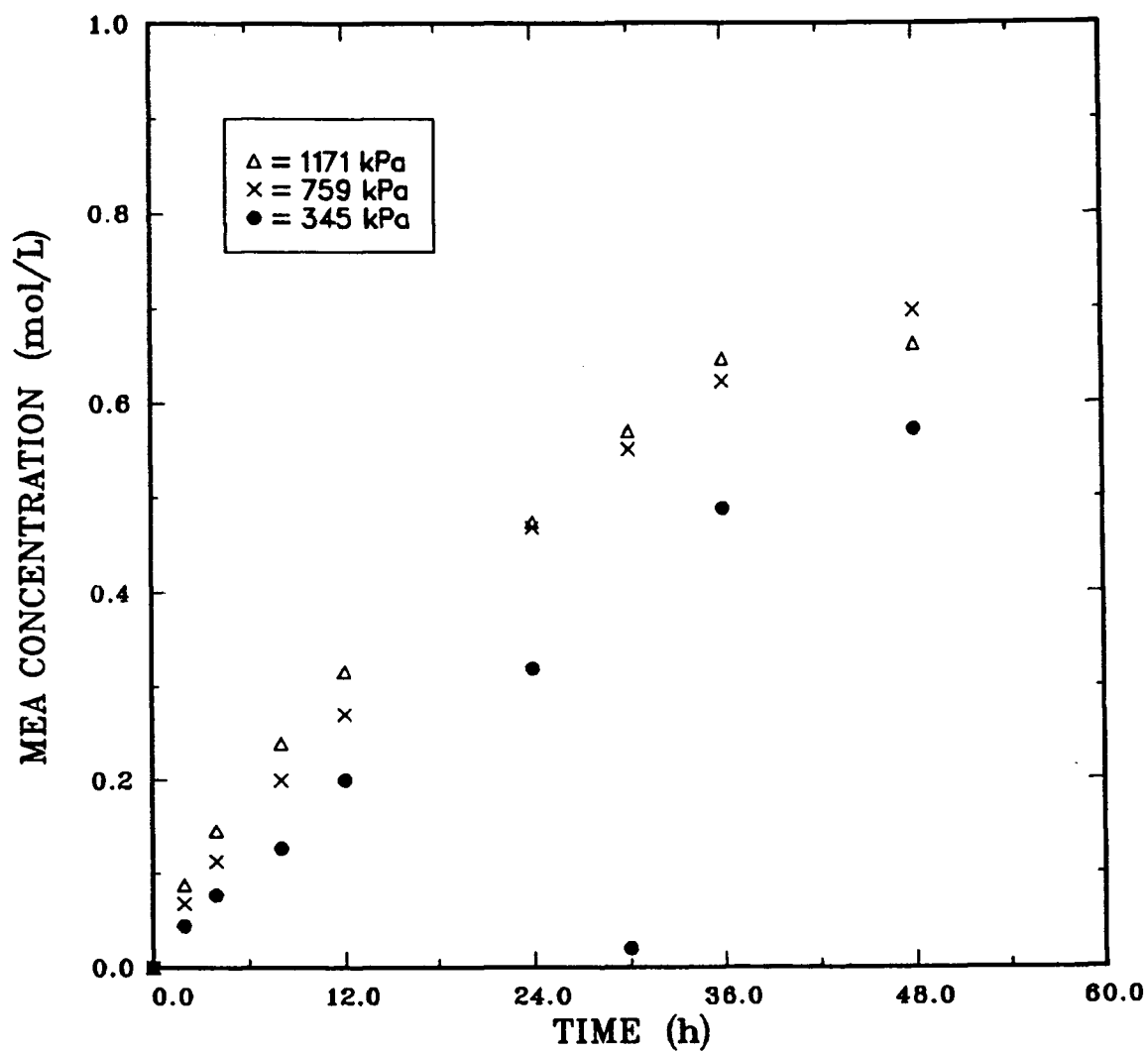


Figure 5.31: MEA concentration as a function of initial COS partial pressure and time ($\text{DEA}_0 = 3\text{M}$, $T = 150^\circ\text{C}$).

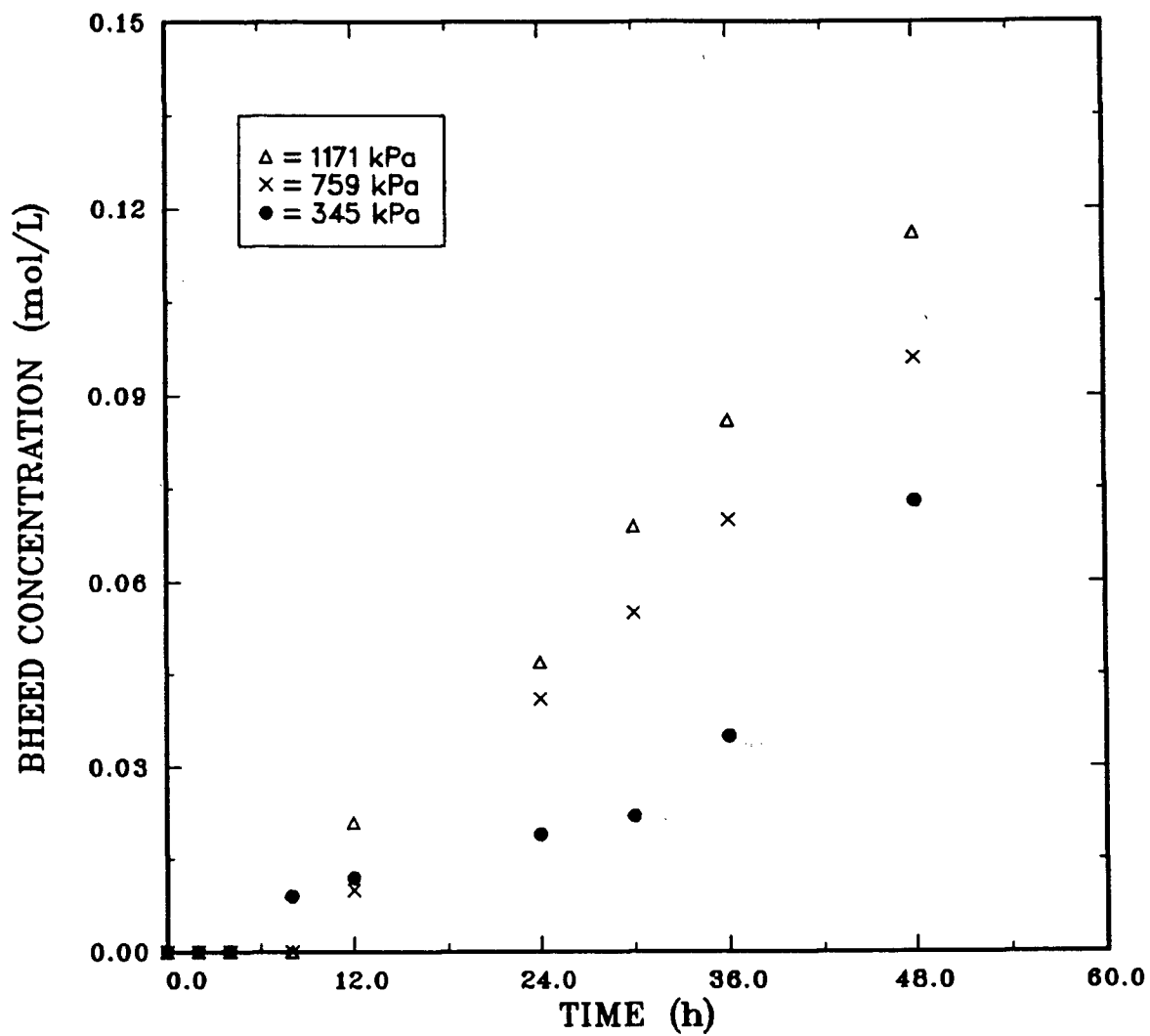


Figure 5.32: BHEED concentration as a function of initial COS partial pressure and time ($\text{DEA}_0 = 3\text{M}$, $T = 150^\circ\text{C}$).

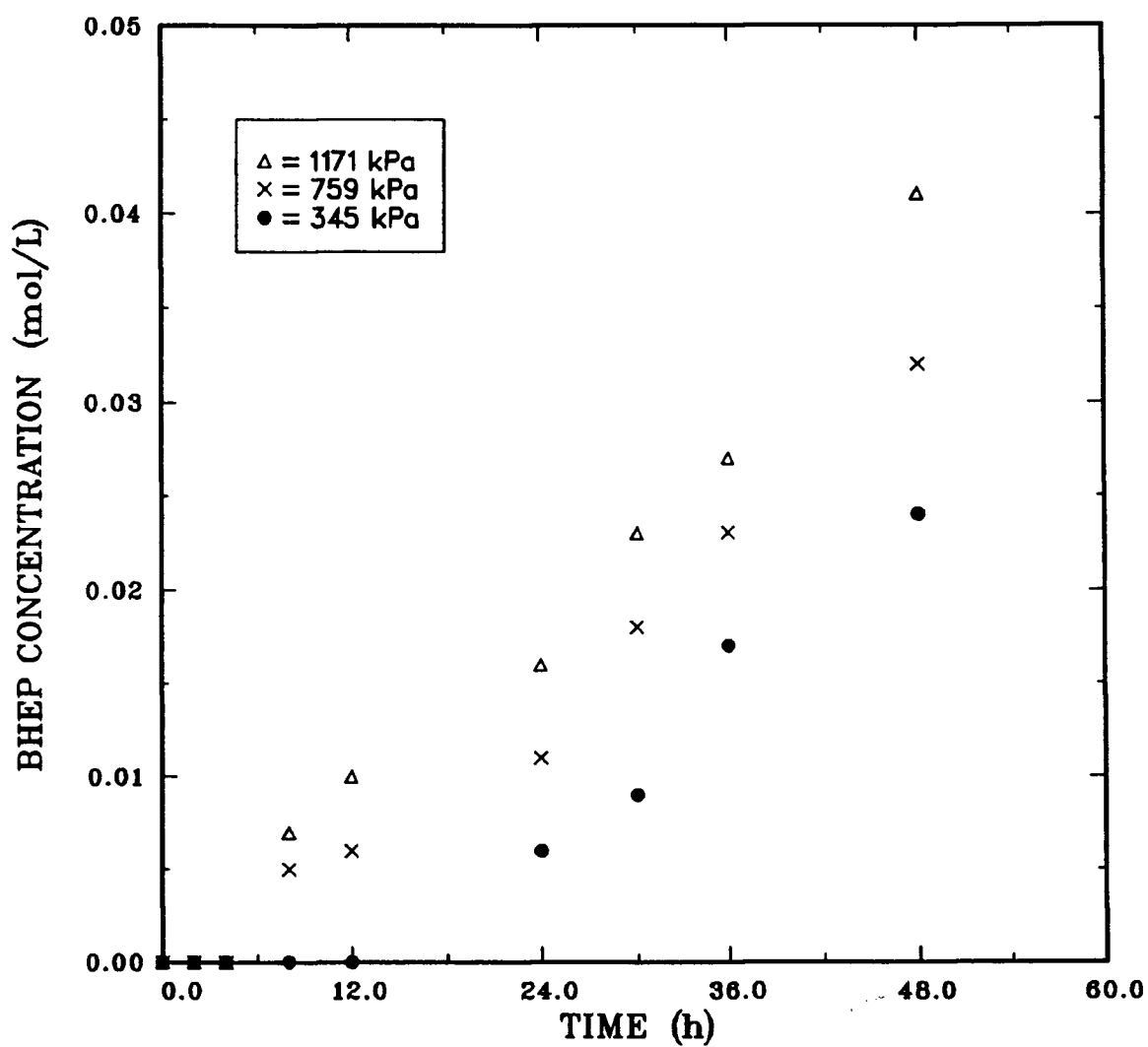


Figure 5.33: BHEP concentration as a function of initial COS partial pressure and time ($\text{DEA}_0 = 3\text{M}$, $T = 150^\circ\text{C}$).

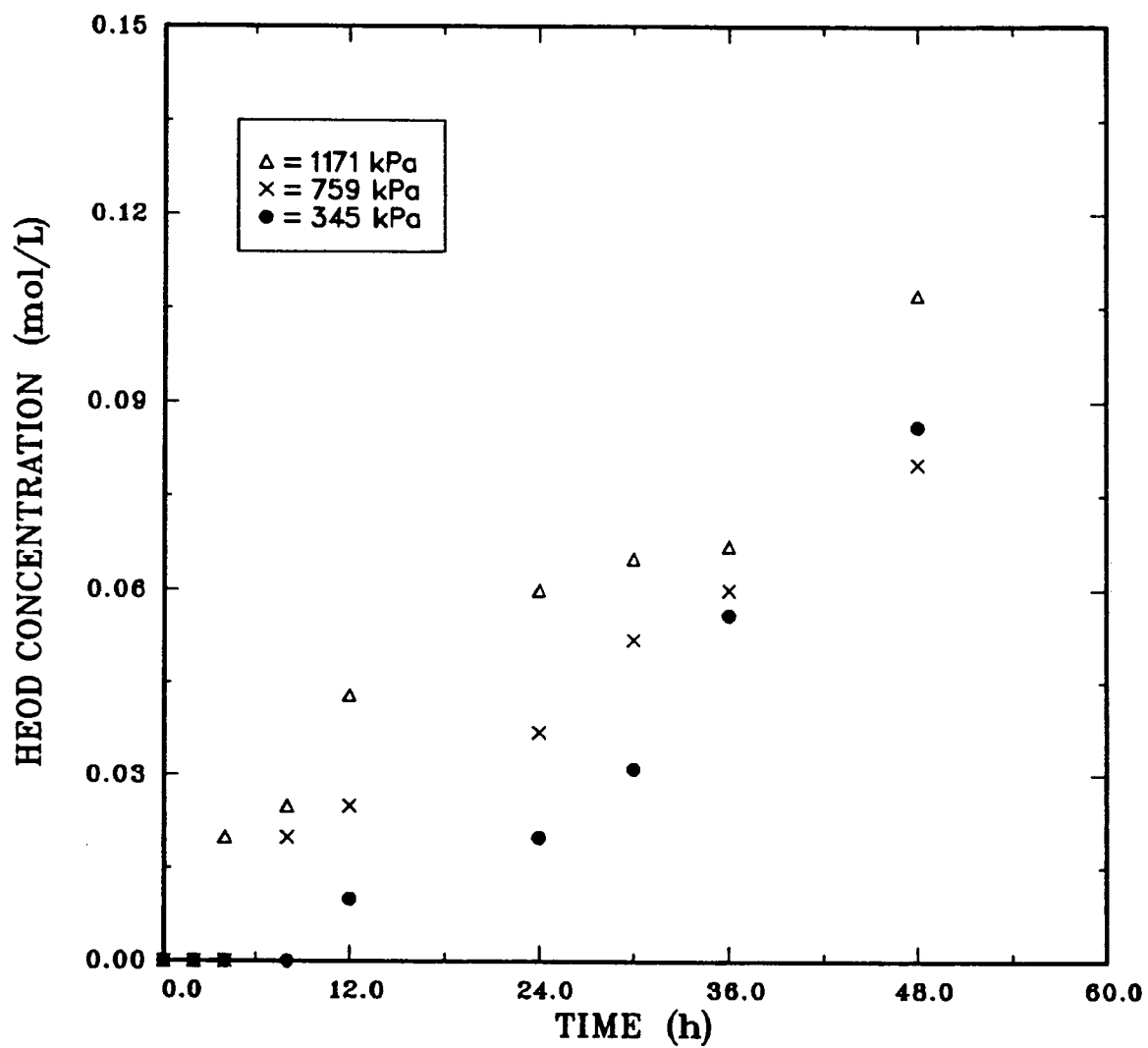


Figure 5.34: HEOD concentration as a function of initial COS partial pressure and time ($\text{DEA}_0 = 3\text{M}$, $T = 150^\circ\text{C}$).

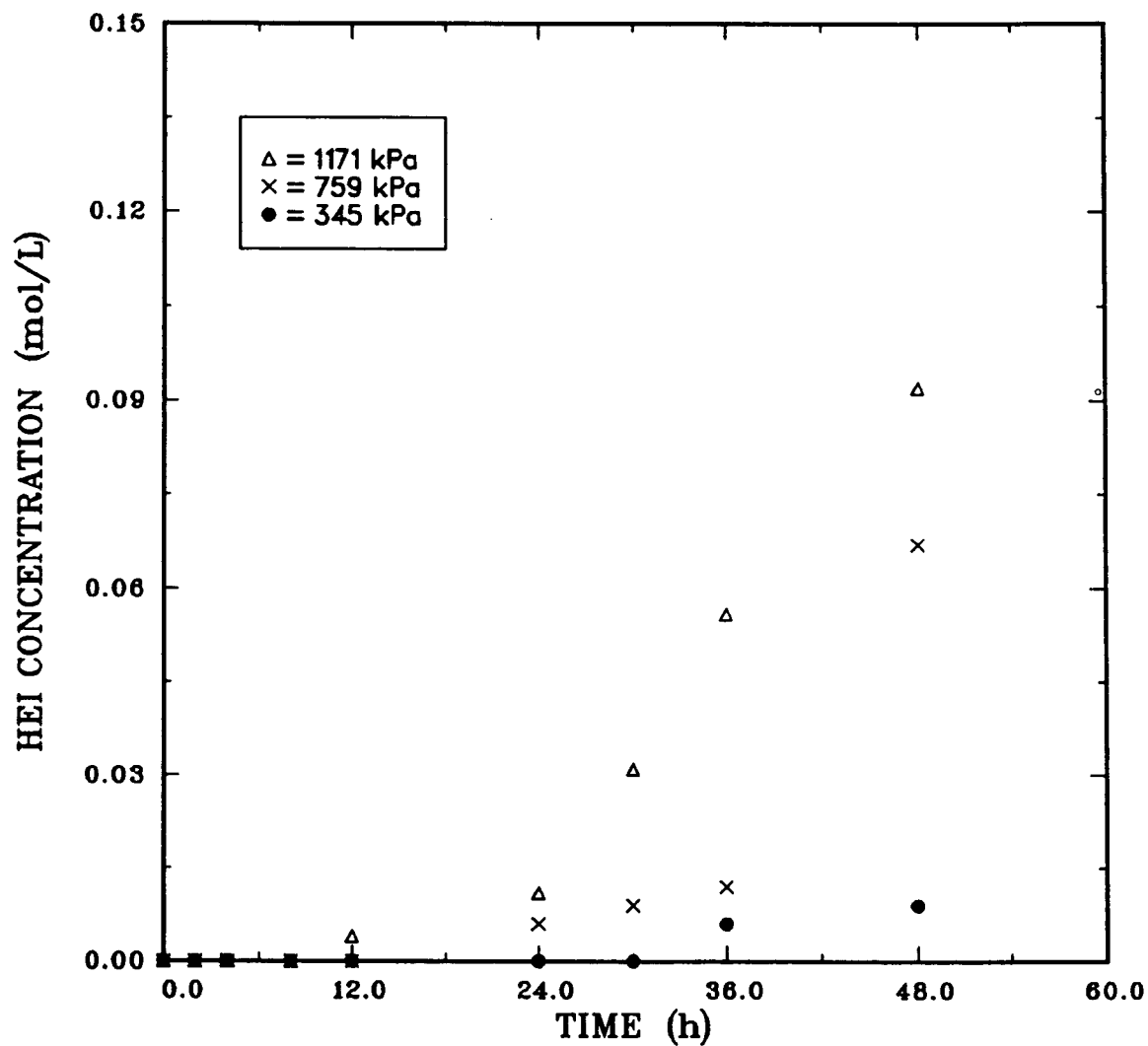


Figure 5.35: HEI concentration as a function of initial COS partial pressure and time ($\text{DEA}_0 = 3\text{M}$, $T = 150^\circ\text{C}$).

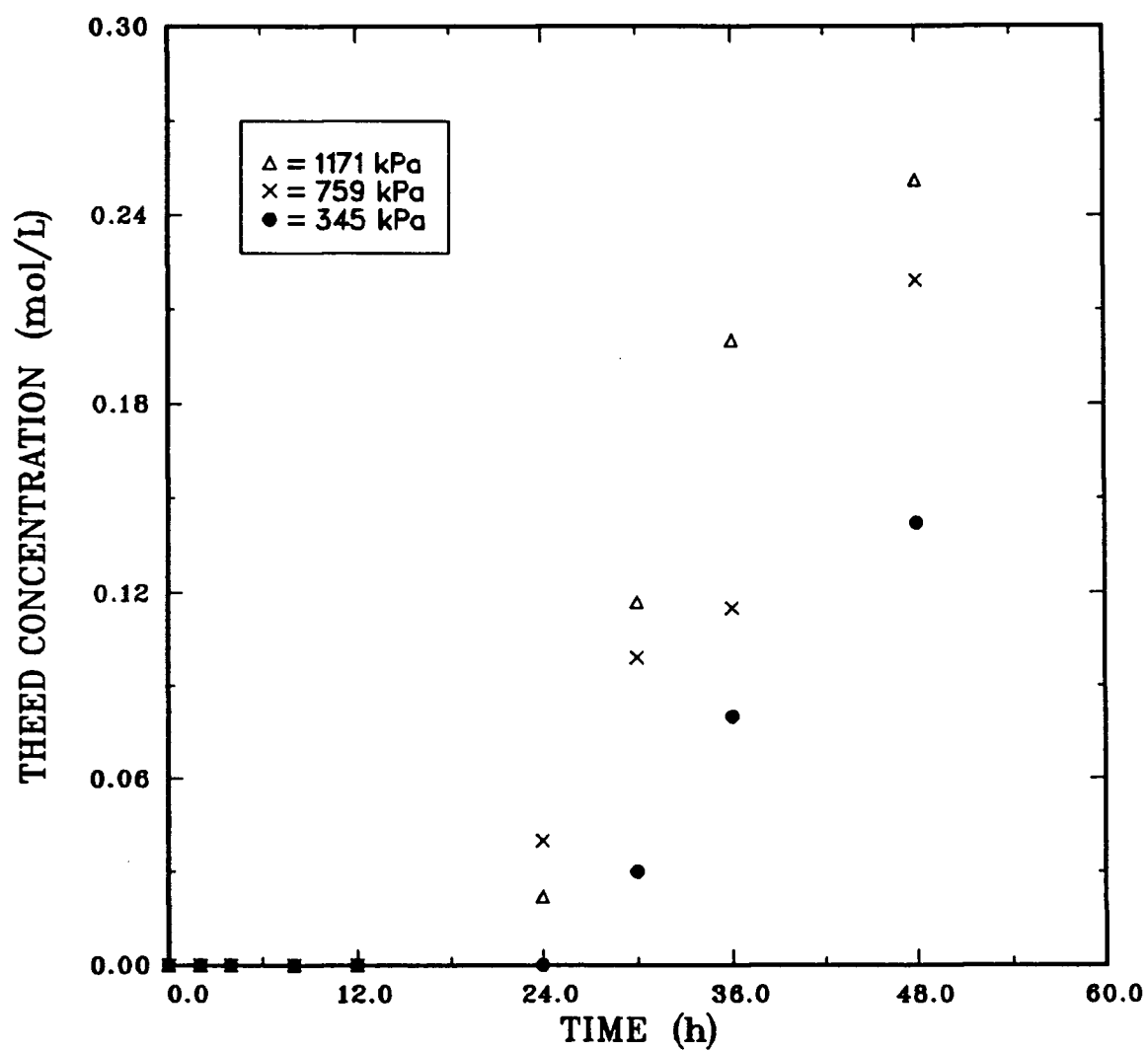


Figure 5.36: THEED concentration as a function of initial COS partial pressure and time ($\text{DEA}_0 = 3\text{M}$, $T = 150^\circ\text{C}$).

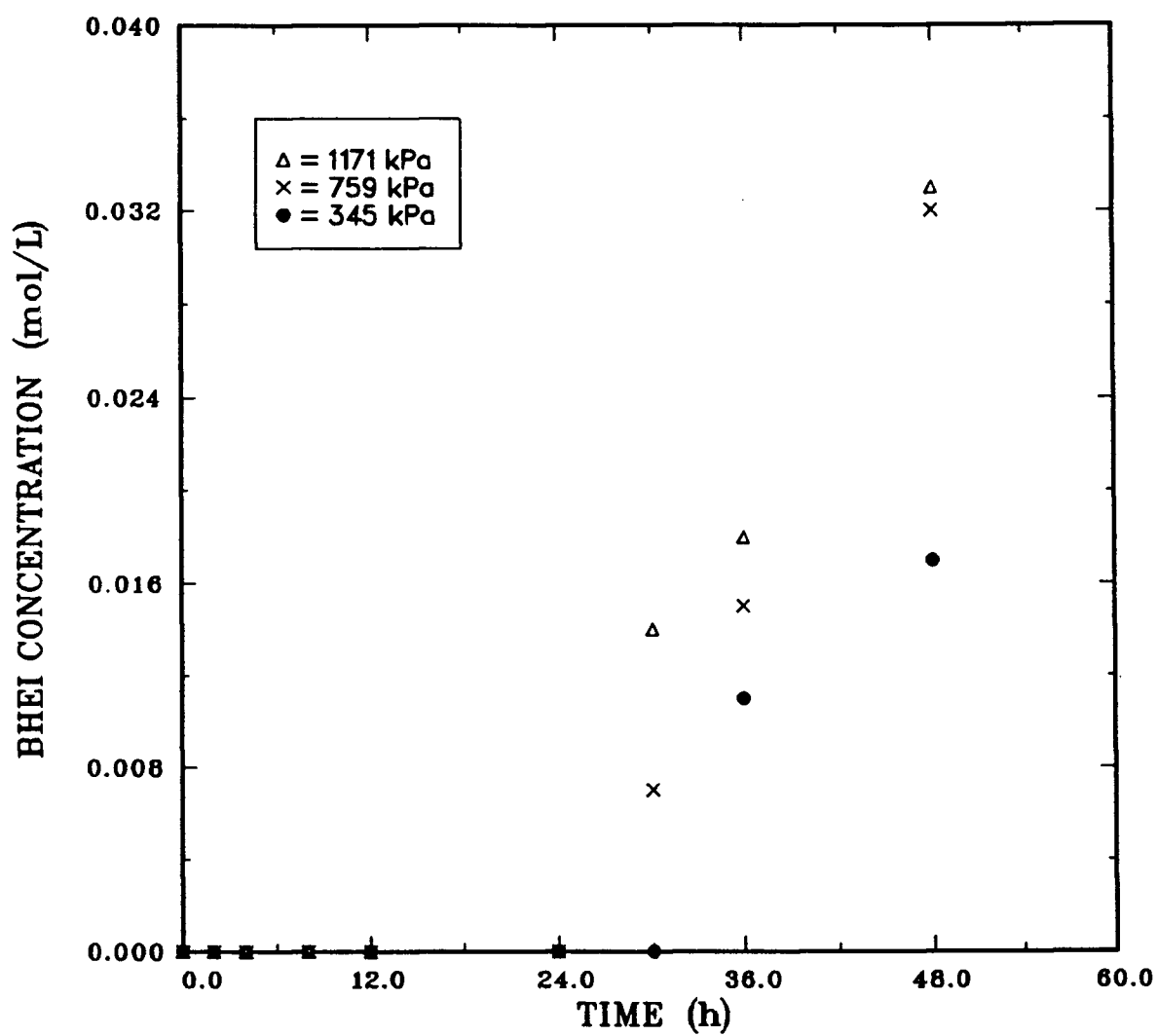


Figure 5.37: BHEI concentration as a function of initial COS partial pressure and time ($\text{DEA}_0 = 3\text{M}$, $T = 150^\circ\text{C}$).

The rates of production and final concentrations of BHEED, BHEP, HEOD, HEI, THEED and BHEI increase with COS partial pressure as shown by Figs. 5.32 to 5.37.

In summary, the rate of DEA degradation is more sensitive to changes in temperature than variations in DEA concentration and COS partial pressure. For example, at an initial concentration of 30 wt%, a change in temperature from 127 to 165 °C resulted in a 5 fold increase in the rate of degradation. On the other hand, a 2 fold increase in DEA concentration (2 - 4M) caused an increase of 1.76 in the rate of degradation while doubling the COS partial pressure produced a 1.4 fold increase in the rate of degradation. The total concentrations of the degradation products also reflect the rates of degradation. The higher the rates, the higher the total concentrations of the degradation products.

By comparing the degradation rate constant of 0.0173 h^{-1} for a CO_2 -DEA system (Table C.43) with the value of 0.0131 h^{-1} for a similar COS-DEA system (Table C.17), it is seen that the rate of degradation in the former is just 1.3 times faster than that of the latter system.

5.2 CS_2 -DEA SYSTEM

5.2.1 EFFECTS OF INITIAL DEA CONCENTRATION

Figures 5.38 - 5.40 show the DEA concentration as a function of time and initial DEA concentration at temperatures of 120, 150 and 165 °C, respectively. The DEA concentration curves consist of an initial

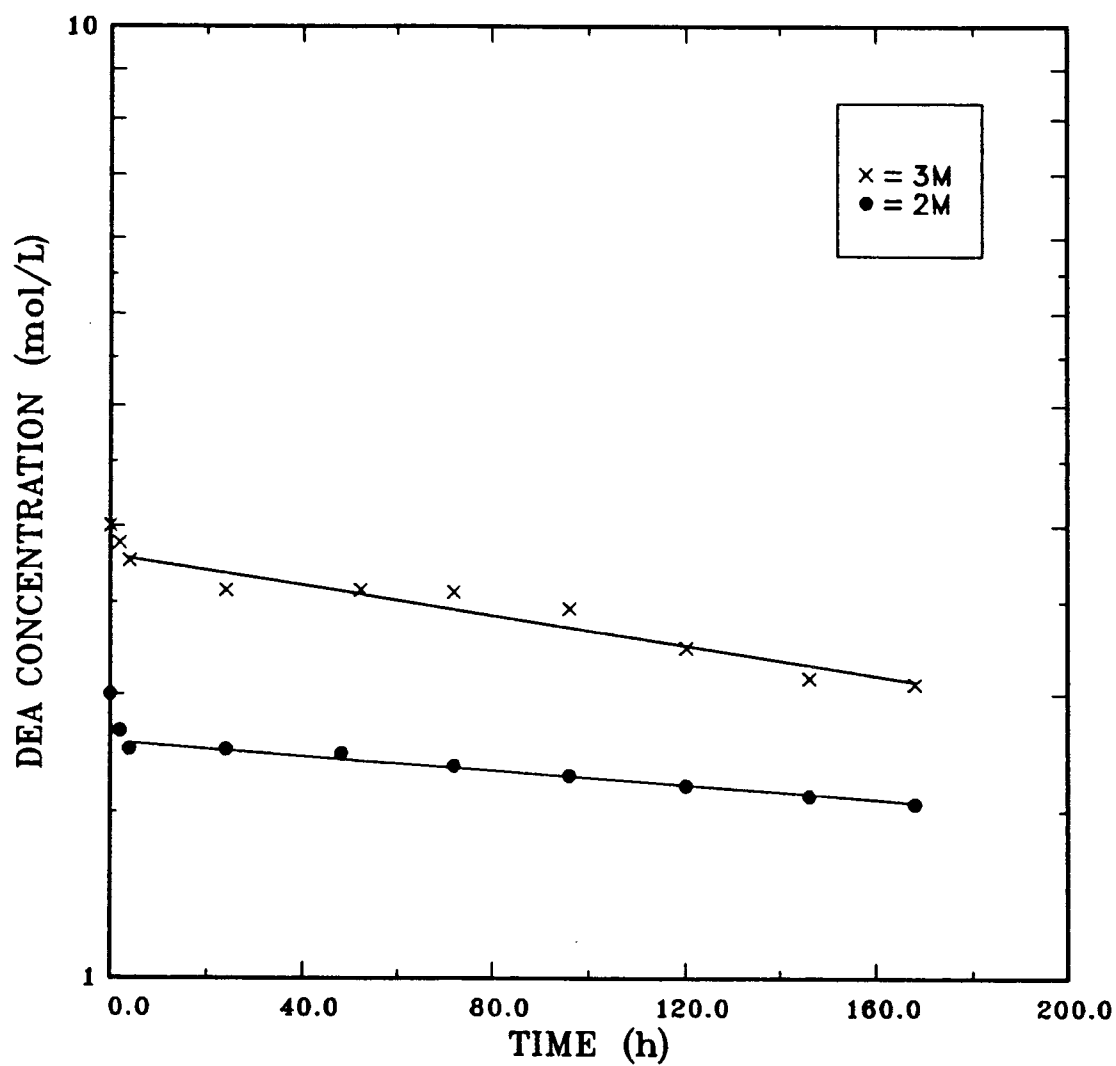


Figure 5.38: DEA concentration as a function of initial DEA concentration and time (CS_2 volume = 6 mL, $T = 120^\circ\text{C}$, CS_2/DEA mole ratios = 0.1 - 0.2).

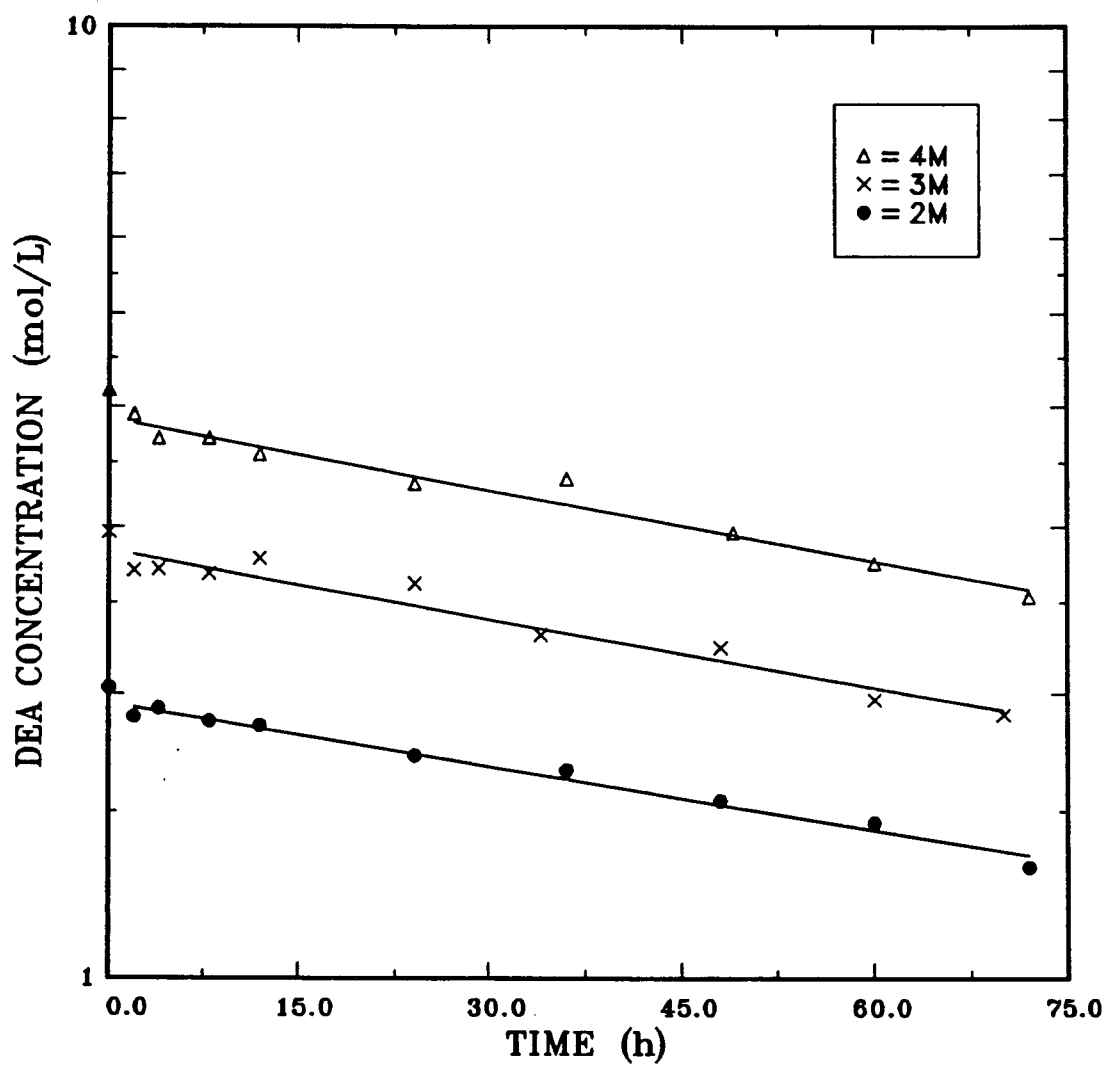


Figure 5.39: DEA concentration as a function of initial DEA concentration and time (CS_2 volume = 6 mL, $T = 150\text{ }^{\circ}C$, CS_2/DEA mole ratios = 0.1 - 0.2).

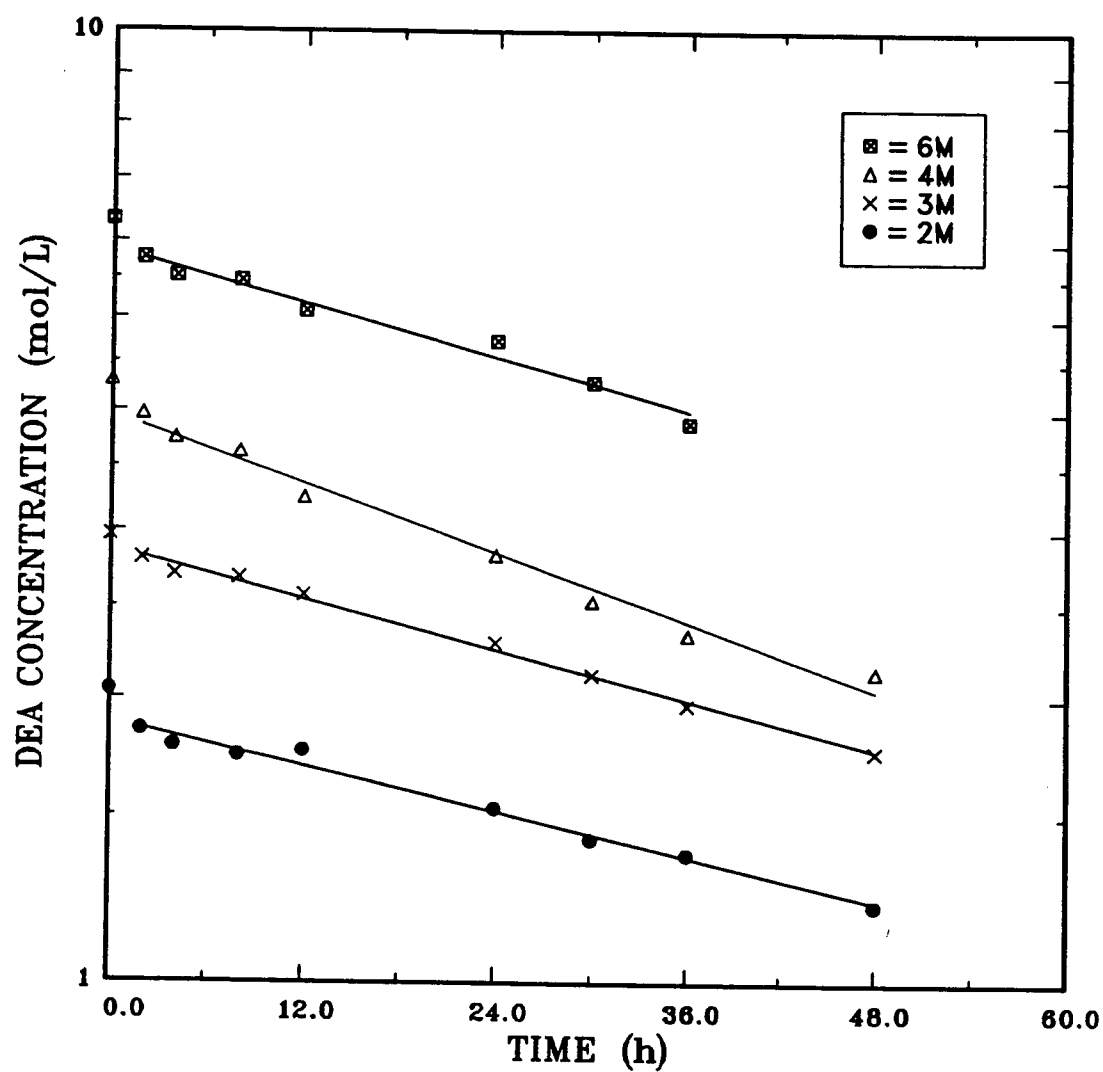


Figure 5.40: DEA concentration as a function of initial DEA concentration and time (CS_2 volume = 6 mL, $T = 165^\circ\text{C}$, CS_2/DEA mole ratios = 0.1 - 0.2).

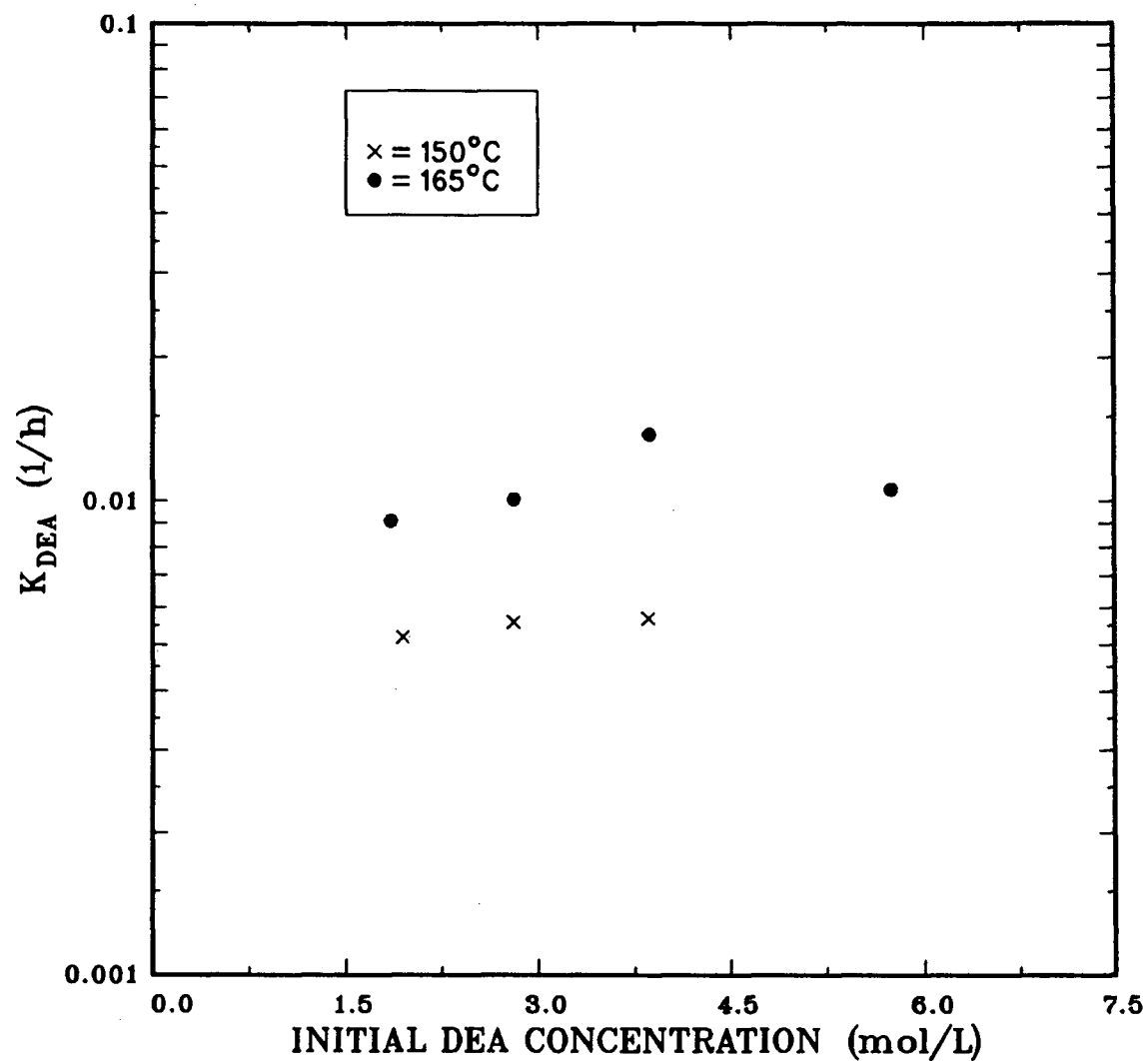


Figure 5.41: Overall degradation rate constant as a function of initial DEA concentration and temperature (CS_2 volume = 6 mL, CS_2/DEA mole ratios = 0.1 - 0.2).

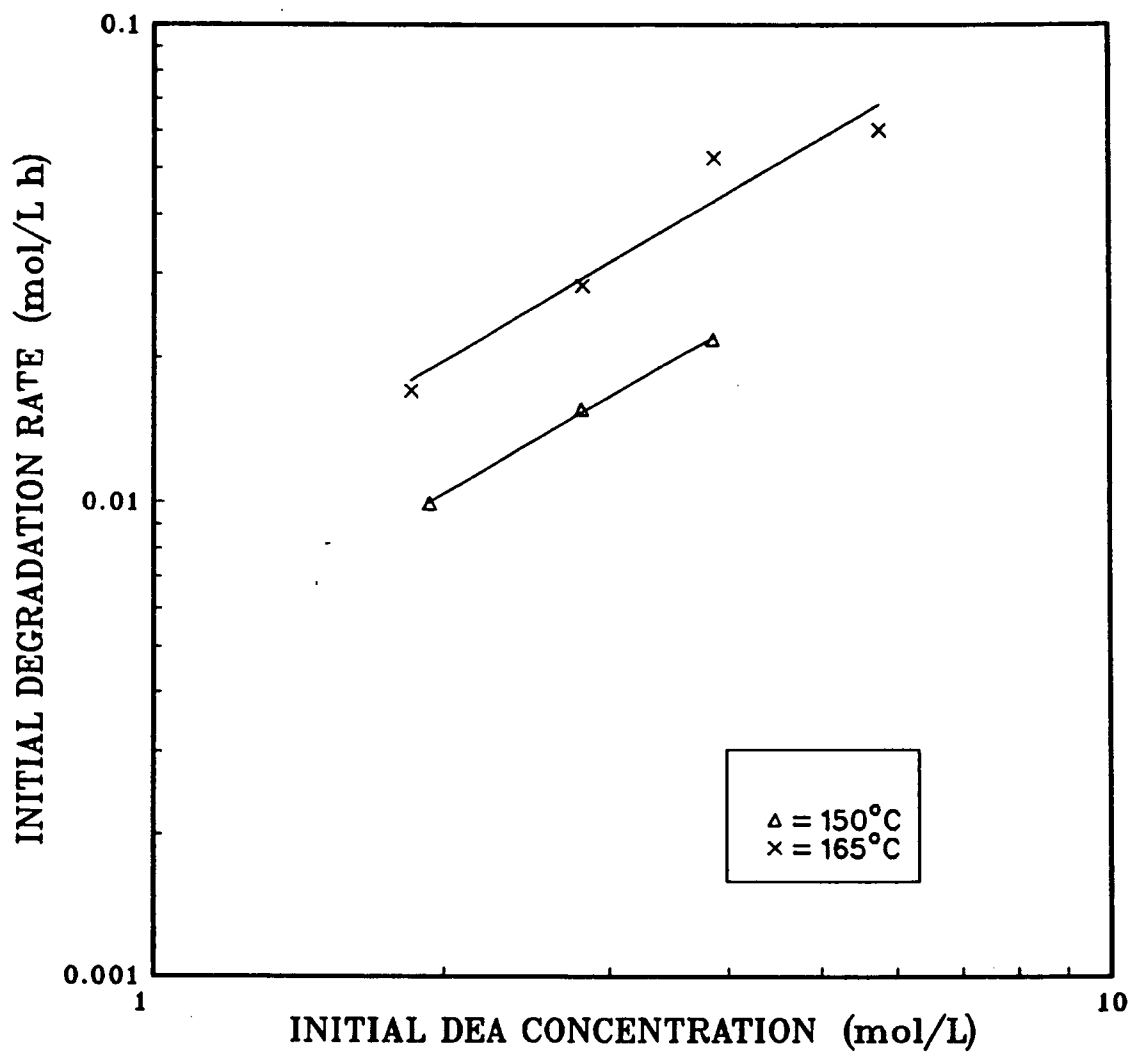


Figure 5.42: Initial degradation rate as a function of initial DEA concentration and temperature (CS_2 volume = 6 mL, CS_2/DEA mole ratios = 0.1 - 0.2).

region of sharp decline and a second region of more moderate decline. This suggests that the degradation occurs via initial fast reactions, which end after a short period of time, followed by slower reactions. The plots in the second region are linear, suggesting that for this region, the initial overall degradation exhibits first order behaviour. The degradation rate constants plotted in Fig. 5.41 show that the rate of degradation is largely independent of the initial DEA concentration at $T = 150^{\circ}\text{C}$. However, at 165°C , a slight concentration dependence is observed. As the DEA concentration increases to 60 wt%, the rate of degradation declines. The explanation offered for a similar observation in the COS-DEA system also applies in this case. A further check on the first order postulate is provided by Fig. 5.42 which is based on the application of Eq. 5.4 to the second region. The curves have slopes of 1.1 thereby again confirming that the overall degradation is consistent with the first order assumption.

The initial rate of MEA formation increases with initial DEA concentration, but within the experimental durations, the final MEA concentrations approach the same value irrespective of the initial DEA concentration (Fig. 5.43). The maxima in the plots conform to previously established trends which suggest that MEA is an intermediate product. The approach to a constant final concentration despite the different maximum concentrations, indicates that MEA depletion is enhanced by high DEA concentration or basicity, as observed in the COS-DEA system.

Figures 5.44 to 5.49 show that the production of the other degradation compounds increases with initial DEA concentration up to 40 wt%. However, between 40 and 60 wt%, a decline is observed for BHEED,

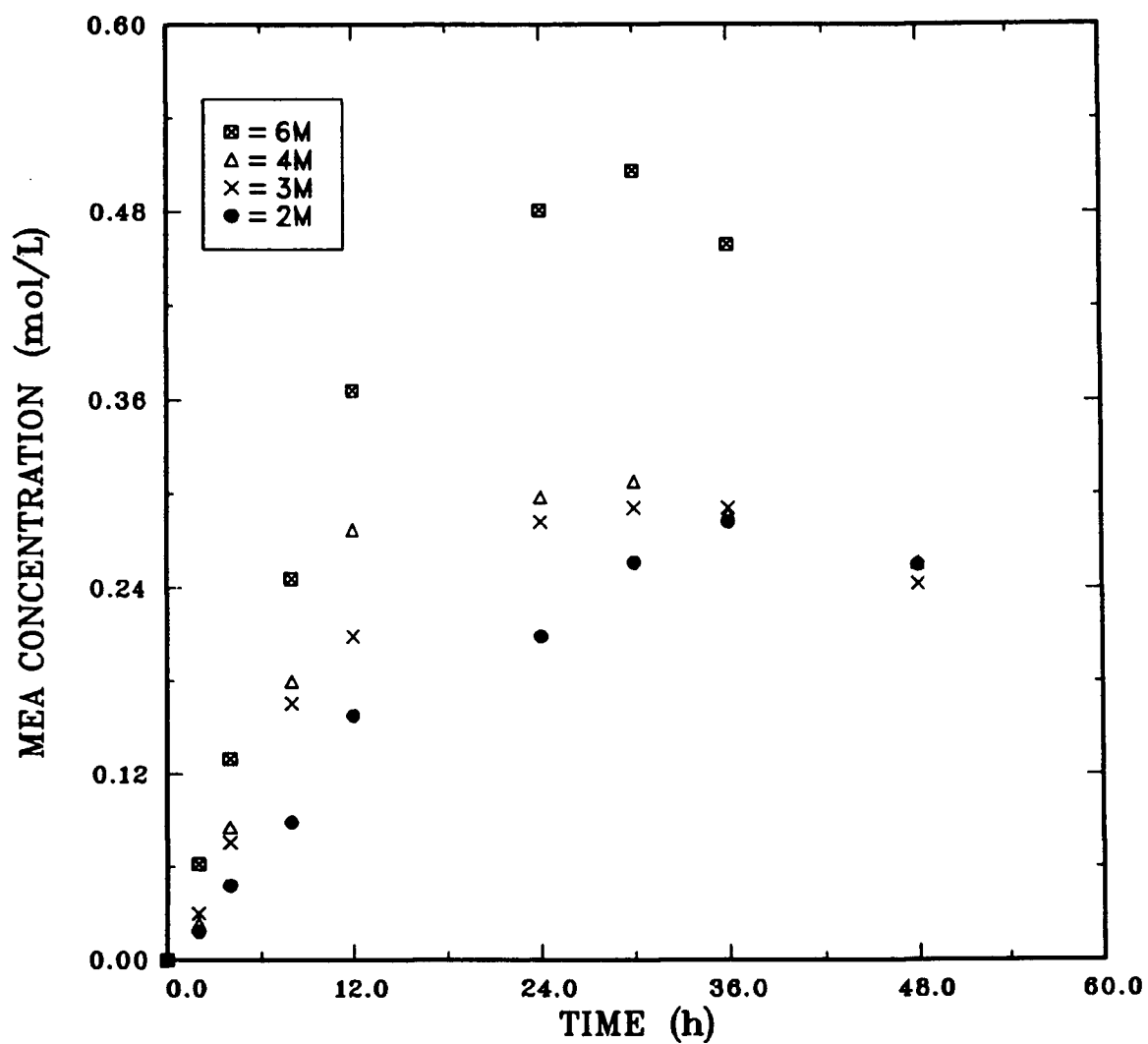


Figure 5.43: MEA concentration as a function of initial DEA concentration and time (CS_2 volume = 6 mL, $T = 165^\circ\text{C}$, CS_2/DEA mole ratios = 0.1 - 0.2).

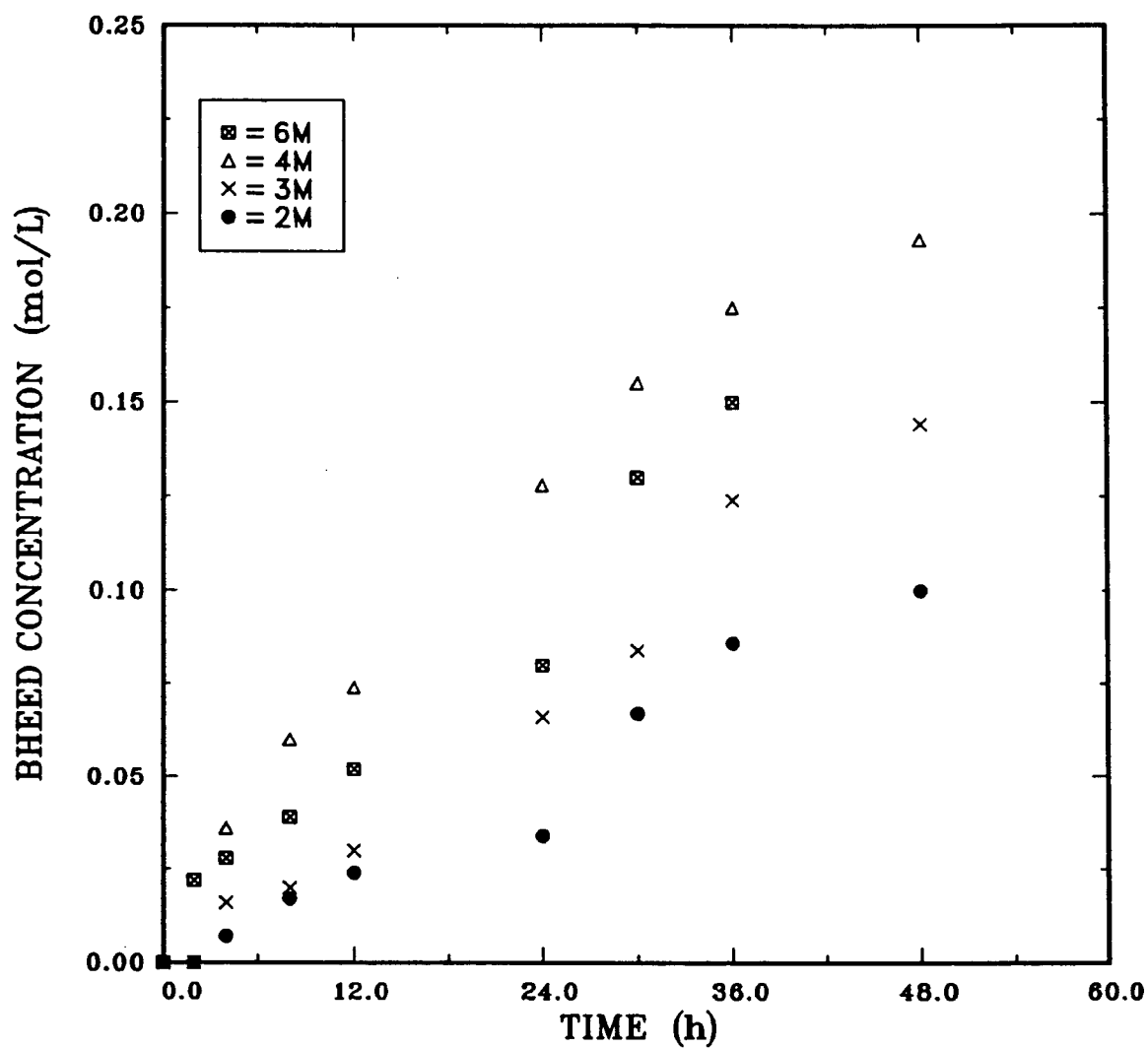


Figure 5.44: BHEED concentration as a function of initial DEA concentration and time (CS_2 volume = 6 mL, $T = 165^\circ\text{C}$, CS_2/DEA mole ratios = 0.1 - 0.2).

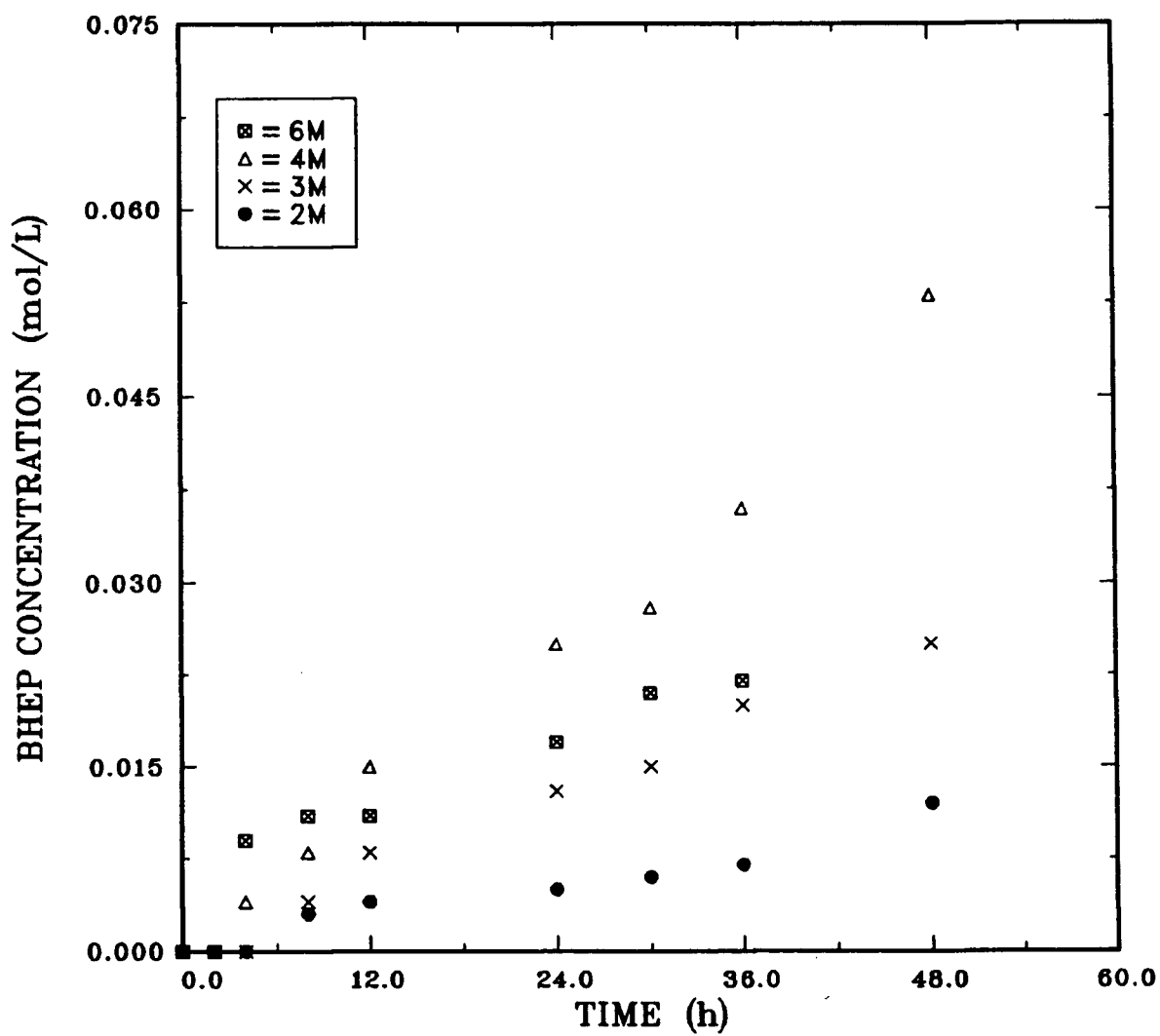


Figure 5.45: BHEP concentration as a function of initial DEA concentration and time (CS_2 volume = 6 mL, $T = 165^\circ\text{C}$, CS_2/DEA mole ratios = 0.1 - 0.2).

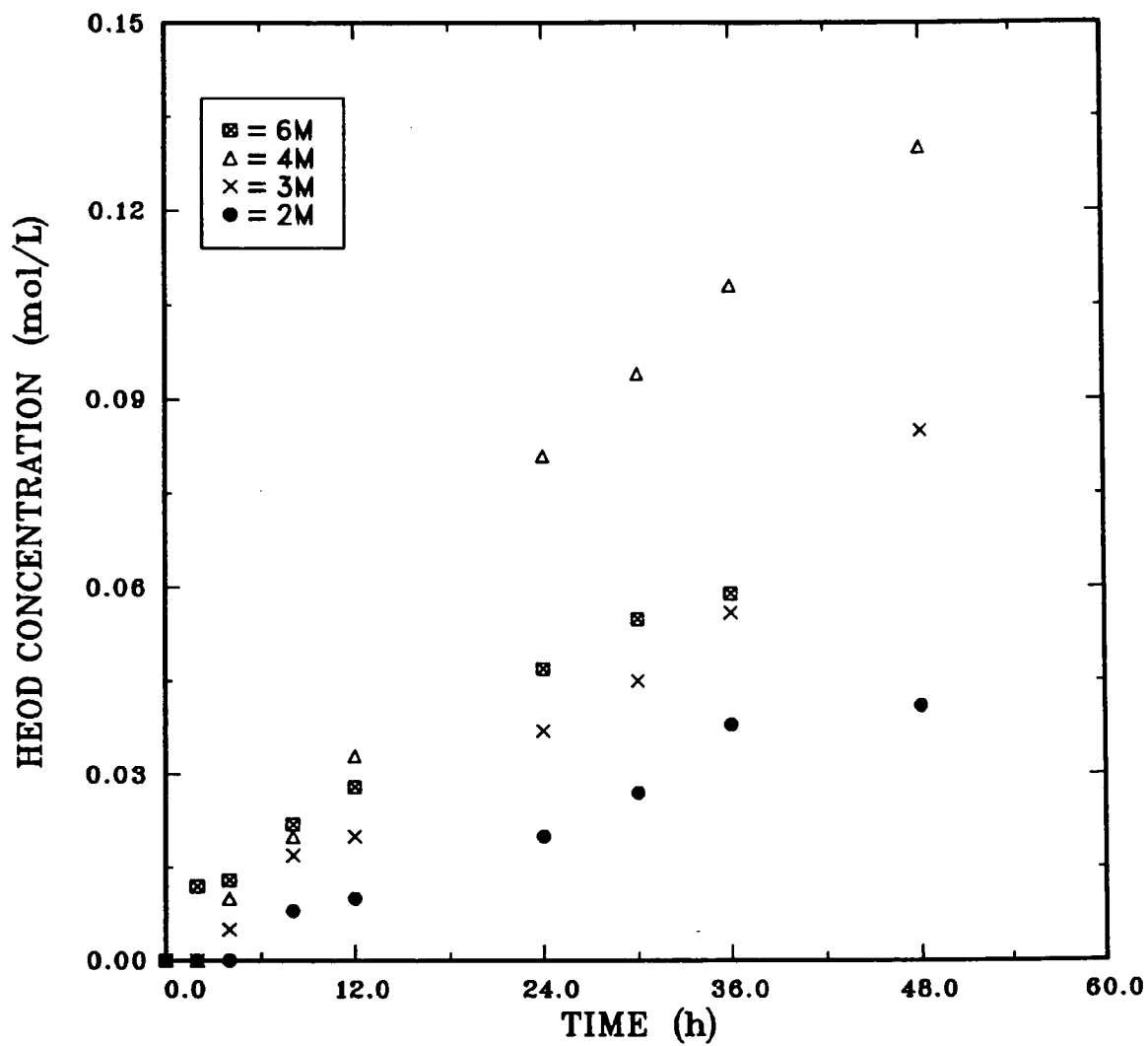


Figure 5.46: HEOD concentration as a function of initial DEA concentration and time (CS_2 volume = 6 mL, $T = 165^\circ\text{C}$, CS_2/DEA mole ratios = 0.1 - 0.2).

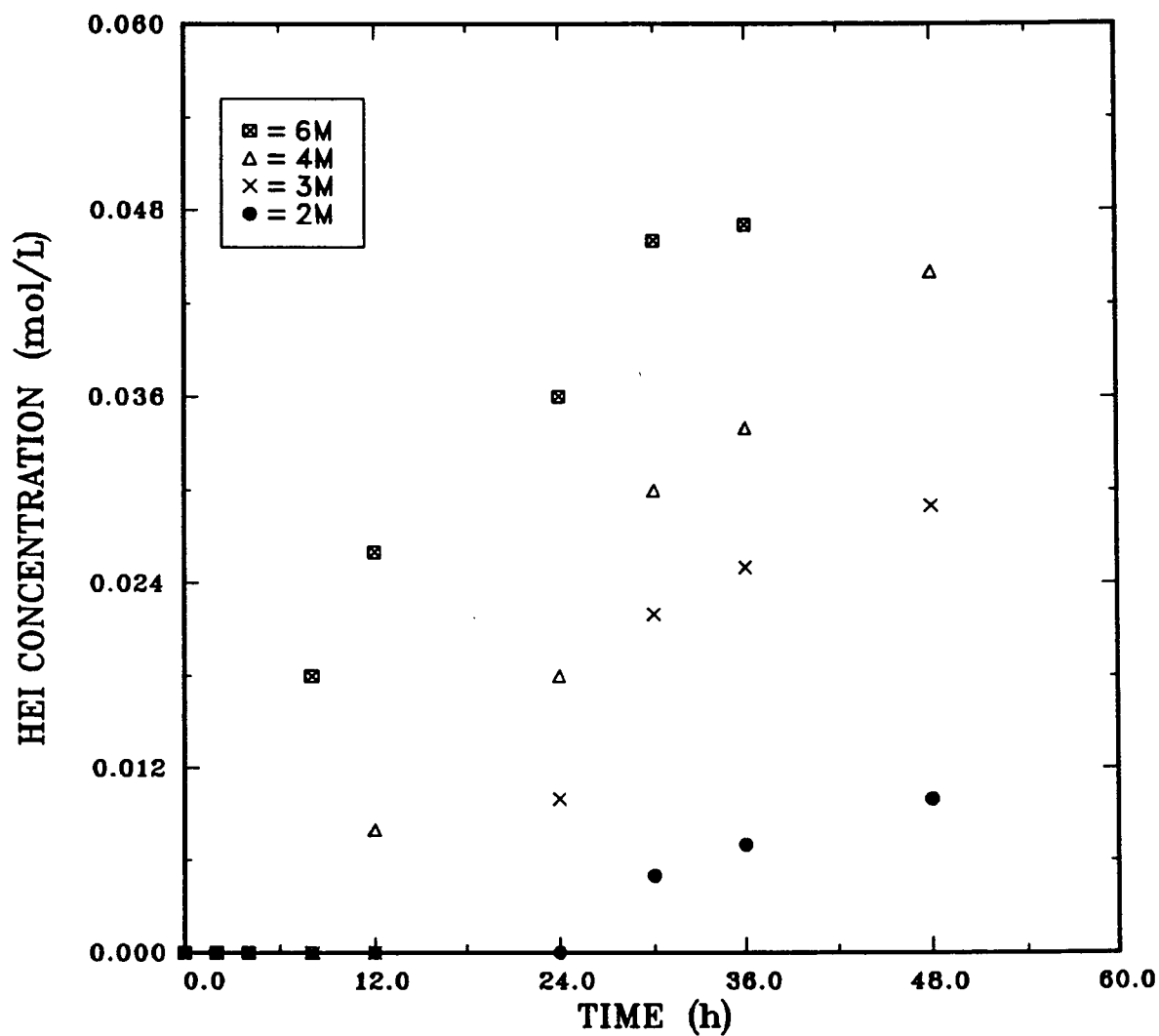


Figure 5.47: HEI concentration as a function of initial DEA concentration and time (CS_2 volume = 6 mL, $T = 165^\circ\text{C}$, CS_2/DEA mole ratios = 0.1 - 0.2).

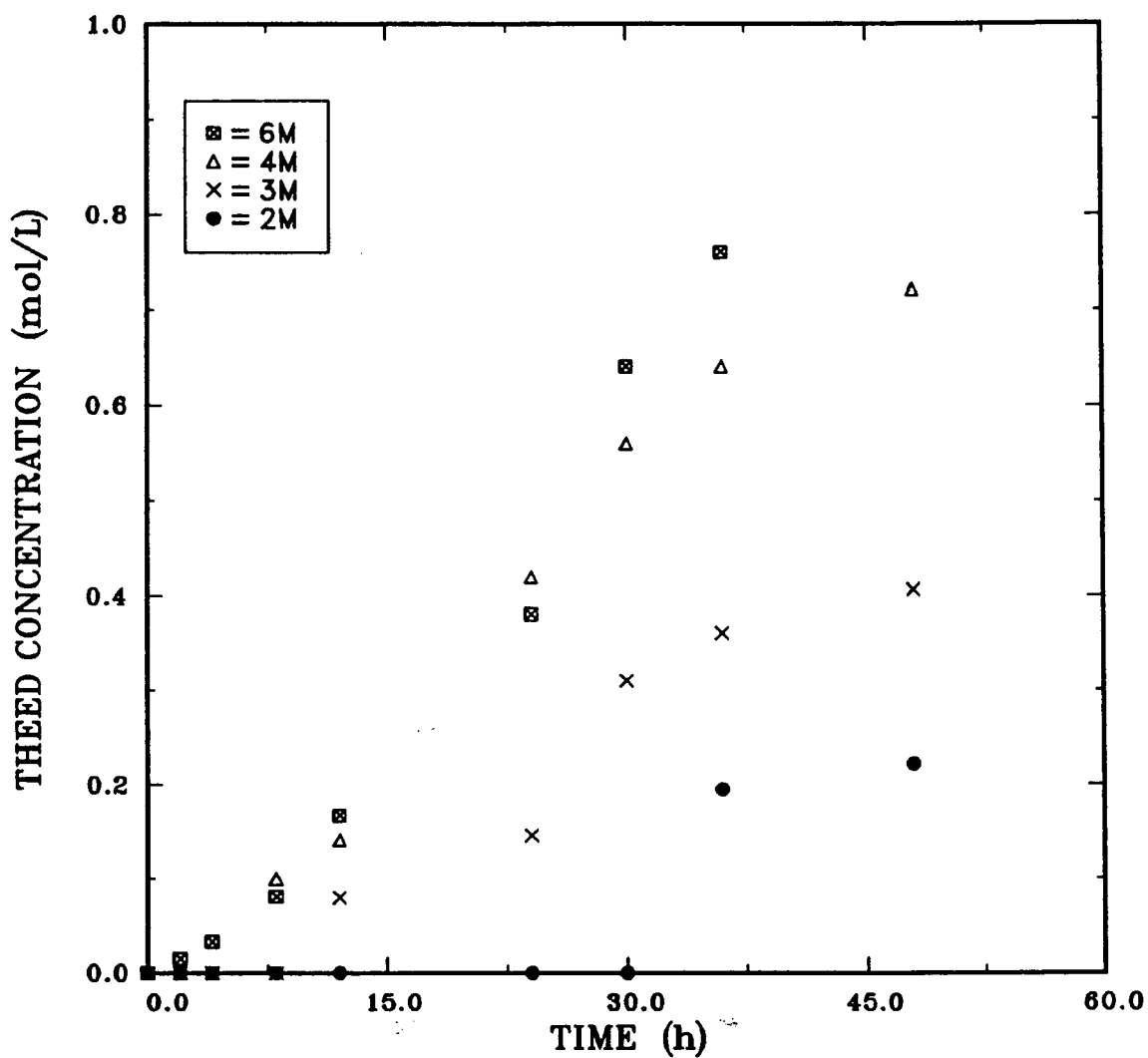


Figure 5.48: THEED concentration as a function of initial DEA concentration and time (CS_2 volume = 6 mL, $T = 165^\circ\text{C}$, CS_2/DEA mole ratios = 0.1 - 0.2).

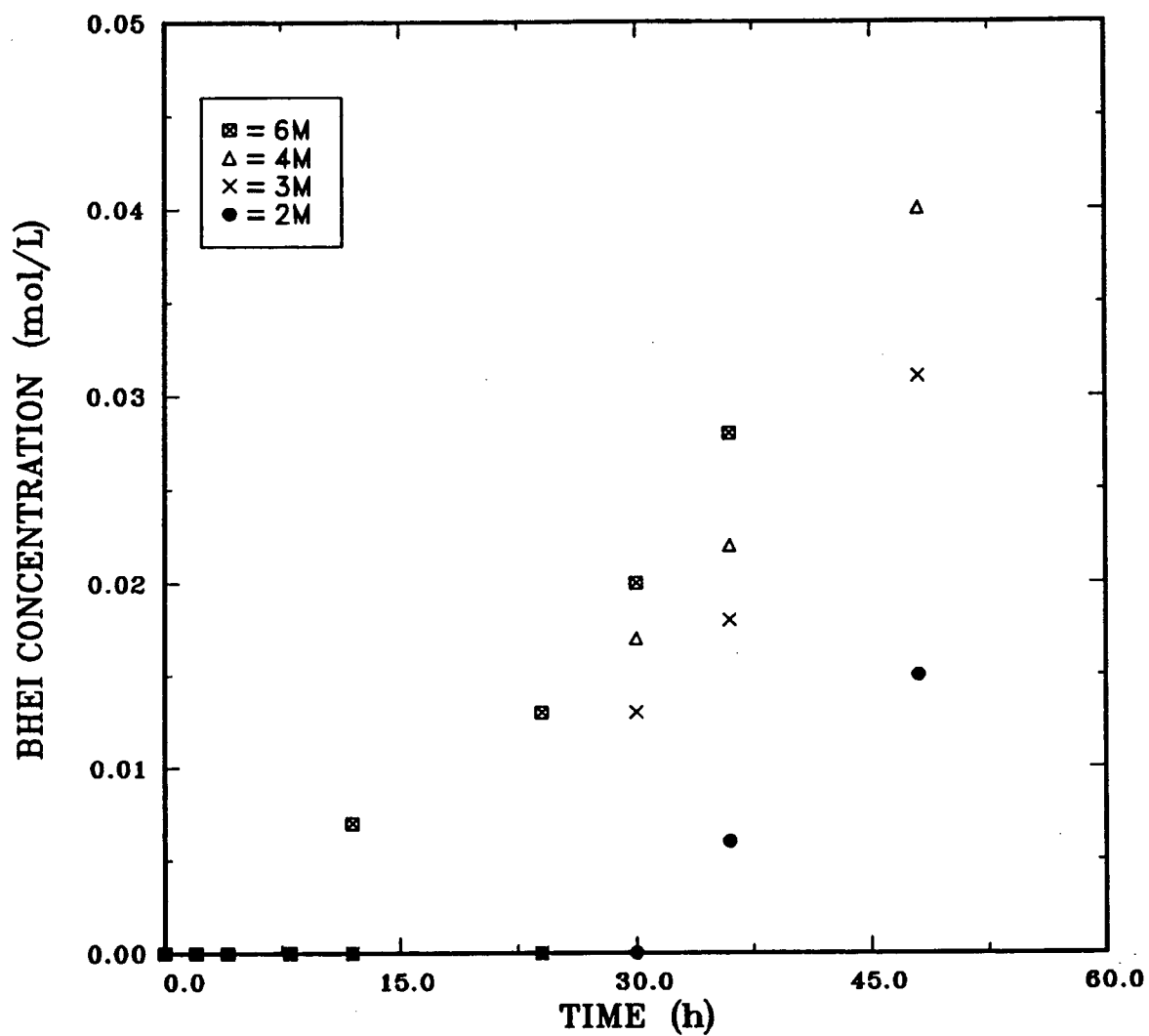


Figure 5.49: BHEI concentration as a function of initial DEA concentration and time (CS_2 volume = 6 mL, $T = 165^\circ\text{C}$, CS_2/DEA mole ratios = 0.1 - 0.2).

BHEP and HEOD (Figs. 5.44 - 5.46), while the concentrations of HEI, THEED and BHEI (Figs. 5.47 - 5.49) continue to rise. These trends suggest that the effect of the declining water content in highly concentrated DEA solutions is more pronounced on some degradation reactions than others.

5.2.2 EFFECTS OF TEMPERATURE

The effects of temperature on DEA degradation are shown in Figs. 5.50 - 5.52 at initial DEA concentrations of 40, 30 and 20 wt%, respectively. The rate of degradation increases with temperature at all levels of initial DEA concentration. Figure 5.53 shows that the temperature dependency of the rate constants obtained from the slopes of the curves in Figs. 5.50 - 5.52 conforms to the Arrhenius expression. This result is consistent with the first order reaction kinetics suggested earlier. However, for $T = 180^{\circ}\text{C}$, degradation is much more rapid and the plot deviate substantially from linearity (see Fig. 5.52). At this temperature (and higher ones), the reactions become more complex, producing far more degradation compounds than at lower temperatures (see chapter 4). Consequently, the overall rate cannot be represented by a simple first order expression. Since the highest operating temperature in DEA plants is far below 180°C , further discussions are limited to runs conducted at $T \leq 165^{\circ}\text{C}$.

The rates of production and depletion of MEA increase with temperature. Thus the final concentration of MEA decreases as temperature increases (Fig. 5.54).

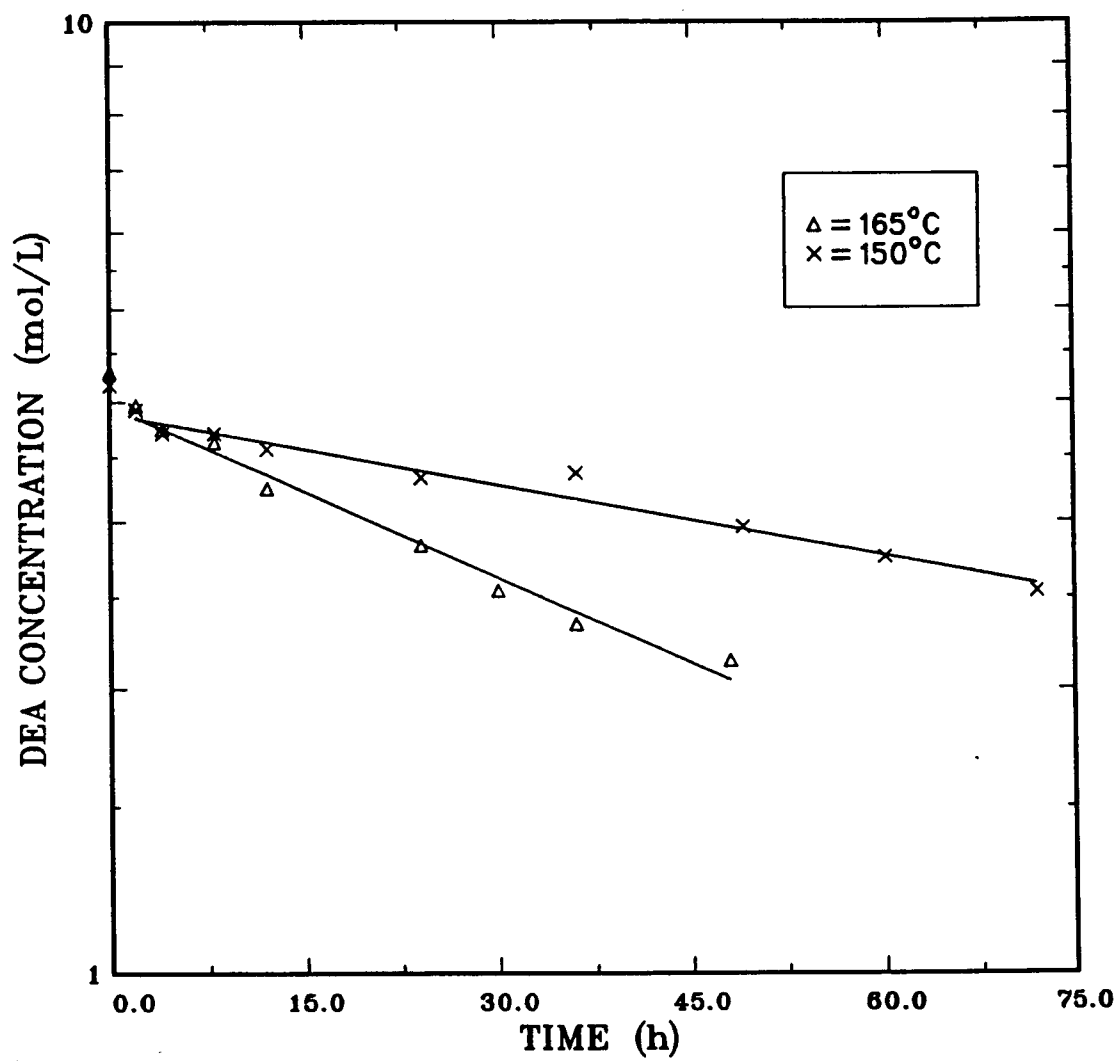


Figure 5.50: DEA concentration as a function of temperature and time
($\text{DEA}_0 = 4\text{M}$, CS_2 volume = 6 mL, CS_2/DEA mole ratio = 0.1).

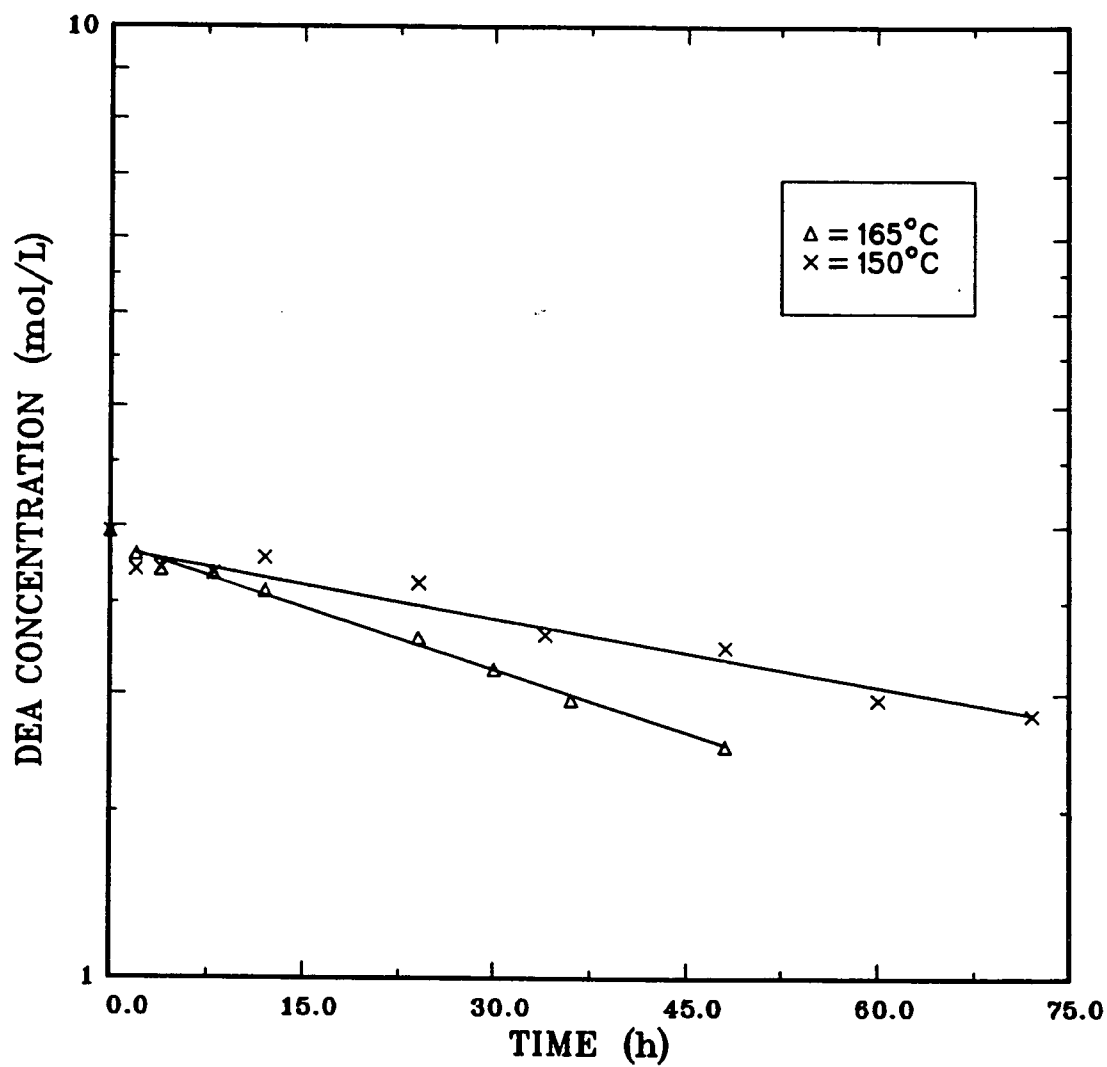


Figure 5.51: DEA concentration as a function of temperature and time
($\text{DEA}_0 = 3\text{M}$, CS_2 volume = 6 mL, CS_2/DEA mole ratio = 0.13).

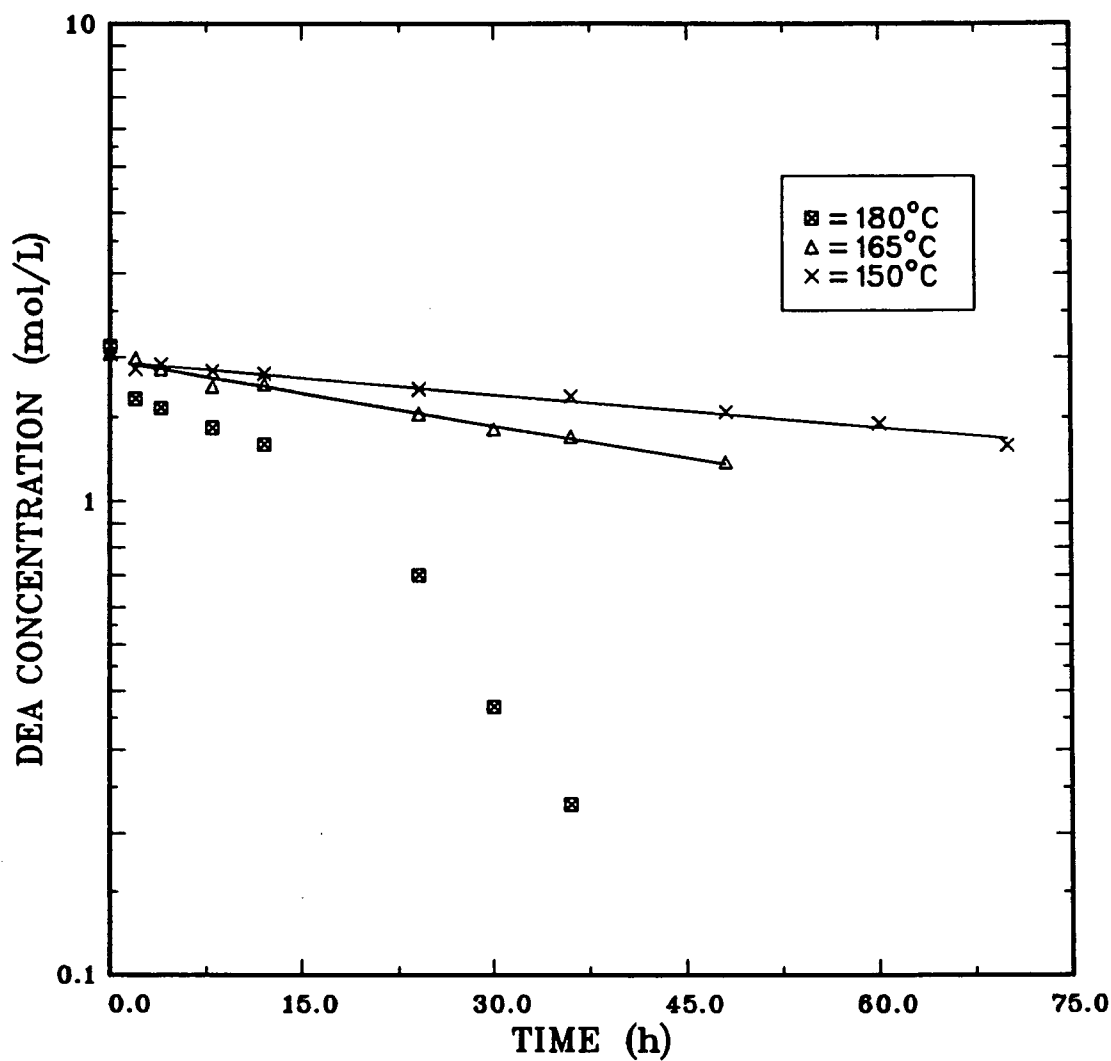


Figure 5.52: DEA concentration as a function of temperature and time
(DEA₀ = 2M, CS₂ volume = 6 mL, CS₂/DEA mole ratio = 0.2).

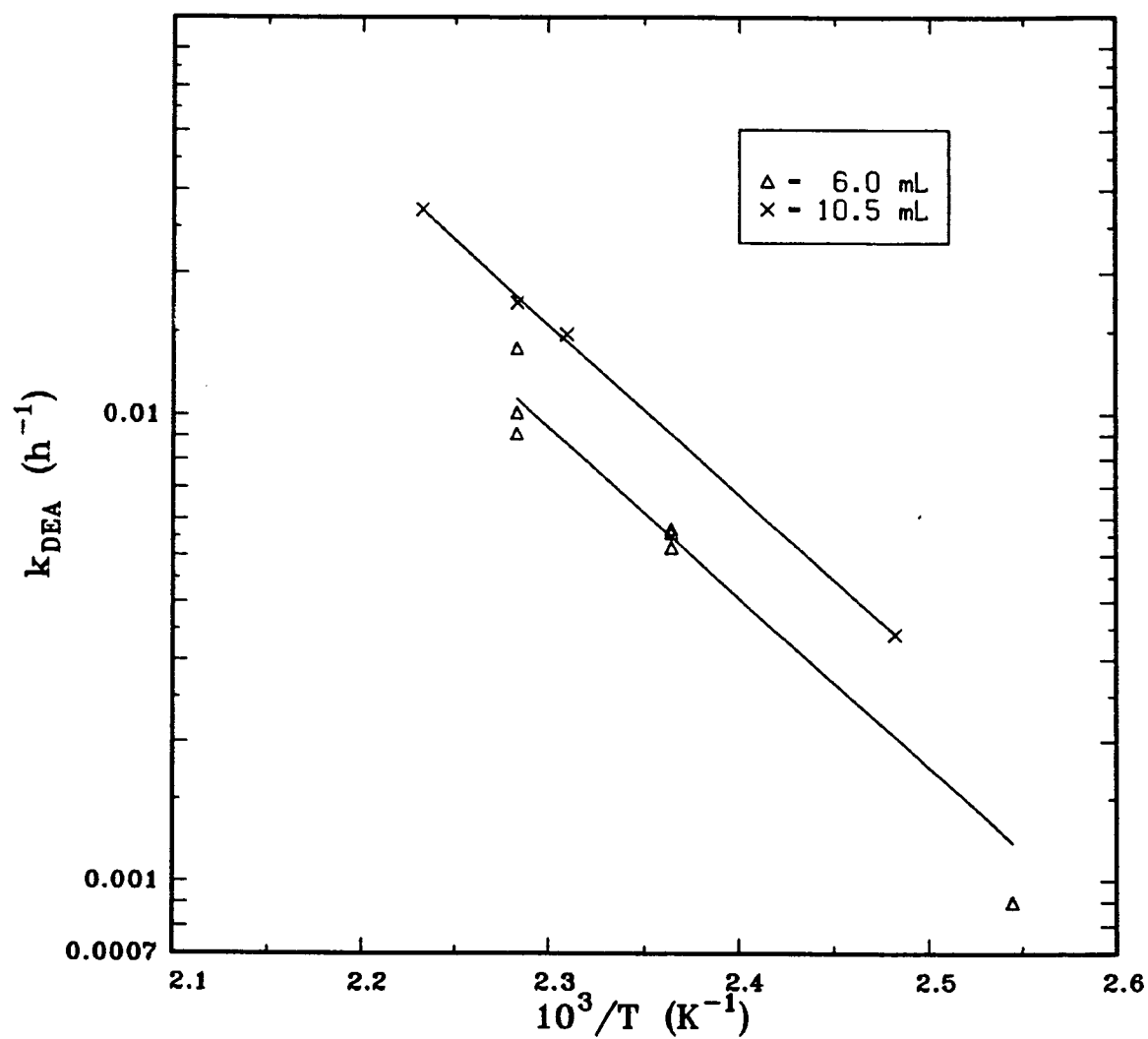


Figure 5.53: Arrhenius plots for the overall degradation rate constant as a function of initial CS_2 volume.

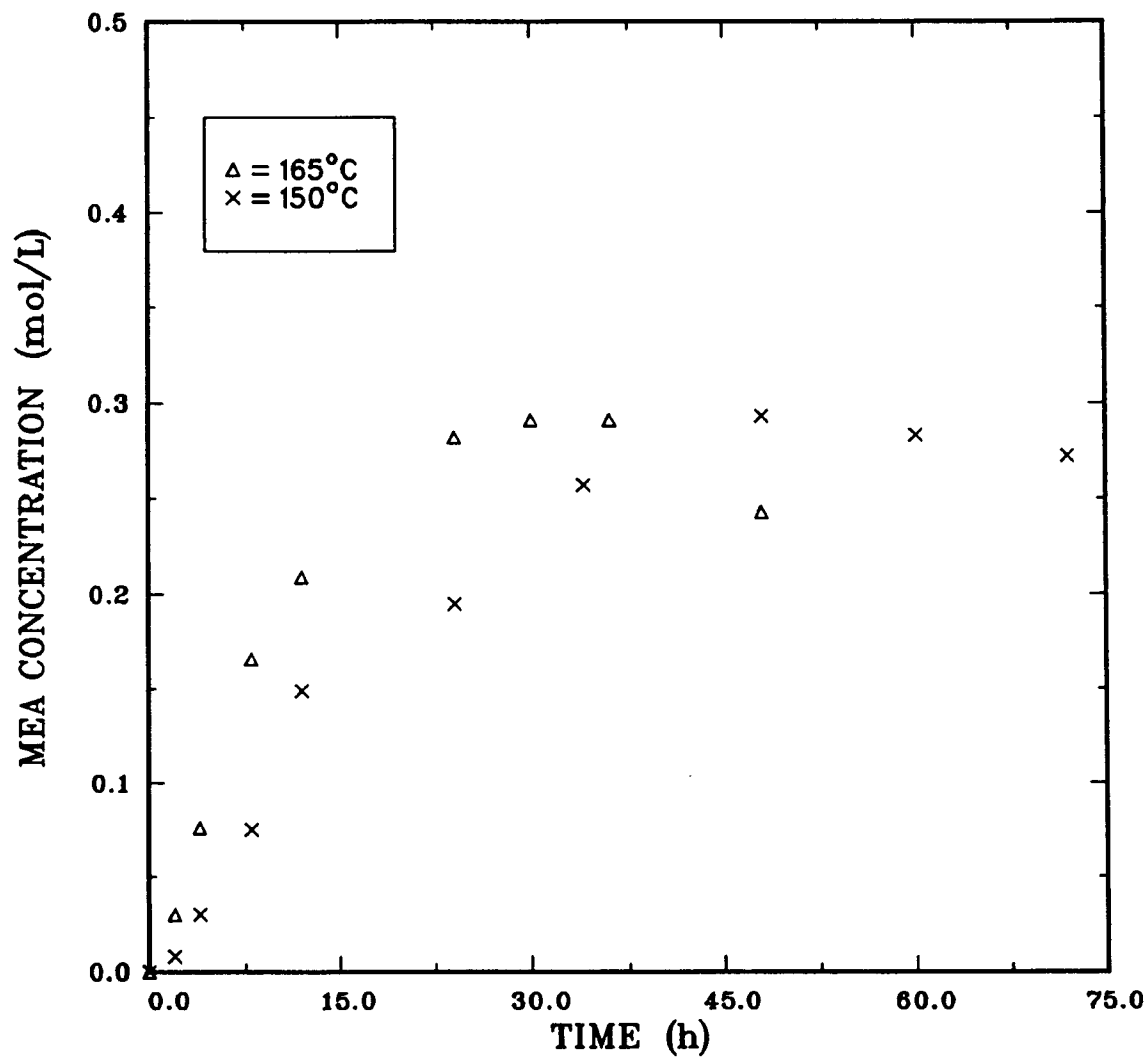


Figure 5.54: MEA concentration as a function of temperature and time
($\text{DEA}_0 = 3\text{M}$, CS_2 volume = 6 mL, CS_2/DEA mole ratio = 0.13).

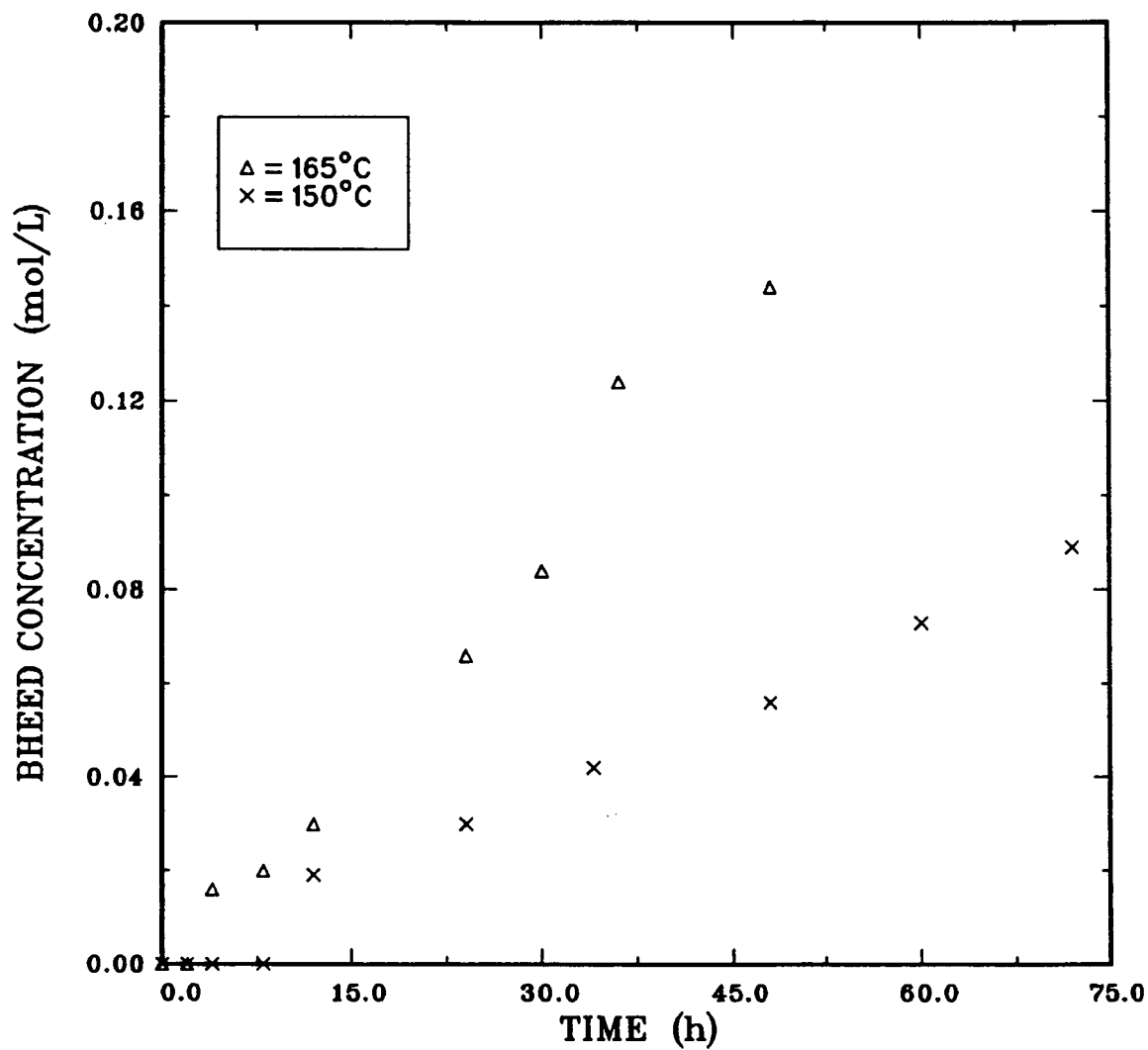


Figure 5.55: BHEED concentration as a function of temperature and time
(DEA₀ = 3M, CS₂ volume = 6 mL, CS₂/DEA mole ratio = 0.13).

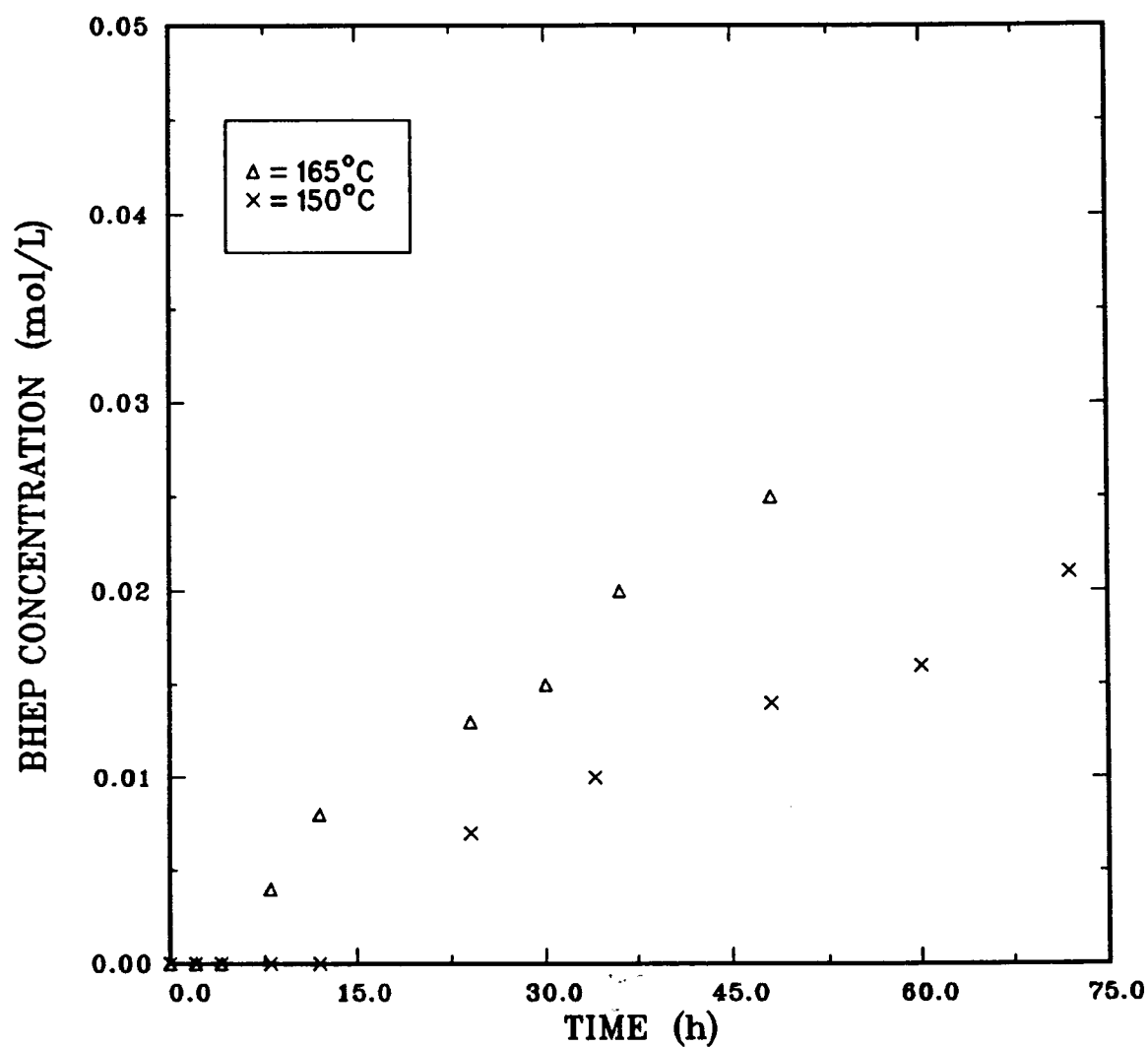


Figure 5.56: BHEP concentration as a function of temperature and time
($\text{DEA}_0 = 3\text{M}$, CS_2 volume = 6 mL, CS_2/DEA mole ratio = 0.13).

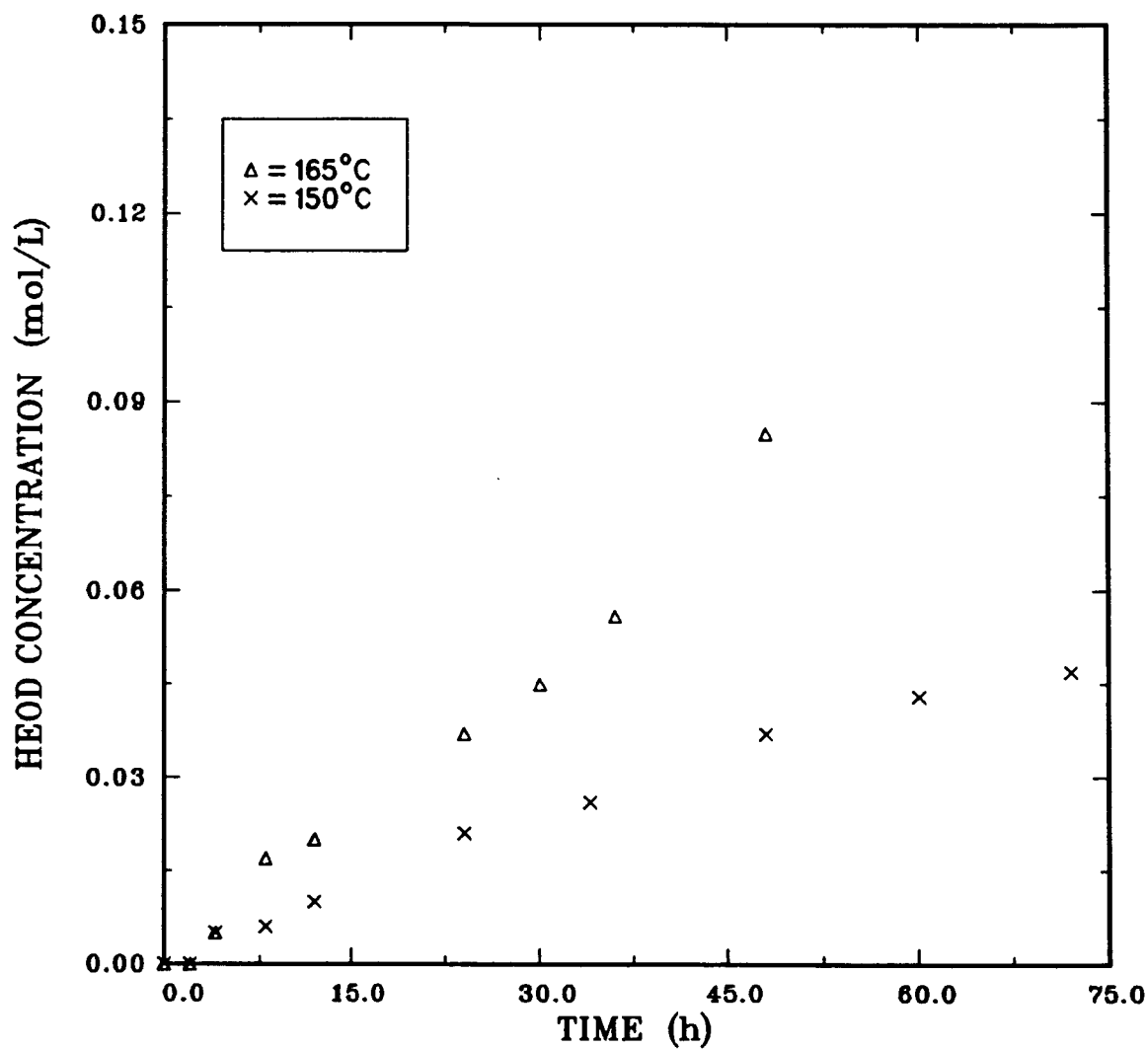


Figure 5.57: HEOD concentration as a function of temperature and time
(DEA₀ = 3M, CS₂ volume = 6 mL, CS₂/DEA mole ratio = 0.13).

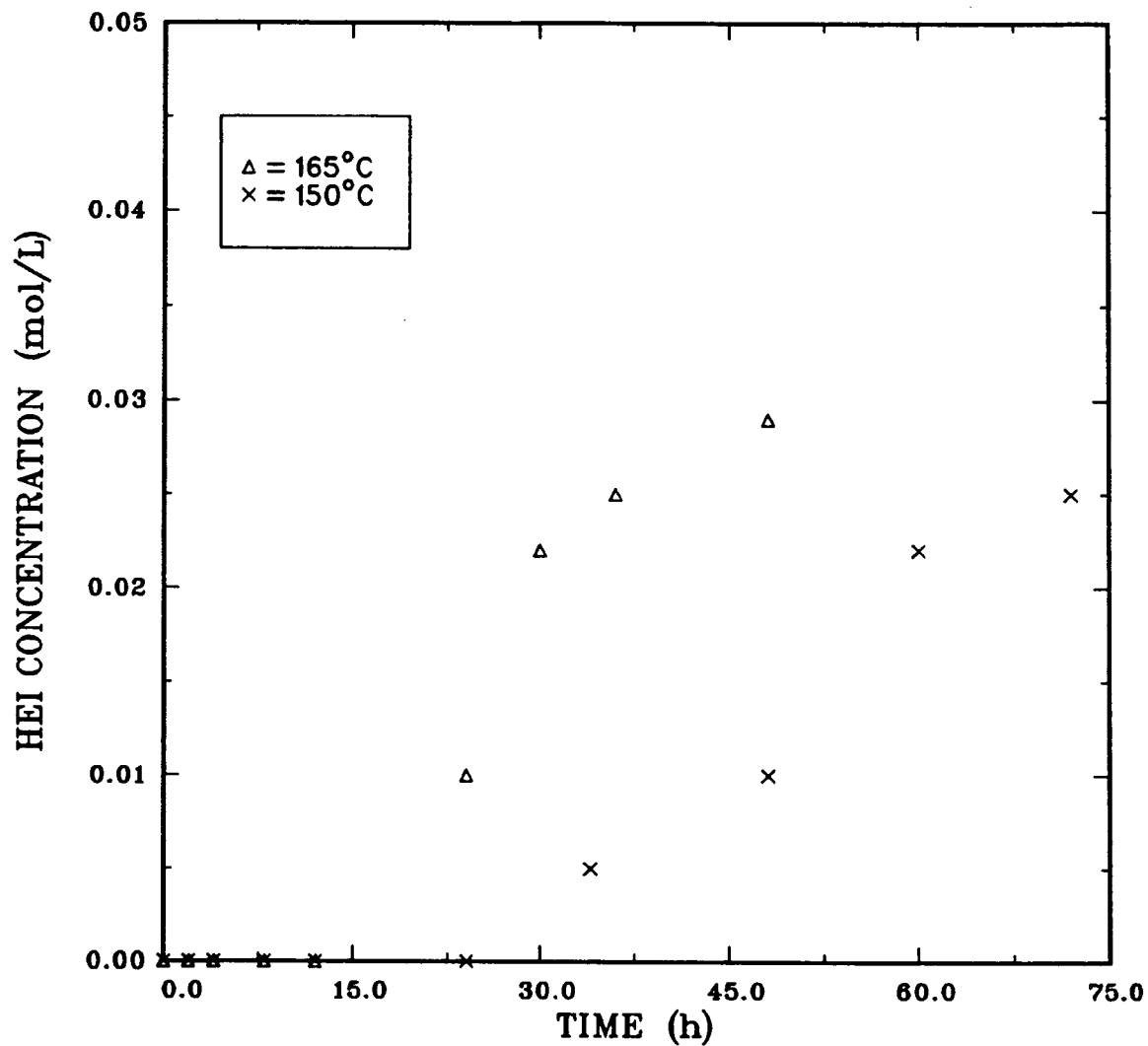


Figure 5.58: HEI concentration as a function of temperature and time
(DEA₀ = 3M, CS₂ volume = 6 mL, CS₂/DEA mole ratio = 0.13).

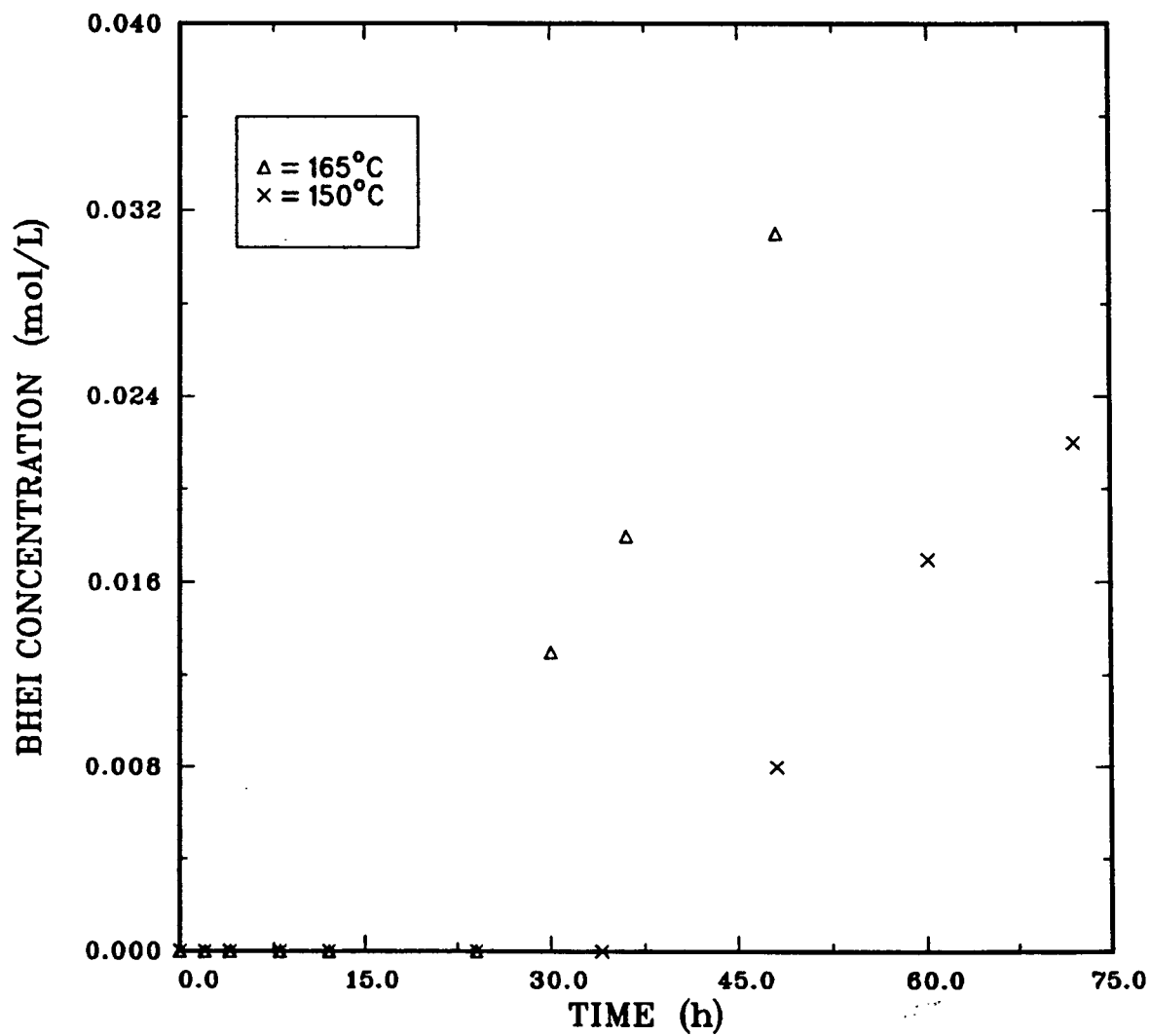


Figure 5.59: BHEI concentration as a function of temperature and time
(DEA₀ = 3M, CS₂ volume = 6 mL, CS₂/DEA mole ratio = 0.13).

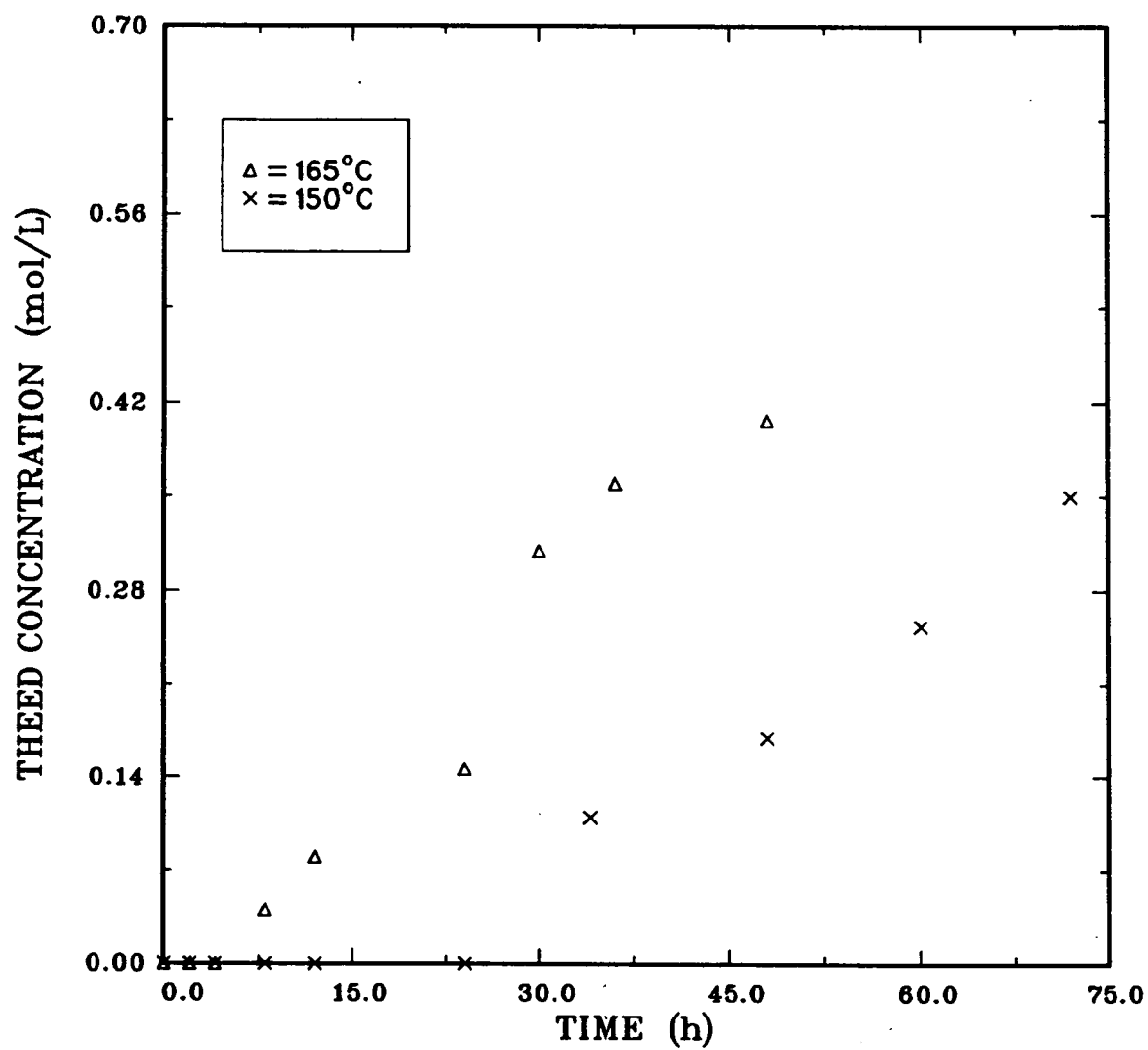


Figure 5.60: THEED concentration as a function of temperature and time
(DEA₀ = 3M, CS₂ volume = 6 mL, CS₂/DEA mole ratio = 0.13).

The rates of formation and final concentrations of BHEED, BHEP, HEOD, HEI and BHEI increase with increasing temperature (see Figs. 5.55 to 5.59). Except for HEI whose concentrations approach a constant value at each temperature level, the concentrations of the other compounds increase throughout the durations of the runs.

The rate of formation of THEED increases with temperature as shown by Fig. 5.60. At 165 °C, the THEED concentration tends to a maxima while at 150 °C, the concentration increased throughout the run. This trend again confirms that the rate of depletion of THEED increases with temperature.

5.2.3 EFFECTS OF INITIAL VOLUME OF CS₂

The curves in Fig. 5.61 represent runs conducted with 250 mL of 3M aqueous DEA solutions and 2.5, 6 and 10.5 mL of CS₂ at 165 °C. The corresponding CS₂/DEA mole ratios are 0.055, 0.133 and 0.233 respectively. The rate of DEA degradation increases with the initial CS₂ volume (or CS₂/DEA mole ratio) in the reactor. The linearity of the plots indicates that the first order reaction kinetics are not altered even at the highest CS₂ volume investigated. The fact that the degradation rate constant increases with CS₂ volume and not with DEA concentration shows that when the concentration of DEA exceeds that of CS₂, the rate of degradation is influenced by the CS₂ volume and not the CS₂/DEA mole ratio. The masses of the solid products recovered from the runs increased with the initial volume of CS₂. Since DEA was in excess

of CS_2 in all the runs, the increase in the mass of solid may be due to the increase in the formation of the dithiocarbamate salt as described by Eqs. 2.14 and 2.15. The increased formation of the salt could also be responsible for the sharper drop in DEA concentration between 0 and 2 hours, in the run conducted with 10.5 mL of CS_2 .

Figure 5.62 shows that the initial rate of MEA formation and the maximum concentration increase with CS_2 volume. The final concentrations of MEA tend to a constant value which is independent of the initial CS_2 volume. This suggests that MEA production and depletion probably attained equilibrium at the operating conditions.

The rates of production and concentrations of BHEED, BHEP, HEOD, HEI and BHEI increase with the initial CS_2 volume as shown by Figs. 5.63 to 5.67, respectively. At each level of CS_2 , the concentration of HEOD tends towards a constant final value which suggests an approach to equilibrium.

THEED production rates and concentrations also increase with initial CS_2 volume. The maxima exhibited in Fig. 5.68, particularly at an initial CS_2 volume of 10.5 mL, is indicative of conversion to other compounds such as BHEP.

Similar to the COS-DEA systems, the degradation reactions were particularly sensitive to changes in temperature. Increasing the temperature from 120 to 165 °C for a 20 wt% solution, caused a 10 fold increase in the degradation rate constant. Doubling the initial DEA concentration from 20 to 40 wt% caused 1.5 and 1.1 fold increases in the rate constant at 165 and 150 °C, respectively. A four fold increase in the volume of CS_2 resulted in 3.6 fold increase in the rate constant.

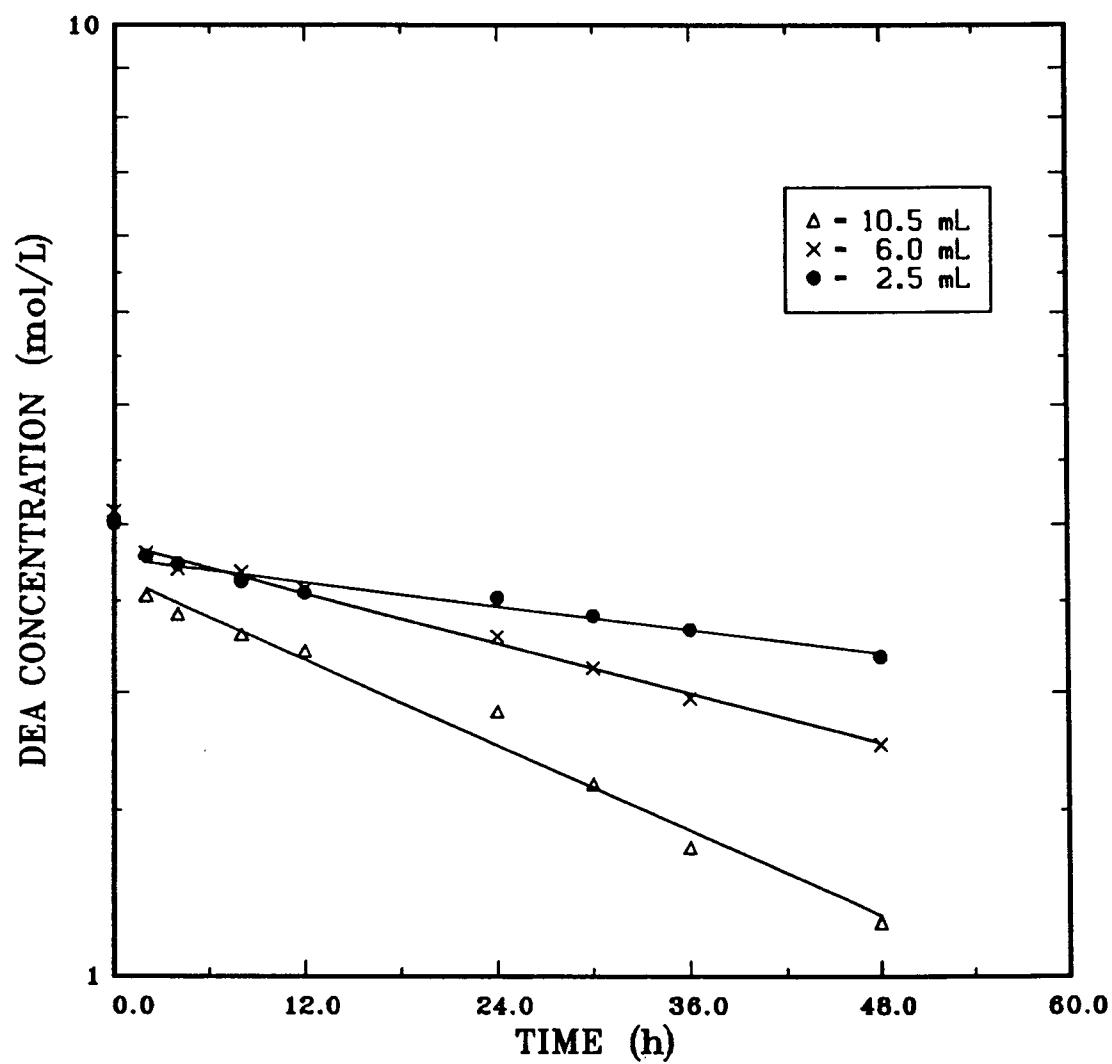


Figure 5.61: DEA concentration as a function of initial CS_2 volume and time ($\text{DEA}_0 = 3\text{M}$, $T = 165^\circ\text{C}$).

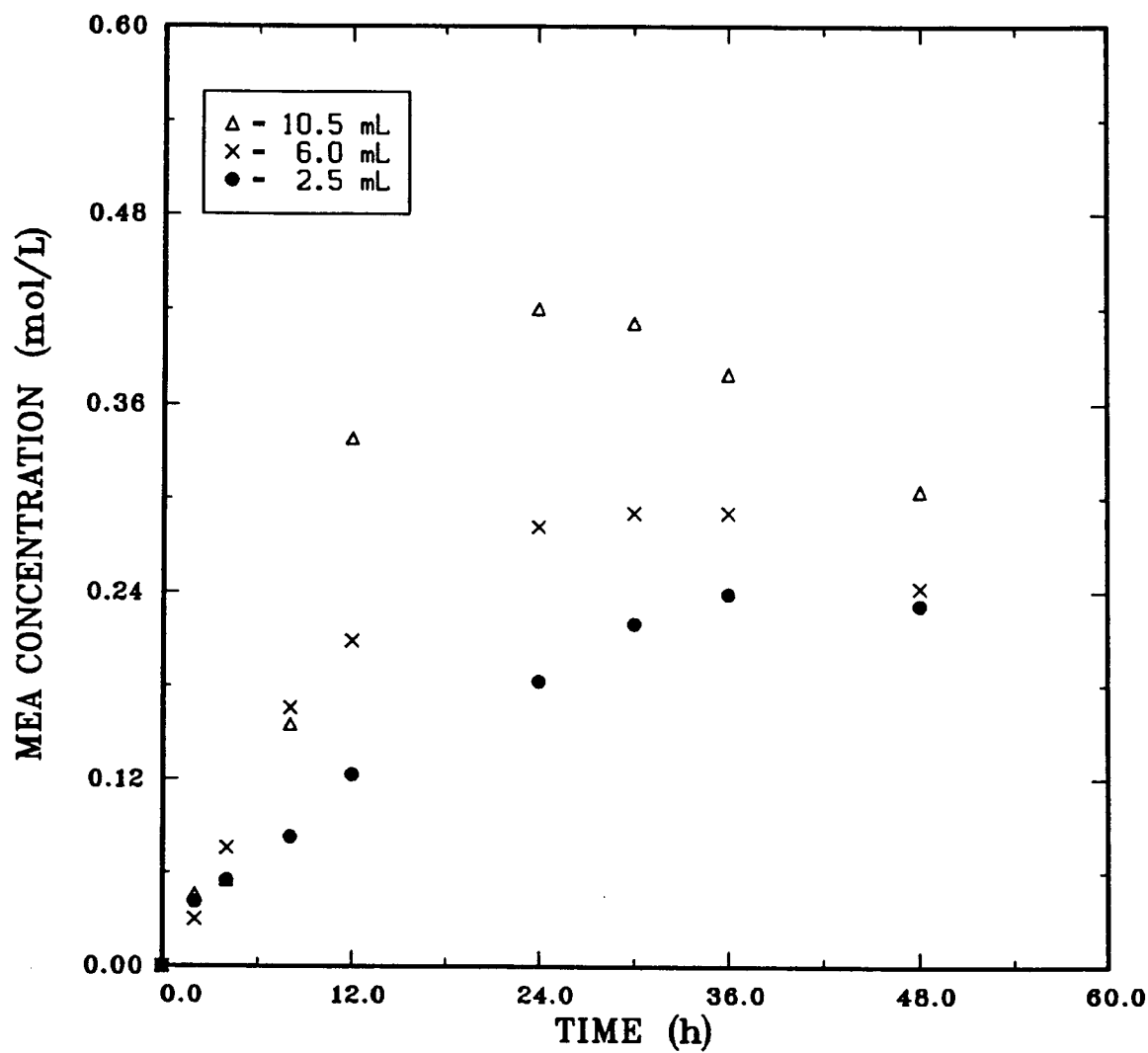


Figure 5.62: MEA concentration as a function of initial CS_2 volume and time ($\text{DEA}_0 = 3\text{M}$, $T = 165^\circ\text{C}$).

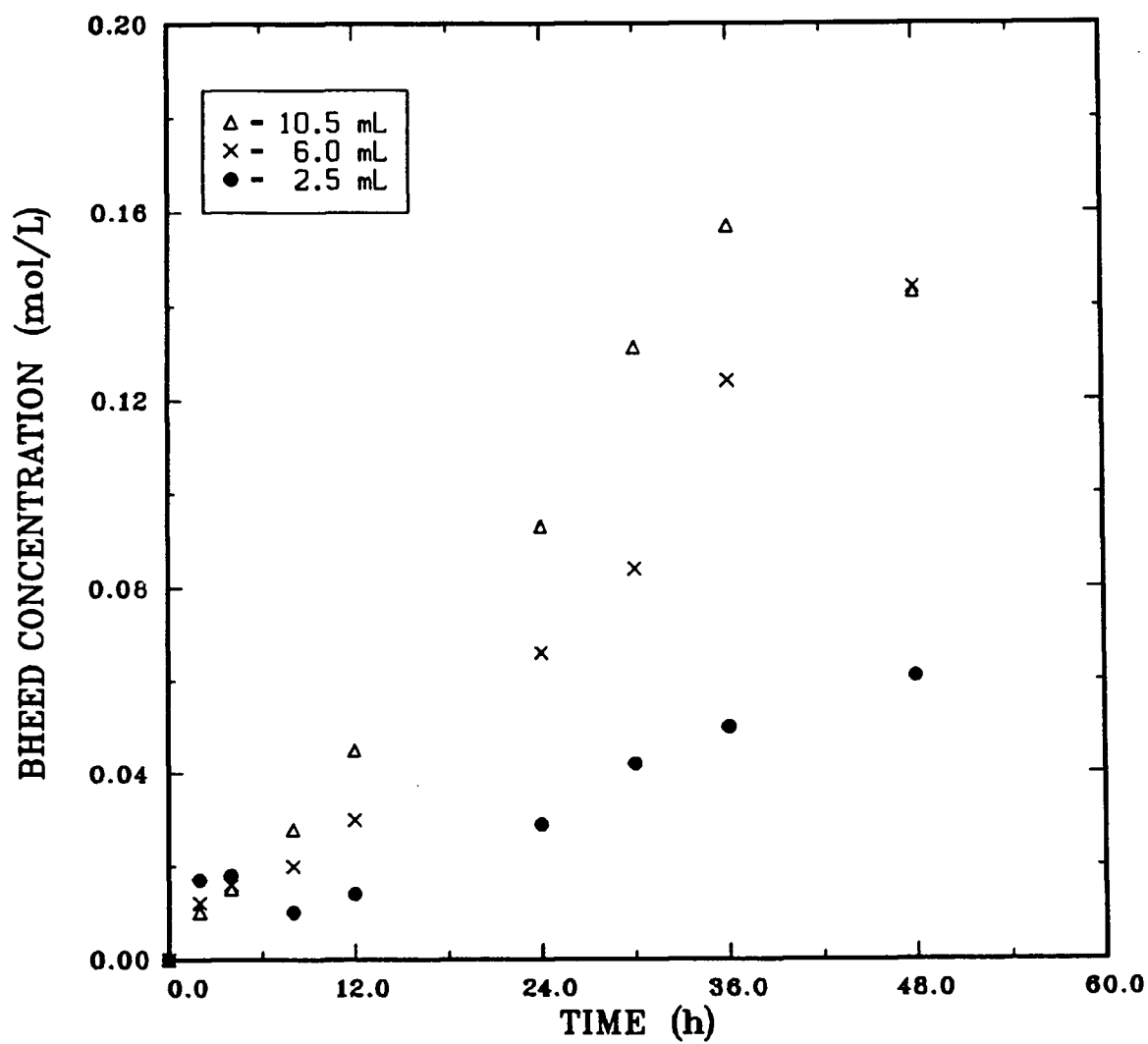


Figure 5.63: BHEED concentration as a function of initial CS₂ volume and time (DEA₀ = 3M, T = 165 °C).

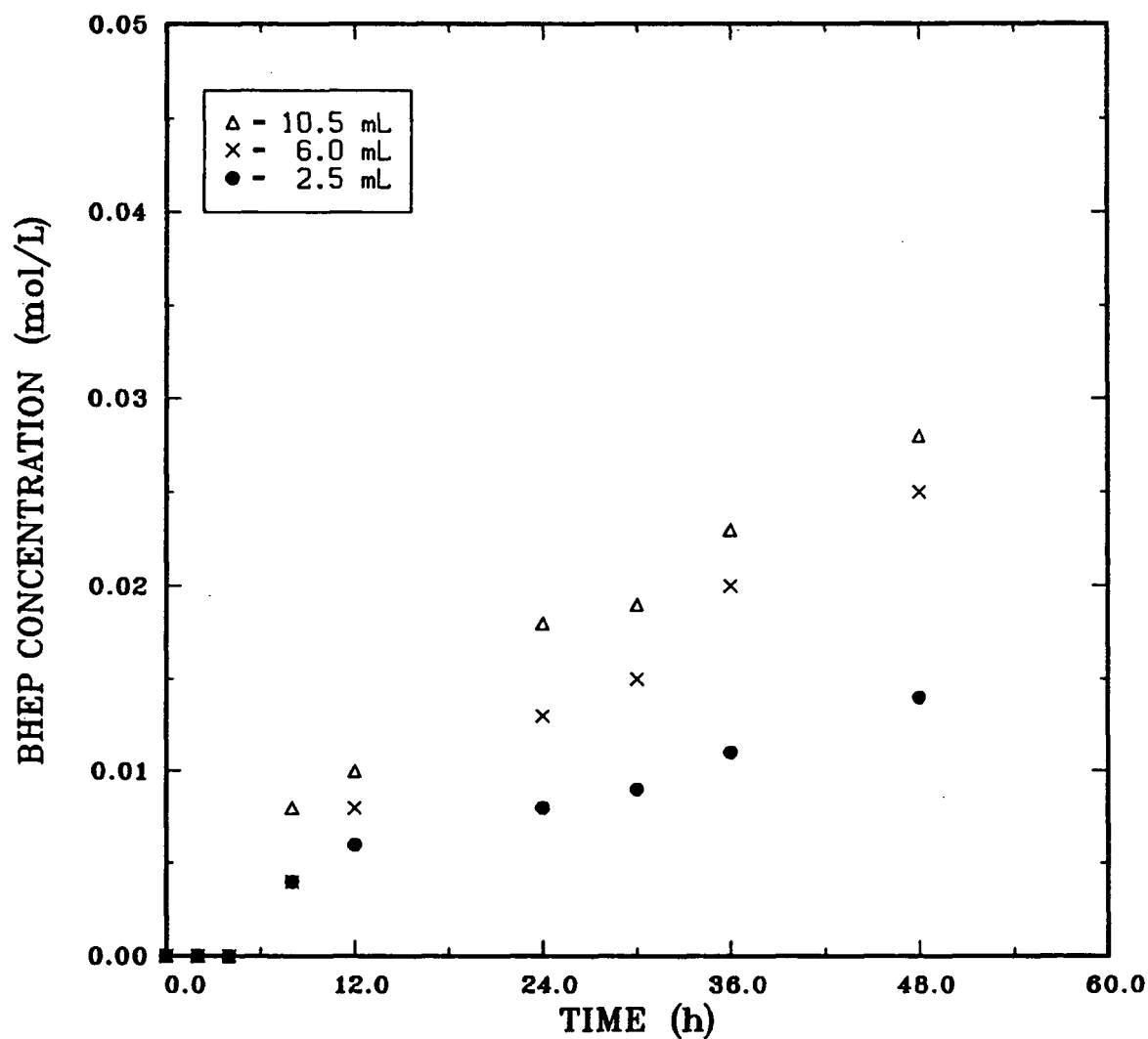


Figure 5.64: BHEP concentration as a function of initial CS_2 volume and time ($\text{DEA}_0 = 3\text{M}$, $T = 165^\circ\text{C}$).

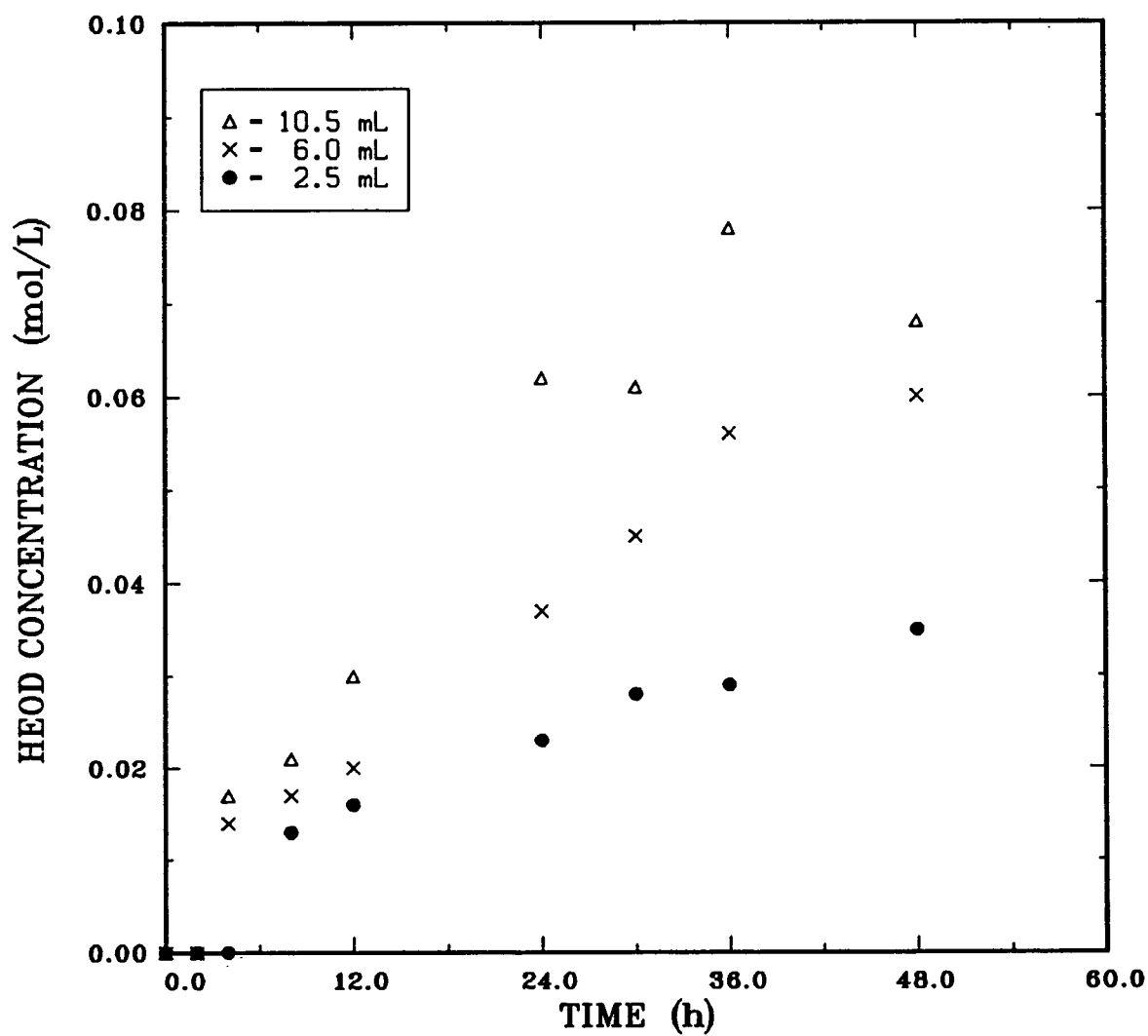


Figure 5.65: HEOD concentration as a function of initial CS₂ volume and time (DEA₀ = 3M, T = 165 °C).

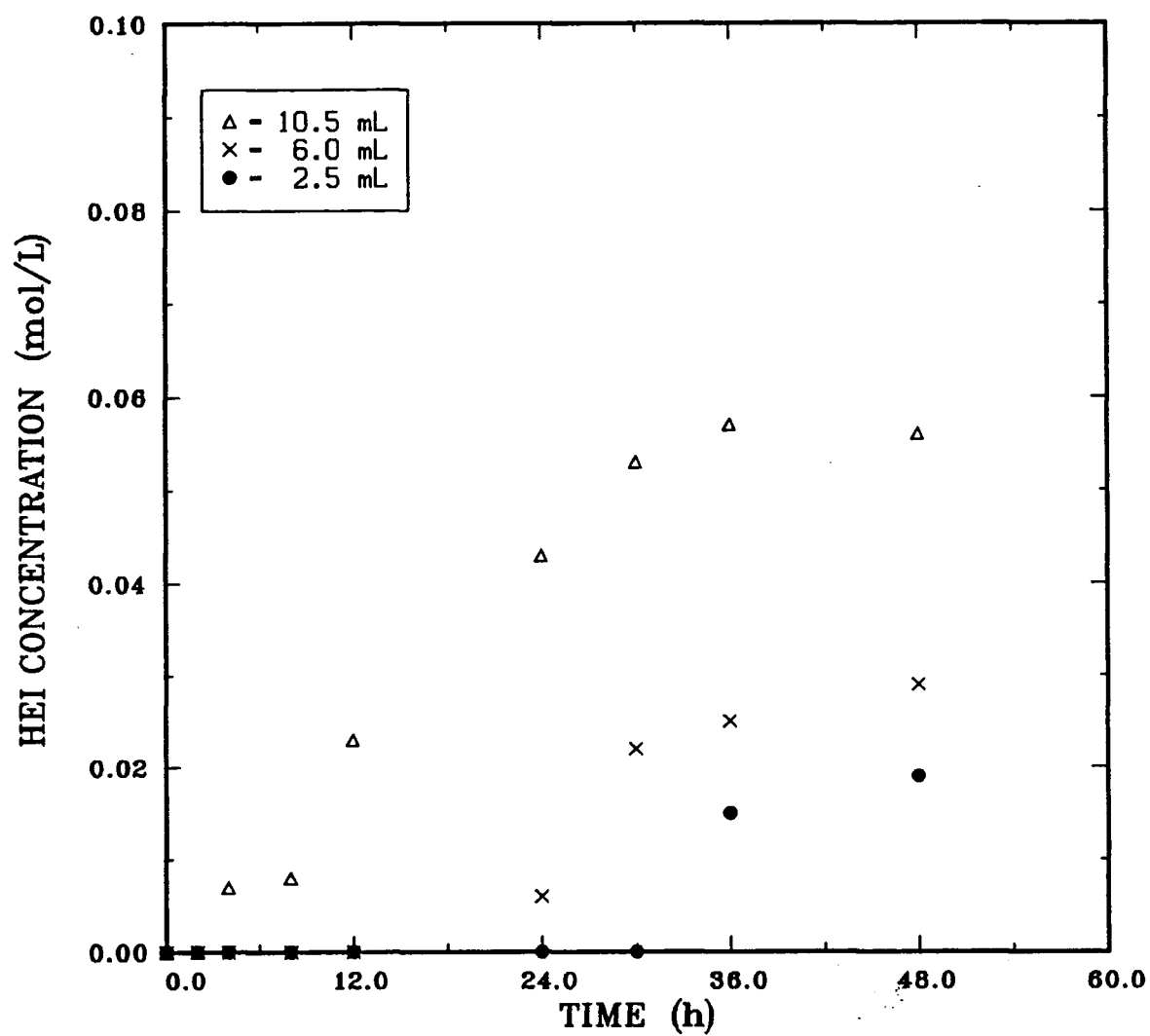


Figure 5.66: HEI concentration as a function of initial CS_2 volume and time ($\text{DEA}_0 = 3\text{M}$, $T = 165^\circ\text{C}$).

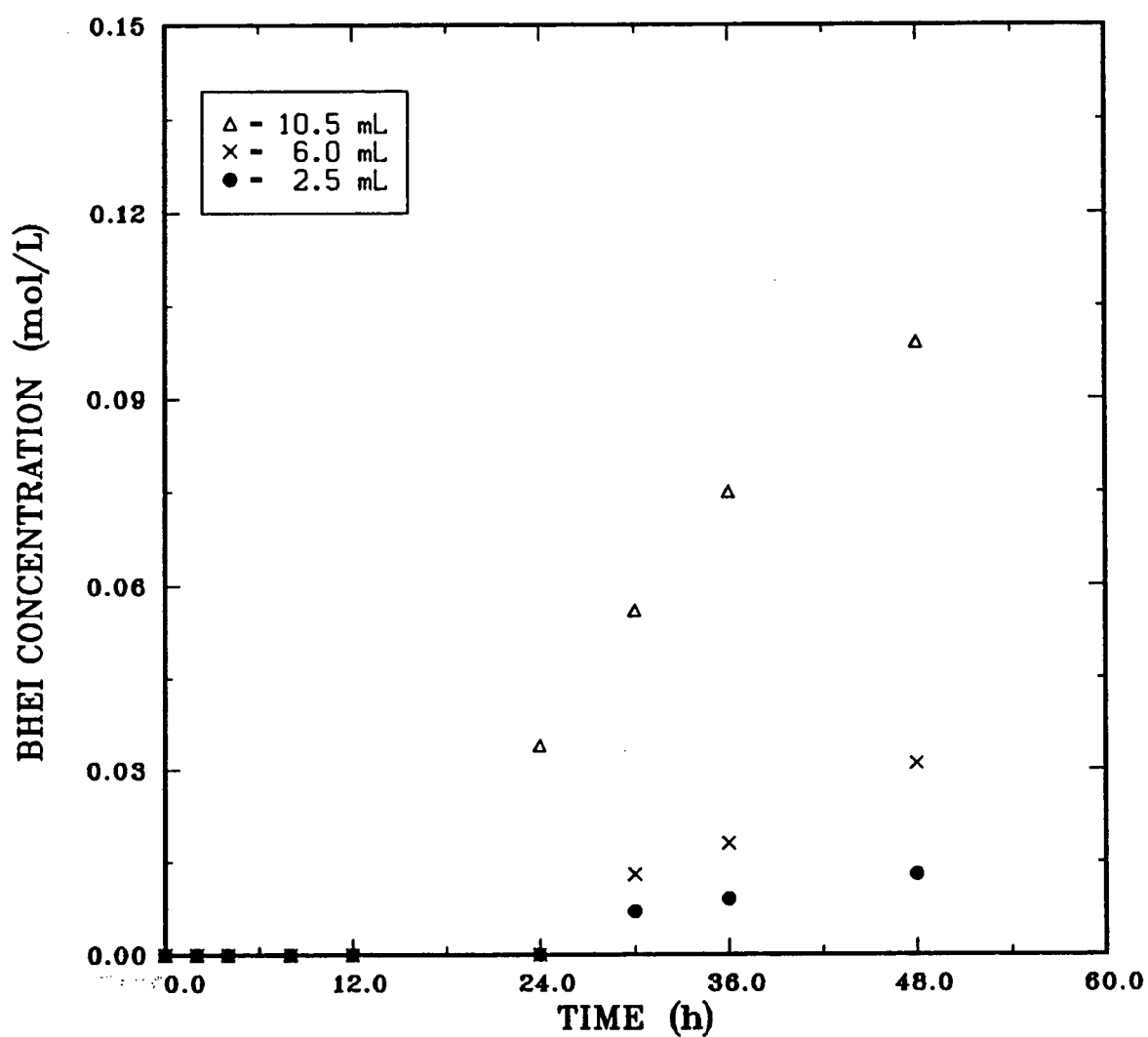


Figure 5.67: BHEI concentration as a function of initial CS_2 volume and time ($\text{DEA}_0 = 3\text{M}$, $T = 165^\circ\text{C}$).

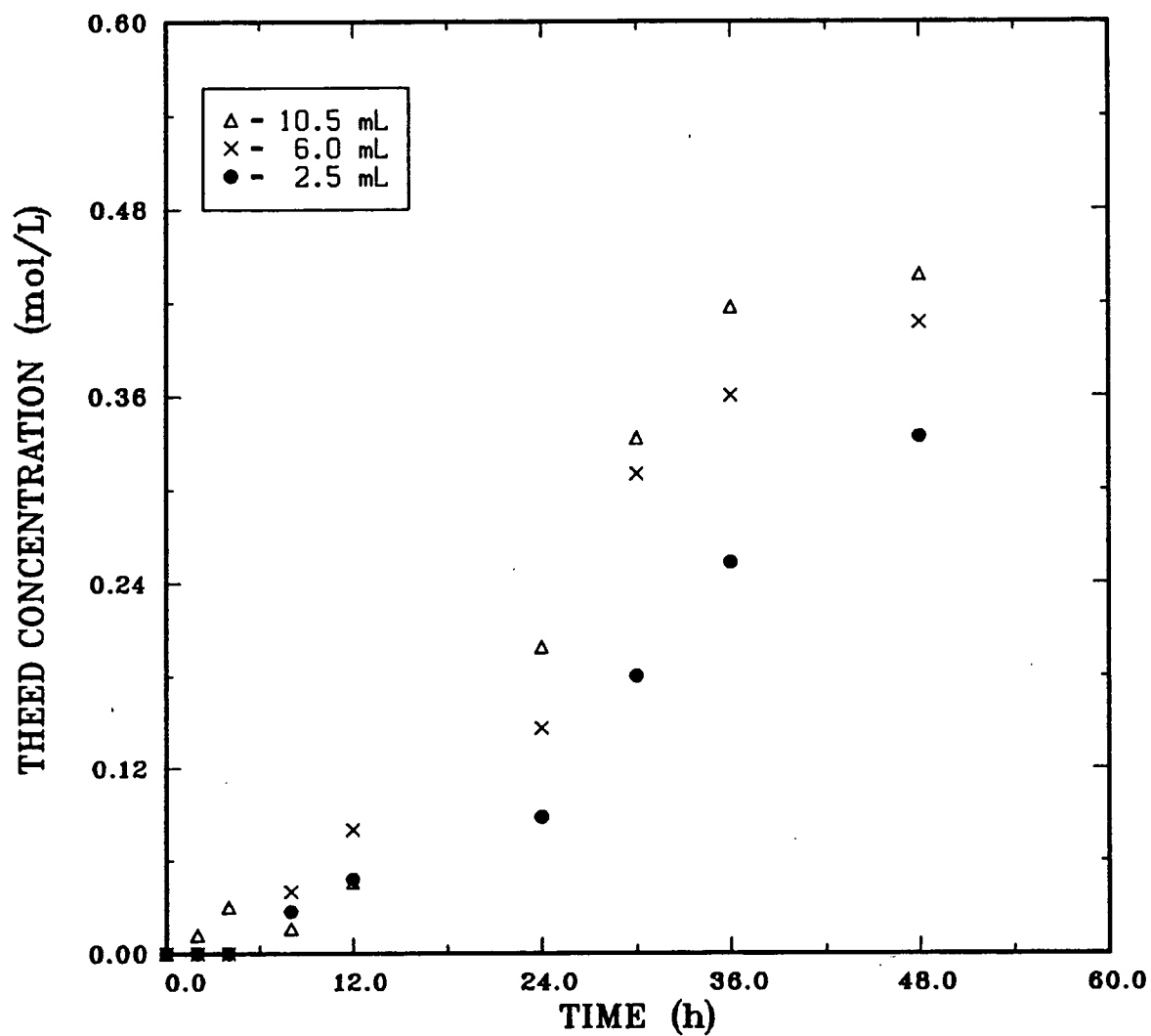


Figure 5.68: THEED concentration as a function of initial CS_2 volume and time ($\text{DEA}_0 = 3\text{M}$, $T = 165^\circ\text{C}$).

The results presented in this chapter indicate that the rate of degradation of DEA in COS-DEA systems is dependent on the initial DEA concentration, while in the CS₂-DEA system it appears not to be. The detection of similar products in both systems, suggests similar reaction mechanisms. Therefore it is necessary to clarify the contradictory findings. It should be noted that the DEA concentrations obtained from the GC analysis are the total DEA in each system. However, degradation is induced primarily by the ionic species such as DEACOO⁻, DEAH⁺, DEACOS⁻, HCO₃⁻ etc. In the case of the CS₂-DEA systems studied, the DEA concentration was always in excess of CS₂. Therefore, a significant portion of CS₂ is tied up in the formation of the dithiocarbamate salt of DEA, leaving very little for conversion via hydrolysis. By contrast, no stable salt is formed in the COS-DEA system. The COS absorbed is subsequently hydrolysed to CO₂ and H₂S. The gases in solution undergo ionisation reactions to generate the ions that induce degradation. Since the solubility of acid gases in amine solutions increase with basicity, the concentration of the ions that induce degradation will increase with DEA concentration. Therefore, the COS-DEA systems, by virtue of containing appreciable concentrations of CO₂, H₂S, COS and their ionic species, have degradation rates that are dependent on the total DEA concentration while the rates of degradation in CS₂-DEA systems which have significantly lower concentrations of such species are independent of total DEA concentration.

It is shown in appendix E that the errors in the reported concentrations are $\pm 5\%$ for DEA while those for the degradation products, particularly THEED, may be up to $\pm 20\%$.

CHAPTER 6

EXPERIMENTS DESIGNED TO ELUCIDATE REACTION MECHANISMS

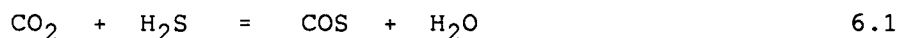
The COS-DEA and CS₂-DEA systems produced numerous degradation products as revealed in Chapter 4. The results presented in Chapter 5 showed that a number of series, parallel and consecutive reactions are occurring in both COS-DEA and CS₂-DEA systems. However, the information is insufficient to develop reaction mechanisms. This chapter presents the results of experiments conducted to highlight the roles of the principal degradation compounds and the acid gases in the degradation process. The information acquired is subsequently used to develop reaction mechanisms.

6.1 EFFECT OF MIXED GASES

Compounds such as BHEP, HEOD and THEED were previously identified as the major degradation products in the CO₂-DEA system (13,14,16). Their presence in the COS-DEA and CS₂-DEA systems is an indication that COS and CS₂ are hydrolysed to CO₂ and H₂S. Both systems therefore contain eventually H₂S and CO₂. Five runs were conducted to establish the role of H₂S and CO₂ in the degradation. Solutions containing 30 wt% DEA were subjected for 48 hours to the following initial gas mixtures at 165 °C and a total pressure of 2.1 MPa: (1) 15.3% H₂S, balance N₂; (2) 14.7% CO₂, balance N₂; (3) 15.2% CO₂, 15.2% H₂S, balance N₂; (4) 30% CO₂, 15% H₂S, balance N₂; (5) 15.5% CO₂, 29.9% H₂S, balance N₂.

Figures 6.1 - 6.8 show the concentrations of DEA and the degradation products resulting from the experiments.

Mixture 1 did not cause any degradation which is consistent with the earlier findings of Choi (12) and Kim and Sartori (13). Mixture 2 produced HEOD, BHEP and THEED (consistent with the results of Kim and Sartori (13) and Kennard and Meisen (14)) whereas Mixtures 3, 4 and 5 yielded MEA, BHEED, BHEP, HEOD, HEI, THEED and BHEI as the major products. Only the mixtures containing H_2S and CO_2 (mixtures 3 - 5) yielded ketones and the solid product. These compounds must therefore be attributed to the sulphur species. The amount of solid products increased with H_2S concentration in the mixture, but was generally small compared to the ones recovered from the COS-DEA and CS_2 -DEA systems. The solids resembled those of the former system. Appreciable amounts of ketones, comparable with those of the COS-DEA systems, were produced in the system containing mixture 5, while only trace amounts were formed in mixtures 3 and 4. The formation of the ketones is therefore enhanced by high H_2S concentration. It could be that under such conditions, the equilibrium shown below is established:



The COS then induces degradation as previously described in chapter 4.

As shown by Fig. 6.1, the rate of DEA degradation increases slightly with H_2S but significantly with CO_2 . This trend can be explained in terms of the solution composition. As the H_2S concentration in the gas mixture increases, the concentration of H_2S in the solution

also increases, resulting in an increase in the ratio of protonated DEA to DEA carbamate. The effect of this is a reduction in the rate of CO_2 induced degradation. Consequently, the concentrations of BHEP, HEOD and THEED decrease with increasing H_2S concentration as shown in Figs. 6.2 - 6.4, respectively. However, the H_2S in the presence of CO_2 enables the formation of MEA, causing a slight increase in the overall rate of degradation. The high concentration of H_2S also inhibits the degradation of MEA through protonation. As a result, the concentration of MEA increases with H_2S concentration, as shown in Fig. 6.5. This in turn, affects the production of BHEED, HEI and BHEI, and their concentrations fall as H_2S concentration increases or CO_2 concentration decreases (Fig. 6.6 - 6.8).

It can be concluded from these results that a mixture of CO_2 and H_2S which has the relative proportions used in this study, is capable of inducing degradation reactions leading to the formation of MEA in aqueous DEA solutions. The MEA undergoes further reactions to produce compounds such as BHEED, HEI and BHEI while BHEP, HEOD and THEED are produced from DEA. Hydrogen sulphide therefore affects DEA degradation even though most of the principal degradation products do not contain sulphur.

The increased rate of degradation with H_2S concentration contradicts the findings of Choi (12) and Kim and Sartori (13). In the latter case, the mole ratio of CO_2 to H_2S was 1.10 to 0.03 or 36.7/1. Given such a high ratio, the deduction that H_2S exerts essentially no effect on the degradation is not surprising.

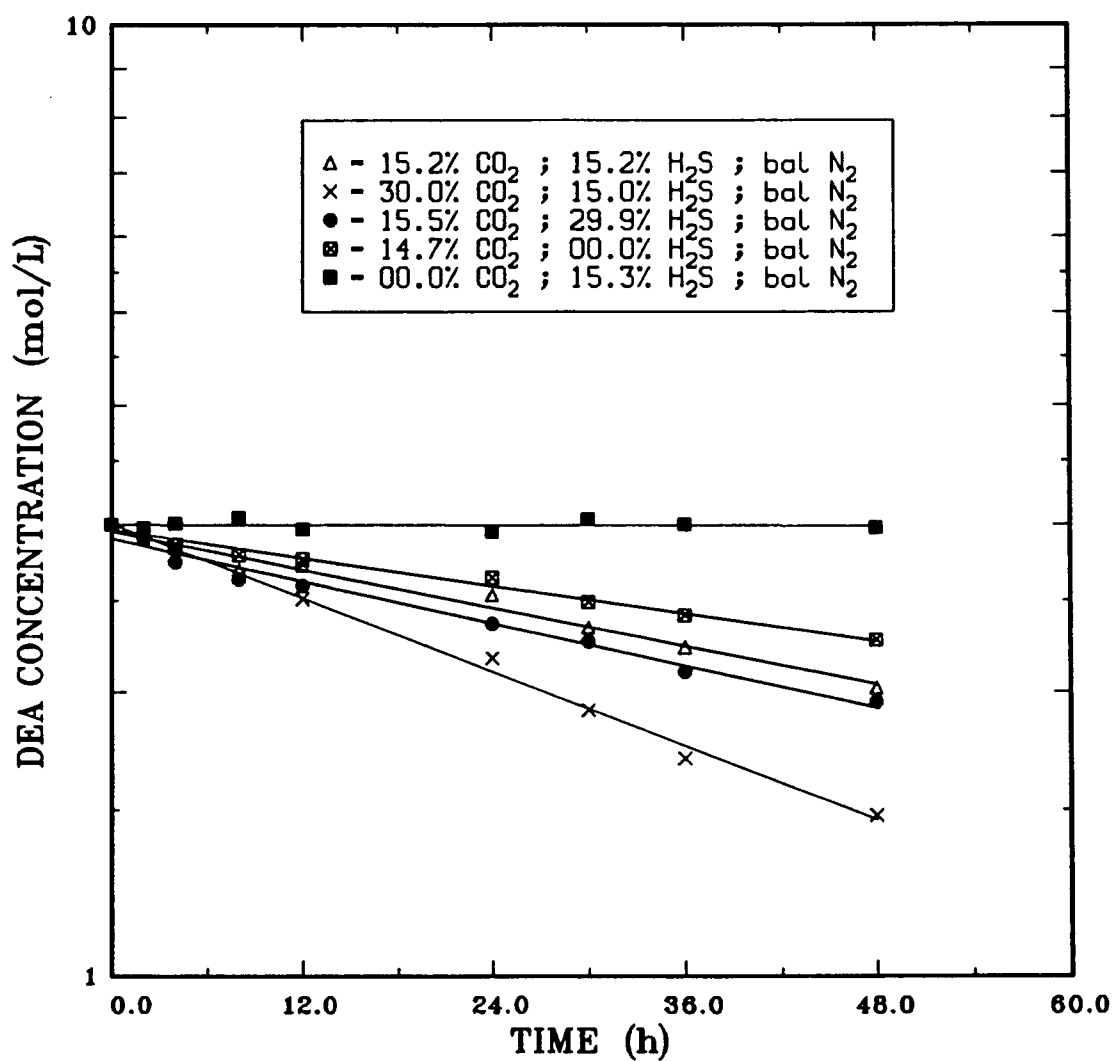


Figure 6.1: DEA concentrations as a function of time and gas composition (DEA₀ = 3M, T = 165 °C).

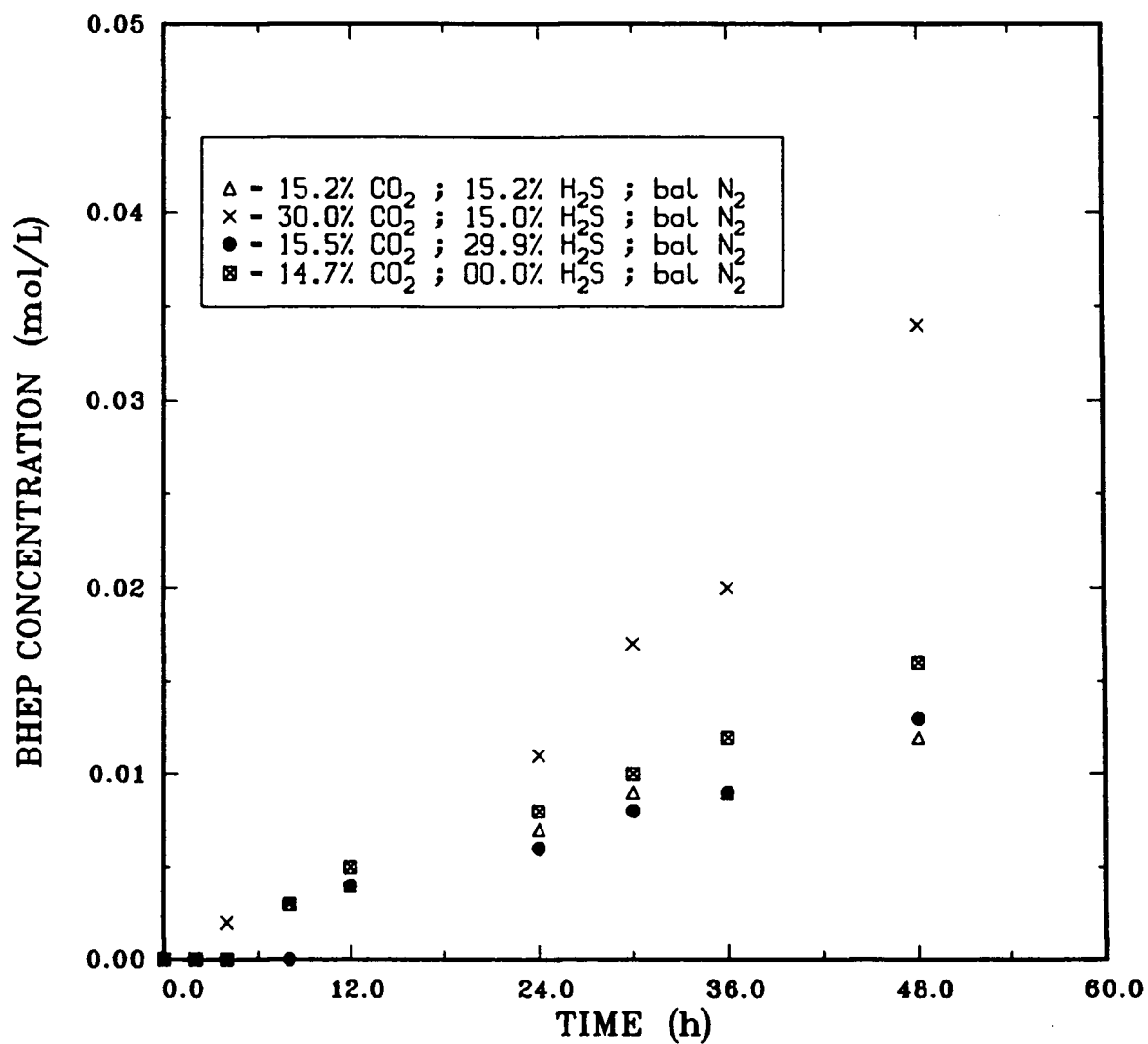


Figure 6.2: BHEP concentrations as a function of time and gas composition ($\text{DEA}_0 = 3\text{M}$, $T = 165^\circ\text{C}$).

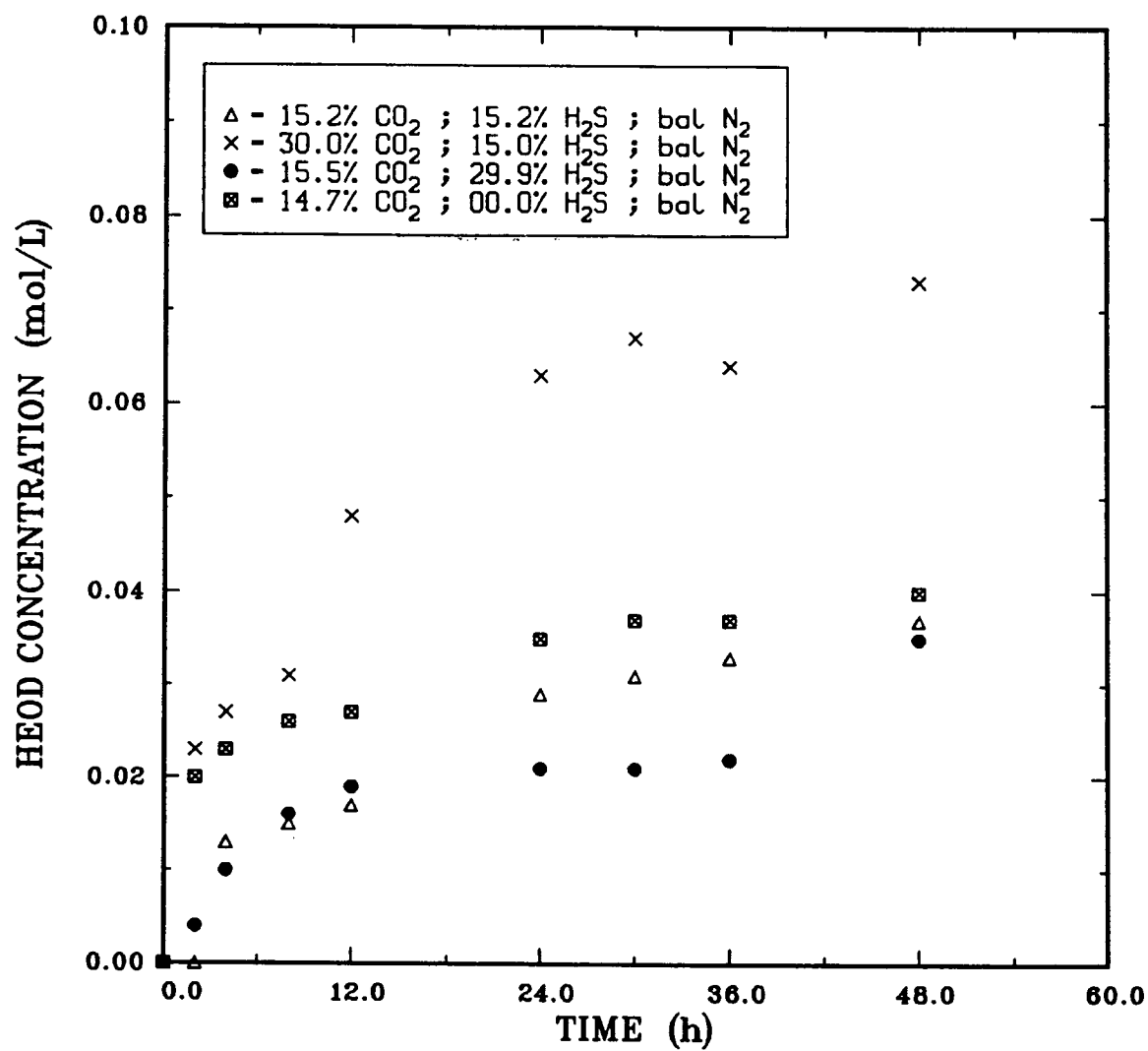


Figure 6.3: HEOD concentrations as a function of time and gas composition (DEA₀ = 3M, T = 165 °C).

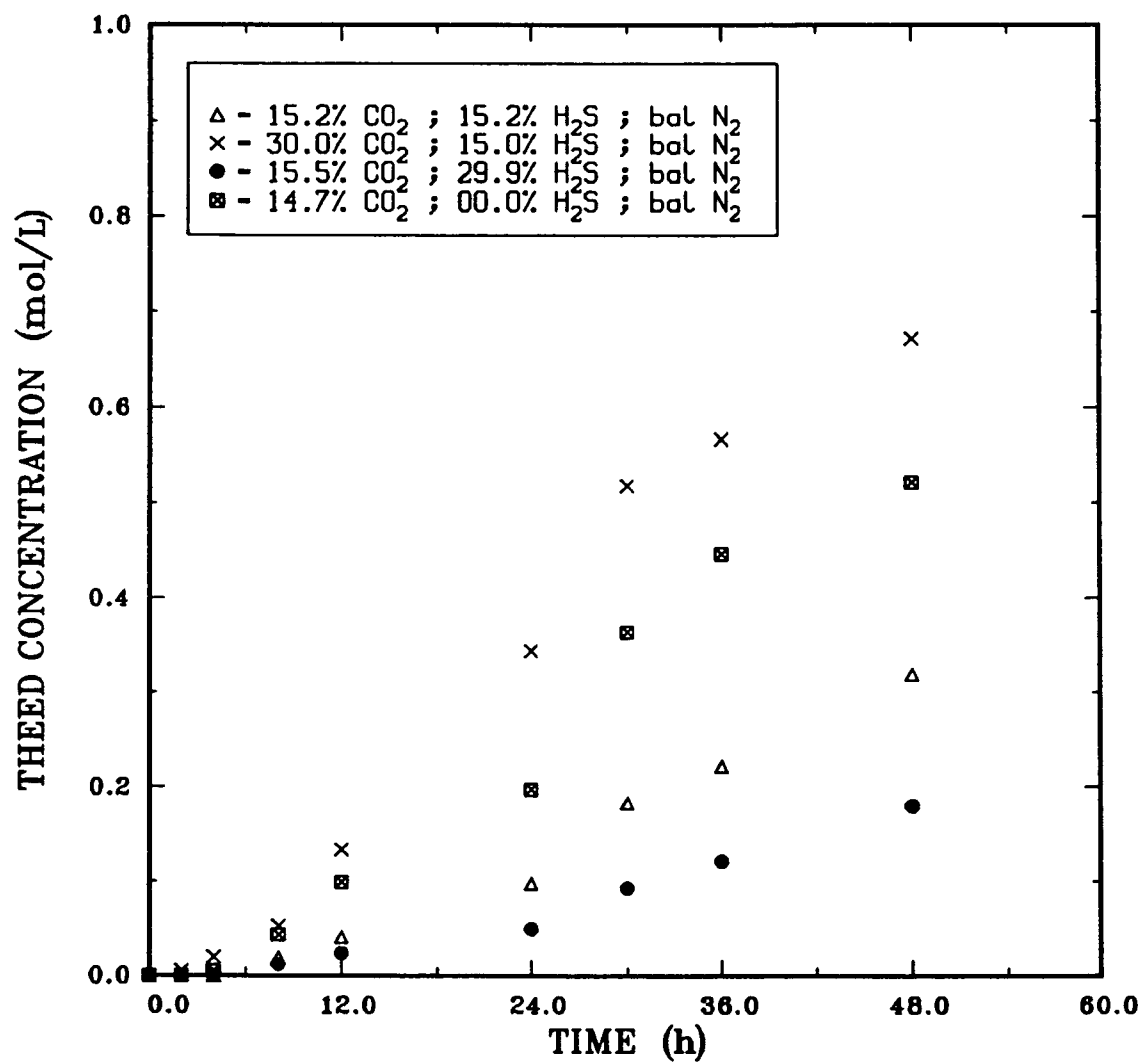


Figure 6.4: THEED concentrations as a function of time and gas composition ($\text{DEA}_0 = 3\text{M}$, $T = 165^\circ\text{C}$).

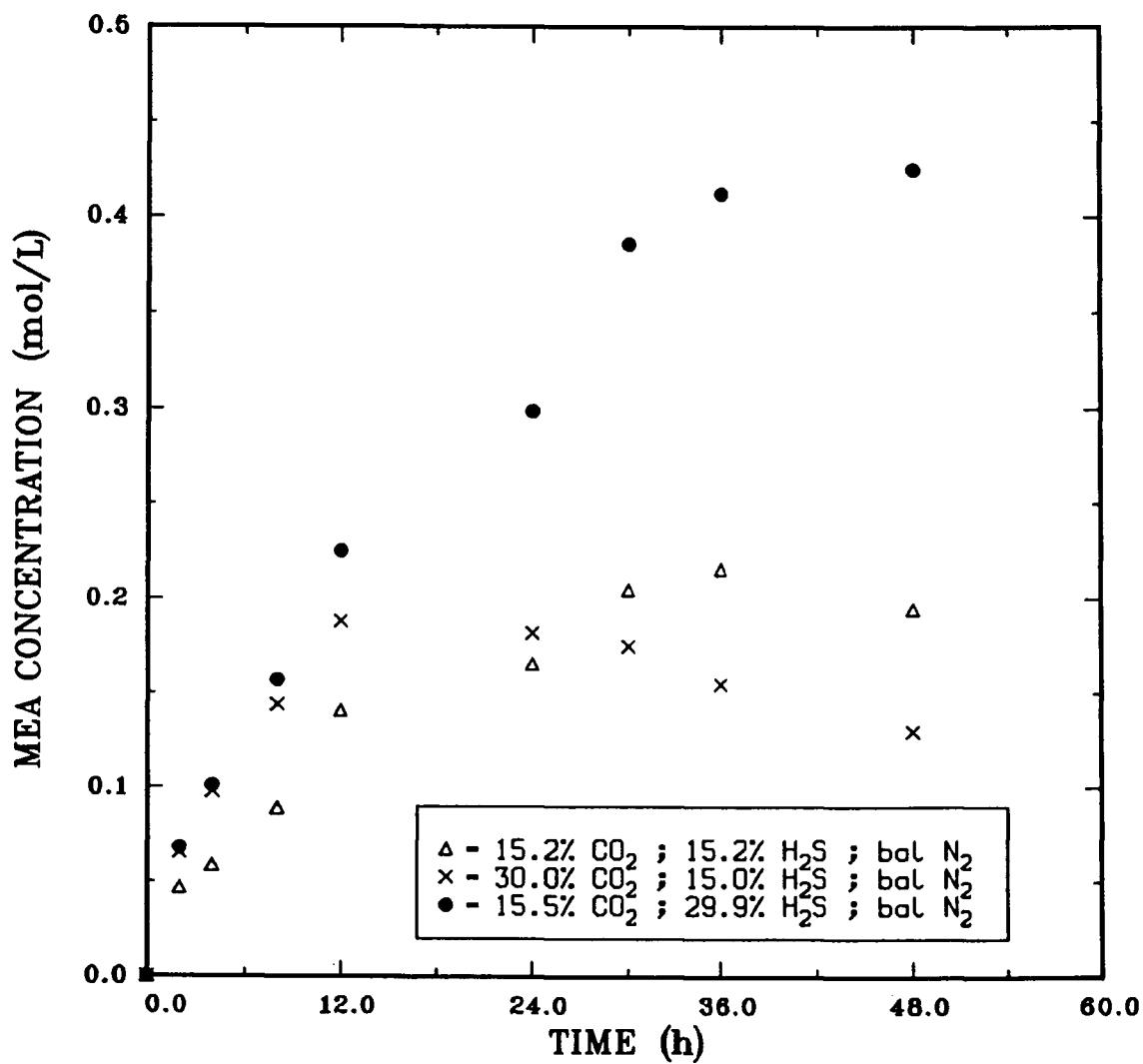


Figure 6.5: MEA concentrations as a function of time and gas composition ($\text{DEA}_0 = 3\text{M}$, $T = 165^\circ\text{C}$).

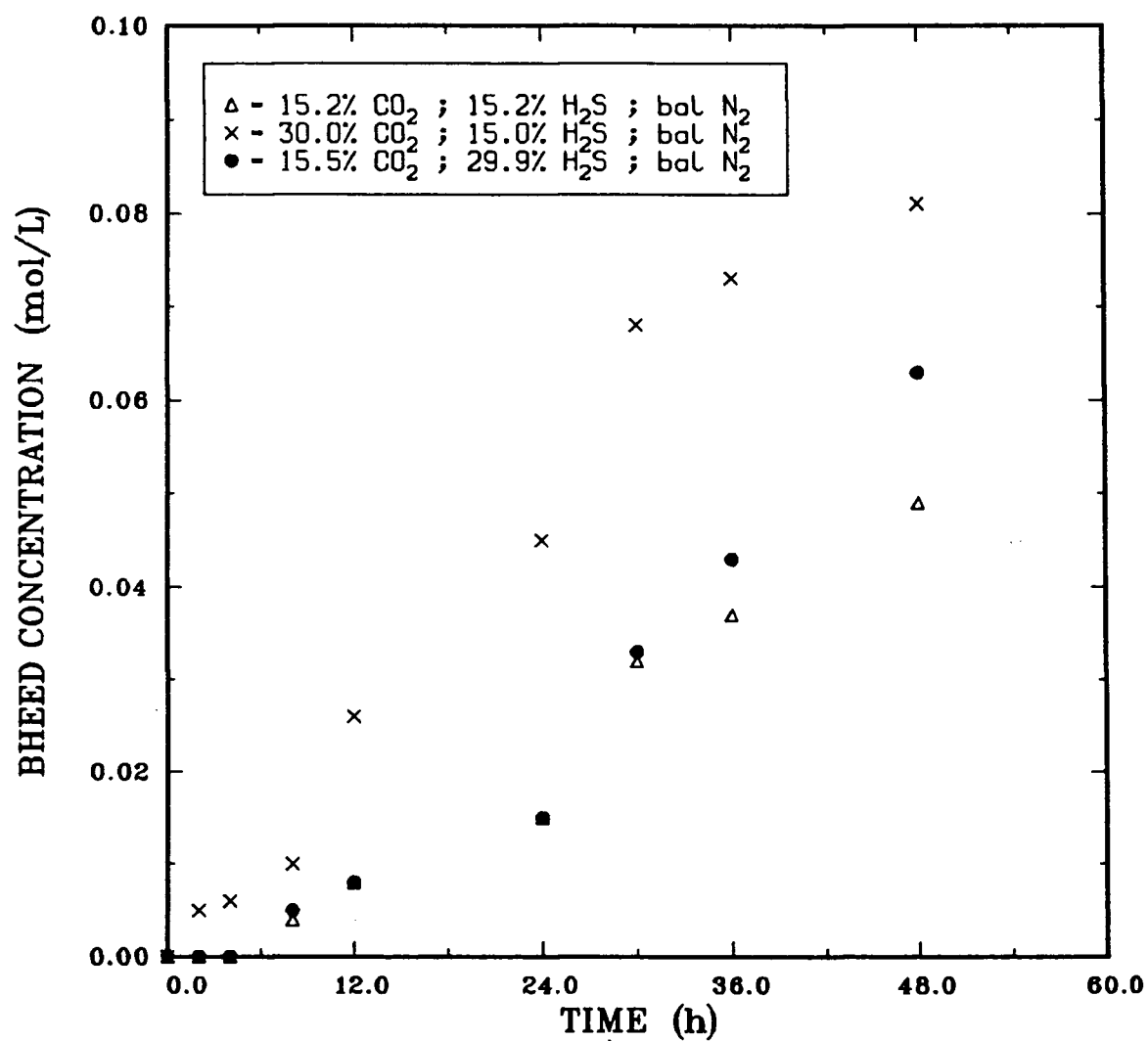


Figure 6.6: BHEED concentrations as a function of time and gas composition ($\text{DEA}_0 = 3\text{M}$, $T = 165^\circ\text{C}$).

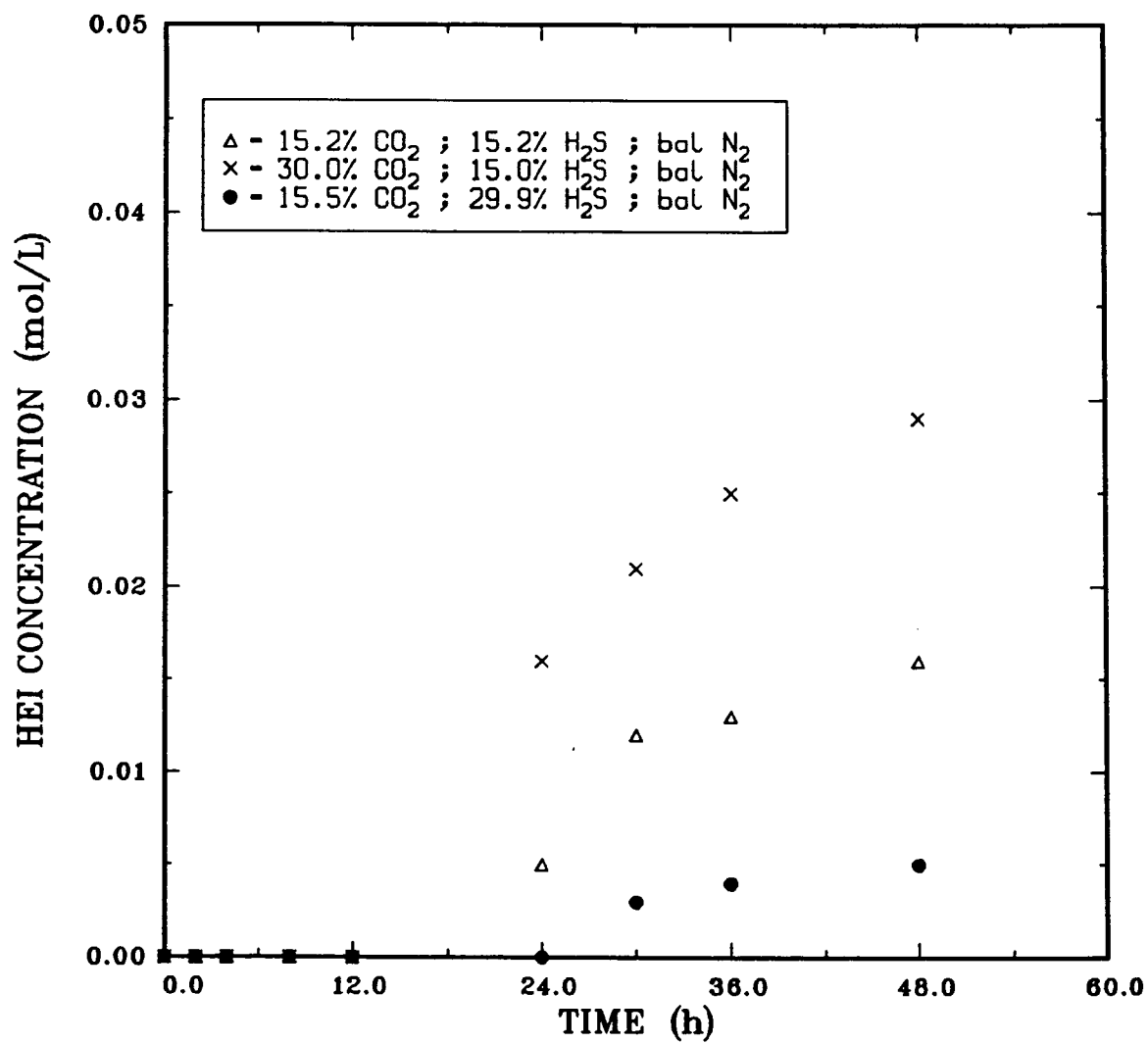


Figure 6.7: HEI concentrations as a function of time and gas composition ($\text{DEA}_0 = 3\text{M}$, $T = 165^\circ\text{C}$).

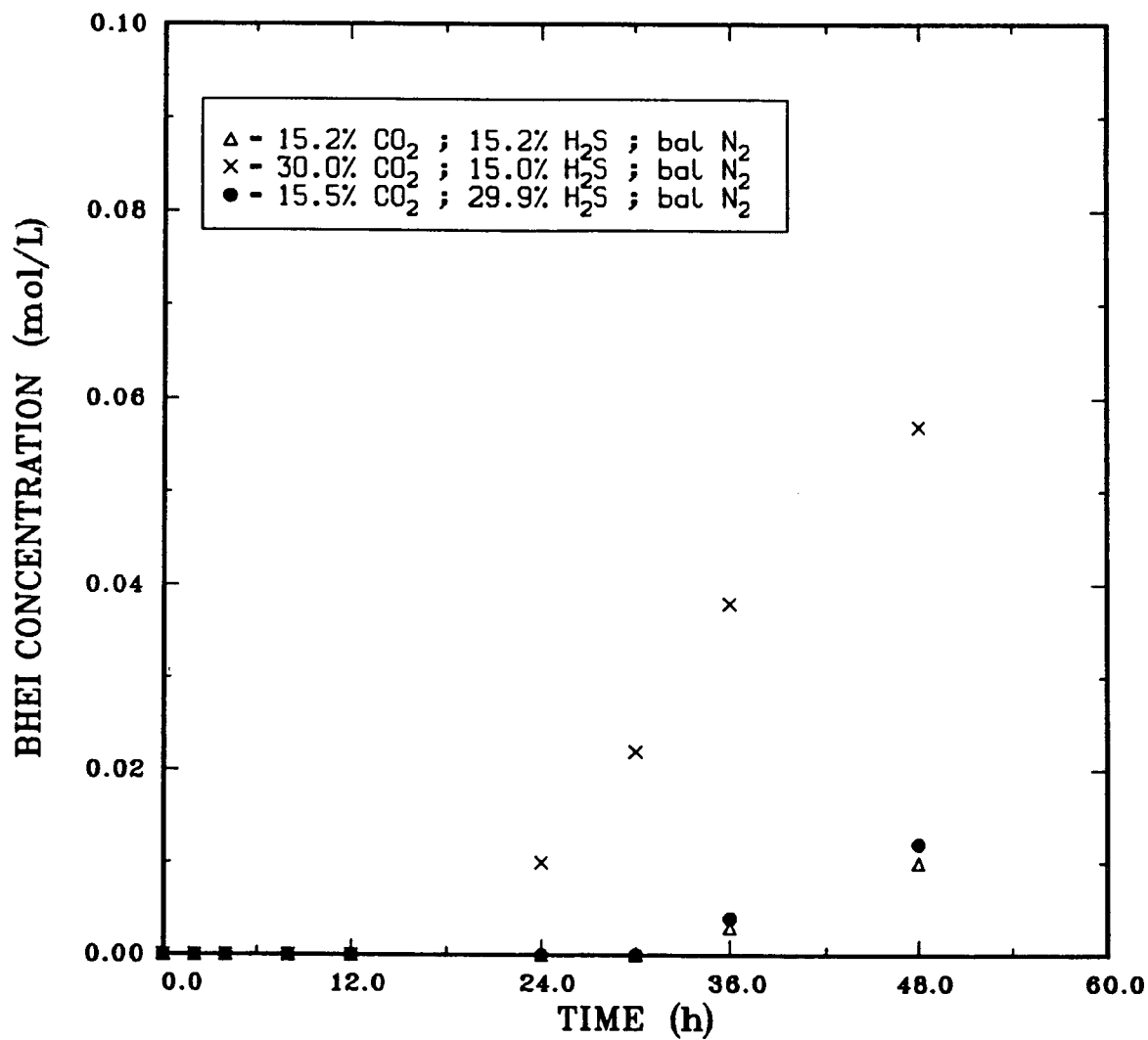


Figure 6.8: BHEI concentrations as a function of time and gas composition ($\text{DEA}_0 = 3\text{M}$, $T = 165^\circ\text{C}$).

The only mixed gas run conducted by Choi (12) was performed by first saturating the solution with 1480 kPa of H_2S at room temperature followed by contact with 4238 kPa of CO_2 at 175°C for 4 hr. The procedure significantly hindered the solubility of CO_2 in the amine solution. Therefore, the reduced rate of DEA degradation compared to a CO_2 run can be linked to the low concentration of CO_2 in the amine solution. Since most of the degradation compounds formed in the study were not identified, a comparison of product spectra with the present study cannot be made.

6.2 EFFECT OF OXYGEN

The formation of ketones was initially thought to be due to oxidation by the 0.1 mole% oxygen impurity in the COS feed. However, the relatively lower solubility of oxygen in water (1) and, by inference, in amine solutions, coupled with the fact that the ketones were formed within half hour of each run make this unlikely. Further, the absence of well known amine oxidative degradation products (viz. formic acid propionic acid and oxalic acid (84)), demonstrates that oxidative degradation was not occurring in the COS-DEA system. In order to remove any doubts in this regard, a run was conducted following the usual procedure, except that the DEA solution used was initially exposed to air for about 16 hours. In addition, the reactor was not purged prior to the commencement of the run. These actions were taken to ensure that oxygen was present in the reactor. Table 6.1 shows the concentrations of acetone, butanone and DEA in this run and in a corresponding run

conducted in a thoroughly purged environment. The similar concentrations in both runs provide conclusive proof that DEA oxidation by molecular oxygen was not responsible for the formation of the ketones.

Table 6.1: Contribution of oxygen to degradation in COS-DEA system
(DEA₀ = 30 wt%, T = 150 °C, P_{COS} = 345 kPa).

TIME	CONCENTRATIONS (MOLES/L)					
	PURGED SYSTEM			UNPURGED SYSTEM		
HOURS	ACET	BUT	DEA	ACET	BUT	DEA
0	0.000	0.000	3.01	0.000	0.000	3.00
2	0.006	0.000	3.06	0.005	0.000	2.98
6	0.007	0.002	2.91	0.007	0.002	2.86
9	0.010	0.006	2.83	0.010	0.007	2.77
12	0.013	0.011	2.76	0.011	0.010	2.69
24	0.016	0.014	2.47	0.019	0.016	2.45
30	0.019	0.016	2.31	0.020	0.015	2.30
36	0.021	0.017	2.18	0.021	0.015	2.17
48	0.015	0.016	1.93	0.022	0.017	1.91

6.3 EFFECTS OF DEGRADATION COMPOUNDS

The effects of the various degradation products on the degradation of DEA were studied by conducting degradation runs with 30% aqueous DEA solutions spiked with the degradation compound of interest. In the runs described in sections 6.3.1 to 6.3.6 below, 0.25 moles of the degradation compound of interest was added to the aqueous DEA solution and the mixture was contacted with 10.5 mL of CS₂ at 180 °C. CS₂ was chosen as the degrading agent because the CS₂-DEA system at 180 °C behaves like the COS-DEA systems at all temperatures used in this study. Therefore, in terms of the water soluble products, the results for a run should be applicable to all the COS-DEA systems investigated and the CS₂-DEA systems at 180 °C. The results from each of these runs were then compared with the results from the corresponding non-spiked (regular) run.

Ethanol and acetaldehyde were classified as minor degradation compounds because of their low concentrations in the degraded DEA solutions. Nevertheless, since they are oxygenated compounds, it was decided to check whether their low concentrations were due to fast transformations to ketones under the reaction conditions.

6.3.1 EFFECT OF ETHANOL

The degradation of the ethanol-spiked solution resulted in higher concentrations of acetone, butanone and acetic acid, but lower concentrations of MEA within the first four hours (see Figs. 6.9a and

6.9b). However, after nine hours the concentrations of the ketones and acetic acid were comparable with their respective concentrations in the regular run, but the MEA concentration remained lower. This result suggests that ethanol enhances the production of acetic acid and ketones, but inhibits MEA production. Considering the fact that ethanol has two carbon atoms as opposed to acetone and butanone which have three and four carbon atoms respectively, it is unlikely that these compounds were produced directly from ethanol. It is probable that ethanol was dehydrogenated to acetaldehyde which, in turn, produced the ketones and acetic acid. The equal concentrations recorded for the ketones and acetic acid in both runs at 9 hr suggest an approach to equilibrium.

6.2.2 EFFECT OF ACETALDEHYDE

As shown by Figs. 6.10a and 6.10b, degradation of the acetaldehyde-spiked solution resulted in significant increases in the rates of production of acetone, acetic acid and butanone within the first four hours. The increases were three fold in the first two hours. The increase in acetic acid concentration was accompanied by an increase in the rate of production of HEA. By the 25th hour, the rates of production of these compounds had decreased such that their concentrations in the spiked and regular runs were comparable. The concentrations of MEA were higher in the spiked run while the DEA concentrations were lower. This run also produced higher concentrations of ETAHEAME. These observations indicate that acetaldehyde is involved in the production of acetic acid, acetone and butanone.

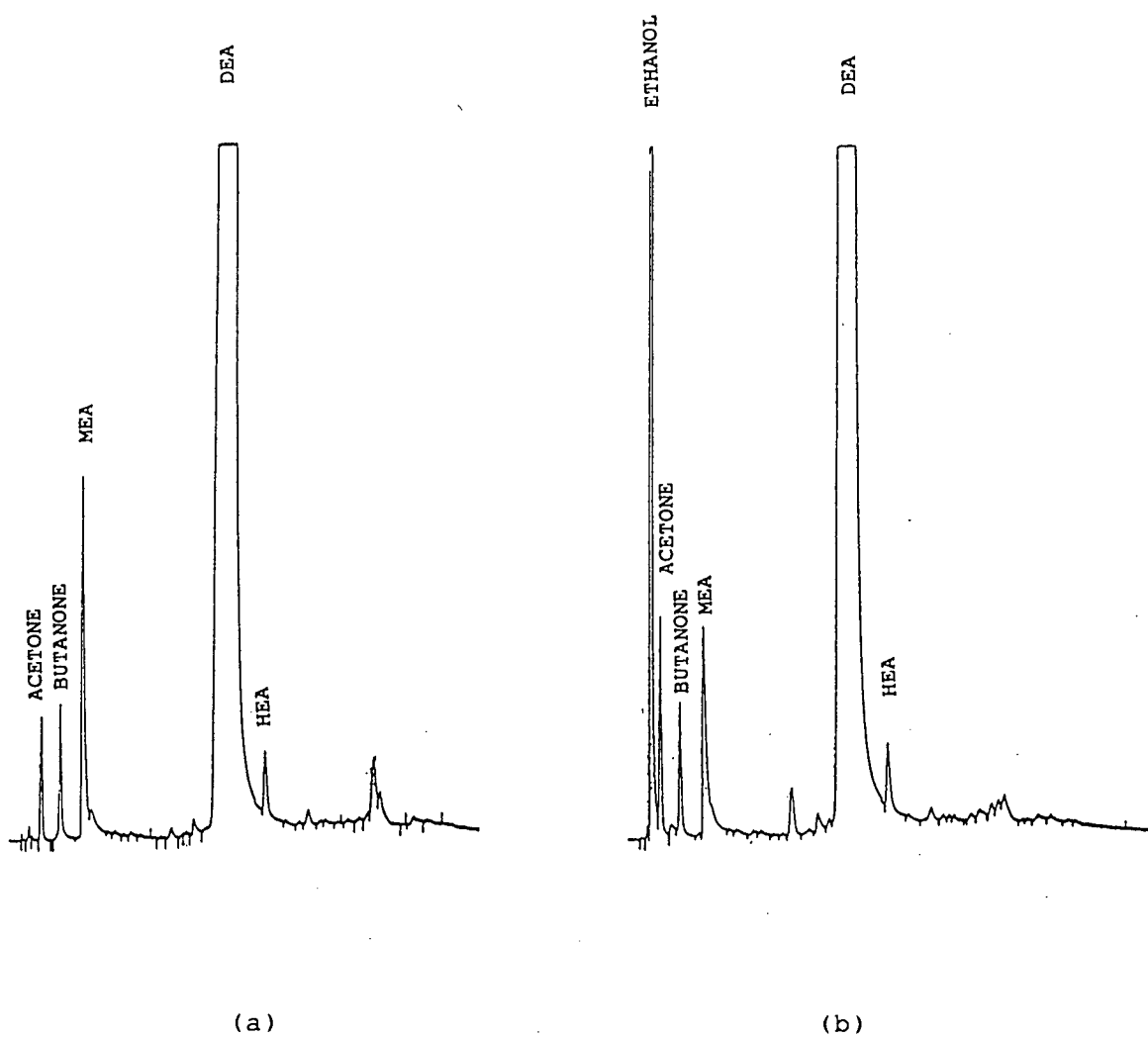


Figure 6.9: Chromatograms of partially degraded DEA solutions of 3M initial concentrations degraded with 10.5 mL of CS₂ at 180 °C (a: regular run; b: ethanol-spiked run).

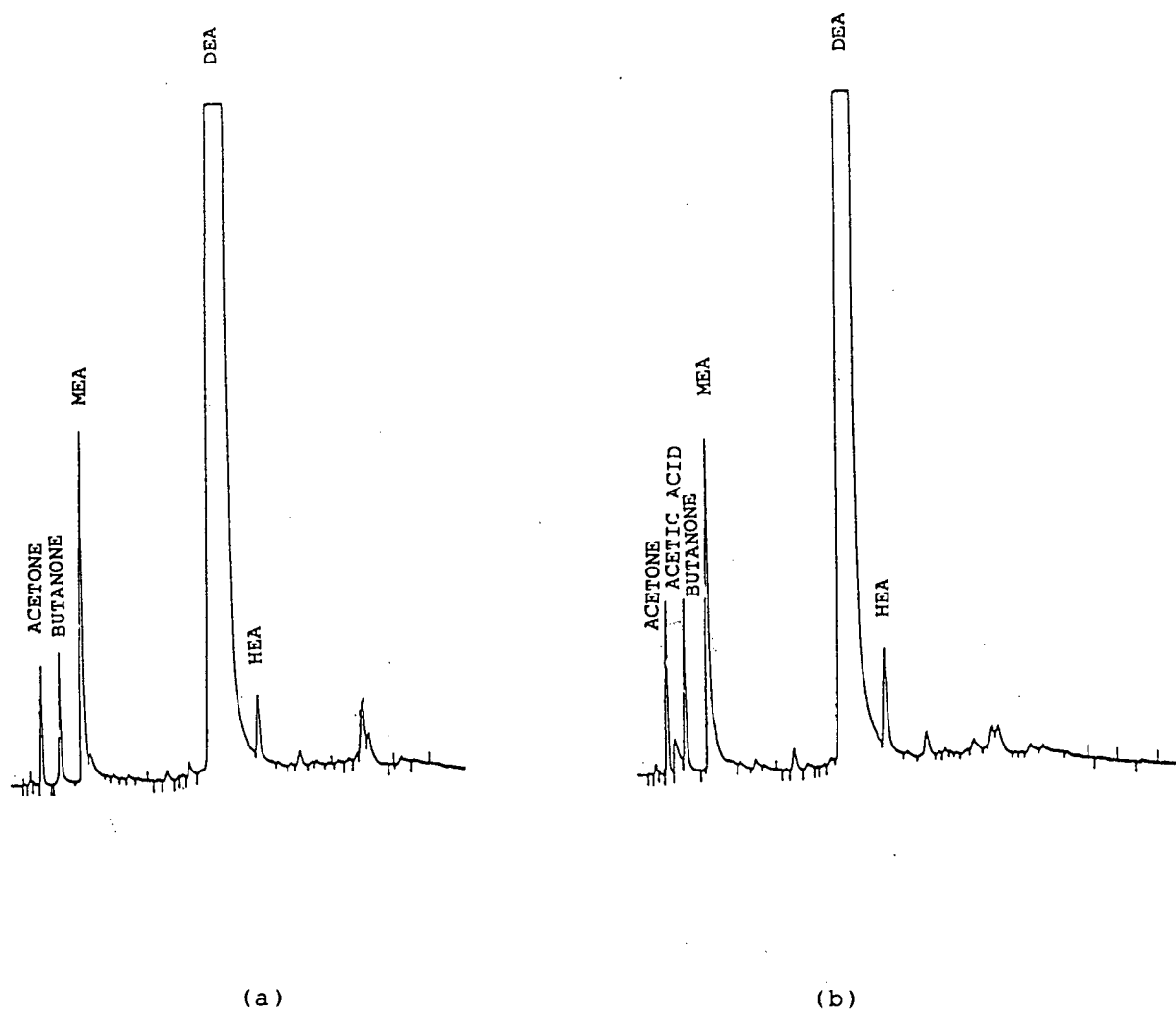


Figure 6.10: Chromatograms of partially degraded DEA solutions of 3M initial concentrations degraded with 10.5 mL of CS₂ at 180 °C (a: regular run; b: acetaldehyde-spiked run).

The comparable concentrations of these compounds at the later stages of both runs may also be due to an approach to equilibrium brought about by some limiting reactants. There was extensive polymerisation of acetaldehyde in the spiked run, thereby reducing the amount available for the reactions. This also contributed to the decline in the production of the ketones at the later stages of the run.

6.3.3 EFFECT OF ACETIC ACID

The results of the acetic acid-spiked run indicate that the ketones were not formed via acetic acid. In fact, their formation was entirely suppressed. However, the rate of degradation of DEA was increased significantly, resulting in much higher concentrations of the high boiling degradation compounds than in the regular run. The MEA concentration was lower due to increased conversion to HEA (see Figs. 6.11a and 6.11b). The formation of MEA implies that the hydroxyethyl group was released from DEA, yet no ketones were formed. This could be due to the fact that under the acidic condition of the run, transformation of the hydroxyethyl radical was inhibited. It probably reacted with acetic acid since it is impossible to remain as such in the liquid phase. A lot of solid product was formed in this run. Kennard (14) observed the rate of DEA degradation by CO_2 to increase with solution pH. Since the acetic acid spiked solution had a lower pH than the solution used for the regular run, the increase in the rate of DEA degradation cannot be attributed to the decrease in solution pH.

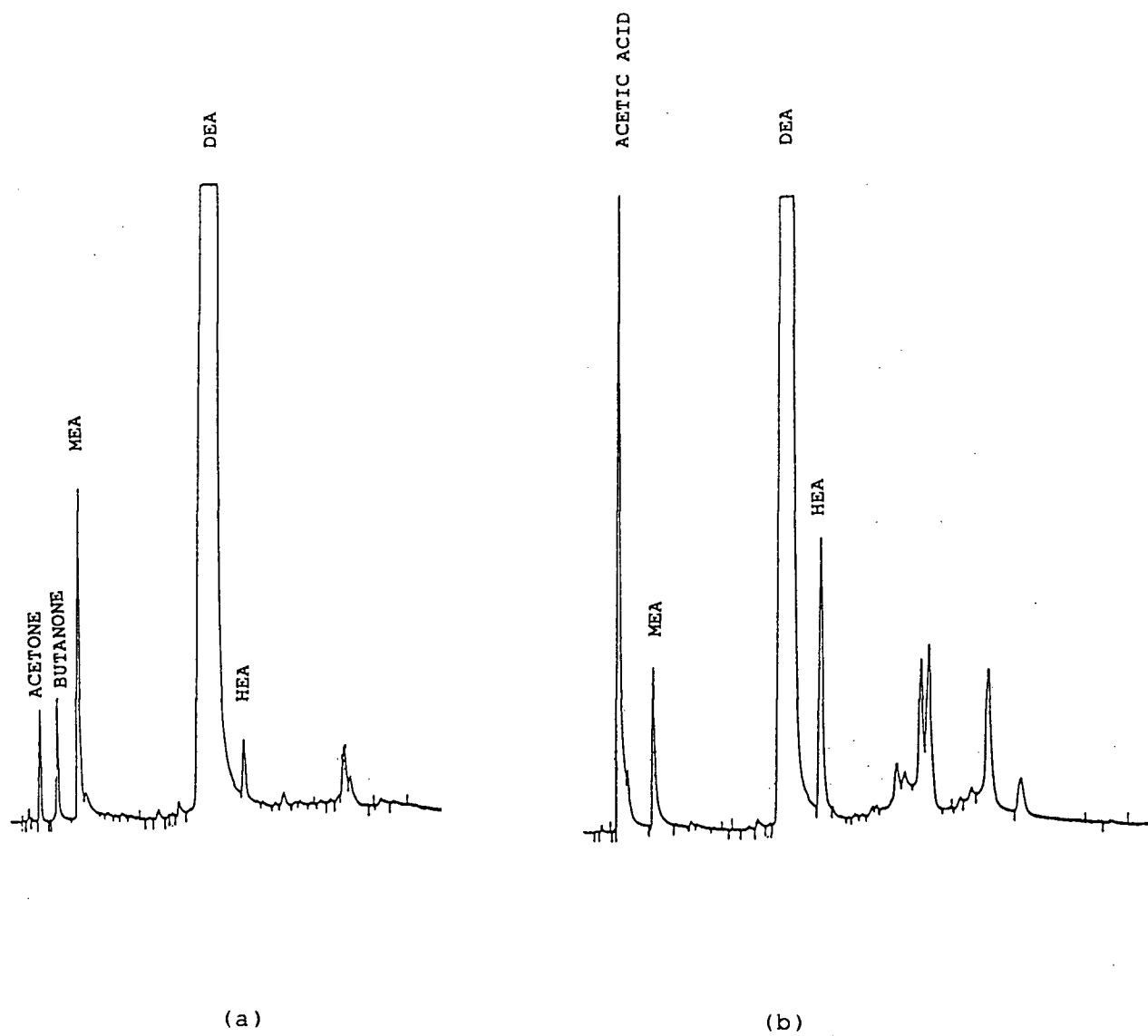


Figure 6.11: Chromatograms of partially degraded DEA solutions of 3M initial concentration degraded with 10.5 mL of CS_2 at 180°C (a: regular run; b: acetic acid-spiked run).

It is not clear at this stage why the acetic acid spiked run resulted in an increased rate of DEA degradation.

6.3.4 EFFECT OF ACETONE

The acetone-spiked run resulted in slightly reduced concentrations of butanone and DEA. In spite of the acetone production expected, the acetone peak in the chromatogram decreased progressively. This suggests that the formation of acetone may involve an equilibrium reaction, such that the presence of acetone at the initial stages shifts the equilibrium against further production of acetone. The rates of production of acetic acid and MEA increased within the first six hours, but by the 25th hour, their concentrations were similar to those obtained in the regular run. Acetone thus seems to affect the initial rates of formation/depletion of MEA and acetic acid only slightly.

6.3.5 EFFECT OF BUTANONE

Higher concentrations of acetone and acetic acid were recorded within the first four hours of the run. By the 12th hour, their rates of production had declined such that acetone concentration was lower than in the regular run while the acetic acid concentration was similar to the concentration in the regular run. Except at 2 hr when the MEA concentration was lower than in the regular run, other samples taken up till the 12th hour showed higher MEA concentration than in the regular run. Similar DEA concentrations were recorded in both runs.

6.3.6 EFFECT OF ETHYLENE GLYCOL

The production of MEA suggested that protonated DEA molecules were losing hydroxyethyl groups. Chakma (18) who had studied the CO_2 -MDEA system at elevated temperatures, suggested that the hydroxyethyl group released from MDEA produced ethylene glycol via ethylene oxide. In this study however, ethylene glycol was not detected. It is known that aldehydes and ketones could be produced from the transformations of substituted diols (85). In order to check whether the apparent absence of ethylene glycol in this study was due to the fast transformation to acetaldehyde or ketones, an ethylene glycol-spiked run was conducted. No increases were observed in the concentrations of the ketones. This indicated that acetaldehyde and ketones were not formed by rapid transformations involving ethylene glycol.

6.3.7 EFFECTS OF ETHYL DIETHANOLAMINE AND ETHYL AMINOETHANOL

Methanol, ethanol, acetaldehyde, acetone, acetic acid and butanone all contain alkyl groups, whereas DEA which was the starting material does not. Examination of the product spectrum of the degraded solutions shows the presence of two alkyl alkanolamines, viz. EDEA and EAE. Therefore, it was decided to check whether or not these compounds could produce the low boiling degradation compounds with alkyl groups. The tests were done by degrading 1M solutions of EDEA and EAE at 180 °C with 10.5 mL of CS_2 . Figures 6.12 and 6.13, which are chromatograms of

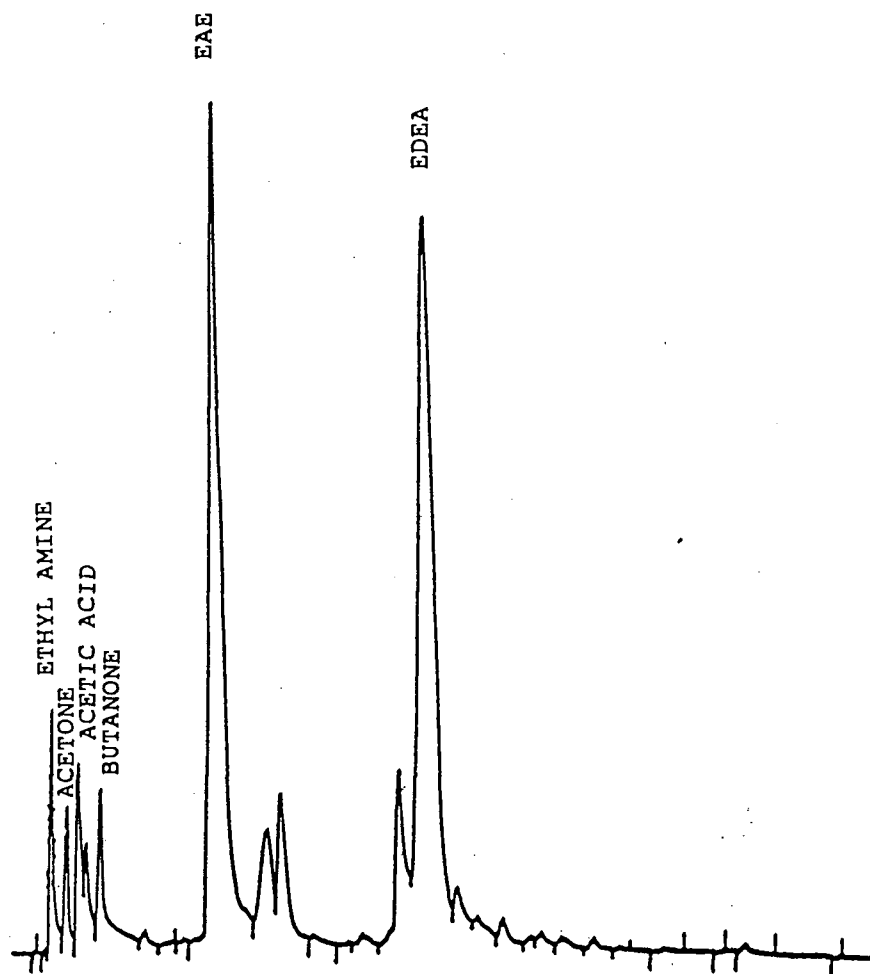


Figure 6.12: Chromatogram of partially degraded EDEA solution of 1M initial concentration degraded with 10.5 mL of CS₂ at 180 °C for 30 hours.

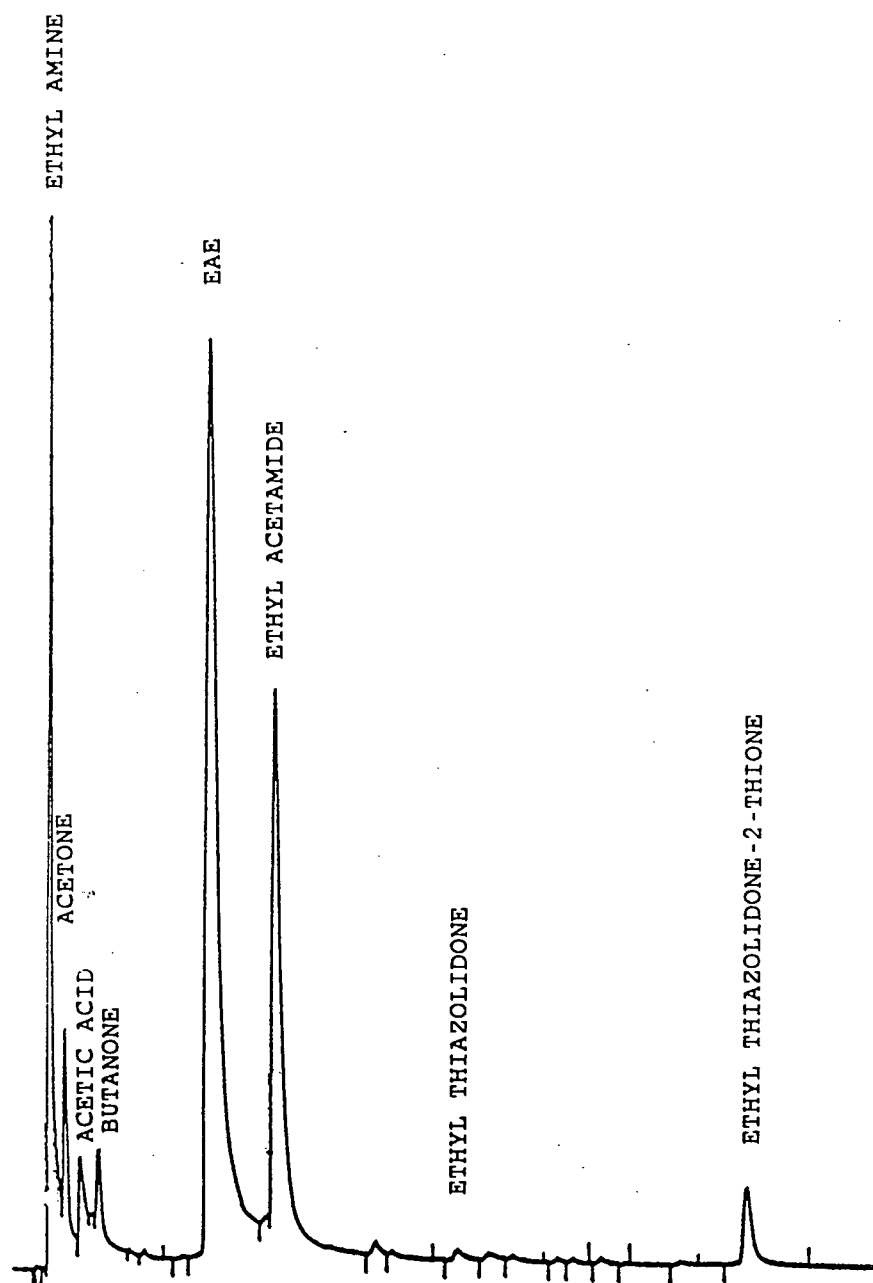


Figure 6.13: Chromatogram of partially degraded EAE solution of 1M initial concentration degraded with 10.5 mL of CS₂ at 180 °C for 24 hours.

samples withdrawn from these runs, show that EDEA and EAE are degraded by CS_2 and by inference COS, to form acetone, acetic acid and butanone among other products. The runs also showed the production of ethyl amine from EAE which in turn was formed from EDEA. This trend is consistent with the loss of a hydroxyethyl group from the parent compound as previously observed in the formation of MEA from DEA. The fact that the hydroxyethyl group was released rather than the alkyl group, coupled with the production of acetic acid and the ketones, demonstrate that these low boiling degradation compounds were formed through complex transformations of the hydroxyethyl radical.

Two further runs were then performed using DEA solutions spiked with EDEA and EAE to check the contributions of these compounds to DEA degradation. As shown by Tables 6.2 and 6.3, spiking with EDEA and EAE caused increases in the rates of production of acetone, butanone and also acetic acid. Acetic acid was not included in the table because the amount formed was only inferred from the GC peak areas. Beyond 12 hours, similar concentrations were recorded for acetone and butanone in the spiked and regular runs. The approach to equilibrium suggests that acetone and butanone may have been produced from some equilibrium reactions. The MEA concentration was initially lower in the spiked runs, but approached the same maximum value as in the regular run. The increased conversion of MEA to HEA in the spiked run, due to the increased production of acetic acid, resulted in a lower final concentration of MEA. The concentrations of DEA are comparable at the initial stages, but at the latter stages of the EDEA spiked run, lower DEA concentrations were recorded than in the regular run.

Table 6.2: Concentrations of DEA and the low boiling degradation compounds in the regular and the EDEA-spiked runs*
 (DEA₀ = 3M, EDEA₀ = 0.25M, T = 180 °C, CS₂ volume = 10.5 mL).

TIME		REGULAR RUN				SPIKED RUN			
HOUR	ACET	BUT	MEA	DEA	ACET	BUT	MEA	DEA	
0	0.00	0.00	0.00	3.10	0.00	0.00	0.00	3.10	
2	0.01	0.00	0.11	3.08	0.04	0.01	0.00	3.05	
4	0.02	0.02	0.23	2.85	0.06	0.03	0.17	2.82	
6	0.06	0.03	0.35	2.54	0.08	0.04	0.33	2.63	
9	0.08	0.04	0.48	2.15	0.08	0.05	0.46	2.29	
12	0.07	0.04	0.57	1.87	0.08	0.05	0.56	1.53	
25	0.03	0.03	0.46	0.88	0.06	0.05	0.45	0.85	
30	0.04	0.04	0.48	0.76	0.05	0.04	0.43	0.59	
48	0.03	0.04	0.35	0.45	0.03	0.04	0.23	0.36	

*The experiments reported in Tables 6.2 and 6.3 were performed in a glass lined reactor.. The reported concentrations are higher than what would be obtained in a reactor without the liner.

Table 6.3: Concentrations of DEA and the low boiling degradation compounds in the regular and the EAE-spiked runs (DEA₀ = 3M, EAE₀ = 0.25M, T = 180 °C, CS₂ volume = 10.5 mL).

TIME		REGULAR RUN			SPIKED RUN			
HOUR	ACET	BUT	MEA	DEA	ACET	BUT	MEA	DEA
0	0.00	0.00	0.00	3.10	0.00	0.00	0.00	3.08
2	0.01	0.00	0.11	3.08	0.04	0.02	0.06	3.00
4	0.02	0.02	0.23	2.85	0.05	0.03	0.18	2.69
6	0.06	0.03	0.35	2.54	0.06	0.04	0.33	2.49
9	0.08	0.04	0.48	2.15	0.07	0.04	0.46	2.24
12	0.07	0.04	0.57	1.87	0.06	0.04	0.56	2.00
25	0.03	0.03	0.46	0.88	0.04	0.04	0.46	1.03
30	0.04	0.04	0.48	0.76	0.04	0.04	0.44	0.75
48	0.03	0.04	0.35	0.45	0.02	0.04	0.25	0.43

The EAE run also provides an opportunity to evaluate the gas treating potential of this amine. Sharma and Danckwerts (48) had found EAE to be over 10 times more effective than MEA and DEA in absorbing COS. However, since there were no data on the resistance of EAE to degradation, no definite conclusions could be reached on its gas treating potential.

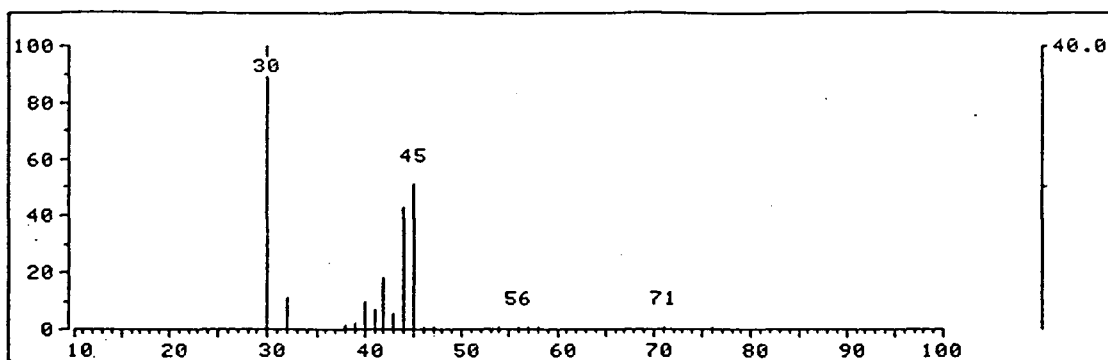


Figure 6.14: EI mass spectrum of the compound identified as Ethyl amine in the partially degraded EAE solution.

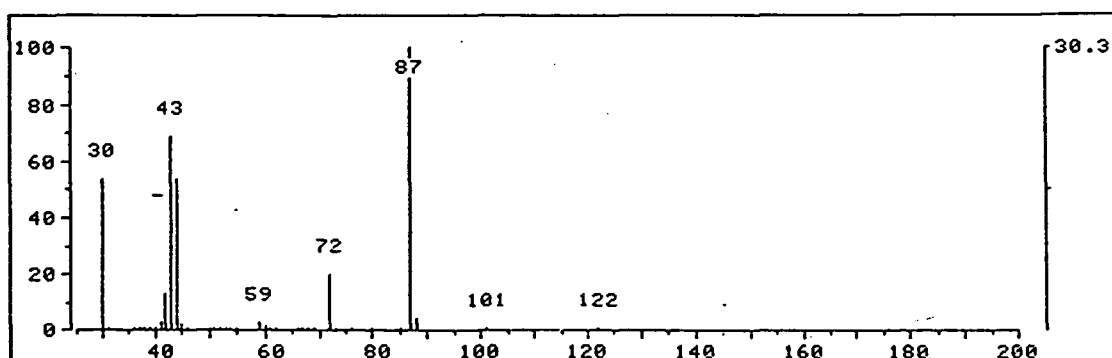


Figure 6.15: EI mass spectrum of the compound identified as Ethyl acetamide in the partially degraded EAE solution.

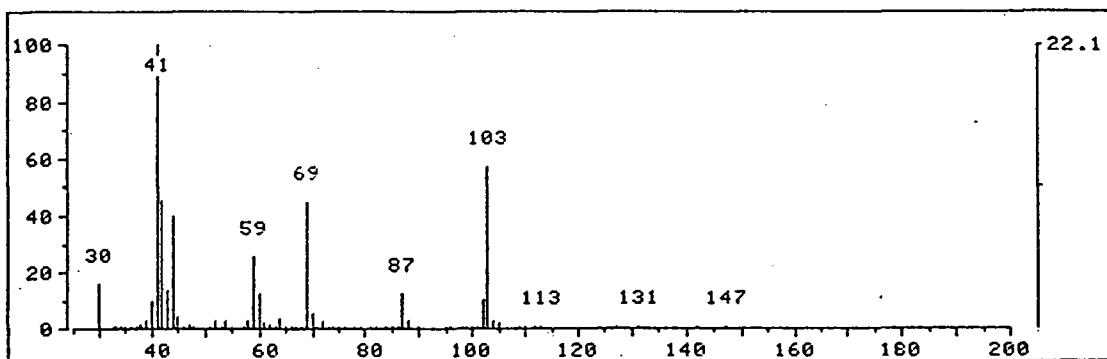


Figure 6.16: EI mass spectrum of the compound identified as Ethyl thiazolidone in the partially degraded EAE solution.

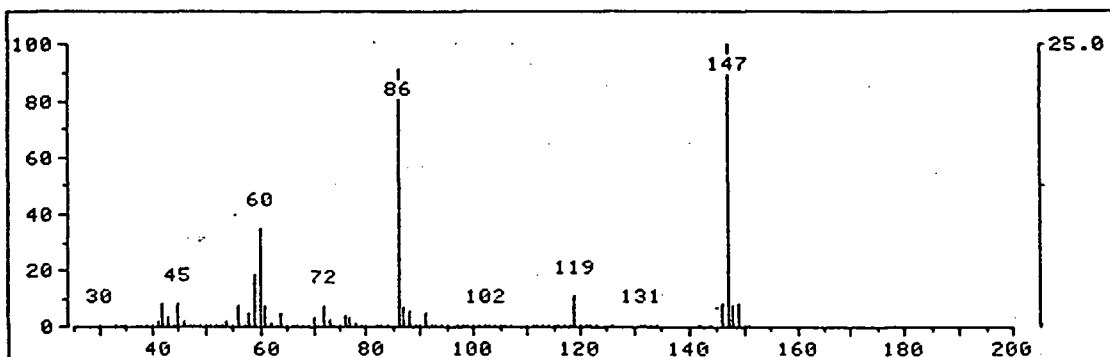


Figure 6.17: EI mass spectrum of the compound identified as Ethyl thiazolidone-2-thione in the partially degraded EAE solution.

The present results show that EAE is degraded by COS and CS₂ just like DEA. In addition to acetone, butanone and acetic acid, other degradation products tentatively identified from the EI mass spectra were ethyl amine, ethyl acetamide, ethyl thiazolidone and ethyl thiazolidone-2-thione. The EI spectra of these compounds are shown in Figs. 6.14 to 6.17.

No solids were formed in the EAE system, hence less fouling occurs. EAE degrades faster than DEA since 65% of the amine was lost in 24 hours compared to a 55% DEA loss under similar conditions. Since the major degradation compounds have ring structures, the amine could be recovered by the addition of a base, as is done in the case of HEOD (18). Therefore degraded EAE solutions may be amenable to the same chemical purification methods as those used for degraded DEA solutions.

6.3.8 EFFECT OF WATER

The role played by water in the degradation of DEA by COS and CS₂ was investigated by conducting a run with a solution consisting of 30% DEA and 70% MDEA at 150 °C and 345 kPa of COS for 48 hours. The temperature of 150 °C was chosen because it has been shown that MDEA degradation at this temperature is negligible within 48 hours (18).

The samples from this run were very viscous and difficult to draw into the syringe. This affected the reproducibility of the GC analysis. As shown by Fig. 6.18, degradation in the non-aqueous system was significantly reduced, the concentration of the amine being fairly

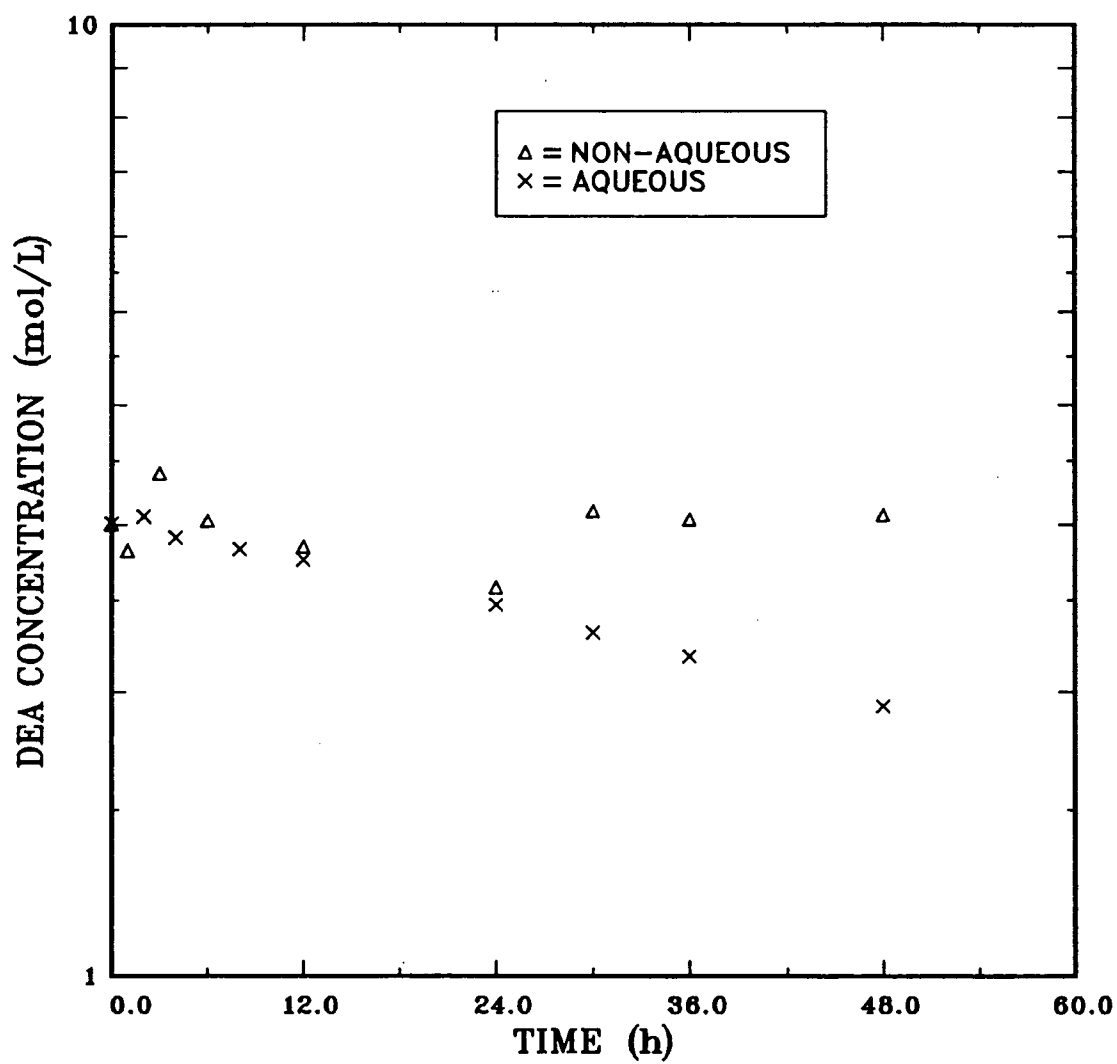


Figure 6.18: Concentrations of DEA as a function of time in aqueous and non-aqueous systems in contact with 345 kPa of COS at 150 °C.

constant. Degradation compounds produced in very low concentrations include BHEP, HEOD, HEI, THEED and ETAHEAME. THEED could have been formed by the direct reaction of DEA with DEA thiocarbamate. Dehydration of THEED to produce BHEP would provide some water for hydrolysis of COS to CO₂ and hence the formation of HEOD. Since MEA was not detected, it is clear that the presence of water is essential for its formation. DEA usually contains some MEA as an impurity. This may be responsible for the small amounts of HEI formed. Degradation products such as BHEED and BHEI were also insignificant in the non-aqueous system and this could be linked to the absence of substantial amounts of MEA. A low boiling compound having the same retention time as acetone, but identified as ethane thiol, was also produced.

In summary, water plays a significant role not only in terms of the rate of degradation, but also in initiating the hydrolysis reactions and consequently the formation of MEA and the other low boiling degradation compounds.

6.3.9 EFFECT OF MONOETHANOLAMINE

Three runs were conducted to study the effects of MEA on DEA degradation. In the first run, an aqueous mixture containing approximately 1M MEA and 3M DEA, was heated and maintained at 165 °C under a blanket of nitrogen for 48 hours. No degradation compounds were formed in this run; this provides an indication that DEA and MEA do not react directly and are not thermally degraded at 165 °C.

The second run was conducted for 32 hours under the same conditions as in the first run except that 758 kPa. of carbon dioxide was used in place of nitrogen. Degradation products such as BHEED, HEOD, BHEP, HEI, THEED and BHEI were formed. As shown in Table C.42 in appendix C, the concentrations of DEA and MEA decreased while those of BHEI, HEI and BHEP increased with time. The HEOD concentration increased to a maximum value and then fell slightly. Both THEED and BHEED concentrations also passed through maxima. Since the degradation of aqueous DEA by CO_2 produces mainly BHEP, HEOD and THEED, the formation of BHEI, BHEED and HEI in aqueous MEA/DEA/ CO_2 system can be attributed to reactions involving MEA, DEA and their respective carbamates.

The behaviour of MEA when subjected to a gas mixture containing CO_2 and H_2S , as was the case in the partially degraded DEA-COS systems, was investigated in the third run. A 2M MEA solution was contacted with a gas mixture containing 15.5% CO_2 , 29.9% H_2S in nitrogen, for 48 h at 165 °C and a partial pressure of 1.55 MPa. Acetone and butanone were detected in the partially degraded solution. The formation of the ketones would imply the presence of ammonia, in accord with the formation of MEA from DEA, EAE from EDEA, and ethyl amine from EAE. The non-detection of ammonia may be due to its high volatility as well as the inability of the FID to detect the gas. Ammonia was probably involved in the formation of the pyridines. HEI was the only high boiling degradation compound formed, albeit at low concentration. This may be as a result of the preferential protonation of MEA thereby limiting the amount of MEA carbamate available to form appreciable

quantities of hydroxyethyl ethylenediamine (HEED) and oxazolidone (OZD), the other degradation products of MEA-CO₂ reactions.

6.3.10 EFFECT OF BHEED

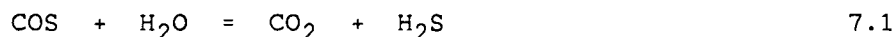
The trends in BHEED and THEED concentrations suggest that they are intermediate compounds. THEED is known to dehydrate to BHEP (13,14). Theoretically, BHEED could dehydrate in a similar manner to produce HEP. BHEED could also react with CO₂ to form BHEI. In order to determine the degradation compounds originating from BHEED, an aqueous solution of 0.2M BHEED was contacted with CO₂ at 180°C. Analysis of reaction samples showed the gradual formation of BHEI and by the 6th hour, the concentration of BHEI was 0.17M. HEP was not detected, but trace amounts of HEOD were formed. It appears that CO₂ reacted with BHEED to form BHEED carbamate, which was then dehydrated to form BHEI. Perhaps in a CO₂ limiting environment, dehydration of BHEED would have produced HEP. BHEED carbamate in aqueous solution may also establish an equilibrium with MEA and DEA carbamate, the latter forming HEOD. The very low concentration of HEOD and the absence of HEP in this run suggests that BHEED, in the presence of excess CO₂, is more likely transformed to BHEI than to HEOD or HEP.

The behaviour of BHEP, HEOD and THEED is well documented by Kennard (16) and the mechanisms for their formation are known. Therefore, no runs were conducted in respect to these compounds.

CHAPTER 7

SOLUBILITY AND HYDROLYSIS OF CARBONYL SULPHIDE

When COS is absorbed into aqueous solutions, it hydrolyzes to CO_2 and H_2S according to the overall reaction:



Thompson et al. (56) have obtained rate constants for the hydrolysis at temperatures between 15 and 47 °C. Sharma (57) has shown that the hydrolysis is catalysed by bases. Thus an aqueous solution originally containing DEA and COS, is eventually made up of the hydrolysis products, unreacted COS and ionic species derived from their interactions with DEA and water. Solubility and hydrolysis proceed relatively faster than amine degradation. Therefore, the extent of degradation is largely determined by the equilibrium composition of the solution prior to the commencement of degradation.

This chapter describes experiments conducted to establish the equilibrium composition of the COS-DEA system before the commencement of significant degradation. The results of the experiments are analysed and an equilibrium model is developed to predict the equilibrium concentrations of COS, H_2S and CO_2 . These results could be used in the development of a kinetic model for DEA degradation by COS, as well as in the design and modelling of COS absorption processes utilizing DEA.

7.1 THEORY

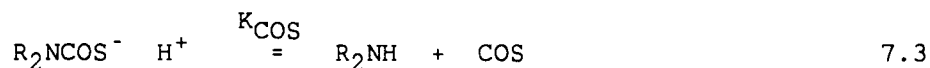
The attainment of equilibrium in a system consisting initially of gaseous COS and an aqueous DEA solution may be regarded as involving the following steps: (i) Physical absorption of COS into water, (ii) Reaction between DEA and absorbed COS to form DEA thiocarbamate, (iii) Hydrolysis of absorbed COS and DEA thiocarbamate to yield CO_2 and H_2S , (iv) Redistribution of COS, CO_2 , H_2S and their associated compounds between the liquid and gas phases. At low temperatures, steps (i) and (ii) are very much faster than (iii) and it is therefore possible to measure absorption without significant hydrolysis during the early stages of contact between COS and aqueous DEA solutions. By contrast, at elevated temperatures, steps (iii) and (iv) are rapid and distinction between absorption and hydrolysis is not easily achieved experimentally.

1. Absorption Regime (Steps i and ii)

The physical absorption of gas i into water may be described by Henry's law, i.e.

$$H_i = P_i/c_i \quad 7.2$$

where P_i and c_i denote the partial pressure and liquid phase concentration of physically absorbed species i , respectively. When component i reacts to form ionic complexes, such as DEA thiocarbamate,



then Henry's law may be written as

$$H_i^* = P_i / c_i^* \quad 7.4$$

where c_i^* now denotes the total (i.e. physically absorbed and chemically bound) concentration of component i in solution.

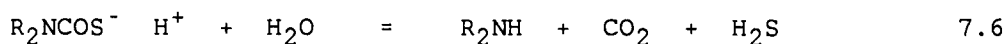
The temperature variation of the Henry's constants may be represented by the Arrhenius expression:

$$\ln \{H_i^*\} = A_i + B_i/T \quad 7.5$$

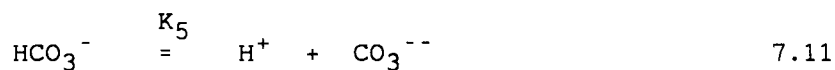
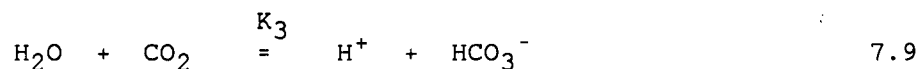
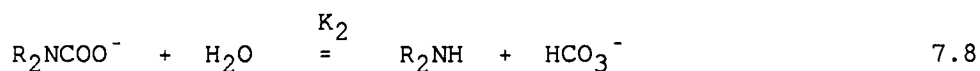
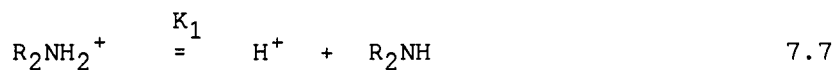
where the constants A_i and B_i can be obtained from least square fits of the semilogarithmic plots of H_i^* vs $1/T$.

2. Hydrolysis Regime (Steps iii and iv)

The DEA thiocarbamate formation is a rapid reaction and the overall COS hydrolysis is therefore governed, in effect, by the hydrolysis of DEA thiocarbamate:



The newly formed CO_2 and H_2S participate in the well known reactions for aqueous DEA solutions (36-41):



Reactions 7.3, 7.7 to 7.13 can be described by a model of the type first proposed by Kent and Eisenberg (39):

$$K_1 = [\text{H}^+] [\text{R}_2\text{NH}] / [\text{R}_2\text{NH}_2^+] \quad 7.14$$

$$K_2 = [\text{R}_2\text{NH}] [\text{HCO}_3^-] / [\text{R}_2\text{NCOO}^-] \quad 7.15$$

$$K_3 = \frac{[H^+][HCO_3^-]}{[CO_2]} \quad 7.16$$

$$K_4 = \frac{[H^+][OH^-]}{[H_2O]} \quad 7.17$$

$$K_5 = \frac{[H^+][CO_3^{--}]}{[HCO_3^-]} \quad 7.18$$

$$K_6 = \frac{[H^+][HS^-]}{[H_2S]} \quad 7.19$$

$$K_7 = \frac{[H^+][S^{--}]}{[HS^-]} \quad 7.20$$

$$K_{COS} = \frac{[R_2NH][COS]}{[R_2NCOS^-][H^+]} \quad 7.21$$

and

$$H_{CO_2} = \frac{P_{CO_2}}{[CO_2]} \quad 7.22$$

$$H_{H_2S} = \frac{P_{H_2S}}{[H_2S]} \quad 7.23$$

$$H_{COS} = \frac{P_{COS}}{[COS]} \quad 7.24$$

where [i] denotes the concentration of component i in solution. As was the case for the Kent-Eisenberg model, Eqs. 7.14 to 7.21 assume an excess of water, unit activity coefficients and incorporate system non-idealities into the equilibrium constants governing the carbamate, thiocarbamate and amine protonation reactions.

In addition to the mass action equations and Henry's law, the following charge and material balances apply:

$$\begin{aligned} \text{Charge: } [R_2NH_2^+] + [H^+] &= [HCO_3^-] + [R_2NCOO^-] + 2[CO_3^{--}] \\ &+ [OH^-] + [HS^-] + 2[S^{--}] + [R_2NCOS^-] \end{aligned} \quad 7.25$$

$$\text{DEA: } m = [R_2NH] + [R_2NCOO^-] + [R_2NCOS^-] + [R_2NH_2^+] \quad 7.26$$

$$\text{H}_2\text{S: } m_{H_2S} = [H_2S] + [HS^-] + [S^{--}] \quad 7.27$$

$$CO_2: \quad m \alpha_{CO_2} = [CO_2] + [HCO_3^-] + [R_2NCOO^-] + [CO_3^{--}] \quad 7.28$$

$$COS: \quad m \alpha_{COS} = [COS] + [R_2NCOS^-] \quad 7.29$$

where m and α_i represent the total DEA concentration and the DEA loading by acid gas i , respectively.

The above 16 equations contain 20 unknown operating variables (14 concentrations: m , $[H^+]$, $[R_2NH]$, $[R_2NH^+]$, $[HCO_3^-]$, $[R_2NCOO^-]$, $[CO_2]$, $[OH^-]$, $[CO_3^{--}]$, $[HS^-]$, $[H_2S]$, $[S^{--}]$, $[R_2NCOS^-]$, $[COS]$; 3 partial pressures: P_{CO_2} , P_{H_2S} , P_{COS} ; 3 loadings: α_{CO_2} , α_{H_2S} , α_{COS}). The system is therefore fully specified provided the equilibrium and Henry's constants are known and four operating variables are given. For most design calculations the latter are the three partial pressures (P_{CO_2} , P_{H_2S} , P_{COS}) and the total DEA concentration (m).

Equations 7.14 to 7.29 were combined to yield four independent model equations:

$$P_{H_2S} = (H_{H_2S} / K_6 K_7) (A [H^+]^2 / (1 + [H^+] / K_7)) \quad 7.30$$

$$P_{CO_2} = (H_{CO_2} / K_3 K_5) (B [H^+]^2 / (1 + [H^+] / K_5 + m [H^+] / K_2 K_5 K')) \quad 7.31$$

$$\begin{aligned}
[H^+] = & A (1 + K_7 / (K_7 + [H^+])) / (1 + m / K_1 K') + \\
& B (1 + K_2 K_5 / (K_2 K_5 + K_2 [H^+] + m [H^+] / K')) \\
& / (1 + m / K_1 K') + K_4 / ([H^+] (1 + m / K_1 K')) + \\
& (C / (m - C)) (1 + H^+ / K_1 + (P_{CO2} / H_{CO2}) (K_3 / (K_2 H^+))) \\
& (m / K') / (1 + m / K_1 K')
\end{aligned} \tag{7.32}$$

$$\begin{aligned}
P_{COS} = & (C / (m - C)) (K_{COS} H_{COS} H^+) (1 + (H^+ / K_1) + \\
& P_{COS} K_3 / (K_2 H_{CO2} H^+))
\end{aligned} \tag{7.33}$$

where:

$$A = m \alpha_{H2S} - P_{H2S} / H_{H2S} \tag{7.34}$$

$$B = m \alpha_{CO2} - P_{CO2} / H_{CO2} \tag{7.35}$$

$$C = m \alpha_{COS} - P_{COS} / H_{COS} \tag{7.36}$$

$$\begin{aligned}
K' = & 1 + [H^+] / K_1 + (K_3 / K_2) (P_{CO2} / (H_{CO2} [H^+])) \\
& + P_{COS} / (K_{COS} H_{COS} H^+)
\end{aligned} \tag{7.37}$$

The variables m , P_{CO2} , P_{H2S} , P_{COS} , α_{CO2} and α_{H2S} could be readily found experimentally. By contrast, α_{COS} was very small under the experimental conditions and therefore difficult to determine accurately.

7.2 EXPERIMENTAL EQUIPMENT AND PROCEDURE

The experiments were conducted with the 600 mL stainless steel reactor described in detail in Chapter 3.

7.2.1 PROCEDURE

100 mL of the aqueous DEA solution of the desired concentration were placed in the reactor which was then sealed tightly. Nitrogen was passed into the reactor to purge the unit of oxygen. The liquid inlet and gas sampling valves were closed and the reactor was heated to the desired operating temperature while stirring its contents. The pressure increase was recorded as the vapour pressure (P_{DEA}) of the aqueous DEA solution at the operating temperature. COS from a pre-weighed steel bomb was passed into the reactor to attain a total pressure P_{T} such that $P_{\text{T}} - P_{\text{DEA}}$ equalled the desired partial pressure of COS. As COS was absorbed into the DEA solution, the total pressure dropped and more COS was added as necessary to maintain the system pressure at P_{T} . Equilibrium COS solubility was deemed to be achieved when the system pressure remained constant for times varying from 7 min at 180 °C to over 25 min at 120 °C, without the addition of COS. At this point, the steel bomb was disconnected from the reactor and re-weighed. Hydrolysis of the dissolved COS to H_2S and CO_2 , and the subsequent exchange of gases between the gas and liquid phases, resulted in a gradual increase of the total reactor pressure. When the pressure reached a constant value thereby indicating true equilibrium, both the gas and liquid

phases were sampled. Gas phase samples were obtained by opening and closing the gas sampling valve thereby trapping the sample gas within a short section of tubing which had been previously purged. The tubing was fitted with a septum and the sample was then drawn into a "pressure-lok" syringe and kept for analysis. Liquid phase samples were forced by the reactor pressure into a stainless steel sampling coil which was then immersed in ice-cold water to reduce the temperature and pressure quickly.

Two sets of experiments were conducted under the following conditions:

Low temperature solubility experiments:

DEA concentration:	0	-	40 wt%
Temperature:	20	-	50 °C
COS partial pressure:	345 kPa		

Elevated temperature hydrolysis experiments:

DEA concentration:	10	-	40 wt%
Temperature:	120	-	180 °C
COS partial pressure:	345	-	1172 kPa

A few equilibrium hydrolysis experiments were also conducted at 40 °C using 30 % DEA solutions and initial COS partial pressures of 72 - 210 kPa.

7.2.2 ACID GAS LOADINGS

Wet chemical methods could not be used for the analysis of the samples because of their non-specificity. Instead, the gas trapping set-up shown in Fig. 7.1 was used to collect the gases dissolved in the liquid samples. The set-up is similar to the "Chittick" apparatus used for the determination of CO_2 in carbonate samples (90). The displacement solution was prepared by dissolving 200 g of NaCl and 2 g of NaHCO_3 in 700 mL of distilled water. 2 mL of Methyl Orange indicator and enough concentrated HCl were added to make the solution acidic. The solution was stirred to remove all dissolved acid gases. This solution was placed in the levelling bulb, gas burette and connecting tubing.

Prior to sample introduction, the levelling bulb was moved up along a tripod stand to bring the level of the displacement solution to the zero mark in the gas measuring burette. The sample inlet valve and sampling points were opened and nitrogen was passed into the system to purge it of oxygen and/or carbon dioxide. The pressure was allowed to build up within the system by quickly closing all outlets before the flow of nitrogen was stopped. The sample inlet valve was then opened and later closed again to raise the displacement solution in the gas burette as high as possible. The levelling bulb was then lowered and a period of about 15 min was allowed to elapse for the pressure and temperature to reach equilibrium. Once the temperature and pressure had stabilized, the level of the displacement solution in the gas burette stayed constant unless the system was leaking. The point at which the pressure in the system equalled atmospheric pressure was established and

recorded as the initial burette reading. A fraction of the cooled sample in the sampling coil was then transferred into the flask. Excess dilute HCl solution (2 M or 5 M) was added from the acid burette and liberated the gases dissolved in the sample. The magnetic stirrer was turned on to ensure complete mixing within the flask. The acid gases displaced the solution in the gas burette until the pressure within the system was equal to atmospheric pressure. Total displacement was usually achieved in less than 30 minutes. To prevent the escape of liberated gases through the acid burette during sample introduction, the displacement solution in the levelling bulb was kept at a lower level than in the gas burette at all times during the displacement of the gases. Thereafter, the levelling bulb was moved up and down several times depending on the volume of gas displaced, to ensure uniform gas composition within the system. The point of equal pressure in both arms of the displacement solution was again determined and recorded as the final burette reading. "Pressure lok" gas syringes were then used to collect gas samples from the two sampling points along the tubing. The pressure within the system was maintained at atmospheric during sampling. The ambient temperature was also monitored.

7.2.3 GAS ANALYSIS

Gas samples withdrawn from the reactor and the gas trapping set-up were analyzed with a Varian (Vista 6000) gas chromatograph equipped with a CD 401 data station. Using helium as the carrier gas, the gas mixture

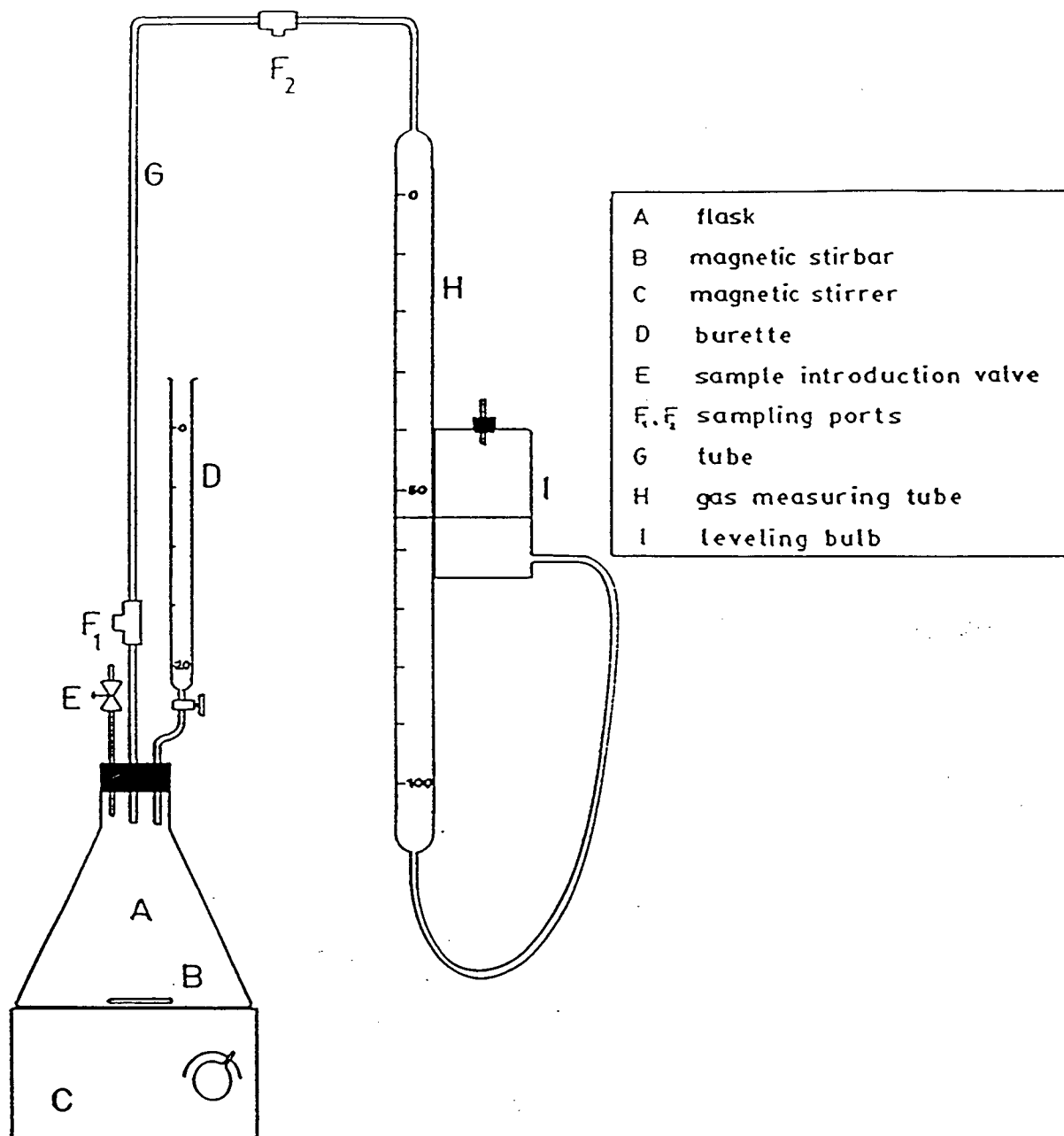


Figure 7.1: Gas trapping set up (86).

was separated in the order N_2 , CO_2 , COS and H_2S by a 6' x 1/8" ID Teflon column containing Chromosil 310 packings (supplied by Supelco Inc., Oakville, Ont.). The GC was operated at 40 °C. Gases eluting from the column were sensed by a thermal conductivity detector (TCD). Each analysis was completed within three minutes. A typical chromatogram is shown in Fig. 7.2. Effluent gases from the GC were absorbed into a 30 wt% MEA solution to prevent pollution of the environment. Peak areas recorded for each compound were converted to volume concentrations using previously prepared calibration plots (see Appendix B). The latter showed linear relationships between concentration and peak area for the range of concentrations encountered in the study.

7.2.4 SOLUBILITY DETERMINATION AT LOW TEMPERATURES

For each run, the quantity of COS fed into the reactor from the steel bomb was determined as the difference between the final and initial weights of the bomb. Using the reactor temperature, pressure and volume as well as the vapour pressure of the DEA solution (P_{DEA}), the moles of COS in the gas phase were determined by the Peng and Robinson equation of state (87). This value was then subtracted from the moles of COS fed into the reactor to obtain the moles of COS dissolved in the liquid phase. The scale used to weigh the bomb is accurate within 0.1 g.

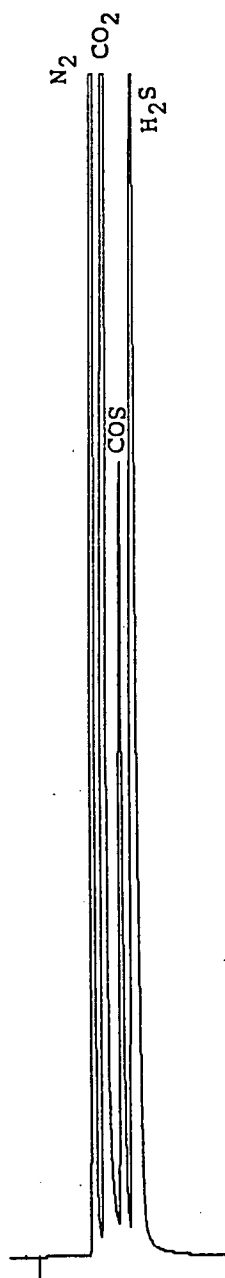


Fig. 7.2: Chromatogram showing a typical separation in the Chromosil 310 teflon packed column.

7.2.5 HYDROLYSIS AT ELEVATED TEMPERATURES

Data obtained from the analyses of the gas and liquid samples were treated as follows:

Gas samples

1. The previously obtained calibration curves were used to convert the GC peak areas to concentrations expressed in vol or mole %.
2. The concentrations were normalized to obtain the mole fraction of each gas on an acidic gas basis.
3. The partial pressure of each gas was calculated from

$$P_i = y_i P_T^*$$

where P_T^* denotes the total partial pressure of the acid gases.

4. The partial pressures were converted to moles using the Peng-Robinson equation of state (87).

Liquid samples

1. The volume of liquid sample transferred to the gas trapping set-up, V_s , was determined as the difference between the volume of the sampling coil and the additive volumes of the residual

liquid in the sampling coil and line connected to the gas trapping set-up.

2. The total volume of gas liberated from the liquid sample, V_d , was the difference between the final and initial burette readings.
3. The total moles of acid gas liberated were calculated using the ideal gas law. This was then multiplied by the ratio V_l/V_g to obtain the total moles of the various gases in the liquid phase of the reactor.
4. Peak areas from GC analyses were converted to vol %, which was then equated to mole % and normalized to obtain the mole fraction of each gas.
5. The moles of the individual gases in the liquid phase of the reactor were calculated by multiplying the total moles of acid gas by its mole fraction.

7.3 RESULTS AND DISCUSSION OF SOLUBILITY AND HYDROLYSIS RUNS

In accordance with expectation, the reactor pressure was found to decline shortly after the introduction to of COS due to its absorption. The decline could be offset by adding more COS. At a certain point in time the system pressure was found to rise again due to hydrolysis until

a final constant pressure was attained. The absorption and hydrolysis regimes were clearly distinguishable at low temperatures, but they overlapped at elevated temperatures.

7.3.1 SOLUBILITY OF COS IN DEA SOLUTIONS AT LOW TEMPERATURES

The Henry's constants for COS are shown in Fig. 7.3 and the corresponding coefficients for Eq. 7.5 are summarized in Table 7.1. Since the Henry's constants were calculated on the premise that, at low temperatures, the hydrolysis of COS in amine solutions is slow, the gas phase was assumed to consist only of COS, nitrogen and water vapour. To check the validity of this assumption, the liquid and gas phase compositions were determined for the absorption of COS in 40 wt% DEA solution at 50 °C (see Run 27 in Tables 7.3 and 7.4). The extent of hydrolysis, calculated as the fraction of the total COS that was present either as CO₂ or H₂S, was about 16%. COS constituted about 90 % of the acid gases in the gas phase. Since the increase in system pressure was used as the indicator of transition to hydrolysis, it is certain that, at the time the system was sampled, some hydrolysis had already occurred. Therefore the extent of hydrolysis at equilibrium solubility will be less than 16%, justifying the assumption of negligible hydrolysis.

The Henry's constants obtained for the COS-H₂O system in the present study may be compared with earlier results. As seen from Table 7.2, the good agreement between the values is an indication of the reliability of the present experimental method and data.

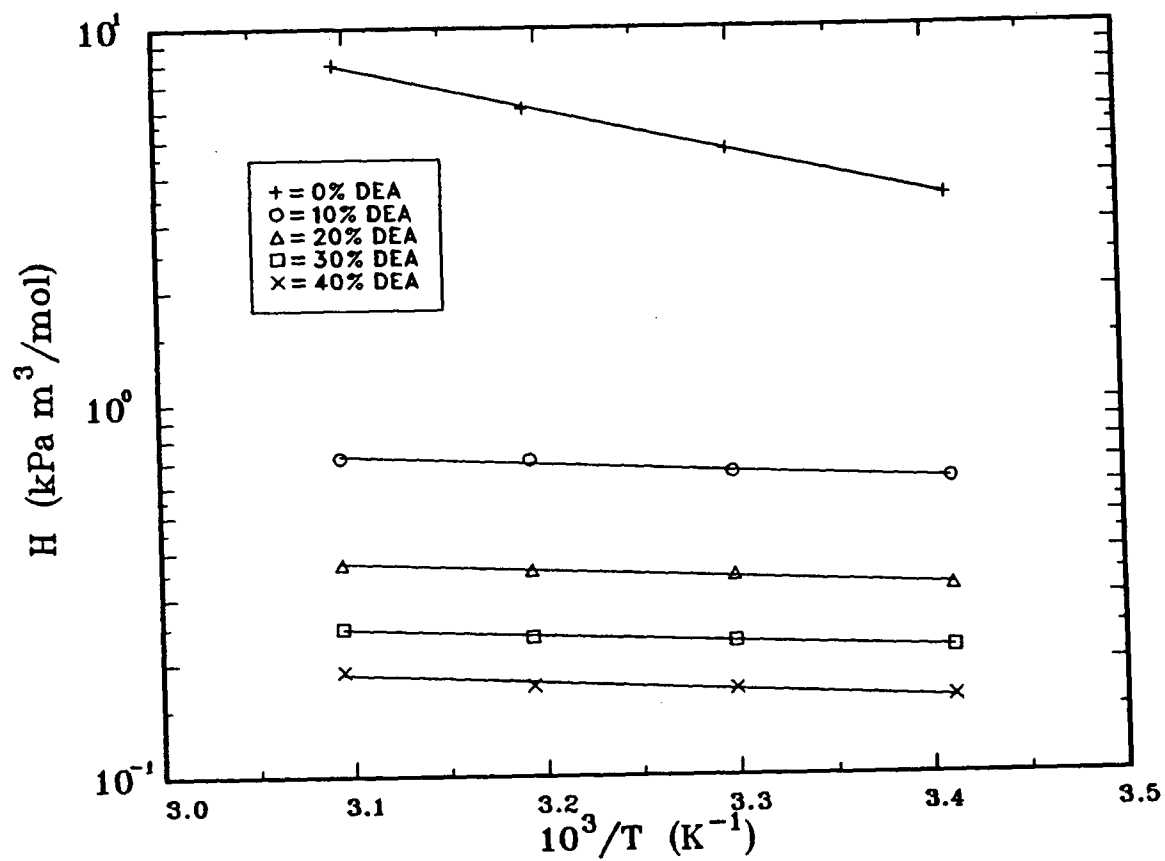


Figure 7.3: Henry's constant as a function of temperature for COS in aqueous DEA solutions.

Table 7.1: Fitting constants in the Henry's law expression for the COS-DEA system ($T = 20 - 50\text{ }^{\circ}\text{C}$).

DEA Conc. wt %	A_{COS}	B_{COS}
0	10.00	-2562.83
10	1.21	-494.73
20	0.50	-478.68
30	-0.10	-416.82
40	-0.11	-504.86

Table 7.2: Henry's constants for the solubility of COS in water.

Henry's constants, H_{COS} (kPa m ³ /mol)			
T °C	Al-Ghawas et al. (50)	Perry and Green (88)	This work
20	3.92	3.99	3.52
30	5.05	5.54	4.70
40	6.59		6.16
50			7.93

Table 7.3: Equilibrium data for the hydrolysis of COS in aqueous DEA solutions. (The compositions are expressed in milli moles.)

RUN #	GAS PHASE			LIQUID PHASE			TOTAL			ERROR %
	CO ₂	COS	H ₂ S	CO ₂	COS	H ₂ S	CO ₂	COS	H ₂ S	
1	31.0	1.6	21.5	23.0	0.2	30.9	54.0	1.8	52.4	1.57
2	31.7	1.4	21.5	17.8	0.3	27.6	49.6	1.7	49.1	0.52
3	28.5	1.5	20.4	9.8	0.4	16.5	38.3	1.9	36.9	1.93
4	31.4	2.7	20.6	14.3	0.2	23.6	45.6	2.8	44.2	1.58
5	32.0	0.7	21.4	12.3	BDL ^a	21.3	44.3	0.7	42.7	1.84
6	33.5	1.7	21.4	15.9	0.1	26.3	49.4	1.9	47.6	1.87
7	62.5	4.2	44.4	38.1	BDL	53.8	100.6	4.2	98.2	1.25
8	65.1	3.9	48.9	51.2	BDL	68.0	116.4	3.9	116.9	0.22
9	61.2	8.1	50.5	63.2	0.3	72.1	124.4	8.4	122.5	0.77
10	64.0	5.8	43.8	29.8	BDL	45.9	93.8	5.8	89.7	2.32
11	87.5	9.8	63.6	34.2	BDL	59.5	121.7	9.8	123.2	0.58
12	112.6	6.8	80.3	46.7	BDL	68.3	159.2	6.8	148.6	3.58
13	29.9	1.5	24.2	51.8	BDL	54.1	81.7	1.5	78.3	2.12
14	46.4	2.2	36.4	53.1	0.3	58.0	99.5	2.5	94.4	2.68
15	33.4	1.2	23.7	41.7	BDL	45.7	75.0	1.2	69.5	4.02
16	52.2	2.2	38.6	46.6	0.5	55.3	98.8	2.7	93.9	2.63
17	68.3	10.4	51.8	48.7	0.3	64.7	17.0	10.7	116.5	0.21
18	51.2	4.3	36.1	18.8	0.7	32.8	70.1	5.0	68.9	0.84
19	66.7	6.3	50.5	24.8	0.6	48.4	91.5	6.9	98.9	3.75
20	36.6	3.1	25.5	32.2	0.2	44.3	68.8	3.3	69.8	0.71
21	54.8	5.5	41.7	36.1	0.4	52.7	90.9	5.9	94.5	1.90
22	71.4	8.9	55.6	37.0	0.4	59.5	108.4	9.2	115.2	2.94
23	50.2	2.0	35.6	29.0	0.6	46.3	79.2	2.6	81.9	1.67
24	35.5	3.7	45.9	106.2	0.9	101.6	141.8	4.5	147.5	1.94
25	26.9	3.1	36.2	107.2	0.6	105.1	134.0	3.7	141.3	2.57
26	16.1	0.7	28.0	96.4	0.3	89.2	112.5	0.7	117.2	2.02
27	1.9	62.1	5.2	24.0	87.0	25.5	25.9	149.1	30.7	7.85

^a BDL indicates that the COS reading was below the detectable limit.

Error is calculated as the % deviation of H₂S or CO₂ concentration from the mean of the CO₂ and H₂S concentrations.

Table 7.4: Equilibrium data for the hydrolysis of COS
(Liquid phase concentrations are expressed in mole/mole DEA).

RUN #	OPERATING CONDITIONS ^a			LIQUID LOADING (mole/mole DEA)			PARTIAL PRESSURE (kPa)		
	C	T	P	CO ₂	COS	H ₂ S	CO ₂	COS	H ₂ S
1	40	150	345	0.058	0.001	0.078	217.23	11.06	150.72
2	40	165	345	0.045	0.001	0.070	230.26	10.17	155.81
3	40	180	345	0.025	0.001	0.042	214.29	11.65	153.07
4	30	165	345	0.049	0.001	0.081	227.59	19.38	149.28
5	20	165	345	0.064	0.001	0.110	232.14	5.41	155.24
6	20	150	345	0.082	BDL ^b	0.135	234.43	12.19	149.61
7	40	150	689	0.097	BDL	0.136	436.48	29.65	309.13
8	40	135	689	0.130	BDL	0.172	438.26	26.19	328.03
9	40	120	689	0.160	BDL	0.182	396.52	52.87	325.87
10	30	150	689	0.102	BDL	0.156	446.81	40.55	305.12
11	30	150	896	0.116	0.001	0.203	609.45	68.71	441.65
12	40	150	1172	0.118	BDL	0.173	781.67	47.93	555.52
13	40	120	345	0.131	BDL	0.137	194.59	9.76	157.43
14	40	120	517	0.134	BDL	0.147	301.41	14.15	235.73
15	30	120	345	0.142	0.001	0.156	217.16	7.72	154.14
16	30	120	517	0.159	BDL	0.188	338.79	14.44	249.75
17	30	120	689	0.166	0.002	0.220	442.08	67.75	334.33
18	20	150	517	0.097	0.002	0.169	358.28	30.38	252.27
19	20	150	689	0.128	0.003	0.249	465.39	44.34	351.66
20	20	120	345	0.166	0.001	0.229	238.19	19.95	165.66
21	20	120	517	0.186	0.002	0.272	355.40	36.04	270.11
22	20	120	689	0.191	0.002	0.307	462.06	57.75	358.81
23	30	150	517	0.099	0.002	0.158	350.85	13.81	248.65
24	30	40	210	0.362	0.003	0.346	183.40	19.01	235.18
25	30	40	141	0.365	0.002	0.358	138.93	16.10	186.08
26	30	40	72	0.328	0.001	0.304	83.21	3.52	144.13
27	40	50	345	0.081	0.294	0.086	9.69	308.37	26.50

^a C = DEA concentration (wt%), T = Temperature (°C),
P = Initial partial pressure of COS (kPa).

^b BDL indicates that the loadings fell below the detectable limit.

7.3.2 HYDROLYSIS OF COS IN DEA SOLUTIONS AT ELEVATED TEMPERATURES

The distribution of the various components in the reactor at equilibrium conditions is shown in Table 7.3. The data are presented in terms of partial pressures and solution loadings, along with the operating conditions, in Table 7.4. By reaction stoichiometry in Eq. 7.1, one mole of COS reacts with one mole of water to produce one mole each of CO_2 and H_2S . Therefore, the total moles of CO_2 and H_2S should be equal in each run. The deviations resulting from the analyses were generally below $\pm 5\%$. Due to the low concentration of COS (particularly in the liquid phase) it was not always possible to detect COS with the TCD. Even when COS was detected, its concentration was so small that the reliability of the results was uncertain.

The experimental results show that H_2S was preferentially dissolved relative to CO_2 and COS. Liquid loadings of carbon dioxide and hydrogen sulphide were generally two orders of magnitude (or more) higher than the COS loadings. The concentrations of hydrogen sulphide and carbon dioxide in the liquid phase also increased with increasing DEA concentration and initial COS partial pressure, but decreased with increasing temperature (Figs. 7.4 and 7.5). Figure 7.6 shows that the $\text{H}_2\text{S}/\text{CO}_2$ ratio in solution, which is a measure of the selectivity for H_2S , decreased with increasing solution concentration, but increased with increasing temperature. This suggests that increasing the amine concentration enhances amine carbamation more than protonation, while increasing the temperature makes carbamation more difficult.

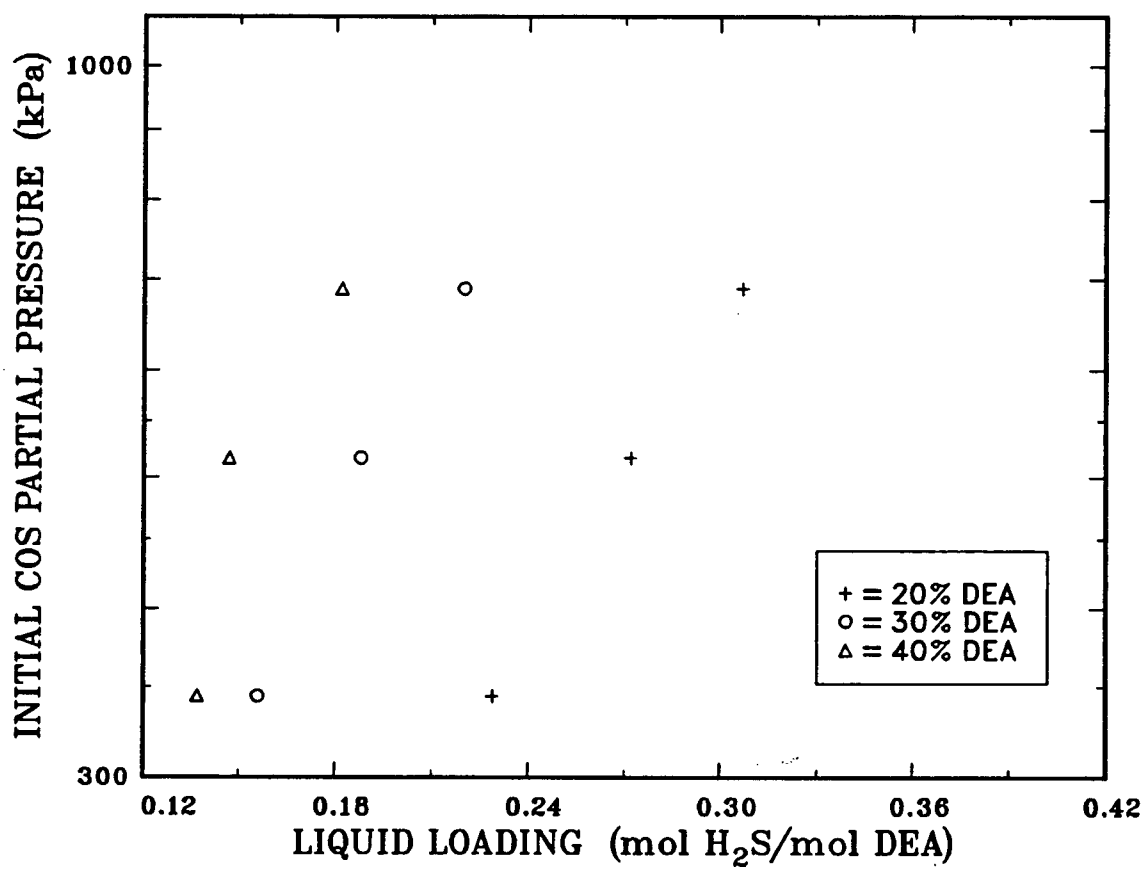


Figure 7.4: H₂S liquid loading as a function of initial COS partial pressure and DEA concentration at 120 °C.

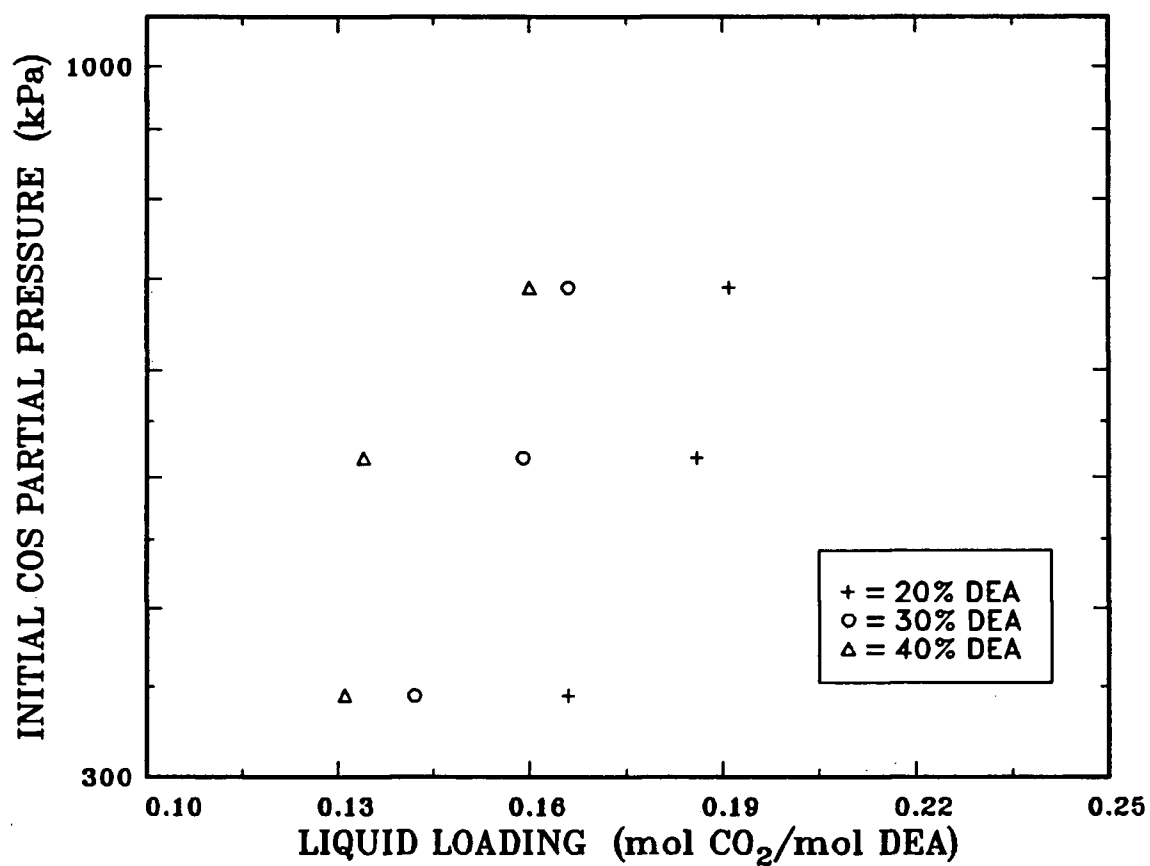


Figure 7.5: CO₂ liquid loading as a function of initial COS partial pressure and DEA concentration at 120 °C.

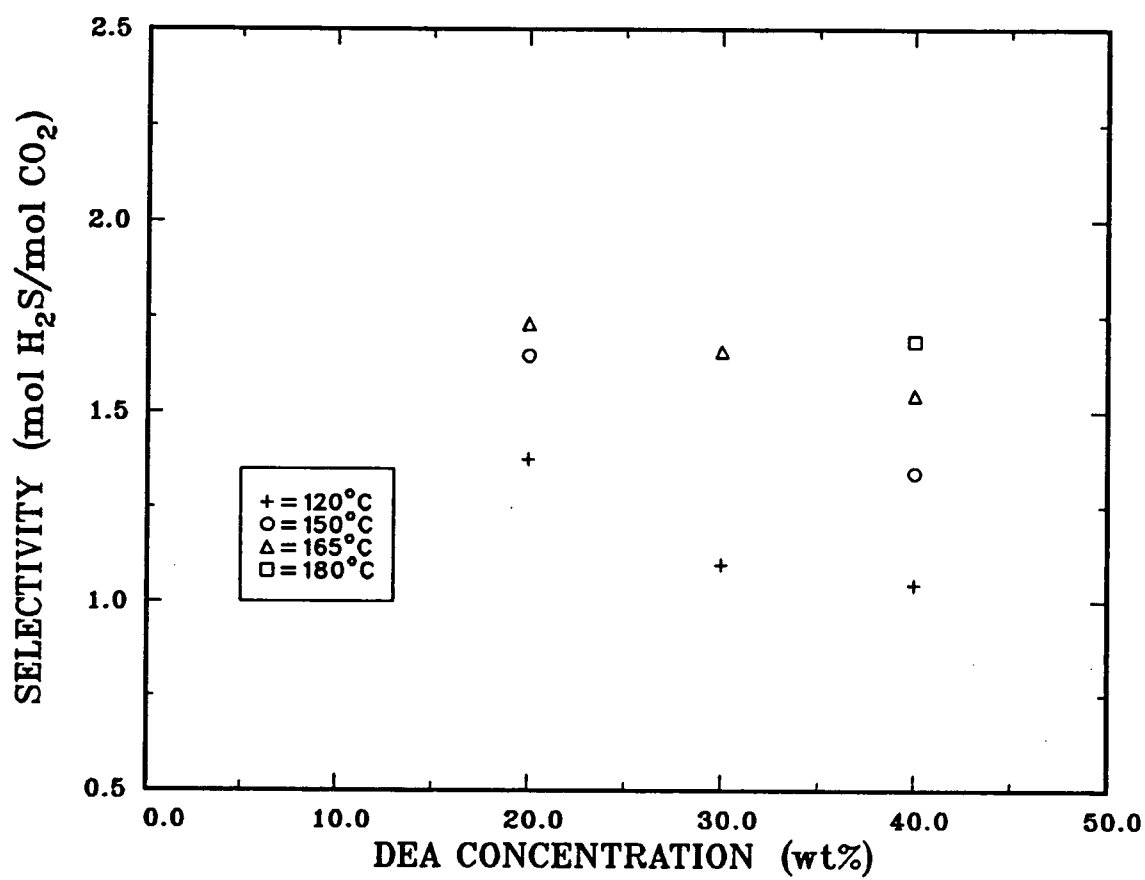


Figure 7.6: Selectivity as a function of temperature and DEA concentration.

The data at 40 °C show comparable concentrations of CO₂ and H₂S in solution, with partial pressures of H₂S being higher than those of CO₂. This is in contrast with the trend at high temperatures where the partial pressure of H₂S was lower than that of CO₂. It appears that at such low temperatures the acid gas loadings were high, causing desorption of H₂S into the gas phase. Desorption of H₂S in amine systems with high H₂S and CO₂ liquid loadings have been reported in the literature (89).

Figures 7.7 and 7.8 show typical plots of partial pressure versus loading. The wider spread of the H₂S plots is indicative of its preferential absorption. Henry's constants plotted against inverse temperature (see Figs. 7.9 and 7.10), were also found to follow the Arrhenius relationship. The plots tend towards a convergence temperature which appears to be lower for H₂S than CO₂. This trend could be linked to the various reactions occurring in the system as well as the higher selectivity of H₂S. When H₂S is absorbed into the amine solution, the absorption takes two forms: chemical and physical absorption. As the temperature increases, the solution becomes more concentrated and the physically dissolved H₂S decreases. At a temperature T_C, which is the convergence temperature, the concentration of the amine solution is very high and physical dissolution becomes negligible. At this temperature, the concentration of the amine solution is almost independent of the initial concentration, resulting in equal absorption of H₂S. Since the equilibrium partial pressure of H₂S is dependent on the solution concentration, the partial pressures at the convergence temperature are also similar. Hence the same Henry's

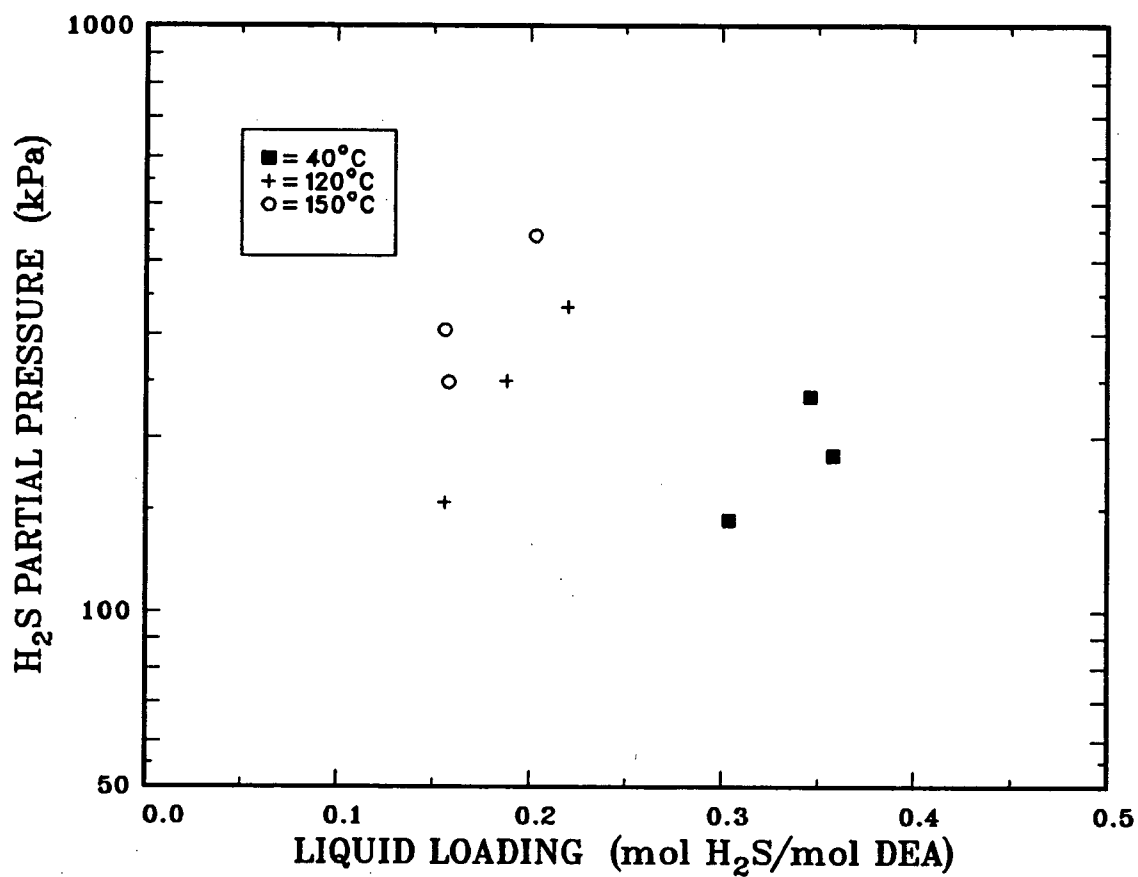


Figure 7.7: Partial pressure of H₂S as a function of liquid loading and temperature for a 30 wt% DEA solution.

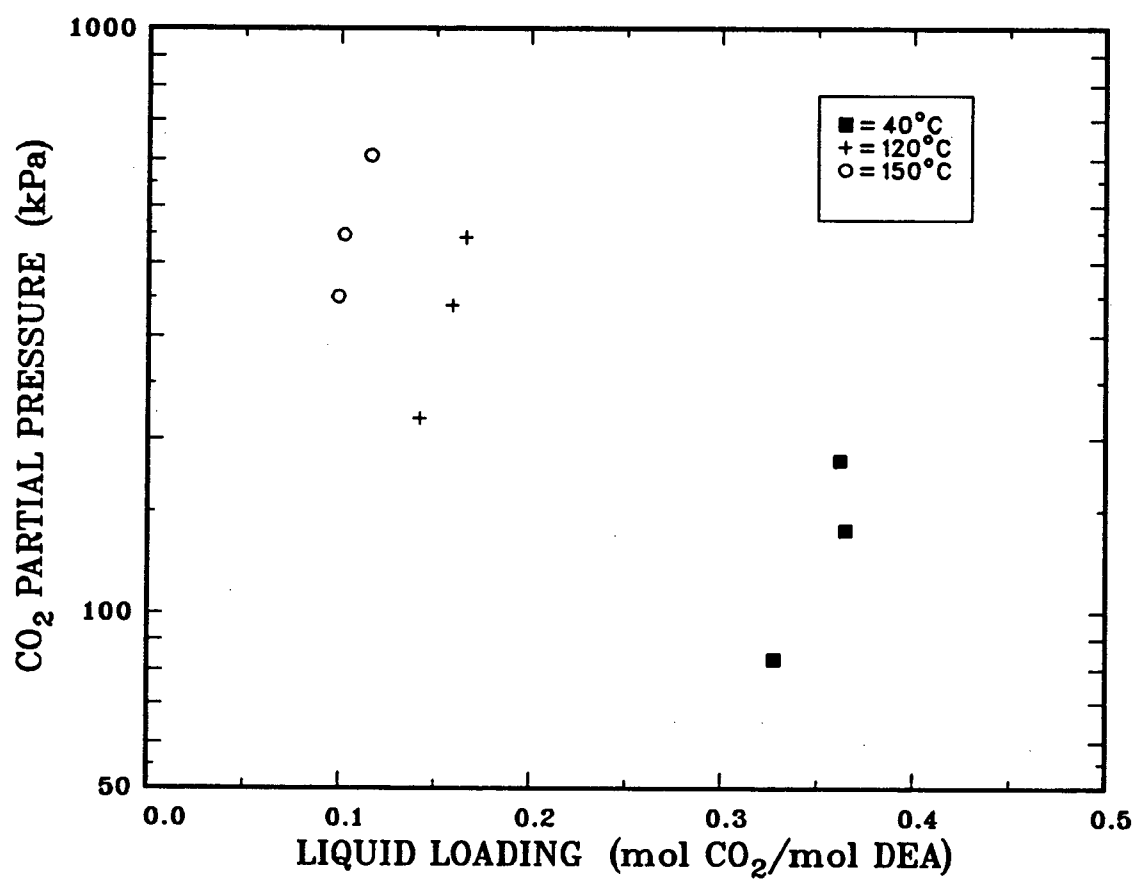


Figure 7.8: Partial pressure of CO₂ as a function of liquid loading and temperature for a 30 wt% DEA solution.

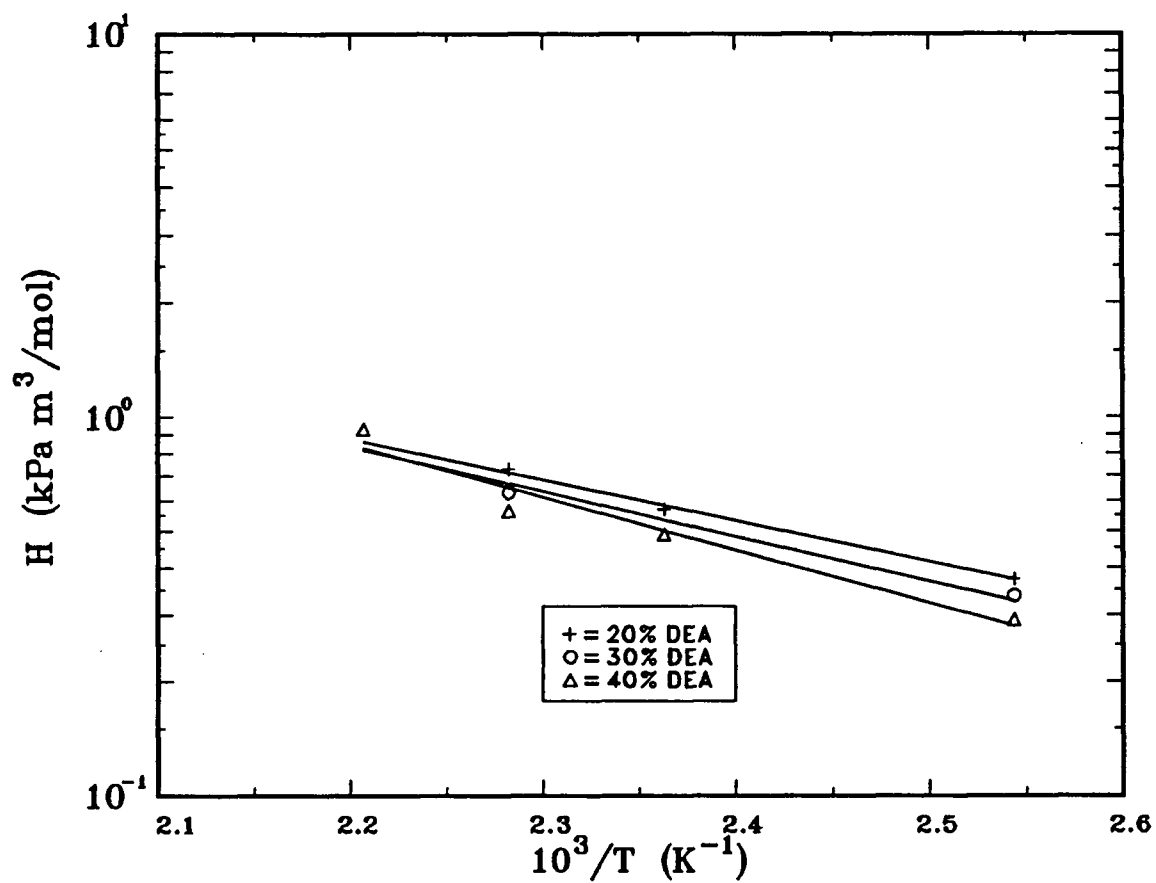


Figure 7.9: Henry's constant for H₂S in aqueous DEA solutions containing also CO₂ and COS.

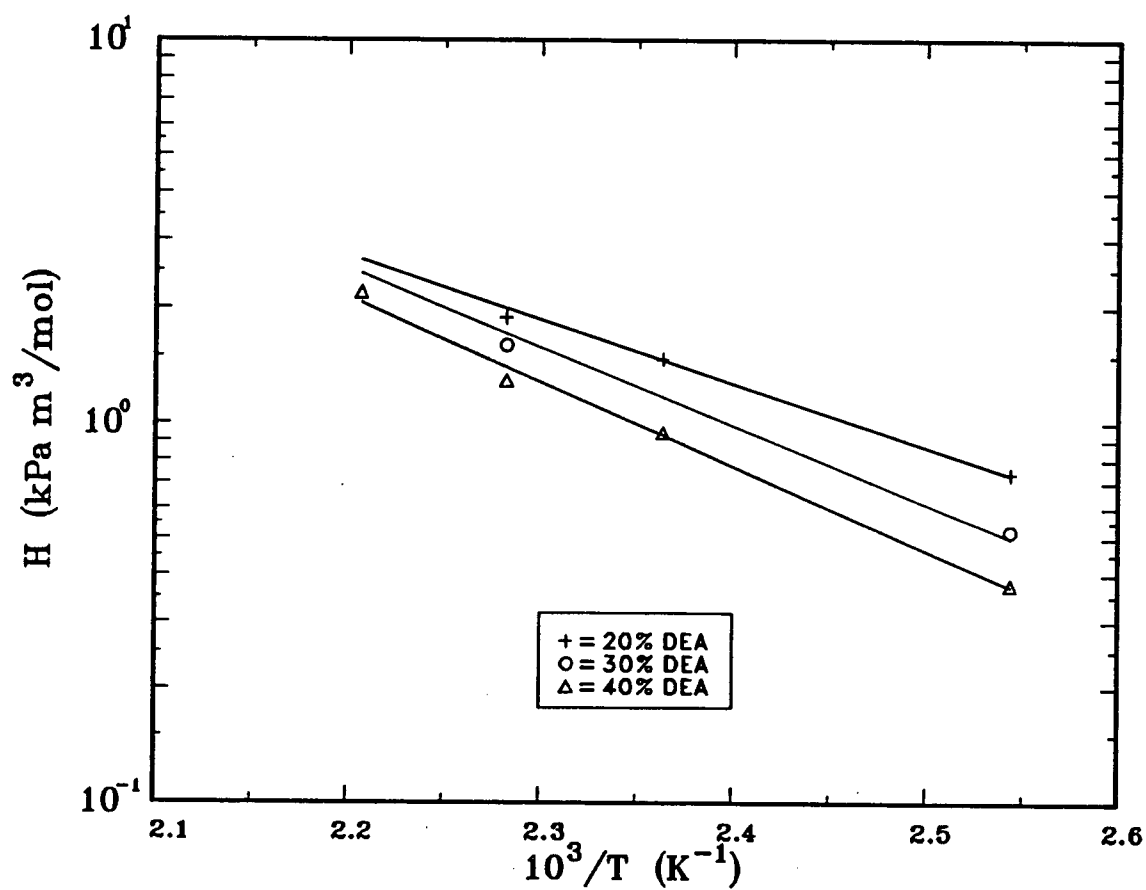


Figure 7.10: Henry's constant for CO₂ in aqueous DEA solutions containing also H₂S and COS.

constants are obtained.

In the case of CO_2 , the gas is also absorbed physically and chemically, chemical absorption being via the carbamate reaction and the hydration of CO_2 . As long as some water is still available in the solution, there will be differences in the amount of hydrated CO_2 . Hence the total CO_2 absorbed and the Henry's constants are still functions of the initial DEA concentration. The convergence temperature corresponds to the temperature at which water is virtually absent from the liquid phase. The presence of a convergence temperature may be peculiar to the current experimental set-up since the vapour space was 500 mL compared to 100 mL of liquid.

Although degradation reactions involving CO_2 could affect its concentration, analysis of liquid samples following the previously outlined procedures (see Chapter 3), indicated such reactions to be negligible within the duration of the experiments.

7.3.3 MODEL PREDICTIONS

In order to use Eqs. 7.30 to 7.33 to predict VLE, it is necessary to limit the unknowns to four. K_3 to K_7 , H_{CO_2} and $H_{\text{H}_2\text{S}}$ are known from the work of Kent and Eisenberg (39), and are given in appendix E. H_{COS} was found in this study by performing COS solubility experiments in pure water at low temperatures and extrapolating the results to higher temperatures by means of Eq. 7.5. The other unknowns are K_1 , K_2 and K_{COS} ; the latter has not been reported previously for the present system. Although K_1 and K_2 have been reported by Kent and

Eisenberg (39), the constants were derived from experimental measurements obtained from amine systems containing single acid gases and operating at temperatures below 140 °C. Since the present system contained CO₂, H₂S and COS and was operated at elevated temperatures, K₁, K₂ and K_{COS} were all calculated from the present experimental data.

The following procedure was used: For each run, the physically dissolved CO₂, H₂S and COS were determined from Eqs. 7.22 to 7.24 and Eq. 7.30 was solved for the H⁺ concentration. Once these four concentrations were known, it was possible to solve Eqs. 7.16 to 7.20 for [HCO₃⁻], [OH⁻], [CO₃²⁻], [HS⁻] and [S²⁻], respectively. The concentration values were then substituted into Eqs. 7.28, 7.29 and 7.25 to obtain [R₂NCOO⁻], [R₂NCOS⁻] and [R₂NH₂⁺]. The free amine concentration, [R₂NH], was calculated from Eq. 7.26. K₁, K₂ and K_{COS} were then determined by substituting the relevant concentrations into Eqs. 7.14, 7.15 and 7.21.

K₁ and K₂ were found to be stronger functions of temperature than amine concentration and partial pressure. The pressure and concentration dependencies were eliminated by finding the arithmetic average of the constants obtained for all runs conducted at the same temperature. K_{COS} on the other hand, exhibited wider scatter and the best fit through the average values was, at best, a marginal function of temperature. The resulting temperature dependencies are:

$$K_1 = \exp(-6.58 - 3979.22 / T)$$

$$K_2 = \exp(6.97 - 2498.39 / T)$$

$$K_{\text{COS}} = \exp(15.90 - 77.31 / T)$$

As shown in appendix E, the present K_1 values are one to two times those reported previously by Kent and Eisenberg (39) while the K_2 values are approximately twice those found by the latter authors. The deviations in the K_1 , K_2 and K_{COS} values are estimated as $\pm 11\%$, $\pm 17\%$ and $\pm 30\%$ respectively.

To test the model, the constants calculated by the above procedure were substituted into Eqs. 7.30 to 7.33 and the equations were solved by means of the non-linear equation solver NDINVT (90)) for the partial pressures corresponding to runs 1 to 26 in Table 7.4. As shown in Table 7.5, the predicted loadings matched the experimental values fairly well.

Even though more robust thermodynamic models, which consider system non-idealities and ionic interactions, have been developed, deviations greater than 20 % still occur between predictions and experimental measurements for mixed gas systems, particularly at high loadings and high temperatures (40,41). Such deviations are mostly due to the lack of literature data for the equilibrium constant for carbamate formation at moderate to high temperatures. It has also been suggested that interaction parameters involving species derived from CO_2 and H_2S , may have to be considered to obtain better predictions at high loadings (40). The fact that the present model gives good predictions for H_2S and CO_2 loadings and is also able to predict COS loadings fairly well, is a significant improvement over the previous equilibrium models which give predictions for CO_2 and/or H_2S loadings alone.

7.3.4 REPRODUCIBILITY

Some experiments were repeated to estimate the errors inherent in the experimental and analytical procedures. For the solubility runs at less than 50 °C, the average error in the Henry's constants was less than ± 3 % for the COS-DEA systems. In the case of the COS-H₂O system, because of the small amount of physically absorbed COS, a ± 1 % error in the amount of COS fed into the reactor, translated to errors of ± 4 % (or more) in the Henry's constants depending on the operating temperature. For the high temperature experiments, errors in the gas, liquid and total moles measurements for H₂S were less than ± 3 %, while CO₂ measurements recorded average errors of about ± 5 %. As stated earlier, the COS concentrations could not be determined with sufficient confidence because of their values and the lack of sensitivity of the thermal conductivity detector.

7.3.5 COS BALANCE

Material balances were performed on COS by comparing the amount introduced into the reactor with the amount reported as COS, CO₂ and H₂S from the analysis of the gas and liquid phases of the reactor. More than 90 % of the COS was accounted for in systems with low to moderate acid gas loadings (0.6 mole/mole DEA). At higher loadings, the figure dropped to about 85 %. This is probably due to the fact that at such loadings, small errors in the determination of the volume of liquid

samples transferred to the gas trapping set-up amplify the errors in the overall figures for the acid gases in the system.

Table 7.5: Predicted and experimental acid gas loadings.

RUN	CARBON DIOXIDE (mol CO ₂ /mol DEA)			HYDROGEN SULPHIDE (mol H ₂ S/mol DEA)			CARBONYL SULPHIDE (mol COS/mol DEA)	
	PRED	EXP	DEV(%)	PRED	EXP	DEV(%)	PRED	EXP
1	0.065	0.058	+12.07	0.087	0.078	+11.54	0.001	0.001
2	0.045	0.045	0.00	0.068	0.070	- 2.86	0.001	0.001
3	0.028	0.025	+12.00	0.050	0.042	+19.05	0.001	0.001
4	0.048	0.049	- 2.04	0.080	0.081	- 1.23	0.002	0.001
5	0.055	0.064	-14.06	0.105	0.110	- 4.55	0.001	0.001
6	0.080	0.082	- 2.44	0.134	0.135	- 0.74	0.001	0.001
7	0.090	0.097	- 7.22	0.129	0.136	- 5.15	0.002	0.001
8	0.127	0.130	- 2.31	0.162	0.172	- 5.81	0.002	0.001
9	0.165	0.160	+ 3.13	0.187	0.182	+ 2.75	0.004	0.001
10	0.097	0.102	- 4.90	0.154	0.156	- 1.28	0.002	0.001
11	0.110	0.116	- 5.17	0.192	0.203	- 5.42	0.003	0.001
12	0.117	0.118	- 0.85	0.180	0.173	+ 4.05	0.002	0.001
13	0.130	0.131	- 0.76	0.130	0.137	- 5.11	0.001	0.001
14	0.153	0.134	+14.18	0.158	0.147	+ 7.48	0.001	0.001
15	0.143	0.142	+ 0.70	0.151	0.156	+ 3.21	0.001	0.001
16	0.167	0.159	+ 5.03	0.194	0.188	+ 3.19	0.001	0.001
17	0.181	0.166	+ 9.04	0.225	0.220	+ 2.27	0.004	0.002
18	0.096	0.097	- 1.03	0.182	0.169	+ 7.69	0.002	0.002
19	0.107	0.128	-16.41	0.222	0.249	-10.84	0.002	0.003
20	0.157	0.166	- 5.42	0.202	0.229	-11.79	0.002	0.001
21	0.178	0.186	- 4.30	0.263	0.272	- 3.31	0.002	0.002
22	0.195	0.191	+ 2.09	0.304	0.307	- 0.98	0.003	0.002
23	0.085	0.099	-14.14	0.139	0.158	-12.03	0.001	0.002
24	0.434	0.362	+19.89	0.286	0.346	-17.34	0.003	0.003
25	0.417	0.365	+14.25	0.261	0.358	-27.09	0.003	0.002
26	0.372	0.328	+13.41	0.257	0.304	+15.46	0.002	0.001

CHAPTER 8

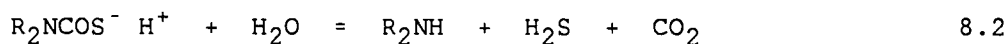
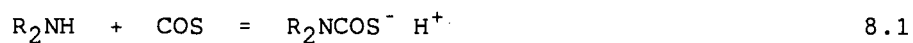
REACTION MECHANISMS

On the basis of observations discussed in Chapters 6 and 7, reaction mechanisms describing the formation of the various degradation compounds can be formulated.

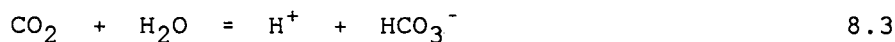
8.1 COS-DEA DEGRADATION

8.1.1 FORMATION OF MEA

The formation of MEA and the low boiling degradation compounds appears to be initiated by the absorption and hydrolysis of COS described by Eqs. 8.1 and 8.2.



The dissolved carbon dioxide gives rise mainly to H^+ and HCO_3^- , whereas hydrogen sulphide yields primarily H^+ and HS^- :

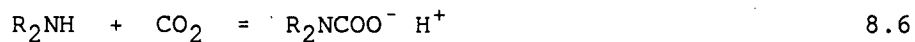


The DEA molecules are readily protonated:

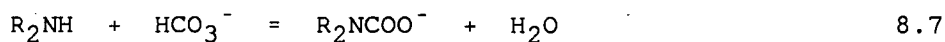


where R denotes $-C_2H_4OH$.

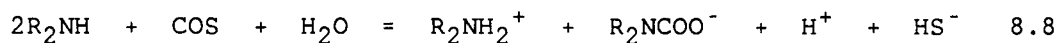
The DEA molecules also react with CO_2 to form DEA carbamate,



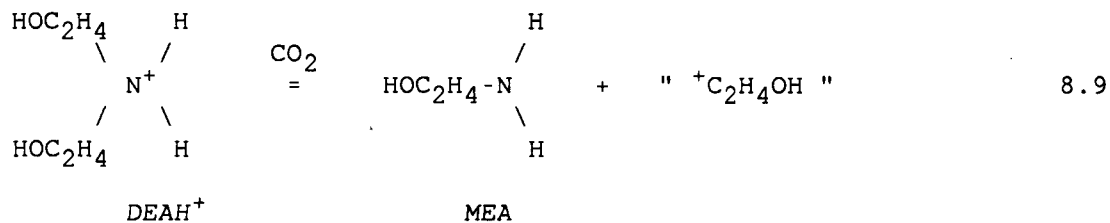
which establishes an equilibrium with the bicarbonate ions:



Equations 8.1 to 8.5 and 8.7 can be combined to give the overall reaction for the COS-DEA system:



The protonated diethanolamine molecule loses one hydroxyethyl group to form MEA:

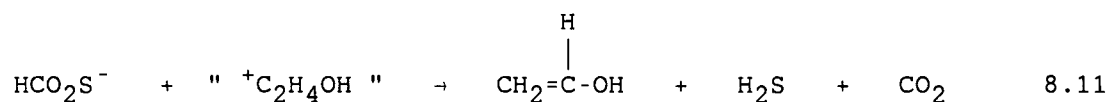


Since MEA was formed only in DEA systems containing both H_2S and CO_2 , the transformation in Eq. 8.9 therefore proceeds only in alkanolamine systems containing both CO_2 and H_2S . Analogous reactions viz: formation of EAE from EDEA and ethyl amine from EAE, suggest that the CO_2 need not be in the carbamate form. The hydroxyethyl group is in quotation marks because it does not exist as such in solution. It is suggested that it is transformed according to the following scheme:

The bisulphide ion formed in Eq. 8.4 reacts with CO_2 to form the thiol of the bicarbonate ion as proposed by Al-Ghawas et al. (50):



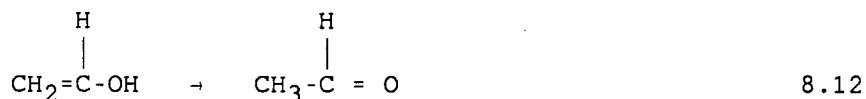
The thiobicarbonate ion then reacts with the hydroxyethyl group to form an enol of acetaldehyde:



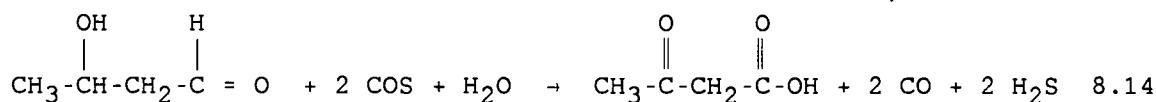
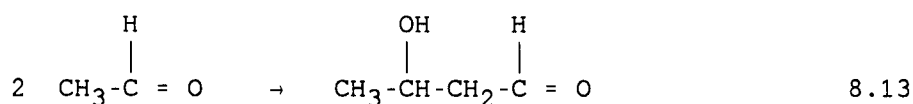
This reaction provides a means for the fast transformation of the hydroxyethyl group released in Eq. 8.9, and is probably the driving force for the formation of MEA. The presence of H_2S and CO_2 in Eq. 8.11 indicates that both compounds are not used up, but only catalyze the transformation of DEA to MEA. Eq. 8.11 also explains the lack of formation of MEA in CO_2 -DEA or H_2S -DEA systems, since such systems cannot form the thiobicarbonate ion.

8.1.2 FORMATION OF ACETALDEHYDE AND KETONES

Acetaldehyde is formed from a fast transformation of its enol:

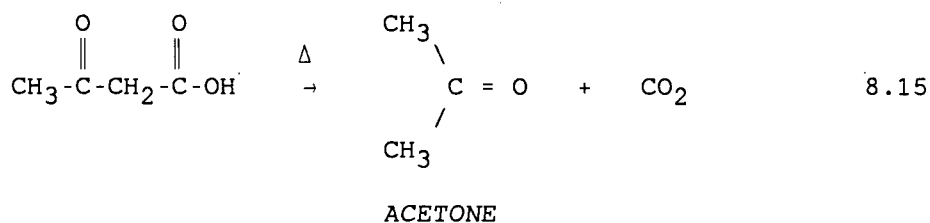


Two moles of acetaldehyde then condense in an aldol reaction, followed by reaction with COS to form an acetoacetic acid:



Acetoacetic acid

The acetoacetic acid breaks down under heat to form acetone:



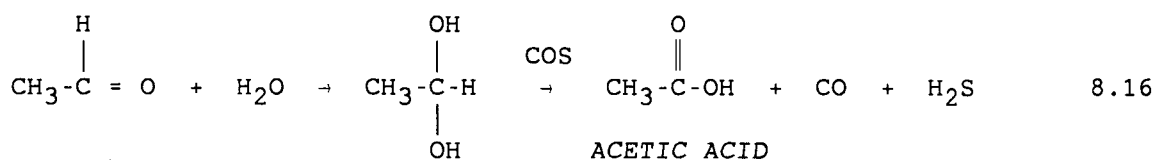
The reactions described by Eqs. 8.11 to 8.15 proceed very fast under the operating conditions used in this study, hence only the end product, acetone was detected in appreciable quantities.

Butanone may be formed by similar reactions, but the reaction steps are not fully understood.

Chakma (18) detected ethylene oxide and ethylene glycol in MDEA solutions degraded by CO_2 and attributed those compounds to the hydroxyethyl group released from protonated MDEA. The lack of formation of ethylene glycol in the present study, despite the release of the hydroxyethyl group, suggests that, given the composition of the solution in the present study, the reaction in Eq. 8.11 is a more favourable route for the transformation of the hydroxyethyl group.

8.1.3 FORMATION OF ACETIC ACID

Acetaldehyde may undergo liquid phase oxidation by COS to produce acetic acid:



Due to the presence of hydrogen sulphide in the solutions it is not unlikely that thioacetic acid was also formed. Some of the chromatograms showed peaks at the shoulders of butanone and MEA peaks.

The mechanisms proposed above can be used to explain some of the trends observed in the ethanol, acetaldehyde and acetic acid spiked runs. Recall that ethanol spiking resulted in reduced MEA concentrations and increased concentrations of the ketones and acetic acid at the

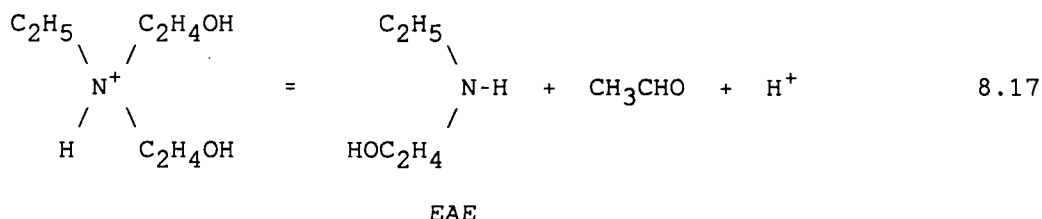
initial stages of the runs. The acetaldehyde spiked run caused increased MEA concentration and significantly higher concentrations of the ketones and acetic acid in the first four hours of the run.

In the ethanol spiked run, ethanol was probably dehydrogenated to acetaldehyde. The absence of suitable catalysts would limit the extent of this reaction. The acetaldehyde produced from ethanol disturbs the existing equilibrium in equation 8.11. This disturbance also affects the equilibrium in equation 8.9 by shifting it away from MEA production. Since acetaldehyde also generates acetic acid which, in turn, converts some MEA to HEA, the equilibrium in equation 8.9 is again shifted, this time in favour of MEA production. The decreases observed in MEA concentration suggest that the overall effect of these disturbances is a shift in equilibrium against MEA production. The same explanations apply to the observed trends in the acetaldehyde spiked run. However, the much higher acetaldehyde concentration and, by inference, higher acetic acid concentration, would cause a greater depletion of MEA via HEA production. Hence the equilibrium eventually shifts in favour of MEA production. The effect of the higher MEA depletion on the equilibrium in equation 8.9 is also the reason for the higher rate of DEA degradation observed in the acetic acid spiked run. This explains the contradictions between this result and an earlier work that reported decreased rate of DEA degradation with increased solution acidity (16). The lack of formation of the ketones in the acetic acid spiked run may be due to a reaction between the hydroxyethyl group and acetic acid. It could also be that acetic acid increased the acidity of the solution such that the

enol of acetaldehyde could not form. The absence of acetaldehyde thus prevented the formation of the ketones.

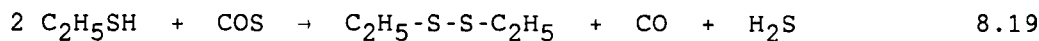
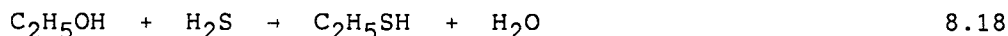
8.1.4 FORMATION OF ETHYL AMINOETHANOL (EAE)

The mechanism for the formation of EAE is similar to that of MEA formation from DEA. It involves the loss of a hydroxyethyl group from a protonated EDEA, the former being rapidly transformed to acetaldehyde via the enol:



8.1.5 FORMATION OF DIETHYL DISULPHIDE

Diethyl disulphide could form by the following reactions:

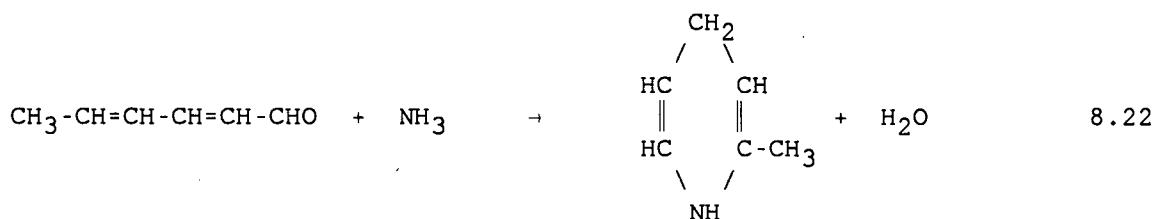
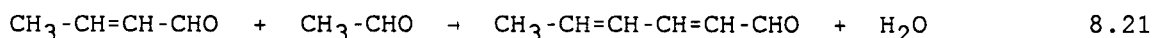
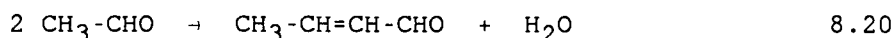


DIETHYL DISULPHIDE

Another minor sulphur compound detected was 1,2 dithiane. From the available information, it is not clear how this compound was formed.

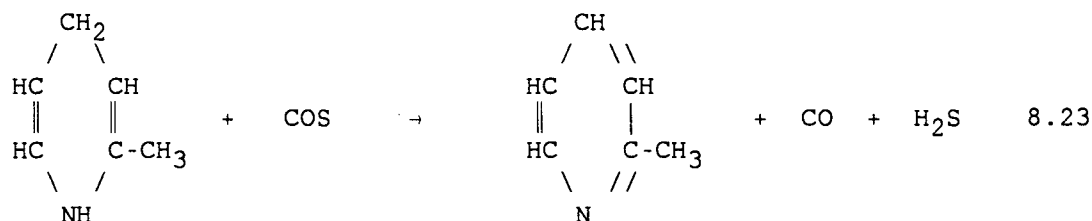
8.1.6 FORMATION OF SUBSTITUTED PYRIDINES

There is sufficient experimental evidence that protonated DEA, EDEA and EAE may lose an hydroxyethyl group to produce the respective lower order amines. Ammonia may be produced from protonated MEA in a similar manner. The high volatility and reactivity of ammonia makes its detection almost impossible under the analytical conditions used in this study. Its formation can be inferred from the presence of pyridine derivatives in the degraded solution. The substituted pyridines were probably formed from the reactions of ammonia with acetaldehyde. Such reactions proceed well with paraldehyde as the starting material, but a much lower yield is obtained with acetaldehyde (91). Methyl pyridine may have formed according to the following condensation reactions:



METHYL DIHYDROPYRIDINE

Methyl dihydropyridine then reacts with COS to form methyl pyridine:

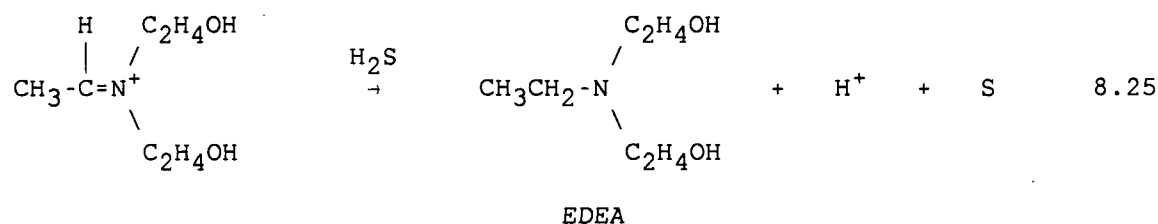
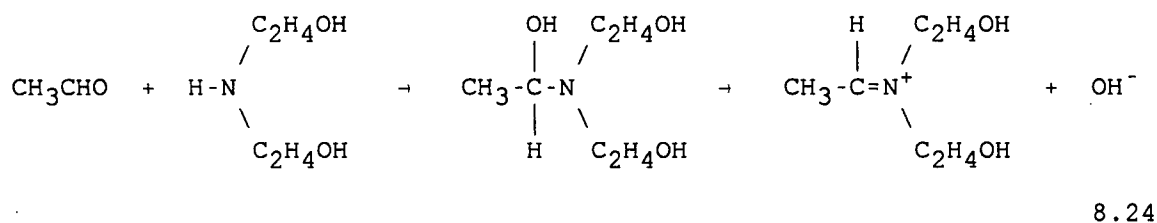


METHYL PYRIDINE

Ethyl methyl pyridine may form by a related condensation, but a precise scheme cannot be offered.

8.1.7 FORMATION OF ETHYLDIETHANOLAMINE (EDEA)

In the presence of nickel catalysts and hydrogen, alkyl amines have been formed from aqueous or alcoholic ammonia and acetaldehyde (92). Production of EDEA may proceed in an analogous manner between DEA and acetaldehyde:

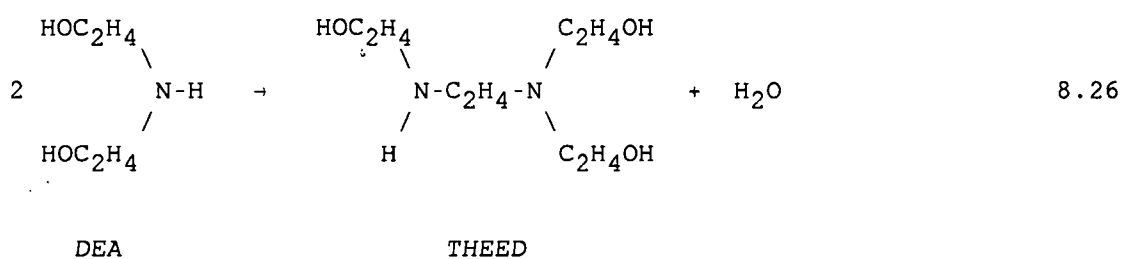


The absence of a catalyst is probably responsible for the low concentrations of EDEA recorded in most of the runs.

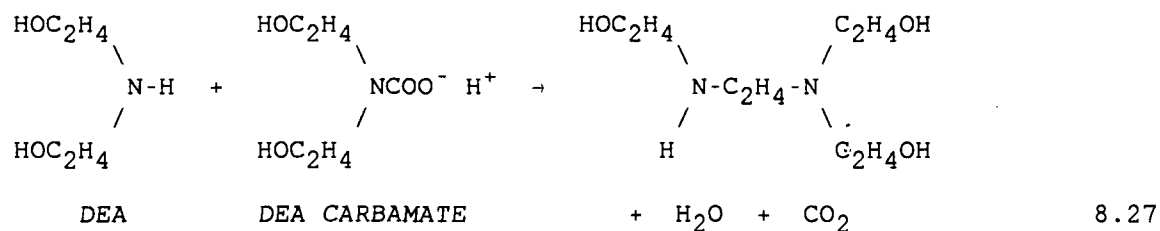
It should be noted that CS_2 may also serve the role of an oxidizing agent where COS appears in the above reaction mechanisms. In such cases, the byproduct will be carbon monosulphide (CS) instead of carbon monoxide (CO).

8.1.8 FORMATION OF N,N,N' -TRIS HYDROXYETHYL ETHYLENEDIAMINE (THEED)

The production of THEED from DEA or DEA and DEA carbamate has already been reported by Kennard and Meisen (14):



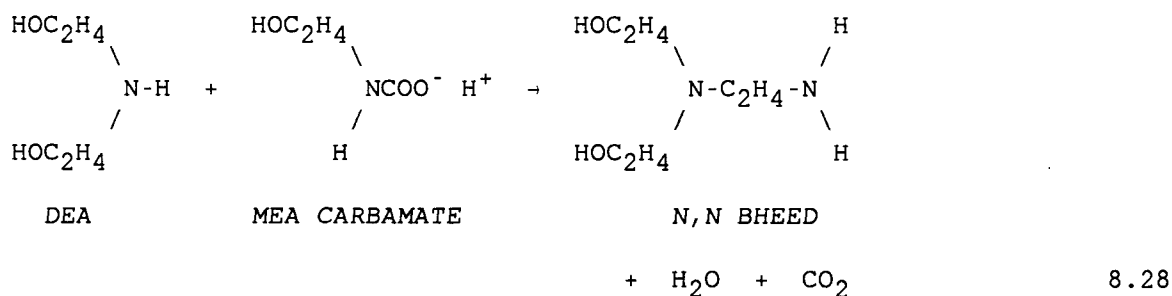
or



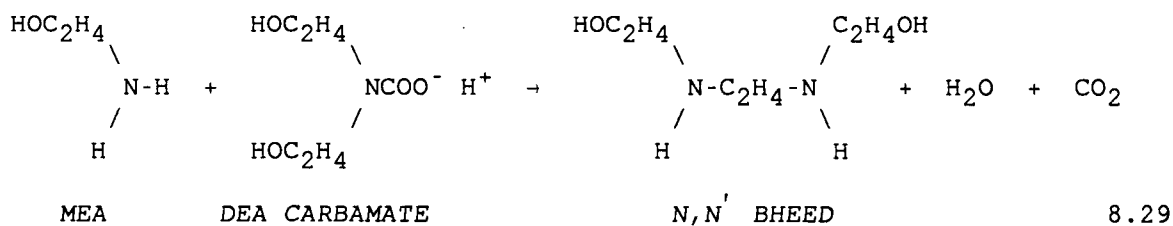
Equation 8.26 represents the thermal route for THEED formation and may be discounted at the temperatures used in this study.

8.1.9 FORMATION OF BIS HYDROXYETHYL ETHYLENEDIAMINE (BHEED)

BHEED was formed from the reaction between MEA and DEA carbamate or vice versa:



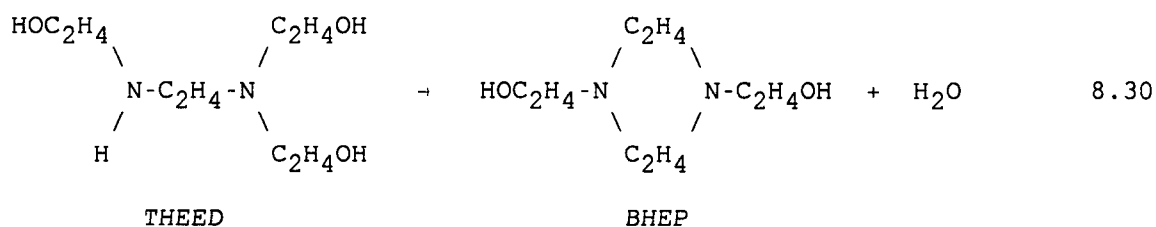
or



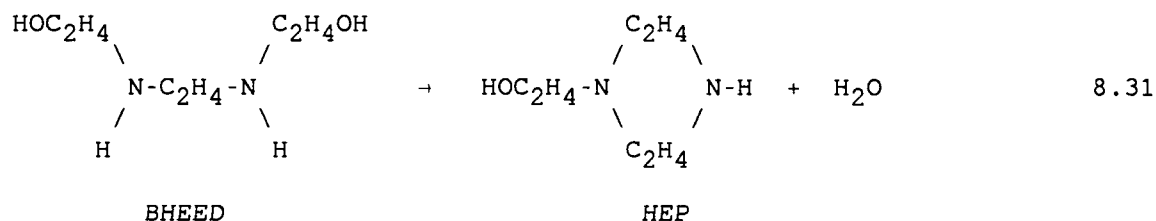
The thermal formation of BHEED (reaction of DEA with MEA) does not proceed readily at the temperatures used in this study. The above equations represent the overall reactions and may, in detail, involve additional ionic steps.

8.1.10 FORMATION OF N,N'-BIS HYDROXYETHYL PIPERAZINE (BHEP) AND
N-HYDROXYETHYL PIPERAZINE (HEP)

Both THEED and BHEED may undergo dehydration, which leads to the formation of BHEP and HEP, respectively:

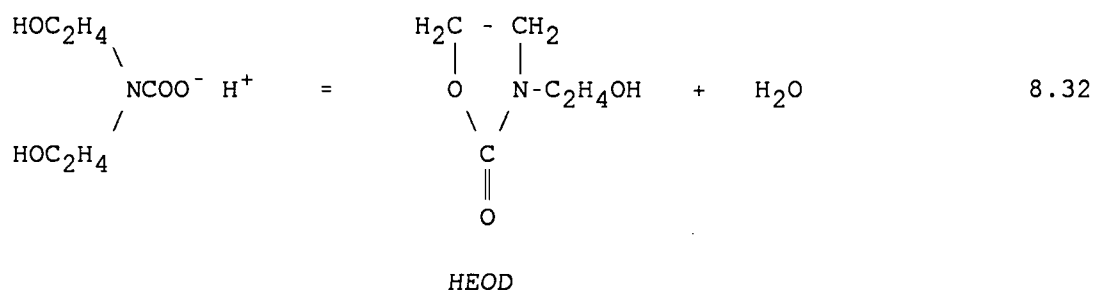


and



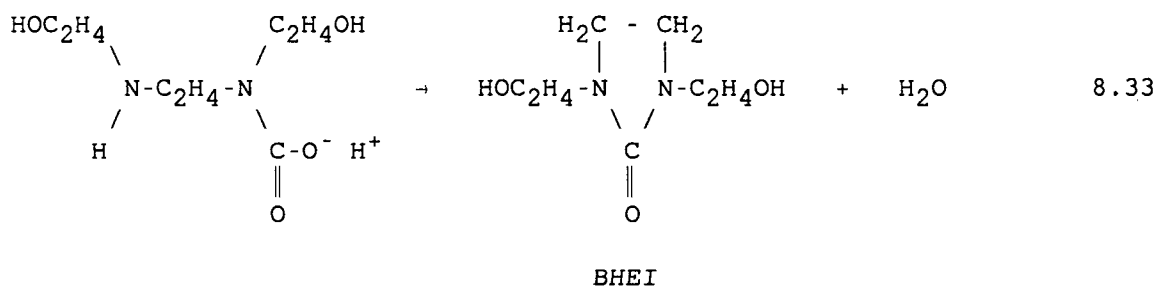
8.1.11 FORMATION OF N-HYDROXYETHYL OXAZOLIDONE (HEOD)

Kim and Sartori (13) and Kennard and Meisen (14) have shown that DEA carbamate dehydrates to HEOD and that an equilibrium exists between both compounds:

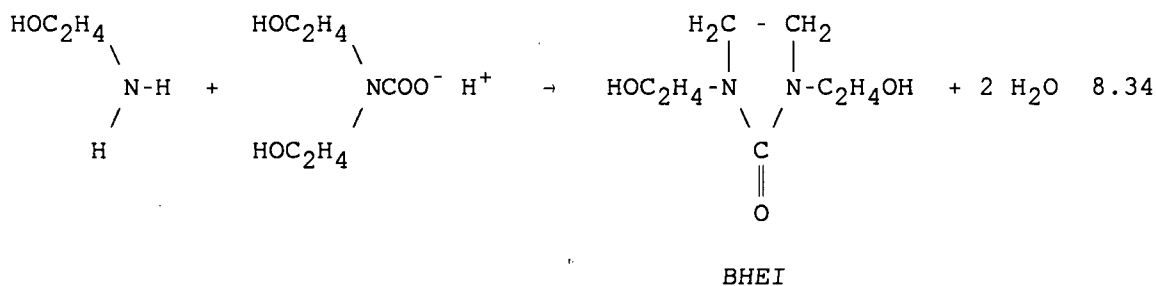


8.1.12 FORMATION OF N,N'-BIS HYDROXYETHYL IMIDAZOLIDONE (BHEI)

BHEI results from the dehydration of BHEED carbamate:



and the reaction between MEA and DEA carbamate:

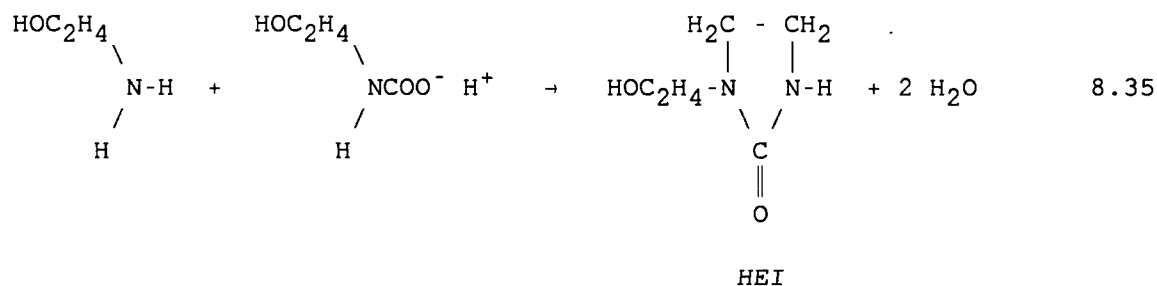


The latter is a two step reaction consisting of the coupling of MEA and DEA carbamate to form an intermediate, and the cyclization of the

intermediate product. BHEED carbamate appears to be the most likely intermediate product and since BHEED was a stable intermediate, the formation of BHEI is better represented by Eq. 8.33. In all the systems studied, the formation of BHEED precedes that of BHEI.

8.1.13 FORMATION OF N-HYDROXYETHYL IMIDAZOLIDONE (HEI)

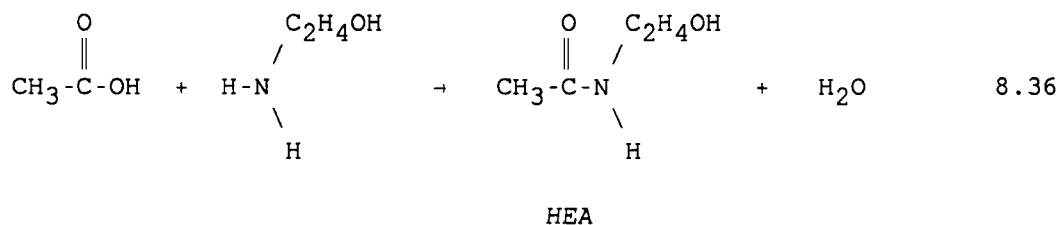
The formation of HEI proceeds via the reaction between MEA and MEA carbamate:



The same reaction could produce hydroxyethyl ethylenediamine (HEED), but this compound was not detected probably due to its transformation to HEI through a reaction similar to Eq. 8.33. Therefore, Eq. 8.35 may involve HEED as an intermediate.

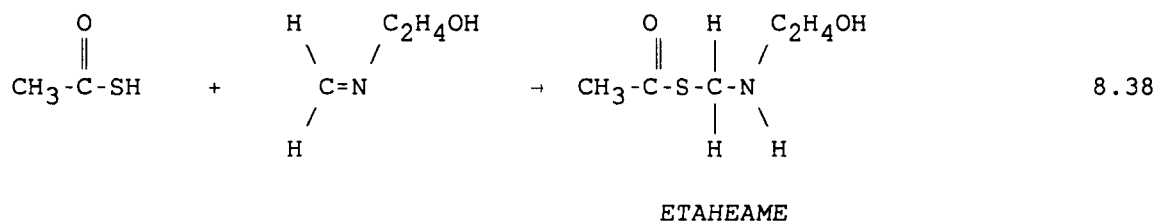
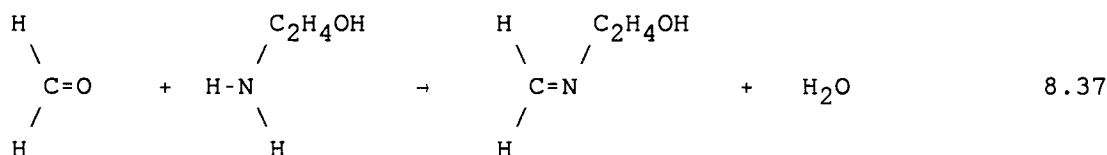
8.1.14 FORMATION OF N-HYDROXYETHYL ACETAMIDE (HEA)

Acetic acid reacts readily with MEA to form HEA:



8.1.15 FORMATION OF ETHANETHIOIC ACID-(S-(HYDROXYETHYL) AMINO) METHYL ESTER (ETAHEAME)

This compound can be synthesized by condensing monoethanolamine, thioacetic acid and formaldehyde in a Mannich reaction (93):

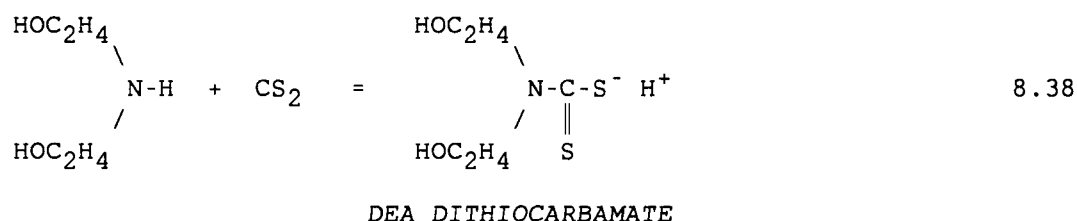


Monoethanolamine was detected in the degraded solution. Thioacetic could have been formed from acetic acid and H₂S. Formaldehyde may have been a

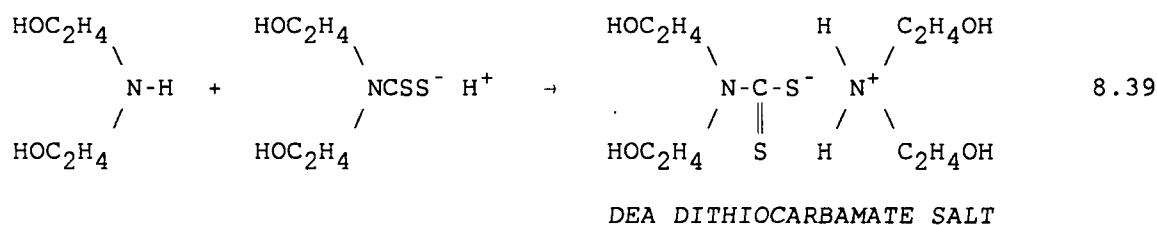
by-product of some reactions related to the ones described above. Thus the three reactants needed to produce this compound appear to be available in the degraded solution.

8.2 CS₂-DEA DEGRADATION

The experimental observations suggest that the mechanism previously developed for the COS-DEA system also applies, to a large extent, to the CS₂-DEA system. In the latter case, amine dithiocarbamate is also formed,



which may react with additional DEA to yield the dithiocarbamate salt of DEA:



At high temperatures such as 180 °C, the dithiocarbamate salt is unstable, reverting to DEA and CS₂. The latter is then hydrolysed to COS, CO₂ and H₂S. CO₂ subsequently undergoes the typical ionization and DEA carbamate formation reactions as shown in Equations 8.4 and 8.5. H₂S is also ionized and forms protonated DEA according to Equations 8.3 and 8.6. The subsequent reactions then proceed as already shown for the COS-DEA system, resulting in the formation of degradation products.

At lower temperatures ($T \leq 165$ °C), the dithiocarbamate salt is sufficiently stable and ties up a greater amount of CS₂. Less CS₂ is left for hydrolysis and consequently, less COS, CO₂ and H₂S are formed compared to the quantities at 180 °C. The much lower concentrations of the acid gases cause degradation to proceed with the formation of very little ketones as observed for some H₂S/CO₂-DEA systems and the CS₂-DEA systems at $T \leq 165$ °C.

The extremely high rate of DEA degradation at 180 °C, relative to 165 °C (see Fig. 5.52), can be attributed to the high concentrations of H₂S and CO₂ resulting from the breakdown of the unstable dithiocarbamate salt. Under this condition, the DEA is preferentially transformed to MEA. The consequence of this is that the concentrations of the compounds formed directly from MEA (e.g. HEI, HEA) were higher at 180 °C than at 165 °C, while the concentrations of compounds resulting from reactions involving DEA (BHEED, HEOD, and THEED) were significantly lower at 180 °C than at 165 °C (see Tables C.26 and C.27 in appendix C).

8.3 FORMATION OF THE SOLID PRODUCTS

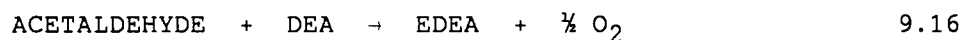
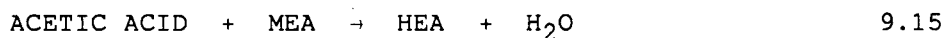
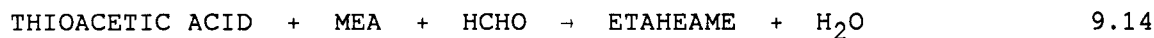
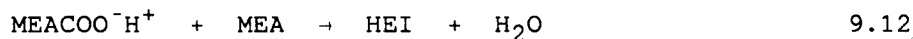
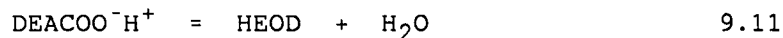
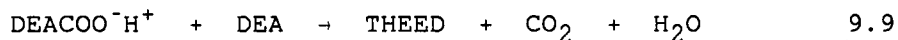
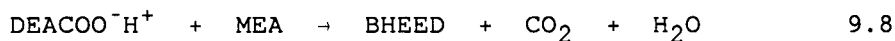
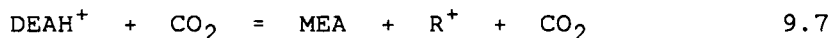
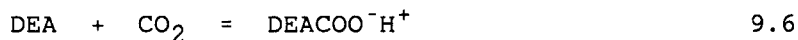
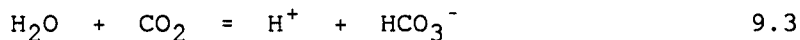
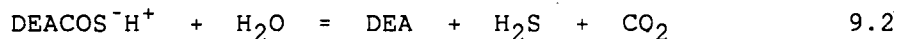
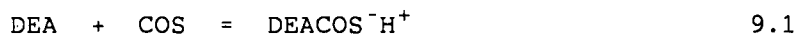
Since the solid products were not conclusively identified, no mechanisms are offered for their formation. Some reaction mechanisms show the formation of elemental sulphur. As well, runs conducted for short durations ($t \leq 12$ h) only produced sulphur deposits but not the solid product. Considering the elements that constitute the solid product, it appears that its formation was the result of reactions involving sulphur, the amine and the hydroxyethyl group.

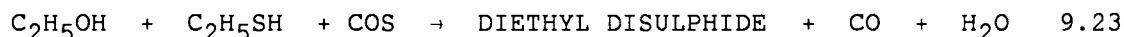
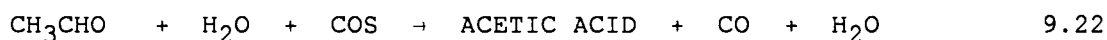
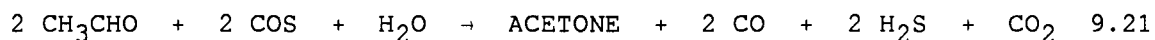
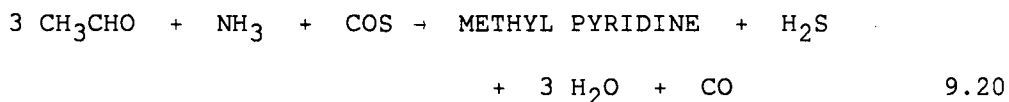
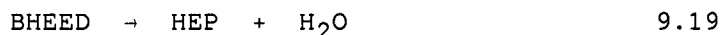
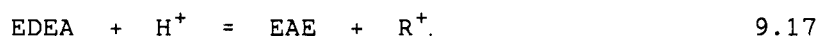
CHAPTER 9

KINETIC MODEL FOR DEA DEGRADATION

9.1 COS INDUCED DEGRADATION OF DEA

The reaction mechanisms proposed in Chapter 8 can be summarized by the following equations:



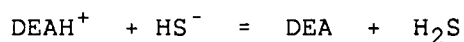


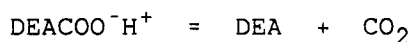
The number of equations demonstrates the complexity of DEA degradation by COS. In order to develop a kinetic model based on the reactions, the following simplifying assumptions are invoked.

* The solubility and hydrolysis reactions governed by Equations 9.1 to 9.6 are much faster than the degradation reactions, and equilibrium acid gas loadings are achieved prior to the commencement of any significant degradation. This simplification has been used successfully in the past (13,14,18).

* With the exception of Equations 9.1 to 9.6, all reactions are considered to be irreversible because the experimental data suggest that for the duration of the experiments, equilibrium was still in favour of products formation (forward reaction).

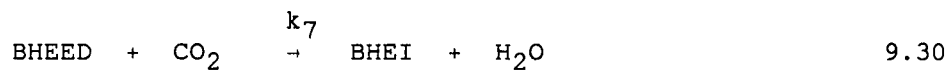
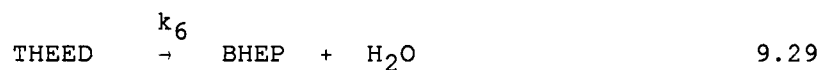
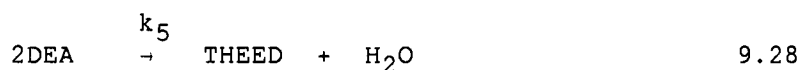
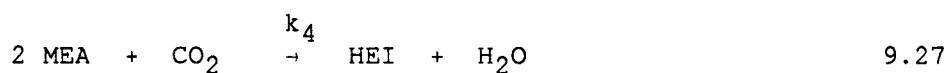
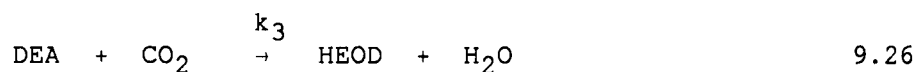
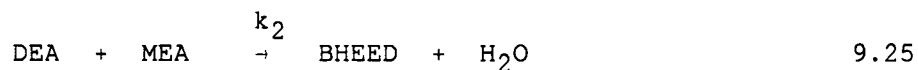
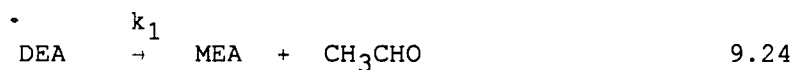
* Ionic species such as DEAH^+ and $\text{DEACOO}^-\text{H}^+$ may be written as:





- * The reaction between MEA and DEACOO^- is equivalent to the reaction between MEACOO^- and DEA.
- * The amine solutions are sufficiently dilute so that the concentration of water can be neglected in the kinetic expressions.
- * When CO_2 or H_2S appears on both sides of an equation, it is considered to act as a catalyst and need not be included in the kinetic expressions.
- * Except for the runs conducted at temperatures above 180°C , the concentrations of ETAHEAME, HEA, EDEA, HEP and the low boiling degradation compounds (except MEA) were generally low. In addition, some of the reactions do not tie up any nitrogen atoms. Therefore, Eqs. 9. 14 - 9.23 are considered as secondary degradation reactions and are neglected in the kinetic expressions.
- * Reactions leading to the formation of solids are neglected because elemental analysis showed that the amount of amine responsible for solids formation is small.

The above assumptions lead to the following simplified set of reactions:



The corresponding rate equations are:

$$\begin{aligned} d[\text{DEA}]/dt &= -k_1 [\text{DEA}] - k_2 [\text{DEA}] [\text{MEA}] \\ &\quad - k_5 [\text{DEA}] - k_3 [\text{DEA}] [\text{CO}_2] \end{aligned} \quad 9.31$$

$$d[\text{MEA}]/dt = k_1 [\text{DEA}] - k_4 [\text{MEA}]^2 [\text{CO}_2] - k_2 [\text{DEA}] [\text{MEA}] \quad 9.32$$

$$d[\text{BHEED}]/dt = k_2 [\text{MEA}] [\text{DEA}] - k_7 [\text{BHEED}] [\text{CO}_2] \quad 9.33$$

$$d[\text{BHEP}]/dt = k_6 [\text{THEED}] \quad 9.34$$

$$d[\text{HEOD}]/dt = k_3 [\text{DEA}] [\text{CO}_2] \quad 9.35$$

$$d[\text{HEI}]/dt = k_4 [\text{MEA}]^2 [\text{CO}_2] \quad 9.36$$

$$d[\text{THEED}]/dt = k_5 [\text{DEA}] - k_6 [\text{THEED}] \quad 9.37$$

$$d[\text{BHEI}]/dt = k_7 [\text{BHEED}] [\text{CO}_2] \quad 9.38$$

where [i] denotes concentration of specie i in units of mol/L.

Equations 9.31 to 9.38 represent the simplified kinetic model for the DEA degradation by COS. Although the CO_2 and H_2S loadings were obtained from the COS solubility and hydrolysis system described by Equations 9.1 to 9.6, these values were assumed to be either constant or not limiting throughout the duration of the runs. Therefore, the acid gas loadings can be lumped into the rate constants. It is recognized that, as degradation proceeds, the concentration of DEA falls thereby causing a reduction in the CO_2 and H_2S solution loadings. However, since MEA and other degradation compounds such as BHEED, THEED and BHEP (94) are also able to absorb acid gases, their presence in the degraded solution will compensate for the reduction in acid gas loadings associated with the reduction in DEA concentration. The acid gas loadings should therefore remain approximately constant. Equations 9.31 - 9.38 are kinetic expressions and do not strictly follow the reaction stoichiometries. For example THEED formation has a molecularity of two with respect to DEA according to Eqs. 9.9 and 9.28, but the first order

kinetic representation in Eq. 9.37 has been found in the past (16,18), to represent experimental data better. This was also the case in the present study.

In order to solve Eqs. 9.31 - 9.38, the rate constants k_1 to k_7 must be known. They were determined by first fitting a 5th order polynomial expression to the concentration - time measurements for DEA, MEA, BHEED, BHEP, HEOD, HEI, THEED and BHEI. In this way, the concentrations for each compound could be found at uniform time intervals. For each experimental run, a non-linear optimization routine, NLPQL (95) was used to search for the set of rate constants k_1 to k_7 which gave the best agreement with the experimental measurements. The objective function, which was minimized in the search, was defined as:

$$\sum_{t=1}^N \sum_{i=1}^8 (Y_{c_i,t} - Y_{e_i,t})^2 / Y_{\max_i}^2 \quad 9.39$$

where $i = 1, 2, \dots, 8$ denotes the compounds (DEA, MEA, BHEED, BHEP, HEOD, HEI, THEED, BHEI, respectively) in the kinetic expressions and $t = 1, 2, \dots, N$ indicates the time at which samples were taken. Y_{c_i} , Y_{e_i} and Y_{\max_i} denote the calculated, experimental and maximum experimental concentrations for compound i , respectively. The term Y_{\max_i} was introduced as a weighting factor to account for the considerable differences between the concentrations of DEA and the degradation

products. A Runge-Kutta differential equation solver (96), was employed to solve the set of differential equations.

As shown in Table D.19 in appendix D, the rate constants obtained from the above procedure were functions of temperature and pressure. Except for k_3 and k_5 , the dependency on the initial DEA concentration did not follow any specific pattern and was therefore attributed to scatter in the experimental data and/or approximations in the NLPQL and Runge-Kutta routines. The variation with concentration was eliminated by taking the average of the constants (except k_3 and k_5) for all runs conducted at the same temperatures and COS partial pressures. For all the runs conducted at an initial COS partial pressure of 345 kPa and temperatures below 165 °C, the rate constants could be represented by the Arrhenius expressions shown below:

k_1	$= 4.353 \times 10^4 \exp (-56,174/RT)$		9.40
k_2	$= 1.525 \times 10^7 \exp (-80,282/RT)$		9.41
k_4	$= 8.554 \times 10^8 \exp (-94,931/RT)$		9.42
k_6	$= 5.398 \times 10^4 \exp (-59,315/RT)$		9.43
k_7	$= 1.412 \times 10^2 \exp (-31,077/RT)$		9.44
k_3	$= 4.029 \times 10^3 \exp (-55,063/RT)$	(for $DEA_0 = 4M$)	9.45
k_3	$= 2.683 \times 10^3 \exp (-54,924/RT)$	(for $DEA_0 = 3M$)	9.46
k_3	$= 1.774 \times 10^2 \exp (-47,272/RT)$	(for $DEA_0 = 2M$)	9.47
k_5	$= 9.900 \times 10^6 \exp (-77,450/RT)$	(for $DEA_0 = 4M$)	9.48
k_5	$= 1.931 \times 10^7 \exp (-82,670/RT)$	(for $DEA_0 = 3M$)	9.49

$$k_5 = 1.343 \times 10^6 \exp (-75,604/RT) \quad (\text{for } \text{DEA}_0 = 2M) \quad 9.50$$

The activation energies are in units of J/mole while the frequency factors and the rate constants are in units of h^{-1} or $\text{L} (\text{mol h})^{-1}$, depending on the order of the reaction. Values of the activation energies are typical of liquid phase reactions (97), but some of the frequency factors are unusually low.

The rate constants k_1 , k_2 , k_3 and k_5 for runs conducted at different pressures were found to be related by the expression:

$$k_{P2} = k_{P1} \times (P_2/P_1)^{0.5} \quad 9.51$$

The pressure variation of k_4 can be represented by the expression:

$$k_{P2} = k_{P1} \times (P_2/P_1)^{1.19} \quad 9.52$$

Rate constants k_6 and k_7 were roughly independent of pressure. Since DEA and MEA have the highest absorption capacities compared to the other compounds, it is not surprising that the rate constants that control the reactions involving these two compounds are the ones affected by changes in pressure.

By using Eqs. 9.40 - 9.52, it was possible to obtain the rate constants governing the degradation reactions conducted under the following operating conditions:

DEA concentration	20	-	40 wt% (appr. 2 - 4M)
Temperature	120	-	165 °C
COS partial pressure	345	-	1172 kPa

The rate constants were then substituted in the kinetic expressions and the expressions were solved with the Runge-Kutta routine (96).

Tables D.1 - D.18 in appendix D, show the predicted and experimental concentrations for DEA and the major degradation compounds. The maximum deviation between the experimental and predicted DEA concentrations was approximately 22%, averaging below 8% at $T \leq 180$ °C. MEA predictions were also good, with an average deviation of about 18%, except for runs conducted at $T \geq 165$ °C where more substantial deviations were recorded. This was due to the fact that some reactions such as the formation of HEA which consume MEA but considered as minor reactions, become appreciable at high temperatures. At such temperatures the experimental concentrations show maxima but the model predictions did not, consequently resulting in deviations that increased with time. In the case of THEED, the model predicted lower concentrations for experimental concentrations greater than 0.2M. The consistently negative deviations suggest that a fairly appreciable degree of error may be associated with the experimental concentrations particularly at high THEED concentrations, since the THEED used for calibration was not pure (see appendix A.2.2). The model predictions for BHEED, BHEP, HEOD, HEI and BHEI were in general, fairly good. However, because of the generally low concentrations of these compounds, a qualitative assesment does not give a fair representation of the model predictions since a difference

of 0.01M between the experimental and predicted concentrations often result in deviations above 25%.

In summary, the model gave satisfactory predictions for the operating conditions indicated above. It should be possible to extend the range of applicability to COS partial pressures lower than 345 kPa without any significant errors. Results of sensitivity analyses (shown in detail in appendix E.2) indicate that the rate constants obtained from the optimisation method are accurate within $\pm 20\%$.

9.2 CS₂ INDUCED DEGRADATION OF DEA

The experimental results suggest that the mechanism previously developed for the COS-DEA system should also apply, to a large extent, to the CS₂-DEA system. At $T \leq 165^\circ\text{C}$, the dithiocarbamate salt formation either reaches completion or attains equilibrium within two hours. During this period, no degradation compounds were formed in appreciable amounts. Subsequently, degradation products began to form. Since the products formed were the same as those found in the COS-DEA system, the reaction mechanism and the rate expressions describing the latter (Eqs. 9.31 - 9.38) should also apply to the CS₂-DEA system.

In addition, the reactions occurring in the first few hours viz. the dithiocarbamate salt formation and the hydrolysis of CS₂ which produces the species that subsequently induce degradation, must be included in the rate expressions. The resulting rate equations that describe the CS₂-DEA system are as follows:

$$\begin{aligned} d[\text{DEA}]/dt &= -k_1 [\text{DEA}] - k_2 [\text{DEA}] [\text{MEA}] - k_5 [\text{DEA}] \\ &\quad - k_3 [\text{DEA}] [\text{CO}_2] - k_9 [\text{DEA}] [\text{CS}_2] \end{aligned} \quad 9.53$$

$$d[\text{MEA}]/dt = k_1 [\text{DEA}] - k_4 [\text{MEA}]^2 [\text{CO}_2] - k_2 [\text{DEA}] [\text{MEA}] \quad 9.54$$

$$d[\text{BHEED}]/dt = k_2 [\text{MEA}] [\text{DEA}] - k_7 [\text{BHEED}] [\text{CO}_2] \quad 9.55$$

$$d[\text{BHEP}]/dt = k_6 [\text{THEED}] \quad 9.56$$

$$d[\text{HEOD}]/dt = k_3 [\text{DEA}] [\text{CO}_2] \quad 9.57$$

$$d[\text{HEI}]/dt = k_4 [\text{MEA}]^2 [\text{CO}_2] \quad 9.58$$

$$d[\text{THEED}]/dt = k_5 [\text{DEA}] - k_6 [\text{THEED}] \quad 9.59$$

$$d[\text{BHEI}]/dt = k_7 [\text{BHEED}] [\text{CO}_2] \quad 9.60$$

$$d[\text{CS}_2]/dt = -k_9 [\text{DEA}] [\text{CS}_2] - k_8 [\text{CS}_2] \quad 9.61$$

$$d[\text{SALT}]/dt = k_9 [\text{DEA}] [\text{CS}_2] \quad 9.62$$

The assumption of excess water still holds and the concentration of water is excluded from Eq. 9.61.

When the salt formation and hydrolysis reactions were discounted, it was possible to obtain the rate constants $k_1 - k_7$ by following the optimisation procedure described earlier. The resulting constants are

given in Table D.20 in appendix D. However, the optimisation routine did not produce reasonable values of k_8 and k_9 when Eqs. 9.53 - 9.62 were solved simultaneously. This may be due to the fact that the concentrations of the dithiocarbamate salt were not determined during the first few hours of each run when DEA was consumed primarily in the salt formation. It could also be that Eq. 9.61 describing the consumption of CS_2 via hydrolysis and the salt formation need to be modified. There is therefore the need to get more experimental data and a better understanding of the reactions occurring within the first few hours of each run, before a model can be developed to cover the degradation reactions as well as the dithiocarbamate salt formation. This aspect will be addressed in a subsequent study.

CHAPTER 10

CONCLUSIONS AND RECOMMENDATIONS

10.1 CONCLUSIONS

10.1.1 COS INDUCED DEGRADATION

1. Carbonyl sulphide degrades DEA to form water soluble degradation products and an insoluble sulphur - rich solid.
2. The reactions in the COS-DEA system can be broken down into three stages. First is the formation of the DEA thiocarbamate which enhances the absorption of COS. Second is the hydrolysis of COS or DEA thiocarbamate and the redistribution of COS, CO₂, H₂S and their associated compounds between the gas and liquid phases to establish system equilibrium. The third stage involves the amine degradation reactions leading to the conversion of DEA to degradation compounds. At low temperatures, stages 1 and 2 can be clearly distinguished, whereas at high temperatures, hydrolysis is fast and distinction between the two stages is not easily observed. Reactions in stage 3 are much slower than those in the first two stages, such that equilibrium solubility and hydrolysis is usually achieved prior to the commencement of any appreciable degradation.

3. Gas and liquid phase compositions were determined for the COS-DEA system on attainment of equilibrium hydrolysis. The equilibrium could be represented by a modified Kent-Eisenberg model which is able to simulate a gas mixture containing COS in addition to CO_2 and H_2S . Previous equilibrium models are limited to the absorption of CO_2 and H_2S mixtures. The modified model is therefore a significant improvement.
4. Even though COS hydrolyses to CO_2 , DEA degradation by COS is distinct because products not previously identified in CO_2 -induced degradation were formed in the COS-DEA system.
5. The major degradation compounds in the COS-DEA system are MEA, BHEED, BHEP, HEOD, HEI, THEED and BHEI.
6. THEED, BHEP and HEOD are produced from degradation reactions involving DEA and the CO_2 generated from the hydrolysis of COS.
7. Protonated DEA (R_2NH_2^+) loses a hydroxyethyl group (R^+) to form MEA. This reaction occurs only in DEA solutions containing both H_2S and CO_2 with the latter acting as a catalyst. Similar transformations occurred in MEA, EAE and EDEA solutions, and may therefore, be generalized for solutions of primary, secondary and tertiary amines.
8. The hydroxyethyl group released during the formation of MEA initiate and undergo some complex reactions leading to the formation of low boiling degradation compounds such as acetaldehyde, ethanol, acetone, acetic acid, butanone, 1,2 dithiane, diethyl disulphide, substituted pyridines as well as HEA and EDEA.

9. MEA degrades to HEI and also reacts with acetic acid to form HEA.
10. BHEI and BHEED are formed from reactions involving MEA, DEA and their carbamates. BHEI is also formed from BHEED carbamate.
11. H_2S alone does not degrade DEA, but its mixture with CO_2 degrades DEA to form MEA as well as other products. For such gas mixtures, the rate of DEA degradation increases slightly with H_2S concentration but significantly with CO_2 concentration.
12. The rate of degradation of DEA by COS increases with solution temperature, amine concentration and COS partial pressure.
13. The degradation of DEA by COS is first order with respect to DEA within the following operating ranges:

DEA concentration: 20 - 40 wt%; Temperature: 120 - 180 °C;

COS partial pressure: 0.34 - 1.17 MPa.

The overall degradation rate constant, k_{DEA} , increased with amine concentration, temperature and COS partial pressure. The temperature dependency could be represented by the Arrhenius expression. At DEA concentrations above 40 wt%, the rate of degradation decreased due to the limitation of water for certain ionic reactions that control the degradation process.

14. A kinetic model based on the simplified reaction mechanism was developed to predict the formation of degradation products as well as the depletion of DEA within the following operating regimes:
 DEA concentration: 20 - 40 wt%; Temperature: 120 - 165 °C;
 COS partial pressure: 0.34 - 1.17 MPa. The fairly good agreement between the experimental values and model predictions validates the reaction mechanism.

10.1.2 CS₂ INDUCED DEGRADATION

1. CS₂ degrades DEA to form water soluble products as well as a dithiocarbamate salt and a sulphur - rich solid.
2. The CS₂ first reacts with DEA to form DEA dithiocarbamate which reacts with another molecule of DEA to form the DEA dithiocarbamate salt. At 180 °C, the salt is unstable, reverting to DEA and CS₂, while at $T \leq 165$ °C, the salt remains in the form of insoluble solid particles. CS₂ is also hydrolysed to COS, CO₂ and H₂S, but the extent of the hydrolysis products is limited by the amount of CS₂ tied up in the salt. When the concentrations of the hydrolysis products are low as was the case at $T \leq 165$ °C, MEA is the only low boiling degradation compound of significance. When the concentrations of the hydrolysis products are high due to the instability of the dithiocarbamate salt at 180 °C, MEA and other low boiling degradation compounds are formed in appreciable quantities. In summary, the degradation products of CS₂-DEA systems are similar to those of the COS-DEA systems and the same reaction mechanism applies for their formation.
3. The rate of degradation increased with amine concentration, temperature and initial CS₂ volume (or CS₂/DEA mole ratio).
4. The degradation of DEA by CS₂ is first order with respect to DEA within the following operating ranges: DEA concentration: 20 - 40 wt%; Temperature: 120 - 165 °C; CS₂ volumes; 2.5 - 10.5 mL (CS₂/DEA mole ratios of 0.055 - 0.233). The overall degradation rate constant increased with temperature and CS₂ volume (CS₂/DEA

mole ratio) but was largely independent of the amine concentration. The temperature dependency of the rate constant was well represented by the Arrhenius expression.

5. The reaction rate constants were determined for the region where amine degradation was controlled mainly by the hydrolysis products i.e. after the formation of the dithiocarbamate salt had ceased. However, there were not sufficient experimental data to develop a model to cover all the reactions occurring in the CS₂-DEA system.
6. The solids formed in the CS₂-DEA system and the COS-DEA system were not conclusively identified, but analysis shows that they are insoluble, high molecular weight, high melting substances, containing ethenyl and sulphur units in covalent bonding.

The COS-DEA and CS₂-DEA systems produced 7 and 8 major degradation compounds, respectively, as well as the solid products. These numbers, when compared with 3 major products for the CO₂-DEA system, demonstrate that the former systems are distinct and more complicated than the latter.

10.2 RECOMMENDATIONS

1. DEA plants should be operated under conditions that minimize degradation. In this respect, temperature control in the heat exchanger and reboiler is essential in making sure that the solution temperature is kept as low as possible and preferably around 120 °C, but certainly not at the expense of efficient

stripping. In particular, skin temperatures of heat transfer surfaces should be monitored, as they are often much higher than the bulk fluid temperatures. Since MEA and diamines are known to be particularly corrosive at high temperatures and in the presence of CO_2 , temperature control is paramount in minimising corrosion. DEA concentration should also be kept at the minimum value necessary to meet the desired treating capacity.

2. Formation of solid products may create fouling deposits in piping, heat exchangers and reboilers. As a result, pressure drops will rise and heat transfer coefficients will fall leading to increased overall energy costs for the plants. Cleaning of piping and heat exchangers is also expensive. It is therefore advisable to provide efficient filtration capabilities to remove the sulphur deposits before they react with other compounds to form the solid product.
3. DEA plants treating gases containing COS and/or CS_2 should be operated under conditions that enhance their hydrolysis to CO_2 and H_2S . Such action would minimise fouling since degradation by a mixture of H_2S and CO_2 does not result in substantial solid formation. Increased basicity by means other than increasing the amine concentration, may achieve this goal.
4. The solid products need to be subjected to further analysis such as Nuclear Magnetic Resonance Spectroscopy (NMR), X-ray diffraction etc. to conclusively determine their identity.
5. Studies should be conducted to evaluate the potential of Ethyl aminoethanol (EAE) and Methyl aminoethanol (MAE) as gas treating

solvents. Both amines have been reported to absorb COS over ten times faster than DEA. The emphasis in the studies should be on the resistance of the amines to degradation by acid gases, their capacity to absorb acid gases, foaming and corrosion tendencies.

6. More detailed studies should be conducted on the degradative effects of mixtures of CO_2 and H_2S on the amines used in gas treating operations. Of particular interest is MDEA which is used for the selective absorption of H_2S from sour gas streams.
7. The formation of the dithiocarbamate salt in the CS_2 -DEA system should be investigated in detail. The data acquired can be combined with those reported in this study to develop a kinetic model that covers all reactions occurring in the CS_2 -DEA system.
8. There appears to be enough information from this and other degradation studies to attempt to develop a purification scheme based on the reversal of the degradation reactions.

NOMENCLATURE

ACET	Acetone (2-Propanone).
BHEED	Bis(hydroxyethyl) ethylenediamine (N,N and N,N' isomers).
BHEI	N,N' -bis(hydroxyethyl) imidazolidone.
BHEP	N,N' -bis(hydroxyethyl) piperazine.
BHEU	N,N' -bis(hydroxyethyl) urea.
BUT	Butanone (Methyl ethyl ketone).
C _i	Concentration of gas i in solution (mol/m ³).
CI	Chemical Ionisation mode of operation in the GC/MS.
CO ₂	Carbon dioxide.
COS	Carbonyl sulphide.
CS ₂	Carbon disulphide.
DEA	Diethanolamine.
DEACOO ⁻	DEA carbamate.
DEACOS ⁻	DEA thiocarbamate.
DEACSS ⁻	DEA dithiocarbamate.
DGA	Diglycolamine.
DIPA	Diisopropanolamine.
EAE	Ethylaminoethanol.
EDEA	Ethyldiethanolamine.
EHEP	Ethyl hydroxyethyl piperazine.
EI	Electron Impact mode of operation in the GC/MS.
ETAHEAME	Ethanethioic acid S (hydroxyethyl) amino methyl ester.
FID	Flame Ionisation Detector.
GC	Gas chromatograph.

GC/MS	Gas chromatograph coupled to a mass spectrometer.
H_i	Henry's constant for the physical solubility of compound i (kPa m ³ /mol).
H_i^*	Henry's constant for the solubility of compound i in aqueous DEA solution (kPa m ³ /mol).
H ₂ S	Hydrogen sulphide.
HEA	N-hydroxyethyl acetamide.
HEI	N-hydroxyethyl imidazolidone.
HEOD	N-hydroxyethyl oxazolidone.
HEP	N-hydroxyethyl piperazine.
IR	Infrared.
$[i]_t$	Liquid phase concentration of specie i in mol/L at time t.
k	Reaction rate constant.
k_{DEA}	Overall DEA degradation rate constant (h ⁻¹).
$k_{\text{AM-CO}_2}$	Second order reaction rate constant for amine-CO ₂ reaction (L/mol s).
$k_{\text{AM-COS}}$	Second order reaction rate constant for amine-COS reaction (L/mol s).
$k_{\text{AM-CS}_2}$	Second order reaction rate constant for amine-CS ₂ reaction (L/mol s).
$k_1 - k_7$	Reaction rate constants in the kinetic expressions for COS-DEA and CS ₂ -DEA degradation.
$K_1 - K_7$	Equilibrium constants governing the ionic reactions in the COS-DEA system (mol/L).
K_{COS}	Equilibrium constant governing the formation of DEA thiocarbamate.

MDEA	Methyldiethanolamine.
MEA	Monoethanolamine.
m	DEA concentration (mol/L).
P_{DEA}	Vapour pressure of aqueous DEA solution (kPa).
P_i	Partial pressure of compound i (kPa).
P_T	Total system pressure (kPa).
P_T^*	Sum of the partial pressures of acid gases.
R	$\text{C}_2\text{H}_4\text{OH}$.
T	Temperature (K or $^{\circ}\text{C}$).
t	Time (h).
TCD	Thermal Conductivity Detector.
TEA	Triethanolamine.
THEED	N,N,N'-tris(hydroxyethyl) ethylenediamine.
TSIM	Trimethyl silyl imidazole.
V_d	Difference between the final and initial burette readings.
V_l	Volume of the liquid phase in the reactor.
V_s	Volume of the liquid sample transferred to the gas trapping set-up.
y_i	Mole fraction of gas i in the gas phase.
$y_{c,i,t}$	Calculated (predicted) concentration of compound i at time t.
$y_{e,i,t}$	Experimental concentration of compound i at time t.
$y_{\text{max},i}$	Maximum experimental concentration of compound i.
α_i	Loading of gas i (mol of gas i / mol DEA).

REFERENCES

1. Kohl, A.L and Riesenfeld, F.C., "Gas Purification", 4th Edition, Gulf Publishing Company, Houston, Texas, (1985).
2. Astarita, G. "Mass Transfer With Chemical Reaction", Elsevier Publishing Company, New York (1967).
3. Bottoms, R.R., U.S. Patent 1,783,901 (1930).
4. Smith, R.F., Travis Chemicals, Calgary, Alberta (1978). Quoted in reference 1.
5. Pauley, R.C. and Hashema, R. "Analysis of Foaming Mechanisms in Amine Plants", Proc. 39th Ann. Gas Conditioning Conf., Norman, Oklahoma; 219-247, (1989).
6. Moore, K.L., "Corrosion Problems in a Refinery Diethanolamine System", Corrosion, N.A.C.E., 16, 111 (1960).
7. Hall, W.D., and Barron, J.G., "Solving Gas Treating Problems - A Different Approach", Proc. 31st Annual Gas Conditioning Conference, Norman, OK, March 2 - 4, 1981.
8. Chakma, A. and Meisen, A., "Corrosivity of Diethanolamine Solutions and Their Degradation Products", Ind. Eng. Chem. Prod. Res. Dev., 25(4), 627 (1986).
9. Chakma, A and Meisen, A., "Degradation of Aqueous DEA Solutions in a Heat Transfer Tube", Can. J. Chem. Eng., 65, 264 (1987).
10. Polderman, L.D. and Steele, A.B., "Why Diethanolamine Breaks Down in Gas Treating Service", Oil Gas J., 54(5), 206(1956).
11. Hakka, L.D., Sing, K.P., Bata G.L., Testart A.G. and Andrejchyshyn W.M., "Some Aspects of Diethanolamine Degradation in Gas Sweetening", Gas Processing/Canada, 61(1), 32 (1968).
12. Choy E.T., "Degradation of DEA Treating Solutions", M.A.Sc. Thesis, University of British Columbia, B.C., (1978).
13. Kim C.J. and Sartori G., "Kinetics and Mechanism of Diethanolamine Degradation in Aqueous Solutions Containing Carbon Dioxide", Int. J. Chem. Kinetics, 16, 1257 (1984).
14. Kennard, M.L. and Meisen, A., "Mechanisms and Kinetics of Diethanolamine Degradation", Ind. Eng. Chem. Fund., 24(2), 129 (1985).

15. Hsu, C.S. and Kim, C.J., "Diethanolamine (DEA) Degradation under Gas-Treating Conditions", *Ind. Eng. Chem. Prod. Res. Dev.*, **24**, 630 (1985).
16. Kennard, M.L., "Degradation of Diethanolamine Solutions", Ph.D. Thesis, University of British Columbia, B.C., (1983).
17. Smith, R.F. and Younger, A.H., "Tips on DEA Treating", *Hydro. Proc.*, **51**(7), 98 (1972).
18. Chakma A., "Studies on DEA and MDEA Degradation", Ph.D. Thesis, University of British Columbia, B.C., (1987).
19. Orbach, H.K. and Selleck, F.T., "The effect of Carbonyl Sulphide on Ethanolamine Solutions", Unpublished Paper (Quoted with permission of F.T. Selleck, Fluor Corporation).
20. Pearce, R.L., Arnold, J.L. and Hall, C.K., "Studies Show Carbonyl Sulfide Problem", *Hydro. Proc.*, **40**(8), 121 (1961).
21. Osenton J.B. and Knight A.R., "Reaction of Carbon Disulphide with Alkanolamines Used in the Sweetening of Natural Gas", Paper Presented at the Fourth Quarterly Meeting of the Can. Gas. Proc. Assoc., Calgary (Nov. 20, 1970).
22. Ferm, R.J., "Chemistry of Carbonyl Sulphide", *Chem. Rev.* **57**, 621 (1957).
23. Kirk-Othmer Encyclopedia of Chemical Technology, 2nd Ed., **19**, 372 (1964).
24. Kirk-Othmer Encyclopedia of Chemical Technology, 2nd Ed., **4**, 370 (1964).
25. Kirk-Othmer Encyclopedia of Chemical Technology, 2nd Ed., **4**, 353 (1964).
26. Kirk-Othmer Encyclopedia of Chemical Technology, 2nd Ed., **19**, 375 (1964).
27. Mason, J.W. and Dodge, B.F., "Equilibrium Absorption of Carbon Dioxide by Solutions of the Ethanolamine", *Trans. Am. Inst. Chem. Eng.*, **32**, 27 (1936).
28. Lee, J.I, Otto, F.D. and Mather, A.E, "Solubility of Carbon Dioxide in Aqueous Diethanolamine Solutions at High Pressures", *J. Chem. Eng. Data*, **17**(4), 465 (1972).
29. Lee, J.I, Otto, F.D. and Mather, A.E, "Solubility of Hydrogen Sulphide in Aqueous Diethanolamine Solutions at High Pressures", *J. Chem. Eng. Data*, **18**(1), 71 (1973).

30. Lee, J.I, Otto, F.D. and Mather, A.E, "Partial Pressures of Hydrogen Sulphide over Aqueous Diethanolamine Solutions", J. Chem. Eng. Data, **18**(4), 420 (1973).
31. Lee, J.I, Otto, F.D. and Mather, A.E, "The Solubility of Mixtures of Carbon Dioxide and Hydrogen Sulphide in Aqueous Diethanolamine Solutions", Can. J. Chem. Eng., **52**, 125 (1974).
32. Lawson, J.D. and Garst, A.W., "Gas Sweetening Data: Equilibrium Solubility of Hydrogen Sulphide and Carbon Dioxide in Aqueous Monoethanolamine and Aqueous Diethanolamine Solutions", J. Chem. Eng. Data, **21**(1), 20 (1976).
33. Kennard, M.L. and Meisen, A., "Solubility of Carbon Dioxide in Aqueous Solutions of Diethanolamine at High Temperatures and Pressures", J. Chem. Eng. Data, **29**(3), 309 (1983).
34. Lal, D., Otto, F.D. and Mather, A.E, "The Solubility of H₂S and CO₂ in a Diethanolamine Solution at Low Partial Pressures", Can. J. Chem. Eng., **63**, 681 (1985).
35. Bhairi, A., Mains, G., and Maddox, R.N., "Experimental Equilibrium Between CO₂ and Ethanolamines", Proc. of Annual Gas Proc. Assoc. Convention, 1985.
36. Atwood, K, Arnold, M.R. and Kindrick, R.C., "Equilibrium For The System, Ethanolamines-Hydrogen Sulphide-Water", Ind. Eng. Chem., **49**(9), 1439 (1957).
37. Danckwerts, P.V. and McNeil, K.M., "The Absorption of Carbon Dioxide Into Aqueous Amine Solutions and The Effects of Catalysis", Trans. Inst. Chem. Eng., **45**, T32 (1967).
38. Klyamer, S.D., Kolesnikova, T.S. and Rodin, Yu.A., Gazov. Prom., **18**(2), 44 (1973).
39. Kent, R.L. and Eisenberg, B., "Better Data For Amine Treating", Hydro. Proc., **55**(2), 87 (1976).
40. Deshmukh, R.D. and Mather, A.E., "A Mathematical Model For Equilibrium Solubility of Hydrogen Sulphide and Carbon Dioxide in Aqueous Alkanolamine Solutions", Chem. Eng. Sci., **36**, 355 (1981).
41. Austgen, D.M., Rochelle, G.T., Peng, X and Chen, C.C., "Model of Vapour-Liquid Equilibrium For Aqueous Acid Gas-Alkanolamine Systems Using the Electrolyte-NRTL Equation", Ind. Eng. Chem. Res., **28**, 1060 (1989).
42. Schultze, W.A., Ruoho, A.A. and Short, G.H., U.S. Patent 2,315,663 (Apr. 1943).

43. Johnson, A.B. and Condit, D.H., U.S. Patent 2,594,311 (Apr. 1952).
44. Schultze, W.A. and Short, G.H., U.S. Patent 2,309,871 (1943).
45. Kerns, J.W. and Beamer, M., U.S. Patent 2,331,342 (Feb. 1943).
46. Reed, R.M., U.S. Patent 2,383,416 (Aug. 1941).
47. Easthergen, J.H. and Allen, H.I., U.S. Patent 2,726,992 (Dec. 1955).
48. Sharma, M.M. and Danckwerts, P.V., "Absorption of Carbonyl Sulphide in Amines and Alaklis", Chem. Eng. Sci., **19**, 991 (1964).
49. Rahman, M.A., "Study of Reactions of Carbon Dioxide and Sulphur Containing Compounds with Ethanolamines", Ph.D Thesis, University of Oklahoma State University, Okla., U.S.A. (1984).
50. Al-Ghawas, H.A., Ruiz-Ibanez, G. and Sandall, O.C., "Absorption of Carbonyl Sulphide in Aqueous Methyldiethanolamine", Chem. Eng. Sci., **44**(3), 631 (1989).
51. Clarke, J.K.A., "Kinetics of Absorption of Carbon Dioxide in Monoethanolamine Solutions at Short Contact Times", Ind. Eng. Chem. Fund., **3**, 239 (1964);
52. Chaudhuri, S.K. and Sharma, M.M., "Absorption of Carbonyl Sulphide in Aqueous Alkaline Solutions: New Strategies", Ind. Eng. Chem. Res., **28**, 870 (1989).
53. Klein, J.P., Oil and Gas J., Sept. 10, 109 (1970).
54. McClure, G.P. and Morrow, D.C., "Amine Process Removes COS from Propane Economically", **77**(27), 106 (1979).
55. Singh, M. and Bullin, J.A., "Determination of Rate Constants for the Reaction Between Diglycolamine and Carbonyl Sulphide", Gas Separation and Purification **2**, 131 (1988).
56. Thompson, H.W., Kearton. C.F. and Lamb, S.A., "Kinetics of the Reaction between Carbonyl Sulphide and Water", J. Chem. Soc. 1033 (1935).
57. Sharma, M.M., "Kinetics of Reactions of Carbonyl Sulphide and Carbon Dioxide with Amines and Catalysis by Bronsted Bases of the Hydrolysis of COS", Trans. Faraday Soc. **61**, 681 (1965).
58. Sharma, M.M. and Danckwerts, P.V., "Fast Reactions of CO₂ in Alkaline Solutions", Chem. Eng. Sci., **18**, 729 (1963).

59. Sharma, M.M. and Danckwerts, P.V., "Catalysis by Bronsted bases of the Reaction between CO_2 and Water", Trans. Faraday Soc., **59**, 386 (1963).
60. Caplow, M., "Kinetics of Carbamate Formation and Breakdown", J. Am. Chem. Soc., **90**, 6795 (1968).
61. Frazier, H.D. and Kohl, A.L., "Selective Absorption of Hydrogen Sulphide From Gas Streams", Ind. Eng. Chem., **42**(11), 2288, 1950.
62. Vidaurri, F.C. and Kahre, L.C., "Recover H_2S Selectively from Sour Gas Streams", Hydrocarbon Processing, **56**(11), 333 (1977).
63. Daviet, G.R., Sundermann, R., Donnelly, S. and Bullin, J.A., "Simulation Values Prove Out in DEA to MDEA Switch", Oil Gas J., **82**(32), 47 (1984).
64. Berlie, E.M., Estep, J.W. and Ronicker, F.J., "Preventing MEA Degradation", Chem. Eng. Prog., **61**(4), 82 (1965).
65. Rahman, M.A., Maddox, R.N. and Mains, G.J., "Reactions of Carbonyl Sulphide and Methyl Mercaptan with Ethanolamines", Ind. Eng. Chem. Res., **28**, 470 (1989).
66. Khotari, P.J. and Sharma, M.M., "Kinetics of Reaction Between CS_2 and Amines", Chem. Eng. Sci., **21**, 391 (1966).
67. Henry, M.S. and Grennert, M., Petroleum Refiner, **34**(6), 177 (1955).
68. Gas Conditioning Fact Book, The Dow Chemical Company, Midland, Michigan, (1962)..
69. Brydia, L.E. and Persinger, H.E., "Quantitative Gas Chromatographic Determination of Ethanolamines as Trifluoroacetyl Derivatives", Anal. Chem., **39**(11), 1318 (1967).
70. Piekos, R., Kobyiczek, K. and Grzybowski, J., "Quantitative Gas Chromatographic Determination of Ethanolamines as Trimethylsilyl Derivatives", Anal. Chem., **47**(7), 1157 (1975).
71. Choy, E.T. and Meisen, A., "Gas Chromatographic Detection of Diethanolamine and its Degradation Products", J Chrom., **187**, 145 (1980).
72. Saha N.C., Jan, S.K. and Dua, R.K., "A Rapid and Powerful Method for the Direct Gas Chromatographic Analysis of Alkanolamines: Application to Ethanolamines", Chromatographia, **10**(7), 368 (1977).

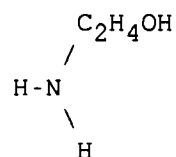
73. Van Wijk, R., "The Use of Poly-Para-2,6-Diphenyl-Phenylene Oxide as a Porous Polymer in Gas Chromatography", *J. Chrom. Sci.*, **8**, 418 (1970).
74. Kennard, M.L. and Meisen, A., "Gas Chromatographic Technique for Analyzing Partially Degraded Diethanolamine Solutions", *J. Chrom.*, **267**, 373 (1983).
75. Robbins G.D. and Bullin J.A., "Analysis of Amine Solutions by Gas Chromatography", Presented at AIChE National Meeting, California, (May 20 - 23, 1984); *Energy Progr.*, **4**, 229 (1984).
76. Chakma, A. and Meisen, A., "Identification of Methyl Diethanolamine Degradation Products by Gas Chromatography and Gas Chromatography-Mass Spectrometry", *J. Chrom.*, **457**, 287 (1988).
77. Pecsok, R., Shields, L.D., Cairns, T. and McWilliam, I.G., "Modern Methods of Chemical Analysis", 2nd Edition, John Wiley & Sons Inc., New York. (1976).
78. Pierce, A.E., "Silylation of Organic Compounds", Pierce Chemical Co., Ill. (1968).
79. EPA/NIH Mass Spectral Data Base, National Stand. Ref. Data Service, Natl. Bur. of Stand., U.S., (1983).
80. Eight Peak Index of Mass Spectra, 2nd Ed., Mass Spectrometry Data Centre, AWRE, Reading, U.K., (1974).
81. Dean, J.A., "Handbook of Organic Chemistry", Chapter 6, McGraw Hill Book Co., New York, (1987).
82. Simmons, W.W (editor), "The Sadtler Handbook of Infrared Spectra", Sadtler Research Laboratories Inc., Pennsylvania, (1978).
83. Reilly, J.T., Schubert, C.N., Lindner, J.R., Donohue, M.D. and Kelly, R.M., "Effect of Heterocyclic Amine Additives on the Absorption Rates of Carbonyl Sulphide and Carbon Dioxide in Aqueous Methyldiethanolamine", *Chem. Eng. Comm.*, **93**, 181 (1990).
84. Blanc, C., Grall, M. and Demarais, G., "Amine Degradation Products Play no Part in Corrosion at Gas Sweetening Plants", *Oil Gas J.*, Nov.15, p128 (1982).
85. Patai, S (editor), "The Chemistry of the Carbonyl Group", Chapter 15, p761, Interscience Publishers, New York (1966).
86. Horowitz, W., AOAC Methods, 12th Edition, George Banta Co., (1975).

87. Peng, D.Y. and Robinson, D.B., "A New Two-Constant Equation of State", *Ind. Eng. Chem. Fund.*, **15**(1), 59 (1976).
88. Perry, R.H. and Green, D.W., "Chemical Engineers Handbook", 6th Edition, McGraw Hill, New York, (1984).
89. Savage, D.W., Funk, E.W., Yu, C.W. and Astarita, G., "Selective Absorption of H_2S and CO_2 in Aqueous Solutions of Methyl-diethanolamine", *Ind. Eng. Chem. Fund.*, **25**, 326 (1986).
90. Moore, C., "UBC NLE - Zeroes of Nonlinear Equations", University of British Columbia Computing Centre Document, Vancouver, BC. (1984).
91. Astle, M.S., "Industrial Organic Nitrogen Compounds", Reinhold Publishing Corporation, New York, 134 (1961).
92. Kirk-Othmer Encyclopedia of Chemical Technology, 2nd Ed., **81**, 77 (1964).
93. Lysenko, N.M., "Condensation of Primary Amines with Paraformaldehyde and Thiocarboxylic Acids", *Zhur. Org. Khimii*, **10** (10), 2049 (1974).
94. Chakma, A. and Meisen, A., "Solubility of CO_2 in Aqueous Methyl-diethanolamine and N,N'-Bis hydroxyethyl piperazine Solutions", *Ind. Eng. Chem. Res.* **26**, 2461 (1987).
95. Vaessen, W., "U.B.C. NLP - Nonlinear Function Optimization", The University of British Columbia Computing Centre Document, Vancouver, B.C., 1983.
96. Moore, C., "U.B.C. RKC - Runge Kutta with Error Control", The University of British Columbia Computing Centre Document, Vancouver, B.C., 1983.
97. Levenspiel, O., "Chemical Reaction Engineering", 2nd edition, John Wiley & Sons Inc., New York, 1972.
98. Drechsel, E.K., "N-Vinyl-2-Oxazolidone", *J. Org. Chem.*, **22**, 849 (1957).
99. Moller, H. and Osberghaus, R., "Cosmetic Agent Containing Moisturizing Agents for Skin" *Ger. Offen* 2,746,650 (April 1979). *Chem. Abst.* 91:128904u.
100. Dawodu, O.F. and Meisen, A., "Amine Degradation by Carbonyl Sulphide and Carbon Disulphide", *Proceedings of the 39th Annual Gas Conditioning Conference*, Norman, Okla., p 9 - 71 (1989).

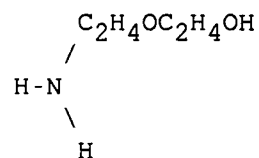
APPENDIX

A.1 ALKANOLAMINES COMMONLY USED INDUSTRIALLY

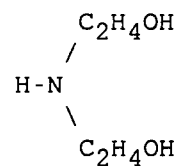
MONOETHANOLAMINE (MEA)



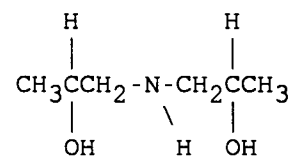
DIGLYCOLAMINE (DGA) OR
B,B'-HYDROXYAMINOETHYL ETHER



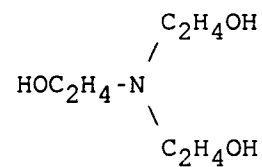
DIETHANOLAMINE (DEA)



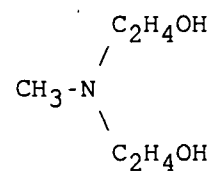
DIISOPROPANOLAMINE (DIPA)



TRIETHANOLAMINE (TEA)



METHYLDIETHANOLAMINE (MDEA)



2-AMINO-2 METHYL-1-PROPANOL (AMP)

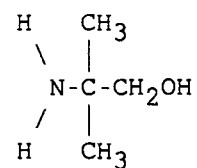


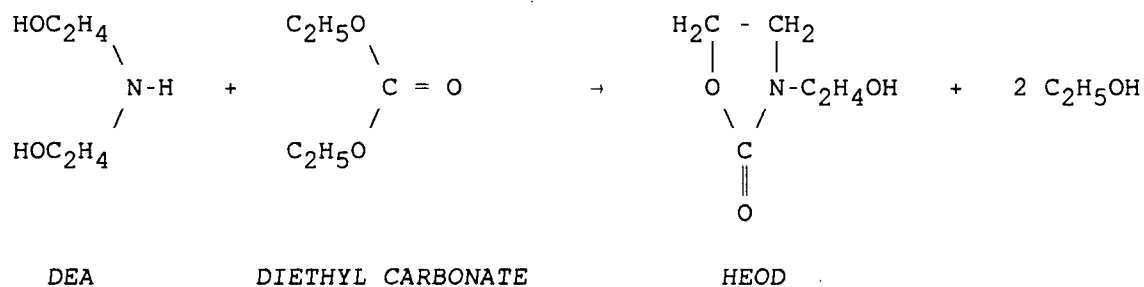
Figure A.1: Structures of alkanolamines used in gas treating operations

A.2 SYNTHESIS OF SELECT DEGRADATION COMPOUNDS

Some of the degradation compounds, HEOD, THEED and BHEI were not available commercially. They had to be synthesized for subsequent calibration of the GC so that their concentrations in the degraded solutions could be quantified. The synthesis methods are described below:

A.2.1 HEOD SYNTHESIS

HEOD was synthesized according to the procedure of Dreschel (98). DEA and diethyl carbonate, the latter in 20% excess on a molar basis, were placed in the glass-lined reactor. The reactor was sealed and the contents stirred for about an hour to thoroughly mix the immiscible liquids. Heat was then applied to bring the temperature of the autoclave to 110 °C and maintained as such for 22 hours. HEOD was expected to be produced according to the reaction:

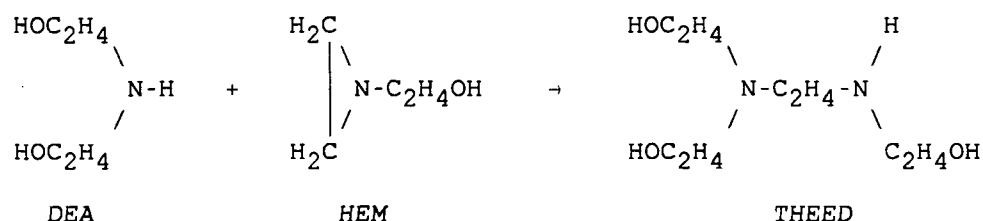


The temperature was then raised and maintained at 130 °C until ethanol production ceased. The gas outlet valve on the autoclave was left open

throughout the duration of the reaction so that the by-product ethanol, continuously flowed out into a collecting beaker. GC analysis of the cooled product showed that it contained mainly HEOD, as well as ethanol and residual diethyl carbonate. The latter two were removed by evaporation in a rotavapor at reduced pressure. The oily, coloured product was purified by mixing with activated carbon and then filtered to give a product which on analysis, contained over 95% HEOD. This final product was used to generate the calibration curve for HEOD.

A.2.2 THEED SYNTHESIS

THEED was synthesized by following the procedure of Kennard (14). 105 g of DEA was reacted with 87 g of N-hydroxyethyl imine (HEM) in the presence of 5 g of aluminium chloride, at 120 °C for 24 hours. The reactants were placed in the autoclave which was then sealed and pressurized to 0.7 MPa with nitrogen. THEED was expected to be produced according to the reaction:

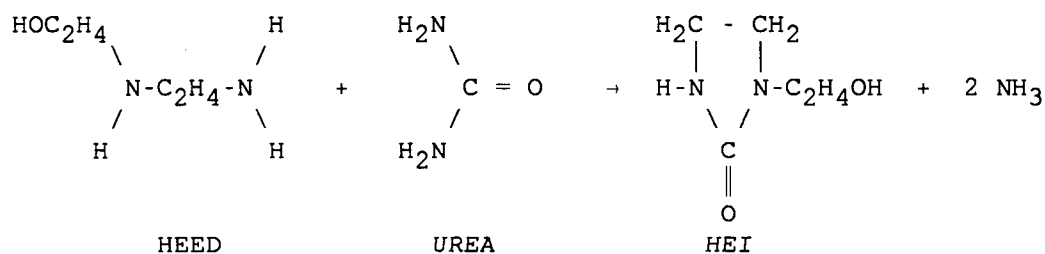


Despite several trials, THEED produced from the reaction was lower than the 70 - 80 % yield obtained by Kennard (16) and Chakma (18). The crude product mixture was purified by column chromatography. The mixture was

first diluted with water and then passed at the rate of 0.5 mL / min, through a 15 mm ID glass column packed to a height of 40 cm with 60 - 200 mesh silica gel. Water was again used as the eluting solvent. The THEED fraction was concentrated in a rotavapor at reduced pressure to give a final product mixture containing approximately 48% THEED, 47% DEA and 5% BHEP on a molar basis. By using the previously prepared calibration curves of DEA and BHEP, it was possible to calculate the concentration of THEED in each solution of the mixture and hence establish the calibration curve for THEED.

A.2.3 HEI SYNTHESIS

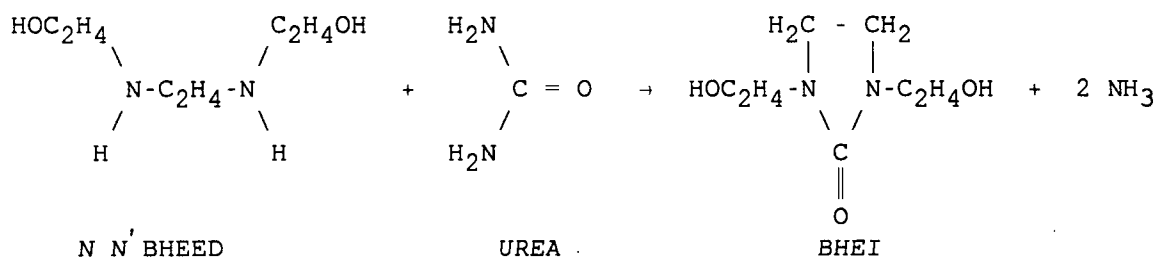
N-hydroxyethyl imidazolidone (HEI) was synthesized according to literature procedure (99). Equimolar amounts of urea and Hydroxyethyl ethylene diamine (HEED) were placed in the reactor and maintained at 200 °C for 4 hours. The following reaction was expected to occur:



GC/MS analysis confirmed the reaction product as HEI. The product was further purified by activated carbon adsorption. GC analysis of the final product indicated a purity of 97%⁺.

A.2.4 BHEI SYNTHESIS

BHEI was synthesized by reacting BHEED with urea (20% excess) at 225 °C for 4 hours in the autoclave. This technique is an adaptation of the procedure for the synthesis of HEI and was expected to generate BHEI according to the reaction:



At the end of the reaction, the ammonia formed was discharged through the gas outlet valve into the fume hood. Analysis of the crude mixture by gas chromatography and GC/MS revealed a BHEI content of over 80%. The mixture was further purified by column chromatography. A 15 mm ID glass column was packed to a height of 40 cm with 70 - 230 mesh silica gel. The impure mixture was slightly diluted with water, transferred to the top of the column and after adsorption, was eluted with water at a flow rate of 0.5 mL/min. The BHEI fractions were concentrated in a rotavapor at reduced pressure. GC analysis showed that the final product had a purity of over 95%.

APPENDIX B

B.1 CALIBRATION OF THE GAS CHROMATOGRAPH

B.1.1 DEGRADATION RUNS

Once the degradation compounds had been identified, it was necessary to quantify them. This was done by preparing calibration curves of GC peak area versus concentration. Commercial compounds were used except in the case of HEOD, HEI, THEED and BHEI which were not available commercially and had to be synthesized (see Appendix A.2). Typical calibration curves for the major compounds are shown in Figs. B.1 - B.10. Calibration equations were generated for each compound from a least squares fit of the concentration and peak areas. These equations were subsequently used to calculate the concentrations of the various compounds in the samples of the degraded solutions once the GC peak areas were known.

As the Tenax columns aged or had to be replaced, new calibration curves were prepared. The frequency of re-calibration depended on the extent of usage of the column. On the average, new curves were prepared after every four or five runs involving 10 sample withdrawals each (this, in turn, corresponds to about 120 to 150 GC injections). Due to the number of curves generated, the calibration usually required about 2 to 3 days.

B.1.2 SOLUBILITY AND HYDROLYSIS RUNS

Known volumes of factory analysed standard mixtures containing H_2S and CO_2 were drawn into pressure lok syringes and diluted with appropriate amounts of nitrogen to obtain the desired concentrations of the gases. In the case of COS the pure gas was withdrawn from the gas cylinder and diluted with nitrogen. The mixtures in the syringes were properly mixed prior to their analysis with the Varian GC containing a TCD. Details of the operating conditions have been provided in Chapter 7. The calibration curves were generated by plotting the peak areas obtained from the GC analysis against the concentration (vol%) of each gas in the mixtures. Typical calibration curves are shown in Figs. B.11

- B.13

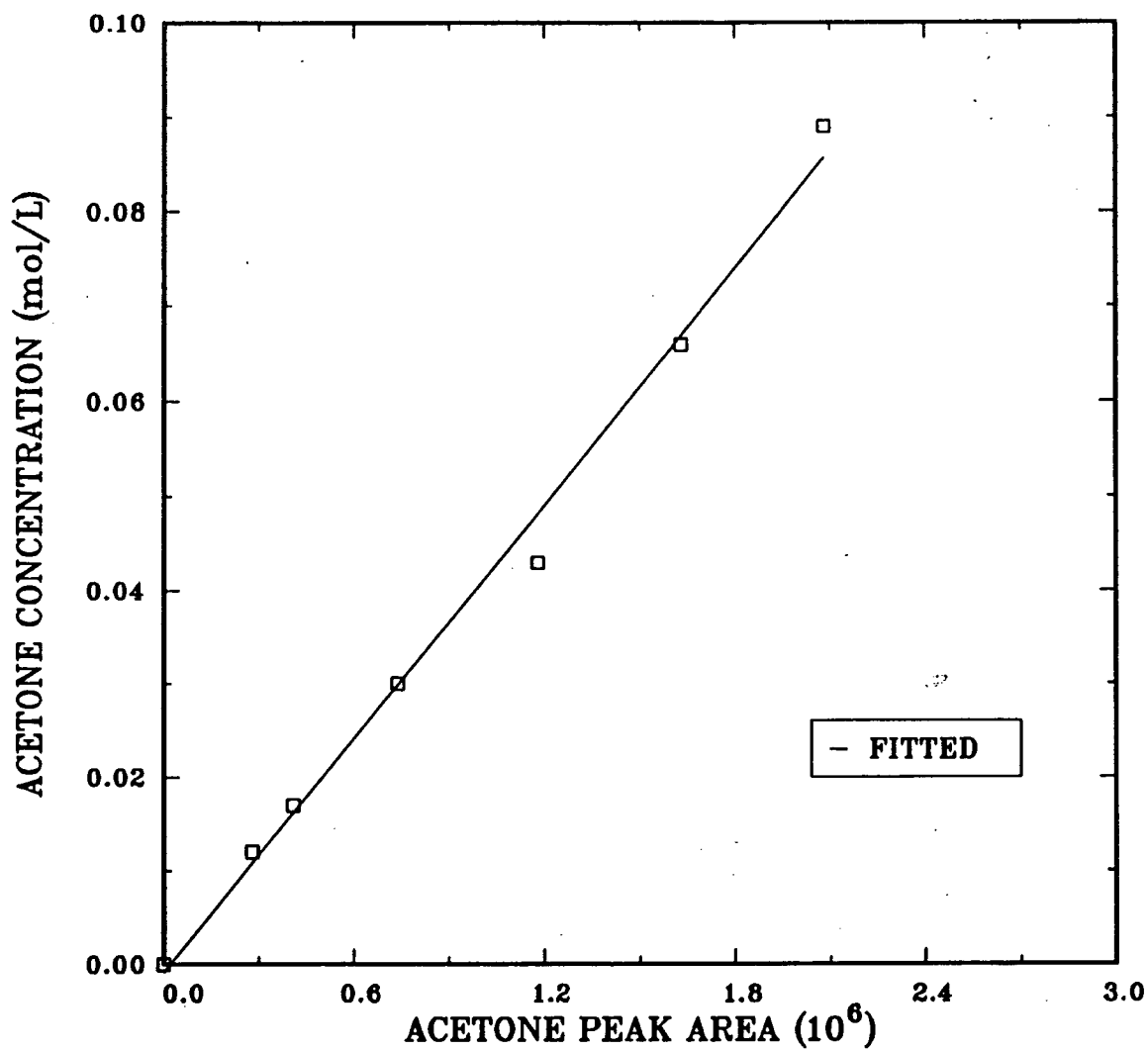


Figure B.1: Calibration curve for acetone.

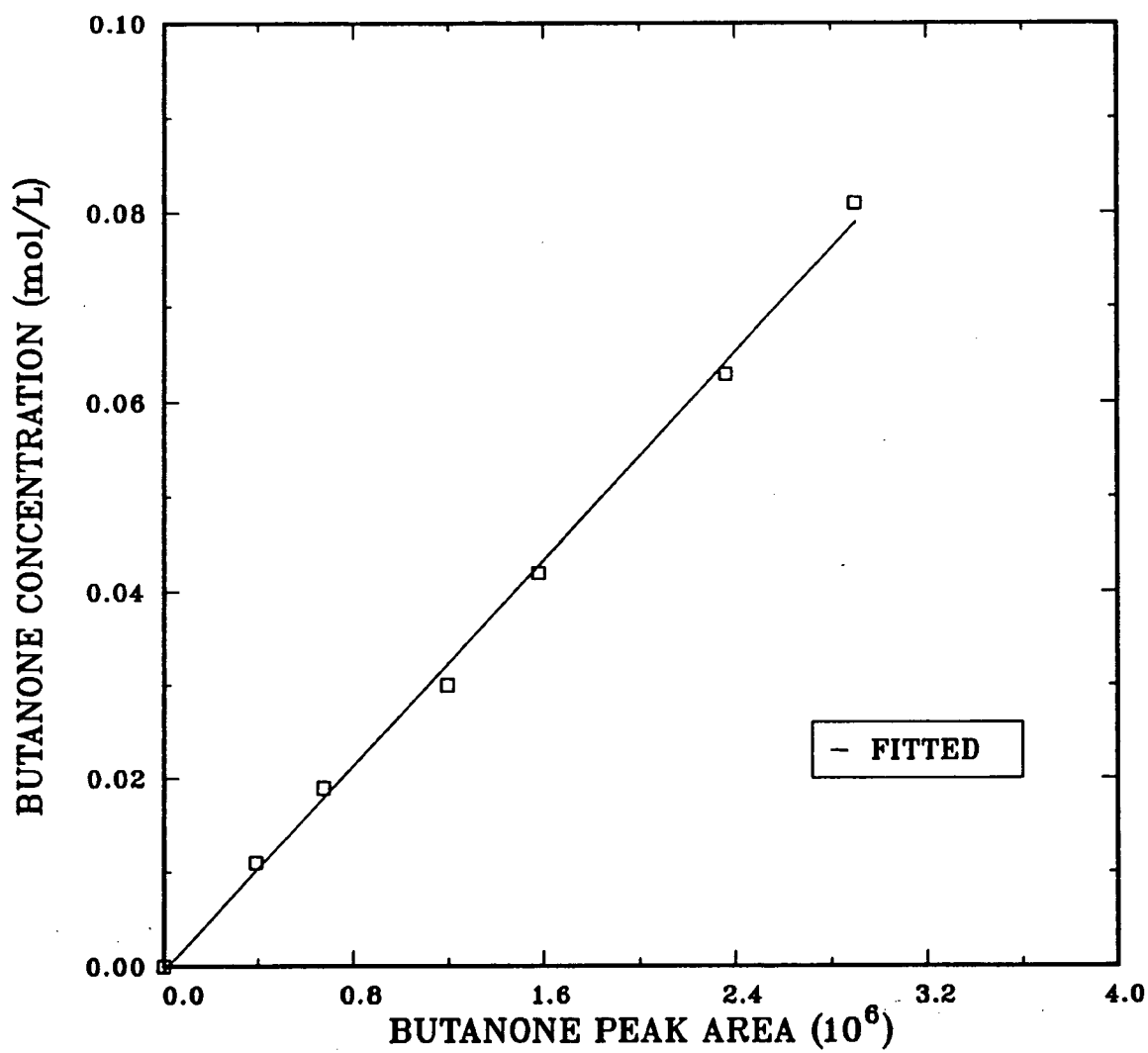


Figure B.2: Calibration curve for butanone.

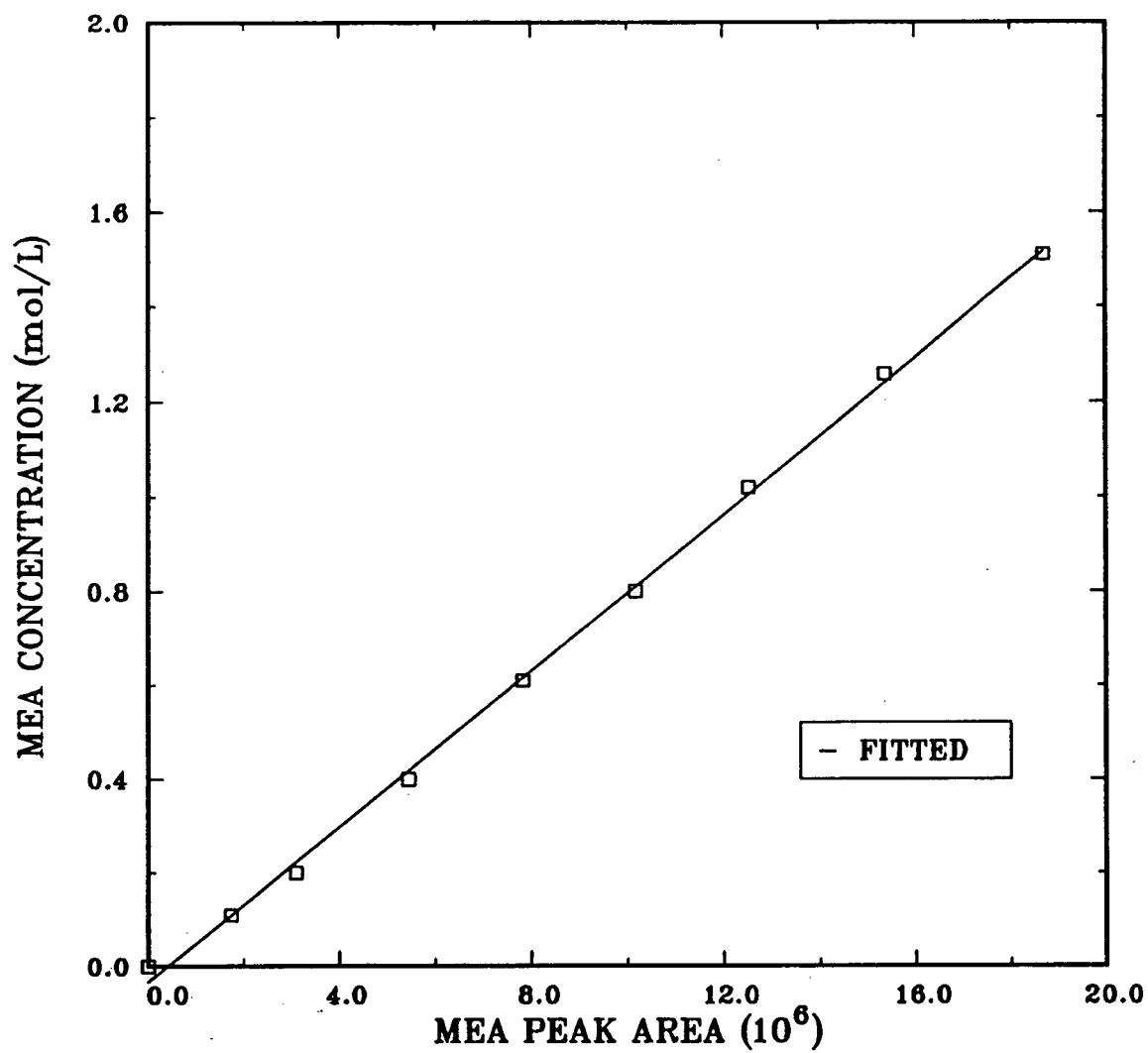


Figure B.3: Calibration curve for MEA.

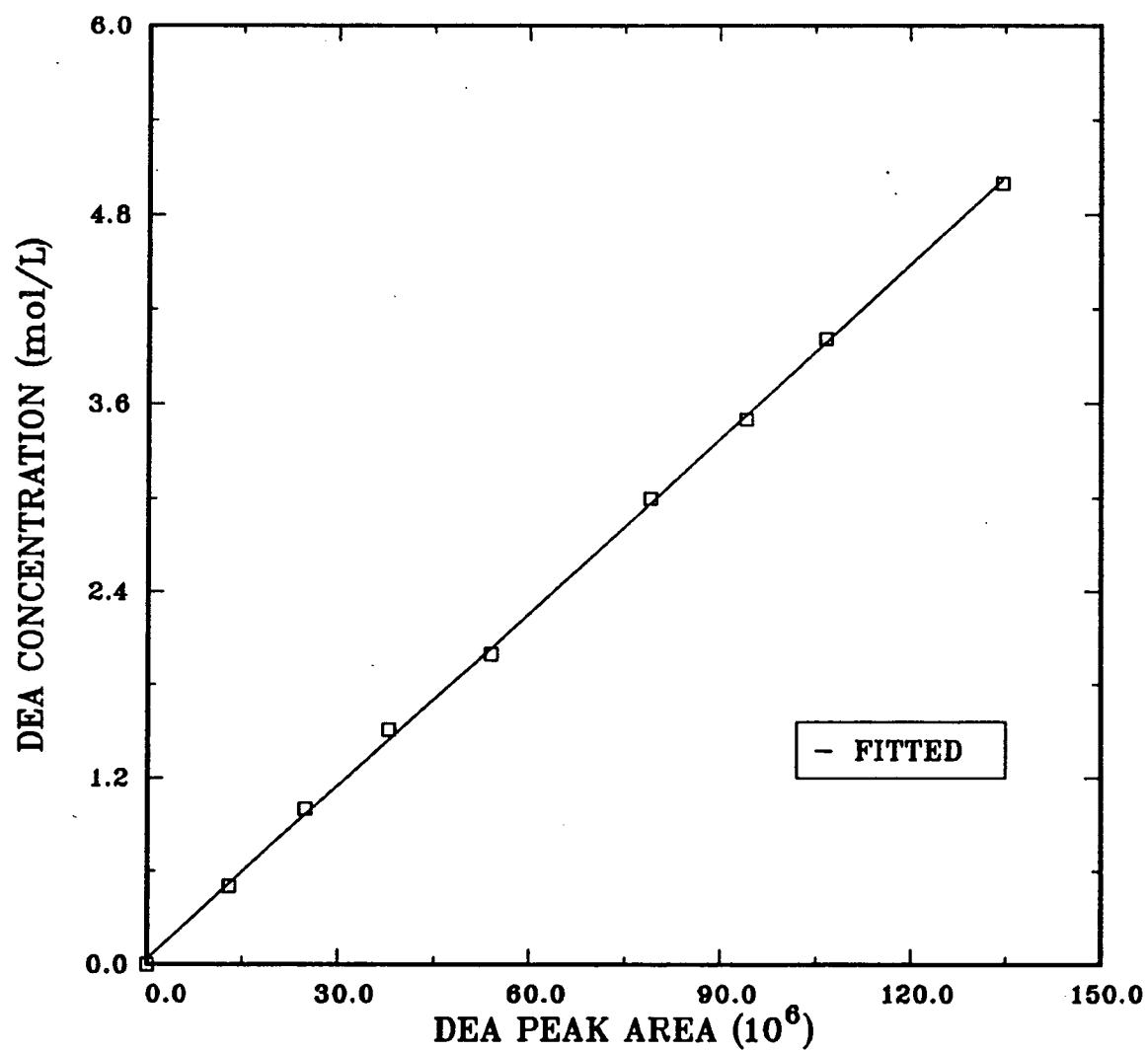


Figure B.4: Calibration curve for DEA.

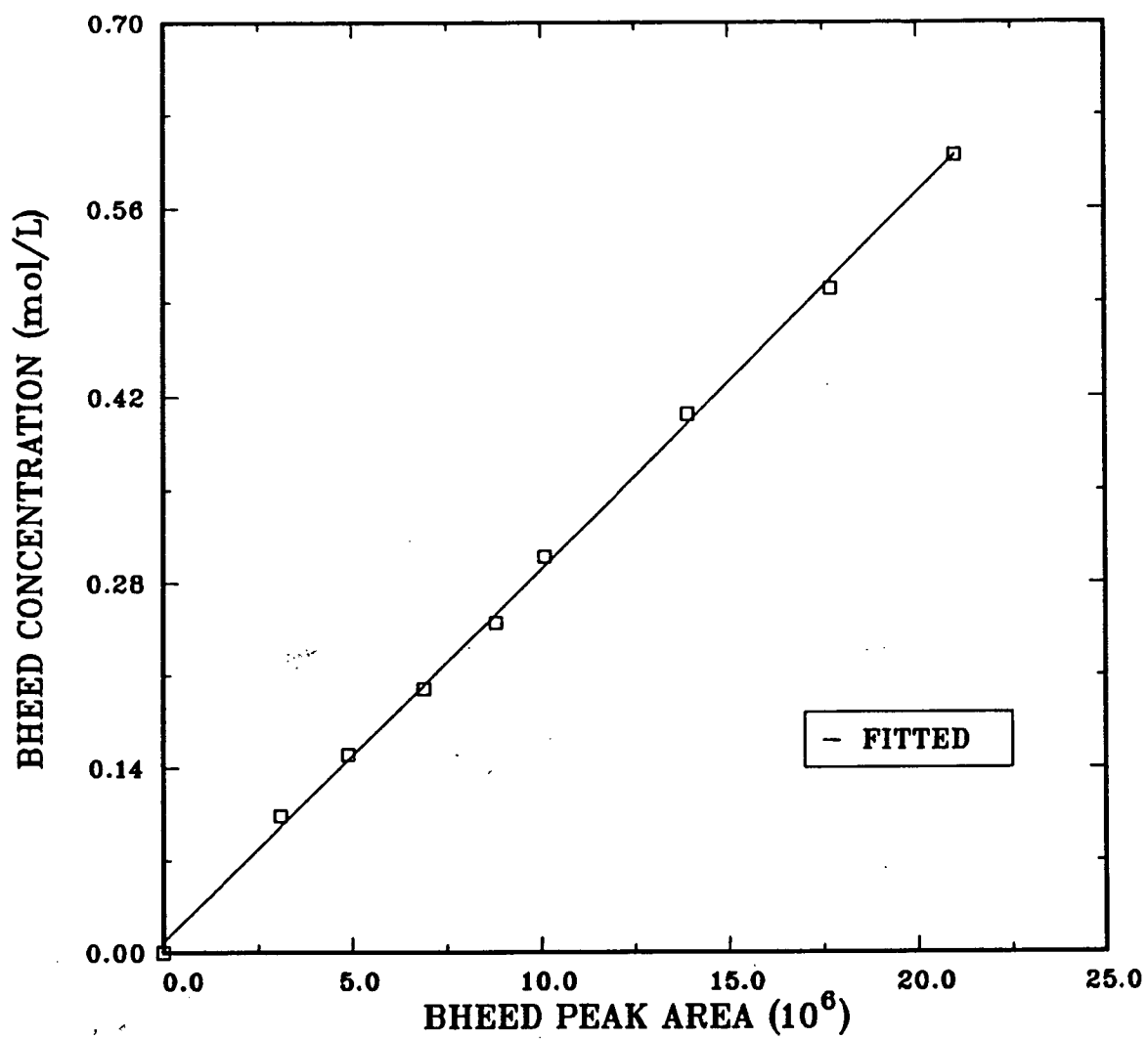


Figure B.5: Calibration curve for BHEED.

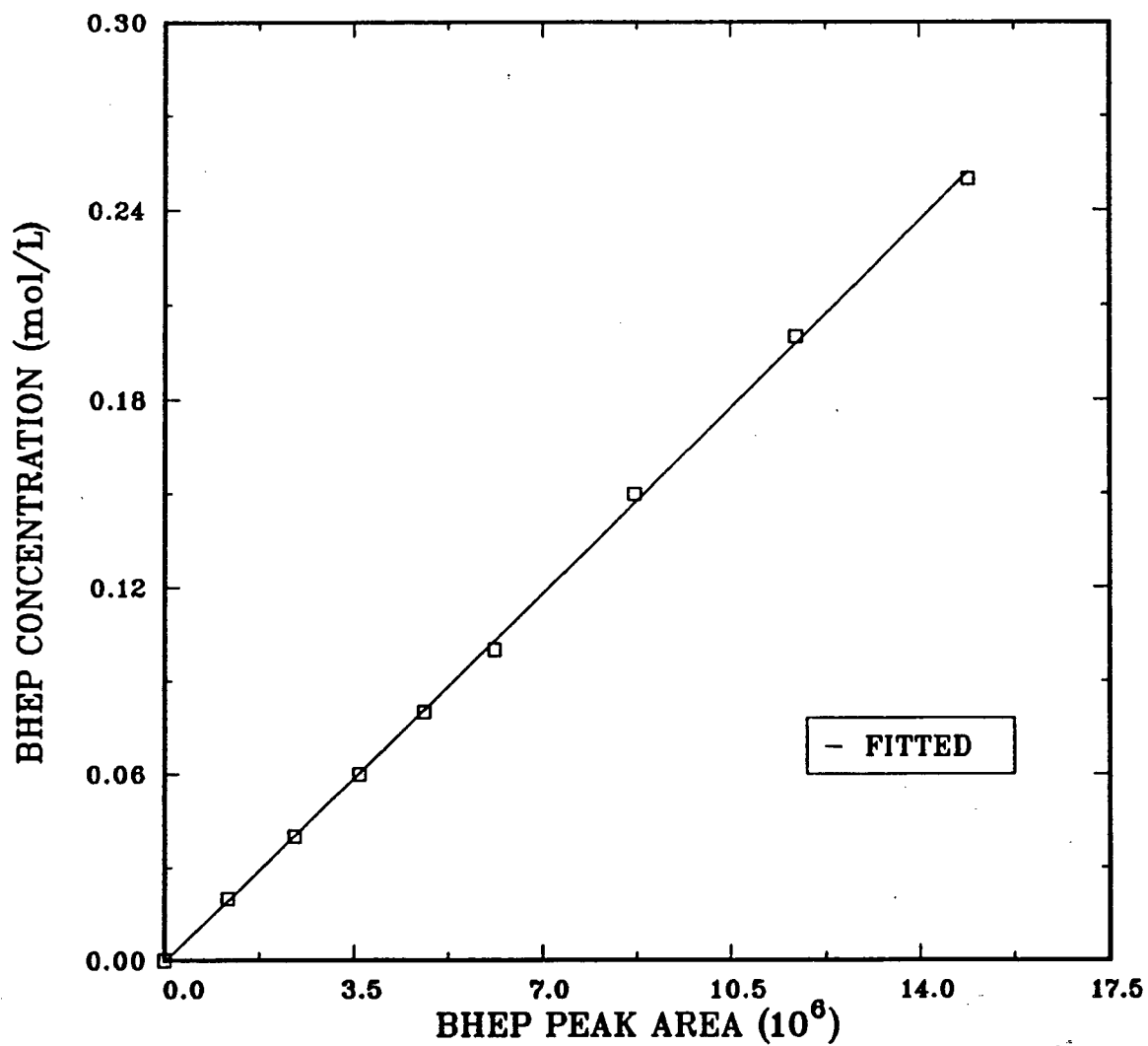


Figure B.6: Calibration curve for BHEP.

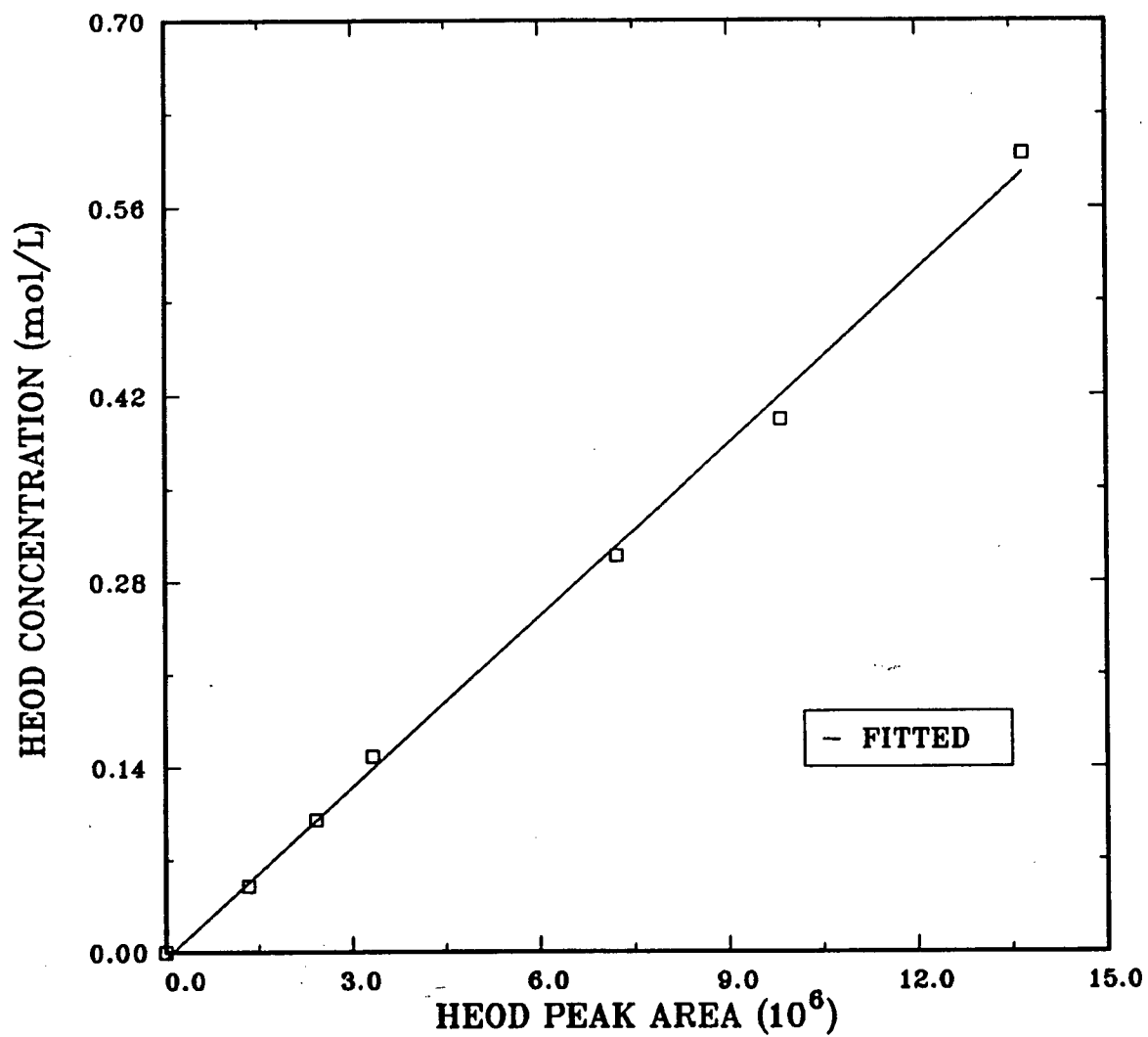


Figure B.7: Calibration curve for HEOD.

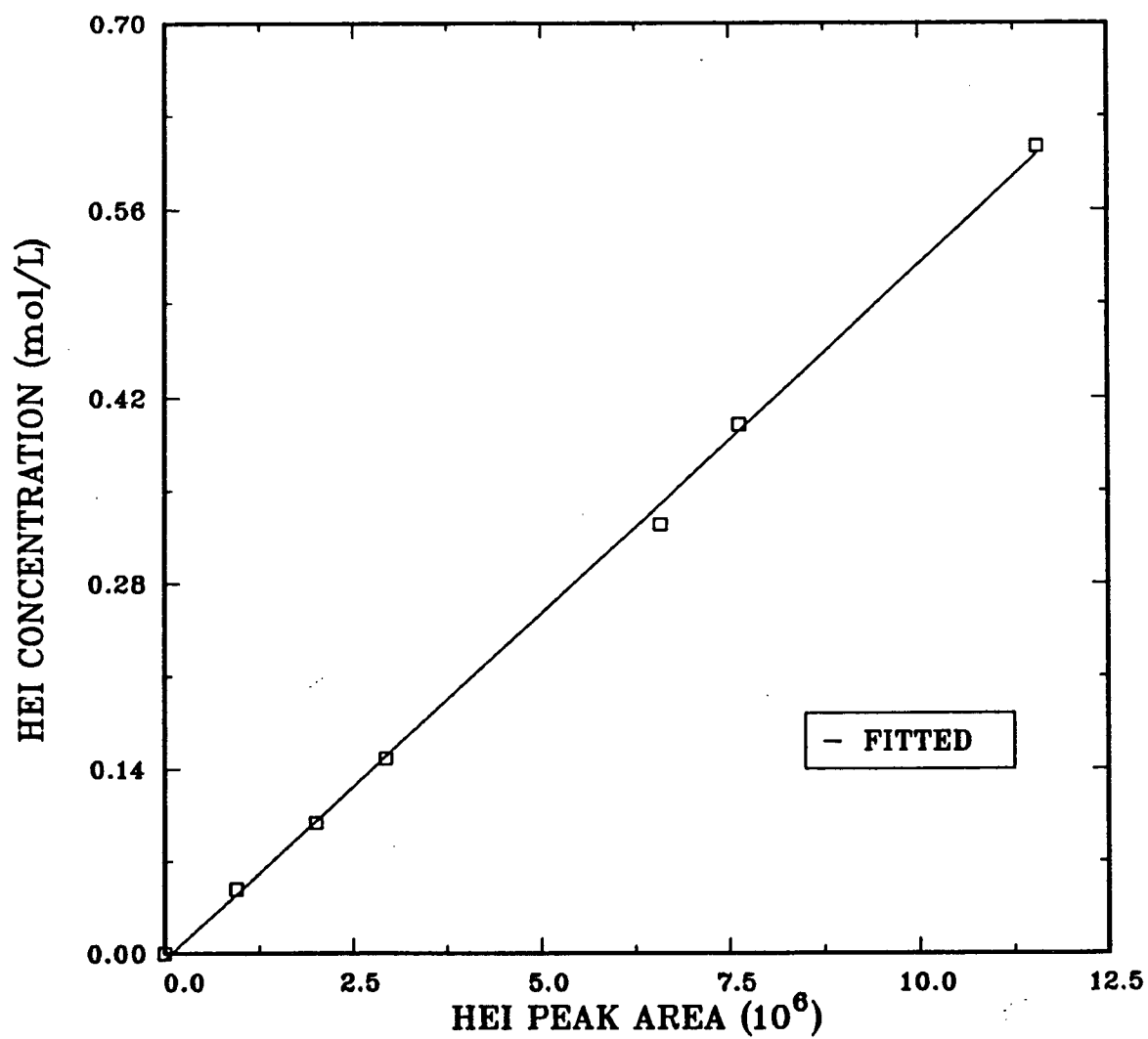


Figure B.8: Calibration curve for HEI.

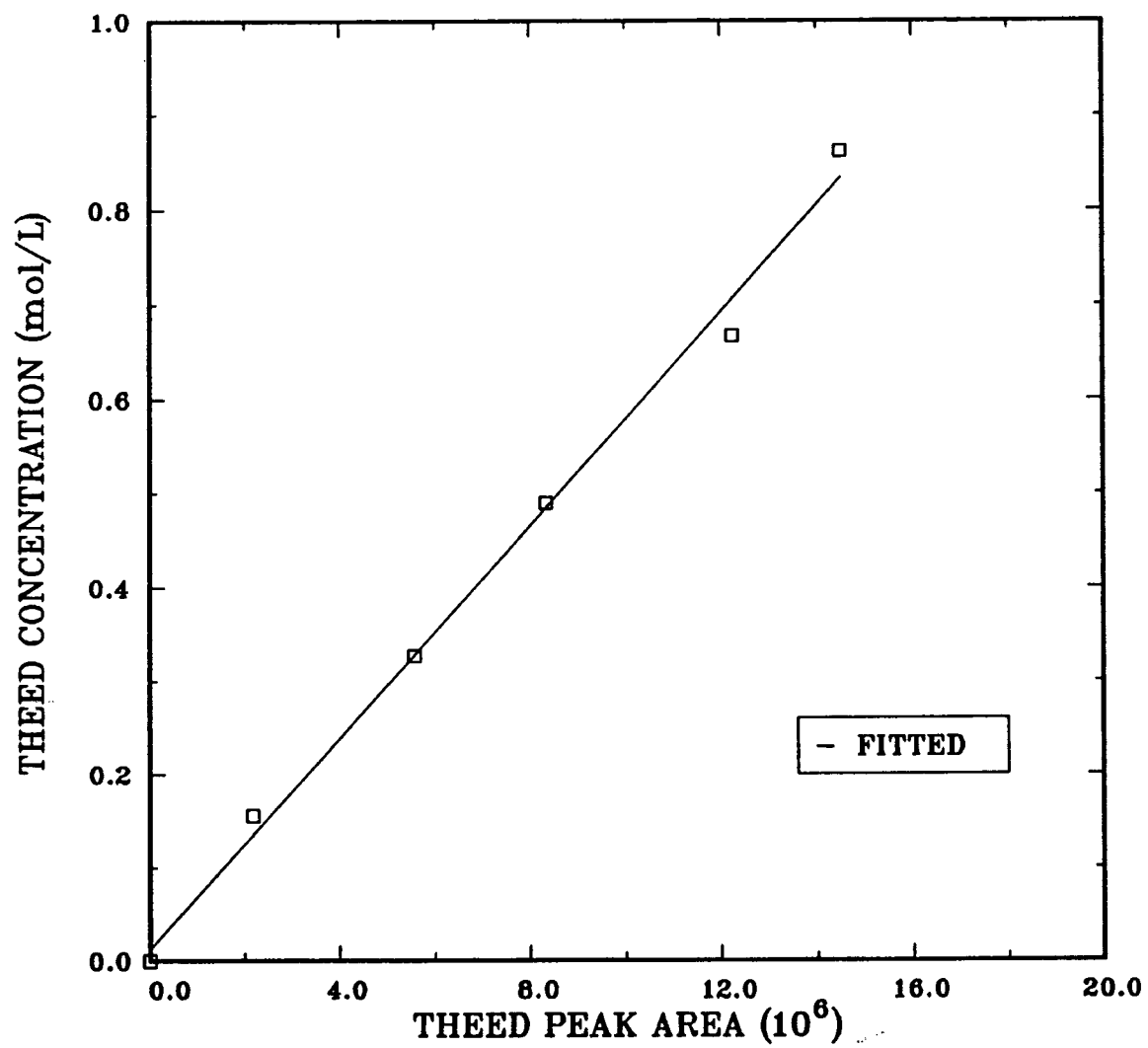


Figure B.9: Calibration curve for THEED.

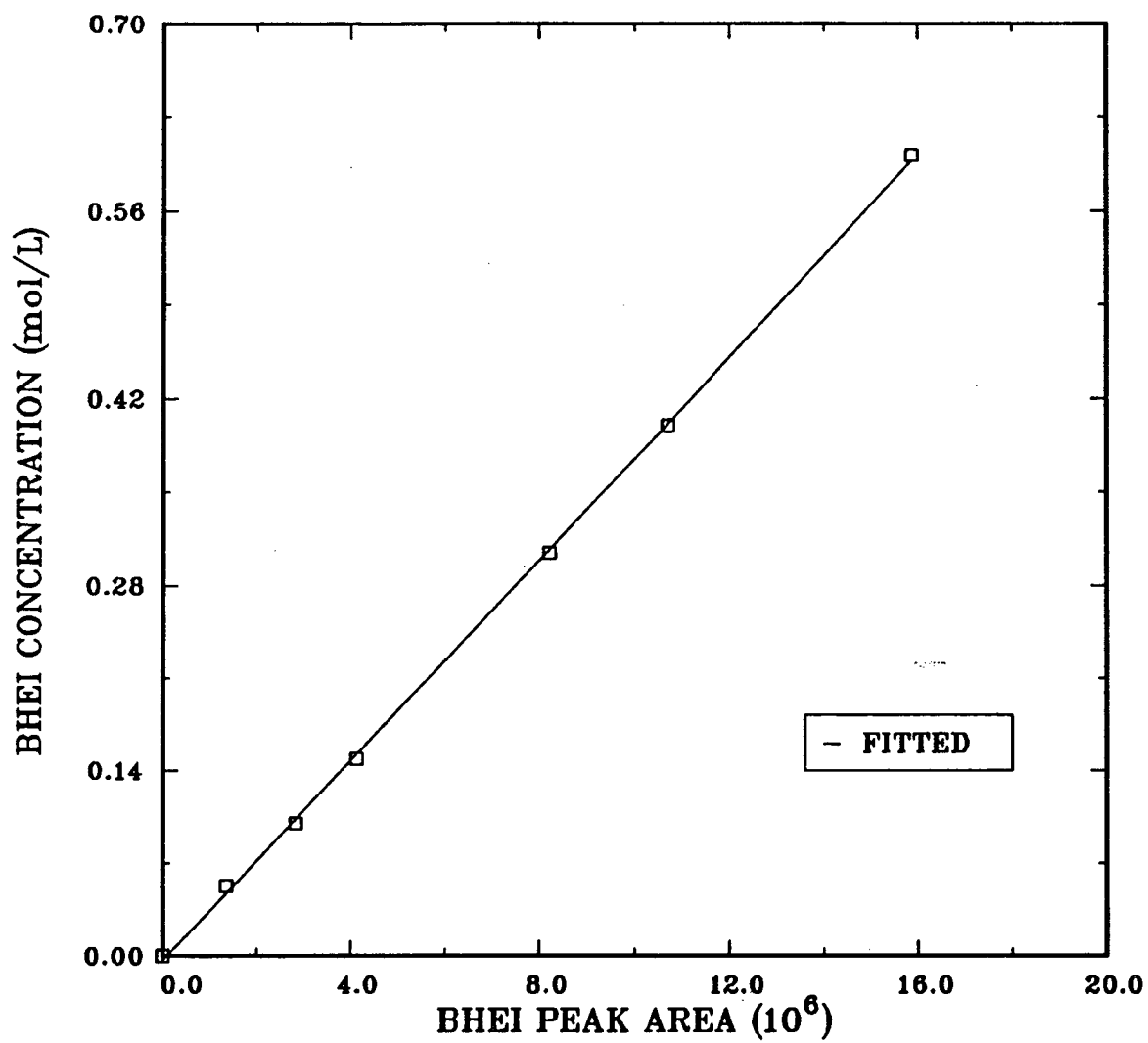


Figure B.10: Calibration curve for BHEI.

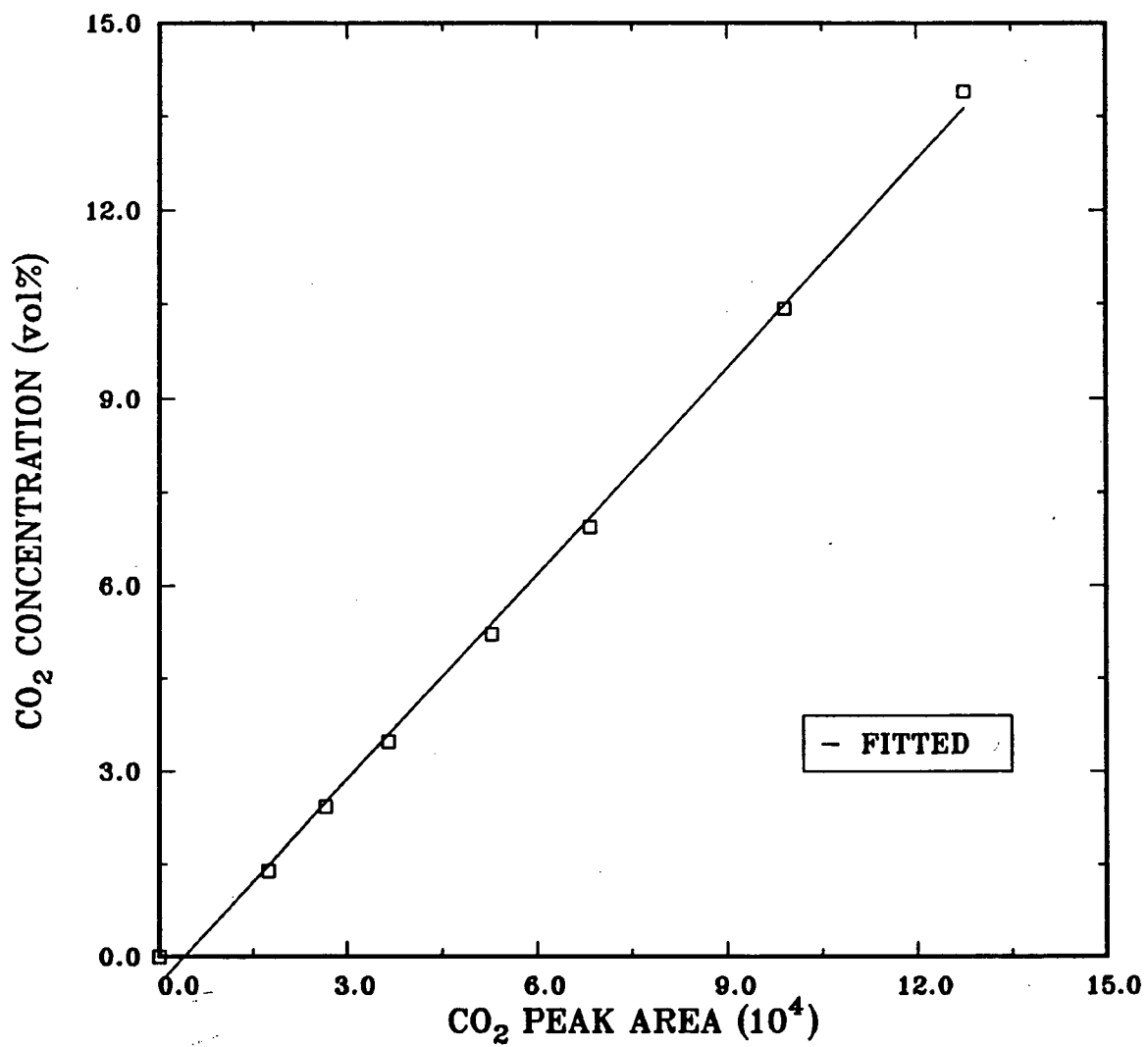


Figure B.11: Calibration curve for CO₂.

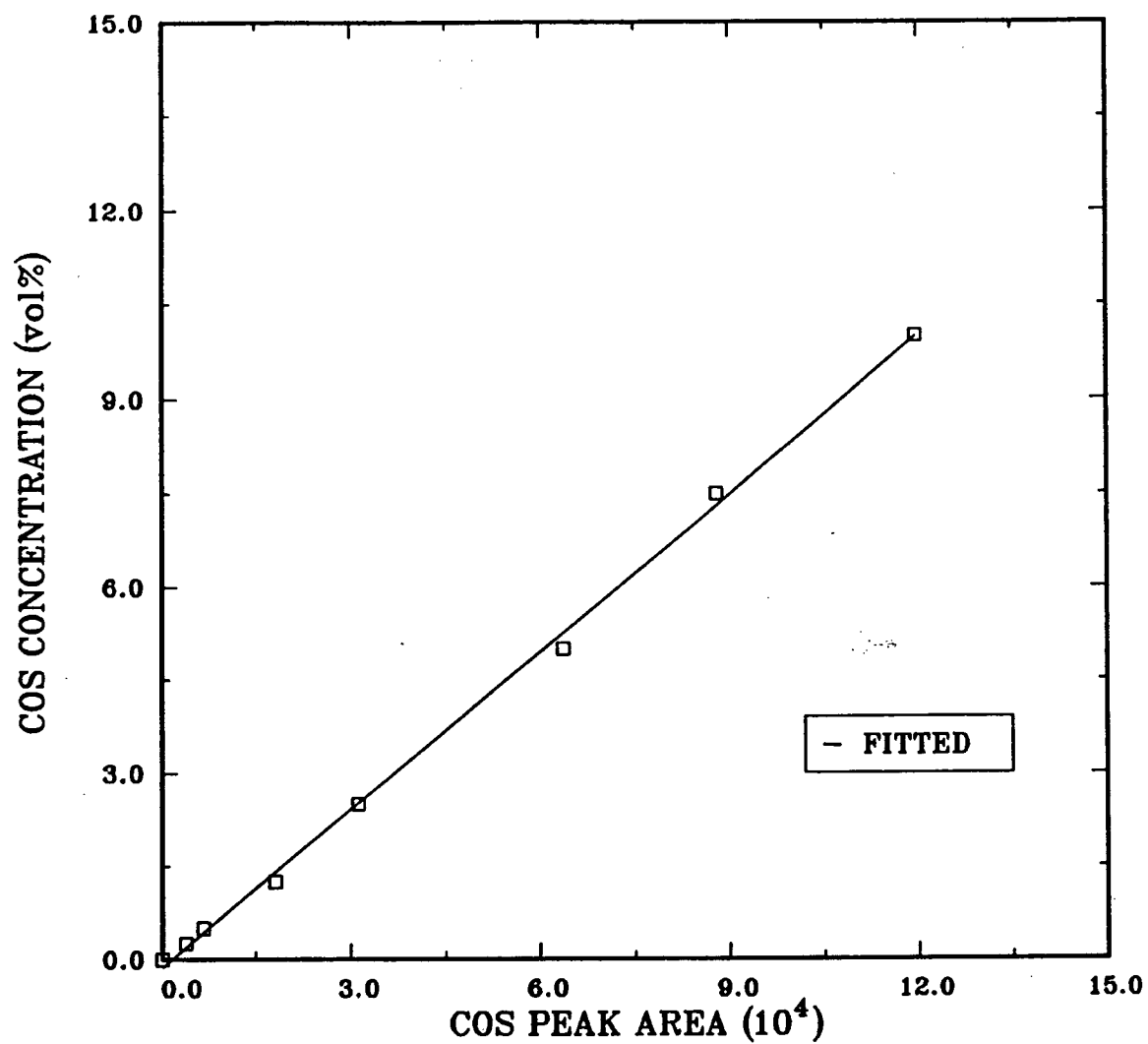


Figure B.12: Calibration curve for COS.

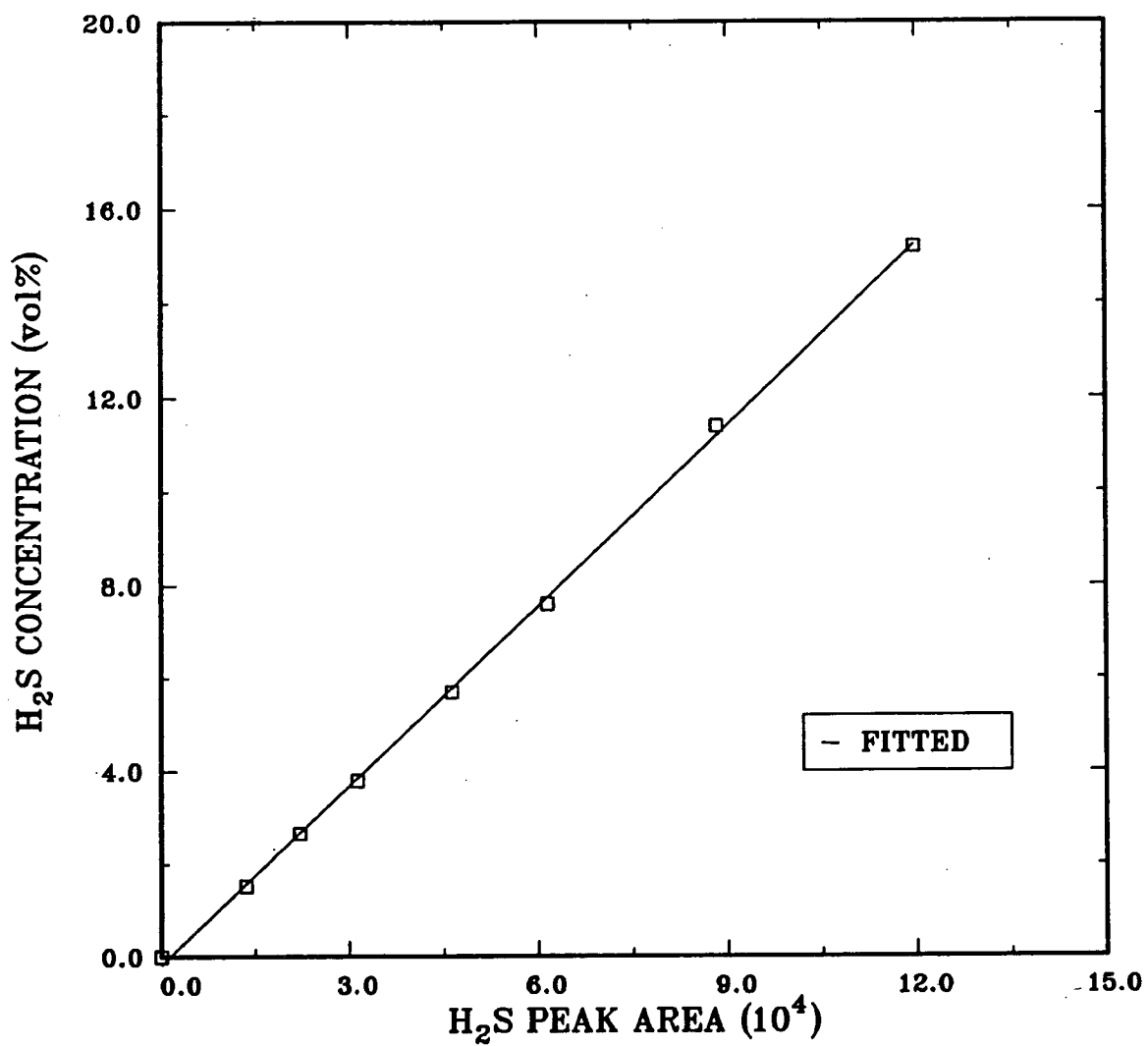


Figure B.13: Calibration curve for H₂S.

B.2 EI SPECTRA OF MINOR DEGRADATION COMPOUNDS IN THE COS-DEA SYSTEM

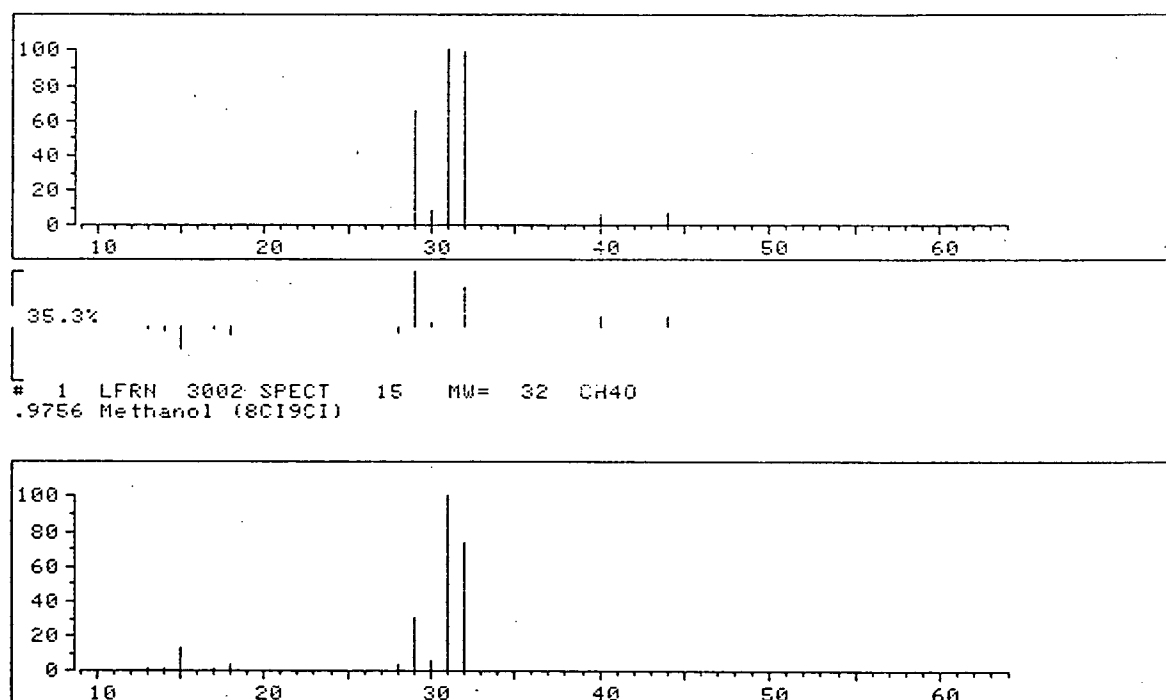


Figure B.14: Sample and library EI spectra of methanol.

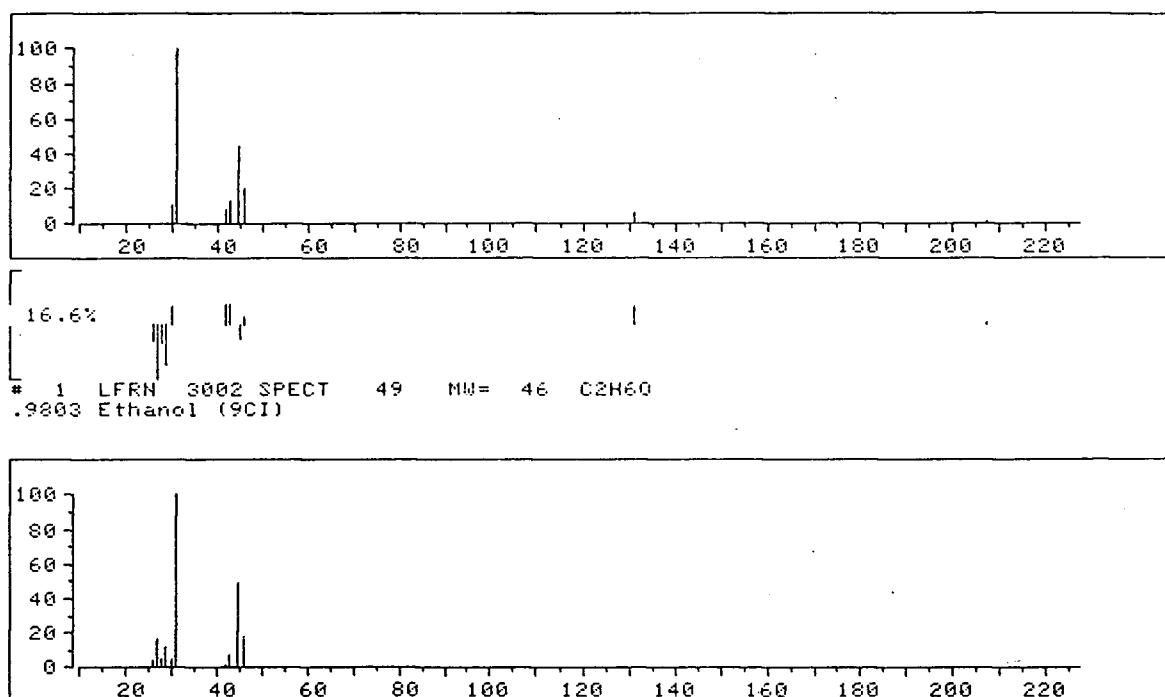


Figure B.15: Sample and library EI spectra of ethanol.

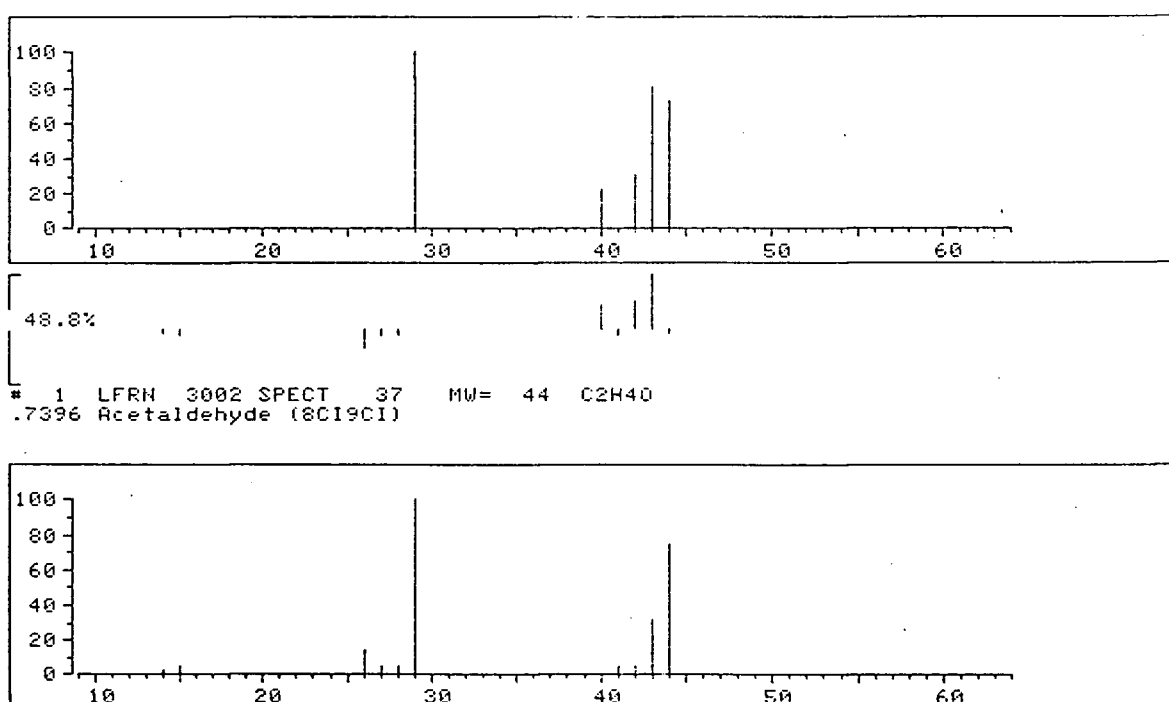


Figure B.16: Sample and library EI spectra of acetaldehyde.

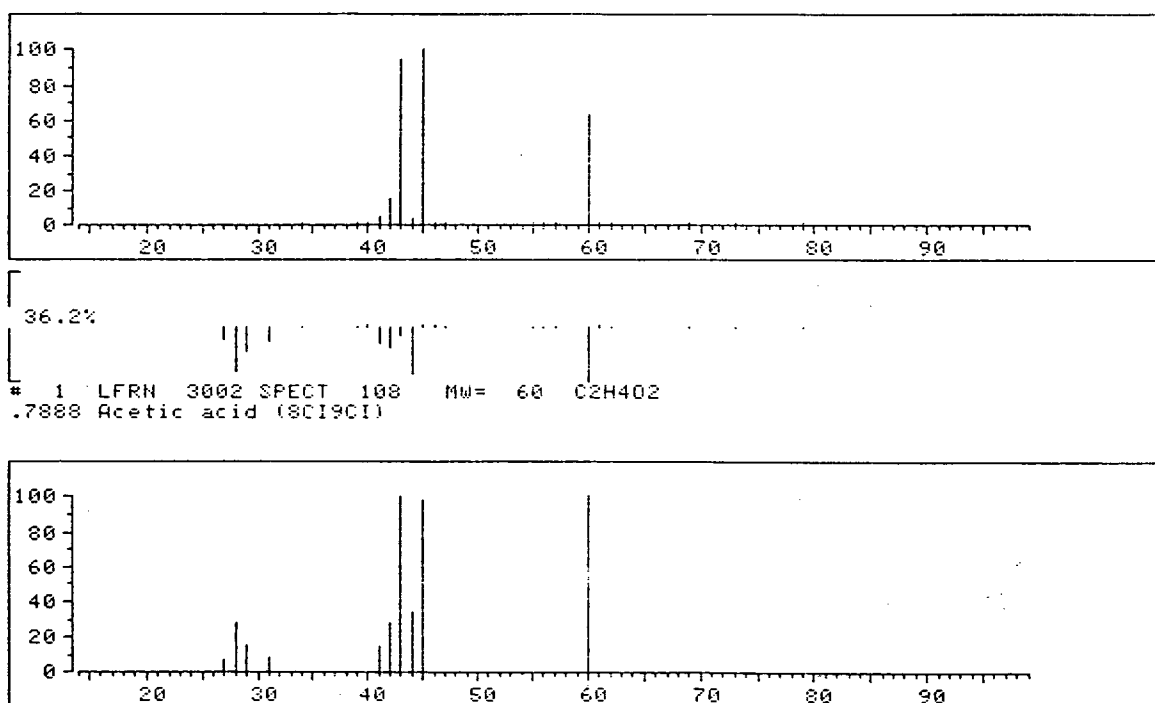


Figure B.17: Sample and library EI spectra of acetic acid.

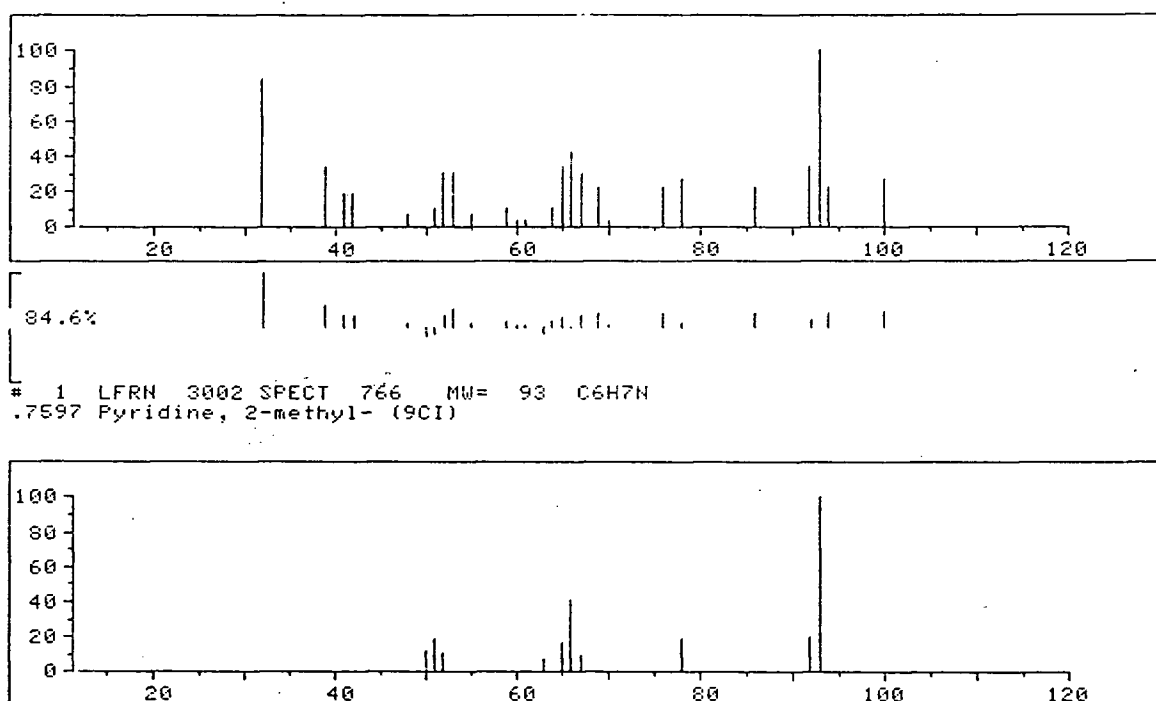
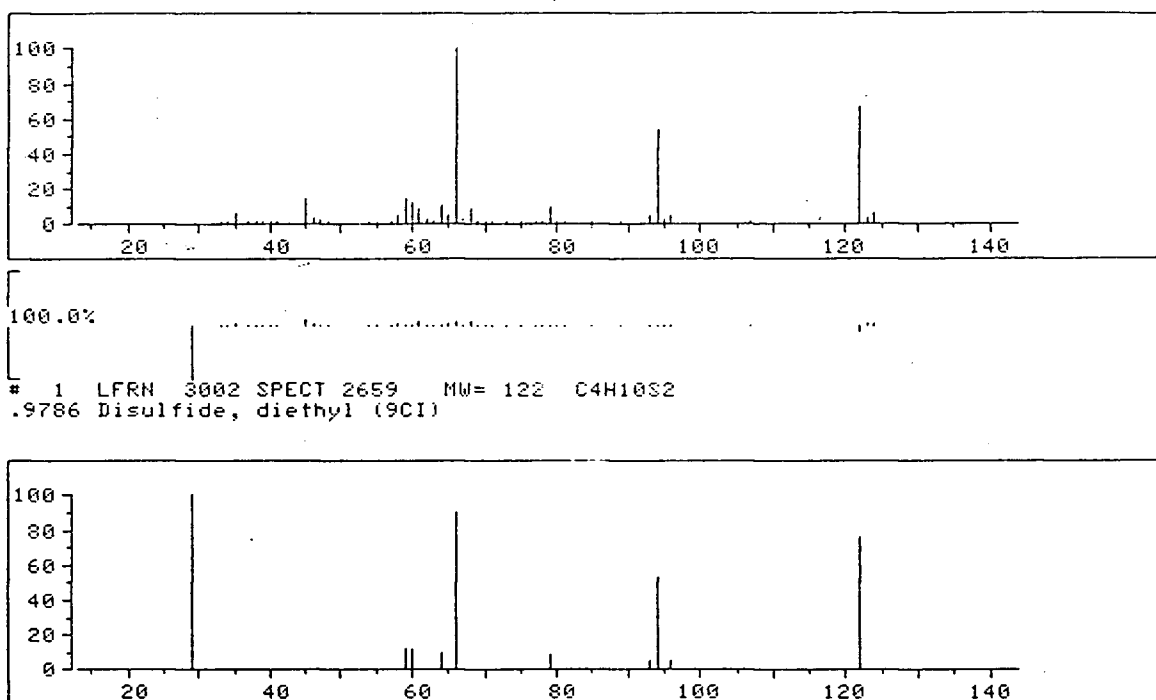


Figure B.18: Sample and library EI spectra of methyl pyridine.



Figur B.19: Sample and library EI spectra of diethyl disulphide.

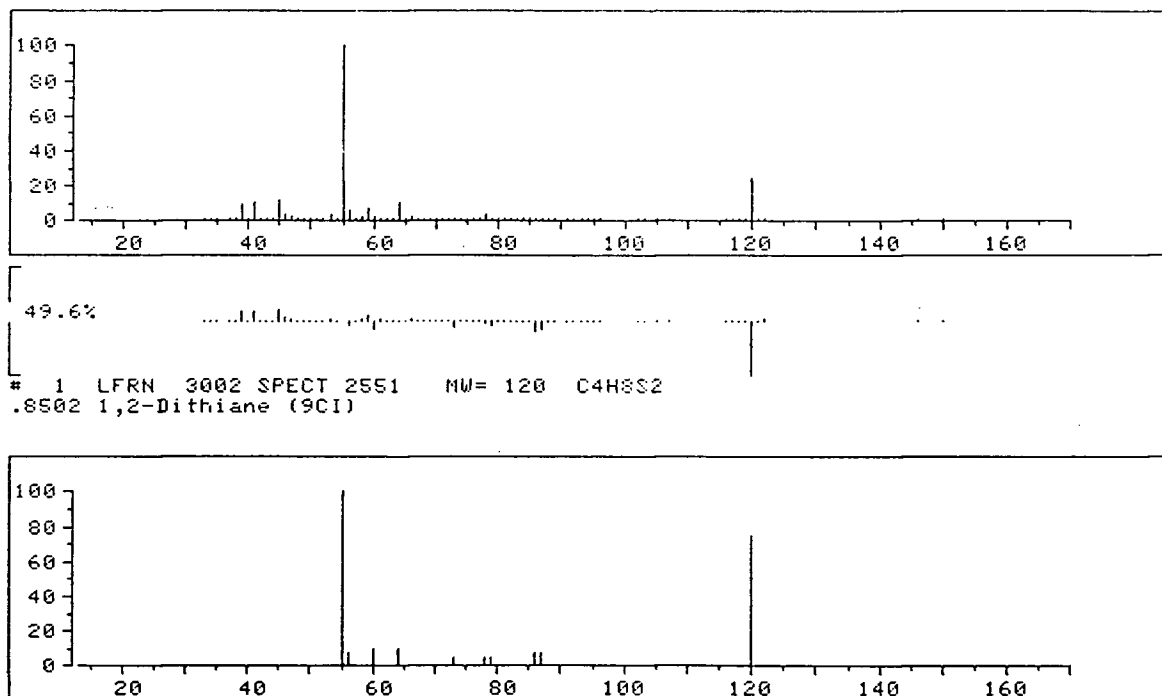


Figure B.20: Sample and EI spectra of 1,2 dithiane.

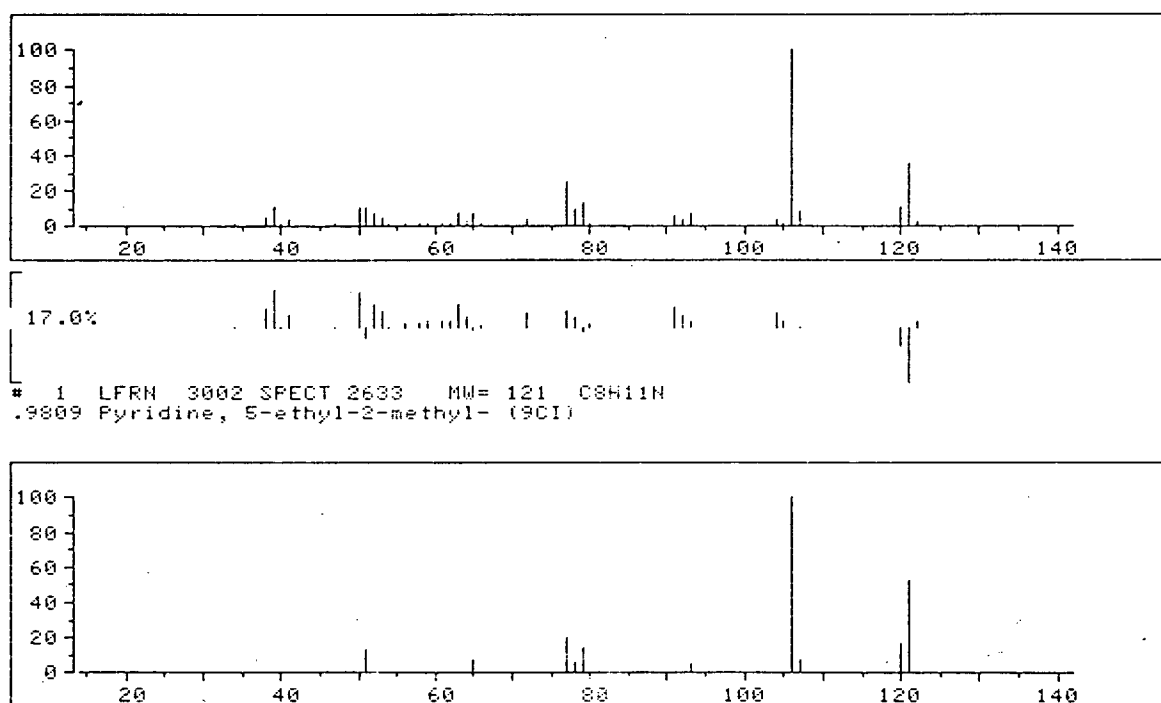
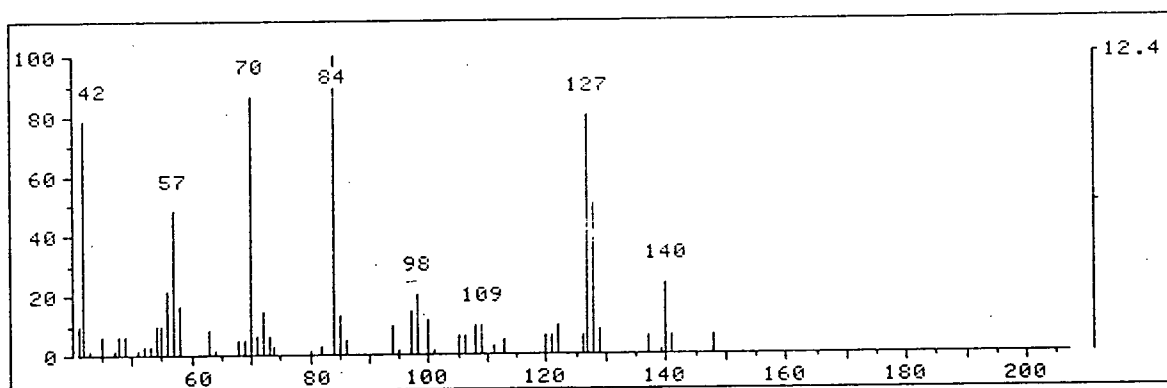
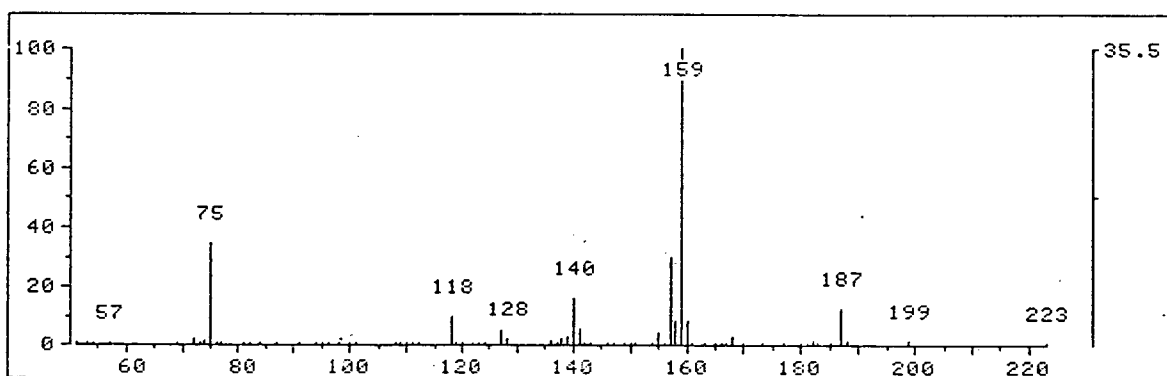


Figure B.21: Sample and library EI spectra of ethyl methyl pyridine.



(a)



(b)

Figure B.22: Mass spectra of EHEP (a: EI; b: CI).

C EXPERIMENTAL CONCENTRATIONS

C.1 COS-DEA SYSTEMS

Table C.1: Concentrations of compounds in COS-DEA system.
 $[\text{DEA}]_0 = 40 \text{ wt\%}$, $T = 165 \text{ }^\circ\text{C}$, $P_{\text{COS}} = 345 \text{ kPa}$.

TIME (H)	CONCENTRATION (mol/L)									
	DEA	ACET	BUT	MEA	BHEED	BHEP	HEOD	HEI	THEED	BHEI
0	4.20	0.000	0.000	0.000	0.000	0.000	0.000	0.000	0.000	0.000
2	4.09	0.010	0.004	0.129	0.000	0.000	0.000	0.000	0.000	0.000
4	3.90	0.013	0.010	0.202	0.014	0.000	0.010	0.000	0.000	0.000
6	3.68	0.015	0.013	0.263	0.020	0.003	0.015	0.000	0.000	0.000
8	3.48	0.017	0.013	0.312	0.028	0.007	0.027	0.000	0.085	0.000
12	3.27	0.019	0.016	0.487	0.046	0.014	0.043	0.000	0.133	0.000
24	2.77	0.015	0.020	0.730	0.156	0.033	0.107	0.069	0.461	0.040
30	2.37	0.013	0.019	0.687	0.211	0.039	0.119	0.096	0.587	0.105
36	2.15	0.011	0.020	0.655	0.233	0.043	0.122	0.108	0.615	0.127
48	1.59	0.010	0.020	0.578	0.286	0.074	0.146	0.131	0.845	0.245

$$k_{\text{DEA}} = 0.0194 \text{ h}^{-1}$$

Table C.2: Concentrations of compounds in COS-DEA system.
 $[\text{DEA}]_0 = 40 \text{ wt\%}$, $T = 160 \text{ }^\circ\text{C}$, $P_{\text{COS}} = 345 \text{ kPa}$.

TIME (H)	CONCENTRATION (mol/L)									
	DEA	ACET	BUT	MEA	BHEED	BHEP	HEOD	HEI	THEED	BHEI
0	4.12	0.000	0.000	0.000	0.000	0.000	0.000	0.000	0.000	0.000
2	4.02	0.008	0.003	0.083	0.000	0.000	0.000	0.000	0.000	0.000
4	3.83	0.009	0.005	0.136	0.010	0.000	0.000	0.000	0.000	0.000
6	3.71	0.011	0.010	0.200	0.017	0.000	0.010	0.000	0.000	0.000
8	3.71	0.013	0.014	0.284	0.024	0.004	0.025	0.000	0.078	0.000
12	3.45	0.015	0.016	0.405	0.036	0.008	0.036	0.000	0.106	0.000
24	3.02	0.013	0.018	0.550	0.116	0.021	0.088	0.052	0.431	0.050
30	2.78	0.011	0.019	0.644	0.172	0.029	0.099	0.065	0.615	0.079
36	2.58	0.011	0.020	0.637	0.209	0.036	0.117	0.070	0.730	0.121

$$k_{\text{DEA}} = 0.0127 \text{ h}^{-1}$$

Table C.3: Concentrations of compounds in COS-DEA system.
 $[\text{DEA}]_0 = 40 \text{ wt\%}$, $T = 150 \text{ }^\circ\text{C}$, $P_{\text{COS}} = 345 \text{ kPa}$.

TIME (H)	CONCENTRATION (mol/L)									
	DEA	ACET	BUT	MEA	BHEED	BHEP	HEOD	HEI	THEED	BHEI
0	4.17	0.000	0.000	0.000	0.000	0.000	0.000	0.000	0.000	0.000
2	4.09	0.007	0.001	0.068	0.000	0.000	0.000	0.000	0.000	0.000
4	3.95	0.009	0.003	0.108	0.007	0.000	0.000	0.000	0.000	0.000
6	3.85	0.011	0.005	0.157	0.014	0.000	0.007	0.000	0.000	0.000
8	3.74	0.013	0.008	0.206	0.021	0.000	0.010	0.000	0.000	0.000
12	3.79	0.016	0.014	0.318	0.029	0.006	0.020	0.000	0.000	0.000
24	3.42	0.021	0.018	0.535	0.043	0.012	0.042	0.000	0.122	0.005
30	3.08	0.020	0.017	0.576	0.053	0.016	0.048	0.000	0.145	0.009
36	2.92	0.019	0.018	0.704	0.073	0.019	0.060	0.009	0.211	0.016
48	2.69	0.019	0.019	0.769	0.141	0.033	0.110	0.012	0.326	0.027
54	2.59	0.020	0.018	0.773	0.173	0.043	0.116	0.020	0.364	0.036

$$k_{\text{DEA}} = 0.0089 \text{ h}^{-1}$$

Table C.4: Concentrations of compounds in COS-DEA system.
 $[\text{DEA}]_0 = 40 \text{ wt\%}$, $T = 127 \text{ }^\circ\text{C}$, $P_{\text{COS}} = 345 \text{ kPa}$.

TIME (H)	CONCENTRATION (mol/L)									
	DEA	ACET	BUT	MEA	BHEED	BHEP	HEOD	HEI	THEED	BHEI
0	4.20	0.000	0.000	0.000	0.000	0.000	0.000	0.000	0.000	0.000
12	4.00	0.012	0.002	0.098	0.000	0.000	0.000	0.000	0.000	0.000
20	3.86	0.018	0.004	0.218	0.005	0.000	0.025	0.000	0.000	0.000
44	3.50	0.020	0.009	0.390	0.020	0.005	0.047	0.000	0.035	0.000
68	3.20	0.020	0.011	0.570	0.038	0.011	0.068	0.011	0.123	0.031
92	2.86	0.022	0.012	0.649	0.050	0.016	0.077	0.013	0.198	0.055
116	2.61	0.019	0.013	0.679	0.091	0.023	0.107	0.015	0.310	0.079
140	2.33	0.024	0.014	0.635	0.128	0.038	0.127	0.028	0.439	0.100
164	2.12	0.023	0.013	0.685	0.160	0.047	0.142	0.036	0.532	0.147

$$k_{\text{DEA}} = 0.0042 \text{ h}^{-1}$$

Table C.5: Concentrations of compounds in COS-DEA system.
 $[\text{DEA}]_0 = 30 \text{ wt\%}$, $T = 190 \text{ }^\circ\text{C}$, $P_{\text{COS}} = 345 \text{ kPa}$.

TIME (H)	CONCENTRATION (mol/L)									
	DEA	ACET	BUT	MEA	BHEED	BHEP	HEOD	HEI	THEED	BHEI
0	3.11	0.000	0.000	0.000	0.000	0.000	0.000	0.000	0.000	0.000
2	2.90	0.010	0.006	0.130	0.000	0.000	0.010	0.000	0.000	0.000
4	2.66	0.013	0.008	0.220	0.000	0.002	0.014	0.000	0.000	0.000
6	2.57	0.016	0.010	0.330	0.010	0.005	0.024	0.000	0.040	0.000
8	2.42	0.013	0.011	0.390	0.020	0.008	0.031	0.017	0.110	0.000
12	2.13	0.012	0.013	0.440	0.040	0.011	0.042	0.020	0.200	0.010
24	1.32	0.012	0.017	0.410	0.150	0.044	0.081	0.039	0.500	0.116
30	1.16	0.013	0.018	0.380	0.180	0.072	0.088	0.049	0.590	0.187
36	1.00	0.010	0.019	0.340	0.190	0.098	0.093	0.054	0.600	0.242
48	0.82	0.008	0.017	0.290	0.170	0.134	0.088	0.066	0.530	0.305

$$k_{\text{DEA}} = 0.0291 \text{ h}^{-1}$$

Table C.6: Concentrations of compounds in COS-DEA system.
 $[\text{DEA}]_0 = 30 \text{ wt\%}$, $T = 170 \text{ }^\circ\text{C}$, $P_{\text{COS}} = 345 \text{ kPa}$.

TIME (H)	CONCENTRATION (mol/L)									
	DEA	ACET	BUT	MEA	BHEED	BHEP	HEOD	HEI	THEED	BHEI
0	3.04	0.000	0.000	0.000	0.000	0.000	0.000	0.000	0.000	0.000
2	2.86	0.007	0.003	0.023	0.000	0.000	0.016	0.000	0.000	0.000
4	2.85	0.010	0.006	0.089	0.000	0.000	0.020	0.000	0.000	0.000
6	2.60	0.012	0.007	0.133	0.000	0.000	0.022	0.000	0.000	0.000
8	2.56	0.013	0.007	0.193	0.000	0.003	0.025	0.000	0.000	0.000
12	2.49	0.012	0.008	0.276	0.008	0.005	0.036	0.000	0.000	0.000
24	2.05	0.010	0.010	0.461	0.038	0.009	0.064	0.016	0.190	0.000
30	1.91	0.010	0.012	0.500	0.112	0.017	0.107	0.023	0.390	0.070
36	1.74	0.010	0.014	0.489	0.138	0.022	0.117	0.029	0.480	0.100
48	1.38	0.009	0.014	0.412	0.175	0.038	0.136	0.034	0.630	0.190
60	1.02	0.007	0.013	0.308	0.157	0.048	0.116	0.034	0.610	0.220

$$k_{\text{DEA}} = 0.0168 \text{ h}^{-1}$$

Table C.7: Concentrations of compounds in COS-DEA system.
 $[\text{DEA}]_0 = 30 \text{ wt\%}$, $T = 165 \text{ }^\circ\text{C}$, $P_{\text{COS}} = 345 \text{ kPa}$.

TIME (H)	CONCENTRATION (mol/L)									
	DEA	ACET	BUT	MEA	BHEED	BHEP	HEOD	HEI	THEED	BHEI
0	3.00	0.000	0.000	0.000	0.000	0.000	0.000	0.000	0.000	0.000
2	3.01	0.007	0.003	0.082	0.000	0.000	0.000	0.000	0.000	0.000
4	2.82	0.010	0.005	0.100	0.012	0.000	0.006	0.000	0.000	0.000
8	2.63	0.013	0.011	0.205	0.016	0.000	0.017	0.000	0.000	0.000
12	2.50	0.016	0.018	0.300	0.021	0.003	0.027	0.002	0.067	0.000
24	2.09	0.024	0.021	0.454	0.047	0.017	0.033	0.008	0.087	0.013
30	1.89	0.024	0.020	0.551	0.066	0.023	0.051	0.016	0.117	0.015
36	1.73	0.022	0.020	0.624	0.088	0.027	0.058	0.022	0.149	0.020
48	1.36	0.016	0.021	0.627	0.127	0.040	0.070	0.039	0.287	0.040

$$k_{\text{DEA}} = 0.0162 \text{ h}^{-1}$$

Table C.8: Concentrations of compounds in COS-DEA system.
 $[\text{DEA}]_0 = 30 \text{ wt\%}$, $T = 160 \text{ }^\circ\text{C}$, $P_{\text{COS}} = 345 \text{ kPa}$.

TIME (H)	CONCENTRATION (mol/L)									
	DEA	ACET	BUT	MEA	BHEED	BHEP	HEOD	HEI	THEED	BHEI
0	3.05	0.000	0.000	0.000	0.000	0.000	0.000	0.000	0.000	0.000
2	3.08	0.007	0.000	0.005	0.000	0.000	0.000	0.000	0.000	0.000
4	2.99	0.008	0.004	0.050	0.000	0.000	0.010	0.000	0.000	0.000
8	2.83	0.010	0.006	0.110	0.000	0.000	0.019	0.000	0.000	0.000
12	2.72	0.014	0.009	0.192	0.004	0.002	0.025	0.000	0.000	0.000
24	2.39	0.016	0.011	0.364	0.010	0.006	0.039	0.000	0.005	0.000
30	2.24	0.014	0.011	0.400	0.020	0.008	0.054	0.003	0.100	0.000
36	2.02	0.013	0.012	0.440	0.030	0.010	0.062	0.006	0.150	0.005
48	1.70	0.010	0.012	0.510	0.070	0.012	0.091	0.022	0.300	0.050

$$k_{\text{DEA}} = 0.0120 \text{ h}^{-1}$$

Table C.9: Concentrations of compounds in COS-DEA system.
 $[\text{DEA}]_0 = 30 \text{ wt\%}$, $T = 150 \text{ }^\circ\text{C}$, $P_{\text{COS}} = 345 \text{ kPa}$.

TIME (H)	CONCENTRATION (mol/L)									
	DEA	ACET	BUT	MEA	BHEED	BHEP	HEOD	HEI	THEED	BHEI
0	3.01	0.000	0.000	0.000	0.000	0.000	0.000	0.000	0.000	0.000
2	3.06	0.006	0.000	0.044	0.000	0.000	0.000	0.000	0.000	0.000
4	2.91	0.007	0.002	0.077	0.000	0.000	0.000	0.000	0.000	0.000
8	2.83	0.010	0.006	0.127	0.009	0.000	0.005	0.000	0.000	0.000
12	2.76	0.013	0.011	0.200	0.012	0.000	0.010	0.000	0.000	0.000
24	2.47	0.016	0.014	0.319	0.019	0.008	0.020	0.000	0.000	0.000
30	2.31	0.019	0.016	0.402	0.022	0.009	0.031	0.000	0.030	0.000
36	2.18	0.022	0.017	0.488	0.035	0.017	0.056	0.006	0.080	0.011
48	1.93	0.015	0.016	0.572	0.073	0.024	0.086	0.009	0.142	0.017

$$k_{\text{DEA}} = 0.0094 \text{ h}^{-1}$$

Table C.10: Concentrations of compounds in COS-DEA system.
 $[\text{DEA}]_0 = 30 \text{ wt\%}$, $T = 127 \text{ }^\circ\text{C}$, $P_{\text{COS}} = 345 \text{ kPa}$.

TIME (H)	CONCENTRATION (mol/L)									
	DEA	ACET	BUT	MEA	BHEED	BHEP	HEOD	HEI	THEED	BHEI
0	3.08	0.000	0.000	0.000	0.000	0.000	0.000	0.000	0.000	0.000
24	2.94	0.010	0.003	0.162	0.000	0.000	0.000	0.000	0.000	0.000
48	2.73	0.019	0.010	0.280	0.000	0.000	0.018	0.000	0.000	0.000
80	2.51	0.019	0.010	0.410	0.000	0.000	0.030	0.003	0.050	0.000
96	2.35	0.020	0.010	0.500	0.005	0.003	0.033	0.005	0.070	0.000
124	2.19	0.022	0.009	0.610	0.017	0.011	0.047	0.006	0.108	0.012
146	1.95	0.016	0.008	0.660	0.029	0.012	0.054	0.008	0.152	0.024
168	1.88	0.018	0.010	0.730	0.057	0.017	0.085	0.018	0.222	0.054
192	1.88	0.020	0.011	0.840	0.082	0.028	0.113	0.024	0.281	0.076

$$k_{\text{DEA}} = 0.0031 \text{ h}^{-1}$$

Table C.11: Concentrations of compounds in COS-DEA system.
 $[\text{DEA}]_0 = 20 \text{ wt\%}$, $T = 195 \text{ }^\circ\text{C}$, $P_{\text{COS}} = 345 \text{ kPa}$.

TIME (H)	CONCENTRATION (mol/L)									
	DEA	ACET	BUT	MEA	BHEED	BHEP	HEOD	HEI	THEED	BHEI
0	1.97	0.000	0.000	0.000	0.000	0.000	0.000	0.000	0.000	0.000
2	1.84	0.007	0.005	0.103	0.000	0.000	0.000	0.000	0.000	0.000
4	1.70	0.008	0.007	0.154	0.000	0.000	0.000	0.000	0.000	0.000
6	1.63	0.009	0.008	0.203	0.000	0.000	0.000	0.000	0.000	0.000
8	1.54	0.008	0.008	0.227	0.015	0.004	0.010	0.000	0.000	0.000
12	1.40	0.011	0.010	0.321	0.024	0.007	0.015	0.007	0.076	0.000
24	1.00	0.011	0.014	0.402	0.059	0.017	0.027	0.031	0.149	0.024
30	0.79	0.008	0.014	0.353	0.110	0.028	0.047	0.071	0.227	0.077
36	0.68	0.008	0.013	0.335	0.121	0.040	0.050	0.088	0.257	0.112

$$k_{\text{DEA}} = 0.0293 \text{ h}^{-1}$$

Table C.12: Concentrations of compounds in COS-DEA system.
 $[\text{DEA}]_0 = 20 \text{ wt\%}$, $T = 180 \text{ }^\circ\text{C}$, $P_{\text{COS}} = 345 \text{ kPa}$.

TIME (H)	CONCENTRATION (mol/L)									
	DEA	ACET	BUT	MEA	BHEED	BHEP	HEOD	HEI	THEED	BHEI
0	1.98	0.000	0.000	0.000	0.000	0.000	0.000	0.000	0.000	0.000
2	1.85	0.004	0.003	0.062	0.000	0.000	0.000	0.000	0.000	0.000
4	1.78	0.005	0.005	0.092	0.000	0.000	0.000	0.000	0.000	0.000
6	1.73	0.007	0.006	0.139	0.000	0.000	0.000	0.000	0.000	0.000
8	1.64	0.008	0.007	0.179	0.013	0.003	0.000	0.000	0.000	0.000
12	1.52	0.009	0.008	0.235	0.015	0.006	0.010	0.000	0.007	0.000
24	1.17	0.011	0.011	0.371	0.031	0.011	0.025	0.014	0.096	0.014
30	1.02	0.009	0.010	0.346	0.054	0.015	0.033	0.032	0.165	0.019
36	0.87	0.009	0.011	0.366	0.089	0.019	0.046	0.052	0.198	0.048
48	0.72	0.008	0.013	0.370	0.093	0.030	0.048	0.076	0.201	0.064

$$k_{\text{DEA}} = 0.0214 \text{ h}^{-1}$$

Table C.13: Concentrations of compounds in COS-DEA system.
 $[\text{DEA}]_0 = 20 \text{ wt\%}$, $T = 165 \text{ }^\circ\text{C}$, $P_{\text{COS}} = 345 \text{ kPa}$.

TIME (H)	CONCENTRATION (mol/L)									
	DEA	ACET	BUT	MEA	BHEED	BHEP	HEOD	HEI	THEED	BHEI
0	1.91	0.000	0.000	0.000	0.000	0.000	0.000	0.000	0.000	0.000
2	1.97	0.004	0.002	0.042	0.000	0.000	0.000	0.000	0.000	0.000
4	1.86	0.005	0.003	0.063	0.000	0.000	0.000	0.000	0.000	0.000
8	1.78	0.007	0.006	0.109	0.000	0.000	0.000	0.000	0.000	0.000
12	1.83	0.008	0.008	0.153	0.012	0.000	0.000	0.000	0.000	0.000
24	1.52	0.010	0.010	0.258	0.016	0.000	0.015	0.000	0.000	0.000
30	1.41	0.010	0.010	0.294	0.018	0.005	0.019	0.004	0.072	0.000
36	1.33	0.010	0.011	0.333	0.027	0.009	0.027	0.007	0.088	0.014
48	1.15	0.010	0.012	0.410	0.052	0.014	0.038	0.013	0.127	0.022

$$k_{\text{DEA}} = 0.0110 \text{ h}^{-1}$$

Table C.14: Concentrations of compounds in COS-DEA system.
 $[\text{DEA}]_0 = 20 \text{ wt\%}$, $T = 150 \text{ }^\circ\text{C}$, $P_{\text{COS}} = 345 \text{ kPa}$.

TIME (H)	CONCENTRATION (mol/L)									
	DEA	ACET	BUT	MEA	BHEED	BHEP	HEOD	HEI	THEED	BHEI
0	1.96	0.000	0.000	0.000	0.000	0.000	0.000	0.000	0.000	0.000
2	1.92	0.003	0.000	0.000	0.000	0.000	0.000	0.000	0.000	0.000
4	1.88	0.004	0.001	0.039	0.000	0.000	0.000	0.000	0.000	0.000
8	1.85	0.007	0.003	0.081	0.000	0.000	0.005	0.000	0.000	0.000
12	1.88	0.009	0.006	0.120	0.000	0.000	0.010	0.000	0.000	0.000
24	1.70	0.010	0.010	0.200	0.014	0.001	0.012	0.000	0.000	0.000
30	1.55	0.010	0.009	0.234	0.015	0.003	0.017	0.000	0.000	0.000
36	1.62	0.012	0.011	0.295	0.017	0.004	0.019	0.002	0.000	0.000
48	1.42	0.013	0.012	0.316	0.016	0.005	0.019	0.004	0.000	0.008
60	1.26	0.015	0.013	0.351	0.017	0.008	0.020	0.006	0.061	0.012

$$k_{\text{DEA}} = 0.0070 \text{ h}^{-1}$$

Table C.15: Concentrations of compounds in COS-DEA system.
 $[\text{DEA}]_0 = 20 \text{ wt\%}$, $T = 135 \text{ }^\circ\text{C}$, $P_{\text{COS}} = 345 \text{ kPa}$.

TIME (H)	CONCENTRATION (mol/L)									
	DEA	ACET	BUT	MEA	BHEED	BHEP	HEOD	HEI	THEED	BHEI
0	1.99	0.000	0.000	0.000	0.000	0.000	0.000	0.000	0.000	0.000
24	1.82	0.008	0.003	0.100	0.000	0.000	0.000	0.000	0.000	0.000
48	1.74	0.009	0.006	0.157	0.000	0.000	0.000	0.000	0.000	0.000
72	1.56	0.012	0.008	0.215	0.000	0.000	0.010	0.000	0.000	0.000
96	1.35	0.011	0.009	0.251	0.013	0.000	0.016	0.000	0.000	0.000
120	1.30	0.009	0.009	0.317	0.024	0.007	0.019	0.000	0.000	0.000
144	1.12	0.011	0.009	0.315	0.031	0.009	0.032	0.000	0.077	0.015
168	1.12	0.011	0.009	0.386	0.039	0.010	0.030	0.000	0.091	0.017
192	0.96	0.009	0.008	0.430	0.040	0.012	0.035	0.015	0.145	0.025
216	0.90	0.010	0.008	0.440	0.035	0.011	0.034	0.020	0.123	0.025

$$k_{\text{DEA}} = 0.0038 \text{ h}^{-1}$$

Table C.16: Concentrations of compounds in COS-DEA system.
 $[\text{DEA}]_0 = 20 \text{ wt\%}$, $T = 127 \text{ }^\circ\text{C}$, $P_{\text{COS}} = 345 \text{ kPa}$.

TIME (H)	CONCENTRATION (mol/L)									
	DEA	ACET	BUT	MEA	BHEED	BHEP	HEOD	HEI	THEED	BHEI
0	2.00	0.000	0.000	0.000	0.000	0.000	0.000	0.000	0.000	0.000
10	1.97	0.006	0.000	0.021	0.000	0.000	0.013	0.000	0.000	0.000
22	1.85	0.008	0.003	0.062	0.000	0.000	0.014	0.000	0.000	0.000
46	1.82	0.010	0.006	0.151	0.000	0.000	0.018	0.000	0.000	0.000
70	1.63	0.009	0.007	0.220	0.000	0.000	0.018	0.000	0.000	0.000
94	1.50	0.010	0.008	0.306	0.004	0.000	0.026	0.000	0.035	0.000
118	1.62	0.011	0.008	0.414	0.009	0.000	0.040	0.000	0.054	0.000
142	1.35	0.010	0.008	0.422	0.015	0.005	0.047	0.000	0.058	0.018
166	1.23	0.009	0.007	0.451	0.028	0.010	0.054	0.010	0.133	0.033

$$k_{\text{DEA}} = 0.0029 \text{ h}^{-1}$$

Table C.17: Concentrations of compounds in COS-DEA system.
 $[\text{DEA}]_0 = 30 \text{ wt\%}$, $T = 150 \text{ }^\circ\text{C}$, $P_{\text{COS}} = 759 \text{ kPa}$.

TIME (H)	CONCENTRATION (mol/L)									
	DEA	ACET	BUT	MEA	BHEED	BHEP	HEOD	HEI	THEED	BHEI
0	2.93	0.000	0.000	0.000	0.000	0.000	0.000	0.000	0.000	0.000
2	2.90	0.007	0.001	0.068	0.000	0.000	0.000	0.000	0.000	0.000
4	2.84	0.011	0.003	0.113	0.000	0.000	0.000	0.000	0.000	0.000
8	2.75	0.015	0.008	0.200	0.000	0.005	0.020	0.000	0.000	0.000
12	2.60	0.019	0.013	0.270	0.010	0.006	0.025	0.000	0.000	0.000
24	2.29	0.037	0.021	0.468	0.041	0.011	0.037	0.006	0.069	0.000
30	2.12	0.027	0.018	0.551	0.055	0.018	0.052	0.009	0.089	0.007
36	1.86	0.028	0.018	0.622	0.070	0.023	0.060	0.012	0.103	0.015
48	1.55	0.025	0.018	0.697	0.096	0.032	0.080	0.067	0.197	0.032

$$k_{\text{DEA}} = 0.0131 \text{ h}^{-1}$$

Table C.18: Concentrations of compounds in COS-DEA system.
 $[\text{DEA}]_0 = 30 \text{ wt\%}$, $T = 150 \text{ }^\circ\text{C}$, $P_{\text{COS}} = 1172 \text{ kPa}$.

TIME (H)	CONCENTRATION (mol/L)									
	DEA	ACET	BUT	MEA	BHEED	BHEP	HEOD	HEI	THEED	BHEI
0	2.95	0.000	0.000	0.000	0.000	0.000	0.000	0.000	0.000	0.000
2	2.90	0.009	0.000	0.088	0.000	0.000	0.000	0.000	0.000	0.000
4	2.87	0.015	0.001	0.146	0.000	0.000	0.020	0.000	0.000	0.000
8	2.70	0.022	0.009	0.239	0.000	0.007	0.025	0.000	0.000	0.000
12	2.48	0.026	0.013	0.316	0.021	0.010	0.043	0.004	0.000	0.000
24	2.00	0.030	0.015	0.474	0.047	0.016	0.060	0.011	0.022	0.000
30	1.82	0.039	0.015	0.570	0.069	0.023	0.065	0.031	0.117	0.014
36	1.61	0.035	0.013	0.646	0.086	0.027	0.067	0.056	0.200	0.018
48	1.25	0.033	0.014	0.661	0.116	0.041	0.107	0.092	0.251	0.033

$$k_{\text{DEA}} = 0.0180 \text{ h}^{-1}$$

Table C.19: Concentrations of compounds in COS-DEA system.
 $[\text{DEA}]_0 = 60 \text{ wt\%}$, $T = 165 \text{ }^\circ\text{C}$, $P_{\text{COS}} = 345 \text{ kPa}$.

TIME (H)	CONCENTRATION (mol/L)									
	DEA	ACET	BUT	MEA	BHEED	BHEP	HEOD	HEI	THEED	BHEI
0	6.21	0.000	0.000	0.000	0.000	0.000	0.000	0.000	0.000	0.000
2	6.24	0.016	0.005	0.156	0.000	0.000	0.025	0.000	0.000	0.000
4	5.96	0.022	0.012	0.273	0.027	0.008	0.032	0.000	0.042	0.000
8	5.46	0.026	0.016	0.424	0.039	0.015	0.041	0.000	0.168	0.000
12	5.00	0.022	0.017	0.549	0.105	0.032	0.080	0.024	0.305	0.000
24	4.05	0.016	0.017	0.655	0.224	0.055	0.174	0.089	0.799	0.070
30	3.53	0.009	0.018	0.682	0.321	0.064	0.177	0.133	1.190	0.141

$$k_{\text{DEA}} = 0.0194 \text{ h}^{-1}$$

Table C.20: Concentrations of compounds in COS-DEA system.
 $[\text{DEA}]_0 = 30 \text{ wt\%}$, $T = 150 \text{ }^\circ\text{C}$, $P_{\text{COS}} = 345 \text{ kPa}$.
 (Run conducted to determine the effect of oxygen)

TIME (H)	CONCENTRATION (mol/L)									
	DEA	ACET	BUT	MEA	BHEED	BHEP	HEOD	HEI	THEED	BHEI
0	3.00	0.000	0.000	0.000	0.000	0.000	0.000	0.000	0.000	0.000
2	2.98	0.005	0.000	0.059	0.000	0.000	0.000	0.000	0.000	0.000
4	2.86	0.007	0.002	0.085	0.000	0.000	0.000	0.000	0.000	0.000
8	2.77	0.010	0.007	0.143	0.000	0.006	0.000	0.000	0.000	0.000
12	2.69	0.011	0.010	0.198	0.000	0.007	0.018	0.000	0.000	0.000
24	2.45	0.017	0.016	0.330	0.021	0.010	0.023	0.000	0.000	0.000
30	2.30	0.020	0.015	0.380	0.024	0.013	0.026	0.007	0.036	0.000
36	2.17	0.021	0.015	0.436	0.054	0.020	0.078	0.009	0.073	0.012
48	1.91	0.022	0.017	0.531	0.073	0.033	0.107	0.012	0.121	0.016

$$k_{\text{DEA}} = 0.0096 \text{ h}^{-1}$$

C.2 CS₂-DEA SYSTEMS

Table C.21: Concentrations of compounds in CS₂-DEA system.
 [DEA]₀ = 40 wt%, T = 165 °C, CS₂ volume = 6.0 mL.

TIME (H)	CONCENTRATION (mol/L)							
	DEA	MEA	BHEED	BHEP	HEOD	HEI	THEED	BHEI
0	4.30	0.000	0.000	0.000	0.000	0.000	0.000	0.000
2	3.97	0.023	0.000	0.000	0.000	0.000	0.000	0.000
4	3.75	0.086	0.036	0.004	0.010	0.000	0.000	0.000
8	3.63	0.180	0.060	0.008	0.020	0.000	0.010	0.000
12	3.25	0.277	0.074	0.015	0.033	0.008	0.141	0.000
24	2.83	0.298	0.128	0.025	0.081	0.018	0.420	0.000
30	2.54	0.308	0.155	0.028	0.094	0.030	0.560	0.017
36	2.34	0.287	0.175	0.036	0.108	0.034	0.640	0.022
48	2.14	0.256	0.193	0.053	0.130	0.044	0.721	0.040

$$k_{\text{DEA}} = 0.0138 \text{ h}^{-1}$$

Table C.22: Concentrations of compounds in CS₂-DEA system.
 [DEA]₀ = 40 wt%, T = 150 °C, CS₂ volume = 6.0 mL.

TIME (H)	CONCENTRATION (mol/L)							
	DEA	MEA	BHEED	BHEP	HEOD	HEI	THEED	BHEI
0	4.16	0.000	0.000	0.000	0.000	0.000	0.000	0.000
2	3.93	0.012	0.000	0.000	0.000	0.000	0.000	0.000
4	3.71	0.043	0.000	0.000	0.007	0.000	0.000	0.000
8	3.71	0.126	0.000	0.000	0.008	0.000	0.000	0.000
12	3.57	0.188	0.010	0.008	0.015	0.000	0.032	0.000
24	3.33	0.253	0.047	0.011	0.034	0.010	0.010	0.000
36	3.37	0.309	0.070	0.016	0.051	0.018	0.310	0.000
49	2.96	0.326	0.095	0.024	0.052	0.028	0.384	0.011
60	2.75	0.292	0.141	0.030	0.100	0.031	0.422	0.016
72	2.53	0.295	0.163	0.034	0.108	0.032	0.520	0.022

$$k_{\text{DEA}} = 0.0057 \text{ h}^{-1}$$

Table C.23: Concentrations of compounds in CS₂-DEA system.
 [DEA]₀ = 30 wt%, T = 165 °C, CS₂ volume = 6.0 mL.

TIME (H)	DEA	MEA	BHEED	BHEP	HEOD	HEI	THEED	BHEI
CONCENTRATION (mol/L)								
0	2.96	0.000	0.000	0.000	0.000	0.000	0.000	0.000
2	2.80	0.030	0.000	0.000	0.000	0.000	0.000	0.000
4	2.70	0.076	0.016	0.000	0.005	0.000	0.000	0.000
8	2.68	0.166	0.020	0.004	0.017	0.000	0.040	0.000
12	2.57	0.209	0.031	0.008	0.020	0.000	0.080	0.000
24	2.29	0.282	0.066	0.013	0.037	0.010	0.146	0.000
30	2.12	0.291	0.084	0.015	0.045	0.022	0.310	0.013
36	1.97	0.291	0.124	0.020	0.056	0.025	0.360	0.018
48	1.76	0.243	0.144	0.025	0.085	0.029	0.407	0.031

$$k_{\text{DEA}} = 0.0101 \text{ h}^{-1}$$

Table C.24: Concentrations of compounds in CS₂-DEA system.
 [DEA]₀ = 30 wt%, T = 150 °C, CS₂ volume = 6.0 mL.

TIME (H)	DEA	MEA	BHEED	BHEP	HEOD	HEI	THEED	BHEI
CONCENTRATION (mol/L)								
0	2.96	0.000	0.000	0.000	0.000	0.000	0.000	0.000
2	2.72	0.008	0.000	0.000	0.000	0.000	0.000	0.000
4	2.71	0.030	0.000	0.000	0.000	0.000	0.000	0.000
8	2.68	0.075	0.000	0.000	0.006	0.000	0.000	0.000
12	2.78	0.149	0.019	0.000	0.010	0.000	0.000	0.000
24	2.62	0.195	0.030	0.007	0.021	0.000	0.000	0.000
34	2.31	0.257	0.042	0.010	0.026	0.005	0.110	0.000
48	2.24	0.293	0.056	0.014	0.037	0.010	0.170	0.008
60	1.97	0.283	0.073	0.016	0.043	0.022	0.254	0.017
70	1.90	0.272	0.089	0.021	0.047	0.025	0.350	0.022

$$k_{\text{DEA}} = 0.0056 \text{ h}^{-1}$$

Table C.25: Concentrations of compounds in CS₂-DEA system.
 [DEA]₀ = 30 wt%, T = 120 °C, CS₂ volume = 6.0 mL.

TIME (H)	CONCENTRATION (mol/L)							
	DEA	MEA	BHEED	BHEP	HEOD	HEI	THEED	BHEI
0	3.00	0.000	0.000	0.000	0.000	0.000	0.000	0.000
2	2.88	0.000	0.000	0.000	0.000	0.000	0.000	0.000
4	2.76	0.000	0.000	0.000	0.005	0.000	0.000	0.000
24	2.57	0.042	0.000	0.000	0.012	0.000	0.000	0.000
52	2.57	0.088	0.017	0.003	0.016	0.000	0.008	0.000
72	2.56	0.149	0.020	0.004	0.018	0.000	0.013	0.000
96	2.46	0.176	0.022	0.006	0.020	0.000	0.013	0.000
120	2.24	0.221	0.025	0.005	0.018	0.000	0.021	0.000
146	2.08	0.260	0.034	0.007	0.026	0.000	0.048	0.000
168	2.05	0.289	0.032	0.008	0.030	0.006	0.056	0.008

$$k_{\text{DEA}} = 0.0018 \text{ h}^{-1}$$

Table C.26: Concentrations of compounds in CS₂-DEA system.
 [DEA]₀ = 20 wt%, T = 180 °C, CS₂ volume = 6.0 mL.

TIME (H)	CONCENTRATION (mol/L)									
	DEA	ACET	BUT	MEA	BHEED	BHEP	HEOD	HEI	THEED	BHEI
0	2.11	0.000	0.000	0.000	0.000	0.000	0.000	0.000	0.000	0.000
2	1.64	0.001	0.000	0.040	0.000	0.000	0.000	0.000	0.000	0.000
4	1.57	0.004	0.002	0.048	0.000	0.000	0.000	0.000	0.000	0.000
8	1.43	0.019	0.011	0.121	0.012	0.005	0.009	0.007	0.000	0.000
12	1.32	0.032	0.022	0.179	0.018	0.012	0.012	0.013	0.000	0.000
24	0.70	0.051	0.042	0.215	0.055	0.017	0.015	0.024	0.000	0.000
30	0.37	0.050	0.047	0.246	0.045	0.013	0.011	0.035	0.000	0.000
36	0.23	0.044	0.047	0.221	0.041	0.012	0.013	0.046	0.008	0.010

TIME (H)	CONCENTRATION (mol/L)		
	EAE	HEA	EDEA
0	0.000	0.000	0.000
2	0.000	0.000	0.000
4	0.000	0.000	0.000
8	0.000	0.000	0.000
12	0.018	0.060	0.000
24	0.050	0.143	0.037
30	0.060	0.132	0.025
36	0.052	0.110	0.018

Table C.27: Concentrations of compounds in CS₂-DEA system.
 [DEA]₀ = 20 wt%, T = 165 °C, CS₂ volume = 6.0 mL.

TIME (H)	DEA	MEA	BHEED	BHEP	HEOD	HEI	THEED	BHEI
0	2.04	0.000	0.000	0.000	0.000	0.000	0.000	0.000
2	1.99	0.018	0.000	0.000	0.000	0.000	0.000	0.000
4	1.89	0.048	0.023	0.000	0.000	0.000	0.000	0.000
8	1.74	0.089	0.030	0.003	0.014	0.000	0.000	0.000
12	1.76	0.158	0.034	0.004	0.019	0.000	0.000	0.000
24	1.53	0.209	0.034	0.005	0.020	0.000	0.000	0.000
30	1.42	0.256	0.067	0.006	0.027	0.005	0.150	0.000
36	1.37	0.282	0.086	0.007	0.038	0.007	0.195	0.006
48	1.21	0.255	0.100	0.012	0.041	0.010	0.222	0.015

$$k_{\text{DEA}} = 0.0091 \text{ h}^{-1}$$

Table C.28: Concentrations of compounds in CS₂-DEA system.
 [DEA]₀ = 20 wt%, T = 150 °C, CS₂ volume = 6.0 mL.

TIME (H)	DEA	MEA	BHEED	BHEP	HEOD	HEI	THEED	BHEI
0	2.03	0.000	0.000	0.000	0.000	0.000	0.000	0.000
2	1.89	0.000	0.000	0.000	0.000	0.000	0.000	0.000
4	1.93	0.007	0.000	0.000	0.000	0.000	0.000	0.000
8	1.87	0.024	0.000	0.000	0.000	0.000	0.000	0.000
12	1.85	0.052	0.000	0.000	0.005	0.000	0.000	0.000
24	1.72	0.095	0.000	0.000	0.014	0.000	0.000	0.000
36	1.66	0.133	0.005	0.001	0.015	0.000	0.000	0.000
48	1.54	0.168	0.015	0.011	0.018	0.000	0.000	0.000
60	1.46	0.202	0.031	0.013	0.026	0.006	0.058	0.023
72	1.31	0.196	0.039	0.014	0.029	0.016	0.084	0.040

$$k_{\text{DEA}} = 0.0052 \text{ h}^{-1}$$

Table C.29: Concentrations of compounds in CS₂-DEA system.
 [DEA]₀ = 20 wt%, T = 120 °C, CS₂ volume = 6.0 mL.

TIME (H)	CONCENTRATION (mol/L)							
	DEA	MEA	BHEED	BHEP	HEOD	HEI	THEED	BHEI
0	1.90	0.000	0.000	0.000	0.000	0.000	0.000	0.000
2	1.78	0.000	0.000	0.000	0.000	0.000	0.000	0.000
4	1.75	0.000	0.000	0.000	0.000	0.000	0.000	0.000
24	1.66	0.019	0.000	0.000	0.013	0.000	0.000	0.000
48	1.64	0.052	0.006	0.000	0.015	0.000	0.000	0.000
72	1.60	0.074	0.008	0.004	0.016	0.000	0.000	0.000
96	1.56	0.101	0.011	0.005	0.017	0.000	0.000	0.000
120	1.52	0.145	0.019	0.005	0.021	0.000	0.000	0.000
144	1.48	0.191	0.023	0.006	0.020	0.000	0.013	0.000
168	1.45	0.220	0.024	0.007	0.022	0.005	0.014	0.000

$$k_{\text{DEA}} = 0.009 \text{ h}^{-1}$$

Table C.30: Concentrations of compounds in CS₂-DEA system.
 [DEA]₀ = 60 wt%, T = 165 °C, CS₂ volume = 6.0 mL.

TIME (H)	CONCENTRATION (mol/L)							
	DEA	MEA	BHEED	BHEP	HEOD	HEI	THEED	BHEI
0	6.32	0.000	0.000	0.000	0.000	0.000	0.000	0.000
2	5.76	0.062	0.022	0.000	0.012	0.000	0.015	0.000
4	5.52	0.130	0.028	0.009	0.013	0.000	0.033	0.000
8	5.47	0.246	0.039	0.011	0.022	0.018	0.081	0.000
12	5.09	0.366	0.052	0.011	0.028	0.026	0.167	0.007
24	4.74	0.481	0.080	0.017	0.047	0.036	0.381	0.013
30	4.30	0.506	0.130	0.021	0.055	0.046	0.640	0.020
36	3.90	0.459	0.150	0.022	0.059	0.047	0.760	0.028

$$k_{\text{DEA}} = 0.0106 \text{ h}^{-1}$$

Table C.31: Concentrations of compounds in CS₂-DEA system.
 [DEA]₀ = 30 wt%, T = 165 °C, CS₂ volume = 2.5 mL.

TIME (H)	CONCENTRATION (mol/L)							
	DEA	MEA	BHEED	BHEP	HEOD	HEI	THEED	BHEI
0	3.01	0.000	0.000	0.000	0.000	0.000	0.000	0.000
2	2.78	0.041	0.017	0.000	0.000	0.000	0.000	0.000
4	2.73	0.055	0.018	0.000	0.000	0.000	0.000	0.000
8	2.62	0.083	0.021	0.004	0.013	0.000	0.027	0.000
12	2.55	0.123	0.024	0.006	0.016	0.000	0.048	0.000
24	2.52	0.183	0.029	0.008	0.023	0.000	0.088	0.000
30	2.41	0.220	0.042	0.009	0.028	0.000	0.180	0.007
36	2.33	0.239	0.050	0.011	0.029	0.015	0.253	0.009
48	2.18	0.232	0.061	0.014	0.035	0.019	0.334	0.013

$$k_{\text{DEA}} = 0.0048 \text{ h}^{-1}$$

Table C.32: Concentrations of compounds in CS₂-DEA system.
 [DEA]₀ = 30 wt%, T = 165 °C, CS₂ volume = 10.5 mL.

TIME (H)	CONCENTRATION (mol/L)							
	DEA	MEA	BHEED	BHEP	HEOD	HEI	THEED	BHEI
0	3.07	0.000	0.000	0.000	0.000	0.000	0.000	0.000
2	2.53	0.046	0.010	0.000	0.000	0.000	0.012	0.000
4	2.42	0.055	0.015	0.000	0.017	0.007	0.013	0.000
8	2.30	0.155	0.028	0.008	0.021	0.008	0.016	0.000
12	2.21	0.338	0.045	0.010	0.030	0.023	0.046	0.000
24	1.91	0.420	0.093	0.018	0.062	0.043	0.199	0.034
30	1.60	0.411	0.131	0.019	0.061	0.053	0.333	0.056
36	1.37	0.379	0.157	0.023	0.078	0.057	0.417	0.075
48	1.14	0.305	0.143	0.028	0.068	0.056	0.438	0.099

$$k_{\text{DEA}} = 0.0173 \text{ h}^{-1}$$

Table C.33: Concentrations of compounds in CS₂-DEA system.
 [DEA]₀ = 30 wt%, T = 190 °C, CS₂ volume = 10.5 mL.

TIME (H)	CONCENTRATION (mol/L)									
	DEA	ACET	BUT	MEA	BHEED	BHEP	HEOD	HEI	THEED	BHEI
0	3.11	0.000	0.000	0.000	0.000	0.000	0.000	0.000	0.000	0.000
2	2.72	0.038	0.023	0.060	0.000	0.000	0.000	0.000	0.000	0.000
4	2.29	0.053	0.035	0.200	0.020	0.010	0.035	0.000	0.000	0.000
6	1.96	0.079	0.050	0.350	0.026	0.016	0.040	0.000	0.000	0.000
12	1.21	0.081	0.052	0.480	0.058	0.029	0.052	0.045	0.110	0.074
24	0.86	0.057	0.044	0.540	0.096	0.041	0.067	0.086	0.170	0.093
30	0.58	0.045	0.041	0.520	0.110	0.042	0.066	0.137	0.190	0.127
36	0.42	0.036	0.041	0.450	0.110	0.045	0.066	0.200	0.160	0.172
48	0.25	0.031	0.040	0.380	0.100	0.055	0.068	0.230	0.155	0.232

The EAE, HEA and EDEA formed in this run were not quantified.

Table C.34: Concentrations of compounds in CS₂-DEA system.
 [DEA]₀ = 30 wt%, T = 175 °C, CS₂ volume = 10.5 mL.

TIME (H)	CONCENTRATION (mol/L)							
	DEA	MEA	BHEED	BHEP	HEOD	HEI	THEED	BHEI
0	3.11	0.000	0.000	0.000	0.000	0.000	0.000	0.000
2	2.55	0.036	0.000	0.000	0.015	0.000	0.000	0.000
4	2.43	0.086	0.017	0.005	0.040	0.000	0.000	0.000
6	2.27	0.173	0.026	0.008	0.050	0.002	0.000	0.000
12	1.88	0.321	0.060	0.008	0.069	0.007	0.125	0.010
24	1.37	0.290	0.132	0.027	0.092	0.046	0.450	0.122
30	1.13	0.280	0.142	0.035	0.090	0.050	0.500	0.155
36	1.01	0.267	0.153	0.046	0.095	0.056	0.540	0.190
48	0.78	0.220	0.141	0.067	0.087	0.069	0.530	0.272

$$k_{\text{DEA}} = 0.0272 \text{ h}^{-1}$$

Table C.35: Concentrations of compounds in CS₂-DEA system.
 [DEA]₀ = 30 wt%, T = 160 °C, CS₂ volume = 10.5 mL.

TIME (H)	CONCENTRATION (mol/L)							
	DEA	MEA	BHEED	BHEP	HEOD	HEI	THEED	BHEI
0	3.08	0.000	0.000	0.000	0.000	0.000	0.000	0.000
2	2.62	0.010	0.000	0.000	0.000	0.000	0.000	0.000
4	2.57	0.030	0.000	0.000	0.000	0.000	0.000	0.000
6	2.54	0.080	0.007	0.000	0.020	0.000	0.000	0.000
8	2.50	0.140	0.013	0.001	0.027	0.000	0.000	0.000
12	2.43	0.240	0.020	0.002	0.034	0.000	0.000	0.000
24	1.93	0.360	0.040	0.003	0.057	0.014	0.170	0.025
30	1.78	0.350	0.090	0.011	0.088	0.030	0.290	0.058
36	1.65	0.370	0.110	0.013	0.096	0.032	0.390	0.083
48	1.31	0.280	0.120	0.021	0.091	0.041	0.450	0.120
60	1.13	0.280	0.130	0.029	0.096	0.047	0.530	0.160

$$k_{\text{DEA}} = 0.0148 \text{ h}^{-1}$$

Table C.36: Concentrations of compounds in CS₂-DEA system.
 [DEA]₀ = 30 wt%, T = 130 °C, CS₂ volume = 10.5 mL.

TIME (H)	CONCENTRATION (mol/L)							
	DEA	MEA	BHEED	BHEP	HEOD	HEI	THEED	BHEI
0	3.08	0.000	0.000	0.000	0.000	0.000	0.000	0.000
2	2.76	0.000	0.000	0.000	0.000	0.000	0.000	0.000
4	2.77	0.000	0.000	0.000	0.000	0.000	0.000	0.000
24	2.51	0.031	0.000	0.000	0.000	0.000	0.000	0.000
48	2.44	0.123	0.000	0.000	0.000	0.000	0.000	0.000
72	2.24	0.242	0.013	0.002	0.031	0.000	0.038	0.000
98	2.08	0.340	0.027	0.004	0.043	0.009	0.122	0.000
120	1.93	0.410	0.032	0.004	0.048	0.013	0.157	0.024
144	1.81	0.444	0.045	0.005	0.069	0.016	0.209	0.031

$$k_{\text{DEA}} = 0.0034 \text{ h}^{-1}$$

C.3 OTHER SYSTEMS.

Table C.37: Gas mixture of 15% H₂S in nitrogen was contacted with 30 wt% aqueous DEA solution for 48 h. No degradation occurred.

Table C.38: Concentrations of compounds in aqueous DEA solution degraded with a gas mixture containing 14.7% CO₂ in nitrogen (DEA₀ = 3.0 mol/L; T = 165 °C; P_{gas mixture} = 1.55 MPa).

TIME (H)	CONCENTRATION (mol/L)			
	DEA	BHEP	HEOD	THEED
0	3.00	0.000	0.000	0.000
2	2.96	0.000	0.020	0.000
4	2.86	0.000	0.023	0.005
8	2.79	0.003	0.026	0.044
12	2.76	0.005	0.027	0.099
24	2.64	0.008	0.035	0.197
30	2.49	0.010	0.037	0.364
36	2.41	0.012	0.037	0.447
48	2.27	0.016	0.040	0.522

$$k_{\text{DEA}} = 0.0056 \text{ h}^{-1}$$

Table C.39: Concentrations of compounds in aqueous DEA solution degraded with a gas mixture containing 15.2% CO₂ and 15.2% H₂S in nitrogen (DEA₀ = 3.0 mol/L; T = 165 °C; P_{gas mixture} = 1.55 MPa).

TIME (H)	CONCENTRATION (mol/L)							
	DEA	MEA	BHEED	BHEP	HEOD	HEI	THEED	BHEI
0	3.00	0.000	0.000	0.000	0.000	0.000	0.000	0.000
2	2.94	0.047	0.000	0.000	0.000	0.000	0.000	0.000
4	2.79	0.059	0.000	0.000	0.013	0.000	0.000	0.000
8	2.69	0.089	0.004	0.003	0.015	0.000	0.019	0.000
12	2.72	0.141	0.008	0.004	0.017	0.000	0.041	0.000
24	2.53	0.166	0.015	0.007	0.029	0.005	0.098	0.000
30	2.34	0.205	0.032	0.009	0.031	0.012	0.183	0.000
36	2.23	0.216	0.037	0.010	0.033	0.013	0.222	0.003
48	2.02	0.195	0.049	0.012	0.037	0.016	0.319	0.010

$$k_{\text{DEA}} = 0.0077 \text{ h}^{-1}$$

Table C.40: Concentrations of compounds in aqueous DEA solution degraded with a gas mixture containing 30.0% CO₂ and 15.0% H₂S in nitrogen (DEA₀ = 3.0 mol/L; T = 165 °C; P_{gas mixture} = 1.55 MPa).

TIME (H)	CONCENTRATION (mol/L)							
	DEA	MEA	BHEED	BHEP	HEOD	HEI	THEED	BHEI
0	3.00	0.000	0.000	0.000	0.000	0.000	0.000	0.000
2	2.91	0.066	0.005	0.002	0.023	0.000	0.005	0.000
4	2.84	0.098	0.006	0.002	0.027	0.000	0.020	0.000
8	2.65	0.144	0.010	0.003	0.031	0.000	0.053	0.000
12	2.51	0.188	0.026	0.005	0.048	0.000	0.133	0.000
24	2.17	0.182	0.045	0.011	0.063	0.016	0.344	0.010
30	1.91	0.175	0.068	0.017	0.067	0.021	0.518	0.022
36	1.70	0.155	0.073	0.020	0.064	0.025	0.567	0.038
48	1.48	0.130	0.081	0.034	0.073	0.029	0.672	0.057

$$k_{\text{DEA}} = 0.0150 \text{ h}^{-1}$$

Table C.41: Concentrations of compounds in aqueous DEA solution degraded with a gas mixture containing 15.5% CO₂ and 29.9% H₂S in nitrogen (DEA₀ = 3.0 mol/L; T = 165 °C; P_{gas mixture} = 1.55 MPa).

TIME (H)	CONCENTRATION (mol/L)									
	DEA	ACET	BUT	MEA	BHEED	BHEP	HEOD	HEI	THEED	BHEI
0	3.00	0.000	0.000	0.000	0.000	0.000	0.000	0.000	0.000	0.000
2	2.90	0.004	0.001	0.068	0.000	0.000	0.000	0.000	0.000	0.000
4	2.74	0.006	0.003	0.101	0.000	0.000	0.005	0.000	0.000	0.000
8	2.63	0.007	0.005	0.157	0.005	0.000	0.010	0.000	0.012	0.000
12	2.59	0.010	0.008	0.225	0.008	0.004	0.016	0.000	0.024	0.000
24	2.36	0.009	0.009	0.299	0.015	0.006	0.021	0.000	0.050	0.000
30	2.26	0.009	0.011	0.386	0.033	0.008	0.021	0.003	0.093	0.000
36	2.10	0.008	0.011	0.412	0.043	0.009	0.022	0.004	0.121	0.004
48	1.95	0.007	0.012	0.425	0.063	0.013	0.035	0.005	0.180	0.012

$$k_{\text{DEA}} = 0.0085 \text{ h}^{-1}$$

Table C.42: Concentrations of compounds in aqueous DEA solution initially containing MEA. (DEA₀ = 2.90 mol/L; MEA₀ = 1 mol/L; T = 165 °C; P_{CO2} = 758 kPa).

TIME (H)	CONCENTRATION (mol/L)							
	DEA	MEA	BHEED	BHEP	HEOD	HEI	THEED	BHEI
0	2.90	0.964	0.000	0.000	0.000	0.000	0.000	0.000
2	2.67	0.890	0.041	0.003	0.118	0.000	0.028	0.000
4	2.25	0.821	0.085	0.006	0.130	0.000	0.177	0.019
6	2.15	0.801	0.137	0.008	0.154	0.000	0.301	0.035
8	1.94	0.740	0.155	0.012	0.148	0.000	0.335	0.047
11	1.83	0.732	0.198	0.017	0.161	0.000	0.442	0.081
20	1.40	0.568	0.211	0.034	0.164	0.010	0.512	0.188
26	1.12	0.477	0.218	0.048	0.120	0.012	0.566	0.258
32	0.94	0.396	0.204	0.066	0.119	0.015	0.661	0.384

$$k_{\text{DEA}} = 0.0338 \text{ h}^{-1}$$

Table C.43: Concentrations of compounds in aqueous DEA solution degraded with CO₂ (DEA₀ = 3.00 mol/L; T = 150 °C; P_{CO2} = 759 kPa).

TIME (H)	CONCENTRATION (mol/L)			
	DEA	BHEP	HEOD	THEED
0	3.00	0.000	0.000	0.000
2	2.73	0.004	0.083	0.000
4	2.63	0.006	0.163	0.000
8	2.49	0.007	0.205	0.182
12	2.32	0.010	0.261	0.311
24	1.93	0.021	0.291	0.413
30	1.73	0.029	0.302	0.670
36	1.53	0.038	0.301	0.772

$$k_{\text{DEA}} = 0.0173 \text{ h}^{-1}$$

APPENDIX D

D. COMPARISON BETWEEN EXPERIMENTAL AND PREDICTED CONCENTRATIONS

Table D.1: $[\text{DEA}]_0 = 40 \text{ wt\%}$, $T = 165 \text{ }^\circ\text{C}$, $P_{\text{COS}} = 345 \text{ kPa}$.

TIME (H)	CONCENTRATIONS (mol/L)							
	DEA		MEA		BHEED		BHEP	
	EXPT	PRED	EXPT	PRED	EXPT	PRED	EXPT	PRED
0	4.25	4.25	0.000	0.000	0.000	0.000	0.000	0.000
6	3.68	3.86	0.265	0.220	0.016	0.013	0.003	0.002
12	3.29	3.49	0.483	0.383	0.055	0.036	0.014	0.008
18	2.98	3.15	0.638	0.514	0.105	0.064	0.025	0.017
24	2.71	2.83	0.711	0.621	0.157	0.093	0.033	0.028
30	2.43	2.53	0.706	0.706	0.203	0.118	0.039	0.042
36	2.13	2.27	0.649	0.775	0.239	0.140	0.043	0.057
42	1.84	2.03	0.584	0.829	0.266	0.157	0.052	0.075
48	1.59	1.81	0.578	0.871	0.285	0.170	0.074	0.094

TIME (H)	HEOD		HEI		THEED		BHEI	
	EXPT	PRED	EXPT	PRED	EXPT	PRED	EXPT	PRED
0	0.000	0.000	0.000	0.000	0.000	0.000	0.000	0.000
6	0.015	0.027	0.000	0.005	0.019	0.145	0.000	0.003
12	0.047	0.051	0.010	0.007	0.153	0.266	0.003	0.007
18	0.080	0.073	0.036	0.012	0.321	0.372	0.020	0.016
24	0.105	0.092	0.066	0.020	0.467	0.463	0.049	0.029
30	0.119	0.110	0.092	0.031	0.566	0.542	0.088	0.046
36	0.123	0.125	0.112	0.045	0.628	0.608	0.136	0.068
42	0.127	0.139	0.124	0.060	0.695	0.665	0.190	0.093
48	0.146	0.152	0.130	0.078	0.844	0.712	0.244	0.120

Table D.2: $[\text{DEA}]_0 = 40 \text{ wt\%}$, $T = 160 \text{ }^\circ\text{C}$, $P_{\text{COS}} = 345 \text{ kPa}$.

TIME (H)	CONCENTRATIONS (mol/L)							
	DEA		MEA		BHEED		BHEP	
	EXPT	PRED	EXPT	PRED	EXPT	PRED	EXPT	PRED
0	4.13	4.13	0.000	0.000	0.000	0.000	0.000	0.000
6	3.75	3.82	0.217	0.167	0.016	0.006	0.002	0.001
12	3.47	3.52	0.382	0.310	0.036	0.021	0.008	0.005
18	3.24	3.24	0.499	0.431	0.070	0.040	0.015	0.010
24	3.01	2.98	0.577	0.534	0.118	0.061	0.022	0.018
30	2.78	2.73	0.622	0.622	0.171	0.081	0.028	0.027
36	2.58	2.50	0.642	0.695	0.209	0.100	0.036	0.037

TIME (H)	HEOD		HEI		THEED		BHEI	
	EXPT	PRED	EXPT	PRED	EXPT	PRED	EXPT	PRED
0	0.000	0.000	0.000	0.000	0.000	0.000	0.000	0.000
6	0.011	0.022	0.000	0.001	0.023	0.106	0.000	0.001
12	0.039	0.042	0.005	0.002	0.113	0.201	0.004	0.003
18	0.067	0.061	0.022	0.005	0.258	0.287	0.019	0.008
24	0.087	0.078	0.047	0.009	0.436	0.363	0.046	0.015
30	0.100	0.094	0.069	0.015	0.610	0.431	0.082	0.026
36	0.117	0.108	0.069	0.023	0.731	0.491	0.120	0.040

Table D.3: $[\text{DEA}]_0 = 40 \text{ wt\%}$, $T = 150 \text{ }^\circ\text{C}$, $P_{\text{COS}} = 345 \text{ kPa}$.

TIME (H)	CONCENTRATIONS (mol/L)							
	DEA		MEA		BHEED		BHEP	
	EXPT	PRED	EXPT	PRED	EXPT	PRED	EXPT	PRED
0	4.15	4.15	0.000	0.000	0.000	0.000	0.000	0.000
6	3.89	3.95	0.166	0.120	0.016	0.003	0.001	0.001
12	3.70	3.75	0.303	0.228	0.026	0.009	0.005	0.002
18	3.53	3.55	0.420	0.326	0.033	0.019	0.008	0.005
24	3.35	3.36	0.521	0.415	0.041	0.030	0.012	0.008
30	3.15	3.18	0.609	0.495	0.055	0.042	0.016	0.012
36	2.95	3.01	0.683	0.567	0.076	0.055	0.020	0.017
42	2.76	2.84	0.740	0.633	0.104	0.067	0.025	0.022
48	2.63	2.68	0.772	0.691	0.138	0.078	0.032	0.028
54	2.62	2.53	0.772	0.744	0.174	0.089	0.043	0.035

TIME (H)	HEOD		HEI		THEED		BHEI	
	EXPT	PRED	EXPT	PRED	EXPT	PRED	EXPT	PRED
0	0.000	0.000	0.000	0.000	0.000	0.000	0.000	0.000
6	0.008	0.016	0.000	0.000	0.000	0.069	0.000	0.000
12	0.017	0.030	0.000	0.000	0.015	0.130	0.000	0.001
18	0.026	0.044	0.000	0.001	0.052	0.186	0.002	0.003
24	0.036	0.058	0.001	0.003	0.102	0.239	0.005	0.006
30	0.050	0.070	0.002	0.005	0.157	0.288	0.010	0.010
36	0.067	0.082	0.005	0.007	0.214	0.333	0.015	0.016
42	0.085	0.093	0.009	0.011	0.270	0.375	0.021	0.024
48	0.104	0.104	0.014	0.015	0.321	0.414	0.028	0.033
54	0.119	0.114	0.019	0.020	0.366	0.450	0.036	0.043

Table D.4: $[\text{DEA}]_0 = 40 \text{ wt\%}$, $T = 127 \text{ }^\circ\text{C}$, $P_{\text{COS}} = 345 \text{ kPa}$.

TIME (H)	CONCENTRATIONS (mol/L)							
	DEA		MEA		BHEED		BHEP	
	EXPT	PRED	EXPT	PRED	EXPT	PRED	EXPT	PRED
0	4.20	4.20	0.000	0.000	0.000	0.000	0.000	0.000
24	3.80	3.90	0.228	0.192	0.009	0.004	0.002	0.001
48	3.45	3.62	0.439	0.360	0.020	0.014	0.005	0.003
72	3.13	3.35	0.588	0.509	0.037	0.026	0.011	0.007
96	2.83	3.09	0.657	0.639	0.062	0.039	0.018	0.013
120	2.55	2.85	0.662	0.753	0.095	0.050	0.027	0.019
144	2.30	2.62	0.649	0.853	0.132	0.060	0.038	0.026

TIME (H)	HEOD		HEI		THEED		BHEI	
	EXPT	PRED	EXPT	PRED	EXPT	PRED	EXPT	PRED
0	0.000	0.000	0.000	0.000	0.000	0.000	0.000	0.000
24	0.025	0.025	0.000	0.000	0.007	0.073	0.000	0.004
48	0.048	0.049	0.004	0.001	0.050	0.139	0.011	0.007
72	0.068	0.070	0.009	0.003	0.124	0.199	0.034	0.013
96	0.088	0.090	0.014	0.005	0.223	0.252	0.057	0.022
120	0.108	0.109	0.019	0.009	0.336	0.300	0.081	0.035
144	0.129	0.126	0.027	0.015	0.450	0.343	0.109	0.052

Table D.5: $[\text{DEA}]_0 = 30 \text{ wt\%}$, $T = 190 \text{ }^\circ\text{C}$, $P_{\text{COS}} = 345 \text{ kPa}$.

TIME (H)	CONCENTRATIONS (mol/L)							
	DEA		MEA		BHEED		BHEP	
	EXPT	PRED	EXPT	PRED	EXPT	PRED	EXPT	PRED
0	3.08	3.08	0.000	0.000	0.000	0.000	0.000	0.000
6	2.56	2.53	0.320	0.298	0.008	0.034	0.004	0.005
12	2.09	2.03	0.444	0.483	0.048	0.090	0.012	0.019
18	1.68	1.62	0.455	0.593	0.100	0.138	0.025	0.038
24	1.36	1.28	0.416	0.654	0.148	0.169	0.045	0.063
30	1.14	1.01	0.372	0.685	0.180	0.184	0.071	0.090
36	1.00	0.79	0.343	0.695	0.192	0.184	0.099	0.118
42	0.91	0.62	0.326	0.692	0.188	0.176	0.123	0.148
48	0.84	0.49	0.299	0.681	0.175	0.162	0.134	0.178

TIME (H)	HEOD		HEI		THEED		BHEI	
	EXPT	PRED	EXPT	PRED	EXPT	PRED	EXPT	PRED
0	0.001	0.001	0.000	0.000	0.000	0.000	0.000	0.000
6	0.023	0.030	0.006	0.003	0.049	0.148	0.000	0.007
12	0.045	0.053	0.018	0.019	0.198	0.258	0.016	0.024
18	0.064	0.072	0.031	0.049	0.368	0.338	0.057	0.054
24	0.079	0.087	0.041	0.088	0.507	0.392	0.116	0.095
30	0.089	0.098	0.049	0.133	0.586	0.427	0.182	0.142
36	0.093	0.107	0.053	0.181	0.602	0.447	0.246	0.191
42	0.092	0.115	0.058	0.229	0.570	0.456	0.293	0.239
48	0.089	0.120	0.064	0.277	0.533	0.456	0.307	0.283

Table D.6: $[\text{DEA}]_0 = 30 \cdot \text{wt}\%$, $T = 170^\circ\text{C}$, $P_{\text{CO}_2} = 345 \text{ kPa}$.

TIME (H)	CONCENTRATIONS (mol/L)							
	DEA		MEA		BHEED		BHEP	
	EXPT	PRED	EXPT	PRED	EXPT	PRED	EXPT	PRED
0	3.02	3.02	0.000	0.000	0.000	0.000	0.000	0.000
6	2.68	2.76	0.138	0.171	0.000	0.011	0.001	0.002
12	2.43	2.51	0.275	0.313	0.007	0.027	0.004	0.005
18	2.23	2.27	0.385	0.429	0.029	0.048	0.006	0.010
24	2.07	2.05	0.461	0.523	0.060	0.069	0.010	0.016
30	1.91	1.84	0.497	0.599	0.096	0.089	0.016	0.024
36	1.74	1.65	0.496	0.660	0.132	0.106	0.023	0.032
42	1.56	1.48	0.462	0.708	0.163	0.118	0.030	0.041
48	1.38	1.33	0.409	0.746	0.182	0.128	0.038	0.051
54	1.19	1.19	0.350	0.775	0.182	0.134	0.044	0.062
60	1.02	1.06	0.309	0.797	0.156	0.136	0.048	0.073

TIME (H)	HEOD		HEI		THEED		BHEI	
	EXPT	PRED	EXPT	PRED	EXPT	PRED	EXPT	PRED
0	0.000	0.000	0.000	0.000	0.000	0.000	0.000	0.000
6	0.016	0.016	0.000	0.001	0.000	0.076	0.000	0.003
12	0.035	0.030	0.002	0.003	0.021	0.127	0.000	0.006
18	0.055	0.043	0.008	0.008	0.108	0.172	0.002	0.013
24	0.076	0.054	0.016	0.016	0.226	0.210	0.021	0.024
30	0.097	0.065	0.023	0.026	0.355	0.243	0.053	0.038
36	0.116	0.074	0.029	0.039	0.478	0.271	0.097	0.056
42	0.131	0.082	0.033	0.055	0.579	0.294	0.147	0.077
48	0.139	0.090	0.034	0.072	0.643	0.313	0.193	0.099
54	0.135	0.097	0.035	0.091	0.656	0.328	0.223	0.123
60	0.115	0.103	0.034	0.111	0.606	0.340	0.221	0.148

Table D.7: [DEA]₀ = 30 wt%, T = 165 °C, P_{CO2} = 345 kPa.

TIME (H)	CONCENTRATIONS (mol/L)							
	DEA		MEA		BHEED		BHEP	
	EXPT	PRED	EXPT	PRED	EXPT	PRED	EXPT	PRED
0	3.04	3.04	0.000	0.000	0.000	0.000	0.000	0.000
6	2.75	2.82	0.169	0.149	0.012	0.005	0.000	0.001
12	2.49	2.61	0.283	0.275	0.022	0.017	0.004	0.003
18	2.27	2.41	0.376	0.383	0.032	0.033	0.010	0.006
24	2.08	2.21	0.463	0.475	0.047	0.051	0.017	0.010
30	1.90	2.03	0.549	0.552	0.066	0.067	0.022	0.015
36	1.73	1.86	0.622	0.618	0.088	0.083	0.028	0.020
42	1.55	1.71	0.661	0.673	0.110	0.096	0.033	0.026
48	1.36	1.56	0.627	0.718	0.127	0.107	0.040	0.033

TIME (H)	HEOD		HEI		THEED		BHEI	
	EXPT	PRED	EXPT	PRED	EXPT	PRED	EXPT	PRED
0	0.000	0.000	0.000	0.000	0.000	0.000	0.000	0.000
6	0.013	0.013	0.000	0.000	0.011	0.046	0.000	0.001
12	0.023	0.026	0.001	0.001	0.041	0.088	0.002	0.003
18	0.030	0.037	0.004	0.004	0.071	0.125	0.007	0.007
24	0.038	0.047	0.009	0.009	0.097	0.158	0.012	0.014
30	0.048	0.057	0.015	0.015	0.118	0.187	0.016	0.024
36	0.059	0.066	0.022	0.024	0.145	0.213	0.020	0.037
42	0.068	0.074	0.031	0.034	0.193	0.236	0.027	0.051
48	0.070	0.081	0.039	0.046	0.288	0.255	0.040	0.068

Table D.8: $[\text{DEA}]_0 = 30 \text{ wt\%}$, $T = 160 \text{ }^\circ\text{C}$, $P_{\text{COS}} = 345 \text{ kPa}$.

TIME (H)	CONCENTRATIONS (mol/L)							
	DEA		MEA		BHEED		BHEP	
	EXPT	PRED	EXPT	PRED	EXPT	PRED	EXPT	PRED
0	3.09	3.09	0.000	0.000	0.000	0.000	0.000	0.000
6	2.91	2.91	0.079	0.127	0.001	0.003	0.001	0.000
12	2.74	2.73	0.186	0.240	0.002	0.012	0.002	0.002
18	2.56	2.56	0.285	0.339	0.006	0.024	0.004	0.004
24	2.39	2.39	0.362	0.427	0.011	0.037	0.006	0.006
30	2.21	2.23	0.409	0.503	0.019	0.051	0.008	0.009
36	2.04	2.08	0.434	0.570	0.031	0.064	0.010	0.013
42	1.87	1.94	0.454	0.629	0.047	0.076	0.011	0.017
48	1.72	1.80	0.498	0.680	0.068	0.087	0.012	0.022

TIME (H)	HEOD		HEI		THEED		BHEI	
	EXPT	PRED	EXPT	PRED	EXPT	PRED	EXPT	PRED
0	0.000	0.000	0.000	0.000	0.000	0.000	0.000	0.000
6	0.014	0.011	0.000	0.000	0.000	0.037	0.000	0.000
12	0.024	0.022	0.000	0.001	0.000	0.070	0.000	0.001
18	0.033	0.032	0.000	0.002	0.000	0.101	0.000	0.004
24	0.041	0.042	0.000	0.005	0.019	0.129	0.000	0.009
30	0.051	0.050	0.002	0.009	0.077	0.154	0.000	0.015
36	0.063	0.059	0.006	0.014	0.157	0.177	0.005	0.024
42	0.076	0.066	0.012	0.021	0.241	0.197	0.018	0.035
48	0.089	0.073	0.020	0.028	0.298	0.216	0.044	0.047

Table D.9: [DEA]₀ = 30 wt%, T = 150 °C, P_{CO2} = 345 kPa.

TIME (H)	CONCENTRATIONS (mol/L)							
	DEA		MEA		BHEED		BHEP	
	EXPT	PRED	EXPT	PRED	EXPT	PRED	EXPT	PRED
0	3.04	3.04	0.000	0.000	0.000	0.000	0.000	0.000
6	2.89	2.92	0.111	0.088	0.005	0.001	0.000	0.000
12	2.75	2.80	0.186	0.171	0.011	0.005	0.001	0.001
18	2.61	2.68	0.252	0.247	0.015	0.011	0.003	0.001
24	2.46	2.57	0.323	0.317	0.019	0.017	0.007	0.002
30	2.32	2.46	0.403	0.382	0.024	0.024	0.011	0.004
36	2.18	2.35	0.485	0.442	0.033	0.032	0.016	0.005
42	2.05	2.25	0.551	0.497	0.049	0.040	0.021	0.007
48	1.93	2.15	0.572	0.548	0.073	0.047	0.024	0.009

TIME (H)	HEOD		HEI		THEED		BHEI	
	EXPT	PRED	EXPT	PRED	EXPT	PRED	EXPT	PRED
0	0.000	0.000	0.000	0.000	0.000	0.000	0.000	0.000
6	0.003	0.008	0.000	0.000	0.000	0.021	0.001	0.000
12	0.005	0.016	0.000	0.000	0.000	0.041	0.000	0.000
18	0.010	0.023	0.000	0.001	0.000	0.060	0.000	0.001
24	0.020	0.030	0.000	0.001	0.002	0.078	0.000	0.003
30	0.035	0.036	0.002	0.003	0.033	0.094	0.003	0.006
36	0.053	0.043	0.006	0.004	0.077	0.110	0.009	0.009
42	0.072	0.049	0.009	0.006	0.122	0.125	0.015	0.014
48	0.086	0.055	0.009	0.009	0.142	0.139	0.017	0.019

Table D.10: $[\text{DEA}]_0 = 30 \text{ wt\%}$, $T = 127^\circ\text{C}$, $P_{\text{COS}} = 345 \text{ kPa}$.

TIME (H)	CONCENTRATIONS (mol/L)							
	DEA		MEA		BHEED		BHEP	
	EXPT	PRED	EXPT	PRED	EXPT	PRED	EXPT	PRED
0	3.09	3.09	0.000	0.000	0.000	0.000	0.000	0.000
24	2.92	2.90	0.157	0.144	0.000	0.002	0.000	0.000
48	2.75	2.73	0.281	0.272	0.000	0.008	0.000	0.001
72	2.57	2.56	0.388	0.388	0.001	0.015	0.000	0.002
96	2.37	2.40	0.489	0.493	0.005	0.023	0.003	0.004
120	2.18	2.24	0.583	0.587	0.013	0.030	0.008	0.006
144	2.00	2.10	0.667	0.672	0.029	0.036	0.013	0.008
168	1.87	1.96	0.726	0.748	0.057	0.042	0.017	0.011

TIME (H)	HEOD		HEI		THEED		BHEI	
	EXPT	PRED	EXPT	PRED	EXPT	PRED	EXPT	PRED
0	0.000	0.000	0.000	0.000	0.000	0.000	0.000	0.000
24	0.002	0.013	0.000	0.000	0.000	0.024	0.000	0.000
48	0.015	0.025	0.001	0.001	0.009	0.044	0.000	0.002
72	0.027	0.037	0.003	0.002	0.036	0.062	0.000	0.005
96	0.036	0.047	0.004	0.003	0.067	0.079	0.001	0.011
120	0.042	0.057	0.005	0.006	0.102	0.094	0.008	0.019
144	0.054	0.067	0.008	0.009	0.148	0.108	0.024	0.028
168	0.085	0.075	0.018	0.013	0.221	0.120	0.054	0.040

Table D.11: [DEA]₀ = 20 wt%, T = 195 °C, P_{COS} = 345 kPa.

TIME (H)	CONCENTRATIONS (mol/L)							
	DEA		MEA		BHEED		BHEP	
	EXPT	PRED	EXPT	PRED	EXPT	PRED	EXPT	PRED
0	1.97	1.97	0.000	0.000	0.000	0.000	0.000	0.000
6	1.62	1.63	0.200	0.241	0.007	0.021	0.002	0.002
12	1.40	1.33	0.321	0.387	0.017	0.057	0.006	0.008
18	1.21	1.07	0.380	0.478	0.038	0.088	0.012	0.016
24	1.00	0.85	0.389	0.530	0.068	0.108	0.018	0.025
30	0.79	0.68	0.365	0.557	0.102	0.117	0.027	0.036
36	0.68	0.54	0.332	0.566	0.123	0.117	0.040	0.048

TIME (H)	HEOD		HEI		THEED		BHEI	
	EXPT	PRED	EXPT	PRED	EXPT	PRED	EXPT	PRED
0	0.000	0.000	0.000	0.000	0.000	0.000	0.000	0.000
6	0.004	0.010	0.003	0.003	0.006	0.051	0.001	0.002
12	0.012	0.018	0.003	0.016	0.052	0.089	0.000	0.014
18	0.021	0.025	0.013	0.041	0.110	0.116	0.002	0.035
24	0.032	0.031	0.036	0.075	0.166	0.134	0.030	0.063
30	0.043	0.035	0.067	0.113	0.214	0.146	0.072	0.096
36	0.051	0.038	0.089	0.155	0.260	0.152	0.113	0.130

Table D.12: [DEA]₀ = 20 wt%, T = 180 °C, P_{COS} = 345 kPa.

TIME (H)	CONCENTRATIONS (mol/L)							
	DEA		MEA		BHEED		BHEP	
	EXPT	PRED	EXPT	PRED	EXPT	PRED	EXPT	PRED
0	1.96	1.96	0.000	0.000	0.000	0.000	0.000	0.000
6	1.71	1.76	0.138	0.159	0.007	0.007	0.001	0.001
12	1.52	1.56	0.244	0.282	0.010	0.023	0.005	0.003
18	1.34	1.38	0.316	0.379	0.016	0.040	0.008	0.005
24	1.18	1.22	0.355	0.454	0.033	0.057	0.012	0.009
30	1.02	1.07	0.365	0.512	0.058	0.071	0.015	0.014
36	0.87	0.94	0.358	0.555	0.085	0.081	0.019	0.019
42	0.76	0.82	0.353	0.587	0.103	0.088	0.023	0.024
48	0.72	0.71	0.370	0.610	0.093	0.091	0.030	0.030

TIME (H)	HEOD		HEI		THEED		BHEI	
	EXPT	PRED	EXPT	PRED	EXPT	PRED	EXPT	PRED
	EXPT	PRED	EXPT	PRED	EXPT	PRED	EXPT	PRED
0	0.000	0.000	0.000	0.000	0.000	0.000	0.000	0.000
6	0.002	0.007	0.000	0.001	0.010	0.028	0.001	0.001
12	0.007	0.013	0.000	0.003	0.036	0.052	0.000	0.004
18	0.015	0.019	0.004	0.010	0.072	0.072	0.002	0.011
24	0.025	0.024	0.014	0.020	0.115	0.088	0.010	0.022
30	0.035	0.028	0.032	0.034	0.159	0.101	0.026	0.036
36	0.044	0.032	0.052	0.050	0.195	0.112	0.044	0.053
42	0.050	0.035	0.070	0.069	0.214	0.120	0.061	0.071
48	0.048	0.038	0.076	0.090	0.202	0.126	0.064	0.091

Table D.13: $[\text{DEA}]_0 = 20 \text{ wt\%}$, $T = 165 \text{ }^\circ\text{C}$, $P_{\text{COS}} = 345 \text{ kPa}$.

TIME (H)	CONCENTRATIONS (mol/L)							
	DEA		MEA		BHEED		BHEP	
	EXPT	PRED	EXPT	PRED	EXPT	PRED	EXPT	PRED
0	1.93	1.93	0.000	0.000	0.000	0.000	0.000	0.000
6	1.87	1.81	0.088	0.100	0.002	0.002	0.000	0.000
12	1.77	1.69	0.155	0.185	0.007	0.008	0.000	0.001
18	1.65	1.58	0.209	0.260	0.012	0.015	0.000	0.002
24	1.53	1.48	0.255	0.327	0.016	0.022	0.002	0.003
30	1.42	1.37	0.295	0.386	0.020	0.030	0.005	0.004
36	1.32	1.28	0.333	0.437	0.025	0.038	0.009	0.006
42	1.23	1.19	0.371	0.483	0.034	0.045	0.012	0.008
48	1.15	1.10	0.410	0.522	0.052	0.051	0.014	0.010

TIME (H)	HEOD		HEI		THEED		BHEI	
	EXPT	PRED	EXPT	PRED	EXPT	PRED	EXPT	PRED
0	0.000	0.000	0.000	0.000	0.000	0.000	0.000	0.000
6	0.000	0.005	0.000	0.000	0.000	0.014	0.001	0.000
12	0.002	0.010	0.000	0.001	0.000	0.027	0.000	0.001
18	0.007	0.014	0.000	0.002	0.000	0.039	0.000	0.003
24	0.013	0.017	0.001	0.004	0.016	0.050	0.000	0.006
30	0.020	0.021	0.003	0.007	0.052	0.059	0.004	0.010
36	0.027	0.024	0.007	0.011	0.097	0.068	0.012	0.016
42	0.033	0.027	0.011	0.016	0.131	0.075	0.020	0.023
48	0.038	0.030	0.013	0.023	0.126	0.082	0.022	0.031

Table D.14: $[\text{DEA}]_0 = 20 \text{ wt\%}$, $T = 150 \text{ }^\circ\text{C}$, $P_{\text{COS}} = 345 \text{ kPa}$.

TIME (H)	CONCENTRATIONS (mol/L)							
	DEA		MEA		BHEED		BHEP	
	EXPT	PRED	EXPT	PRED	EXPT	PRED	EXPT	PRED
0	1.94	1.94	0.000	0.000	0.000	0.000	0.000	0.000
6	1.89	1.87	0.057	0.057	0.000	0.001	0.000	0.000
12	1.83	1.80	0.114	0.111	0.002	0.003	0.000	0.000
18	1.76	1.74	0.164	0.161	0.007	0.005	0.001	0.001
24	1.69	1.67	0.208	0.209	0.012	0.008	0.002	0.001
30	1.62	1.61	0.245	0.254	0.016	0.011	0.003	0.002
36	1.56	1.55	0.276	0.296	0.017	0.014	0.004	0.002
42	1.50	1.49	0.302	0.336	0.017	0.018	0.004	0.003
48	1.43	1.43	0.323	0.373	0.016	0.021	0.005	0.003
54	1.36	1.38	0.339	0.408	0.015	0.024	0.006	0.004
60	1.26	1.32	0.350	0.440	0.017	0.028	0.008	0.005

TIME (H)	HEOD		HEI		THEED		BHEI	
	EXPT	PRED	EXPT	PRED	EXPT	PRED	EXPT	PRED
0	0.000	0.000	0.000	0.000	0.000	0.000	0.000	0.000
6	0.000	0.003	0.000	0.000	0.000	0.008	0.000	0.000
12	0.004	0.006	0.000	0.000	0.000	0.015	0.000	0.000
18	0.008	0.009	0.000	0.000	0.000	0.021	0.000	0.001
24	0.013	0.011	0.000	0.001	0.000	0.027	0.000	0.002
30	0.017	0.014	0.001	0.001	0.000	0.033	0.000	0.003
36	0.019	0.016	0.001	0.002	0.000	0.038	0.001	0.004
42	0.019	0.019	0.003	0.003	0.000	0.043	0.004	0.006
48	0.019	0.021	0.004	0.004	0.002	0.048	0.007	0.009
54	0.019	0.023	0.005	0.006	0.021	0.052	0.010	0.011
60	0.020	0.025	0.006	0.007	0.061	0.057	0.012	0.015

Table D.15: [DEA]₀ = 20 wt%, T = 135 °C, P_{COS} = 345 kPa.

TIME (H)	CONCENTRATIONS (mol/L)							
	DEA		MEA		BHEED		BHEP	
	EXPT	PRED	EXPT	PRED	EXPT	PRED	EXPT	PRED
0	1.98	1.98	0.000	0.000	0.000	0.000	0.000	0.000
24	1.86	1.83	0.097	0.125	0.000	0.003	0.000	0.000
48	1.70	1.69	0.163	0.237	0.000	0.007	0.000	0.001
72	1.54	1.55	0.212	0.335	0.004	0.013	0.001	0.002
96	1.40	1.43	0.254	0.422	0.012	0.018	0.003	0.003
120	1.27	1.31	0.296	0.499	0.022	0.023	0.006	0.005
144	1.16	1.20	0.340	0.566	0.032	0.027	0.009	0.007
168	1.07	1.10	0.383	0.625	0.039	0.030	0.011	0.009
192	0.99	1.00	0.421	0.676	0.041	0.032	0.012	0.011
216	0.89	0.91	0.444	0.720	0.034	0.033	0.011	0.013

TIME (H)	HEOD		HEI		THEED		BHEI	
	EXPT	PRED	EXPT	PRED	EXPT	PRED	EXPT	PRED
0	0.000	0.000	0.000	0.000	0.000	0.000	0.000	0.000
24	0.000	0.007	0.001	0.000	0.000	0.013	0.001	0.001
48	0.002	0.014	0.001	0.001	0.000	0.024	0.000	0.002
72	0.008	0.020	0.000	0.002	0.000	0.034	0.000	0.006
96	0.015	0.026	0.000	0.004	0.000	0.043	0.000	0.011
120	0.022	0.031	0.000	0.007	0.020	0.050	0.004	0.018
144	0.028	0.036	0.001	0.011	0.059	0.057	0.011	0.027
168	0.032	0.040	0.005	0.016	0.104	0.063	0.019	0.037
192	0.034	0.044	0.009	0.022	0.135	0.068	0.025	0.048
216	0.034	0.048	0.014	0.029	0.126	0.072	0.025	0.060

Table D.16: $[\text{DEA}]_0 = 20 \text{ wt\%}$, $T = 127 \text{ }^\circ\text{C}$, $P_{\text{CO}_2} = 345 \text{ kPa}$.

TIME (H)	CONCENTRATIONS (mol/L)							
	DEA		MEA		BHEED		BHEP	
	EXPT	PRED	EXPT	PRED	EXPT	PRED	EXPT	PRED
0	1.99	1.99	0.000	0.000	0.000	0.000	0.000	0.000
24	1.89	1.88	0.067	0.092	0.000	0.001	0.000	0.000
48	1.76	1.78	0.149	0.177	0.000	0.003	0.000	0.001
72	1.62	1.68	0.237	0.256	0.001	0.006	0.000	0.001
96	1.50	1.58	0.322	0.328	0.004	0.010	0.001	0.002
120	1.41	1.49	0.395	0.394	0.009	0.013	0.003	0.003
144	1.32	1.40	0.441	0.455	0.017	0.016	0.006	0.003

TIME (H)	HEOD		HEI		THEED		BHEI	
	EXPT	PRED	EXPT	PRED	EXPT	PRED	EXPT	PRED
0	0.000	0.000	0.000	0.000	0.000	0.000	0.000	0.000
24	0.003	0.006	0.000	0.000	0.000	0.011	0.001	0.000
48	0.011	0.011	0.000	0.000	0.000	0.018	0.000	0.001
72	0.020	0.016	0.000	0.001	0.011	0.025	0.000	0.002
96	0.029	0.020	0.000	0.001	0.029	0.031	0.000	0.005
120	0.039	0.025	0.000	0.003	0.053	0.037	0.005	0.008
144	0.048	0.029	0.003	0.004	0.087	0.043	0.016	0.012

Table D.17: $[\text{DEA}]_0 = 30 \text{ wt\%}$, $T = 150 \text{ }^\circ\text{C}$, $P_{\text{COS}} = 759 \text{ kPa}$.

TIME (H)	CONCENTRATIONS (mol/L)							
	DEA		MEA		BHEED		BHEP	
	EXPT	PRED	EXPT	PRED	EXPT	PRED	EXPT	PRED
0	2.95	2.95	0.000	0.000	0.000	0.000	0.000	0.000
6	2.78	2.77	0.157	0.130	0.000	0.004	0.003	0.000
12	2.63	2.61	0.275	0.241	0.009	0.011	0.005	0.001
18	2.47	2.44	0.375	0.340	0.024	0.021	0.008	0.002
24	2.29	2.29	0.465	0.427	0.040	0.033	0.012	0.004
30	2.09	2.14	0.550	0.504	0.056	0.045	0.017	0.005
36	1.88	2.00	0.624	0.571	0.070	0.057	0.023	0.008
42	1.69	1.86	0.679	0.629	0.082	0.069	0.029	0.010
48	1.55	1.74	0.697	0.680	0.096	0.079	0.032	0.013

TIME (H)	HEOD		HEI		THEED		BHEI	
	EXPT	PRED	EXPT	PRED	EXPT	PRED	EXPT	PRED
0	0.000	0.000	0.000	0.000	0.000	0.000	0.000	0.000
6	0.011	0.011	0.000	0.001	0.000	0.033	0.000	0.000
12	0.023	0.022	0.002	0.002	0.003	0.061	0.000	0.001
18	0.032	0.032	0.004	0.004	0.021	0.086	0.000	0.003
24	0.041	0.041	0.006	0.008	0.048	0.110	0.001	0.006
30	0.050	0.050	0.008	0.013	0.083	0.132	0.007	0.011
36	0.060	0.058	0.013	0.020	0.124	0.151	0.015	0.018
42	0.070	0.066	0.030	0.029	0.169	0.169	0.025	0.025
48	0.080	0.073	0.067	0.040	0.218	0.186	0.032	0.035

Table D.18: $[\text{DEA}]_0 = 30 \text{ wt\%}$, $T = 150 \text{ }^\circ\text{C}$, $P_{\text{COS}} = 1171 \text{ kPa}$.

TIME (H)	CONCENTRATIONS (mol/L)							
	DEA		MEA		BHEED		BHEP	
	EXPT	PRED	EXPT	PRED	EXPT	PRED	EXPT	PRED
0	2.96	2.96	0.000	0.000	0.000	0.000	0.000	0.000
6	2.77	2.74	0.199	0.157	0.003	0.005	0.004	0.000
12	2.51	2.54	0.314	0.290	0.014	0.016	0.009	0.001
18	2.24	2.34	0.396	0.403	0.031	0.030	0.013	0.002
24	2.00	2.15	0.477	0.499	0.050	0.046	0.018	0.004
30	1.80	1.98	0.565	0.579	0.068	0.063	0.022	0.006
36	1.63	1.81	0.649	0.645	0.085	0.078	0.027	0.009
42	1.46	1.66	0.698	0.699	0.101	0.091	0.033	0.012
48	1.25	1.52	0.661	0.742	0.116	0.103	0.041	0.015

TIME (H)	HEOD		HEI		THEED		BHEI	
	EXPT	PRED	EXPT	PRED	EXPT	PRED	EXPT	PRED
0	0.000	0.000	0.000	0.000	0.000	0.000	0.000	0.000
6	0.021	0.014	0.002	0.000	0.000	0.037	0.000	0.000
12	0.041	0.027	0.001	0.003	0.000	0.071	0.000	0.001
18	0.054	0.039	0.003	0.008	0.000	0.102	0.000	0.004
24	0.061	0.050	0.013	0.016	0.033	0.130	0.003	0.009
30	0.064	0.060	0.031	0.028	0.109	0.155	0.010	0.016
36	0.067	0.069	0.055	0.044	0.202	0.178	0.020	0.024
42	0.078	0.078	0.079	0.063	0.269	0.198	0.029	0.035
48	0.107	0.085	0.092	0.085	0.251	0.216	0.033	0.047

Table D.19: Rate constants obtained for the COS-DEA systems using the optimisation routine.

RUN #	OPERATING CONDITIONS*			RATE CONSTANTS ($\times 10^3$) (h^{-1} or $\text{L mol}^{-1} \text{h}^{-1}$)						
	C	T	P	k_1	k_2	k_3	k_4	k_5	k_6	k_7
1	40	165	345	10.40	8.20	1.10	10.90	6.00	3.50	30.60
2	40	160	345	9.50	7.00	1.00	11.00	5.70	3.30	35.10
3	40	150	345	6.00	2.30	0.56	1.00	1.80	4.60	10.80
4	40	127	345	2.10	1.20	0.27	0.80	0.86	1.25	13.20
5	30	190	345	12.40	22.00	1.30	14.40	9.45	7.40	54.00
6	30	170	345	8.20	12.00	1.30	6.00	5.60	2.30	38.00
7	30	165	345	8.40	3.77	0.65	3.80	2.10	7.80	14.70
8	30	160	345	5.10	2.20	0.67	3.00	1.65	3.00	24.20
9	30	150	345	5.50	2.10	0.53	1.60	0.91	10.00	16.00
10	30	127	345	1.90	0.42	0.15	0.41	0.38	1.10	13.60
11	20	195	345	14.40	15.10	0.91	24.90	5.10	8.20	45.80
12	20	180	345	10.20	10.00	0.74	19.10	3.60	5.20	29.70
13	20	165	345	6.40	3.90	0.40	4.20	1.50	5.20	26.30
14	20	150	345	4.40	1.60	0.24	1.80	0.20	13.70	20.00
15	20	135	345	1.60	0.84	0.10	0.57	0.33	1.20	5.00
16	20	127	345	1.90	0.52	0.18	0.31	0.28	0.95	14.00
17	30	150	759	8.20	2.90	0.69	4.00	1.60	8.80	10.00
18	30	150	1171	9.40	3.50	0.92	8.30	2.30	7.90	14.00
19	60	165	345	9.00	6.40	1.30	16.00	6.90	5.30	29.00

*C, T, P refer to DEA concentration (wt%), Temperature ($^{\circ}\text{C}$) and COS partial pressure (kPa), respectively.

Table D.20: Rate constants obtained for the CS₂-DEA systems using the optimisation routine.

RUN #	OPERATING CONDITIONS*			RATE CONSTANTS ($\times 10^3$) (h^{-1} or $\text{L mol}^{-1} \text{h}^{-1}$)						
	C	T	V	k_1	k_2	k_3	k_4	k_5	k_6	k_7
1	60	165	6.0	4.34	2.81	0.33	12.74	3.93	2.00	11.49
2	40	165	6.0	4.42	8.75	0.96	19.10	6.01	2.85	7.58
3	30	165	6.0	5.14	8.97	0.72	15.33	4.42	2.87	9.37
4	20	165	6.0	6.33	10.12	0.64	5.79	2.57	2.71	5.17
5	40	150	6.0	2.64	4.12	0.47	10.08	2.41	2.21	5.60
6	30	150	6.0	3.04	3.88	0.32	7.89	1.86	2.46	8.33
7	20	150	6.0	2.45	2.78	0.25	6.74	0.49	9.81	8.51
8	30	175	10.5	12.90	30.62	1.85	30.95	10.46	4.56	59.25
9	30	165	10.5	9.59	13.88	1.05	18.36	6.03	2.82	25.84
10	30	160	10.5	8.54	14.30	1.38	14.14	5.21	1.77	38.43
11	30	130	10.5	1.58	0.71	0.17	1.77	0.51	0.50	2.40
12	30	165	2.5	3.06	3.99	0.34	13.24	2.80	2.26	9.22

* C, T, V refer to DEA concentration (wt%), Temperature ($^{\circ}\text{C}$) and CS₂ volume (mL), respectively.

APPENDIX E

ERROR AND SENSITIVITY ANALYSIS

E.1 ERROR ANALYSIS

Errors in the GC analysis could arise from any of the following: air bubbles trapped in the injected sample, inconsistency of samples injected into the GC due to the presence of solid particles, GC integration error for very large peaks, fusion of small peaks with larger adjacent ones, and inconsistent sample volume. The effect of the last factor was minimized by using a syringe fitted with a "Chaney adaptor" to ensure the withdrawal of a constant sample volume. In the case of the solubility and hydrolysis runs, gas samples were transferred into a constant volume coil placed between the injection port and the column inlet. Excess volume was discharged through a purge line connected to the coil. This arrangement ensured that the volumes of samples analysed were equal. Each analysis was repeated at least three times and the average of the results was recorded. In general, results of repeated analyses were reproducible within $\pm 10\%$. The precision was even better for calibration samples because they contained no solids.

It is difficult to provide precise values for the various sources of error, but a nitrogen balance gives an estimate of the overall error involved in the degradation experiments. For each degradation run, a nitrogen balance can be expressed as follows:

$$N \text{ (DEA)}_0 = N \text{ (DEA)}_t + N \text{ (DEGRADATION PRODUCTS)}_t$$

$$= N_{(DEA)t} + N_{(MEA)t} + N_{(BHEED)t} + N_{(BHEP)t} + N_{(HEOD)t} + N_{(HEI)t} + N_{(THEED)t} + N_{(BHEI)t} \quad E.1$$

or

$$[DEA]_0 = [DEA]_t + [MEA]_t + 2 [BHEED]_t + 2 [BHEP]_t + [HEOD]_t + 2 [HEI]_t + 2 [THEED]_t + 2 [BHEI]_t \quad E.2$$

where $[i]_t$ denotes the concentration of compound i in mol/L at time t .

In Table E.1, N_L and N_R refer to the L.H.S and R.H.S respectively, of Eq. E.2. The experimental data used in the calculations are provided in appendix C.

Table E.1: Nitrogen balance for the degradation runs.

RUN	N_L	N_R	% DEV*	RUN	N_L	N_R	% DEV
1	4.20	5.48	+30.48	22	4.16	4.48	+ 7.69
2	4.12	5.67	+37.62	23	3.10	3.36	+ 8.39
3	4.17	4.75	+13.91	24	2.96	3.23	+ 9.12
4	4.20	4.79	+14.05	25	3.00	2.59	-13.70
5	3.11	3.61	+16.08	26	2.11	0.87	-58.77
6	3.04	3.58	+17.76	27	2.04	2.22	+ 8.82
7	3.00	3.12	+ 4.00	28	2.03	1.92	- 5.42
8	3.05	3.21	+ 5.25	29	1.90	1.79	- 5.68
9	3.01	3.12	+ 3.65	30	6.32	6.43	+ 1.74
10	3.08	3.43	+10.20	31	3.01	3.33	+10.63
11	1.97	2.30	+16.75	32	3.07	3.04	- 0.98
12	1.98	2.07	+ 4.55	33	3.11	2.24	-27.97
13	1.91	2.05	+ 7.33	34	3.11	3.25	+ 4.50
14	1.96	1.84	- 6.12	35	3.08	3.30	+ 7.14
15	1.99	1.80	- 9.55	36	3.08	2.94	- 4.55
16	2.00	2.16	+ 8.00	37	NO DEGRADATION		
17	2.93	3.18	+ 8.53	38	3.00	3.38	+12.67
18	2.95	3.08	+ 4.41	39	3.00	3.06	+ 2.00
19	6.21	8.09	+30.27	40	3.00	3.43	+14.33
20	3.00	3.06	+ 2.00	41	3.00	2.96	- 1.33
21	4.30	4.63	+ 7.67	42	3.86	4.12	+ 6.74
				43	3.10	3.45	+11.29

*% DEV = $100 \times (N_R - N_L) / N_L$

The deviations are generally below 20%. Higher deviations obtained in some runs are probably due to outdated calibrations and errors in the THEED concentrations when produced in large amounts. It should be recalled that THEED was the only compound not available in the pure form. Runs 26 and 33 were CS₂ runs conducted at temperatures above 180 °C. The high negative deviations in those runs suggest that some products of the reactions were not quantified either because they are very volatile, or could not be detected by the FID. By discounting deviations above 20%, an average deviation of +5.46% is obtained for the degradation runs. This value will be slightly higher when the minor degradation compounds containing nitrogen are included in the balance. Nevertheless, the overall value is an indication of the reliability of the experimental data.

In addition to the nitrogen balance, a measure of the confidence in the DEA concentration data can be obtained from the scatter between the experimental and fitted concentrations. Using the data for the DEA plots in chapter 5, a maximum deviation of $\pm 13\%$ was obtained, with an average of $\pm 3.98\%$ (see Table E.2). This value is close to the 5.46% average deviation obtained from the total nitrogen balance. Therefore, the average deviation in the reported concentrations is estimated at $\pm 5\%$, with a maximum of $\pm 13\%$ for DEA (based on Table E.2) and $\pm 20\%$ for the degradation products (based on the nitrogen balance).

Table E.2 : Maximum deviations in the DEA concentrations reported for the degradation runs.

RUN ^a	% DEVIATION ^b	RUN ^a	% DEVIATION ^b
1	- 4.81	17	- 3.91
2	+ 1.70	18	+ 3.45
3	- 2.73	19	+ 2.53
4	- 1.00	21	- 4.60
5	+12.79	22	- 5.96
7	+ 2.64	23	+ 2.12
9	- 1.83	24	- 5.26
10	+ 3.17	25	- 4.37
11	- 3.25	27	- 3.81
12	+ 3.83	28	+ 3.01
13	- 5.47	29	+ 1.59
14	- 5.20	30	- 3.94
15	+ 4.55	31	+ 2.45
16	- 3.47	32	- 7.94

^a Data used are from the corresponding table in appendix C.

^b % DEVIATION = (Fitted - Experimental)/Experimental

Using a similar approach, the deviations in Table E.3 were generated for the equilibrium constants governing amine protonation (K_1), carbamate formation (K_2) and thiocarbamate formation (K_{COS}). The maximum deviations are $\pm 11\%$, $\pm 17\%$ and $\pm 30\%$ for K_1 , K_2 and K_{COS} , respectively. Table E.4 shows that, for temperatures between 120 and 180 °C, K_1 obtained from the modified Kent-Eisenberg model is one to two times the value obtained from the Kent-Eisenberg model, while K_2 from the former is approximately twice that of the latter.

Table E.3 : Deviations between the experimental and fitted values of the protonation, carbamate and thiocarbamate equilibrium constants.

TEMPERATURE °C	K_1 ($\times 10^7$)			K_2			K_{COS} (10^6)		
	EXPT	FIT	% DEV	EXPT	FIT	% DEV	EXPT	FIT	% DEV
180	3.46	3.18	- 8.09	5.10	4.27	-16.27	7.84	6.77	-13.61
165	2.16	2.39	+10.65	3.02	3.53	+16.89	6.69	6.73	+ 0.60
150	1.73	1.75	+ 1.16	2.60	2.89	+11.15	5.14	6.69	+30.00
120	0.91	0.88	- 2.86	2.00	1.84	- 8.00	7.47	6.60	-11.65

Table E.4 : Comparison of protonation (K_1) and carbamate (K_2) constants from the Kent-Eisenberg and modified Kent-Eisenberg models.

TEMPERATURE °C	FACTOR ^a	
	K_1	K_2
180	1.07	2.20
165	1.23	2.10
150	1.42	2.00
120	1.99	1.79

^a FACTOR is the ratio of the predictions from the modified Kent-Eisenberg model to that from the Kent-Eisenberg model.

E.2 SENSITIVITY ANALYSIS

Tables E.5 and E.6 show the sensitivities of the objective function F , as defined in chapter 9, to +20% and -20% changes

respectively, in the optimal rate constants. F was most sensitive to k_1 , often resulting in changes exceeding 100%. Changes in k_2 to k_7 varied F by less than 20% on the average. Despite the sensitivity of F to k_1 , the changes in the model predictions as a result of changes in the rate constants were always below 20%, and generally below 10%. The accuracy of the reported rate constants should therefore be of the order of $\pm 20\%$.

Table E.5: Sensitivity of the objective function to changes in the rate constants for the COS-DEA systems (% change in $k_1 = +20\%$).

RUN		% CHANGE IN THE OBJECTIVE FUNCTION					
#	k_1	k_2	k_3	k_4	k_5	k_6	k_7
1	+ 14.54	+ 11.66	- 6.38	+ 9.13	-18.61	-13.60	- 0.23
2	+ 11.56	+ 8.50	- 2.41	+ 4.14	+ 2.11	- 0.83	- 0.45
3	+ 28.58	+ 4.10	- 36.85	- 1.30	-32.13	+ 4.91	- 4.76
4	- 34.68	+ 16.90	- 18.51	+ 2.33	+ 2.46	+ 1.90	- 1.27
5	- 82.27	+ 23.97	- 3.14	-33.81	+ 0.50	- 6.36	+ 0.64
6	- 49.67	+ 14.83	+ 9.87	-10.00	+ 3.00	- 4.59	+ 0.78
7	-134.44	- 5.93	- 86.52	-11.90	-24.88	+11.31	-17.78
8	-119.26	- 4.78	+ 1.44	- 2.61	- 6.63	- 2.53	+ 1.69
9	- 2.62	- 1.01	+ 11.18	- 0.21	- 6.03	+ 3.87	- 1.23
10	-119.14	- 10.76	-105.44	+ 0.36	+ 6.38	+ 1.15	+ 0.60
11	-126.50	+ 12.93	+ 0.76	-42.49	+ 2.08	- 3.26	- 0.97
12	-109.70	+ 7.99	+ 4.16	- 4.51	+ 5.97	- 1.39	- 3.61
13	-155.80	+ 4.47	- 1.95	- 4.21	+ 3.97	+ 0.66	+ 0.23
14	-216.07	+ 3.64	- 15.02	+ 0.76	- 9.94	+ 1.98	+ 0.66
15	- 84.23	+ 5.99	- 8.33	- 1.94	+ 1.99	- 0.10	- 1.66
16	- 95.33	+ 0.17	+ 37.52	- 0.32	+ 2.77	+ 0.13	+ 0.28
17	- 0.09	- 4.47	- 12.01	- 0.28	- 6.93	+ 8.31	- 4.01
18	- 42.70	- 5.09	+ 3.43	+ 8.75	+ 0.49	+ 6.94	- 3.41

Table E.6: Sensitivity of the objective function to changes in the rate constants for the COS-DEA systems (% change in $k_i = -20\%$).

RUN		% CHANGE IN THE OBJECTIVE FUNCTION						
#	k_1	k_2	k_3	k_4	k_5	k_6	k_7	
1	- 34.21	-16.82	- 4.61	-10.85	+ 3.81	+ 5.29	- 0.97	
2	- 32.05	-11.17	- 8.72	- 4.47	-12.02	- 2.09	+ 0.17	
3	- 83.58	- 9.41	+ 4.41	+ 0.71	+11.07	-11.69	+ 4.34	
4	- 21.31	-20.82	-19.03	- 2.77	-12.51	- 3.35	+ 0.64	
5	+ 51.95	-34.93	- 0.17	+28.97	- 6.64	+ 2.99	- 2.56	
6	+ 27.60	-20.39	-15.60	+ 6.95	- 6.62	+ 3.06	- 2.25	
7	-114.06	-29.59	+10.37	- 1.67	- 6.92	-19.39	+12.61	
8	+ 57.67	- 2.27	-22.07	+ 0.83	- 0.24	+ 1.36	- 3.09	
9	- 73.78	- 2.69	-32.96	- 0.14	+ 1.26	- 4.35	+ 0.92	
10	-121.11	+ 1.78	+28.59	- 1.70	-13.74	- 2.30	- 3.06	
11	+ 69.64	-25.91	- 2.81	+29.42	- 5.40	+ 1.71	- 1.55	
12	+ 40.57	-20.56	- 9.06	- 9.58	- 9.93	- 0.28	+ 0.99	
13	+ 72.92	-11.67	- 6.40	+ 1.39	- 6.88	- 1.35	- 1.55	
14	+ 20.12	-10.02	- 5.47	- 1.77	+ 6.25	- 2.54	- 1.78	
15	+ 57.35	- 8.07	+ 3.54	+ 0.93	- 2.63	- 0.11	+ 1.50	
16	- 34.22	- 2.27	-55.13	+ 0.05	- 4.07	- 0.34	- 0.82	
17	-147.12	- 7.50	-30.83	- 6.91	- 2.51	- 9.35	+ 2.80	
18	- 99.45	- 8.02	-39.22	-28.04	- 8.50	- 7.78	+ 2.02	

APPENDIX F

PROGRAM LISTINGS

```

C   THIS PROGRAM DETERMINES THE PROTONATION AND CARBAMATION
C   CONSTANTS IN THE MODIFIED K/E MODEL. THE CONSTANTS ARE LATER
C   EXPRESSED AS FUNCTIONS OF TEMPERATURE AND THEN USED TO OBTAIN
C   THE MODEL PREDICTIONS.
C
C   IMPLICIT REAL*8 (A-H,O-Z)
C   DIMENSION DEA(50),PCO2(50),PCOS(50),PH2S(50),YCO2(50),YCOS(50),
C   1YH2S(50),T(50),F(4),ACCEST(4),X(4),
C   COMMON/BLKA/CK1,CK2,CK3,CK4,CK5,CK6,CK7,CK8,CK9,CKC
C   COMMON/BLKB/Y1,Y2,Y3,H1,H2,H3,DEAC,P1,P2,P3
C   EXTERNAL FCN
C
C   INPUT VARIABLES
C
C   DATA A1,A2,A3,A4,A5,A6,A7,A8,A9/-2.551D0,4.8255D0,-241.818D0,
C   1 39.5554D0,-294.74D0,-304.689D0,-657.965D0,104.518D0,22.2819D0/
C   DATA B1,B2,B3,B4,B5,B6,B7,B8,B9/-5.652D3,-1.885D3,298.25D3,
C   1 -98.79D3,364.385D3,387.21D3,916.31D3,-136.81D3,-13.831D3/
C   DATA C1,C2,C3,C4,C5,C6,C7,C8,C9/0.D0,0.D0,-148.53D6,56.88D6,
C   1 -184.16D6,-194.76D6,-490.63D6,73.77D6,6.91D6/
C   DATA D1,D2,D3,D4,D5,D6,D7,D8,D9/0.D0,0.D0,332.6D8,-146.5D8,
C   1 415.8D8,438.1D8,1153.1D8,-174.7D8,-15.6D8/
C   DATA E1,E2,E3,E4,E5,E6,E7,E8,E9/0.D0,0.D0,-282.4D10,+136.1D10,
C   1 -354.3D10,-373.2D10,-1010.2D10,152.2D10,12.0D10/
C   DATA F1,F2,F3,F4,F5,F6,F7,F8/1.0344D0,2.92237D-2,26.207099D0,
C   1 -10.394767D0,3.749716D0,0.19297775D0,9.0006721D-3,74.282674D0/
C   N=4
C
C   INPUT NUMBER OF RUNS
C
C   READ(5,10)NRUN
C   10  FORMAT(I2)
C
C   INPUT DEA CONCENTRATIONS AND TEMPERATURES
C
C   DO 20 I=1,NRUN
C   READ(5,15)DEA(I),T(I)
C   15  FORMAT(F5.3,2X,F6.2)
C   20  CONTINUE
C
C   INPUT PARTIAL PRESSURES (KPa) AND ACID GAS LOADINGS (mol/mol DEA)
C   FOR EACH RUN
C
C   DO 30 I=1,NRUN
C   READ(5,25)YCO2(I),YCO2(I),YH2S(I),PCO2(I),PCOS(I),PH2S(I)
C   25  FORMAT(3(F5.3,2X),3(F6.2,2X))
C   30  CONTINUE
C
C   WRITE(6,35)
C   35  FORMAT(/17X,'PREDICTED AND EXPERIMENTAL ACID GAS LOADINGS'//)
C   WRITE(6,40)
C   40  FORMAT(13X,'CARBON DIOXIDE',10X,'HYDROGEN SULPHIDE',6X,
C   1 'CARBONYL SULPHIDE'//)
C   WRITE(6,45)
C   45  FORMAT(2X,'RUN',3X,'PRED',3X,'EXPT',3X,'DEV (%)',3X,'PRED',
C   13X,'EXTAL',3X,'DEV (%)',3X,'PRED',3X,'EXPT')
C   DO 55 I=1,NRUN
C
C   CALCULATE EQUILIBRIUM CONSTANTS FROM KENT/EISENBERG (K/E) MODEL

```



```

C
C      CK1=DEXP(A1+B1/T(I)+C1/(T(I)**2)+D1/(T(I)**3)+E1/(T(I)**4))
C      CK2=DEXP(A2+B2/T(I)+C2/(T(I)**2)+D2/(T(I)**3)+E2/(T(I)**4))
C      CK3=DEXP(A3+B3/T(I)+C3/(T(I)**2)+D3/(T(I)**3)+E3/(T(I)**4))
C      CK4=DEXP(A4+B4/T(I)+C4/(T(I)**2)+D4/(T(I)**3)+E4/(T(I)**4))
C      CK5=DEXP(A5+B5/T(I)+C5/(T(I)**2)+D5/(T(I)**3)+E5/(T(I)**4))
C      CK6=DEXP(A6+B6/T(I)+C6/T(I)**2+D6/T(I)**3+E6/T(I)**4)
C      CK7=DEXP(A7+B7/T(I)+C7/T(I)**2+D7/T(I)**3+E7/T(I)**4)
C      CK8=(DEXP(A8+B8/T(I)+C8/(T(I)**2)+D8/(T(I)**3)+E8/(T(I)**4)))/7.5025D0
C      CK9=(DEXP(A9+B9/T(I)+C9/(T(I)**2)+D9/(T(I)**3)+E9/(T(I)**4)))/7.5025D0
C
C      SAVE CURRENT PARAMETERS (DEA CONCENTRATION, HENRY'S CONSTANTS,
C      LOADINGS AND PARTIAL PRESSURES AS SINGLE VARIABLES
C
C      DEAC=DEA(I)
C      H1=CK8
C      H2=CK9
C      H3=1.D3*(DEXP(9.2910D0-2313.4324D0/T(I)))
C      Y1=YH2S(I)
C      Y2=YCO2(I)
C      Y3=YCOS(I)
C      IF(Y3.EQ.0.D0) Y3=0.001D0
C      P1=PH2S(I)
C      P2=PCO2(I)
C      P3=PCOS(I)
C
C      CALCULATE CONCENTRATIONS OF SPECIES IN SOLUTION. DONE ONLY WHEN
C      DETERMINING K1, K2 AND KC FROM EXPERIMENTAL DATA
C
C      PK=(P1*CK6/H1)*(1.D0+CK7)
C      HP=PK/(DEAC*Y1-P1/H1)
C      H2S=P1/H1
C      CO2=P2/H2
C      COS=P3/H3
C      HCO3=CK3*CO2/HP
C      CO3=CK5*HCO3/HP
C      HS=CK6*H2S/HP
C      SS=CK7*HS/HP
C      DEACOO=Y2*DEAC-HCO3-CO3-CO2
C      DEACOS=Y3*DEAC-COS
C      DEAH=HCO3+DEACOO+2.D0*CO3+CK4/HP+HS+2.D0*SS+DEACOS-HP
C      DEAF=DEAC-DEACOO-DEACOS-DEAH
C
C      CALCULATE K1,K2,KCOS FROM EXPERIMENTAL DATA
C
C      CK1=DEAF*HP/DEAH
C      CK2=DEAF*HCO3/DEACOO
C      CKC=DEAF*COS/(DEACOS*HP)
C
C      K1,K2,KC AS FUNCTIONS OF TEMPERATURE
C
C      CK1=DEXP(-5.0058-4459.9476/T(I))
C      CK2=DEXP(5.0809-1716.4522/T(I))
C      CKC=DEXP(19.0833-1440.0543/T(I))
C
C      SET INPUT PARAMETERS AND INITIAL GUESSES FOR THE NON LINEAR
C      SOLVER (NDINVT)
C
C      ERR=1.D-12
C      MAXIT=200000

```

```

C
C SET INITIAL GUESS FOR YH2S=X(1),YCO2=X(2),HPLUS=X(3),YCOS=X(4)
C (OR SET INITIAL GUESSES FOR K1,K2,HP,KC)
C
C   X(1)=1.D-1
C   X(2)=1.D-1
C   X(3)=1.D-1
C   X(4)=1.D-3
C
C CALL NDINVT(N,X,F,ACCEST,MAXIT,ERR,FCN,&60)
C
C   X1=X(1)
C   X2=X(2)
C   HP1=X(3)
C   X3=X(4)
C
C CALCULATE DEVIATIONS BETWEEN EXPERIMENTAL VALUES AND MODEL
C PREDICTIONS
C
C   DEV1=((X1-Y1)/Y1)*100.D0
C   DEV2=((X2-Y2)/Y2)*100.D0
C
C SOLUTION
C
C   WRITE(6,50) I,X2,Y2,DEV2,X1,Y1,DEV1,X3,YCOS(I)
50  FORMAT(2X,I2,2(4X,F5.3,3X,F5.3,3X,F7.2),4X,F5.3,4X,F5.3)
55  CONTINUE
C   GO TO 70
60  WRITE(6,65)
65  FORMAT(10X,'ROUTINE FAILURE')
70  STOP
C   END
C
C SUBROUTINE FCN(X,F)
C IMPLICIT REAL*8(A-H,O-Z)
C DIMENSION X(1),F(1)
C COMMON/BLKA/CK1,CK2,CK3,CK4,CK5,CK6,CK7,CK8,CK9,CKC
C COMMON/BLKB/Y1,Y2,Y3,H1,H2,H3,DEAC,P1,P2,P3
C
C THE 4 MODEL EQUATIONS TO BE SOLVED BY NDINVT
C
C   F(1)=P1-(H1/(CK6*CK7))* (DEAC*X(1)-P1/H1)*(X(3)**2)/(1.D0+X(3)/CK7)
C
C   F(2)=P2-(H2/(CK3*CK5))* (DEAC*X(2)-P2/H2)*(X(3)**2)/(1.D0+X(3)/
1CK5+DEAC*X(3)/(CK2*CK5*(1.D0+X(3)/CK1+(P2/(H2*X(3)))*(CK3/CK2)
1+(P3/(H3*CKC*X(3))))))
C
C   F(3)=X(3)*(1.D0+DEAC/(CK1*(1.D0+X(3)/CK1+(P2/(H2*X(3)))*(CK3/CK2
1)+(P3/(CKC*H3*X(3))))))-(DEAC*X(1)-P1/H1)*(1.D0+CK7/(CK7*X(3))
1-(DEAC*X(2)-P2/H2)*(1.D0+CK2*CK5/(CK2*CK5+CK2*X(3)+DEAC*X(3)/
1(1.D0+X(3)/CK1+(P2/(H2*X(3)))*(CK3/CK2)+(P3/(CKC*H3
1*X(3)))))))-CK4/X(3)-((DEAC*X(4)-P3/H3)/(DEAC-(DEAC
1*X(4)-P3/H3)))*(1.D0+X(3)/CK1+(P2/H2)*(CK3/(CK2
1*X(3))))*(DEAC/(1.D0+X(3)/CK1+(CK3/(CK2*X(3))
1*P2/H2+P3/(CKC*X(3)*H3)))
C
C   F(4)=P3-H3*((DEAC*X(4)-P3/H3)/(DEAC-(DEAC*X(4)-P3/H3)))
1*(CKC*X(3)*(1.D0+X(3)/CK1+(P2/H2)*(CK3/(CK2*X(3)))))
C
C RETURN
C END

```

```

C
C  PROGRAMME TO DETERMINE THE RATE CONSTANTS IN THE KINETIC
C  EXPRESSIONS FOR THE COS-DEA AND CS2-DEA SYSTEMS
C
      IMPLICIT REAL*8 (A-H,O-Z)
      DIMENSION A11(50),A12(50),A13(50),A14(50),A15(50),A21(50),
1A22(50),A23(50),A24(50),A25(50),A31(50),A32(50),A33(50),A34(50),
1A35(50),A41(50),A42(50),A43(50),A44(50),A45(50),A51(50),A52(50),
1A53(50),A54(50),A55(50),A61(50),A62(50),A63(50),A64(50),A65(50),
1A71(50),A72(50),A73(50),A74(50),A75(50),A81(50),A82(50),A83(50),
1A84(50),A85(50),RKL(50),RKU(50),X(80),Y(10),NT(50),RC(10)
C  1YY(50,50)
      COMMON/BLKA/YC(80,80),YF(80),YE(80,80),YMAX(8)
      COMMON/BLKB/RK(15)
      COMMON DX,N,NE
      INTEGER FLAG
      INTEGER FAIL
C
C  Input maximum values of rate constants for each search (RC) and
C  time for each run (NT) in hours. Values different from those
C  below may be input through READ statements
C
      DATA RC/0.01D0,0.02D0,0.03D0,0.04D0,0.05D0,0.06D0,
1 0.07D0,0.08D0,0.09D0,0.10D0/
      DATA NT/48,36,54,48,60,3*48,168,36,2*48,60,216,30,2*48,166,168,
1 164/
C
C  Input the numbers of runs (NRUN), equations (NE)
C  and variables (NVAR)
C
      READ(5,10)NRUN,NE,NVAR
10  FORMAT(3(I2,2X))
C
C  Input initial guesses of rate constants, RK(1).....RK(8).
C
      READ(5,15) (RK(L),L=1,7)
15  FORMAT(7(F3.1,1X))
C
C  Input the five polynomial fitting constants for DEA (1) and the
C  degradation compounds (2-8)
C
      DO 25 I=1,NRUN
      READ(5,20)A11(I),A12(I),A13(I),A14(I),A15(I)
20  FORMAT(5(2X,E15.8))
25  CONTINUE
      DO 30 I=1,NRUN
      READ(5,20)A21(I),A22(I),A23(I),A24(I),A25(I)
30  CONTINUE
      DO 35 I=1,NRUN
      READ(5,20)A31(I),A32(I),A33(I),A34(I),A35(I)
35  CONTINUE
      DO 40 I=1,NRUN
      READ(5,20)A41(I),A42(I),A43(I),A44(I),A45(I)
40  CONTINUE
      DO 45 I=1,NRUN
      READ(5,20)A51(I),A52(I),A53(I),A54(I),A55(I)
45  CONTINUE
      DO 50 I=1,NRUN
      READ(5,20)A61(I),A62(I),A63(I),A64(I),A65(I)
50  CONTINUE

```

```

DO 55 I=1,NRUN
  READ(5,20) A71(I),A72(I),A73(I),A74(I),A75(I)
55 CONTINUE
  DO 60 I=1,NRUN
    READ(5,20) A81(I),A82(I),A83(I),A84(I),A85(I)
60 CONTINUE
C
C Calculate exptal concentrations at selected times, using a fourth
C order polynomial fitting equation derived in a previous programme.
C
  DO 65 I=1,8
    YMAX(I)=0.D0
65 CONTINUE
C
  DX=4
  X(1)=0.D0
  DO 135 L=1,NRUN
    L=1
    N=1+NT(L)/DX
    DO 70 J=1,N
      JM=J-1
      IF(J.GE.2) X(J)=X(JM)+DX
C
      YE(1,J)=A11(L)+A12(L)*X(J)+A13(L)*X(J)**2+A14(L)*X(J)**3
      1+A15(L)*X(J)**4
      IF(YE(1,J).LT.0.D0) YE(1,J)=0.D0
      YC(1,J)=YE(1,J)
      YMAX(1)=DMAX1(YMAX(1),YE(1,J))
C
      YE(2,J)=A21(L)+A22(L)*X(J)+A23(L)*X(J)**2+A24(L)*X(J)**3
      1+A25(L)*X(J)**4
      IF(YE(2,J).LT.0.D0) YE(2,J)=0.D0
      YC(2,J)=YE(2,J)
      YMAX(2)=DMAX1(YMAX(2),YE(2,J))
C
      YE(3,J)=A31(L)+A32(L)*X(J)+A33(L)*X(J)**2+A34(L)*X(J)**3
      1+A35(L)*X(J)**4
      IF(YE(3,J).LT.0.D0) YE(3,J)=0.D0
      YC(3,J)=YE(3,J)
      YMAX(3)=DMAX1(YMAX(3),YE(3,J))
C
      YE(4,J)=A41(L)+A42(L)*X(J)+A43(L)*X(J)**2+A44(L)*X(J)**3
      1+A45(L)*X(J)**4
      IF(YE(4,J).LT.0.D0) YE(4,J)=0.D0
      YC(4,J)=YE(4,J)
      YMAX(4)=DMAX1(YMAX(4),YE(4,J))
C
      YE(5,J)=A51(L)+A52(L)*X(J)+A53(L)*X(J)**2+A54(L)*X(J)**3
      1+A55(L)*X(J)**4
      IF(YE(5,J).LT.0.D0) YE(5,J)=0.D0
      YC(5,J)=YE(5,J)
      YMAX(5)=DMAX1(YMAX(5),YE(5,J))
C
      YE(6,J)=A61(L)+A62(L)*X(J)+A63(L)*X(J)**2+A64(L)*X(J)**3
      1+A65(L)*X(J)**4
      IF(YE(6,J).LT.0.D0) YE(6,J)=0.D0
      YC(6,J)=YE(6,J)
      YMAX(6)=DMAX1(YMAX(6),YE(6,J))
C
      YE(7,J)=A71(L)+A72(L)*X(J)+A73(L)*X(J)**2+A74(L)*X(J)**3

```

```

1+A75(L)*X(J)**4
IF(YE(7,J).LT.0.D0)YE(7,J)=0.D0
YC(7,J)=YE(7,J)
YMAX(7)=DMAX1(YMAX(7),YE(7,J))
C
  YE(8,J)=A81(L)+A82(L)*X(J)+A83(L)*X(J)**2+A84(L)*X(J)**3
1+A85(L)*X(J)**4
IF(YE(8,J).LT.0.D0)YE(8,J)=0.D0
YC(8,J)=YE(8,J)
YMAX(8)=DMAX1(YMAX(8),YE(8,J))
70 CONTINUE
C
C Input parameters for optimization routine. The routine NLPQL0 is
C used to optimize the values of the rate constants by minimising
C the square of the differences between experimental and calculated
C concentrations for all compounds for each integration interval
C used in Runge-Kutta (RKC)
C
C
C Upper and lower bounds of the rate constants
C
  DO 130 KOUNT=1,10
  DO 75 J=1,NVAR
75 RK(J)=1.D-4
  DO 80 LL=1,NVAR
  RKL(LL)=0.D0
  RKU(LL)=RC(KOUNT)
80 CONTINUE
C
C Other optimisation parameters
C
  ME=0
  M=0
  MMAX=0
  MAXIT=15000
  MXFLSE=200
  LOG=20000
  ACCUR=1.D-6
  SCBOU=1.D3
C
  CALL NLPQL0(M,ME,NVAR,RK,F2,RKL,RKU,ACCUR,SCBOU,MXFLSE,MAXIT,
1LOG,FAIL)
  WRITE(6,85)FAIL,F2
85 FORMAT('0RETURN CODE FROM NLPQL0:',I6/
1'FINAL FUNCTION VALUE:',1PG16.8/)
  DO 125 KK=1,2
  IF(KK.EQ.2)GO TO 95
  K1=1
  K2=4
  WRITE(6,90)
90 FORMAT(/3X,'TIME',7X,'DEA',11X,'MEA',10X,'BHEED',9X,'BHEP')
  GO TO 105
95 K1=5
  K2=8
  WRITE(6,100)
100 FORMAT(/3X,'TIME',7X,'HEOD',10X,'HEI',10X,'THEED',9X,'BHEI')
105 WRITE(6,110)
110 FORMAT(4X,'(H)',3X,'EXPT',3X,'PRED',3X,'EXPT',3X,'PRED',3X,
1'EXPT',3X,'PRED',3X,'EXPT',3X,'PRED')
  DO 120 I=1,N,3

```

```

        WRITE(6,115)X(I),(YE(J,I),YC(J,I),J=K1,K2)
115  FORMAT(2X,F5.1,8(3X,F4.2))
120  CONTINUE
125  CONTINUE
130  CONTINUE
135  CONTINUE
      STOP
      END
C
C
      SUBROUTINE FUNK(TI,Y,F)
      IMPLICIT REAL*8(A-H,O-Z)
      DIMENSION Y(1),F(1)
      COMMON/BLKA/YC1(80,80),YF(80),YE(80,80),YMAX(8)
      COMMON/BLKB/RK(15)
      COMMON/RKCS/OK
      LOGICAL OK
      IF(.NOT.OK) STOP
C
      F(1)=-RK(1)*Y(1)-RK(2)*Y(1)*Y(2)-RK(3)*Y(1)-RK(5)*Y(1)
      F(2)=RK(1)*Y(1)-RK(2)*Y(1)*Y(2)-RK(4)*Y(2)**2
      F(3)=RK(2)*Y(1)*Y(2)-RK(7)*Y(3)
      F(4)=RK(6)*Y(7)
      F(5)=RK(3)*Y(1)
      F(6)=RK(4)*Y(2)**2
      F(7)=RK(5)*Y(1)-RK(6)*Y(7)
      F(8)=RK(7)*Y(3)
C
      RETURN
      END
C
C
      SUBROUTINE FUNC(M,ME,MMAX,NVAR,F2,G,RK)
      IMPLICIT REAL*8(A-H,O-Z)
      DIMENSION RK(15),T(20),S(20),P(20),F(20),Y(20)
      COMMON/BLKA/YC1(80,80),YF(80),YE(80,80),YMAX(8)
      COMMON DX,N,NE
      EXTERNAL FUNK
C
      EPS=1.D-6
      TI=0.D0
      TF=DX*N
      H=(TF-TI)/256.D0
      HMIN=1.D-3*H
      DO 10 J=1,NE
        Y(J)=YE(J,1)
10    CONTINUE
      TF=DX
C
C    Call RKC routine
C
      DO 20 JJ =2,N
        CALL DRKC(NE,TI,TF,Y,F,H,HMIN,EPS,FUNK,T,S,P)
      DO 15 J=1,NE
        YC1(J,JJ)=Y(J)
15    CONTINUE
      TF=TF+DX
20    CONTINUE
      SUM1=0.D0
      DO 30 L=1,8

```

```
SUM=0.D0
DO 25 II=1,N
SUM=SUM+(YE(L,II)-YC1(L,II))**2
25 CONTINUE
IF(YMAX(L).EQ.0.D0) SUM1=SUM1+SUM
IF(YMAX(L).GT.0.D0) SUM1=SUM1+SUM/YMAX(L)**2
30 CONTINUE
C
F2=SUM1
C
RETURN
END
```